

MTA doktori értekezés

**A sejtmembrán gyógyszertranszporterei: módszerfejlesztéstől a
szerkezet-hatás vizsgálatokig**

Laczka Csilla

Enzimológiai Intézet, TTK, ELKH

Budapest

2021

ELŐSZÓ

Akadémiai doktori értekezésemben a PhD fokozatom megszerzése utáni kutatásom eredményeit mutatom be. Ezek, témájukat tekintve két csoportra oszlanak. Az ABCG2 fehérjével kapcsolatos kutatásaimat még Sarkadi Balázs és Váradi András irányításával, illetve útmutatásai alapján készítettem, posztdoktori éveimben már levelező szerzőként jegyezve az ezekből született publikációkat. Ezúton is köszönöm nekik a sok segítségét és az évtizedek óta tartó támogatást! A dolgozatom második részében a vezetésemmel, önállóan megkezdett kutatási irányban, az OATP-k vizsgálata terén született eredményeinket mutatom be.

Tartalomjegyzék

ELŐSZÓ.....	2
ÖSZEFOGLALÁS	5
RÖVIDÍTÉSEK JEGYZÉKE.....	6
I. IRODALMI BEVEZETŐ.....	9
Membrántranszporterek a farmakokinetikában	9
Az ABCG2 fehérje	12
Az ABCG2 térszerkezete.....	14
Az ABCG2 fehérje szerepe az emberi szervezetben	15
Az ABCG2 fehérje és farmakokinetika	16
Az ABCG2 polimorf változatai.....	17
Az ABCG2 expressziójának, működésének és lokalizációjának szabályozása	19
A lipidkörnyezet hatása az ABCG2 fehérje működésére	19
Az OATP fehérjecsalád.....	20
Az első OATP felfedezése.....	21
Nevezéktan	21
Az OATP-k működési mechanizmusa.....	22
OATP-k szerkezete és poszttranszlációs szabályozása.....	24
Gyógyszertranszporter OATP-k	25
Az OATP-k betegséget okozó mutációi	28
OATP-k SNP-i	28
OATP-k a tumorokban	29
ABC és OATP transzporterek <i>in vitro</i> vizsgálatának módszerei.....	31
II. CÉLKITŰZÉSEK	33
III. MÓDSZEREK	34
IV. EREDMÉNYEK ÉS MEGVITATÁSUK	43
IV/A. A humán ABCG2 fehérje vizsgálata: szubsztrátfelismerés, koleszterin általi szabályozás, antitest kötődés jellemzése és új gyógyszerkölsönhatások feltárása	43
IV/A.1. Az ABCG2 fehérje mutációs forró pontjának vizsgálata	43
IV/A.2. Az ABCG2 koleszterin-szenzor régiójának azonosítása felé	46
IV/A. 2.1. Az LxxL szteroidkötő motívum szerepe.....	46
IV/A. 2.2. A CRAC motívum szerepe a koleszterinérzékelésben	50
IV/A.3. Az ABCG2 és tirozin kináz gátlószerek közötti kölcsönhatás vizsgálata	55
IV/A.4. Egy ABCG2-specifikus antitest jellemzése.....	56
IV/A.4.1. Gátlószerek és nukleotid analógok hatása az 5D3 kötődésére.....	57
IV/A. 4.2. Az 5D3 antitest kötődéséhez nem szükséges a kovalens ABCG2 dimer megléte.....	60
IV/B. A humán Organikus Anion Transzporter Polipeptidek vizsgálata: új módszerek, új gyógyszerkölsönhatások és mechanizmus kutatás.....	65

IV/B. 1. Az OATP-k vizsgálatára alkalmas új fluoreszcens módszerek kidolgozása.....	65
IV/B.1.1. OATP-k vizsgálata rovarsejtekben, egy általános OATP szubsztrát azonosítása.....	65
IV/B. 1.2. Multispecifikus OATP-ket kifejező humán sejtes modellek létrehozása és új fluoreszcencia- alapú vizsgálati módszerek kidolgozása	70
IV/B. 1.2.1. OATP-ket termelő sejtek kiválogatása festékfelvétel alapján.....	72
IV/B.1.2.2. Hepatociták OATP-inek vizsgálata.....	73
IV/B.1.2.3 Az első fluoreszcencia-alapú „add-és-mérd” módszer multispecifikus OATP-k vizsgálatára	77
IV/B. 1.2.4. Kompetitív ellenáramlásos módszer a szubsztrátok és nem transzportálódó inhibitorok elkülönítésére.....	80
IV/B. 2. OATP1B1 és MRP2 együttes vizsgálatára alkalmas fluoreszcens módszer kidolgozása	83
IV/B. 3. Új vegyület-OATP kölcsönhatások azonosítása	86
IV/B. 3.1. Extrahepatikus OATP-k vizsgálatára alkalmas fluoreszcens módszer kidolgozása, új gyógyszerkölcsönhatás kimutatása	86
IV/B. 3.2. OATP2B1 és ösztrom szarmazékok kölcsönhatásának vizsgálata.....	89
IV/B. 3.3. „Újrahasznosított” Covid-19 elleni gyógyszerek és OATP-k.....	92
V. AZ ÚJ TUDOMÁNYOS EREDMÉNYEK ÖSSZEFOGLALÁSA	94
VI. KÖVETKEZTETÉSEK ÉS KITEKINTÉS.....	96
VII. A DISSZERTÁCIÓ ALAPJÁT KÉPEZŐ KÖZLEMÉNYEK	107
VIII. A DISSZERTÁCIÓHOZ KAPCSOLÓDÓ TOVÁBBI KÖZLEMÉNYEK	111
IX. KÖSZÖNETNYILVÁNÍTÁS.....	113
X. IRODALOMJEGYZÉK	114
XI. A DOLGOZAT ALAPJÁT KÉPEZŐ KÖZLEMÉNYEK EREDETI VERZIÓI.....	126

ÖSZEFoglalás

A sejtmembrán transzporterei membránba ágyazott fehérjék, amelyek összehangolt működése szükséges a sejt és a szervezet homeosztázisának fenntartásához. A membrántranszporterek egy része gyógyszerhatóanyagokat is felismer és befolyásolja ezek szervezeten belüli sorsát (abszorpció, disztribúció, metabolizmus és elimináció, ADME). A gyógyszertranszporterek aktivitásának megváltozása például mutációk, polimorfizmusok, vagy szubsztrátjaik és/vagy inhibitoraik együttes alkalmazása miatt, megváltozott farmakokinetikát és nem várt, akár toxikus mellékhatásokat eredményezhet (ADME-Tox). Ezt felismerve ma már a nemzetközi szabályozó hatóságok több gyógyszertranszporterrel való kölcsönhatás vizsgálatát is előírják a gyógyszerfejlesztés korai, preklinikai fázisában. Ilyen kitüntetett szerepe van többek között az ABC (ATP Binding Cassette) családba tartozó ABCG2 transzporternek és a Solute Carrier (SLC) fehérjecsaládba tartozó, a májban kifejeződő Organikus anion transzporter polipeptideknek (OATP1B1 és OATP1B3).

A doktori értekezésem alapját képező kutatások az ABCG2 fehérje és az OATP fehérjecsalád vizsgálatára irányultak. Az egyik célkitűzésünk az ABCG2 fehérje működésének és szabályozásának megértése volt, amely kapcsán vizsgáltam az ABCG2 fehérje szubsztrátfelismerésben és koleszterinérzékelésben részt vevő régióit. Tanulmányoztam továbbá egy, az ABCG2 fehérjét a sejt felszínen felismerő antitest kötődésének mechanizmusát. Munkám másik célkitűzése a humán OATP fehérjecsalád vizsgálata volt. Ennek során többféle, fluoreszcencia-alapú és új megközelítésen alapuló mérési módszert dolgoztunk ki, amely alkalmas ezeknek a transzportereknek az érzékeny kimutatására és akár nagy áteresztőképességű tesztelésére. Végezetül, az ABCG2 transzporter és az OATP fehérjecsalád több tagjának új kölcsönhatásait tártuk fel ismert gyógyszerhatóanyagokkal vagy korábban transzporter kölcsönhatásban nem jellemzett vegyületekkel. Az ABCG2 fehérjével kapcsolatos eredményeimre azóta számos további alkalmazás épült. Az OATP transzporterekre kidolgozott fluoreszcencia-alapú módszereink pedig jó alternatívái lehetnek az eddigi, radioaktív próbákra alapuló módszereknek és széleskörű felhasználást nyerhetnek.

RÖVIDÍTÉSEK JEGYZÉKE

ABC: ATP Binding Cassette, jellegzetes ATP-kötő domént tartalmazó fehérjecsald neve

ABCG2: az ABCG fehérjecsald másodikként felfedezett tagja, alternatív nevei: ABCP, BCRP, MXR

ABCP: placenta-specifikus ABC (ABCG2 alternatív neve)

Ace: 8-acetoxi-1,3,6-trihidroxipirandin, fluorogén OATP szubsztát

ADME: abszorpció, disztribúció, metabolizmus és elimináció

ADME-Tox: abszorpció, disztribúció, metabolizmus, elimináció és toxicitás

AF405: Alexa Fluor 405 fluoreszcens OATP szubsztát

AMP-PNP: adenilil-imidodifoszfát, nem hidrolizálódó ATP analóg

BCRP: breast cancer resistance protein, emlőtumor rezisztencia fehérje (ABCG2 alternatív neve)

BB: benzbromaron

BSA: bovine serum albumin, marha szérum albumin

BSEP: bile salt export pump, epesó transzporter (ABCB11)

BSP: bromoszulfoftalein, OATP inhibitor/szubsztát

CRAC: cholesterol recognition amino acid consensus, koleszterinkötő motívum

CsA: cyclosporin A

CYP: citokróm P450 enzimesald

DDI: drug-drug interaction, gyógyszer-gyógyszer kölcsönhatás

DHEAS: dehidroepiandroszteron-szulfát

E1S: ösztron-3-szulfát

EGFR: epidermal growth factor receptor, epidermális növekedési faktor receptor

EMA: European Medicines Agency, európai gyógyszerügynökség

Ex/Em: excitáció/emisszió

FDI: food-drug interaction, élelmiszer-gyógyszer kölcsönhatás

FDA: US Food and Drug Administration, amerikai élelmiszer és gyógyszerbiztonsági hivatal

FL-MTX: fluorezcein-metotrexát

FTC: Fumitremorgin C, Aspergillus fumigatus gombából izolált ABCG2 inhibitor

GFP: green fluorescent protein, zölden fluoreszkáló fehérje

GWAS: genome-wide association study, genomszintű asszociációs vizsgálat

HTS: high-throughput screening, nagy áteresztőképességű tesztelés

HSD17 β 1: 17 β -hidroxiszteroid dehidrogenáz 1-es típusú enzim

HUGO: Human Genome Organization, humán gén nevezéktan bizottság

ITS: International Transporter Consortium,

IOV: inside-out vesicle, kifordított membránvezikula

Ko143: specifikus ABCG2 inhibitor neve

LDG: Live/Dead Green viabilitási festék festék

LorD488: Live or Dye 488 viabilitási festék festék

NBD: nucleotide binding domain, az ABC-k nukleotidkötő doménje

MRP: multidrug resistance associated protein, multidrog rezisztencia asszociált fehérje, ABCC

MXR: mitoxantrone resistance protein, mitoxantron-rezisztencia fehérje (ABCG2 alternatív neve)

OATP: Organic anion transporting polypeptides, Organikus Anion Transzporter polipeptid

PFA: paraformaldehid

P-gp: P-glikoprotein (ABCB1)

PMDA: Pharmaceuticals and Medical Devices Agency, Japán gyógyszerügynökség

RAMEB: random metilált β -cyclodextrin

SBE: steroid binding element, szteroidkötő motívum

Sf9: *Spodoptera frugiperda*, hernyó ovárium sejt

SLC: Solute Carrier fehérjecsald

SLCO: Solute Carrier for OATPs, OATP fehérjéket kódoló gén neve

SN-38: kamptotecin analóg, kemoterápiás szer

SNP: single nucleotide polymorphism, egynukleotidos polimorfizmus

STS: szteroid-szulfatáz enzim

TKI: tyrosine kinase inhibitor, tirozin kináz gátló vegyületek gyűjtőneve

TMD: transzmembrán domén

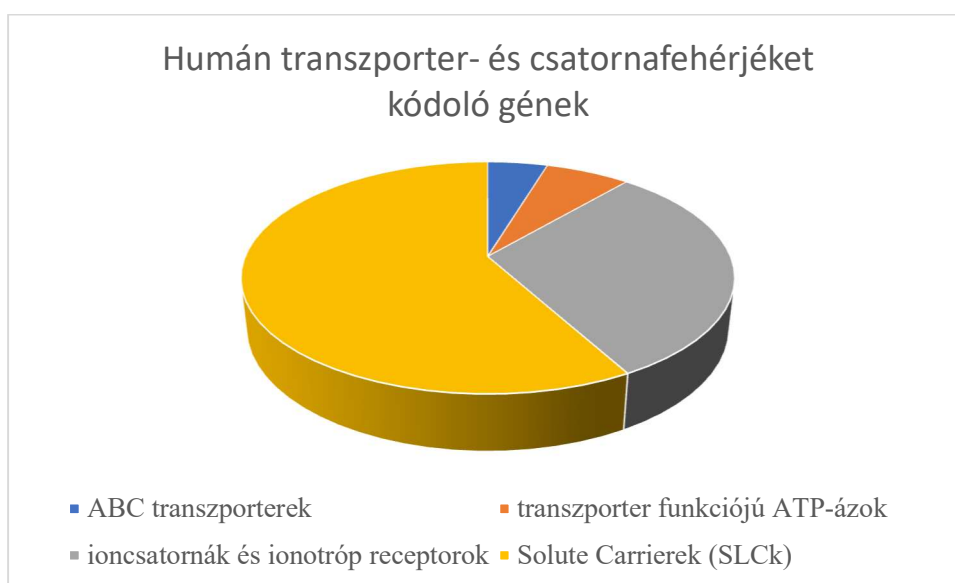
ZV: Zombie Violet viabilitási festék

I. IRODALMI BEVEZETŐ

Membrántranszporterek a farmakokinetikában

Az emberi genomban található gének 10%-a, mintegy 2000 gén membrántranszportert vagy a membrántranszport folyamatokhoz kapcsolt fehérjét kódol (Hediger et al. 2013). A membrántranszporterek a biológiai membránokba ágyazott polipeptidek, amelyek különböző anyagok membránokon át történő, szabályozott transzlokációját végzik. A transzporterek rendkívül sokfélék, és többféle szempont szerint csoportosíthatók. Egyik lehetséges osztályozásuk a működésük és szekvencia azonosságuk alapján történik, ami szerint négy nagy családba sorolhatók:

1) ABC fehérjék: jellegzetes ATP-kötő (ATP Binding Cassette) motívumot tartalmazó, zömében aktív transzporterek; **2) kationok transzporter ATP-ázok;** **3) SoLute Carrierok (SLC-k),** amelyek oldott anyagokat transzportálnak másodlagos aktív transzport vagy facilitált diffúzió által és **4) ioncsatornák** (Hediger et al. 2013).



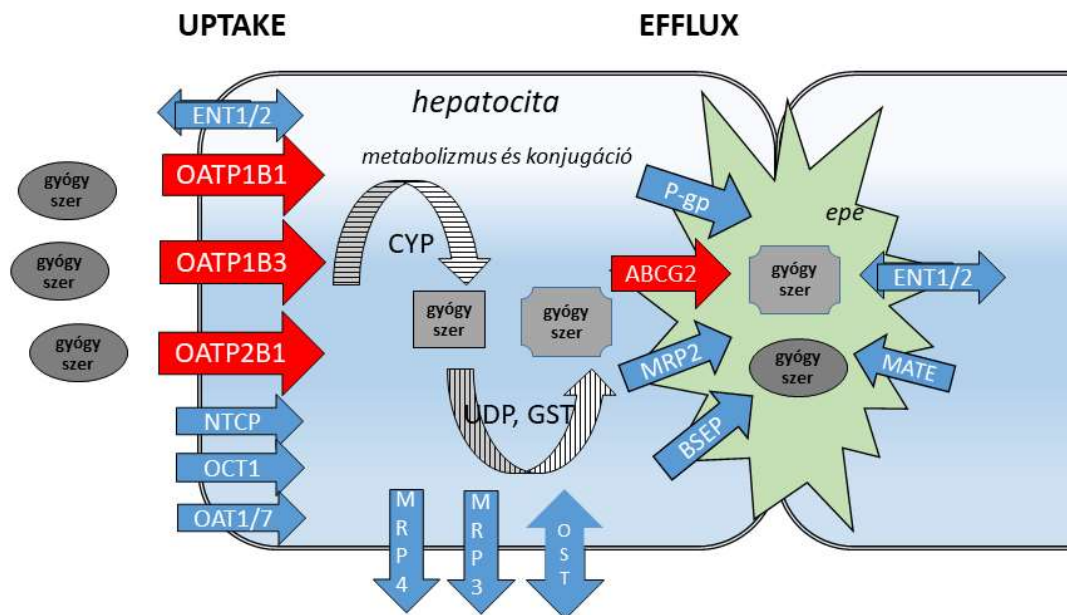
1. ábra: Transzporter- vagy transzport folyamathoz kapcsolt feladatot ellátó fehérjéket kódoló gének az emberi genomban (Hediger et al. 2013). Az SLC-k a legnépesebb transzporter családot alkotják, közel 500 génnel az emberi genomban.

A transzporterek összehangolt működése szükséges a sejt és a szervezet homeosztázisának fenntartásához. Egy részük azonban, jellemzően a multispecifikus transzporterek, nem csak az endogén eredetű anyagok (vitaminok, hormonok, tápanyagok) transzportjában vesz

részt, hanem számos exogén eredetű vegyület, köztük gyógyszerhatóanyagok szervezeten belüli sorsát is befolyásolja.

Az első gyógyszertranszporterként azonosított fehérje a P-glikoprotein volt (ABCB1, P-gp) (Gottesman and Ling 2006; Juliano and Ling 1976; Dano 1973). A P-gp 1976-os felfedezése, majd génjének 1986-os klónozása óta számos, a gyógyszerek szervezeten belüli sorsát, **ADME (abszorpció, disztribúció, metabolizmus és elimináció)** befolyásoló transzportert azonosítottak (International Transporter et al. 2010; Keogh 1996). A gyógyszertranszporterek az ABC és SLC fehérjecsaldokból kerülnek ki, alapvető feladatuk a szervezet potenciálisan veszélyes anyagokkal szembeni védelme. Ebben a bonyolult transzporter hálózatban, az ABC-k és SLC-k kéz a kézben működnek a hepatobiliáris és renális exkrécióban, valamint az epitheliális és endoteliális barrierek védelmében. Ráadásul nem csak gyógyszerészubsztrátjaik és azok metabolitjainak ADME tulajdonságait befolyásolják, de fontosak a szervezet hormonháztartásának és tápanyagellátásának szabályozásában is.

A gyógyszertranszporterek aktivitásának megváltozása például mutációk, polimorfizmusok, vagy szubsztrátjaik és/vagy inhibitoraik együttes alkalmazása miatt, megváltozott farmakokinetikát és nem várt, akár toxikus mellékhatásokat eredményezhet (ADME-Tox). Ezt felismerve ma már a nemzetközi szabályozó hatóságok, így az FDA (US Food and Drug Administration), az EMA (European Medicines Agency) és a PMDA (Pharmaceuticals and Medical Devices Agency, Japan), együttműködve a nemzetközi transzporter konzorciummal (International Transporter Consortium, ITS), ajánlásaikban részletesen leírják, hogy mely transzporterek vizsgálándók a gyógyszerfejlesztés során (International Transporter et al. 2010; https://www.ema.europa.eu/en/documents/scientific-guideline/guideline-investigation-drug-interactions-revision-1_en.pdf ; <https://www.fda.gov/files/drugs/published/In-Vitro-Metabolism--and-Transporter--Mediated-Drug-Drug-Interaction-Studies-Guidance-for-Industry.pdf>). Az ajánlásban közel 30 transzporter szerepel. Az ABC családból a P-gp, ABCG2, néhány MRP (multidrog rezisztencia asszociált) fehérje és a BSEP (bile salt export pump, epesó transzporter) vizsgálata javasolt. A többi transzporter pedig a népes SLC szupercsaládból kerül ki, többek között a májban kifejeződő (Organikus anion transzporter polipeptid) OATP1B1 és OATP1B3 fehérjék. A 2. ábrán a máj igazolt gyógyszertranszportereit foglaltam össze.



2. ábra: A májsejtek nemzetközi ajánlások alapján vizsgálandó gyógyszertranszporterei (Zamek-Gliszczyński et al. 2018) alapján. Pirossal az általam vizsgált transzportereket emeltem ki.

ABC fehérjék: **P-gp** (P-glikoprotein, ABCB1), **MRP** (multidrog rezisztencia asszociált fehérjék, ABCC), **BSEP** (bile salt export pump, epesó transzporter, ABCB11).

SLC-k (SoLute Carriers, oldott anyag transzporterek): **OATP** (Organikus anion transzporter polipeptidek, SLCO), **OCT** (Organic cation transporter, szerves kation transzporter, SLC22A), **OAT** (Organic anion transporter, szerves anion transzporter, SLC22A), **ENT** (equilibrative nucleoside transporter, ekvilibratív nukleozid transzporter, SLC29A), **MATE** (Multidrug and toxin extrusion protein, gyógyszer és toxin transzporter, SLC47A), **NTCP** (sodium- taurocholate cotransporting polypeptide, Na-függő taurokolát transzporter, SLC10A), **OST α/β** (Organic solute transporter, Na-független epesó transzporter, SLC51A).

Az ábrán a gyógyszerek átalakításában részt vevő enzimeket is jelöltem, CYP: Citokróm P450 enzimcsalád, UDP: UDP-glükuronil-transzferáz, GST: glutation S-transzferáz.

Eddigi kutatómunkám fókuszában az ABCG2 fehérje és az SLC fehérje szupercsaládba tartozó Organikus anion transzporter polipeptidek (OATP-k) voltak, így a továbbiakban ezekről adok irodalmi áttekintést.

Az ABCG2 fehérje

Az ABCG2 fehérjét, mintegy húsz évvel a P-gp felfedezése után, 1998-1999-ben azonosították. Felfedezését követően hamar az érdeklődés középpontjába került (amit az eddig megjelent több ezer publikáció is jelez), hiszen nem csak a farmakokinetika fontos szereplője, hanem számos fiziológias folyamatban is részt vesz (lásd később, illetve bővebben (Kerr, Haider, and Gelissen 2011)), és működése a tumorok multidrog rezisztenciájáért is felelős (Robey et al. 2018; Kerr, Haider, and Gelissen 2011). PhD tanulmányaim során már a kezdetekkor csatlakozhattam az ABCG2 kutatásához. Az elsők között voltunk a fehérje jellemzésében, az ehhez szükséges modell sejtek és *in vitro* vizsgálati módszerek megalkotásában (Ozvegy et al. 2001; Ozvegy, Varadi, and Sarkadi 2002).

Az ABCG2 fehérjét kódoló gén felfedezése: három név (BCRP, MXR, ABCP), ugyanazon fehérje

Az ABCG2 fehérjét kódoló gént egymástól függetlenül, szinte egyidőben, három kutatócsoport is klónozták. Allikmets és munkatársai a méhlepényben mutatták ki egy addig ismeretlen ABC fehérje expresszióját és placenta-specifikus ABC-nek, ABCP nevezték (Allikmets et al. 1998). A másik két csoport pedig kemoterápiás szerrel (mitoxantron és doxorubicin) szelektált emlőtumor eredetű, illetve vastagbél karcinóma sejtvonalban mutatta ki egy új fehérje overexpresszióját (Doyle et al. 1998; Miyake et al. 1999). Ennek megfelelően az egyik csoport emlőtumor rezisztencia fehérjének (BCRP, breast cancer resistance protein) (Doyle et al. 1998), a másik csoport pedig mitoxantron-rezisztencia fehérjének (MXR, mitoxantrone resistance protein) nevezte el az új transzportert (Miyake et al. 1999). A humán gén nevezéktan bizottság (HUGO) ajánlása alapján a fehérje hivatalos neve ABCG2 (<http://www.gene.ucl.ac.uk/users/hester/abc.html>), így én ezt az elnevezést használom végig az értekezésemben.

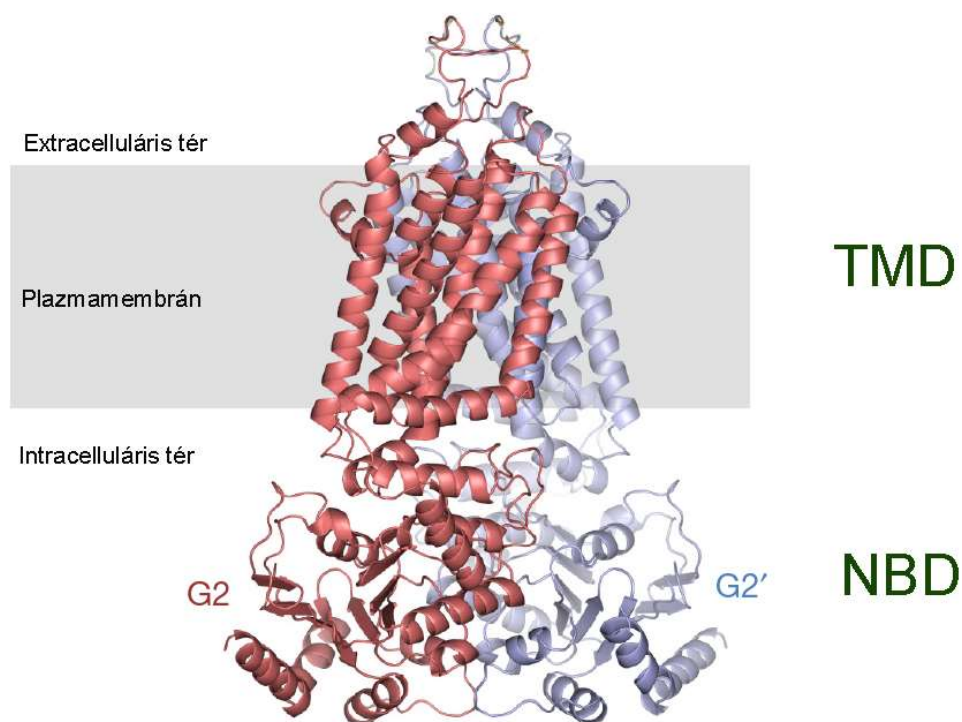
Az ABCG2 fehérje felépítése

A humán ABC fehérjecsalád 48 tagot számlál, amelyeket szekvenciájuk hasonlósága és doménsorrendjük alapján 7 (A-G) alcsaládba sorolnak (Dean 2005; Dean and Allikmets 1995). Az ABC fehérjék nevüket jellegzetes nukleotidkötő doménjükéről kapták. Ez a domén felelős a MgATP megkötéséért és hidrolíziséért, ami az aktivitásukhoz szükséges konformációs változás energiaszükségletét biztosítja. Az ABC család tagjai zömében transzporterek, de a DNS hibajavításban vagy transzlációs faktorként működő ABC-k is ismertek (ABC E és F család) (Fostier et al. 2021; Navarro-Quiles, Mateo-Bonmati, and Micol 2018). Az ABC-kre jellemző nukleotidkötő domén (NBD) a más ATP-kötő fehérjékben is megtalálható Walker A és Walker B motívumokon kívül a csak erre a családra jellemző ún. ABC signature vagy „C-loop” (LSGGQ) motívumot is tartalmazza. Az ABC fehérjék másik fontos „építőeleme” a transzmembrán (TM) domén, amely minimum 6 transzmembránon átívelő helikális struktúrából áll. Ám kivételek is akadnak. Az ABCE és ABCF fehérjék nem tartalmaznak transzmembrán régiót, ezek a fehérjék nem transzporterek. Az ABCC/MRP családban pedig az „alap” 12 hélixen kívül egy extra, 5 hélixből álló transzmembrán egység is megtalálható (Bakos et al. 2000). A transzmembrán domén (TMD) szekvenciája nem konzervált, itt nagyobb mértékű azonosság csak az azonos alcsaládba tartozó ABC-knél mutatható ki. Az egyre nagyobb számban ismertté váló ABC térszerkezet fényében felmerült, hogy a TMD szerkezete alapján kellene az ABC-ket csoportosítani, hiszen az eltérő TMD struktúrák eltérő működési mechanizmust eredményeznek (Thomas et al. 2020).

Az ABCG2 fehérje az **ABCG alcsalád** tagja. Az ABCG fehérjék (G1, G2, G4, G5 és G8) ún. „fél” transzporterek, az ABC-k működéséhez szükséges NBD és a 6 TM hélixet tartalmazó TMD-ből mindössze egyet-egyet tartalmaznak (3. ábra), a működőképes transzporter „egység” dimerizációval alakul ki. Az ABCG2 homodimerként működik (Kage et al. 2002; Ozvegy et al. 2001). Az ABCG alcsaládba tartozó, homo- és heterodimerként (is) működő ABCG1 és ABCG4 fehérjékkel nem alkot működőképes dimert (Cserepes et al. 2004; Hegyi and Homolya 2016). Az ABCG család másik két tagja, ABCG5 és ABCG8 pedig heterodimerként funkcionál.

Az ABCG2 térszerkezete

Az első nagyfelbontású ABCG2 térszerkezeteket kriogén elektronmikroszkópia (cryo-EM) segítségével 2017-2018-ban határozták meg (Taylor et al. 2017; Manolaridis et al. 2018; Jackson et al. 2018) (3. ábra), amit még további, eltérő konformációkban rögzített szerkezetek követtek (Orlando and Liao 2020).



3. ábra: Az ABCG2 térszerkezete ATP nélküli állapotban (PDBID: 5NJ3) (Taylor et al. 2017). A két ABCG2 monomert piros és lila szín jelzi.

Ezek alapján a két ABCG2 monomer TM hélicei közösen egy nagyobb, központi és egy felső, kisebb üreget formálnak, amit egymástól egy dileucin „dugó” zár el (lásd még VI. fejezet 41. ábra). Ezen a két üregen át halad a szubsztrát a transzport során. A felső üreg kialakításában a 3. extracelluláris hurok is részt vesz. Ennek a stabilizálásában az általam is vizsgált, 592. és 608. ciszteinek (lásd az Eredmények A.4.2. fejezete) fontosak (Taylor et al. 2017).

A térszerkezet ismeretében számos, korábban a mutációk és polimorfizmusok alapján tapasztalt, az ABCG2 működését érintő jelenséget meg tudtak magyarázni, például a leggyakoribb polimorfizmus által okozott szerkezetbeli változást, amiről alább írok. Munkám során én is több ABCG2 mutánst vizsgáltam, ezek térbeli elhelyezkedését és az

észlelt fenotípus változások lehetséges magyarázatát később, az Következtetések és kitekintés c. fejezetben tárgyalom.

Az ABCG2 fehérje szöveti expressziója

Az ABCG2 fehérje az emberi szervezet számos szövetében termelődik (Kerr, Haider, and Gelissen 2011). Jellegzetesen a határoló funkciót ellátó szöveinkben és szerveinkben: vér-agy gát, vékonybél, placenta, illetve a méregtelenítésben és a kiválasztásban kulcsfontosságú szervekben, így a májban és a vesében fordul elő legnagyobb mennyiségben (Zhang et al. 2003; Maliepaard et al. 2001).

Az ABCG2 fehérje szerepe az emberi szervezetben

Az ABCG2 egy ún. „efflux” transzporter, szubsztrátjait ATP hidrolízis energiájának terhére (aktív transzporter) az őt kifejező sejtekből az extracelluláris tér felé szállítja.

Az **ABCG2 fehérje multispecifikus transzporter**, számtalan, eltérő fizikokémiai tulajdonságú vegyületet felismer és transzportál (Kerr, Haider, and Gelissen 2011; Szafraniec et al. 2014). Általánosan megállapítható, hogy az ABCG2-vel kölcsönhatásba lépő vegyületek: 1) nagyméretű (7-20 szénatomot tartalmazó) szerves molekulák, 2) tartalmaznak hidrofób és aromás régiót, 3) pozitív és/vagy negatívan töltést, 4) hidrogén akceptor vagy donor atomokat, továbbá gyakran tartalmaznak 5) O és N heteroatomot.

Az ABCG2 egyik elsőként azonosított gátlószere az *Aspergillus fumigatus* gombából izolált toxin, a Fumitremorgin C (FTC). Az FTC azóta széles körben alkalmazott, szintetikus analógja a specifikus nanomoláris ABCG2 inhibitor a Ko143 (Allen et al. 2002). A Ko143 felfedezése óta több, célzottan tervezett inhibitor vizsgáltak, többek között azzal a céllal, hogy olyan ABCG2 gátlószert fejlesszenek, amely szemben a Ko143-al, nem toxikus, így *in vivo* alkalmazásra kerülhet például a tumorok kemoterápia rezisztenciájának kivédésében. Ezek közül néhány tanulmányban kutatócsoportunk is aktívan részt vett (Guragossian et al. 2021; Winter et al. 2013).

Az ABCG2 több endogén szubsztrát transzportjában és ezek metabolitjainak szervezetből való kiürülésében vesz részt. **Legfontosabb endogén szubsztrátjai** ösztrogén konjugátumok (ösztro-3-szulfát, ösztradiol-17 β D-glükuronid), porfirinek (hem), B2 vitamin, folsav és húgysav.

Porfirin transzport: A klorofill egyik bomlásterméke, a pheophorbide A volt az egyik első ABCG2 szubsztrát, amit azonosítottak. Az *Abcg2* (a humán ABCG2 egér ortológ) -hiányos egerekben a pheophorbide A felhalmozódott és fényérzékennyé tette a fénynek kitett testrészt (az állatok fülei szenvedtek sérülést) (Jonker et al. 2002). Később a humán ABCG2 fehérjénél is kimutatták, hogy egyik fontos fiziológiás szubsztrátja a porfirin és annak származékai. Az ABCG2 a hematopoetikus őssejtekben (is) magas expressziót mutat (őssejt markernek is tekinthető). Szerepe oxigénhiányos környezetben ezeknek a sejteknek a védelme a fokozott protoporfirin IX felhalmozódással szemben (Krishnamurthy et al. 2004).

Az ABCG2 húgysav transzporter: Az ABCG2 másik fontos endogén szubsztrátja a húgysav. 2009-ben Woodward és kollégái GWAS (genome-wide association study) során az ABCG2 Q141K polimorfizmusát a köszvény kialakulásának egyik fontos faktoraként azonosították (Woodward et al. 2009). A vese proximális tubulusaiban kifejeződő ABCG2 a húgysav vizeletbe történő szállításában vesz részt, valamint fontos a szerepe a bélbe történő húgysav-ürítésben is. Ha ez a funkció sérül, például egy mutáció miatt, akkor a vér húgysav szintje megnő, és fokozódik a köszvény kialakulásának kockázata. Az elmúlt évtizedben intenzíven vizsgálják az ABCG2 farmakológiai modulátorait, annak érdekében, hogy a csökkent ABCG2 aktivitás következtében kialakuló köszvényes betegeken segíteni tudjanak (Woodward et al. 2013).

Az ABCG2 további fontos szerepe a B₂ (és egyéb) vitaminok szekréciója az anyatejbe (van Herwaarden et al. 2007).

Az ABCG2 fehérje és farmakokinetika

Az ABCG2 számos, gyógyszerként alkalmazott vegyületet transzportál (antivirális szerek, folsav antagonisták, kemoterápiás szerek, sztatinok, stb.) (Lee et al. 2015). Szubsztrátfelismerése nagyban átfed az ABC fehérjecsaldó multispecifikus tagjával (P-gp, MRP1) és az OATP (lásd később) fehérjékével. *Abcg2* knock-out egereken végzett vizsgálatok során több xenobiotikummal szemben igazolták az ABCG2 protektív szerepét (Vlaming, Lagas, and Schinkel 2009) nem csak a felnőtt szervezet, hanem a magzat védelmében is (Jonker et al. 2000). Azóta számos tanulmányból tudjuk, hogy az ABCG2 a farmakokinetika fontos szereplője, befolyásolja gyógyszer-szubsztrátjai vékonybélből

történő felszívódását, hepatikus eliminációját és a vér-agy gáton történő átjutását (Schnepf and Zolk 2013; Lee et al. 2015). Az ABCG2 az immunrendszerrel analógiába állított „kemoimmunitás” rendszer része, amelynek tagjai multispecifikus ABC fehérjék és amely a szervezetünk általános, xenobiotikumokkal szembeni védelmét látja el (Sarkadi et al. 2006). Mindezekből következik, hogy az ABCG2 kiemelten fontos szereplője az ADME-Tox folyamatoknak, FDA, EMA és PMDA ajánlás alapján a gyógyszerfejlesztés preklinikai fázisában vizsgálendő (http://www.fda.gov/drugs/scienceresearch/researchareas/pharmacogenetics/ucm083378.htm).

ABCG2 a tumorokban

Az ABCG2 nem csak szisztémásan, hanem lokálisan is befolyásolhatja szubsztrátjai hatékonyságát. Az ABCG2-t felfedezésekor *in vitro* gyógyszerrezisztenciát okozó fehérjeként azonosították (Doyle et al. 1998; Miyake et al. 1999). Később számos, a kemoterápiában használt vegyületről kimutatták, hogy azok ABCG2 szubsztrátok, és az ABCG2 *in vitro* körülmények között megvédi a fehérjét kifejező sejteket ezekkel a szerekkel szemben, tehát a kemoterápia hatásosságát lokálisan, a tumorokban kifejeződve is akadályozhatja (Polgar, Robey, and Bates 2008). Azóta rákos betegek adatainak elemzése alapján tudjuk, hogy a hematológiai és tüdő eredetű tumorok magas ABCG2 szintje rossz prognózissal társul (Heyes, Kapoor, and Kerr 2018; Kerr, Haider, and Gelissen 2011). Sőt, a transzkriptóm analízissel történt vizsgálatok alapján (TCGA, The Cancer Genome Atlas) egyéb tumorokban is magas expresszióval van jelen az ABCG2 (Robey et al. 2018).

Az ABCG2 polimorf változatai

Az ABCG2 fehérje nagyszámú polimorf allélja ismert (ezekről itt található részletes összefoglalás (Heyes, Kapoor, and Kerr 2018)). Nemrégiben, egy új osztályozási rendszert is javasoltak, ami figyelembe veszi, hogy a variáns milyen módon eredményezi az ABCG2 megváltozott működését, például megváltozott transzkripció, mRNS, illetve fehérje stabilitás, vagy nem megfelelő celluláris elhelyezkedés miatt (Homolya 2021). Az ABCG2

fehérjét kódoló gén két leggyakoribb polimorf allélja a V12M változatot eredményező rs2231137, c.34G>A (0,2, illetve 0,06 allél frekvenciával az ázsiai, illetve a kaukázusi népcsoportban) és a Q141K cserét eredményező rs2231142, c.421C>A (0,17 és 0,098 allél frekvenciával az ázsiai, illetve a kaukázusi népcsoportban). A **V12M változat** saját *in vitro* vizsgálataink alapján nem befolyásolja lényegesen az ABCG2 működését (Morisaki et al. 2005), míg mások csökkent aktivitást tapasztaltak a V12M változatnál (Mizuarai, Aozasa, and Kotani 2004). Az ellentmondást akkor az eltérő sejtes modellekkel magyaráztuk, de későbbi vizsgálatok is azt erősítették meg, hogy a V12M változat nem befolyásolja jelentősen az ABCG2 működését, legalábbis nem okoz csökkent aktivitást (Heyes, Kapoor, and Kerr 2018).

A másik, leggyakoribb változat, **Q141K** azonban igazoltan csökkent ABCG2 funkciót eredményez. A Q141K változat több aspektusában is defektív: 1) a fehérje aktivitása csökkent (lásd például saját eredményeinket (Morisaki et al. 2005) és 2) a fehérje expressziója alacsonyabb (például szintén saját publikációnk (Saranko et al. 2013)). Mindezek levezethetők a nem megfelelő térszerkezetből adódó fokozott lebomlásra (Furukawa et al. 2009). A Q141 az NBD-ben helyezkedik el, egy α -hélixben található, amely az amfipatikus 1. TM-el alakít ki kölcsönhatást. A Lys változat (Q141K polimorfizmus) ezt a kölcsönhatást torzítja és eredményezi a fehérje hibás feltekeredését (Taylor et al. 2017). A Q141K változat nem csak megváltozott farmakokinetikát okozhat, hanem a köszvényes esetek 10%-áért is felelős (Woodward et al. 2009).

Az ABCG2 a vörösvértestekben is kifejeződik. Több, jellemzően korai stop kodont eredményező polimorf változat homozigóta vagy compound heterozigóta formában az ABCG2 fehérje teljes hiányához vezet, amely a Junior^r vércsoportot eredményezi (Zelinski et al. 2012; Saison et al. 2012). Ezek az emberek azonban egészségesek, bár több esetben endogén és exogén szubsztátjaik megváltozott farmakokinetikája jellemzi őket. A Sarkadi Balázs (Enzimológiai Intézet TTK) vezette kutatócsoport eredményei alapján az ABCG2 mennyisége a vörösvértest membránokban kvantitálható, és alkalmas az ABCG2 csökkent expresszióját eredményező polimorf allél kiszűrésére (Kasza et al. 2012; Zambo et al. 2018). Erről a diagnosztikus eszközzel még bővebben írok a Következtetések és kitekintés című fejezetben.

Az ABCG2 expressziójának, működésének és lokalizációjának szabályozása

Az ABCG2 transzkripciós és transzlációs szabályozását, sejten belüli vándorlásának állomásait, lebomlásának útjait, poszttranszlációs módosulását, egyéb, a működését szabályozó faktorokat számtalan tanulmányban vizsgálták (a transzkripciós faktorok szerepéről az alábbi összefoglaló cikkekben lehet bővebben olvasni (Gorczyca and Aleksunes 2020; Mozner et al. 2019). Itt csak a leglényegesebb ismereteket foglalom össze ezzel kapcsolatban. Kitérek viszont az ABCG2 lipidek általi szabályozására, mert kutatómunkám során az Eredmények fejezetben ismertett szerkezet-funkció vizsgálatokkal ennek megértését is céloztuk.

Az ABCG2 transzkripciós szintű szabályozásában igazoltan részt vesznek a szteroid hormon receptorok: ER α / β (ösztrogén receptor), PR α / β (progeszteron receptor), és xenobiotikum, illetve hipoxia aktiválta/érzékelő transzkripciós faktorok: AHR (aryl hydrocarbon receptor), CAR/PXR (constitutive androstane receptor és preneane x receptor), NFR2 (nuclear factor erythroid 2-related factor 2) (Gorczyca and Aleksunes 2020). Prof. Nagy László (Debreceni Egyetem) kutatócsoportjával együttműködve mi igazoltuk először, hogy a lipid aktiválta transzkripciós faktor PPAR (peroxisome proliferator activator receptor) aktiválása fokozza az ABCG2 transzkripcióját és expresszióját dendritikus sejtekben (Szatmari et al. 2006).

Az ABCG2 fehérje egy glikoprotein, az N-glikoziláció az N596-n történik (Diop and Hrycyna 2005), ennek hiánya azonban nem befolyásolja a fehérje működését. Az ABCG2 foszforilálódik is, a T362A Pim-1 általi foszforilációja fokozza működését (Xie et al. 2008).

Az ABCG2 sejten belüli vándorlását („trafficking”), expresszióját és „életidejét” befolyásoló faktorokat számos tanulmány vizsgálta. Ezekről bővebben itt lehet olvasni (Mozner et al. 2019).

A lipidkörnyezet hatása az ABCG2 fehérje működésére

Intenzíven vizsgált terület, hogy a membránkörnyezet, pontosabban annak koleszterin és egyéb lipid tartalma hogyan befolyásolja az ABCG2 működését. Az ABCG család tagjai növényi lipid (szterol) (ABCG5/ABCG8 heterodimer) és koleszterin (ABCG1 és ABCG4) transzporterek (Kerr et al. 2021). Ezzel szemben az ABCG2 nem transzportálja a

koleszterint (Tarling and Edwards 2011), viszont a koleszterinnek fontos szabályozó szerepe van a fehérje működésében.

Storch és mtsai. mutatták ki először, hogy az ABCG2 koleszterinben és szfingolipidben gazdag lipid raftokban található, és hogy a sejtmembrán koleszterin szintjének csökkentése (ciklodextrinnel való inkubálással (Szente and Szejtli 1999)) csökkent ABCG2 aktivitást eredményez (Storch et al. 2007). Ezzel összhangban kutatócsoportunk kimutatta, hogy az emlős sejtek plazmamembránjához képest alacsony (5-8 μg koleszterin/mg membránfehérje) membránkoleszterin-tartalmú rovarsejtekben az ABCG2 fehérje aktivitása fokozható, amennyiben a rovarsejt membránokat az emlős sejtekben mérhető koleszterin szintre (40-60 μg koleszterin/mg membránfehérje) töltjük ciklodextrinbe csomagolt koleszterinnel való együtt inkubálással (Telbisz et al. 2007). Hasonló felfedezésre jutott egy másik kutatócsoport is (Pal et al. 2007). Később, rekonstituált proteoliposzómákat alkalmazva kimutattuk, hogy az ABCG2 működéséhez >20% w/w koleszterintartalom szükséges (Telbisz et al. 2013). Ezek alapján az Sf9 rovarsejt alapú vezikulák koleszterin-töltött változatát érdemes használni annak érdekében, hogy az ABCG2 fehérje maximális aktivitását és az *in vivo* kölcsönhatásokat jobban tükröző gyógyszer interakciókat lehessen mérni.

Az ABCG2 mikrokörnyezete tehát finomszabályozást jelent az ABCG2 működésében (Hegedus et al. 2015). Az ABCG2 térszerkezetének meghatározásakor mind a szubsztrátkötő zsebben, mind pedig a fehérje sejtmembrán felé néző hidrofób redőiben azonosítottak koleszterin molekulákat (Jackson et al. 2018; Taylor et al. 2017). Ezek pontos elhelyezkedését és szerepét később, a Következtetések és kitékintés c. fejezetben tárgyalom, illetve erről itt lehet bővebben olvasni (Kerr et al. 2021).

Az OATP fehérjecsalád

Az endogén és exogén eredetű anyagok, köztük a különböző gyógyszerek transzportjának, az ABC gyógyszertranszportereken kívüli, azokkal jól szabályozott összhangban működő szereplői az SLC fehérjék közül kerülnek ki. Az SLC-k a legnépesebb transzporter szuperfamilia, amely több, egymással nem rokon fehérje/gén családra tagolódik. Az emberi genomban közel 500 SLC gén található, amelyek 65 SLC családba tartoznak (Hediger et al. 2013) és <http://slc.bioparadigms.org/>). Ezekben mindössze annyi a közös, hogy a kódolt fehérjék oldott anyagok membránon át történő szállítását végzik, és nem elsődlegesen aktív

transzporterek (Hediger et al. 2013). Munkám során az OATP (SLCO gének által kódolt) fehérjékkel foglalkoztam, így részletesen csak ezt a családot tárgyalom a következő fejezetekben.

Az első OATP felfedezése

Az első OATP fehérjét (patkány Oatp) 1994-ben azonosították, amikor a BSP (bromoszulfoftalein) patkány májba történő Na⁺-független felvételéért felelős transzportert keresték (Jacquemin et al. 1994). Az azonosított transzporter ráadásul multispecifikusnak bizonyult, a BSP mellett epesók transzportját is eredményezte. Egy évvel később az első humán OATP-t is klónozták, OATP1A2 (Kullak-Ublick et al. 1995), majd sorra azonosították a többi emberi OATP-t kódoló gént. Érdekes módon, szemben az ABC fehérjékkel, az OATP-k csak az állatvilágban találhatók meg.

Nevezéktan

Kezdetben az OATP-eket kódoló géneket az SLC21A családba sorolták, és a nevezéktanuk sem volt egységes (lásd 1. táblázat és (Hagenbuch and Meier 2003; Hagenbuch and Stieger 2013)). 2004-ben azután a HUGO ajánlás alapján az OATP kódoló géneket egy külön, SLCO névvel („solute carrier family of the OATPs”) illetett családba tették és meghatározták az elveket, amely az OATP családokat ($\geq 40\%$ szekvencia azonosság, OATP 1, 2, stb.) és alcsaládokat ($\geq 60\%$ szekvencia azonosság, OATP 1A, 1B, stb.) kijelöli, illetve amely szerint egy-egy OATP ebbe a rendszerbe besorolódik (Hagenbuch and Meier 2004). Az emberi genomban 11 SLCO gént azonosítottak, illetve van egy 12. tag is, SLCO1B7. Az SLCO1B7-t pszeudogénként azonosították, ám nemrégiben egy kutatócsoport kimutatta, hogy a szomszédos SLCO1B3 génről és az SLCO1B7-ről átíródhat egy „kiméra” mRNS, ami funkcionális OATP transzportert eredményezhet (Malagnino et al. 2018). Mások azonban eddig ezt még nem erősítették meg. A 11 (12) humán SLCO génről több, mint 11 (12) fehérje keletkezik, ugyanis néhány OATP-nél alternatív transzkripció vagy splicing miatt többféle fehérje-kódoló mRNS képződhet (Pomari et al. 2009; Knauer et al. 2013; Huber et al. 2007). Az izoformák az eddigi adatok alapján szubsztrátfelismerésükben nem, de polarizált sejten belüli lokalizációjukban és

szöveti expressziójukban eltérhetnek egymástól. Ilyen a tumor-specifikus OATP1B3-V1 izoforma is, amelyről később írok.

1. táblázat: Humán OATP-k nevezéktana, szervezetben belüli kifejeződése és szubsztrátjai (Kovácsics, Patik, and Ozvegy-Laczkó 2017)

Gén jelölése (SLCO)	Fehérje (OATP)	Alternatív elnevezés	Szöveti expresszió*	Szubsztrátfelismerés
SLCO1A2	OATP1A2	OATP-A, OATP	általánosan előfordul (vér-agy gát, neuronok)	multispecifikus
SLCO1B1	OATP1B1	OATP-C, OATP2, LST-1	kizárólag hepatociták	multispecifikus
SLCO1B3	OATP1B3	OATP8, LST-2	kizárólag hepatociták	multispecifikus
SLCO1B7	?	LST-3 TMI2	?	?
SLCO1C1	OATP1C1	OATP-F, tiroid transzporter	agy, here	tiroid hormonok (T3, rT3, T4)
SLCO2A1	OATP2A1	PGT, prosztaglandin transzporter	általánosan előfordul	prosztaglandinok
SLCO2B1	OATP2B1	OATP-B	vékonybél, hepatociták, vér-agy gát, vázizom sejtek	multispecifikus
SLCO3A1	OATP3A1 v_1 and v_2 (izoformák elnevezése)	OATP-D	általánosan előfordul (neuronok, choroid plexus, here)	szteroid hormonok, prosztaglandinok
SLCO4A1	OATP4A1	OATP-E	általánosan előfordul	szteroid és tiroid hormonok
SLCO4C1	OATP4C1	OATP-H	vese proximális tubulusai	digoxin
SLCO5A1	OATP5A1	OATP-J	emlő	feltérképezetlen
SLCO6A1	OATP6A1	OATP-Y, GST (gonad-specific transzporter), CT48 (cancer testis antigen)	here	feltérképezetlen

*: A szöveti expressziónál csak azokat a szerveket, szöveteket soroltam fel, ahol fehérjeszinten kimutatták az adott OATP jelenlétét.

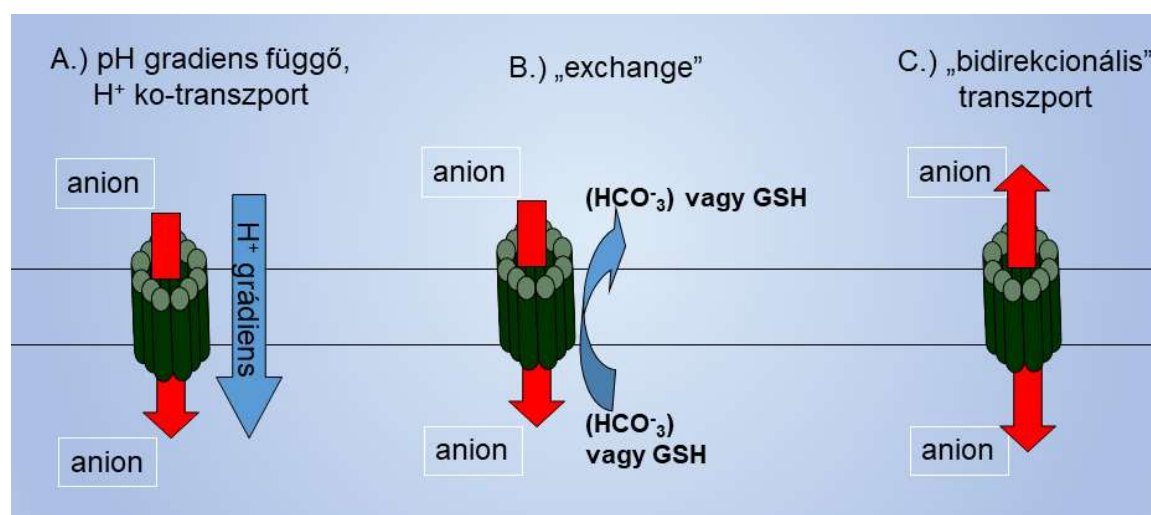
Az OATP-k működési mechanizmusa

Az OATP fehérjét Na^+ - és ATP-független szerves anion cserélőként („exchanger”) definiálják. Működésük pontos mechanizmusa azonban, a nagyszámú irodalmi adat ellenére, vagy éppen ezért, még nem egyértelműen ismert. Ellenionként leírták a bikarbonátot (HCO_3^-) (Satlin, Amin, and Wolkoff 1997) és a glutationt (GSH) (Li et al. 1998), ugyanakkor az ellenion OATP fehérjékként és szubsztrátonként eltérő lehet (Hagenbuch and Stieger 2013). Az sem tisztázott még, hogy vajon képesek-e koncentrálni szubsztrátjaikat a sejtben, tehát másodlagos aktív transzporterként a koncentráció gradiens ellenében is képesek-e működni (Hagenbuch and Stieger 2013). Ha valóban exchangerként működnek, akkor az is kérdés, hogy vajon a nagyméretű szerves szubsztrátjaik sejtből való kiáramlását is segítik-e, működhetnek-e efflux transzporterként. Az OATP3A1 fehérjénél kimutatták például, hogy az taurokolát kiáramlását generálja (Pan et al. 2018), de más

OATP-nél a közelmúltig ezt nem igazolták. Nemrégiben azonban egy svájci csoport új OATP vizsgálati módszert dolgozott ki, amely az OATP szubsztrátok kicserélődésén alapszik (Schafer, Bock, and Meyer Zu Schwabedissen 2018; Schafer et al. 2020). Ez alapján az OATP-ken keresztül egy szubsztrát távozhat is a sejtekből (erről bővebben az Eredmények IV/B.1.2.4. fejezetében lehet olvasni).

Az OATP-k vizsgálatokor megfigyelték, hogy a külső savas pH több OATP működését is fokozza (Leuthold et al. 2009; Kobayashi et al. 2003). Leutold és kollégái leírták, hogy a szubsztrátkötő hely részét képező, az OATP-k 3. transzmembrán hélixében található, kozervált His protonálódása segíti elő a negatívan töltött szubsztrátok transzportját. Saját eredményeink alapján ezt, legalábbis az OATP1C1 fehérjénél, cáfoltuk (Bakos, Nemet, et al. 2020; Patik et al. 2015), és másokkal együtt arra a megállapításra jutottunk, hogy nincs általánosan érvényes transzport mechanizmus: a magas extracelluláris protonkoncentráció stimuláló hatása nem minden OATP-re vagy minden OATP szubsztrátra érvényes (Bakos, Nemet, et al. 2020; Patik et al. 2015).

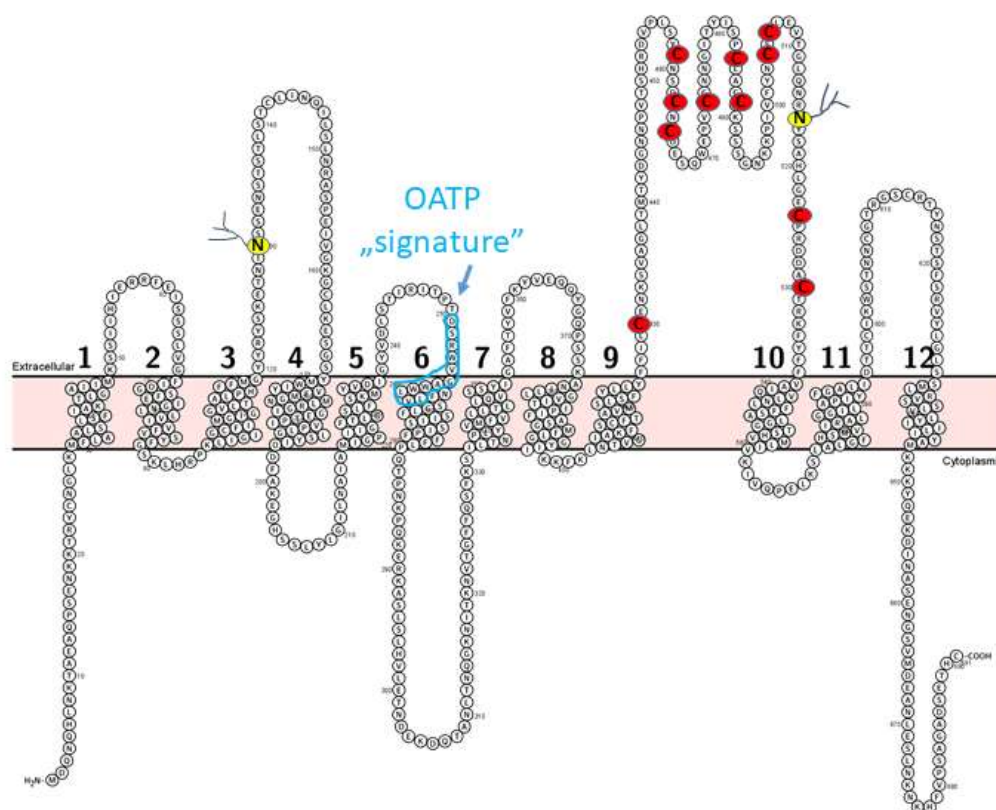
Végezetül, az OATP1B1, OATP1B3 és OATP2B1 fehérjéknél megfigyelték, hogy egyik szubsztrát fokozhatja a másik transzportját (Koenen et al. 2012; Kindla et al. 2011; Grube et al. 2006). Saját vizsgálatunkban az OATP3A1 fehérjénél mutattuk ki, hogy egy kumarin származék és az ösztro-3-szulfát (E1S) kölcsönösen aktiválják egymás transzportját és együttesen képesek transzportálódni (Bakos, Tusnady, et al. 2020).



4. ábra: Az OATP-k transzport működésének lehetséges mechanizmusai

OATP-k szerkezete és poszttranszlációs szabályozása

Az OATP-k 643-724 aminosavból felépülő polipeptidek. Térszerkezetüket kísérletesen még nem sikerült meghatározni, bár többféle modell is született (Meier-Abt, Mokrab, and Mizuguchi 2005), az egyik legutóbbi a csoportunk kísérletes adatai alapján (Tuerkova et al. 2021). Membrántopológia becslés alapján az OATP-k 12 membránon átívelő hélixből és az őket összekötő intra- és extracelluláris hurkokból állnak (5. ábra). A család tagjaira jellemző az ún. „OATP superfamily signature”: D-X-RW-(I,V)-GAWW-X-G-(F,L)-L szekvencia (Hagenbuch and Meier 2004), amely a 3. extracelluláris hurok és a 6. TM hélix határán található, és valószínűleg a szubsztrátfelismerésben van szerepe. Jellegzetes építőelemük még a nagy (közel 100 aminosavból álló) 5. extracelluláris hurok, amely ciszteinekben gazdag és a Kazal-2 típusú szerin-proteáz inhibitorokban megtalálható motívumot tartalmazza. Proteáz inhibitor funkciót az OATP fehérjéknél azonban még nem mutattak ki. Viszont a ciszteinek által létrehozott diszulfid hidak a fehérjeszerkezet stabilizálásában játszhatnak szerepet (Hanggi et al. 2006).



5. ábra: A humán OATP1B1 (Uniprot Q9Y6L6) membrántopológiája. Az OATP „signature” motívumot késsel jelöltem, az extracelluláris ciszteinek pirossal, az

igazolt N-glikozilációs helyek pedig sárgával jelölve láthatók. A TM hélixeket számok (1-12) jelölik. Az ábra a Protter program segítségével készült (Omasits et al. 2014).

Az OATP-k működésének és sejten belüli lokalizációjának (polarizált sejtek apikális vagy bazolaterális membránjában, esetleg lizoszómában való elhelyezkedés) általános szabályozása még nem pontosan ismert. Többnyire csak a család részletesen vizsgált tagjaira van adat. Kimutatták például, hogy az N-glikozilációnak, PKC általi foszforilációnak vagy a PDZ motívumon keresztüli fehérje-fehérje kapcsolatoknak van szerepük az OATP-k lokalizációjában (összefoglaló cikk (Lee, Ha, and Sugiyama 2020), de ezek sem általános érvényű szabályok, hiszen a PDZ motívum például nincs meg a hepatikus OATP1B1 és OATP1B3 fehérjékben.

Gyógyszertranszporter OATP-k

Az OATP-k nagyméretű (>300 Da), negatívan töltött vagy amfipatikus szerves molekulákat transzportálnak. Sőt, nevükkel ellentétben például a pozitívan töltött doxorubicin is OATP1A/1B szubsztrát (Lee et al. 2017). A 11 humán OATP szubsztrátfelismerése alapján két csoportba sorolható: 1) multispecifikus és 2) specializált OATP-k. Hozzá kell azonban tenni, hogy a kevésbé jellemzett OATP-kenél a szubsztrátok köre bővíthet, kellő adat hiányában nem tudhatjuk, hogy azok részt vesznek-e gyógyszerek transzportjában.

Az OATP-k számos endogén szubsztrátot szállítanak: epesók, szteroid és tiroid hormonok, prosztaglandinok, bilirubin (1. táblázat). Az OATP2A1 fehérjét például prosztaglandin (PG) transzporternek is nevezik (Kanai et al. 1995), a makrofágokban a PGE2 excitózisában vesz részt (Shimada et al. 2015). Az OATP1C1 tiroid hormon transzporter, az OATP4C1 fehérjénél pedig a digoxint tekintik „tipikus” szubsztrátnak (Kovacsics, Patik, and Ozvegy-Laczka 2017).

Már az első OATP klónozásakor kiderült, hogy az többféle, kémiai szerkezetében eltérő molekulát képes szállítani (Jacquemin et al. 1994). Később, az *in vitro* és *in vivo* adatok számának növekedésével több OATP-ről igazolódott, hogy sokféle molekulát, köztük gyógyszereket képes szállítani (Roth, Obaidat, and Hagenbuch 2012; Hagenbuch and

Stieger 2013), meghatározza ezek szervezeten belüli sorsát és gyógyszer-gyógyszer (DDI: drug-drug interaction) vagy élelmiszer-gyógyszer (FDI: food-drug interaction) kölcsönhatásokban vehet részt (Kovácsics, Patik, and Ozvegy-Laczkó 2017). Ennek egyik legismertebb példája, amikor a gemfibrozil és cerivasztatin együttes alkalmazása több páciensben súlyos, akár fatális rhabdomyolízishez vezetett. A gemfibrozil ugyanis egyszerre gátolta az OATP1B1 és a CYP2C8 működését (Shitara et al. 2004), ami megemelte a cerivasztatin vérbeli koncentrációját. Ez alapján a cerivasztatin forgalmazását megszüntették. Azóta tudjuk, hogy a sztatinek farmakokinetikájában az OATP-knek, együtt a CYP enzimekkel és az ABCG2 fehérjével, döntő szerepe van (Hirota, Fujita, and Ieiri 2020).

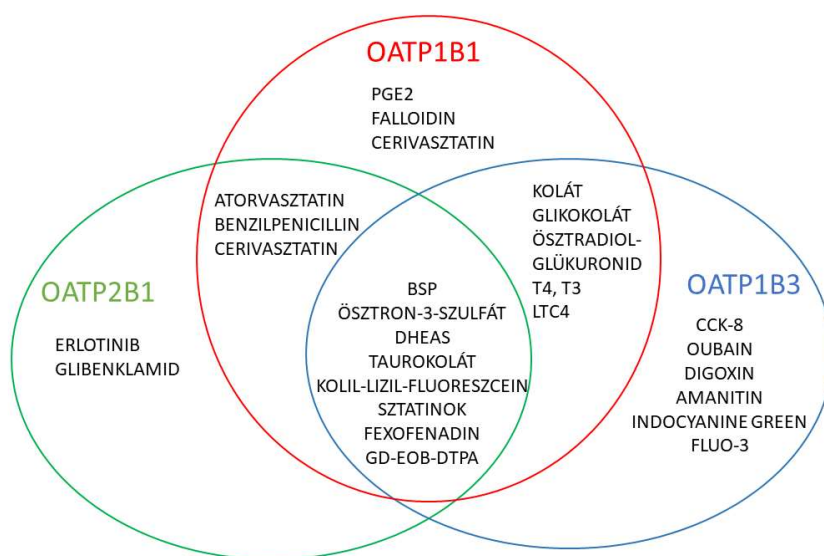
A multispecifikus, gyógyszerek ADME-Tox paramétereit befolyásoló OATP-k az OATP1A2, OATP1B1, OATP1B3 és OATP2B1 fehérjék.

Az **OATP1A2** legnagyobb mennyiségben a vér-agy gát endotél sejtjeinek lumenális oldalán található meg (Gao et al. 2000). Ezen kívül kimutatták még a kolangiocitákban, neuronokban és a vese disztális tubulus sejtjeiben (Hagenbuch and Stieger 2013). Az OATP1A2 a vékonybél enterocitáiban is kifejeződik (Shitara et al. 2013), de az OATP2B1-hez képest csekély mennyiségben, így a vékonybélből történő gyógyszerfelszívódásban szerepe vitatott (Drozdik et al. 2014). Az OATP1A2 viszont befolyásolhatja szubsztrátjai központi idegrendszerbe való bejutását, így lehetséges farmakológiai célpont a központi idegrendszert célzó vegyületek célbajuttatásában (Urquhart and Kim 2009; Ronaldson and Davis 2013). Expressziós mintázata alapján fontos szerepe van továbbá a szubsztrátjainak az epéből, illetve a vizeletből történő reabszorpciójában.

Az **OATP2B1** igazoltan részt vesz szubsztrátjai vékonybélből történő felvételében (Shitara et al. 2013), ezen kívül megtalálható a hepatociták szinuszoidális oldalán (Kullak-Ublick et al. 2001), az OATP1A2-vel azonosan a vér-agy gát endotél sejtjeiben (Gao et al. 2000), és még számos endotél vagy epitél eredetű sejtben (Hagenbuch and Stieger 2013). Szubsztrátfelismerése nagyban átfed az OATP1B fehérjékkel (7. ábra), de szerepe a gyógyszerek hepatikus felvételében még nem egyértelműen igazolódott.

Az **OATP1B1** és **OATP1B3** fehérjék expressziója a hepatocitákra korlátozódik (Konig et al. 2000; Abe et al. 2001), bár az OATP1B3 fehérjét a hasnyálmirigy béta sejtjeiben is kimutatták (Meyer Zu Schwabedissen et al. 2014). Ez a két fehérje az OATP család két legjobban jellemzett tagja, az FDA, EMA és PMDA ajánlásai alapján

gyógyszerkölsönhatásban vizsgálandó, amennyiben a gyógyszerjelölt molekula hepatikus eliminációját valószínűsítik. Az OATP1B1 és OATP1B3 szekvenciája 80%-ban azonos, szubsztrátfelismerésük nagyban átfed (6. ábra), egymás funkcióját valószínűleg nagyban át tudják venni. Ezt mutatja, hogy géneik együttes, mindkét fehérje funkciójának elvesztését eredményező mutációi okozzák a Rotor szindróma, a szérumban megnövekedett konjugált bilirubin és a vizeletben megemelkedett koproporfirin szinttel járó tünetegyüttes kialakulását (van de Steeg et al. 2012). Átfedő szubsztrátfelismerésük miatt, nem overexpressziós rendszerekben működésük elkülönítése nem triviális.



6. ábra: Hepatocelluláris OATP-k néhány közös és specifikus szubsztrátja. Forrás: (Kullak-Ublick et al. 2001; Bauer et al. 2018; Letschert et al. 2006; Nozawa, Imai, et al. 2004; Izumi et al. 2016; Nakanishi and Tamai 2012) és <http://www-metabase.ch.cam.ac.uk/metabaseui/>. BSP: bromoszulfoftalein, CCK-8: kolekisztokinin-oktapeptid, DHEAS: dehidroepiandrosteron-szulfát, Fluo-3: fluoreszcens festék, LTC4: leukotrién C4, PGE2: prosztaglandin E2, T3: trijód-tironin, T4: tiroxin.

A multispecifikus OATP-k többféle, a táplálékunkban előforduló anyagot, például flavonoidokat (Mohos, Fliszar-Nyul, Ungvari, Kuffa, et al. 2020; Mohos, Fliszar-Nyul, Ungvari, Bakos, et al. 2020; Li, Lu, and Paxton 2012), gomba toxinokat (Choudhuri and Klaassen 2020) is felismernek. Az OATP1B3 felel például az α -amanitin májbeli felvételéért, így működésének gátlása terápiás lehetőség a gombamérgezés okozta máj

toxicitás megelőzésében (Letschert et al. 2006). A táplálékunkban megtalálható hatóanyagok befolyásolják az OATP szubsztrát gyógyszerek farmakokinetikáját, például a flavonoidok intenzíven vizsgált *in vivo* inhibitorai az OATP2B1-nek (Shirasaka et al. 2013).

Az OATP-k betegséget okozó mutációi

Az **OATP1C1** az MCT8 (SLC16A2) monokarboxilát transzporterrel együtt a tiroid hormonok vér-agy gáton történő átjutásában és a neuronok és glia sejtek tiroid hormon felvételében fontos. Az MCT8 betegség okozó mutációi korábbról is ismertek (Dumitrescu et al. 2004), nemrégiben azonban fény derült az OATP1C1 fontos szerepére a központi idegrendszer tiroid hormon ellátásában. Egy neurodegeneratív tüneteket mutató tinédzserben az OATP1C1 transzporter D252N cserét okozó, és csökkent T3 transzportot eredményező mutációját azonosították. A fiatal beteg tüneteit, a kieső OATP1C1 funkciót pótolva, sikeresen tudták enyhíteni Triac (T3 analóg adásával) (Stromme et al. 2018).

A prosztaglandin transzporter **OATP2A1** mutációi egy recesszíven öröklődő, csont- és bőrdeformitással járó betegséget, PHO-t (primary hypertrophic osteoarthropathy) okoznak (Zhang et al. 2012) és

<https://www.omim.org/entry/601460?search=slco2a1&highlight=slco2a1>.

Az OAT1B1 és OATP1B3 együttes mutációi pedig a Rotor szindrómát eredményezik (lásd fenn).

OATP-k SNP-i

Az OATP-k, különösen az intenzíven vizsgált multispecifikus OATP1A/1B és OATP2B1 fehérjék variánsairól bőséges irodalmi adat áll rendelkezésünkre. A farmakogenomikai tanulmányok (GWAS és genotípus elemzések) nagyban hozzásegítettek az OATP-k farmakokinetikában betöltött szerepének megértéséhez. Ezekről kiváló összefoglaló cikkek születtek (Yoshida, Maeda, and Sugiyama 2013; Gong and Kim 2013; Nakanishi and Tamai 2012), itt csak a farmakokinetikai szempontból jelentős OATP SNP-ket foglalom össze.

Az **OATP1B1 rs4149056 (V174A)** változata csökkent transzporter aktivitást okoz. Számos GWAS alapján a sztatinok, olmesartan (vérnyomáscsökkentő), atrasentan (diabétesz gyógyszer), lopinavir (HIV gyógyszer), SN-38 (kamptotecin analóg, kemoterápiás szer), fexofenadine (allergiában alkalmazott antihisztamin) és a tacrolimus (immunszuppresszáns) magasabb plazmakoncentrációját eredményezi (Niemi, Pasanen, and Neuvonen 2011; Group et al. 2008).

Az **OATP1B3** fehérjénél az irodalmi adatok ellentmondásosak az SNP-k és megváltozott farmakokinetika terén (Kovacsics, Patik, and Ozvegy-Laczka 2017; Nakanishi and Tamai 2012), sőt, még az *in vitro* eredmények sem egyértelműek. Az rs4149117 (**S112A**) és rs7311358 (**M233I**) változatok például gyakran kapcsolatosan öröklődnek (1* allél) (Namgoong et al. 2015), ráadásul ez a változat a leggyakoribb a kaukázusi és ázsiai populációban. Viszont az *in vitro* adatok ellentmondásosak a téren, hogy az 1* allél által kódolt változat megváltoztatja-e az OATP1B3 aktivitását (Hamada et al. 2008; Schwarz et al. 2011). Tehát itt további vizsgálatok lehetnek szükségesek.

Az OATP1A2 és az OATP2B1 fehérjék SNP-iről sokféle adat látott már napvilágot. Ezek eredményei azonban sokszor ellentmondók, így nehéz állást foglalni a téren, hogy valamelyik polimorf változat igazoltan megváltozott farmakokinetikát eredményezne (Kovacsics, Patik, and Ozvegy-Laczka 2017).

Érdekes módon azonban, mind az OATP1B3, mind pedig az OATP2B1 csökkent szteroid hormon transzportot eredményező SNP-i kedvezőbb prognózist jelentenek prosztatatarákos betegekben. Ezt annak tulajdonítják, hogy a tesztoszteron (OATP1B3 szubsztrát) illetve a DHEAS (dehidroepiandroszteron-szulfát, OATP1B3 és OATP2B1 szubsztrát) csökkent felvétele lassíthatja a tumor növekedését (Wright et al. 2011; Hamada et al. 2008).

OATP-k a tumorokban

Az OATP-k fokozott expresszióját figyelték meg többek között emlő, tüdő, prosztatata és vastagbél eredetű tumorokban (erről több összefoglaló cikk született, többek között (Schulte and Ho 2019; Buxhofer-Ausch et al. 2013; Obaidat, Roth, and Hagenbuch 2012; Kovacsics, Patik, and Ozvegy-Laczka 2017), ami fokozott tápanyag- és hormonfelvételt eredményezve elősegítheti a tumorok progresszióját. Ezt támasztja alá, hogy hormonfüggő tumor eredetű sejtvonalakban az OATP-k jelenléte magasabb ösztro-3-szulfát felvételt eredményez (Meyer zu Schwabedissen et al. 2008; Nozawa, Suzuki, et al. 2004; Banerjee,

Allen, and Bendayan 2012). Ezzel összhangban, az OATP1B3 és OATP2B1 csökkent működést eredményező SNP-i (lásd előző fejezet) kedvezőbb prognózist jelentenek prosztatarákban. Ebből kifolyólag, az OATP-k működésének gátlása lehetséges rákterápiás stratégia lehet. Saját csoportunk, a Szegedi Tudományegyetemmel (Dr. Mernyák Erzsébet csoportja) együttműködve több szteroid-alapú OATP2B1 inhibitort vizsgált, amelyek új startégiát jelenthetnek a hormonfüggő tumorok kezelésében (lásd bővebben *Eredmények IV/B.3.2. fejezete és (Jojart et al. 2021; Jojart et al. 2018; Laczko-Rigo et al. 2020; Laczko-Rigo et al. 2021))*).

Mivel az OATP-k kemoterápiás szereket is felismernek, működésük által ezek a gyógyszerek elvben feldúsíthatók a tumorokban (Liu and Li 2014; Obaidat, Roth, and Hagenbuch 2012). Ebből a szempontból különösen jó célpont lehet a csak tumorokban kifejeződő OATP1B3-V1 izoforma, ami a májspecifikus OATP1B3 tumorokban alternatív transzkripció miatt keletkező variánsa (Furihata, Sun, and Chiba 2015). A kutatók azonban megosztottak a téren, hogy az OATP1B3-V1 változat működőképes-e (Thakkar et al. 2013; Imai et al. 2013) vagy esetleg más, a transzport működéshez nem köthető mechanizmussal (p53 útvonal gátlása) járul hozzá a tumorok fokozott túléléséhez (Lee et al. 2008). Mindenesetre, tumorspecifikus expressziója és a vérben lévő extracelluláris vezikulákban való megjelenése alapján az OATP1B3-V1 szérum markere lehet a vastagbélráknak (Morio et al. 2018).

Mivel a tumorokra jellemző a savas mikrokörnyezet, a másik, a kemoterápiás szerek tumorspecifikus feldúsításában kiaknázható jelölt az OATP2B1, amely hatékonyabban működik savas extracelluláris közegben (Nozawa, Imai, et al. 2004). Az OATP2B1 citosztikus szubsztrátjainak feltárása érdekében, kutatócsoportunk egy 100 tagból álló, az FDA által jóváhagyott molekulakönyvtárat szűrte le, amely során több vegyületet azonosítottunk, amelyekkel szemben az OATP2B1 jelenléte érzékenyítette a sejteket (Windt et al. 2019).

A tumorok OATP-inek további jelentősége, hogy azok diagnosztikus eszközök is lehetnek. Xenograft kísérletekben igazolták az indocyanine green, az FDA által például májfunkció ellenőrzésre jóváhagyott fluoreszcens festék, OATP1B3 általi felvételét (Wu, Huang, and Hsiao 2019). Továbbá az MRI kontraszt anyag Gd-EOB-DTPA (Gadolinium-ethoxybenzyl-diethylenetriamine pentaacetic acid) is az OATP1B3 (és az OATP1B3-V1) szubsztrátja (Narita et al. 2009; Leonhardt et al. 2010; Imai et al. 2013).

ABC és OATP transzporterek *in vitro* vizsgálatának módszerei

Az ABCG2, OATP1B1, OATP1B3 és OATP2B1 fehérjék kölcsönhatásai a nemzetközi ajánlások alapján a gyógyszerfejlesztés korai, *in vitro* fázisában vizsgálandók. Az ABC fehérjék és OATP-k *in vitro* vizsgálatában alkalmazott módszereket korábban összefoglaló cikkeinkben összegyűjtöttük (Szakacs et al. 2008; Kovacsics, Patik, and Ozvegy-Laczkó 2017). Itt a főbb, rutinszerűen alkalmazott eljárásokat azok főbb sajátosságaival tárgyalom. Kiemelem viszont azokat a módszereket, amelyek fejlesztésében részt vettem.

2. táblázat: Az ABCG2 és OATP-k *in vitro* vizsgálatában alkalmazott módszerek

	ép sejtés mérés				mérések izolált vezikulákon			
	transzport		antitest kötődés	sejt proliferáció vagy életképesség mérés	ATP-áz aktivitás mérés	transzport		antitest kötődés
	direkt	indirekt				direkt	indirekt	
ABCG2	R, MS, Fl		Fl	Fl, Kol.	Kol.	R, MS, Fl	R, MS, Fl	Fl
OATP-k	R, MS, Fl		-	Fl, Kol.	-	-	-	-

R: radioaktív detektálás, MS: tömegspektrometriás mérés, Fl: fluoreszcencia-alapú mérés, Kol: kolorimetria

Transzport aktivitás mérés: Általánosságban elmondható, hogy a rutinszerűen alkalmazott *in vitro* módszerek többsége valamilyen tesztvegyület transzportját követi nyomon. A szubsztrát felvételét lehet mérni ép sejten az OATP működésének követése céljából, vagy kifordított membránvezikulán ABC transzporterek vizsgálatára. Ép sejtes ABC transzporter vizsgálatban a szubsztrát kipumpálását követik nyomon. Vezikula-alapú mérést az OATP fehérjékre még nem dolgoztak ki, valószínűleg azért, mert a működési mechanizmusuk, a transzport hajtóereje nem tisztázott.

A tesztvegyület lehet fluoreszcens transzporter szubsztrát, radioaktívan jelzett szubsztrát, illetve nem jelzett vegyületnél tömegspektrometriás meghatározást is használnak. Az **indirekt módszer** során a tesztvegyület transzportjának gátlása az egyik „olvasat”. Ez a vizsgált anyag és a transzporter közötti kölcsönhatás meglétét jelzi, és lehet kompetitív gátlás (transzportálódó szubsztrátnál) vagy nem-, illetve unkompetitív gátlás is (nem transzportálódó inhibitornál). Kutatómunkám során jelentős hozzájárulást tettünk az OATP-k vizsgálatára alkalmas fluoreszcens módszerek megalkotásában, ezt részletesen az Eredmények IV/B. fejezetében mutatom be.

Amennyiben a vizsgált vegyület radioaktív formája nem áll rendelkezésre, illetve a vegyület nem fluoreszcens, **direkt transzportját** tömegspektrometriával lehet meghatározni. Citotoxikus vagy citosztatikus szubsztrátok azonosítására további lehetőséget nyújtanak a **sejtproliferációs vagy életképesség vizsgálatok**. Az ABCG2 működése megvédi, míg az OATP-k működése érzékenyíti a sejteket a citotoxikus szubsztráttal szemben.

Az ABC transzporterek, köztük az ABCG2 vizsgálatának másik lehetősége az **ATP-áz aktivitás** mérés. Az ABCG2 fehérjét jól mérhető alap ATP-áz aktivitás jellemzi. Ez a hozzáadott szubsztrát nélkül mért aktivitás, amit a transzportálódó szubsztrát fokozhat, míg a transzporter inhibitorai gátolnak. Az ATP-áz mérés olvasata azonban bonyolultabb. Vannak igazolt szubsztrátok, melyek gátolják az ATP-áz aktivitást, és például a nem transzportálódó koleszterin is fokozhatja azt (lásd Eredmények IV/A.2. fejezet).

Konformáció-szenzitív antitest vizsgálatán alapuló módszer: Az ABCG2 fehérjénél rendelkezésre áll egy konformáció-szenzitív antitest (5D3, (Zhou et al. 2001)). Kutatómunkám során (lásd Eredmények IV/A.4.2. fejezete) többek között ezt az antitestet jellemeztem, ami elvezetett egy új módszer kifejlesztéséhez, amit „5D3 shift assay”-nek nevezünk el (Telbisz et al. 2012). Ez egy további eszköz az ABCG2-vel kölcsönható szubsztrátok és inhibitorok elkülönítésére (lásd bővebben Következtetések és kitekintés c. fejezet). Ezen kívül az 5D3 antitest segítségével, ahogy korábban már említésre került, a vörösvértestek ABCG2 tartalma kvantitatívan meghatározható.

II. CÉLKITŰZÉSEK

I. Az ABCG2 fehérjével kapcsolatos kutatásaimnak a fehérje működésének és szabályozásának megértése volt a fő célja.

I.1. Ennek során a szubsztrátfelismerést és a koleszterinérzékelést befolyásoló fehérje régiókat vizsgáltuk mutáns változatok jellemzésével. Célunk volt

- a. az ABCG2 fehérje mutációs forró pontjának feltérképezése és
- b. az ABCG2 koleszterin-szenzor régiójának felderítése.

I.2. Célunk volt továbbá egy, az ép sejtekben kifejeződő ABCG2 fehérjét felismerő antitest kötődési mechanizmusának vizsgálata.

II. Kutatómunkám további részében a humán OATP transzporter család vizsgálatára alkalmas fluoreszcencia-alapú módszerek kidolgozása volt a cél, amely

- a. alkalmas a humán OATP fehérjék vizsgálatára
- b. lehetővé teszi a máj OATP1B1 és ABCG2 vagy MRP2 fehérjéinek együttes vizsgálatát
- c. közepes áteresztőképességű és megbízható mérési módszert ad
- d. automatizálható.

III. Végezetül célunk volt új hatóanyag- ABCG2 és OATP transzporter kölcsönhatások feltárása.

III. MÓDSZEREK

Értekezésem célja az új tudományos eredményeim bemutatása, ezért az alkalmazott módszerekről jelen dolgozatban csak rövid leírást adok. A kísérletes módszerek részletei megtalálhatók a csatolt közleményeimben.

Az ABCG2 fehérjével kapcsolatos kísérletekben használt módszerek

- **ABCG2 mutánsokat hordozó plazmidkonstrukciók elkészítése**

Az ABCG2 R482X, L555A, L558A, L555/558A vagy CRAC Tyr (Y413S, Y459S, Y469S/F, Y570, Y645S/F) mutánsait tartalmazó bakulovírus transzfer vektorokat (pAcUW21-L/ABCG2) PCR-alapú irányított mutagenézist követő kazettacserével készítettük el. A mutagenézishez használt oligonukleotidok szekvenciái az eredeti közleményekben megtalálhatók (Gal et al. 2015; Ozvegy-Laczka, Koblos, et al. 2005; Telbisz et al. 2014). A fehérje tisztításához hexahisztidin címkével ellátott ABCG2-t (illetve annak L558A vagy L555/558A verzióját) állítottuk elő rovarsejtekben a pAcUW21-L/His6-ABCG2 vektor segítségével (Telbisz et al. 2013; Telbisz et al. 2014). A plazmidokban lévő ABCG2 cDNS bázissorrendjét szekvenálással minden esetben ellenőriztük.

Az emlős sejtekben való expresszióhoz többféle vektorkonstrukciót használtunk.

A CRAC Tyr mutánsok HEK-293 sejtekben való expressziójához a pSB-CMV-ABCG2, általunk korábban létrehozott plazmidot (Saranko et al. 2013), az ABCG2 C592A, C603A, ill. C608A mutánsokat termelő HEK-293 sejtek előállításához a pCIN4 plazmidot használtuk (Henriksen et al. 2005), amit együttműködés keretében kaptunk meg. Ezekbe a plazmidokba a mutációkat hordozó DNS szakaszokat a megfelelő rekombináns bakulovírus vektorokból klónoztuk át (Gál és mtsai, 2015).

A vad típusú ABCG2-t a PLB985 és HEK-293 sejtekbe retrovirális transzdukcióval jutattuk be, amihez a SPsAGS plazmidot használtuk (Ujhelly et al. 2003).

- **Sejtvonalak és sejttenyésztés**

A különböző kísérletek során többféle, ABCG2 fehérjét termelő sejtvonalat használtunk (HEK-293, PLB985, MDCKII). Az A431 és HEK-293 sejteket az ATCC-től (American Type Culture Collection) szereztük be. A PLB985 (PLB) sejteket Dr. M. Dinauer (Department of Microbiology and Immunology, Indiana University School of Medicine, Indianapolis, IN, USA), az MCF-7 szülői és mitoxantron-szelektált (MCF-7/MX) sejteket Dr. Susan E. Bates (Cancer Therapeutics Branch, Center for Cancer Research, NCI, National Institutes of Health, Bethesda, MD, USA) bocsátotta rendelkezésünkre.

A sejttenyésztés az adott sejtvonalnak megfelelő standard körülményen történt. Az emlős sejtvonalakat jellemzően 10% főtális borjú szérummal (FBS), 2 mM L-glutaminnal és penicillin/sztreptomycin antibiotikumokkal kiegészített DMEM (Gibco, ThermoFisher Scientific) médiumban növesztettük, 37°C-on, 5% CO₂ tartalom mellett. Az Sf9 (*Spodoptera frugiperda*, Invitrogen) rovarsejteket 10% FBS és penicillin/sztreptomocint tartalmazó TNM-FH (Sigma) médiumban tenyésztettük 27°C-on.

A HEK-293 és A431 sejtek transzfekciójához Fugene6 reagenst (Promega), az MDCKII sejtek transzfekciójához pedig Lipofectamin 2000 (ThermoFisher Scientific) reagenst használtunk.

A PLB-ABCG2 sejtek előállításához retrovirális transzdukciót használtunk (Ujhelly et al. 2003).

- **Egyéb sejtvonalak**

A P-gp, illetve MRP1 fehérjéket termelő humán mielomonocita eredetű sejtvonalak (HL60-MDR1 és HL60-MRP1) és az MDCKII-MRP2 sejtvonal korábbi munka során készültek (Hollo et al. 1996; Bakos et al. 2000).

- **Rekombináns bakulovírusok előállítása**

Az ABCG2 változatok cDNS-ét hordozó rekombináns bakulovírusokat a BaculoGold (PharMingen, BD Biosciences) kit segítségével állítottuk elő Sf9 rovarsejtekben.

- **Membránpreparátumok készítése**

Három nappal a vírusfertőzést követően az Sf9 rovarsejteket összegyűjtöttük, hipotóniás oldatban lizáltuk, homogenizáltuk, majd a membránpreparátumot differenciál centrifugálással választottuk el (eredeti leírás (Sarkadi et al. 1992)). A

membránpreparátumokat felhasználásig -80°C -on tároltuk. A koleszterin hatásának vizsgálatához a membránpreparátumhoz koleszterin-RAMEB-et (random metilált β -cyclodextrin, Cyclolab) adtunk 2 mM végkoncentrációban (átlagosan 4,4% koleszterintartalommal) a centrifugálás előtt, vagy közvetlenül az aktivitás mérést megelőzően (Telbisz et al. 2014).

- **Az ABCG2 szolubilizálása, tisztítása és rekonstrukciója proteoliposzómákban**

Az Sf9 rovarsejtekben termeltetett ABCG2 fehérjét 1% (v/v) DDM (dodecil maltozid)-ot tartalmazó 0,4 % E. coli lipid extraktumban (Avanti Polar Lipids) szolubilizáltuk. A His-címkével ellátott ABCG2 fehérjét Ni-NTA (nitrilotriacetát, His-select, Sigma) oszlopon tisztítottuk, majd az eluálás után a fehérjét 0-0,4 mM koleszterinnel kiegészített E.coli lipid extraktumban rekonstituáltuk (Telbisz et al. 2013).

- **ABCG2 transzporter expressziójának ellenőrzése**

Western blot

A membránpreparátumok, proteoliposzómák vagy sejtlizátumok fehérjetartalmát Lowry módszerrel határoztuk meg, majd a fehérjéket SDS-poliakrilamid gélen választottuk el és PVDF (polivinidilén-difluorid) membránra blottoltuk át. Az ABCG2 detektálásához a BXP-21 antitestet használtuk (Maliepaard et al. 2001), amit George Scheffer és Rik Scheper (Department of Pathology, Free University, Medical Center, Amszterdam, Hollandia) bocsátott rendelkezésünkre.

ABCG2 sejtfelszíni expressziójának kimutatása áramlási citometriával

Az ABCG2 sejtfelszíni expresszióját Sf9 rovarsejtekben és emlős sejtekben 5D3 antitesttel követtük nyomon. Ehhez vagy kettős jelölést (5D3 kötést követően fikoeritrinnel konjugált anti-egér antitestet) használtunk (Ozvegy-Laczka, Varady, et al. 2005), vagy az Alexa647 festékkel konjugált 5D3 segítségével direkt jelölést alkalmaztunk (Ozvegy-Laczka et al. 2008). Negatív kontrollként ABCG2-t nem termelő sejteket és izotípus kontroll (egér IgG2b) jelölést használtunk. A sejtek fluoreszcenciáját áramlási citometriával követtük nyomon, amihez FACSCalibur (Becton Dickinson) vagy Attune Next (Applied Biosystems, Life Technologies) készülékeket használtunk. Az 5D3 antitest jellemzésénél az antitest hozzáadását megelőzően a következő kezeléseket alkalmaztuk: formaldehid fixálás (0,005-1%), fehérje keresztkötőkkel történt kezelés (1 mM BMPH, 0,5 mM

BMPEO₃, 1 mM PMPI, 2 mM EDC, 2 mM sEGS, 2 mM sMBS), részletes leírás (Ozvegy-Laczka et al. 2008).

- **ABCG2 kimutatása immunfluoreszcens jelölést követően konfokális mikroszkópiával**

A HEK-ABCG2 sejteket 8-lyukú kamrára osztottuk ki, és 48 órán át növesztettük. A mérés napján a sejteket mostuk, 1% formaldehiddel fixáltuk, majd a formaldehid eltávolítását követően allofikocianinnal konjugált 5D3 antitesttel (R&D Systems) jelöltük.

A HEK-ABCG2 sejtek BXP-21 antitest jelölése fixálást és permeabilizálást (4% formaldehid és metanol) követően történt (Ozvegy-Laczka et al. 2008).

A sejteket Olympus FV500-IX konfokális lézerpásztázó mikroszkópban analizáltuk.

- **5D3 antitest kötődés vizsgálata membránvezikulákon**

Az ABCG2 fehérjét tartalmazó membránpreparátumot 5D3 antitesttel, majd mosást és centrifugálást követően fikoeritrin konjugált anti-egér másodlagos antitesttel (1 µg/ml) inkubáltuk. Újabb mosást és centrifugálást követően a membránok fluoreszcenciáját Fluoroskan II (Labsystems) készülékben olvastuk le. Amikor az ATP hidrolízis különböző fázisait vizsgáltuk, a membránokat az 5D3 antitest hozzáadása előtt 2 mM Na-vanadáttal, 1µM Ko143-mal, 10 mM AMP, MgADP, MgAMP-PNP vagy MgATP-vel előinkubáltuk (Ozvegy-Laczka, Varady, et al. 2005).

- **Koleszterin töltés vagy kivonás**

A rovarsejtek vagy membránpreparátumok koleszterinnel való „feltöltése” 30 perces 2 mM koleszterin-RAMEB-bel történt inkubálással történt. A HEK-293 sejten végzett kísérleteknél 30 percen át inkubáltuk a sejteket koleszterin-mentes („üres”) RAMEB-bel (Gal et al. 2015; Telbisz et al. 2014).

- **ATP-áz aktivitás mérés**

Az ATP-áz aktivitás méréséhez Sf9 rovarsejtekből izolált membránvezikulákat használtunk. Az ABCG2 fehérjét tartalmazó membránpreparátumot inkubáltunk a vizsgált szubsztrát jelenlétében vagy hiányában, 3,3 mM Mg-ATP-vel. A felszabaduló inorganikus foszfátot kolorimetriás módszerrel határoztuk meg. Az ATP hidrolízis ABC fehérjékre

jellemző komponensét a 2 mM Na-ortovanadát jelenlétében mért háttérérték levonásával határoztuk meg (Ozvegy-Laczka, Koblos, et al. 2005). Amikor a koleszterin hatását vizsgáltuk, a membránokat előinkubáltuk 2 mM kolesztrein-RAMEB-bel (vagy a membránpreparálás során előzőleg koleszterinnel „feltöltött” membránokat használtunk) (Telbisz et al. 2014).

- **Transzport aktivitás mérés**

Vezikuláris transzport

Az ABCG2 aktivitását kifordított Sf9 membránvezikulákban radioaktív (10-3000 μM ^3H -methotrexát vagy 25 μM ösztadiol-17 β D-glükuronid (Telbisz et al. 2014; Ozvegy-Laczka, Koblos, et al. 2005)) vagy fluoreszcens szubsztrát (10 μM Lucifer Yellow (Szekely et al. 2020)) segítségével vizsgáltuk. Az ABCG2 fehérjét tartalmazó preparátumot inkubáltunk a radioaktív vagy fluoreszcens szubsztráttal 4 mM Mg-ATP (vagy kontrollként 4 mM AMP) és/vagy 1 μl Ko143 jelenlétében. Az ATP- vagy inhibitor-szenzitív aktivitást határoztuk meg.

Transzport mérések ép sejteken

Áramlási citometria: Az ABCG2 aktivitásának ép sejteken történő nyomon követésére rhodamine 123 és Hoechst 33342 fluoreszcens festékeket, vagy fluoreszcens citosztatikumokat (doxorubicin, mitoxantron) használtunk. A rhodamine 123, doxorubicin vagy mitoxantron fluoreszcenciáját FACSCalibur citométerben mértük. Az elpusztult sejteket propidium-jodid festés alapján azonosítottuk (Gal et al. 2015; Ozvegy-Laczka, Koblos, et al. 2005).

ABCG2 Hoechst 33342 festék felvétele: A Hoechst 33342 festék (1 μM) felvételét valós időben követtük a fluoreszcencia (excitáció: 350 nm, emisszió: 460) mérésével küvettás fluoriméterben (Perkin Elmer LS 50B). Az aktivitást az 1 μM Ko143, specifikus ABCG2 inhibitor jelenlétében mért fluoreszcencia növekedéshez viszonyítva határoztuk meg (Özvegy és mtsai, 2005). Aktivitás: $(F_i - F_0)/F_i * 100$, ahol, F_i : 1 μM Ko143 jelenlétében mért fluoreszcencia növekedés, F_0 : hozzáadott inhibitor nélkül mért fluoreszcencia növekedés. A tirozin kináz gátló Iressa és Gleevec tesztelésénél a Hoechst 33342 festék hozzáadása előtt előinkubáltuk a sejteket az adott vegyülettel.

- **Sejttúlélés vizsgálatok**

A HEK-ABCG2 sejtek viabilitását PrestoBlue reagens (ThermoFisher Scientific) segítségével határoztuk meg.

OATP fehérjék vizsgálata

- **OATP fehérjéket hordozó plazmidkonstrukciók elkészítése**

Az Sf9 rovarsejtben történt expresszióhoz bakulovírus transzfer vektorokat (pAcUW-L/OATP) használtunk. Ezeket a kutatócsoportunkban készítettük el, részletes leírása itt megtalálható (Patik et al. 2015).

Az emlős sejtés expresszióhoz transzpozon alapú génbevitelt, illetve lentivirális transzdukciót használtunk. Az ehhez szükséges plazmidokat (pSB-CMV/OATP vagy pRRL-CMV-MCS-IRES- Δ CD4/OATP) szintén a kutatócsoportunkban hoztuk létre, bővebb leírás itt található (Patik et al. 2018).

Az OATP2B1 fehérjét kifejező A431 sejtvonal létrehozásához az sejteket Fugene HD (Promega) reagenssel transzfektáltuk. A többi OATP-t (OATP1A2, OATP1C1, OATP1B1, OATP1B3) lentivirális transzdukcióval juttattuk be az A431 vagy HEK-293 sejtekbe (Patik et al. 2018; Bakos, Nemet, et al. 2020).

Az MDCKII-OATP1B1, MDCKII-MRP2-OATP1B1 és MDCKII-OATP1B1-ABCG2 sejtek előállításához szintén lentivirális transzdukciót alkalmaztunk (Szekely et al. 2020).

Western blot

A Western blot az ABCG2 fehérjénél leírtak szerint történt. Az **OATP** 1A2, 1B1, 1B3, 1C1, 2B1, 3A1_v1 és 4A1 fehérjéket felismerő antitesteket Prof. Bruno Stieger (University of Zürich, Svájc) bocsátotta a rendelkezésünkre (Kullak-Ublick et al. 2001). Az OATP2A1 (HPA013742), OATP4C1 (HPA036516), OATP5A1 (HPA025062), OATP6A1 (HPA054126) vagy OATP1B3 fehérjékre specifikus antitestet (AMAb91231) az Atlas Antibodies cégtől szereztük be.

- **OATP-k transzport aktivitásának meghatározása Sf9 rovarsejtekben**

A rekombináns bakulovírusokat a megfelelő plazmidkonstrukciók (pAcUW-L/OATP) segítségével az ABCG2-nél leírtak szerint állítottuk elő. Az Sf9 sejteket a mérést 40 órával

megelőzően a megfelelő OATP cDNS-ét tartalmazó rekombináns bakulovírussal transzfektáltuk. A méréskor a sejteket mosást követően Na-fluoresceinnel, fluoresceinmetotrexáttal vagy Zombie Violet festékkel (a festékmennyiségeket az ábraalírásokban feltüntettem) inkubáltuk. Különböző pH-jú puffereket vizsgáltunk (pH 4,5-8,4), annak érdekében, hogy az adott festék felvételéhez optimális körülményt megtaláljuk. Az inhibitorok tesztelésénél azokat a festék hozzáadását megelőzően adtuk a sejtekhez. A reakció végén 1 µg/ml propídium-jodidot adtuk a sejtekhez, hogy az elpusztult sejteket a méréskor azonosítani tudjuk. A sejtek fluoreszcenciáját Attune áramlási citométerben (*Attune Acoustic focusing, Life Technologies*) detektáltuk. Csak az élő (propídium-jodid negatív) sejteket vizsgáltuk.

- **OATP-t termelő sejtek kiválogatása**

Az OATP 1A2, 1B1, 1B3, 1C1 vagy 2B1 fehérjéket kifejező sejtek kiválogatását a Live/Dead Green (LDG, ThermoFisher Scientific) festék felvétele alapján végeztük BD FACSaria III Cell Sorter (BD Biosciences) segítségével. Röviden, a sejteket 0,1 µl LDG festékkel inkubáltuk 30 percen át pH 5.5 pufferben, majd mostuk és sejtenyésző médiumban felvéve őket, megmértük a fluoreszcenciájukat. Az LDG⁺ sejteket kiválogattuk és friss sejtenyésző médiumban (DMEM) növesztettük tovább. Az OATP expressziót és funkciót Western blot vagy festékfelvétel alapján teszteltük (Patik et al. 2018).

OATP-k transzport aktivitásának mérése áramlási citometriával

Az OATP-ket termelő A431, HEK-293 vagy MDCKII sejteket a fluoreszcens festékkel inkubáltuk. A sejtek fluoreszcenciáját Attune áramlási citométerben mértük meg (Bakos, Nemet, et al. 2020; Patik et al. 2018).

Mikrolemez alapú mérés, „klasszikus” módszer

Az OATP-t termelő (és kontroll) A431 sejteket a mérést megelőző napon 96-lyukú lemezre osztottuk ki. Másnap a konfluens sejtréteget mostuk és amennyiben inhibitor vizsgálat történt, az inhibitorral előinkubáltuk (37°C, 5 perc). Ezután hozzáadtuk a vizsgálni kívánt festéket és megfelelő ideig (10-30 percig) 37°C-on inkubáltuk, majd a festéket eltávolítottuk, a sejteket mostuk és a fluoreszcenciát leolvastuk (Enspire, fluoreszcens lemezolvasó, Perkin Elmer). Minden új festékszubsztrát vizsgálatokor minimum kétféle pH-jú puffert teszteltünk (pH 5,5 és pH 7,4), annak érdekében, hogy a transzporthoz az ideális körülményt megtaláljuk (Bakos, Nemet, et al. 2020; Patik et al. 2018).

z-faktor számítás

$$\text{z-faktor} = 1 - \left(\frac{(3 \times \text{Szórás}_{\text{negatív kontroll}} + 3 \times \text{Szórás}_{\text{pozitív kontroll}})}{(\text{Átlag}_{\text{pozitív kontroll}} - \text{Átlag}_{\text{negatív kontroll}})} \right)$$

- **Mikrolemez alapú mérés, „add-és-mérd” módszer**

A méréshez OATP-t termelő A431 sejteket használtunk. A fentiekben leírt klasszikus módszer szerint jártunk el, azzal a kivétellel, hogy az Ace (8-acetoxi-1,3,6-hidroxipirandin, VWR International) fluorogén (nem fluoreszcens) OATP szubsztrátot nem távolítottuk el a mérés során, hanem a fluoreszcenciát folyamatosan (a lemezolvasónkban állandó 37°C biztosított) mértük vagy pedig az inkubációs idő leteltével olvastuk le (Ungvari et al. 2021).

- **Kompetitív ellenáramlás és efflux mérések**

A mérés OATP-t termelő A431 sejteken történt, és két fő lépésből áll. Az első lépésben a 96-lyukú lemezre előző nap kihelyezett sejteket feltöltöttük a szubsztráttal (5 vagy 20 μM Ace), 37°C-on 10-30 percig történő inkubálással. A mérés második fázisában a sejteket tovább inkubáltuk Ace-val és a vizsgált vegyületekkel (benzbromaron, bromoszulfoftalein, CsA vagy ösztron-3-szulfát), vagy transzport pufferben (Ace nélkül) a vizsgált vegyületekkel, illetve azok nélkül. A mérés végén a sejtekről eltávolítottuk a puffert, majd a fluoreszcenciát Enspire fluoreszcens lemezolvasóban olvastuk le (Ungvari et al. 2021).

- **Transzcelluláris transzport mérés polarizált MDCKII sejteken**

A fluoreszcens festékek sejten át történő (transzcelluláris) transzportját kettős transzfektáns MDCKII-OATP1B1-ABCG2, MDCKII-OATP1B1-MRP2, a megfelelő egyszeres transzfektáns és kontroll MDCKII sejteken mértük. A sejteket a mérést megelőzően féligáteresztő filteren (6,5 mm átmérő, 0,4 μm pórusméret (VWR Kft.)) 4 napon át növesztettük. A mérés kezdetekor a sejttel benőtt filtereket 24-lyukú lemezre helyeztük. A mérés a vizsgálandó festékszubsztrát alsó kompartmenthez (bazolaterális-apikális irányú transzport), vagy a felső, a sejtréteget tartalmazó kompartmenthez (apikális-bazolaterális irányú transzport) való hozzáadásával indult. Az ellentétes oldali kompartmentből történt mintavételt követően a fluoreszcenciát Enspire fluoreszcens lemezolvasóban mértük meg (Szekely et al. 2020).

- **Sejttúlélés vizsgálatok**

Az OATP2B1 vizsgálatokor mCherry vagy GFP fluoreszcens fehérjéket kifejező A431 sejteket használtunk (Windt et al. 2019). A sejteket 120 órán át inkubáltuk a vizsgált ösztrom származékokkal, majd a sejtek fluoreszcenciáját Enspire fluoreszcens lemezolvasóban mértük meg (Laczkó-Rigó és mtsai, 2021).

Az A431-OATP1A2 sejteken végzett citotoxicitás méréseknél szulforodamin B festést használtunk.

- **Triciálás és transzport mérés**

A tríciummal jelölt 2-bromo-13 α -ösztromot együttműködő partnerünk (Tömböly Csaba, Kémiai Biológiai Laboratórium, SZBK) szintetizálta. A vegyület transzportját A431-OATP2B1 (és kontroll) sejtekben mértük a sejteket 1-100 μM ^3H -2-bromo-13 α -ösztrommal inkubálva. A sejtekben felhalmozódott ^3H -2-bromo-13 α -ösztrom radioaktivitás mérés alapján határoztuk meg (Laczkó-Rigó és mtsai, 2021).

A közleményekben és a dolgozatomban szereplő ábrák minden esetben minimum három független biológiai kísérletből származnak, és azok átlagát (\pm szórás) mutatják. A Western blot és áramlási citometriás mérések reprezentatívak, de ezeket is minden esetben legalább 3 független kísérletben megismételtük.

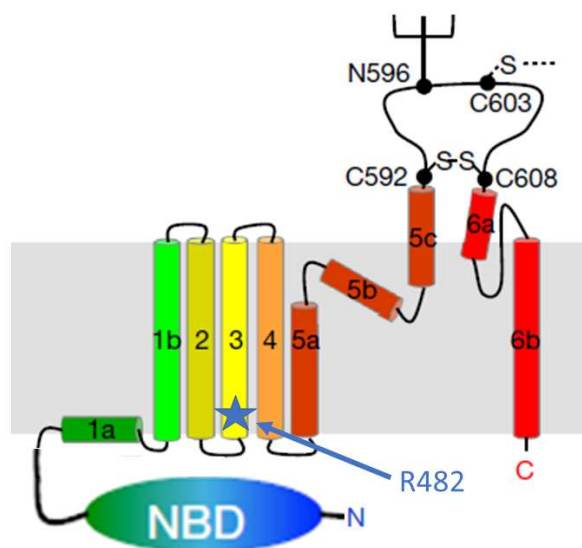
IV. EREDMÉNYEK ÉS MEGVITATÁSUK

IV/A. A humán ABCG2 fehérje vizsgálata: szubsztrátfelismerés, koleszterin általi szabályozás, antitest kötődés jellemzése és új gyógyszerkölcsonhatások feltárása

IV/A.1. Az ABCG2 fehérje mutációs forró pontjának vizsgálata

*Az R482 egyedi szubsztrátfelismerést biztosít
(Özvegy-Laczka és mtsai, 2005, 1. sz. közlemény)*

Amint az az ABCG2 fehérjét kódoló gén azonosításakor kiderült, a citosztatikummal (mitoxantron vagy doxorubicin) szelektált, különböző egér és emlős eredetű sejtekben több esetben az R482-t érintő, pontmutáns (R482 G, T, S illetve M) ABCG2 változatok keletkeztek és szelektálódtak ki (Doyle et al. 1998; Miyake et al. 1999; Allen, Jackson, and Schinkel 2002).



7. ábra: Az R482 pozíciója az ABCG2 fehérjében. A topológia a térszerkezet alapján készült és egy monomert ábrázol. Az R483 a 3. TM hélixben helyezkedik el. NBD: nukleotidkötő domén. Az ábrán az N-glikozilációs hely és a 3. extracelluláris hurok

diszulfid hídjainak kialakításában fontos ciszteinek is láthatók. Kép forrása (Taylor et al. 2017)

Korábbi munkám során, más kutatócsoportokkal egyidőben kimutattam, hogy az R482 T, S, M vagy G variánsok funkciónyereses („gain of function”) mutánsok, fokozott aktivitással és a vad-típustól eltérő szubsztrátfelismeréssel bírnak, ami megmagyarázza miért szelektálódhattak ki ezek a variánsok az *in vitro* gyógyszerselekció hatására (Honjo et al. 2001; Ozvegy, Varadi, and Sarkadi 2002) (ez a PhD munkám részét képezte, így ezeket az eredményeket itt nem tárgyalom). A felfedezés folytatásaként részletesen vizsgáltuk, hogy az ABCG2 fehérje 482. pozíciójában található aminosav minősége hogyan befolyásolja a fehérje működését. Ezért, eltérő oldallánc karakterrel rendelkező mutáns változatokat, R482 I, M, S, D, N, K és Y, állítottunk elő, azokat rovarsejtekben termeltettük és jellemeztük. A fehérjék mennyiségét és sejtfelszíni expresszióját ellenőrizve megállapítottuk, hogy mindegyik mutáns expresszálódik és a plazmamembránban helyezkedik el (lásd bővebben az 1.sz. csatolt közlemény (Ozvegy-Laczka, Koblos, et al. 2005)).

Az ABCG2 változatok működőképességét először ATP-áz aktivitás méréssel ellenőriztük. Ez a módszer a fehérje ATP hidrolizáló képességét méri, amely a szubsztrát transzportjához szükséges energiát biztosítja. Megállapítottuk, hogy az összes R482X változat aktív, a vad típussal összevethető ATP-áz aktivitással rendelkezik, amit a fehérje specifikus inhibitora, a Ko143 gátol.

A mutánsok további jellemzése során korábban azonosított fluoreszcens vagy radioaktívan jelzett ABCG2 szubsztrátok transzportját követtük nyomon. A 3. táblázatban foglaltam össze az ATP-áz és transzport mérések eredményét, azok részletei megtalálhatók a (Ozvegy-Laczka, Koblos, et al. 2005) közleményben.

3. táblázat: Sf9 rovarsejtekben termelt ABCG2 R482X mutánsok aktivitása és szubsztrátspecifitása

R482X	Transzport aktivitás			
	ATP hidrolízis	metotrexát	rhodamine 123	Hoechst 33342
R (vad típus)	+	+	-	+
K	+	-	-	-
Y	+	-	-	-
G	+	-	+	+
S	+	-	+	+
T	+	-	+	+
I	+	-	+	+
D	+	-	+	+
M	+	-	+	+
N	+	-	+	+

Az ATP hidrolízis és ³H-metotrexát transzport meghatározása Sf9 membránvezikulákon történt. A rhodamine 123 (2 μM) vagy Hoechst 33342 (2 μM) festékek transzportját Sf9 rovarsejteken vizsgáltuk áramlási citometriával vagy kivettás fluoriméterben. +: van mérhető aktivitás, -: nincs aktivitás.

Eredményeink alapján a mutánsok 2 csoportra oszthatók: a vad típushoz képest fokozott, illetve csökkent működéssel rendelkezők.

- Az R482 G, S, T, I, M, N és D változatok funkcionyeréses mutánsoknak tekinthetők a rhodamine 123 transzportáló képességük alapján (amire a vad típus nem képes). Érdekes módon azonban itt szabályszerűséget nem tudunk felfedezni az aminosav oldallánc fizikokémiai tulajdonságai és a megváltozott működés között. A legtöbb mutáns megváltoztatta az ABCG2 szubsztrátfelismerését. Miwa és mtsai alapján, ezek nem csak szubsztrátfelismerésükben, hanem aktivitásukban is meghaladhatják a vad típusú fehérjét, azaz fokozott rezisztenciát eredményezhetnek például mitoxantron és SN-38 ellen (Miwa et al. 2003).
- Az R482 K és Y mutánsok aktivitása jelentősen lecsökkent, az R482K változatnál csak ATP-áz aktivitás volt mérhető. Később kimutattuk, hogy a rovarsejtekben termelt ABCG2 működését fokozza a sejtmembrán koleszterinnel való feltöltése

(lásd IV/A. 2. fejezet). Azonban az R482K és R482Y mutánsoknál, ilyen körülmények mellett is csak elenyésző transzport aktivitást tudunk mérni (Telbisz et al. 2014).

- Megállapítottuk, hogy a vad típus (R482) csak rá jellemző, egyedi szubsztrátfelismeréssel rendelkezik, a metotrexát egyedül ennek a variánsnak szubsztrátja.

A metotrexát egy folsav antagonistája. Chen és mtsai kimutatták, hogy a folsavat a vad típusú ABCG2 képes transzportálni, az R482G és R482T változatok nem (Chen et al. 2003), így elképzelhető, hogy a folsav vagy egyéb fiziológiás szubsztrát az, aminek a transzportjára csak a vad típusú ABCG2 képes. Azonban a többi mutánst ilyen szempontból nem jellemeztük, és tudomásom szerint mások sem vizsgálták, így ez egyelőre nyitott kérdés maradt.

IV/A.2. Az ABCG2 koleszterin-szenzor régiójának azonosítása felé

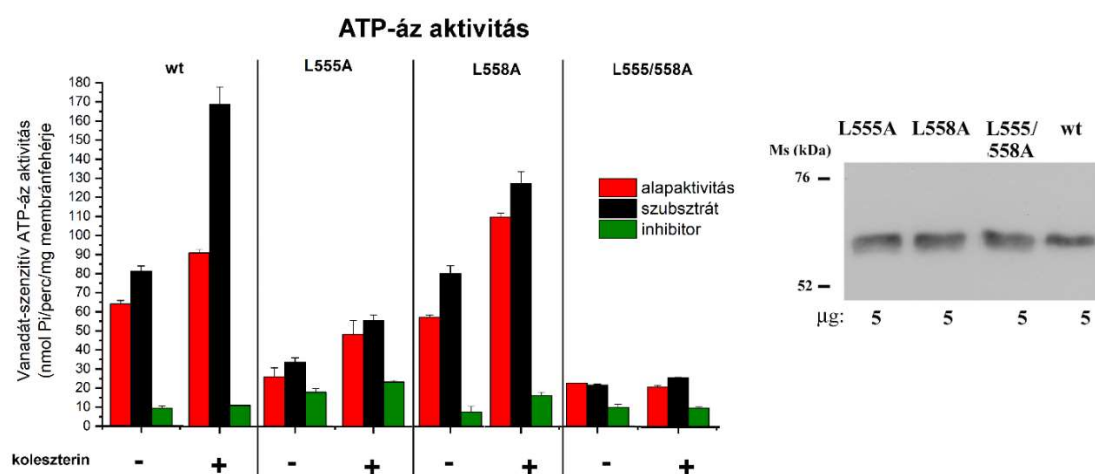
Kutatócsoportunk (Telbisz et al. 2007) másokkal egyidőben (Pal et al. 2007) kimutatta, hogy a koleszterinnek fontos szabályozó szerepe van az ABCG2 működésében. Sőt, tisztított, rekonstituált proteoliposzómák segítségével az ABCG2 működéséhez szükséges koleszterin mennyiséget is sikerült meghatározni (Telbisz et al. 2013). Az ABCG2 koleszterin „érzékelésében” részt vevő aminosavakat, fehérje régiókat azonban, amikor e munka készült, nem ismertük. A következő két fejezetben azt a munkánkat mutatom be, amellyel két, feltételezett szteroidkötő motívum szerepét vizsgáltuk.

IV/A. 2.1. Az LxxL szteroidkötő motívum szerepe

Az LxxL régió az ABCG2 szubsztrátfelismerését és stabilitását változtatja meg (Telbisz és mtsai, 2014, 2.sz. közlemény)

Az L/MxxLxxL, illetve a rövidebb LxxL szekvencia egy igazolt szteroidkötő motívum (SBE, steroid binding element, x: tetszőleges aminosav). Ez a motívum vesz részt például a progeszteron receptor progeszteron kötésében (Williams and Sigler 1998). Az ABCG2 fehérjében a rövidebb, LxxL motívum található meg. Velamakanni és mtsai. korábban kimutatták, hogy az LxxL leucinjainak alaninra történő cseréje a szteránvázas progeszteron és ösztadiol-17 β D-glükuronid felismerésének/transzportjának elvesztését eredményezi (Velamakanni et al. 2008). Munkám során az ABCG2 LxxL egyszeres és kétszeres Leu-Ala mutánsait jellemeztem koleszterinérzékelés és szubsztrátfelismerés szempontjából.

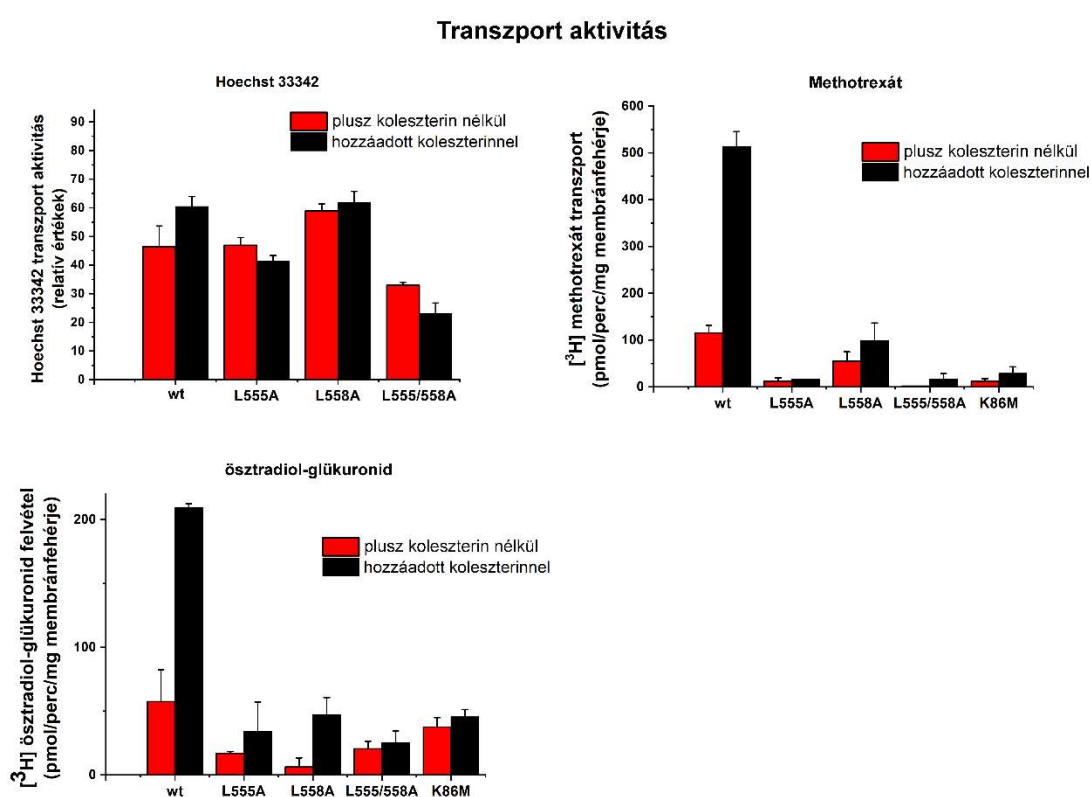
Ezek a kísérletek szintén Sf9 rovarsejteken zajlottak, mivel ez a rendszer számos eszközt nyújt az ABCG2 vizsgálatára. Ráadásul, ebben a rendszerben a membránkoleszterin hatása egyszerűen vizsgálható, mert az alacsony koleszterintartalmú rovarsejtek ciklodextrinbe „csomagolt” koleszterinnel való inkubálással „feltölthetők” (lásd Módszerek fejezet). ATP-áz aktivitás mérésekben (8. ábra) az L555A és L555/558A mutánsokat, figyelembe véve az expressziós szintjeiket, jelentős mértékben csökkent ATP-áz aktivitás jellemezte, amit koleszterin hozzáadásával sem lehetett jelentősen fokozni. A koleszterinnel nem töltött membránokban az L558A egyszeres mutáns ATP-áz aktivitása a vad típusal összemérhető volt. Viszont a hozzáadott koleszterin hatására, a vad típusra jellemző, szubsztrát jelenlétében fokozódó aktivitás e mutánsnál is elmaradt.



8. ábra: Koleszterin hatása az LxxL mutánsok működésére. Bal oldali panel: Az Sf9 rovarsejtekben termelt ABCG2 variánsok ATP hidrolízisét hozzáadott koleszterin nélküli (-) és koleszterinnel „töltött” (2 mM koleszterin-RAMEB hozzáadásával, +) membránokon mértük. Alapaktivitás: hozzáadott szubsztrát vagy inhibitor nélkül mért ATP-áz aktivitás.

Szubsztrátként $1 \mu\text{M}$ quercetint, inhibitoroként pedig $10 \mu\text{M}$ Ko143-t használtunk. **Jobb oldali panel:** Az ABCG2 mutánsok expresszióját Western blot és specifikus antitest (BXP-21) segítségével ellenőriztük. wt: vad típus

A mutánsokat transzport mérésekben is jellemeztük és az alkalmazott szubsztráttól függően eltérő eredményt kaptunk (9. ábra). A csökkent ATP-áz aktivitás ellenére mindhárom LxxL mutáns transzportálta az ABCG2 szubsztrát Hoechst 33342 festéket, működésüket azonban a koleszterin nem fokozta (9. ábra).



9. ábra: Koleszterin hatása az LxxL mutánsok transzport aktivitására. A Hoechst 33342 festék ($2 \mu\text{M}$) felvételét ABCG2-t termelő Sf9 rovarsejteken mértük Enspire küvettás fluoriméterben. Az ábra a ($1 \mu\text{M}$) Ko-143 inhibitor-szenzitív aktivitást mutatja (lásd bővebben Módszerek fejezet). A radioaktívan jelzett metotrexát ($100 \mu\text{M}$) és ösztradiol- $17\beta\text{D}$ -glükuronid ($25 \mu\text{M}$) felvételét Sf9 rovarsejtekből izolált membránvezikulákon határoztuk meg. Az ábrán az ATP-szenzitív aktivitás látható. wt: vad típus, K86M: katalitikus domén mutáns, negatív kontroll.

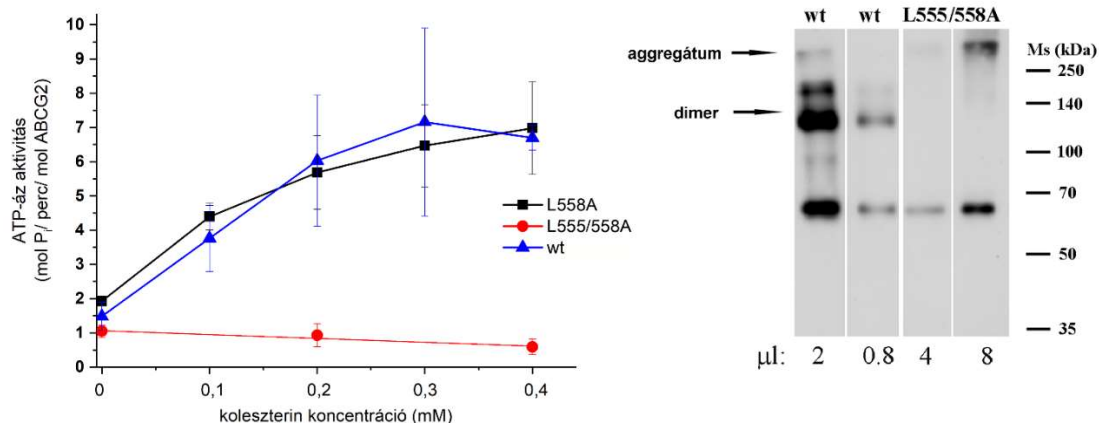
A sejtek, illetve a vezikulák koleszterinnel való feltöltéséhez 2mM koleszterin-RAMEB-et használtunk.

Érdekes módon, annak ellenére, hogy az L558A mutáns ATP-áz aktivitása a koleszterinnel nem töltött membránokban összevethető volt a vad típuséval, metotrexát és ösztradiol-17 β D-glükuronid transzport során nem csak az L555A és L555/558A mutánsok, hanem az L558A mutáns is inaktívnak bizonyult, transzport aktivitást még koleszterin-töltött vezikulákon sem tudtunk mérni (9. ábra). Mindezek arra utalnak, hogy a szubsztrátfelismerése (is) sérült ezeknek a mutánsoknak. Mivel azonban ezekben a kísérletekben a koleszterin hatását nem sikerült egyértelműen tisztázni, további kísérleteket végeztünk.

Mérések tisztított, rekonstituált proteoliposzómákon

Korábban az R482G mutánst vizsgálva észrevettük, hogy rovarsejtekben (alacsony koleszterin szintnél, 5-8 μ g koleszterin/mg membránfehérje) aktivitását koleszterin hozzáadásával nem lehet fokozni. Viszont, amikor a fehérjét tisztítottuk és jól definiált lipidösszetételű proteoliposzómákban rekonstituáltuk, azt tapasztaltuk, hogy az R482G változat koleszterinérzékelése a vad típushoz képest fokozott, már kis mennyiségű koleszterin is képes működését stimulálni (Telbisz et al. 2013).

Annak érdekében, hogy az LxxL mutánsok koleszterinérzékelését jól definiált membránkörnyezetben vizsgálhassuk, az L558A és L555/558A mutánsokat tisztítottuk és különböző koleszterintartalmú liposzómákban rekonstituáltuk. Amint azt a 10. ábra mutatja, az L558A variáns koleszterinérzékenysége nem tért el a vad típusétól. Az L555/558A dupla mutáns tisztításakor, azt csak kis mennyiségben sikerült előállítanunk, és függetlenül a koleszterin mennyiségtől, aktivitást sem tudtunk mérni. Mindennek magyarázata lehet a fehérje csökkent stabilitása és az ABCG2 működéséhez nélkülözhetetlen homodimer kialakulásának hiánya (10. ábra, Western blot).



10. ábra: ABCG2 expressziója és működése tisztított rekonstituált proteoliposzómákban. **ATP-áz aktivitás:** ATP-hidrolízis 1 mg/ml *E. coli* lipid extraktumban rekonstituált proteoliposzómákban hozzáadott szubsztrát nélkül, különböző mennyiségű koleszterin jelenlétében. **Western blot:** Az ABCG2 fehérje dimerként működik, amit egy intermolekuláris diszulfid híd stabilizál (lásd később). Western bloton, ahol az ABCG2-t a BXP-21 antitesttel mutattuk ki, ez a dimer látható. Az L555/558A dupla mutánsnál azonban a tisztítást és rekonstitúciót követően a dimert nem tudtuk detektálni. wt: vad típus

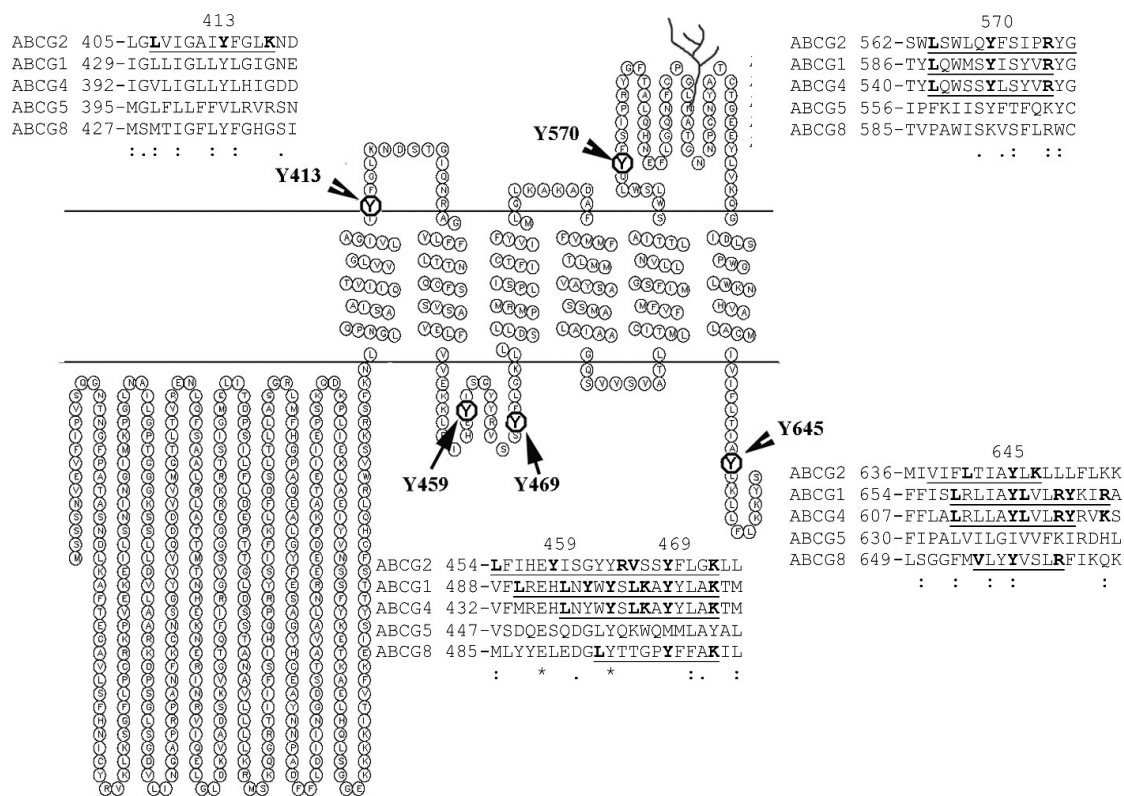
Mindezek alapján megállapítottuk, hogy az L555 és L558 fontos az ABCG2 fehérje szubsztrátfelismerésében, és e két leucin együttes mutációja csökkent aktivitást és valószínűleg a fehérje csökkent stabilitását okozza. Később, a térszerkezet ismeretében az általunk észlelt fenotípus változásokra sikerült magyarázatot találni. Ezt a Következtetések és kitekintés c. fejezetben írom le.

IV/A. 2.2. A CRAC motívum szerepe a koleszterinérzékelésben

Egyes, feltételezett CRAC motívumba eső tirozinok az ABCG2 stabilitását változtatják meg (Gál és mtsai, 2015, 3. sz. közlemény)

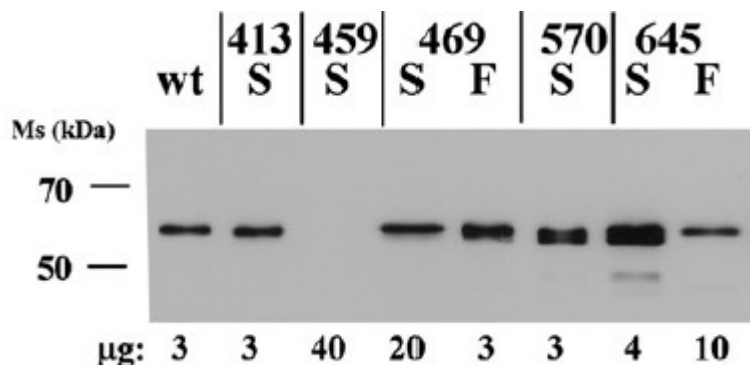
Az ún. “CRAC” (cholesterol recognition amino acid consensus) motívum, amelyet a következő mintázat jellemez: L/V-(x)₍₁₋₅₎-Y-(x)₍₁₋₅₎-R/K (x: tetszőleges, nem konzervált aminosav), számos koleszterint kötő fehérjében megtalálható (Lacapere and Papadopoulos

2003; Epanand 2008). A CRAC motívum egy igen „laza” szekvencia, nagy számban fordul elő az ABCG2 fehérjében is. Mivel azonban a koleszterin a sejtmembránban található, membrántopológia alapján a nem membránközeli régiókban lévő CRAC motívumokat kizártuk, mint a koleszterinnel közvetlen kölcsönhatásba eső régiók. Így öt lehetséges CRAC szekvenciát azonosítottunk (11. ábra). Fontos hangsúlyozni, hogy ez a mutagenézis munka, illetve a korábbi, az IV/A.1-2. fejezetben tárgyaltak az ABCG2 térszerkezetének meghatározása előtt készültek. Az azóta ismertté vált ABCG2 térszerkezet alapján a mutációk elhelyezkedését, és a kísérleteink alapján tett megállapításaink (új) értelmezését a Következtetések és kitekintés c. fejezetben tárgyalom.



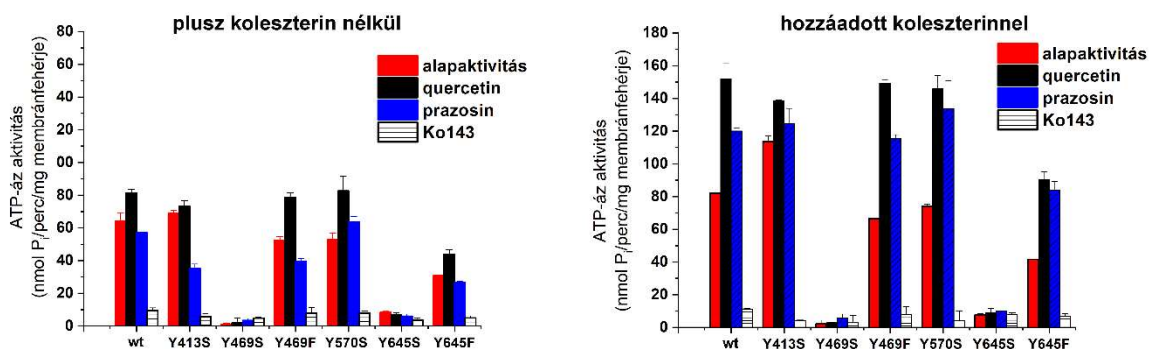
11. ábra: Az ABCG2 topológiája a CRAC motívumokkal. Az ábrán a lehetséges CRAC motívumok központi tirozinjait és a szélső, konzervált aminosavakat emeltem ki. Látható még az ábrán az N-glikozilációs hely. Az ABCG család tagjainak szekvenciáit a Clustalw programmal hasonlítottam össze (<https://www.ebi.ac.uk/Tools/msa/clustalw2/>). Az ABCG2 topológiáját* a CCTOP programmal határoztam meg (Tusnady and Simon 2001). *: a topológia becslés a térszerkezet meghatározása előtt készült

Mivel korábban igazolták, hogy a CRAC motívum központi Tyr-ja döntő szerepet játszik a koleszterin felismerésben (Martinez-Abundis et al. 2011; Epanand 2008), mi ezt cseréltük le Ser (és/vagy Phe)-re.



12. ábra: ABCG2 Tyr mutánsok expressziója Sf9 rovarsejtekben. Az Sf9 membránvezikulumokban az ABCG2-t Western blot és az ABCG2-specifikus BXP-21 antitest segítségével mutattuk ki. wt: vad típus

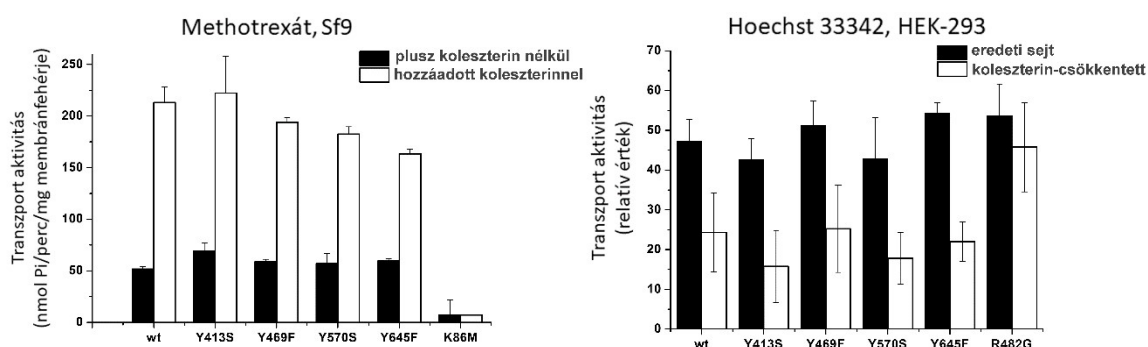
A Y459S mutáns kivételével mindegyik fehérje változatot sikerült expresszálnunk Sf9 rovarsejtekben (12. ábra). A Y469S és Y645S változatok aktivitása azonban a jól detektálható fehérjeexpresszió ellenére elveszett (14. ábra). Ezért a Y469F és Y645F változatokat is elkészítettük. Ezek a mutánsok, a Y413S és Y570S változatokhoz hasonlóan, már jól mérhető alap ATP-áz aktivitással rendelkeztek (13. ábra).



13. ábra CRAC Tyr mutánsok ATP-áz aktivitása Sf9 membránvezikulákban. Az ABCG2 mutánsok aktivitását Sf9 membránvezikulákon, hozzáadott koleszterin nélkül vagy 2 mM koleszterin-RAMEB kezelést követően mértük 1 μ M quercetin, 100 μ M prazosin vagy 1 μ M Ko143 jelenlétében vagy hiányában (alapaktivitás). Az ábra az ABCG2-specifikus, 2 mM Na-ortovanadát-szenzitív aktivitást mutatja. wt: vad típus

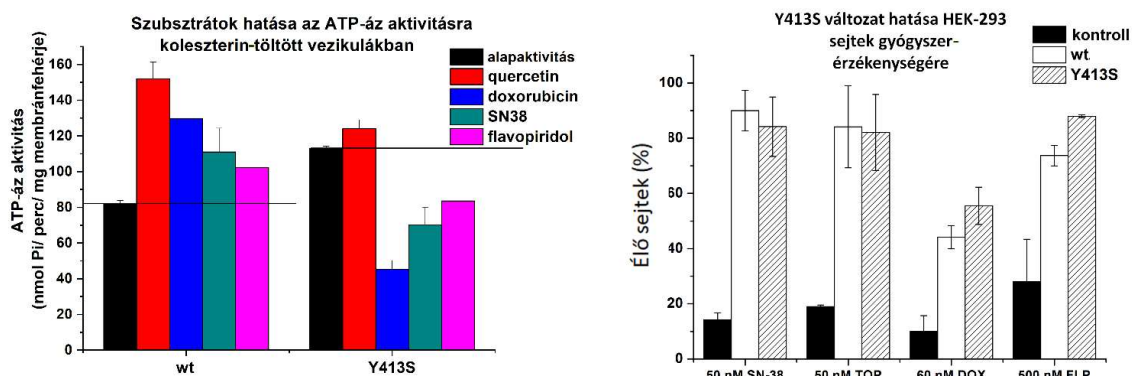
Az ATP-áz aktivitás mérések alapján a koleszterin-töltés, a vad típushoz hasonlóan, jelentősen fokozta a mutánsok aktivitását, az inaktív mutánsok (Y469S és Y645S) viszont hozzáadott koleszterin jelenlétében is inaktívnak bizonyultak.

Ezután a Tyr mutánsok transzport aktivitását mértük meg. A rovarsejteken végzett transzport kísérletekben mindegyik, aktív Tyr mutáns működését fokozta a koleszterin (14. ábra). Sőt, HEK-293 sejtvonalakon (40-60 μg koleszterin/mg membránfehérje), ahol a koleszterin depléció hatását tudtuk nézni, mindegyik aktív mutáns (és a vad típus) működése csökkent a sejtmembrán koleszterintartalmának csökkentésével (14. ábra).



14. ábra Metotrexát és Hoechst 33342 transzportja. A triciált metotrexát (50 μM) transzportját ABCG2-t termelő Sf9 sejtekből izolált membránvezikulákon mértük koleszterin-RAMEB jelenlétében, illetve a nélkül. Az ábrán az ATP-szenzitív aktivitás látható. A Hoechst 33342 (2 μM) transzportját HEK-293 sejteken vizsgáltuk „üres” RAMEB-bel történt koleszterin deplécióval, illetve a nélkül (eredeti sejt). A Ko-143 inhibitor-szenzitív aktivitást ábrázoltam (bővebben Módszerek fejezet). wt: vad típus, K86M: katalitikus domén mutáns, negatív kontroll.

A vad típushoz képest eltérő működést egyedül a Y413S változatnál tapasztaltunk. E mutánsnál a koleszterin-töltés jelentősen (mintegy kétszeresére) fokozta az alap (hozzáadott szubsztrát nélkül mért) ATP-áz aktivitást (13. ábra), amit a szubsztrátok nem, vagy csak kevésbé stimuláltak a vad típushoz képest, vagy csökkentettek (15. ábra). Azonban, citotoxicitási mérések alapján megállapítottuk, hogy ez a mutáns is hatékonyan transzportálja a vizsgált citosztatikumokat (doxorubicin, topotecan, SN-38 és flavopiridol) és védi az őt kifejező sejteket (15. ábra). Szubsztrátfelismerése tehát nem tér el jelentősen a vad típusétól.



15. ábra Y431S mutáns szubsztrátfelismerésének vizsgálata. Bal oldali panel: Az ATP-áz aktivitás méréseket 2mM koleszterin-RAMEB-bel töltött, ABCG2-t tartalmazó Sf9 membránvezikulákon végeztük, 5 μ M quercetin, 50 μ M doxorubicin (DOX), 20 μ M SN-38 (kamptotecin analóg) vagy 50 μ M flavopiridol (FLP) jelenlétében, illetve a nélkül. A 2 mM Na-ortovanadát-szenzitív komponenst ábrázoltam.

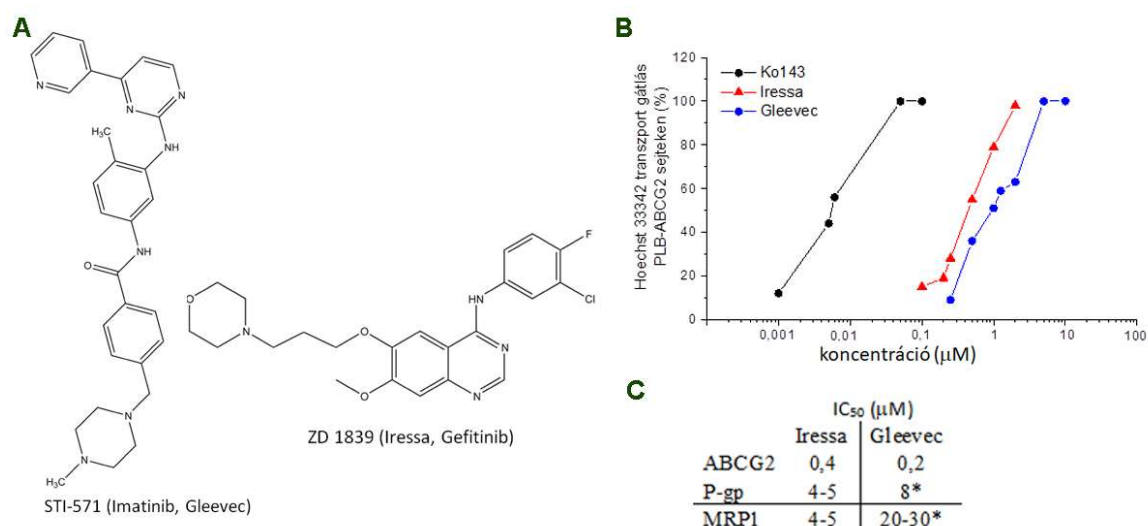
Jobb oldali panel: ABCG2-t termelő HEK-293 sejtek túlélése 72 órás SN-38, topotecan (TOP), doxorubicin vagy flavopiridol kezelést követően. Kontroll: „üres” vektorral transzfektált, ABCG2-t nem overexpresszáló HEK-293 sejt. wt: vad típus.

Az ABCG2 izolált membránvezikulumokban mutatott magas alap ATP-áz aktivitásának oka még nem pontosan tisztázott, endogén szubsztrát jelenléte vagy „szétkapcsolt” (transzport aktivitástól függetlenített) működés állhat a háttérben. Ráadásul, igazoltan transzportálódó szubsztrátok (például a Hoechst 33342 festék) is képesek azt gátolni/csökkenteni. Hasonlóan, az Y413S alap ATP-áz aktivitását csökkentették ugyan a vizsgált citosztatikumok, azonban a citotoxicitás mérések alapján szubsztrátjai e mutáns fehérjének (is). Érdekes módon az Y413S változat alap ATP-áz aktivitását jelentősen fokozta a koleszterin, azonban Tarling és munkatársai (Tarling and Edwards 2011) eredményei alapján az ABCG2, ellentétben az ABCG1 fehérjével, nem képes koleszterint transzportálni. Így azt gondoljuk, hogy a Y413 a koleszterinérzékelésben fontos, oly módon, hogy a fehérje transzport és ATP hidrolizáló működésének (részleges) szétkapcsolását eredményezi.

IV/A.3. Az ABCG2 és tirozin kináz gátlók közötti kölcsönhatás vizsgálata

A Gefitinib és Iressa az ABCG2 hatékony gátlói (Özvegy-Laczkó és mtsai, 2004, Özvegy-Laczkó és mtsai, 2005, 4-5. sz. közlemények)

A tirozin kinázok (TK) megváltozott működése a sejtek malignus átalakulásához vezethet. A tirozin kinázokra ható specifikus gátlók (TKI-k, tirozin kináz inhibitorok) fejlesztése áttörést jelentett a tumoros betegek kezelésében. Azóta is több rák típus (például krónikus mieloid leukémia, nem kissejtes tüdőrák vagy emlőrák) kezelésében használnak TKI-kat elsővonalas vagy kiegészítő terápiaként (Jiao et al. 2018). Azonban, a TKI-k alkalmazásakor is felléphet rezisztencia, amit okozhat a multispecifikus ABC-k, a P-gp vagy az ABCG2 fehérje jelenléte. Amikor e munka készült, több TKI-ról is tudtuk, hogy azok a P-gp szubsztrátjai, azonban az ABCG2 szerepéről a TKI-k felismerésében még kevés adat állt rendelkezésre, jelen munka ezért úttörőnek számított. Munkám során a Gleevec/Imatinib (krónikus mieloid leukémiában alkalmazott Bcr-Abl kináz gátló, az első, az FDA által jóváhagyott TKI (Jiao et al. 2018)) és az Iressa/Gefitinib (nem-kissejtes tüdőrákban szenvedő betegek kezelésére használt EGFR gátló) gyógyszereket teszteltem membránvezikula-alapú, illetve sejtes módszerekkel (16. ábra).



16. ábra: A Gleevec és Iressa az ABCG2 hatékony inhibitorai. A) A vizsgált vegyületek szerkezete. B) Hoechst 33342 festék felvétel gátlása PLB-ABCG2 sejteken. C) Iressa és Gleevec kölcsönhatása ABC gyógyszertranszporterekkel. Az IC₅₀ értékeket ABCG2

Hoechst 33342 transzport gátlás, illetve P-gp-t vagy MRP1-t termelő sejteken (HL60-MDR1 és HL-60-MRP1 (Hollo et al. 1996)) mért calcein-AM transzport gátlás alapján határoztuk meg.

**: korábban a kutatócsoportban mért adatok alapján (Hegedus et al. 2002)*

Elsőként mutattuk ki, hogy az Iressa és Gleevec az ABCG2 hatékony gátlószerei, és ez a gátlás minimum egy nagyságrenddel felülmúlja a vizsgált TKI-k P-gp és MRP1 fehérjéket gátló affinitását. Eredményeink alapján a TKI-k befolyásolhatják az ABC szubsztrátok farmakokinetikáját, és az ABCG2 működését gátolva növelhetik a tumorok gyógyszerérzékenységét. Ugyanakkor alacsony koncentrációban az Iressa fokozta az ABCG2 ATP-áz aktivitását, ami arra utal, hogy transzportálódó szubsztrátja a fehérjének, az ABCG2 tehát a tumorokat rezisztenssé teheti az Iressával szemben.

A TKI-k és ABC fehérjék kapcsolatának vizsgálata azóta is intenzíven kutatott terület (a 4.sz. közleményem 2021. 09. 17-i állapot szerint 281 független idézést kapott). Mi magunk is több irányban folytattuk ezt a kutatást, amelyet a Következtetések és kitekintés című fejezetben mutatok be.

IV/A.4. Egy ABCG2-specifikus antitest jellemzése

Az ABCG2 fehérje érzékeny kimutatása több területen is fontos, például

- 1.) az őssejtek vizsgálatában, amelyeknek az ABCG2 az egyik markere (Krishnamurthy et al. 2004; Scharenberg, Harkey, and Torok-Storb 2002),
- 2.) az ABCG2-t kifejező tumorok azonosításában, ami a megfelelő terápia megválasztását segítheti, illetve
- 3.) ABCG2 polimorfizmusok érzékeny, vérből történő gyors kimutatására (Kasza et al. 2012).

2001-ben Sorrentino és munkatársai előállították az első, és eddig egyetlen olyan antitestet (5D3), amely az ABCG2-t az intakt sejtek felszínén ismeri fel (Zhou et al. 2001). Kutatómunkám során jelentős felismeréseket tettem az ABCG2 és az 5D3 antitest közötti

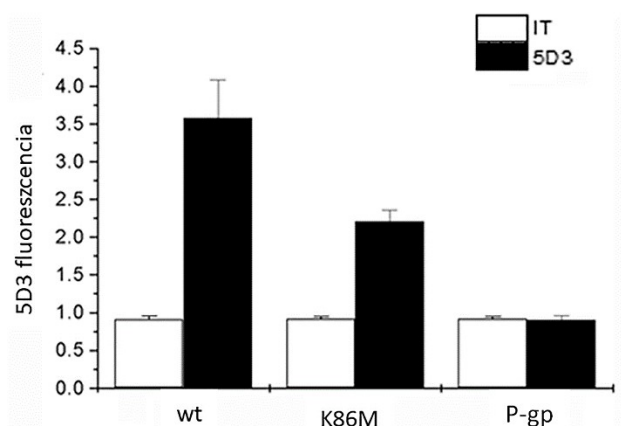
kölcsönhatás mechanizmusának megismerésében. Ezeket az eredményeket a következő két fejezetben foglalom össze, kitérve arra is, hogy eredményeim az 5D3 antitest milyen további alkalmazási területeit nyitották meg.

IV/A.4.1. Gátlószerek és nukleotid analógok hatása az 5D3 kötődésére

*Az 5D3 egy konformáció-szenzitív antitest
(Özvegy-Laczka és mtsai, 2005, 6. sz. közlemény)*

Az 5D3 antitest kötődését többféle, ABCG2-t termelő sejtvonalon jellemeztük, és megvizsgáltuk, hogy különböző inhibitorok és szubsztrátok hogyan befolyásolják azt. Azt tapasztaltuk, hogy az ABCG2 működésének gátlása a Ko143 inhibitorral jelentősen fokozza az antitest kötődést, míg a Na-ortovanadát (Vi) csökkenti azt (Ozvegy-Laczka, Varady, et al. 2005). Ez arra utal, hogy a két gátlószert eltérő ABCG2 konformációt eredményez, ami az 5D3 kötődését befolyásolja. A Ko143 az ABCG2 specifikus, nagy affinitású inhibitora (Allen et al. 2002). A Vi általános ATP-áz inhibitor, amely az ATP hidrolízis során keletkező foszfát helyét elfoglalva rögzíti az ATP-áz fehérjét egy átmeneti, nukleotid csapdázott állapotban (Ozvegy, Varadi, and Sarkadi 2002).

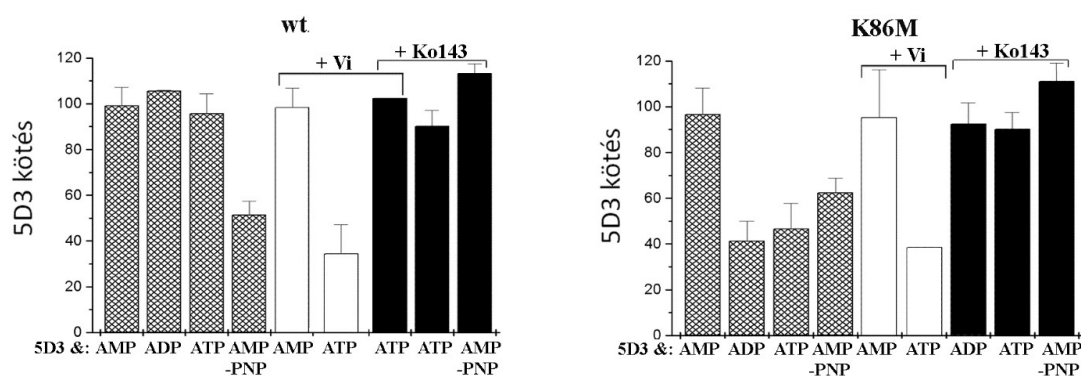
Mivel a két inhibitor eltérően befolyásolta az 5D3 kötődését, további vizsgálatokban annak jártunk utána, hogyan változik az 5D3 kötődése az ATP hidrolízis során.



17. ábra: Az 5D3 antitest kötődésének vizsgálata ABCG2 fehérjét termelő Sf9 rovarsejtekből izolált membránpreparátumokon. Az ABCG2 fehérjét (wt és K86M) vagy a negatív kontroll P-glikoproteint tartalmazó rovarsejt membránpreparátumokat 5D3 antitesttel (1 µg/ml) vagy izotípus kontrollal (IT) és fluoreszcensen jelölt másodlagos

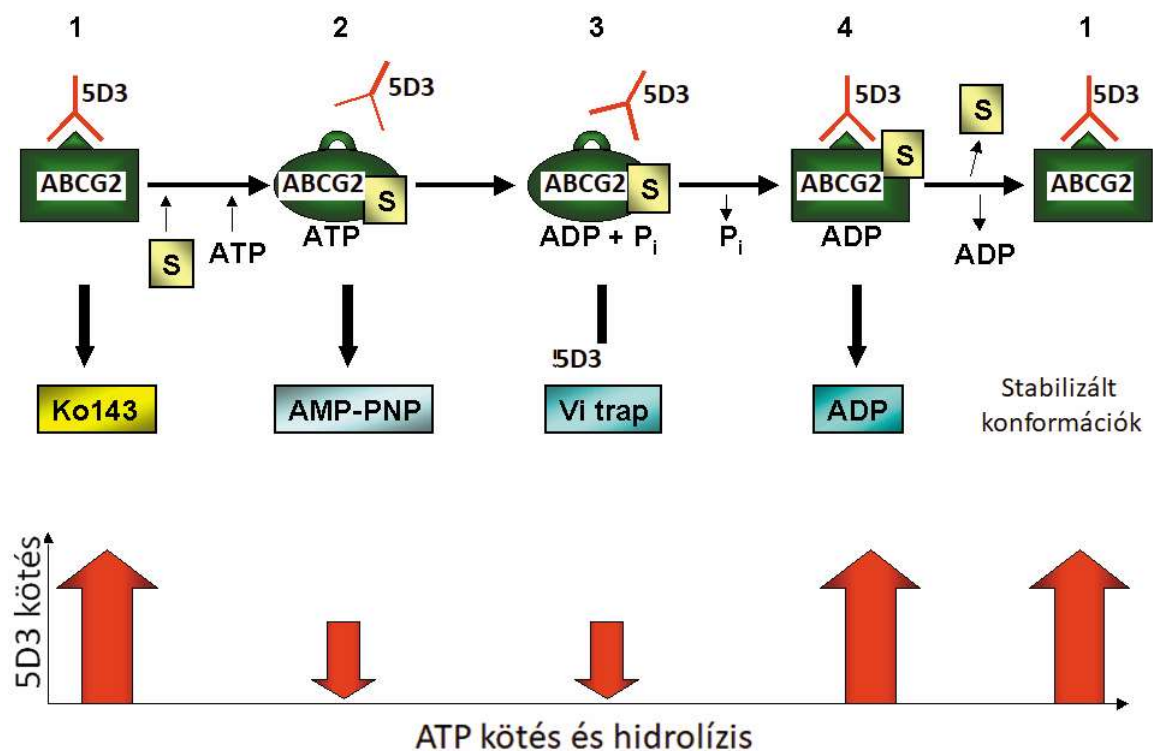
antitesttel inkubáltuk, majd az antitest kötődést fluoreszcencia mérés alapján határoztuk meg. wt: vad típusú ABCG2, K86M: ATP hidrolízisre nem képes mutáns, P-gp: P-glikoprotein.

Ezekben a kísérletekben rovarsejtekből izolált membránpreparátumokat alkalmaztunk, amely az ép sejtes vizsgálatokhoz hasonlóan, lehetővé teszi az 5D3 kötés vizsgálatát (17. ábra), ugyanakkor az ép sejtes mérésekkel szemben előnye, hogy a fehérje intracelluláris régióihoz kötődő ligandumok hatása is vizsgálható. A membránpreparátumok segítségével jellemeztük különböző nukleotid analógok hatását az 5D3 kötődésére (18. ábra).



18. ábra: Az 5D3 antitest kötődésének vizsgálata Sf9-ABCG2 membránvezikulákon. A rovarsejt membránpreparátumokat 5D3 antitesttel (1 µg/ml) inkubáltuk. K86M: ATP hidrolízisre nem képes mutáns. A Na-ortovanadátot (Vi, 2mM), Ko143 inhibitort (1 µM), illetve a nukleotidokat 10 mM-os koncentrációban alkalmaztuk önmagukban vagy kombinációban. wt: vad típus.

A fenti eredmények alapján az alábbi modellt hoztuk létre:



19. ábra: Az ABCG2 egyes konformációs állapotainak és az 5D3 antitest kötődés kapcsolata

Nukleotidmentes állapotban, illetve a hidrolizálható ATP jelenlétében az 5D3 epitópja jól hozzáférhető. Amennyiben egy kötődő, de nem hidrolizálható analógot, AMP-PNP adunk a rendszerhez, vagy megakasztjuk az ATP hidrolízist annak köztes állapotában (a Vi belép a felszabaduló P_i helyére és „csapdázza” az ADP-t) az 5D3 kötődése csökken. Kontroll kísérletekben, az ATP hidrolízisben akadályozott K86M katalitikus domén mutánszt vizsgáltuk. Azt tapasztaltuk, hogy a K86M mutánsnál a Vi 5D3 kötődést fokozó hatása elmarad, viszont azt az ATP és ADP is csökkentette, jelezve, hogy ezekkel a nukleotidokkal a K86M mutáns kapcsolatba lép (18. ábra).

Ezután többféle, igazolt ABCG2 szubsztrát hatását is megvizsgáltuk. Azt tapasztaltuk, hogy alacsony koncentrációban adva a szubsztrátok nem befolyásolták az 5D3 kötődést, míg magasabb, már gátló koncentrációban a flavopiridol fokozta azt (lásd részletesen (Ozvegy-Laczka, Varady, et al. 2005)). Később egy önálló tanulmányban, amelyben

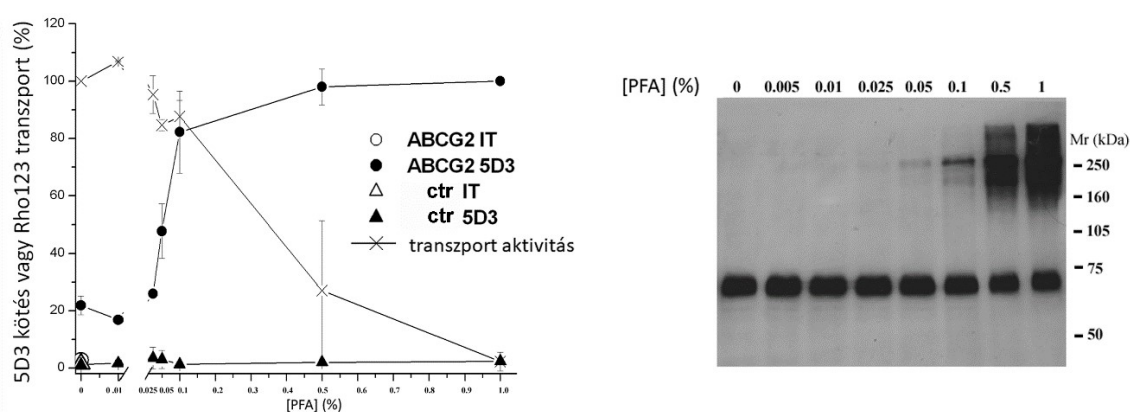
társszerzőként vettem részt, kimutattuk, hogy az 5D3 kötődés vizsgálata alkalmas arra, hogy a transzportáló szubsztrátokat és inhibitorokat elkülönítsük egymástól és erre alapozva egy új vizsgálati módszert hoztunk létre (Telbisz et al. 2012).

IV/A 4.2. Az 5D3 antitest kötődéséhez nem szükséges a kovalens ABCG2 dimer megléte

*Az 5D3 antitest epitópja az ABCG2 monomeren,
a 3. külső, intramolekuláris diszulfid híddal
rögzített hurokban található (Özvegy-Laczka és
mtsai, 2008, 7. sz. közlemény)*

Az ABCG2 homodimerként működik. A két ABCG2-t egy diszulfid híd kovalensen rögzíti a homodimerben, azonban ez nem szükséges a fehérje működéséhez (saját vizsgálataink (Özvegy-Laczka et al. 2008) és (Henriksen et al. 2005)). A két ABCG2-t összekötő intermolekuláris S-S hídon kívül létezik egy, a fehérje nagy, extracelluláris hurkát rögzítő, intramolekuláris S-S híd is. Mivel az 5D3 antitest epitópja nem volt ismert, nem tudhattuk, hogy azt a két ABCG2 közösen hozza-e létre. Ennek eldöntése érdekében különböző fehérje keresztkötők és ABCG2 mutánsok vizsgálatával jellemeztük az 5D3 kötődését.

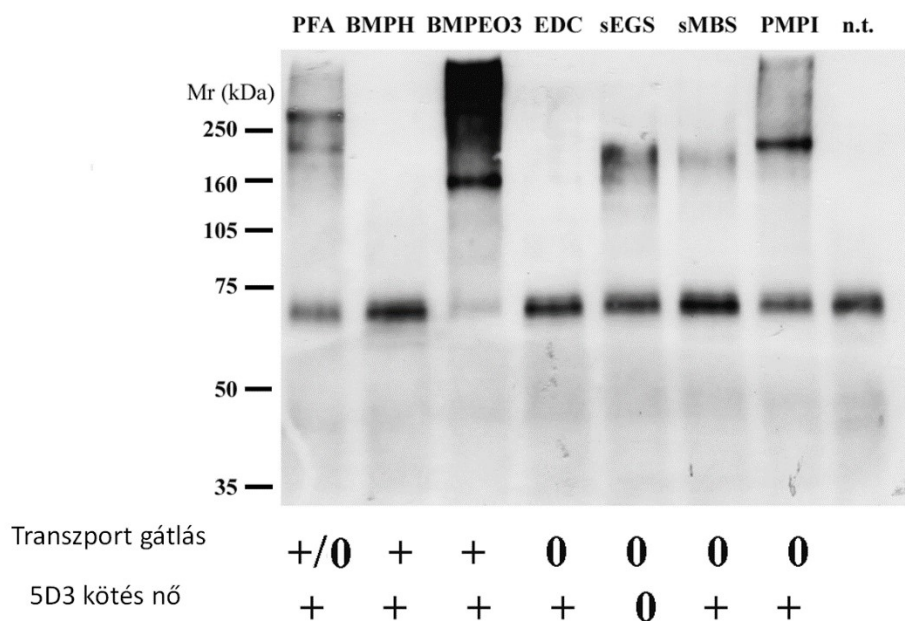
Először a formaldehid hatását vizsgáltuk egyszerre követve az ABCG2 működőképességét, az 5D3 kötődését és a kovalens ABCG2 dimerek kialakulását (20. ábra).



20. ábra: Formaldehid hatása az ABCG2 működésére és az 5D3 antitest kötődésére. Bal oldali panel: HEK-ABCG2-R482G sejteket kezeltünk növekvő koncentrációjú formaldehiddel (PFA), majd mosást követően mértük az 5D3 antitest kötődését, illetve a rhodamine 123 festék transzportját. Az 5D3 kötődést az 1 % PFA jelenlétében mért

fluoreszcens jel %-ában ábrázoltuk. A transzport aktivitást (2 μ M rhodamine 123 transzport) a referencia inhibitor (1 μ M Ko143) jelenlétében mért fluoreszcenciához viszonyítottuk. Ctr: ABCG2-t nem termelő („üres” pCIN4 vektorral transzfektált) HEK-293 sejt. IT: izotípus kontroll (egér IgG2b). **Jobb oldali panel:** ABCG2 kimutatása Western blot és a BXP-21 antitest segítségével növekvő mennyiségű PFA-val kezelt HEK-ABCG2-R482 sejtekben.

Azt tapasztaltuk, hogy már alacsony, az ABCG2 dimer keresztlinketését még nem eredményező formaldehid koncentráció is maximális 5D3 kötődést eredményez. Ez arra utalt, hogy a kovalens dimer megléte nem szükséges az 5D3 kötődéshez. Ennek további vizsgálatához többféle, nem sejt permeábilis keresztlinkető ágenst is megvizsgáltunk. Elemeztük azok hatását a kovalens dimer kialakulására, a fehérje funkciójára és az 5D3 kötődésre (21. ábra).

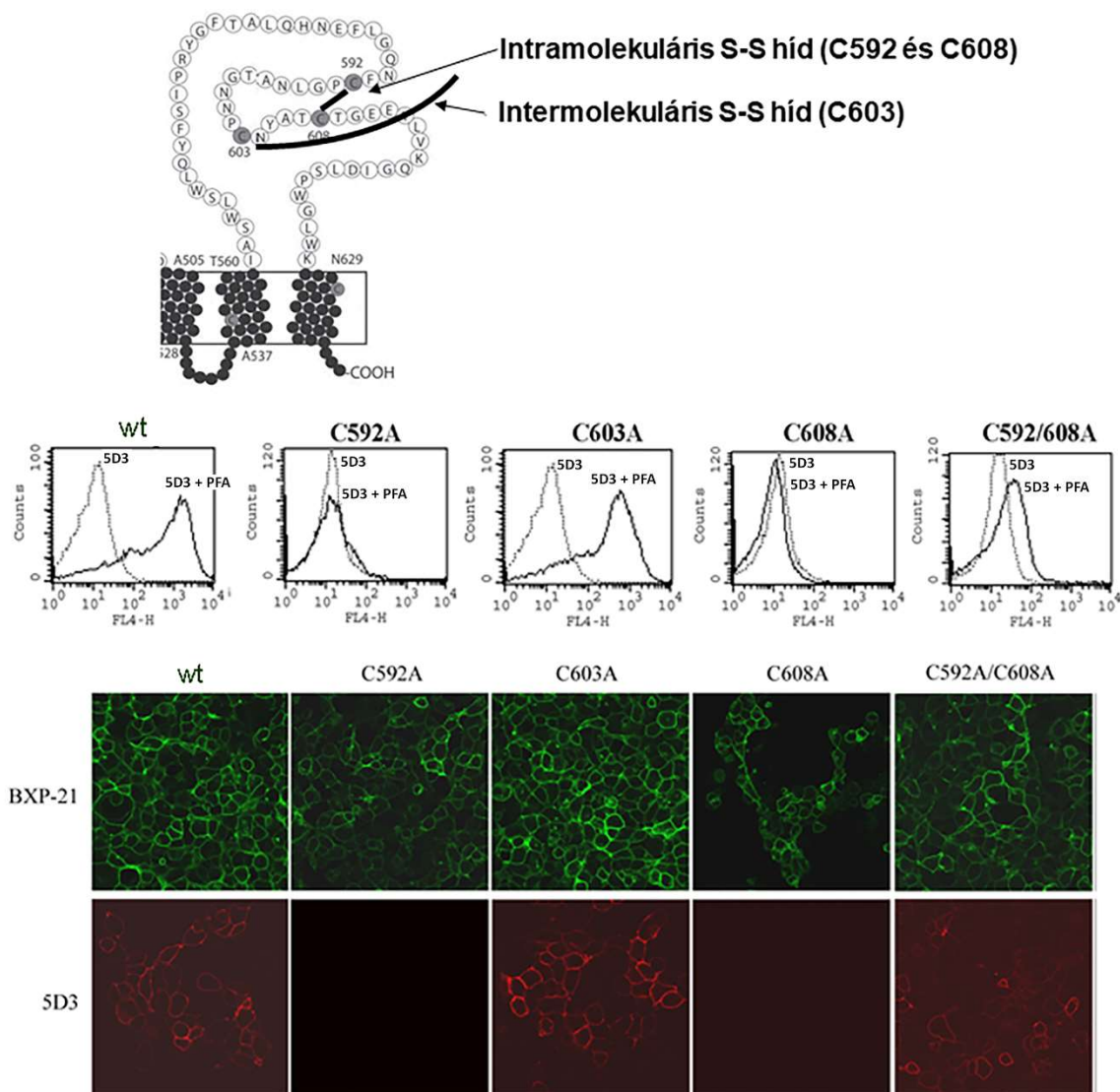


21. ábra: Fehérje keresztlinketők hatása az ABCG2 működésére, az 5D3 antitest kötődésére és az ABCG2 kovalens dimerjének kialakulására. HEK-ABCG2-R482G sejteket inkubáltunk inhibitorral (5 μ M FTC, Fumitremorgin C, ABCG2 gátlószer) vagy a keresztlinketőkkel: 0,5 mM BM[PEO]3, 1,8-bis-maleimidotriethyleneglycol; 1 mM BMPH, N-[1,8-bis-maleimidopropionic acid]hydrazide, trifluoroacetic acid salt; 2 mM EDC, [1-ethyl-3-(3-dimethylaminopropyl)carbodiimide hydrochloride]; 1 mM PMPI, N-(p-maleimidophenyl)isocyanate; 2 mM sEGS: sulfo-EGS, ethylene glycol bis(sulfosuccinimidyl succinate); 2 mM sMBS: sulfo-MBS, m-maleimidobenzoyl-N-hydroxysuccinimide ester. Ezt követően a sejteket 5D3 antitesttel vagy rhodamine123

festékkel inkubáltuk, és a fluoreszcenciát áramlási citométerben detektáltuk. A kovalens ABCG2 dimer megjelenését Western blot (BXP-21 antitest) segítségével vizsgáltuk. n.t.: kezeletlen kontroll. 0: nincs változás. +: 5D3 kötődés nő vagy az ABCG2 aktivitás gátolt.

Amint azt a 21. ábra mutatja, két ABCG2 kovalens keresztkötése nem szükséges, de nem is elegendő az 5D3 kötődéséhez és/vagy a transzport funkció gátlásához. Mindezek a kísérletek azt mutatták, hogy az ABCG2 monomeren lévő epitóp rögzítése az, ami elősegíti az 5D3 kötődését.

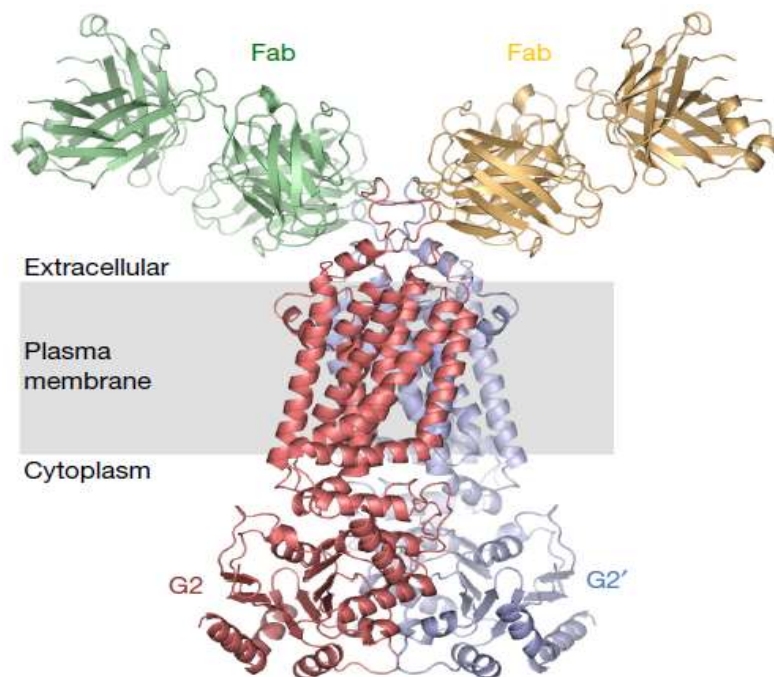
Az ABCG2 fehérjében a két ABCG2 kovalens összekapcsolódásáért a C603-t felelős, illetve az ABCG2 fehérjére (és az ABCG alcsaládra) jellemző nagy extracelluláris hurokban megtalálható másik 2 Cys pedig intramolekuláris diszulfid hidat hoz létre. Annak érdekében, hogy eldöntsük, vajon ezek szerepelnek-e az 5D3 epitóp kialakításában, ezeket a ciszteineket cseréltük ki Ala-ra. A mutánsokat jellemeztük expresszió, funkció és 5D3 kötődés szempontjából (22. ábra).



22. ábra: A 3. extracelluláris hurokban található Cys-ek szerepe az 5D3 epitóp kialakításában. Felső ábra: A vizsgált Cys-ek elhelyezkedése és a közöttük kialakuló diszulfid hidak. Középső panel: 5D3 kötődés formaldehid fixált és natív (nem fixált) ABCG2-t kifejező HEK-293 sejteken áramlási citometriával meghatározva. Alsó panel: HEK-ABCG2 sejtek jelölése BXP-21 (nem konformáció-szenzitív, egy intracelluláris epitópot felismerő ABCG2-specifikus) antitesttel vagy 5D3 antitesttel. A BXP-21 jelölést megelőzően a sejteket permeabilizáltuk (4% PFA és metanol). Az 5D3 jelölésnél 1% PFA-val fixáltuk a sejteket. A képek Olympus FV500-IX konfokális lézerpásztazó mikroszkóppal készültek.

Mindezek, és az itt nem bemutatott (de a 7. sz. (Ozvegy-Laczkó et al. 2008) közleményben megtalálható), az 5D3 Fab fragmentjével végzett vizsgálatok alapján megállapítottuk, hogy az 5D3 epitóp az ABCG2 monomeren található, valószínűleg a 3. nagy extracelluláris

hurokban helyezkedik el, és azt a C592 és C608 között kialakuló diszulfid híd stabilizálja. Később ezt az ABCG2 térszerkezete alapján, ahol az 5D3 antitestet használták, hogy a fehérjét egy adott konformációban rögzítsék, megerősítették (Taylor et al. 2017) (és 23. ábra).



23. ábra: Az ABCG2 fehérje 5D3 Fab által rögzített szerkezete. A kép forrása (Taylor et al. 2017).

IV/B. A humán Organikus Anion Transzporter Polipeptidek vizsgálata: új módszerek, új gyógyszerkölsönhatások és mechanizmus kutatás

Az **Organikus Anion Transzporter Polipeptidek (OATP)** az emberi sejtek membránjában jelen lévő szerves ion cserélők ("exchangerek"). Működésük az epesó-, bilirubin- és hormonháztartás fenntartásában fontos. Emellett a 11 tagot számláló OATP fehérjecsalád több multispecifikus tagja meghatározó szereplője az ADME-Tox folyamatoknak. Megváltozott működésük nem várt mellékhatásokat eredményezhet, ezért ezen multispecifikus OATP-k vizsgálatát a gyógyszerfejlesztés során nemzetközi szervezetek írják elő. Ezen kívül a tumorokban kifejeződő OATP-k a rákterápia lehetséges célpontjai.

Az általam 2013-ban megkezdett és azóta vezetett kutatás fő célja olyan érzékeny és költséghatékony vizsgálati módszerek fejlesztése volt, amelyek az OATP-k gyógyszerkölsönhatásainak, azaz szubsztrátjaik és inhibitoraik egyszerű felderítését, működésük, illetve tumorokban betöltött szerepük megértését segítik. A létrehozott módszerek segítségével felismeréseket tettünk az OATP-k működéséről és új molekula entitások és az OATP-k közötti kölsönhatásokat mutattunk ki. A következő fejezetekben a kutatócsoportom által a fenti témakörökben elért saját eredményeit mutatom be.

IV/B. 1. Az OATP-k vizsgálatára alkalmas új fluoreszcens módszerek kidolgozása

IV/B.1.1. OATP-k vizsgálata rovarsejtekben, egy általános OATP szubsztrát azonosítása

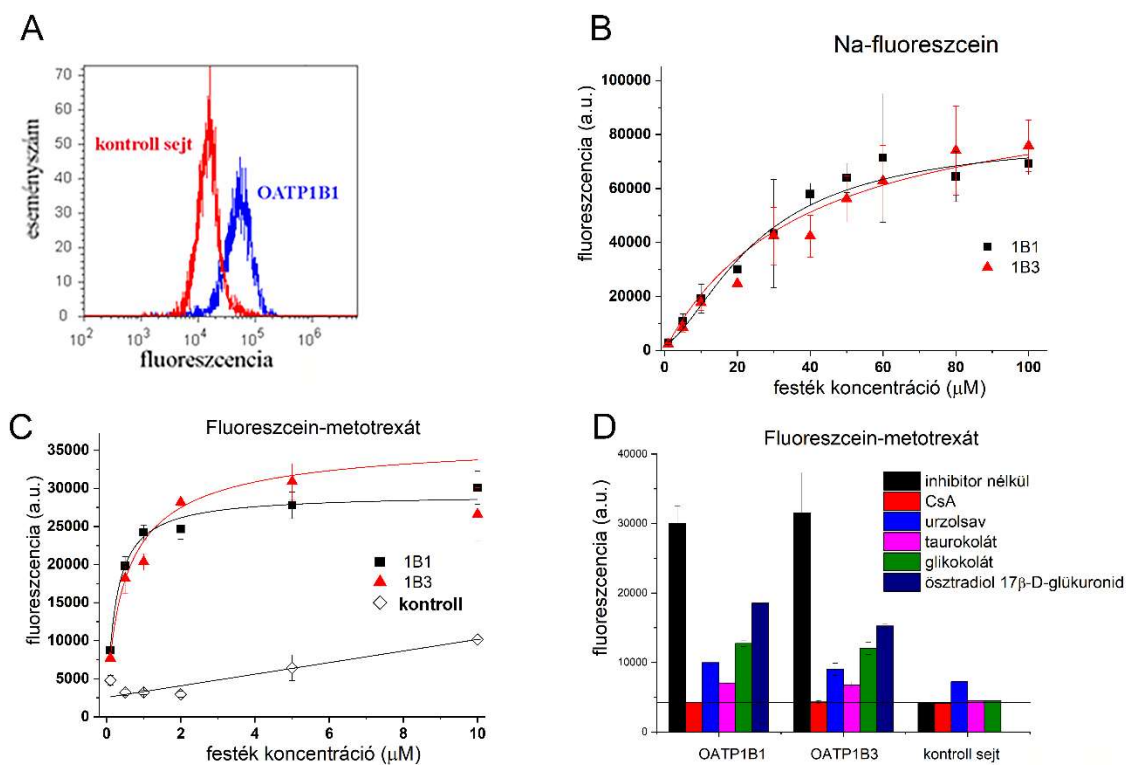
A humán OATP-k rovarsejtekben működőképes formában termeltethetők és Na-fluoreszcinnel vizsgálhatók (Patik és mtsai, 2015, 8. sz. közlemény)

A kutatómunkánk egyik fő célkitűzése olyan fluoreszcencia-alapú módszer(ek) fejlesztése volt, amely(ek) alkalmas(ak) az OATP-k vizsgálatára. Ilyen módszer a kutatás

megkezdésekor csak a májspecifikus OATP1B1 és OATP1B3 fehérjékre volt elérhető, de ezek a korábbi módszerek (legalábbis az OATP1B1 fehérjénél) nem feleltek meg a nagy áteresztőképességű tesztelés (high-throughput screening, HTS) követelményeinek (Gui et al. 2010).

Az OATP-kel kapcsolatos kutatásunk kezdeti lépéseként olyan sejtes modellt terveztünk létrehozni, amelynek segítségével az OATP fehérjecsalád összes tagjának a tesztelése ugyanazon sejtes háttér mellett lehetséges. A rovarsejt rendszer előnye, hogy általában nagy mennyiségben lehet a segítségével humán membránfehérjéket előállítani, és szemben a bakteriális vagy élesztő alapú expressziós rendszerekkel, a termeltetett plazmamembrán fehérje a rovarsejtekben a megfelelő membránba lokalizálódik és működőképes. Az általunk alkalmazott bakulovírus alapú rendszer hátránya viszont, hogy a sejtek a fertőzés következtében pár napon belül pusztulni kezdenek, tehát csak tranziens expresszió érhető el, így az ép sejtes mérések kihívást jelentenek. Az ABCG2 fehérjével kapcsolatos kutatásaim során viszont felfedeztem, hogy a megfelelő „időablakot” megtalálva, amikor a bakulovírus fertőzött sejtek jelentős százalékának sejtmembránja még ép, ezeknek a sejteknek egy fluoreszcens marker (például propidium-jodid) alapján áramlási citometriával történő elkülönítése lehetővé teszi az ép, élő sejteken történő méréseket. Ezt alkalmaztuk az OATP-k vizsgálatánál is.

Először a rovarsejt rendszer OATP-k vizsgálatára való alkalmasságát az eddig legrészletesebben vizsgált OATP1B1 és OATP1B3 fehérjék jellemzésével kezdtük. A Na-fluoresceint és a fluorescein-metotrexátot korábban leírták, mint OATP1B1/3 szubsztrátok (Gui et al. 2010; De Bruyn et al. 2011). Áramlási citometria segítségével jellemeztük tehát ezek felvételét az OATP1B1 vagy OATP1B3 fehérjéket termelő rovarsejtekben. Amint az a 24. ábrán látható, tipikus, transzporter-mediált festékfelvételt mértünk a rovarsejt rendszerben, amit a korábban leírt, az OATP-kel kölcsönható vegyületek gátoltak, megerősítve, hogy a festékek valóban az OATP1B1/3 működése által dúsulnak a sejtekben.

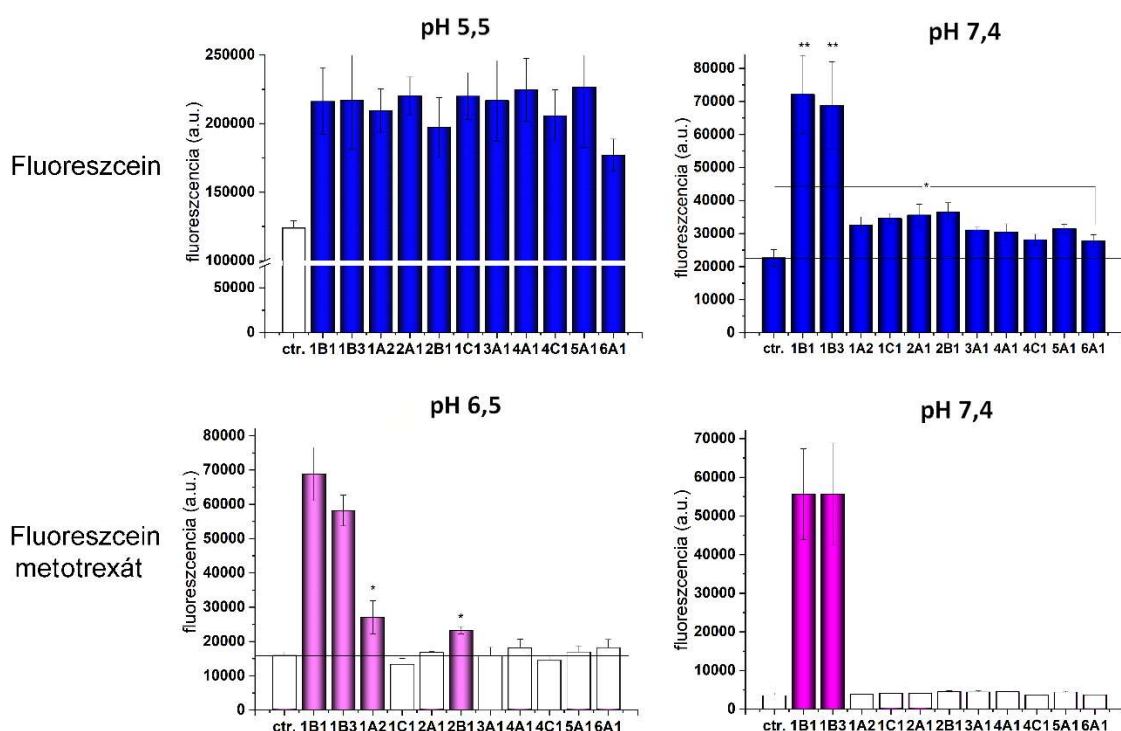


24. ábra: OATP1B1 és OATP1B3 vizsgálata Sf9 rovarsejtekben. *A) fluoreszcein-metotrexát (1 μM) felvétele kontroll és OATP1B1-et kifejező sejtekben. B) Na-fluoreszcein 1 μM felvétele. A kontroll sejtekben mért értékeket levontuk és a különbséget ábráztoltuk. C) fluoreszcein-metotrexát felvétele. D) 1 μM fluoreszcein-metotrexát felvételének gátlása. CsA: cyclosporin A (20 μM), urzolsav (20 μM), taurokolát és glikokolát (150 μM), ösztradiol-17β-D-glükuronid (50 μM). A kísérletek pH 7,4-en történtek. Kontroll: OATP-t nem termelő, bakulovírussal fertőzött Sf9 sejt A fluoreszcenciát áramlási citométerben határoztuk meg.*

Ezután létrehoztuk a többi humán OATP termelésére is alkalmas bakulovírust, és ellenőriztük a fehérjék expresszióját (Patik és mtsai., 2015).

A transzporterek működését kétféle, savas és semleges pH-n is vizsgáltuk, mivel korábban számos közleményben kimutatták, hogy az OATP-k működését a savas extracelluláris milió fokozza (Leuthold et al. 2009). Az OATP-k overexpressziója minden esetben fokozott Na-fluoreszcein felvételt eredményezett, és magasabb aktivitást mértünk savas (pH 5.5) pufferben, beleértve a kontrollként használt OATP1B1 és OATP1B3 fehérjéket is (25. ábra). A fluoreszcein-metotrexát festékkel az OATP1B1/3-n kívül az OATP1A2 és OATP2B1 fehérjéket kifejező rovarsejtekben mértünk aktivitást, de ez utóbbi kettő esetében

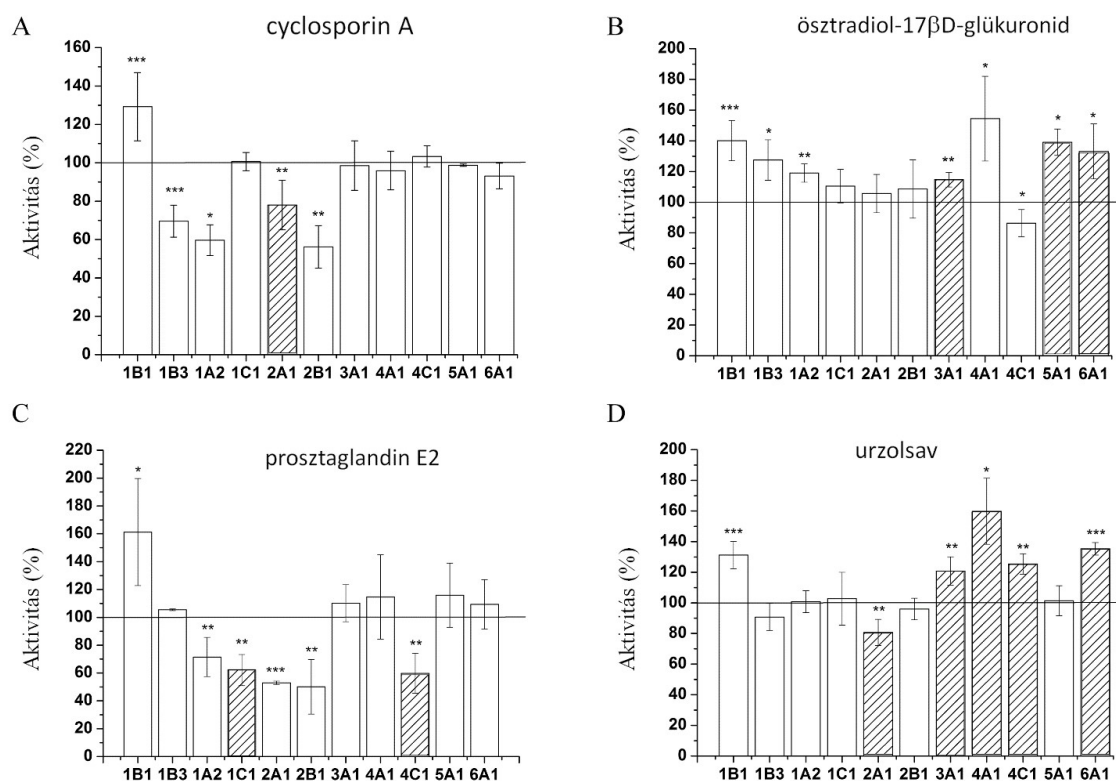
funkció csak savas pH-n (pH 6.5) volt detektálható (27. ábra). Ezek alapján megállapítottuk, hogy a rovarsejt rendszer és az általános OATP szubsztrátként azonosított Na-fluoreszcein alkalmas a teljes humán OATP család vizsgálatára. A fluoreszcein-metotrexátot pedig új OATP1A2 és OATP2B1 szubsztrátként azonosítottuk.



25. ábra: Fluoreszcens festék-felvétel Sf9 sejtekben termeltetett humán OATP-ken. A festékeket 1 μ M koncentrációban alkalmaztuk, a tarszport puffer pH-ját az ábra mutatja. Ctr: OATP-t nem kódoló bakulovírussal fertőzött Sf9 sejt. A festékek fluoreszcenciáját áramlási citométerrel határoztuk meg.

Az OATP-k általi transzport pH-függése ismert jelenség, amely függhet egyrészt a szubsztrát töltöttségétől, másrészt a konzervált His protonálódásától (erről bővebben írtam Az OATP-k transzport mechanizmusa c. fejezetben). A fluoreszcein tartalmaz egy karboxil és egy fenol csoportot, amelyek ionizálódhatnak. pH 6,4 és pH 5 között a monoanion forma van jelen, míg pH 6,4 felett a dianion. Méréseink során a monoanion forma esetében detektáltunk nagyobb jel intenzitást, de részletes kinetikai mérések hiányában (az OATP1B1 és OATP1B3 kivételével a K_m és V_{max} értékek nem kerültek meghatározásra) azt nem lehet eldönteni, hogy ez affinitásbeli vagy transzport kapacitásbeli különbséget jelent-e.

Végezetül, az új „rendszer” próbájaként néhány, korábban valamelyik OATP-vel kölcsönható vegyületet teszteltünk (26. ábra).



26. ábra: Na-fluorescein transzport vizsgálata Sf9 sejtekben termeltetett OATP-ken. A bakulovírus fertőzött sejteket 1 μM Na-fluoresceinnel inkubáltuk potenciális OATP inhibitorok jelenlétében: 20 μM cyclosporin A, 50 μM ösztradiol 17-β-D-glükuronid, 5 μM prosztaglandin E2 or 20 μM urzolsav vagy a nélkül. A fluoreszcenciát áramlási citométerben mértük. Az aktivitást a kontroll (OATP-t nem termelő) Sf9 sejtekben mért fluoreszcenciát levonva határoztuk meg és az inhibitor nélkül mért értékhez viszonyítva ábrázoltuk. A csíkozott oszlopok az új, eddig nem azonosított kölcsönhatásokat mutatják.

OATP-specifikus transzport esetén azt várjuk, hogy az ismert inhibitor gátolni fogja a transzportot. Néhány vegyületnél azonban nem gátlást, hanem fokozást mértünk (például cyclosporin A az OATP1B1 működését, vagy az urzolsav több OATP-ét fokozta) (28. ábra). Ezt a jelenséget korábban mások is megfigyelték (Grube et al. 2006; Gui et al. 2010; Gui et al. 2008). Magyarázata lehet allosztérikus modulálás vagy a két vegyület együttes

transzportja (Bakos, Tusnady, et al. 2020). Méréseink alapján ezek a festékek alkalmasak lehetnek indikátorként az OATP-vel kölcsönható molekulák azonosítására/tesztelésére.

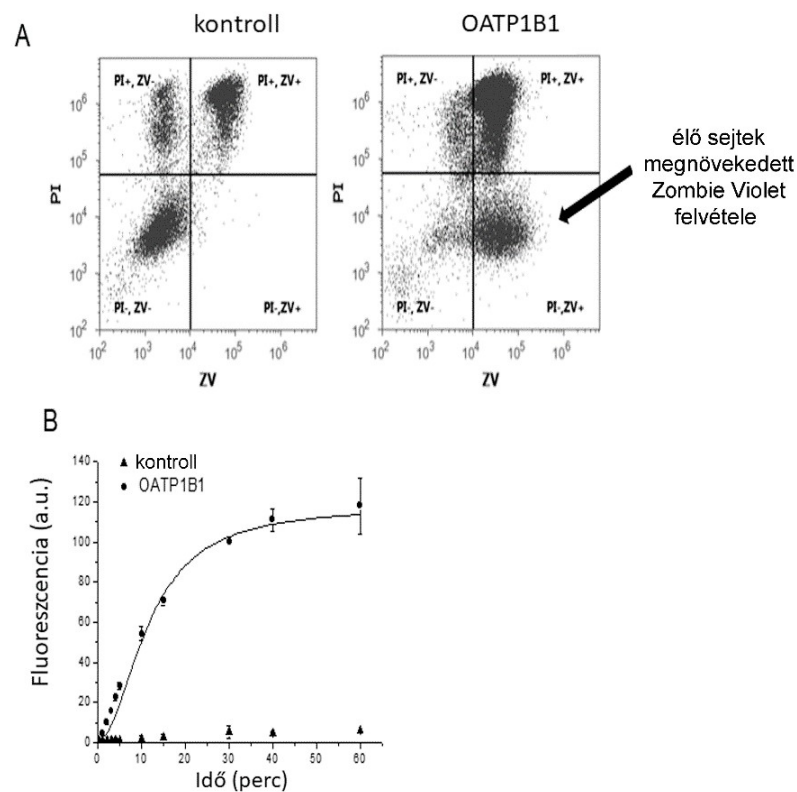
IV/B. 1.2. Multispecifikus OATP-ket kifejező humán sejtes modellek létrehozása és új fluoreszcencia-alapú vizsgálati módszerek kidolgozása

Fluoreszcens viabilitási festékek egy csoportja alkalmas a hepatikus OATP-k kiválogatására és működésének vizsgálatára (Patik és mtsai, 2018, 9. sz. közlemény)

Annak ellenére, hogy a rovarsejt rendszer alkalmasnak bizonyult a teljes humán OATP család vizsgálatára, közepes áteresztőképességű funkcionális mérések kidolgozása is a célunk volt, hiszen molekulakönyvtárak tesztelésénél ez elengedhetetlen. Erre azonban a fent ismertetett tranziens expressziós rendszer nem alkalmas (például, mert az expresszió kísérletről kísérletre változhat és többnapos előkészület szükséges egy mérés előtt). Ezért az OATP fehérjéket stabilan kifejező emlős sejtvonalakat hoztunk létre és további, az OATP-k által esetlegesen felismert, de a fluoreszcenciánál kedvezőbb tulajdonságú (alacsony passzív sejtbeli felvétel, esetleg pH-független fluoreszcencia) fluoreszcens molekulákat teszteltünk.

Modell sejtneként az adherens, humán epidermális karcinóma sejtvonalat, A431 választottuk, mivel korábban számos ABC transzporternél magas expressziót tudtunk elérni ezekben a sejtekben, továbbá ezek a sejtek a sejtenyészítő flakóhoz erősen letapadnak, ami a tervezett mikrolemez alapú mérésekhez, a szükséges mosási lépések miatt, elengedhetetlen. A humán OATP-ket overexpresszáló sejtvonalak létrehozásánál azonban azt tapasztaltuk, hogy nem minden OATP-t tudtunk nagy mennyiségben termeltetni, és az expresszió a sejt kultúrában az idő előrehaladtával csökkent. Ezt a jelenséget már mások is leírták, és bár pontos okát még nem sikerült megfejtetni, azt valószínűsítik, hogy az OATP-k túlműködése miatt a sejtek metabolizmusa felborul (Cesar-Razquin et al. 2015). A stabilan magas expressziót azonban végül több OATP-re is sikerült elérnünk (lásd IV/B.1.2.1. fejezet).

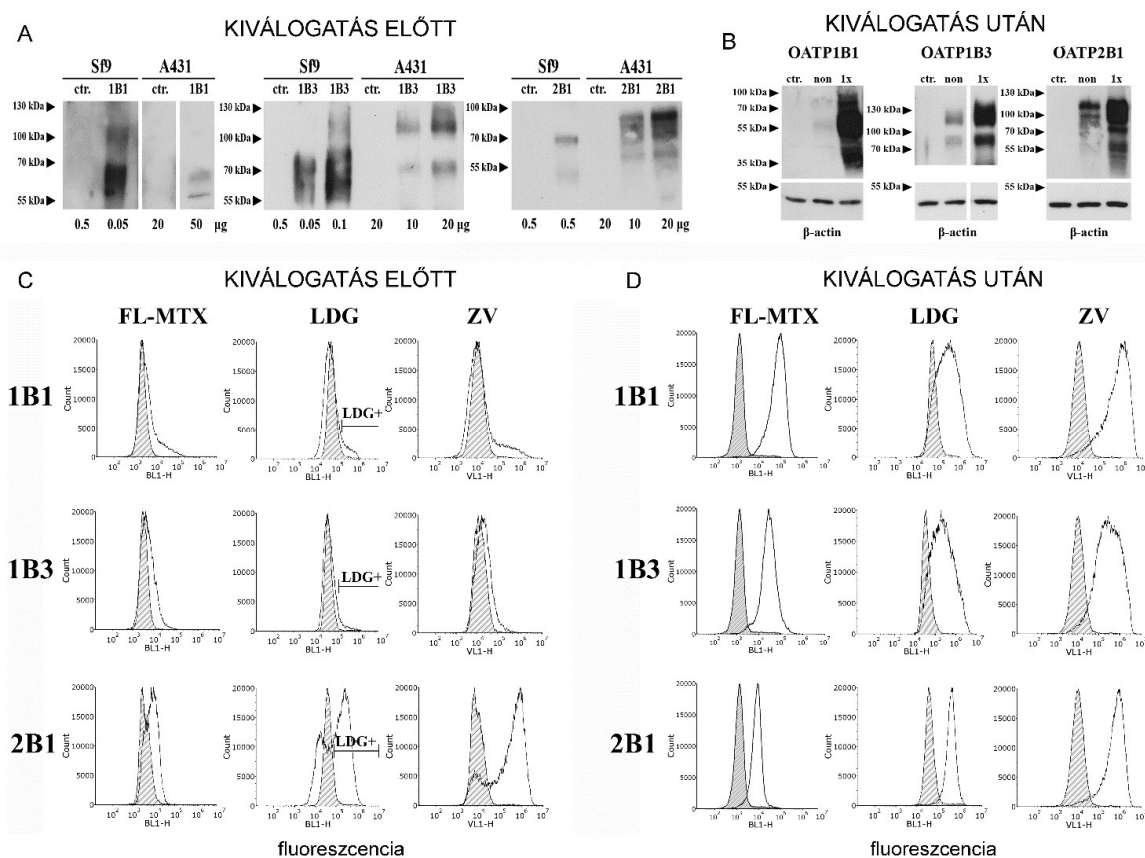
Nem sejtporózható szubsztrátokat keresve, első körben olyan vegyületeket válogattunk ki, amelyek, szemben a Na-fluoresceinnel, alacsony passzív sejtbeli felvételt mutatnak. Így esett a választásunk olyan életképesség (viabilitás) mérésére fejlesztett festékekre, amelyek az élő sejtek plazmamembránján passzívan nem tudnak átjutni. A felfedezés onnan eredt, hogy jelentős Zombie Violet (ZV) viabilitási festék felhalmozódást tapasztaltunk az OATP, 1B1, 1B3 és 2B1 fehérjéket termelő, de a szintén a viabilitási markerként használt propidium-jodid negatív (ép plazmamembránú) sejtekben, ami arra utalt, hogy a ZV festéket ezek az OATP-k transzportálhatják (27. ábra).



27. ábra: ZombieViolet viabilitási festék felvétele OATP1B1 termelő sejtekben. A) A kontroll és OATP1B1 termelő Sf9 sejteket ZombieViolet (ZV) festékkel inkubáltuk (pH 5.5). Az átjárható plazmamembránú sejteket propidium-jodid (PI, 1 µg/ml) festéssel különítettük el. **B)** Zombie Violet időfüggő felvétele kontroll és OATP1B1 termelő Sf9 sejtekben. A fluoreszcenciát áramlási citometriával határoztuk meg.

IV/B. 1.2.1. OATP-ket termelő sejtek kiválogatása festékvétel alapján

A viabilitási festékek (és kontrollként a fluoreszcein-metotrexát) felvételét tehát először a multispecifikus, a gyógyszerek transzportjában bizonyítottan részt vevő OATP-k, 1A2, 1B1, 1B3 és 2B1 fehérjéket termelő A431 sejteken teszteltük. Azonban, az OATP2B1 kivételével, csak alacsony festékvételt tudtunk kimutatni, ami nem meglepő, figyelembe véve a rovarsejtekhez képest lényegesen alacsonyabb OATP expressziót az A431 (és az itt nem bemutatott HEK-293) emlős sejtekben (28. ábra).



28. ábra: Fluoreszcens festékek felvétele és az OATP expresszió nyomon követése A431 sejtekben. A, B) Western blot OATP1B1-, OATP1B3- vagy OATP2B1-termelő Sf9 és A431 sejteken. Teljes sejtizátumokat analizáltunk az adott OATP-re specifikus antitesttel. C, D) fluoreszcens festékek felvétele A431 sejtekben Live/Dead Green (LDG) viabilitási festékkel történt kiválogatás előtt és után. Az A431 sejteket Zombie Violet (ZV), fluoreszcein-metotrexát (FL-MTX) vagy LDG festékkel inkubáltuk, pH 5,5 pufferben. Az OATP-t nem overexpresszáló sejteket a telt hisztogramok ábrázolják. A fluoreszcenciát áramlási citométerben detektáltuk.

Korábbi tapasztalataink alapján a vizsgálni kívánt transzportert termelő sejtek működésük alapján kiválogathatók például fluoreszcens szubsztrát felvétele alapján és áramlási citometria segítségével. Az ABCG2 fehérjénél például a Hoechst 33342 festéket használtuk korábban a sejtek kiválogatására (itt az ABCG2 működése a festék kipumpálását okozza, és a Hoechst 33342 festékre negatív sejteket eredményez). Miután megállapítottuk, hogy a ZV és Live/Dead Green (LDG) viabilitási festékek nem toxikusak az A431 (és az itt nem bemutatott HEK-293, illetve MDCKII) sejtek számára, elképzelésünk az volt, hogy kihasználva a festékek fokozott felhalmozódását az OATP-t tartalmazó sejtekben, azok kiválogathatók lesznek. Amint azt a 28. ábra mutatja, az LDG festék segítségével valóban sikerült az OATP 1B1, 1B3 és 2B1 fehérjéket kifejező sejteket dúsítani (és az OATP1A2, OATP1C1 fehérjéket is, lásd (Bakos, Nemet, et al. 2020)). Az így létrehozott OATP-ket termelő A431 sejtekben az OATP-k működését fluoreszcein-metotrexát (FL-MTX), ZV és LDG festékek felvétele alapján teszteltük. A kiválogatott sejtek megnövekedett OATP expressziót és funkciót mutattak, amely a sejteket mintegy 8 hétig tenyésztésben tartva is megmaradt.

IV/B.1.2.2. Hepatociták OATP-inek vizsgálata

Az így létrehozott modell sejteken ezután további viabilitási festékeket teszteltünk (4. táblázat) és az előzőekben bemutatott ZV és LDG festékeken kívül további festékszubsztrátokat azonosítottunk.

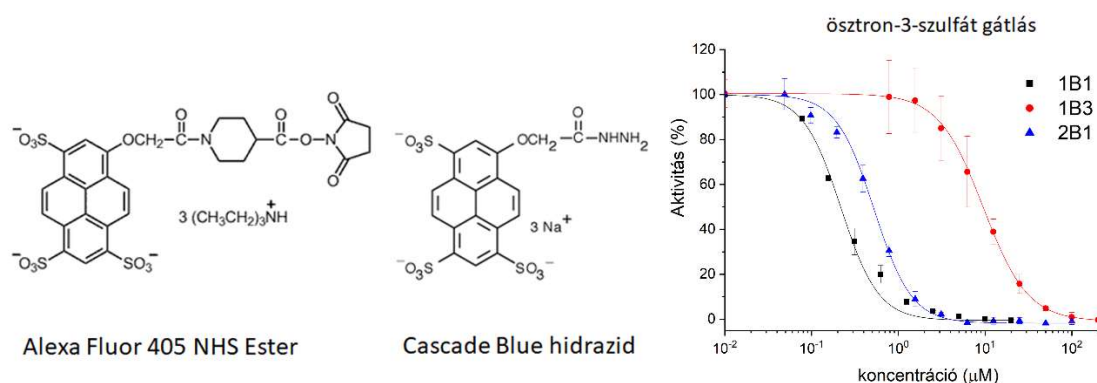
4. táblázat: Hepatociták OATP-inek festékszubsztrátjai

Forgalmazó	Festék fantázianeve	Ex/Em optimum (nm)	Transzport A431 sejteken
BioLegend	Zombie Green	488/515	-
	Zombie Violet	405/423	OATP1B1, OATP1B3, OATP2B1
Thermo Fisher (Life Technologies)	Live/Dead Blue	350/450	gyenge OATP1B1, OATP1B3, OATP2B1
	Live/Dead Aqua	367/526	-
	Live/Dead Violet	416/451	OATP1B1, OATP1B3, OATP2B1
	Live/Dead Yellow	400/575	-
	Live/Dead Green	495/520	OATP1B1, OATP1B3, OATP2B1
	Live/Dead Red	595/615	-
	Live/Dead Far-red	650/665	-
	Live/Dead near-IR	750/775	-
	Alexa Fluor 405 NHS Ester	401/421	OATP1B1, OATP1B3, OATP2B1
	Cascade Blue Hydrazide	400/419	OATP1B1, OATP1B3, OATP2B1

A festéktranszportot OATP-ket kifejező és kontroll A431 sejtekben teszteltük. Ex/Em: a méréskor használt, optimális excitációs és emissziós hullámhossz. -: nincs OATP-specifikus festékfelvétel.

Az új festékszubsztrátok máj OATP-specifikus transzportját a festékfelvétel kinetikájának, OATP-specifikus inhibitorral való gátolhatóságának vizsgálatával igazoltuk és jellemeztük (lásd bővebben a Patik és mtsai, 2018, 9. sz. csatolt közleményben).

Azonban a gyártók megkeresésünk ellenére sem tették hozzáférhetővé a viabilitási festékek képletét és koncentrációját, így megbízható, reprodukálható módszert ezekre a festékekre, hiába „szerepeltek” kiválóan a méréseinkben, nem alapozhattunk. Ezért, a membrán impermeabilitás és hasonló fluoreszcencia spektrum alapján további, ismert képletű vegyületeket kerestünk. Így választottuk ki a Cascade Blue hidrazid és Alexa Fluor 405 (AF405) festékeket (29. ábra).



29. ábra: Szulfopirén alapú OATP szubsztrát festékek és az azok használatán alapuló módszer.

CascadeBlue (OATP1B1, OATP2B1) vagy AF405 (OATP1B3) festékek felvétele OATP-ket kifejező és kontroll A431 sejteken 96-lyukú lemezen mérve ismert OATP szubsztrát, ösztrom-3-szulfát jelenlétében. A festékfelvétel mérése fluoreszcens lemezolvasó segítségével történt. Az új festékszubsztrátok indikátorként használva alkalmasak OATP-kel kölcsönható vegyületek azonosítására.

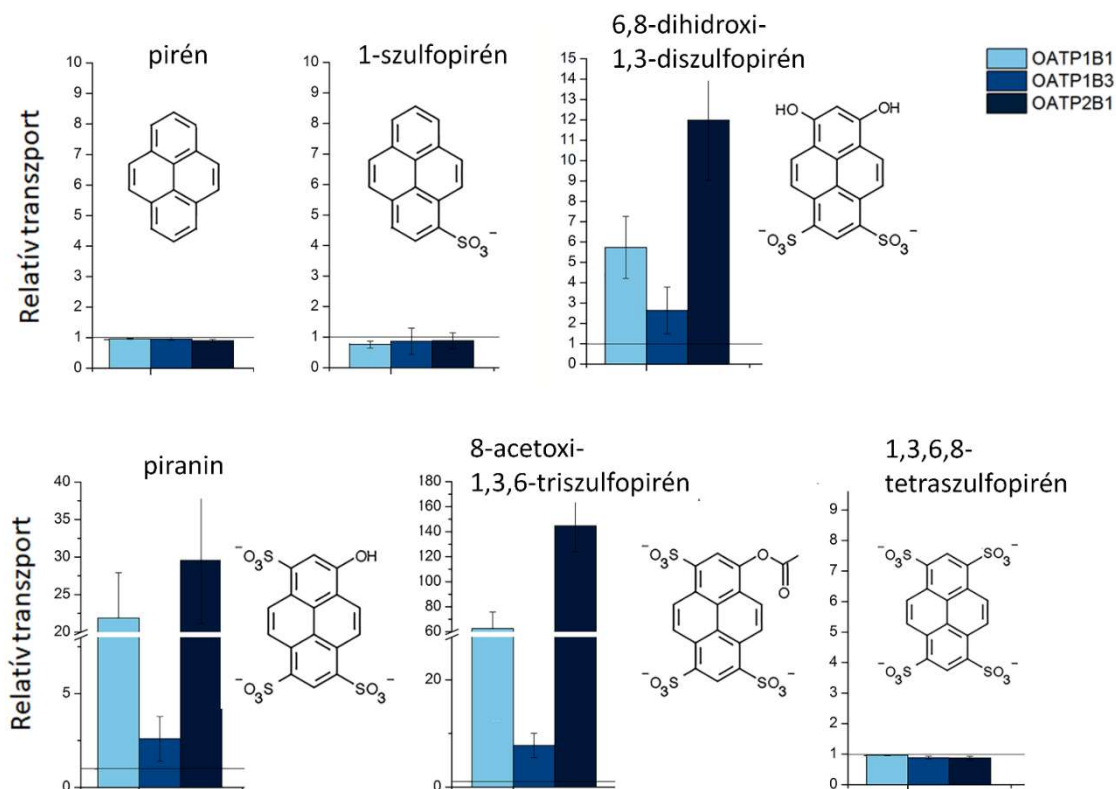
Ezek transzportját részletesen jellemeztük, az OATP-ket (1B1, 1B3 vagy 2B1) stabilan kifejező A431 sejt vonalak segítségével, és a módszert 96-lyukú lemezre adaptáltuk. Ennek lényege, hogy kis térfogatban, kevés anyagigénnyel és félig automatizálva kivitelezhető a mérés, tehát alkalmas OATP fehérjékkel kölcsönható molekulák közepes

áteresztőképességű tesztelésére. Megállapítottuk, hogy a HTS követelményeknek megfelelő jel-zaj arány és reprodukálhatóság jellemzi a CascadeBlue és AF405 festékfelvételt (z-faktor $> 0,5$ (Zhang, Chung, and Oldenburg 1999), lásd a konkrét értékeket a Patik és mtsai, 2018, 9.sz. közleményben), és máj OATP (1B1, 1B3, 2B1) szubsztrát/inhibitor kölcsönhatás tesztelésre alkalmas (Patik et al. 2018) (29. ábra).

Az általunk kidolgozott fluoreszcencia-alapú módszer volt az első mikrolemezre adaptált módszer az OATP2B1 fehérjére. Habár mások korábban kidolgoztak hasonló módszert az OATP1B1/3 fehérjékre, a mi teszrendszerünk ezeket felülmúlta megbízhatóság (z-faktor) terén, ami egyrészt a kiválogatott/dúsított sejtvonalaink magas OATP expressziójának, másrészt az új szubsztrátok kedvező tulajdonságainak köszönhető.

E munka folytatásaként, a Cascade Blue olcsóbb alternatíváját keresve azonosítottuk a piranint, mint megbízható hepatikus OATP szubsztrátot (lásd bővebben a Székely és mtsai, 2020, 12. sz. közleményben).

Mivel a Cascade Blue, AF405 és piranin egyaránt szulfonált pirén származékok, ezért, annak érdekében, hogy eldöntsük, mely szerkezeti elemek fontosak ezek OATP-k általi felismerésében, további pirénvázis vegyületeket is teszteltünk (30. ábra).



30. ábra: Pirénavázis festékek transzportja A431-OATP sejteken. A festékek (20 μM , pH 5.5) transzportját OATP1B1, OATP1B3 vagy OATP2B1-et kifejező (és kontroll) A431 sejteken teszteltük. A kontroll sejtekben mért fluoreszcencia értékekhez (=1) viszonyított aktivitást ábrázoltam.

A pirénavázis vegyületek transzportját a hepatocelluláris OATP-eket kifejező A431 sejteken teszteltük. A 6,8-dihidroxi-1,3-piréndiszulfonátot és a piranin 8-acetoxi változatát (8-acetoxi-1,3,6-triszulfopirén) új OATP szubsztrátként azonosítottuk. Megállapítottuk, hogy minimum 2, de maximum 3 szulfonát csoport kell az OATP1B1, OATP1B3 és OATP2B1 általi felismeréshez (Ungvári és mtsai, 2021, 10. sz. közlemény).

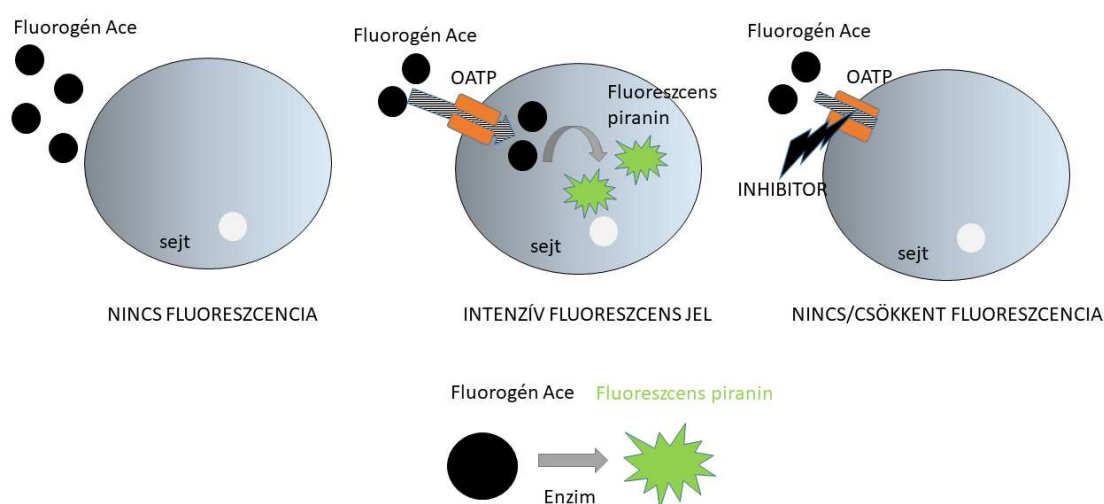
IV/B.1.2.3 Az első fluoreszcencia-alapú „add-és-mérd” módszer multispecifikus OATP-k vizsgálatára

Az acetoxi-pirandin alkalmas a hepatocelluláris OATP-k működésének és inhibitor kölcsönhatásainak valós idejű nyomonkövetésére (Ungvári és mtsai., 2021, 10. sz. közlemény) és PCT/HU2020/050062

A kutatócsoportomban létrehozott sejtes modellek és mikrolemez alapú mérések lehetővé teszik a máj OATP-k és lehetséges szubsztrátjaik vagy inhibitoraik közepes áteresztőképességű azonosítását. Egy nagy áteresztőképességű módszer kidolgozásához azonban egy olyan szubsztrát lenne ideális, amelynek sejten kívüli és sejten belüli állapota, például eltérő fluoreszcencia intenzitásuk vagy spektrumuk miatt, elkülönül. Mintegy 25 évvel ezelőtt Sarkadi Balázs és munkatársai az ABC gyógyszertranszporterekre (P-gp és MRP-k) ilyen szubsztrátot már azonosítottak (Hollo et al. 1996; Hollo et al. 1994). A fluoreszcens Ca^{2+} indikátor calcein festék nem fluoreszkáló (fluorogén) acetoximetil analógját (CAM) viabilitási festékként alkalmazzák, mivel a fluorogén CAM bejut a sejtekbe és az élő sejtek észterázai fluoreszcens calceinné alakítják. Így a sejtek életképessége fluoreszcenciájuk alapján mérhető. Azonban, Sarkadi és mtsai. felfedezése alapján, a calcein és/vagy CAM P-gp és MRP1/2 szubsztrátok, az ezeket az ABC fehérjéket kifejező sejtekből a festék kiáramlik, és azok nem fluoreszkálnak. A P-gp vagy MRP transzporterek gátlószereinek hatására viszont a sejtek ismét „világítani” fognak. Ezzel a módszerrel a P-gp és MRP-k működése és szubsztrát/inhibitor interakciói a festék kimosása nélkül, valós időben és akár nagy áteresztőképességgel követhetők (Glavinas et al. 2011). Munkánk során az OATP szubsztrátok fluorogén analógját kerestük, olyan céllal, hogy a CAM módszerhez hasonló, az OATP-k működésének valós idejű mérésére alkalmas szubsztrátot találjunk (a CAM passzív felvétele miatt nem alkalmas az OATP-k vizsgálatára). Választásunk a pirandin acetoxi származékára (8-acetoxi-1,3,6-triszulfopiridin) esett, amit a továbbiakban Ace-nak nevezek. Ennek két oka volt:

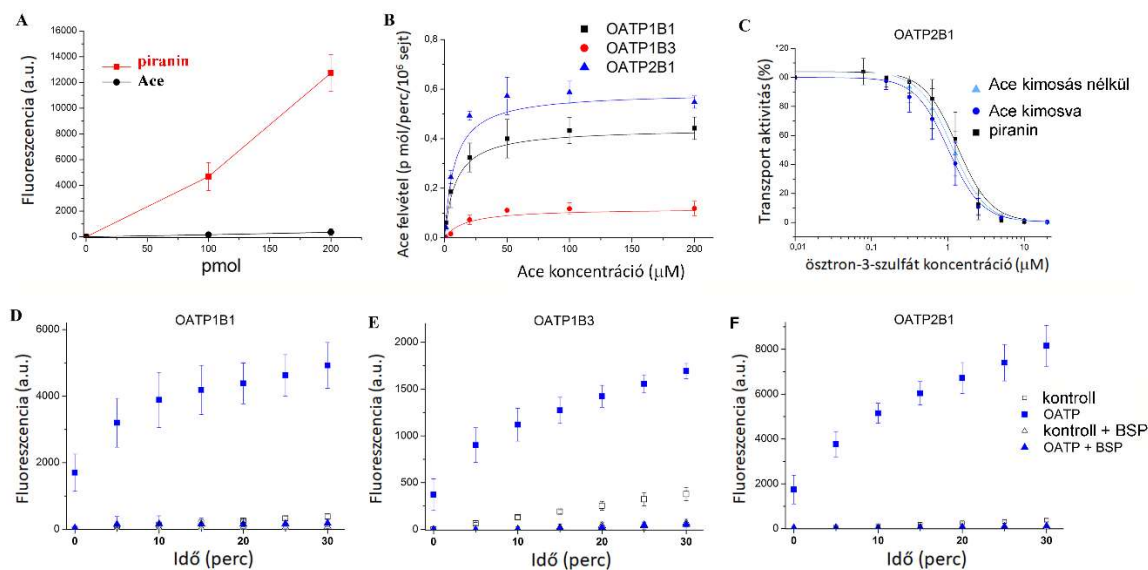
- 1.) Az acetoxi módosítás jellemzően fluorogénné teszi az eredetileg fluoreszcens molekulát (Lavis, Chao, and Raines 2011), és méréseink alapján az Ace hepatocelluláris OATP szubsztrát (lásd 30. ábra).
- 2.) A piranin egy pH indikátor, abszorbancia maximuma változik a pH függvényében (Gan et al. 1998)), pH 7 alatt 460 nm-en történő excitációnál fluoreszcenciája 20x-ad részére csökken. Ráadásul a fluorogén Ace sejtmentes közegben alig fluoreszkál, míg észteráz hasítást követően (például az élő sejtekbe bejutva) fluoreszcens piraninná alakul.

Ebből a kettős „erősítésből” (pH érzékeny fluoreszcencia és Ace-piranin átalakulás) adódóan azt gondoltuk, hogy a sejten kívüli, savas (pH 5.5) közegben alkalmazott Ace, a sejtben (pH 7,4) piraninná alakulva olyan jelentős fluoreszcencia növekedést fog eredményezni az OATP-t kifejező sejtekben, ami a sejten kívül feleslegben alkalmazott Ace eltávolítását nem teszi szükségessé (31. ábra).



31. ábra: Az Ace-piranin átalakuláson alapuló valós idejű OATP vizsgálati módszer működési elve

Az Ace tesztelésekor a fluoreszcencia változást az OATP-t kifejező (és kontroll) sejtekben valós időben mértük. Amint azt a 32. ábra mutatja, jelentős fluoreszcencia változást mértünk az OATP-t kifejező sejtekben, amit jellegzetes transzporter-mediálta telítési kinetika és OATP-inhibitor érzékenység jellemez.



32. ábra: Az Ace transzportjának valós idejű mérése OATP-ket kifejező A431 sejteken.

A) piranin és Ace fluoreszcenciája sejtmentes közegben B) Ace koncentráció-függő transzportjának valós idejű követése A431-OATP sejteken, pH 5.5 Az aktivitást a kontroll sejtekben mért aktivitást levonva határoztuk meg. D-F) Ace valós idejű transzportjának követése A431-OATP és kontroll sejteken. 10 μM (OATP1B1 és OATP2B1) vagy 20 μM (OATP1B3) Ace festékkel történt az inkubáció, 10 μM bromoszulfoftalein (BSP) jelenlétében vagy a nélkül, ctr: kontroll sejt. C) Ace és piranin-alapú módszer összehasonlítása. A431-OATP2B1 sejteket növekvő koncentrációjú ösztron-3-szulfát jelenlétében inkubáltuk 20 μM piranin vagy 10 μM Ace festékekkel, pH 5.5 pufferben. A mérés végén a fluoreszcenciát az Ace festék eltávolítása nélkül mértük (Ace nem kimosva), illetve eltávolítva az Ace és/vagy a piranint. A fluoreszcenciát fluoreszcens lemezolvasóban (Ex/Em: 460/510 nm) detektáltuk.

Végezetül, ismert, OATP-kel kölcsönható vegyületeket tesztelve összehasonlítottuk a piranin és Ace vegyületekre alapozott módszerek megbízhatóságát, ez utóbbit kétféleképpen (nem kimosva a reakció végén a sejtekről és eltávolítást követően, „klasszikus” transzport méréssel) is tesztelve. Ezek alapján az Ace ugyanolyan megbízhatónak bizonyult, mint a piranin, illetve a korábban alkalmazott radioaktív tesztszubsztrátok (lásd 32. C ábra és 1. táblázat az Ungvári és mtsai., 2021, 10. sz. csatolt közleményben).

Mivel tudomásunk szerint ez az első add-és-mérid módszer az OATP-k vizsgálatára, a módszer nemzetközi szabadalmaztatását is elindítottuk (PCT/HU2020/050062, A REAL-TIME, ADD-AND-READ FLUORESCENCE-BASED ASSAY FOR TESTING FUNCTION AND DRUG INTERACTIONS OF OATP TRANSPORTERS).

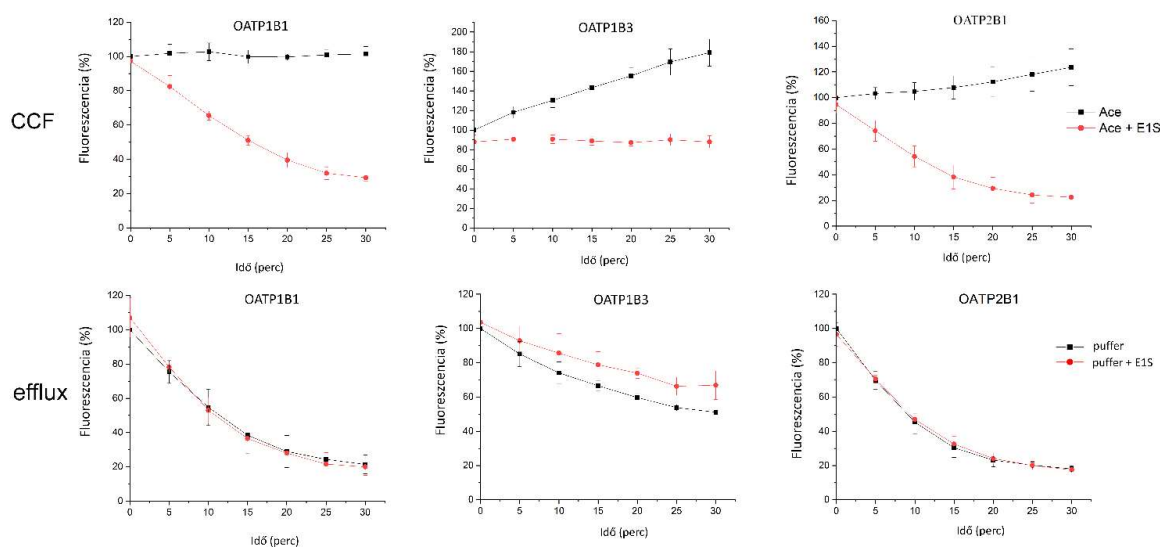
IV/B. 1.2.4. Kompetitív ellenáramlásos módszer a szubsztrátok és nem transzportálódó inhibitorok elkülönítésére

Az acetoxi-pirandin alkalmas az OATP1B1 szubsztrátjainak és inhibitorainak elkülönítésére (Ungvári és mtsai., 2021, 10. sz. közlemény)

Az OATP-k vizsgálatában a fluoreszcens szubsztrátok mindinkább teret nyernek (Izumi et al. 2016; De Bruyn et al. 2011; Gui et al. 2010), azonban az ezek használatán alapuló indirekt módszerek csak a vegyület és OATP közötti kölcsönhatás meglétét mutatják ki, annak természetére, transzportálódó vagy nem transzportálódó inhibitorról van-e szó, nem világítanak rá (legalábbis ennek meghatározása bonyolult kinetikai méréseket igényel). Pedig a máj OATP-k szubsztrátjainak szűrése például a máj toxicitás előrejelzése szempontjából is fontos lehet. Annak ellenére, hogy az OATP-k pontos működési mechanizmusa nem ismert, az általánosan elfogadott nézet, hogy cserélőként (exchanger) működve szubsztrátjaik sejtbeli felvételét és onnan történő exportját is képesek katalizálni. Sőt, az ellenion nem csak bikarbonát lehet, hanem egyik szubsztrát a másikra kicserélődhet (Schafer, Bock, and Meyer Zu Schwabedissen 2018). Erre alapozva nemrégiben kidolgoztak egy módszert (kompetitív ellenáramlásos módszer, CCF: competitive counterflow), amellyel a tesztvegyület transzportjában egyensúlyi állapotot kialakítva, majd a vizsgálandó vegyületet a tesztvegyület mellett feleslegben (IC_{50} 10x-es koncentrációja) adva, a vizsgált vegyületről eldönthető, hogy az szubsztrátja vagy inhibitor-e az OATP2B1 és OATP1A2 fehérjéknek (Schafer, Bock, and Meyer Zu Schwabedissen 2018; Schafer et al. 2020). Ugyanis a transzportálódó szubsztrát ki tud cserélődni a tesztvegyületre, és annak kiáramlását fogja okozni, míg a transzport folyamat gátlószere (nem kompetitív inhibitor) nem generál tesztvegyület kiáramlást. Ez az eljárás nem igényli a tesztvegyület költséges radioaktív jelölését vagy tömegspektrometriás

detektálását, tehát ezekhez a módszerekhez képest egy olcsóbb alternatívát jelent. A Schaefer és mtsai. által korábban leírt módszer azonban szintén radioaktív vegyületet használ teszt/indikátor szubsztrátként, ráadásul hasonló módszer a májban legjelentősebb OATP-k, az OATP1B1 és OATP1B3 fehérjékre vizsgálataink kezdetekor még nem volt elérhető.

A kutatásunk során OATP szubsztrátként azonosított fluorogén Ace-t használva megvizsgáltuk, hogy ez a vegyület alkalmas-e tesztsubszttrátként CCF vizsgálatban (33. ábra). Ehhez két feltételnek kellett teljesülnie: 1) egyensúlyi állapot elérése a festék transzportjában, 2) a festék, illetve annak intracelluláris származéka a piranin képes legyen a sejtekből kiáramlani az OATP-k működése által.

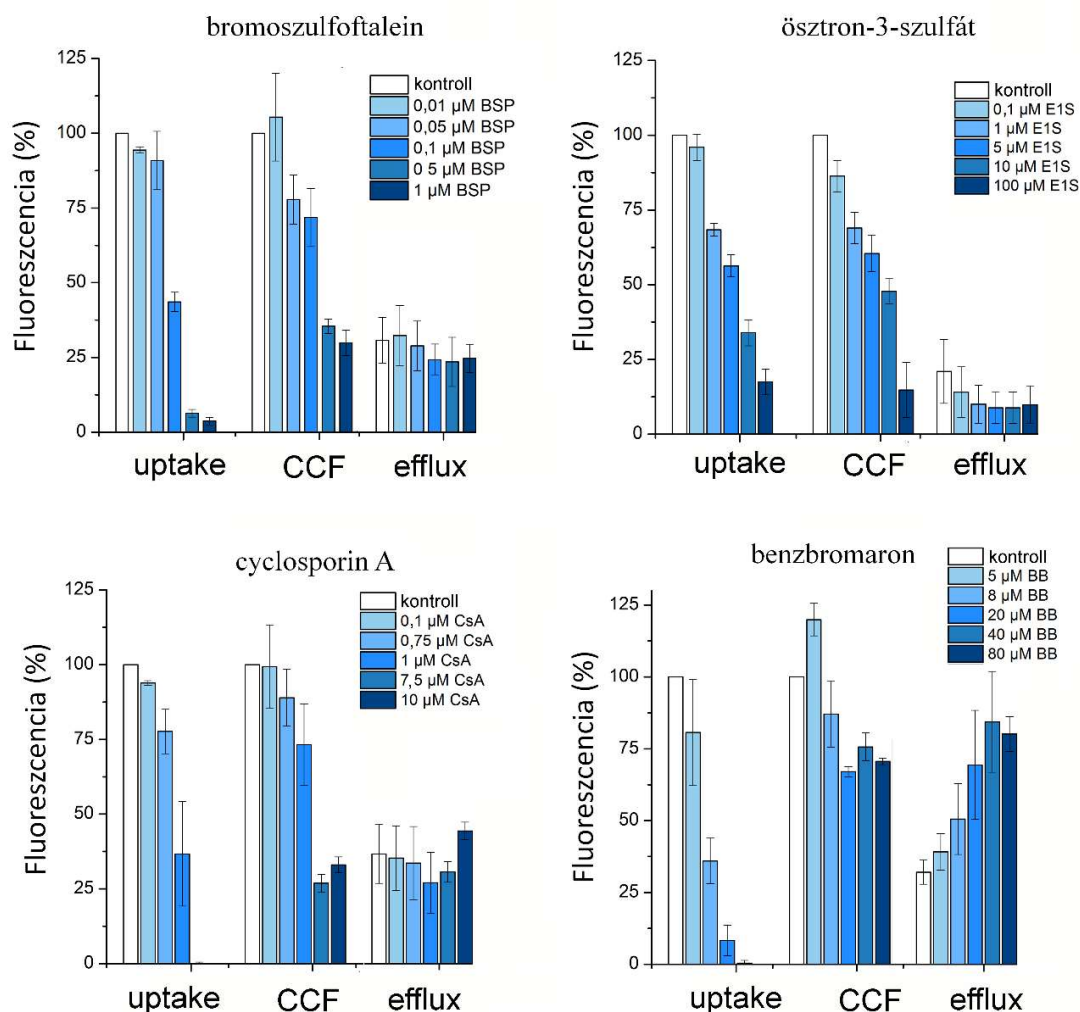


33. ábra: Az Ace, mint CCF próba alkalmasságának tesztelése A431-OATP sejteken. Az OATP-ket kifejező sejteket 5 μ M (OATP1B1, OATP2B1) vagy 20 μ M OATP1B3) Ace-val feltöltöttük, majd valós időben követtük a fluoreszcencia változást. CCF (Kompetitív ellenáramlás): a mérés második szakaszában Ace vagy Ace + 50 μ M ösztron-3-szulfát (E1S) volt jelen. Efflux (kiáramlás): a mérés második szakaszában puffer, vagy puffer és 50 μ M E1S volt jelen (lásd bővebben a Módszerek fejezetben). A fluoreszcencia mérésére Enspire lemezolvasót használtunk, Ex/Em: 460/510 nm.

Eredményeink alapján az OATP1B1 és OATP2B1 fehérjéknél mindkét feltétel teljesült, és az igazolt OATP szubsztrát E1S fokozta a festék kiáramlást a CCF beállításban, míg az efflux-ot nem gátolta (33. ábra). (Az OATP1B3 fehérjét kifejező sejtekben a transzport

nem jutott el az egyensúlyi állapotig, így ott további tesztszubsztrátok vizsgálatára van szükség).

Ezután az OATP1B1-et kifejező sejtekben tovább vizsgálódva igazolt és feltételezett OATP szubsztrátokat teszteltünk párhuzamosan vizsgálva a vegyületeket „klasszikus” festékvétel mérve, CCF és efflux módozatban, széles koncentrációtartományban (34. ábra).



34. ábra: OATP szubsztrátok és inhibitorok tesztelése klasszikus (uptake), CCF és efflux módszerrel. Uptake: A431-OATP1B1 sejteket előinkubáltunk a vizsgált vegyülettel (BSP, EIS, CsA vagy BB) majd a festéket hozzáadtuk (Ace), és a reakció végén a fluoreszcens jel alapján meghatároztuk a transzport aktivitást. Control: csak Ace. **CCF:** A431-OATP1B1 sejteket előinkubáltunk az Ace-val, majd azt eltávolítottuk és növekvő koncentrációjú vizsgált vegyület + Ace-t adtunk a sejtekhez. Végül a festéket eltávolítottuk és a

fluoreszcenciát megmértük. *Control*: a második fázisban csak Ace volt jelen. **Efflux**: A mérés első szakasza a CCF-nél leírtak szerint történt. A második fázisban a sejteket pufferben inkubáltuk (*control*) vagy a vizsgált vegyület jelenlétében. *BSP*: bromoszulfoftalein, *E1S*: ösztron-3-szulfát, *CsA*: cyclosporin A, *BB*: benzbromaron.

Méréseink alapján az E1S-hez hasonlóan az igazolt OATP1B1 szubsztrát bromoszulfoftalein (BSP) is generált festék kiáramlást és kicserélődött a piraninra. Ezekhez az igazolt szubsztrátokhoz hasonlóan viselkedett a cyclosporin A is, a korábban csak OATP inhibitorként definiált (immunszuppresszáns) gyógyszer. Tehát ez vizsgálataink alapján lehetséges szubsztrátja az OATP1B1 fehérjének. A benzbromaron (köszvény kezelésére használt gyógyszer) viszont nem transzportálódó OATP1B1 inhibitor.

Az általunk létrehozott módszer szintén újdonság a hepatocelluláris OATP-k vizsgálatában, így az a nemzetközi szabadalmi bejelentésünk egyik igénypontját képezi (PCT/HU2020/050062).

IV/B. 2. OATP1B1 és MRP2 együttes vizsgálatára alkalmas fluoreszcens módszer kidolgozása

A szulfopirének és a szulforodamin 101 alkalmasak az OATP1B1 és MRP2 együttes vizsgálatára (Székely és mtsai., 2020, 11. sz. közlemény) és PCT/ HU2020/050014

Kettős (vagy többszörös) transzfektáns sejt vonalakat, amelyek például a májban kifejeződő uptake és efflux transzportereket termelnek (akár többet is közülük, esetleg metabolikus enzimekkel (CYP) kombinálva), széleskörben alkalmaznak a transzcelluláris transzport folyamatok modellezésére. Ezekben a modellekben az egyik tipikus kombináció az OATP1B1 és MRP2, illetve az OATP1B1 és ABCG2 együttes vizsgálata, hiszen ezek átfedő szubsztrátfelismeréssel rendelkeznek és összehangolt működésük biztosítja több endogén és exogén eredetű vegyület (például bilirubin, sztatinok) hatékony hepatikus eliminációját. A módszer a közös szubsztrát apikális-bazolaterális irányú transzportjának mérésén alapszik, amire korábban csak radioaktív próbák álltak rendelkezésre.

Mivel az OATP1B és az MRP2, illetve ABCG2 fehérjék szubsztrátfelismerése nagyban átfed, feltételeztük, hogy az általunk felfedezett fluoreszcens OATP szubsztrátok között is akadhat az ABC-k által is transzportált közös festékszubsztrát, aminek segítségével ezeknek a máj transzportereknek a működése egy rendszerben tanulmányozható.

Ezekbe a vizsgálatokba a korábban azonosított fluoreszcens OATP festékszubsztrátokat vontuk be (5. táblázat). A festékek ABCG2, illetve MRP2 általi transzportját rovarsejtekből izolált fordított orientációjú vezikulákon (IOV) teszteltük. Az IOV-k használatára azért volt szükség, mert az általunk azonosított OATP szubsztrátok nem jutnak be passzívan a sejtekbe. Az 5. táblázat alapján megállapítottuk, hogy számos festék szubsztrátja az MRP2 fehérjének, míg az ABCG2 a Live/Dead Violet, LorD488 és CascadeBlue festékeket transzportálja.

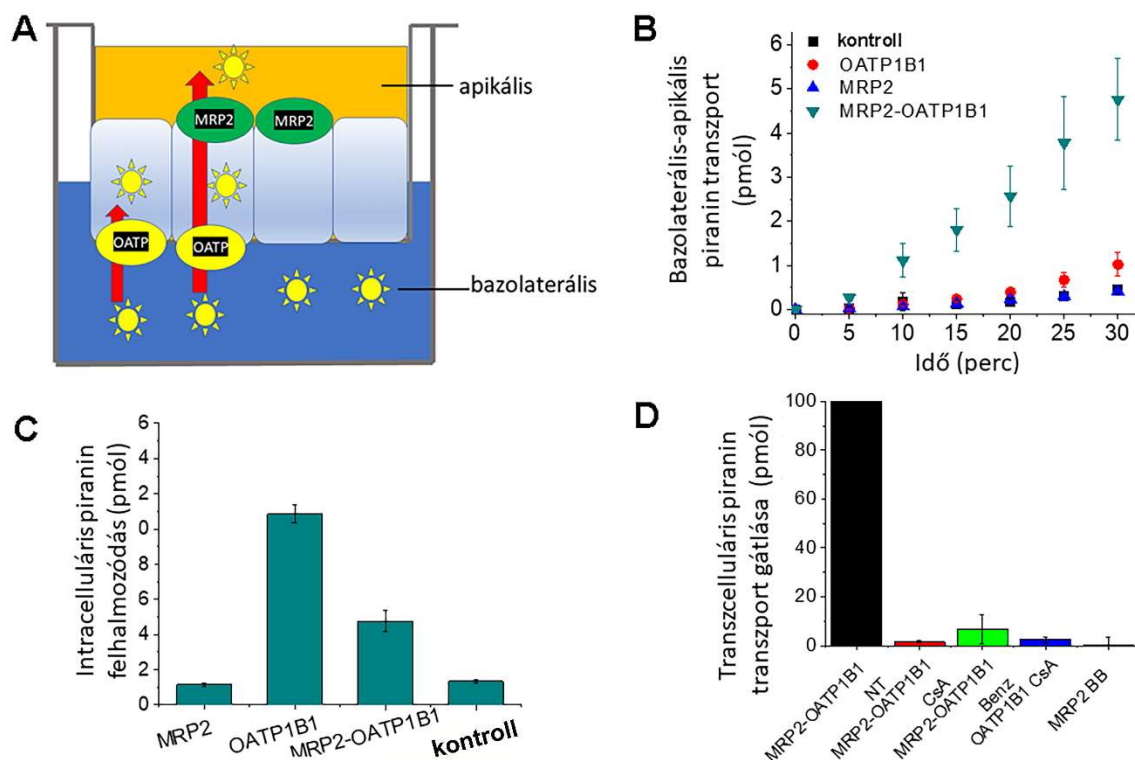
5. táblázat: OATP1B1 és ABC szubsztrátok

Forgalmazó	Festék fantázianeve	OATP1B1	MRP2	ABCG2
Biolegend	Zombie Violet	+	+	-
ThermoFisher Scientific	Live/Dead Violet	+	+	+
	Live/Dead Green	+	+	-
	Alexa Fluor 405	+	+	-
	Cascade Blue Hidrazid	+	+	+
Biotium	LorD488	-	-	+
Sigma Aldrich	szulforodamin 101	+	+	-
	piranin	+	+	-

A festékek transzportját A431-OATP1B1 sejteken, illetve MRP2 vagy ABCG2-t tartalmazó Sf9 membránvezikulákon határoztuk meg.

A polarizálható kutya vese eredetű sejtvonal, MDCKII rutinszerűen alkalmazott eszköze az epiteliális transzport folyamatok modellezésének. Létrehoztuk tehát a kettős

transzsfektáns, OATP1B1 és MRP2, vagy OATP1B1 és ABCG2 fehérjéket kifejező MDCKII sejteket (és megfelelő kontrolljaikat), majd a polarizált sejteken teszteltük a közös szubsztrátként azonosított festékek (piranin, szulfurodamin 101, és Cascade Blue hidrazid) transzcelluláris transzportját (35. ábra).



35. ábra: Piranin transzcelluláris transzportja MDCKII-OATP1B1-MRP2 sejteken. A) Transzcelluláris transzport működési elve **B)** piranin (5 μ M) transzcelluláris transzportja, illetve **C)** intracelluláris akkumulációja MDCKII-OATP1B1, MDCKII-MRP2, MDCKII-MRP2-OATP1B1, illetve kontroll MDCKII (Ctr.) sejteken. **D)** Transzcelluláris piranin transzport inhibitorok jelenlétében, 5 μ M pyranine, 10 μ M cyclosporin A (CsA) vagy 40 μ M benzobromarone (BB).

Amint az a 35. ábrán látható, a piranin (és az itt nem bemutatott, de a Székely és mtsai, 2021, 11.sz. közleményben, illetve a szabadalmi bejelentésben szereplő Cascade Blue hidrazid, Ace és szulfurodamin 101) festékeket alkalmazva, ki tudtuk mutatni a festék apikális-bazolaterális irányú transzportját, amit megfelelő inhibitorokkal gátolni lehetett. Ezen kívül kontroll kísérletekben megállapítottuk, hogy a festékek az ellentétes irányban nem jutnak át a sejteken, tehát az (egy)sejt réteg megfelelően „zárt”, nem sejtközötti transzport okozza a mért jelet. Azt is igazoltuk, hogy a vizsgált festékek valóban sejt impermeábilisak, OATP nélkül nem jutnak be a sejtekbe. Ilyen módon, a piranin, Ace,

Cascade Blue hidrazid és szulforodamin 101 festékekről megállapítottuk, hogy alkalmasak OATP1B1 és MRP2 együttes vizsgálatára.

A kidolgozott módszer alkalmas lehet hepatociták OATP és MRP2 működésének tesztelésére, illetve új hatóanyagok OATP, illetve MRP2 fehérjével való kölcsönhatásának együttes, egy rendszerben történő tesztelésére. Mivel ez az első bizonyított fluoreszcens módszer az előző alkalmazásokra, annak nemzetközi szabadalmaztatását elindítottuk (PCT PCT/HU2020/050014 “Fluorescence method for assessing transport activity of OATPs and MRP2”, a Európai Szabadalmi Hivatal (EPO) pozitív jelentését ezzel kapcsolatban már megkaptuk).

Érdekes módon az ABCG2 fehérje IOV mérések alapján szubsztrátjaként azonosított festék, Cascade Blue hidrazid ABCG2 általi kiáramlását nem tudtuk megerősíteni. Ennek több magyarázata lehet: 1) az ABCG2 expresszió nem volt kellően magas a sejtekben, 2) a Cascade Blue átalakul a sejtekben, és a metabolitot az ABCG2 már nem ismeri fel. Mindezek eldöntése további vizsgálatokat igényel, amire azonban eddig nem volt módunk.

IV/B. 3. Új vegyület-OATP kölcsönhatások azonosítása

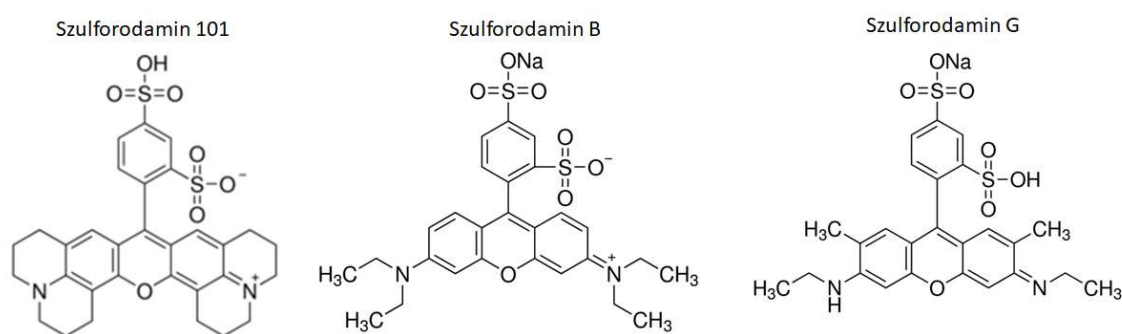
IV/B. 3.1. Extrahepatikus OATP-k vizsgálatára alkalmas fluoreszcens módszer kidolgozása, új gyógyszerkölcsönhatás kimutatása

Szulforodamin festékekkel az OATP1A2 és OATP1C1 fehérjék vizsgálhatók. Az elacridar, P-glikoprotein inhibitor OATP1A2 szubsztrát (Bakos és mtsai, 2020, 12. sz. közlemény)

Habár a nemzetközi gyógyszer- és szabályozó hatóságok irányelvei alapján az OATP1A2 vizsgálata nem szükséges a gyógyszerfejlesztés során, ez a fehérje is befolyásolhatja gyógyszerzsubsztrátjai farmakokinetikáját, azok epéből és vizeletből való visszaszívódásának (reabszorpció), illetve a vér-agy gáton történő áthaladásának elősegítésével (Zhou et al. 2015). Az OATP1C1 fehérje az OATP család kevésbé jellemzett tagja, viszonylag kevés igazolt szubsztráttal. Működése azonban, mint az pár éve kiderült

(Stromme et al. 2018), fontos a központi idegrendszer sejtjeinek tiroid hormon (T3) ellátásában, így az OATP1C1 farmakológiai célpont. Munkánk kezdetekor, hasonlóan a hepatocelluláris OATP-khez, ezekre a fehérjékre sem volt elérhető érzékeny, fluoreszcencia-alapú tesztrendszer. Mivel számtalan közös OATP szubsztrát ismert (szteroid hormonok, epesók, tiroid hormonok), a hepatocelluláris OATP-knél azonosított festékeket teszteltük OATP1A2 és OATP1C1 szubsztrátként. Így azonosítottuk szubsztrátjukként az LDG festéket, aminek segítségével, hasonlóan a hepatocelluláris OATP-khez, az OATP1A2 és OATP1C1 termelő sejteket is ki tudtuk válogatni (lásd részletesen a 12. sz. közleményben). Ezeket a sejteket felhasználva több életképesség festéket, illetve szulforodaminokat teszteltünk.

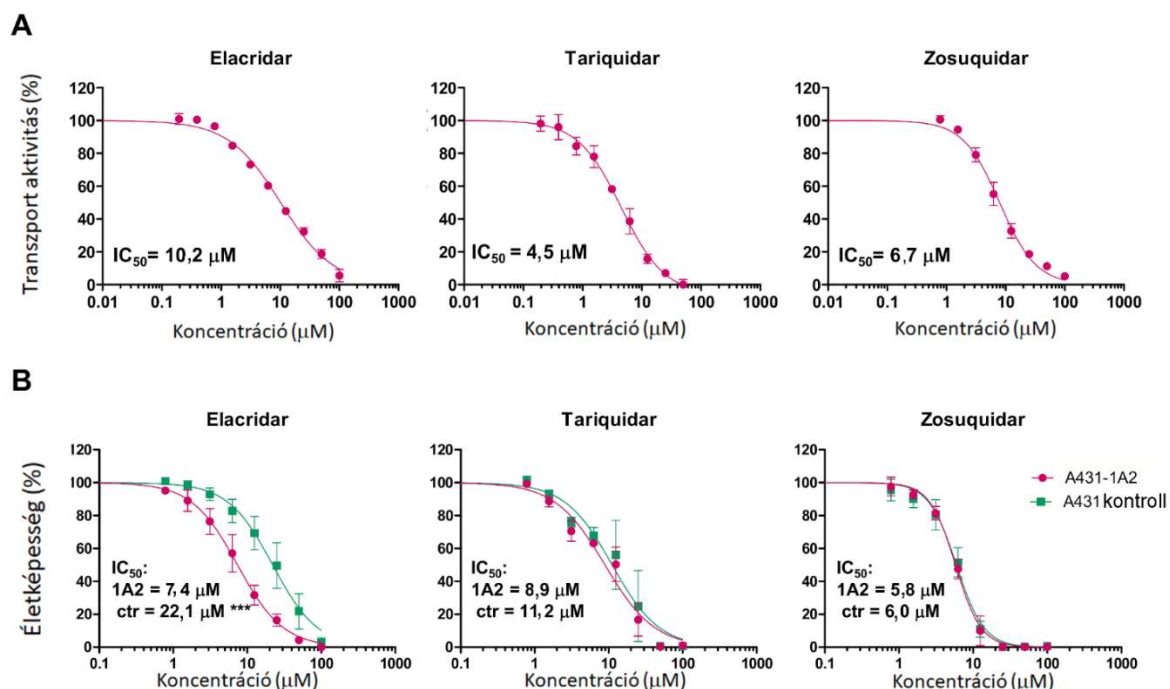
A szulforodamin 101 festék egy széleskörben alkalmazott asztrocita marker (Nimmerjahn et al. 2004). Sőt, több tanulmányban leírták, hogy egér Oatp-k felelősek a sejtbeli felvételért (Hagos and Hulsmann 2016; Yaguchi et al. 2019). Habár az egér Oatp-k expressziós mintázatukat és szubsztrátfelismerésüket tekintve sem feleltethetők meg egy az egyben humán ortológjaiknak (sok esetben nincs is ortológjuk), felmerült, hogy ezt a festéket a humán OATP-k is felismerhetik. Munkánk során többféle szulforodamin (36. ábra) transzportját jellemeztük HEK-OATP1A2, HEK-OATP1C1 és A431-OATP1A2 sejteken (ezt itt nem részletezem, a Bakos és mtsai, 2020, 12. sz. publikációnkban részletes bemutatásra került).



36. ábra: A munkánk során OATP1A2 és OATP1C1 szubsztrátként azonosított szulforodaminok képlete

Röviden, igazoltuk többek között, hogy a szulforodamin B, G és 101 festékek alkalmasak az OATP1A2 és OATP1C1 fehérjékkel kölcsönható vegyületek tesztelésére. Ennek keretében az OATP1A2 fehérjénél az elacridar, tariquidar és zosuquidar, harmadik

generációs P-gp gátlószerekkel új kölcsönhatást mutattunk ki, azok az OATP1A2 inhibitorai. További citotoxicitási mérések alapján pedig megállapítottuk, hogy az elacridar OATP1A2 szubsztrát, az OATP1A2 működése által dúsulhat a sejtekben és azok fokozott pusztulását okozhatja (37. ábra).



37. ábra: Harmadik-generációs P-glikoprotein inhibitorok kölcsönhatása az OATP1A2 fehérjével. A) SR101 festék (1 μM) felvételének gátlása A431-OATP1A2 sejteken B) Harmadik-generációs P-gp inhibitorok hatása az A431 kontroll (ctr) és OATP1A2-t kifejező (A431-1A2) sejtek életképességére, szulforodamin B festődés alapján meghatározva.

Az elacridart (több más 3. generációs P-gp inhibitorral) olyan céllal fejlesztették, hogy a többek között a vér-agy gát endotél sejteiben kifejeződő P-gp és ABCG2 működését gátolva, elősegítse a központi idegrendszer tumorjait célzó terápiás szerek hatékonyabb átjutását a vér-agy-gáton. Azonban a klinikai kipróbálás során ezek a szerek sorra megbuktak, például mert neurotoxicitást okoztak (Rubin et al. 2002; Palmeira et al. 2012). Vizsgálataink alapján az elacridar fokozottan bejuthat a sejtekbe az OATP1A2 működése által, ami nem várt toxicitást eredményezhet. Hozzá kell azonban tenni, hogy az OATP1A2-vel kimutatott kölcsönhatás nem feltétlenül következik be *in vivo* körülmények között, hiszen ezeknek a P-gp inhibitoroknak a vérbeli koncentrációja (1-2 μM) jelentősen

elmarad az OATP1A2-re mért gátlásuktól (IC_{50} 4-10 μ M). Viszont lokálisan kialakulhat olyan koncentráció, ami az OATP1A2 működésének gátlásához vezet. Ráadásul az általunk kimutatott kölcsönhatás rámutat arra, hogy a P-gp inhibitorok között lehetnek az OATP1A2 működését is gátló vegyületek, amelyek megváltozott farmakokinetikát okozhatnak.

IV/B. 3.2. OATP2B1 és ösztrom szarmazékok kölcsönhatásának vizsgálata

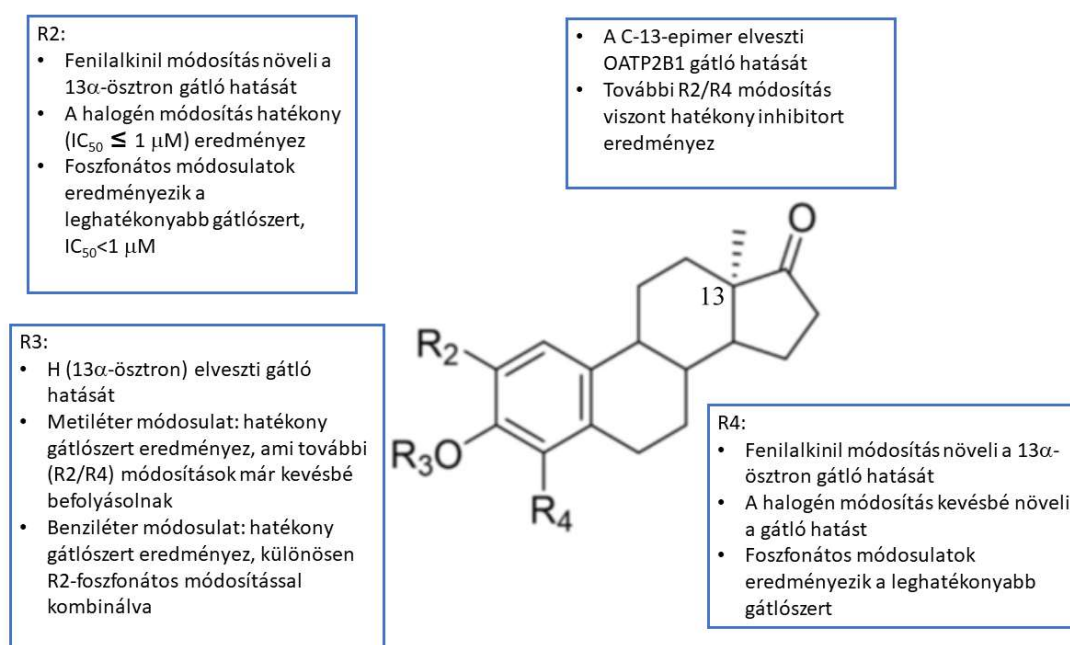
A 13α -ösztrom hatékony és szelektív inhibitorai az OATP2B1 fehérjének (Laczko-Rigó és mtsai, 2020 és 2021, 13-14. sz. közlemények)

Az OATP2B1 fehérje többféle tumorban megnövekedett expressziót mutat (Kovacsics, Patik, and Ozvegy-Laczka 2017). *In vitro* vizsgálatokkal igazolták, hogy működése megnövekedett E1S és DHEAS felvétellel jár, ami az emlő eredetű tumoros sejtvonalak proliferációját fokozza (Matsumoto et al. 2015). Ráadásul, prosztata rákkal diagnosztizált betegek genotípus elemzésével megállapították, hogy a csökkent OATP2B1 funkciót eredményező polimorf változat rs12422149, GG allél (R312Q) kedvezőbb prognózissal, hosszabb betegségmentes túléléssel (DFS, disease-free survival) társul (Wright et al. 2011). A nemi hormonfüggő tumorok kezelésének egyik startégiája a lokális ösztrogén szintézis gátlása. Az ebben az útvonalban résztvevő aromatáz és STS (szteroid szulfatáz) enzimek inhibitorait (például exemestane, letrozole aromatáz gátlók és az Irosustat/ STX64/667 coumate STS gátló) a klinikumban alkalmazzák. Azonban ezeknél a szereknél probléma lehet az ösztrogén hatás, illetve gyakran megfigyelték, hogy a kezelés hatására a tumorokban az ösztrogén szintézis alternatív útvonalai aktiválódnak (Rizner, Thalhammer, and Ozvegy-Laczka 2017), ami a terápia hatástalanságát eredményezi.

Dr. Mernyák Erzsébet (Szegedi Tudományegyetem, Szerves kémia tanszék) munkacsoportjában évek óta fejlesztenek (terveznek és szintetizálnak) olyan ösztrom szarmazékokat, amelyek a lokális ösztrogén szintézisben fontos enzimek, szteroid szulfatáz (STS) és/vagy 17β -hidroxiszteroid-dehidrogenáz 1 (HSD17 β 1) gátlószerrei, de ösztrogén hatással nem rendelkeznek, az ösztrogén receptorhoz nem kötődnek (Bacsa et al. 2015). Ezek a természetes ösztrom epimerjei, amelyekben a 13-as szénatomon lévő metilcsoport

alfa pozícióban található (13α -öszttronok). Az 13α -öszttronok alternatív startégiát jelenthetnek a nemi hormonfüggő tumorok elpusztításában, ráadásul a szterán váz több pozícióban módosítható, ami szerkezet-hatás vizsgálatokhoz és célzott inhibitorok fejlesztéséhez ideális.

Az OATP2B1 nemi hormon transzporter, ezért kíváncsiak voltunk arra, hogy a természetes öszttron 13α epimerjét, illetve annak származékait is felismeri-e. Először, az előző fejezetekben leírt fluoreszcens módszereink segítségével különböző 13α -epiöszttron származékokat tartalmazó molekulakönyvtárat teszteltünk. Számos 13α -epiöszttron változatot találtunk, amelyek hatékonyan (mikromólos IC_{50} értékkel) gátolták az OATP2B1 működését (Laczkó-Rigo et al. 2020). Ezek alapján szerkezet-funkció összefüggéseket állapítottunk meg, amelyeket a 38. ábrán összegztek.

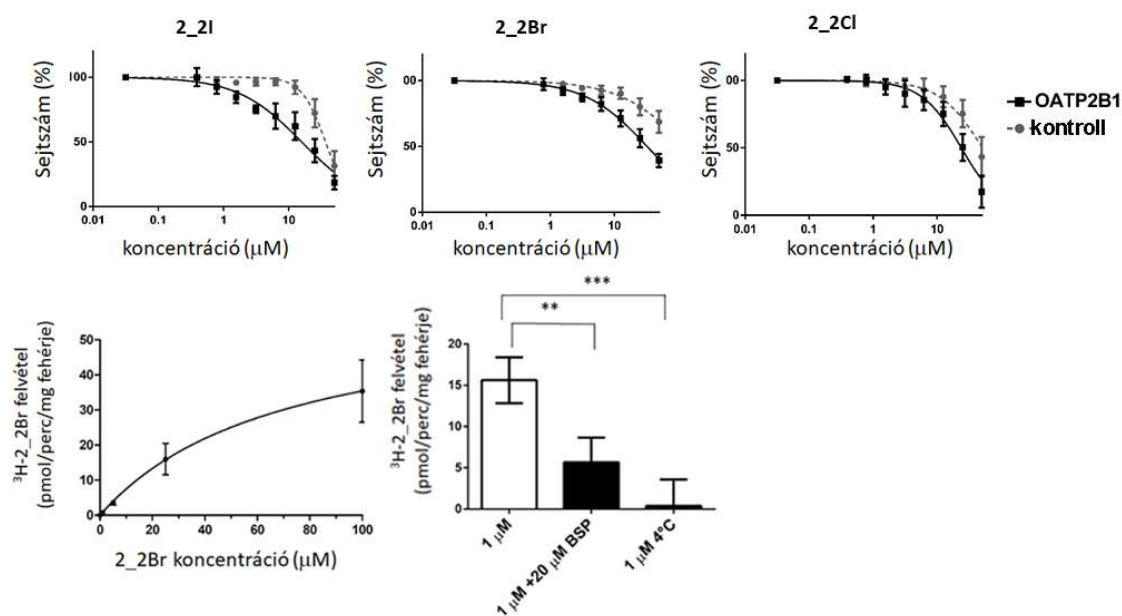


38. ábra: Az OATP2B1 transzport működés gátlása alapján megállapított szerkezet-hatás összefüggések összefoglalása. A transzport gátlás mérések és a vegyületek IC_{50} értékei a közleményeinkben találhatóak meg (Laczkó-Rigó és mtsai, 2020 és 2021, 13. és 14. sz. közlemények).

Az újonnan azonosított öszttronvázas inhibitorok az OATP2B1 gátlószerek új csoportját képviselik, amelyek az OATP2B1 általi hormonfelvétel gátlás egyik lehetséges stratégiája lehetnek a hormonfüggő tumorok elpusztításában. Sőt, alternatívaként felmerül, hogy amennyiben ezek a szerek hatékony enzimgátlók, például az STS vagy HSD1 enzimek

működését gátolják, akkor az OATP2B1 fehérjét kifejező tumorokban dúsulva szintén célzott terápiás lehetőséget adnak. Az általunk azonosított 13α -epiösztion halogénmódosulatai HSD17 β 1 gátlószerként is, ráadásul, ezek szelektív OATP2B1 inhibitorok, az OATP1B1 és OATP1B3 működését nem gátolják (Tuerkova et al. 2021).

Annak érdekében, hogy az OATP2B1 inhibitor 13α -epiösztionok között lehetséges szubsztrátokat azonosítsunk (hiszen az indirekt módszerrel a kompetitív és nem kompetitív gátlószerket nem különítettük el), további vizsgálatainkban az OATP2B1 gátlószerként azonosított 13α -ösztionokat sejtproliferációs vizsgálatban is teszteltük. Ily módon a potenciálisan toxikus OATP2B1 szubsztrátokat terveztük azonosítani (Windt et al. 2019). E kísérletek során megállapítottuk a 2. szénatomon halogénnel módosított 13α -ösztionok szelektív, OATP2B1-függő antiproliferatív hatását (39. ábra). A kontroll sejthez képest legspecifikusabb hatást kifejtő változat, 2-bromo- 13α -ösztion radioaktívan jelzett változatát felhasználva igazoltuk, hogy ez a vegyület az OATP2B1 működése által dúsulhat a sejtekben (Laczkó-Rigó és mtsai, 2021). Így egy kettős, enzim-inhibitor OATP2B1-szubsztrát vegyületet azonosítottunk.



39. ábra: 2-halogénezett 13α -ösztionok szelektív antiproliferatív hatása és transzportja A431-OATP2B1 sejteken. Felső panelek: A 2-halogénezett 13α -ösztionok antiproliferatív hatását 120 óra után határoztuk meg. Alsó panelek: Triciált 2-bromo- 13α -ösztion (2_2Br) felvétele A431 sejtekben. 2_2Br koncentráció-függő felvétele, illetve 1 μ M 2_2Br felvétele

BSP (bromoszulfoftalein) OATP inhibitort jelenlétében, illetve 4°C-on. Az aktivitást a kontroll A431 sejtekben mért 2₂Br felvételt levonva határoztuk meg.

IV/B. 3.3. „Újrahasznosított” Covid-19 elleni gyógyszerek és OATP-k

*A Covid-19 elleni terápiában alkalmazott
antivirális szerek gátolhatják a multispecifikus
OATP-k működését (Telbisz és mtsai., 2021, 15.
sz. közlemény)*

Második éve küzd a világ a SARS-CoV-2 vírus okozta Covid-19 betegséggel. A betegek kezelésének egyik legbiztonságosabb módja a már korábban a szabályozó szervezetek által engedélyezett antivirális, vagy más célra fejlesztett gyógyszerek „újrahasznosítása”. Ilyen gyógyszerek többek között az antivirális favipiravir, ritonavir, lopinavir és remdesivir (Veklury). Azonban a Covid-19 betegek nagy része a valamilyen alapbetegséggel küzdő, más gyógyszert is szedő emberek közül kerül(t) ki. A többféle gyógyszer együttes adásának következményét azonban nem volt idő tesztelni, pedig ezek együttesen adva komoly mellékhatásokat válthatnak ki. Együtműködésben Sarkadi Balázs és Telbisz Ágnes csoportjával (TTK, Enzimológiai Intézet), illetve a Solvo Biotechnológiai Zrt.-vel (Budapest) egy, a gyógyszertranszporterek széles tárházát lefedő *in vitro* vizsgálatban vettünk részt az általunk fejlesztett módszerekkel. Ennek során a favipiravir kivételével hatékony gátlást mértünk a multispecifikus OATP-kre (OATP1A2, OATP1B1, OATP1B3 és OATP2B1). Figyelembe véve maximális plazmakoncentrációjukat (6. táblázat) az ivermectin kivételével a három antivirális szer, lopinavir, ritonavir és remdesivir is okozhatnak OATP-mediálta gyógyszer-gyógyszer kölcsönhatásokat, ami további vizsgálatokat tesz indokolttá. A favipiravir egyik OATP-t sem gátolta, így használatakor OATP-közvetítette gyógyszer kölcsönhatást nem várunk (Telbisz és mtsai, 2021, Ambrus és mtsai, 2021*).

*: közleményjegyzékben az MTMT lezárásakor még nem szerepelt, így nem tüntettem fel a dolgozat alapjául szolgáló közlemények között

6. táblázat: OATP-k működésének gátlása potenciális Covid-19 ellenes szerekkel

anti-COVID-19 gyógyszerek	mechanizmus	Transzporter gátlás IC ₅₀ (μM)				maximális plazma koncentráció (μM)
		OATP1A2	OATP1B1	OATP1B3	OATP2B1	
ivermectin	klorid csatorna és GABA receptor gátló (parazitellenes szer)	5,2	≥20	1,4	8,6	0,052
lopinavir	(HIV) proteáz inhibitor	1,5	1,1	2,6	1	11-20
ritonavir	(HIV) proteáz inhibitor	2,3	1,4	1,5	1,4	1-1,73
remdesivir	virális RNS- polimeráz gátló (Hepatitis C és Ebola ellen fejlesztve)	3,8	2,9	4,3	3,8	3,7
favipiravir	virális RNS- polimeráz gátló (influenza ellenes szer)	nincs hatás	nincs hatás	nincs hatás	nincs hatás	nincs hatás

V. AZ ÚJ TUDOMÁNYOS EREDMÉNYEK ÖSSZEFOGLALÁSA

1. Jellemeztük az ABCG2 mutációs forró pontját, és megállapítottuk, hogy az R482, vad típusú változat egyedi, csak rá jellemző szubsztrátfelismeréssel rendelkezik, és több, funkcionyeréses R482 mutánst azonosítottunk.
2. Az ABCG2 koleszterin-szenzor régiójának felderítése érdekében több lehetséges szteroidkötő motívumot vizsgáltunk.
 - a. Megállapítottuk, hogy az LxxL szteroidkötő motívum leucinjai az ABCG2 fehérje szubsztrátfelismerését és aktivitását befolyásolják. Szerepük lehet továbbá a fehérje megfelelő térszerkezetének kialakításában.
 - b. A potenciális koleszterin-felismerő CRAC motívumok Tyr-jai közül hármát azonosítottunk, amelyek a fehérje expresszióját és/vagy működését befolyásolják.
 - c. Eredményeink és a későbbi térszerkezet alapján az LxxL és CRAC motívumok nem vesznek részt közvetlenül a koleszterinérzékelésben, közvetett (allosztérikus) hatásuk azonban nem kizárható.
3. Jellemeztük egy ABCG2-t felismerő antitest (5D3) kötődését:
 - a. Megállapítottuk, hogy az 5D3 egy konformáció-érzékeny antitest, ami az ABCG2 inhibitor-kötött formáját ismeri fel, az ATP hidrolízis kezdeti fázisaiban megrekedt ABCG2 fehérjéhez viszont kevésbé tud kötődni.
 - b. Megállapítottuk, hogy az 5D3 antitest epitópja az ABCG2 fehérje monomeren, a 3. extracelluláris hurokban található, és az epitóp rögzítésében az intramolekuláris diszulfid híd vesz részt.
4. Többféle specifikus és általános fluoreszcens OATP szubsztrátot azonosítottunk.
5. OATP-ket nagy mennyiségben kifejező sejteket állítottunk elő fluoreszcens festék felhalmozódása és a sejtek kiválogatása alapján.
6. Érzékeny, fluoreszcencia-alapú, közepes áteresztőképességű módszert dolgoztunk ki több OATP vizsgálatára.
7. Kidolgoztuk az MRP2 és OATP1B1 hepatikus transzporterek együttes vizsgálatára alkalmas fluoreszcencia-alapú módszert.

8. Kidolgoztuk az első, fluorogén szubsztrát felvételén alapuló módszert, amely lehetővé teszi a hepatocelluláris OATP-k valós idejű vizsgálatát.
9. Igazoltuk, hogy az OATP1B1 efflux transzporterként is működhet és két, akár nagyméretű szerves molekula kicserélésére is képes. Erre alapozva a szubsztrátok és nem transzportálódó inhibitorok elkülönítésére alkalmas (kompetitív ellenáramláson alapuló) módszert dolgoztunk ki.
10. Az OATP2B1 új inhibitorait és egy potenciális új szubsztrátját azonosítottuk.
11. Új transzporter-gyógyszer kölcsönhatásokat mutattunk ki:
 - a. Elsőként fedeztük fel, hogy az ABCG2 a klinikumban is alkalmazott tirozin kináz gátlószereket, Gleevec és Iressa felismeri.
 - b. Egyes, a COVID-19 elleni terápiában is alkalmazott antivirális szerek a multispecifikus OATP 1A2, 1B1, 1B3 és 2B1 fehérjék inhibitorai.
 - c. A harmadik generációs P-glikoprotein inhibitorok az OATP1A2 gátlószerei, és az elacridar potenciális OATP1A2 szubsztrát.

Az OATP-k vizsgálatára kifejlesztett új módszerek szabadalmaztatását elindítottuk, két nemzetközi bejelentésünk van bírálati szakaszban.

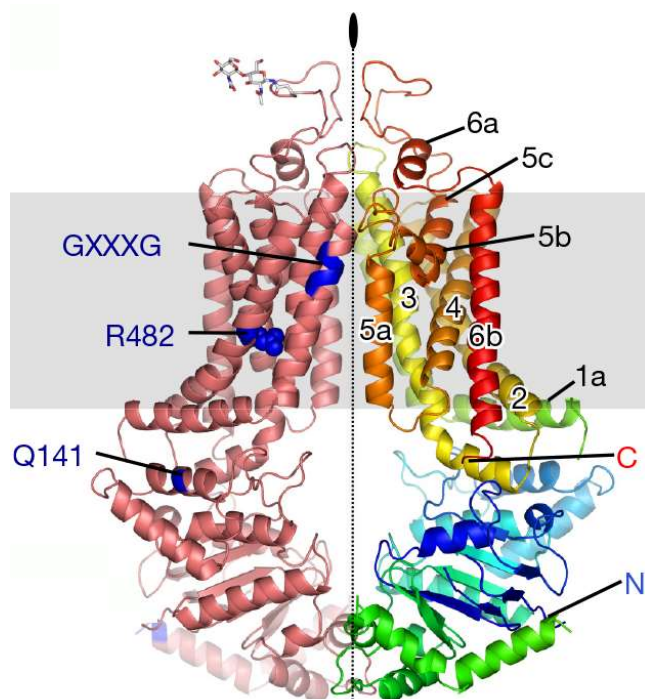
VI. KÖVETKEZTETÉSEK ÉS KITEKINTÉS

1. Mutációk az azóta ismert ABCG2 térszerkezet fényében

Az első nagyfelbontású ABCG2 térszerkezetek 2017/18-ban és 2020-ban láttak napvilágot (Manolaridis et al. 2018; Jackson et al. 2018; Taylor et al. 2017; Orlando and Liao 2020). Ezek az ABCG2 különböző, rögzített konformációit mutatják. Munkám egy része az ABCG2 fehérje egyes régióinak a fehérje működésében és koleszterin általi szabályozásában betöltött szerepének megértésére irányult. Az ABCG2 mutánsok vizsgálata kapcsán tett megállapításainkat a később ismertté vált térszerkezetek fényében itt tárgyalom.

Az R482 elhelyezkedése és szerepe:

Eredményeim alapján, az R482 kulcsfontosságú az ABCG2 szubsztrátfelismerésében (Ozvegy-Laczka, Koblos, et al. 2005). Az ismert térszerkezet alapján az R482 a 3. TM hélix része, de nem a központi, szubsztrátkötő üreg felé néz, direkt kölcsönhatást a szubsztrátokkal nem mutat (40. ábra). Taylor és mtsai alapján a 4. TM hélixben lévő S521-el alkot hidrogén kötést (Taylor et al. 2017). Orlando és mtsai pedig a 2. TM hélixszel való közelségét írták le (Orlando and Liao 2020). Tehát az R482-nek nem közvetlenül a szubsztrátfelismerésben van szerepe, hanem a központi üreget formáló hélixek megfelelő térszerkezetének kialakításában.



40. ábra: Az ABCG2 térszerkezete és az R482 elhelyezkedése, forrás (Taylor et al. 2017). Az ábrán az ABCG2 homodimer szerkezete látható (az egyik ABCG2 pirossal, a másik ABCG2 szivárványszínben). Az R482-n kívül kék szín jelöli a gyakori mutációval érintett Q141-t és a korábban a dimerizációban fontosnak gondolt GxxG motívumot. C, és N: a fehérje C és N végei.

Itt fontos hangsúlyozni, hogy a szubsztrátkötő hely nem egy jól definiált pont, azt nem egy “klasszikus” szubsztrátkötő zsebként kell elképzelnünk, hanem a fehérjén áthaladó szubsztrát „útja során” többféle régióval és aminosavval is érintkezik, és azokkal eltérő affinitással lép kölcsönhatásba. Ráadásul a transzport folyamat során a TM régiók mozognak (a publikált térszerkezetek is eltérő konformációkat mutatnak attól függően, hogy a transzportert milyen „állapotban” rögzítették), így például az R482 orientációja is változhat a transzport során. Mindenesetre egyértelmű, direkt kapcsolatot az R482 és a szerkezet meghatározásokkor használt szubsztrátok között nem sikerült kimutatni. Viszont a számítógépes modellek alapján az R482 a központi üreg felé néz, és a mutációja megváltoztatja a TM hélixek orientációját (Laszlo, Sarkadi, and Hegedus 2016).

Az ABCG2 koleszterinérzékelő régiói

Munkám egyik célja volt az ABCG2 koleszterinérzékelő régióinak feltárása. A térszerkezet hiányában olyan, az ABCG2-ben is fellelhető régiókat (LxxL és CRAC) vizsgáltunk (Gal

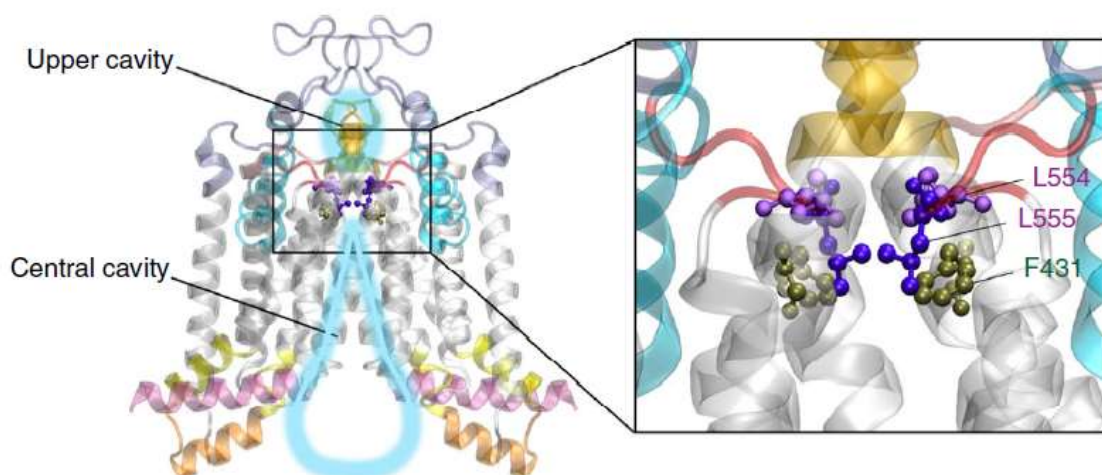
et al. 2015; Telbisz et al. 2014), amelyek más fehérjékben a koleszterin kötésben igazoltan részt vesznek. Azóta, az eddig meghatározott térszerkezetek közül kettőben azonosították az ABCG2-höz kötődő koleszterint. Taylor és mtsai, a szubsztrátkötő zsebben találtak két koleszterin molekulát (Taylor et al. 2017). Mivel azonban a koleszterin az eddigi tudásunk szerint az ABCG2-nek nem transzportálódó szubsztrátja, nincs kizárva, hogy a tisztításkor használt kolátot „látták” a cryo-EM során (Kerr et al. 2021). A másik szerkezetben (PDB 5NJ3) öt, hidrofób barázdába ágyazott koleszterin molekulát találtak ABCG2 monomerenként (Jackson et al. 2018)).

Sőt, az ABCG2 térszerkezetének ismeretében az is felmerült, hogy az NBD részét képező, de a nukleotid kötésben nem szorosan részt vevő A-hurok, amit RI-nek (regulatory insertion) javasolták átnevezni, a koleszterinérzékelésben is részt vehet, a koleszterin membránból való begyűjtésével (Sarkadi, Homolya, and Hegedus 2020). Ez irányú mutagenézis kísérletek azonban tudtommal még nem készültek. Végezetül, molekuladinamikai szimulációval azt találták, hogy a koleszterin a két ABCG2 „fél” TM2 és TM2' hélixeknek citoplazmikus részének záródását befolyásolja. A TM2 hélix közvetlenül részt vesz a szubsztrát kötő zseb kialakításában, így a koleszterin annak az elérhetőségét befolyásolhatja (Nagy et al. 2021).

Az általam vizsgált (LxxL és CRAC) motívumok Leu-jai, illetve Tyr-jai nincsenek olyan „közel” a koleszterinhez, hogy a kötésében részt vegyenek, viszont a térszerkezet alapján fontos szerkezeti elemek részét képezik.

Az LxxL elhelyezkedése:

Az ABCG2 TM hélicei két „üreg” alkotnak, amelyeken a szubsztrát áthalad a transzport során. Az alsó nagyobb (cavity 1 vagy Central cavity) és a felső (cavity 2 vagy Upper cavity) üreg egy dileucin „szelep” zárja el egymástól, ami nyitja, illetve zárja az átjárást a két üreg között. Ezt a szelepet az L554 és L555 alkotja (41. ábra).



41. ábra: A dileucin „szelep” (Khunweeraphong et al. 2019). Az ábra a két szubsztrátkötő üreget („Central cavity” és „Upper cavity”) és az őket elválasztó dileucin „szelepet” mutatja.

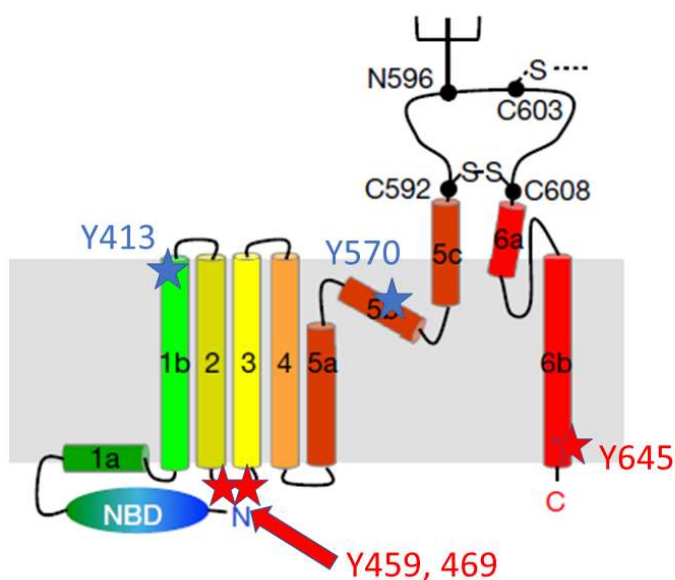
Munkám során jelentős szubsztrátfelismerésembeli különbséget tapasztaltam az L555 mutánsnál (a mutáns nem képes methotrexátot és ösztadiol-17 β D-glükuronidot transzportálni), ami jól magyarázható azzal, hogy ez a Leu a „szelep” részeként szabályozza a szubsztrát átjutását. Ráadásul azt tapasztaltuk, hogy az L555/558 mutáció rontja a fehérje stabilitását, legalábbis a tisztítás és rekonstrukció során. Későbbi mutagenézis vizsgálatainkban több csoport is arra a következtetésre jutott, hogy az L555 kisebb, hidrofób aminosavra történő cseréje alacsonyabb fehérjeexpressziót eredményez és nem csak a szubsztrát két üreg közötti mozgásában fontos, de a fehérje feltekeredéséhez is szükséges (Manolaridis et al. 2018; Khunweeraphong et al. 2019). Ez összhangban van a mi eredményeinkkel.

A térszerkezet alapján viszont az L555 a legközelebbi koleszterintől 12 Å távolságra van, így a térszerkezetek alapján nem lép közvetlen kölcsönhatásba a koleszterinnel, hatása inkább csak allosztérikus lehet (Jackson et al. 2018).

A CRAC motívum:

Vizsgálatainkban a feltételezett CRAC Tyr mutánsok nem változtatták meg az ABCG2 koleszterin érzékelését. Viszont a Y459, Y469 és Y645 Ser mutációi drámai hatással voltak a fehérje expressziójára és funkciójára. A Y459 és Y469 az ún. „coupling hélix” részét képezik, tehát fontosak lehetnek a megfelelő térszerkezet kialakításában. A koleszterinnel

viszont az ismert térszerkezetek alapján nincsenek közvetlen kapcsolatban. A harmadik, az ABCG2 működését döntően befolyásoló Tyr a 645. pozícióban található, és a térszerkezet alapján a mi korábbi topológia becslésünkkel szemben a 6. TM hélix része (42. ábra). A 6. TM hélix azonban nem vesz részt közvetlenül a szubsztrátkötő üreg kialakításában, így az általunk észlelt, az ABCG2 működésének elvesztését eredményező hatás allosztérikus lehet. A Y413 és Y570 a mutánsok (amelyek működésében lényeges eltérést nem tapasztaltunk) az 1. TM hélix extracelluláris tér felé eső részén, illetve a felső üregben találhatók. A térszerkezetek alapján nincsenek szoros kapcsolatban a koleszterinnel. Az Y413S mutáció viszont a szubsztrátfelismerés és az ATP hidrolízis látszólagos szétkapcsolását eredményezte. Ennek okára azonban a térszerkezet alapján sem találtunk magyarázatot.



42. ábra: A CRAC motívumok elhelyezkedése az ABCG2 fehérjében. A „javított” 2D szerkezet az ismert térszerkezet alapján került megalkotásra (Taylor et al. 2017). Az ábrán az N-glikozilációs hely és a 3. extracelluláris hurok diszulfid hidjainak kialakításában fontos ciszteinek is láthatók. A kép alapján (Taylor et al. 2017) készült.

Összegzésként elmondható, hogy az ABCG2 térszerkezet ismeretében sem lehet minden, mutánsok vizsgálatával tett megállapítást megmagyarázni, hiszen egy mutációnak allosztérikus, nem közvetlen hatása is lehet a fehérje konformációjára. Ráadásul a térszerkezetek egy-egy adott konformációs állapotot tükröznek, a transzporter pedig „mozog” a működése során.

3.) A tirozin kináz gátlók és ABCG2 kapcsolata

Munkám során elsőként mutattam ki, hogy a Gleevec és Iressa, klinikumban használt TKI-k kölcsönhatásba lépnek az ABCG2 fehérjével és az Iressa az ABCG2 potenciális szubsztátja (Ozvegy-Laczkó et al. 2004). Ebből a felfedezésből még számos további munkánk született. Létrehoztunk például egy olyan emlős sejtes (A431 humán epidermoid karcinóma) EGF-függő modellt, aminek segítségével igazoltuk, hogy az ABCG2 működése védi a sejteket az Iressa apoptotikus hatásával szemben (Elkind et al. 2005). Később újabb TKI-król igazoltuk, hogy azok ABCG2 szubsztátok (Hegedus, Ozvegy-Laczkó, Apati, et al. 2009; Hegedus, Ozvegy-Laczkó, Szakacs, et al. 2009; Hegedus, Truta-Feles, Antalffy, Brozik, et al. 2012; Hegedus, Truta-Feles, Antalffy, Varady, et al. 2012). Az ABCG2 tehát befolyásolja a TKI-k farmakokinetikáját, és a tumorokat rezisztensé teheti a TKI-k ellen. Akkori eredményeink alapján felvetettük, hogy a polimorfizmusokat is meg kell vizsgálni ezekkel a TKI-kal való kölcsönhatás szempontjából (Ozvegy-Laczkó, Cserepes, et al. 2005). Azóta ezt többen vizsgálták (egy friss összefoglaló erről itt olvasható (Kaehler and Cascorbi 2021)), de egyértelmű összefüggést nem találtak az ABCG2 leggyakoribb polimorfizmusai és a TKI-k farmakokinetikája vagy a terápia hatásossága között (Heyes, Kapoor, and Kerr 2018).

4.) Az 5D3 konformáció-szenzitív antitest további felhasználási területei

Elsőként mutattam ki, hogy az ABCG2 sejtfelszíni epitópját felismerő 5D3 antitest alkalmas az ABCG2 fehérje ATP hidrolízis során bekövetkező konformációs változásainak detektálására. Meghatároztam azokat a körülményeket, amelyek az ABCG2 érzékeny kimutatásához szükségesek (Ozvegy-Laczkó et al. 2008; Ozvegy-Laczkó, Varady, et al. 2005). Munkám során azt is felfedeztem, hogy a szubsztátok és nem transzportálódó inhibitorok eltérően befolyásolják az 5D3 kötődését. Az 5D3 antitest azóta egy széles körben alkalmazott eszközzé „nőtte ki magát”. **1)** A kutatócsoportunk egy új eljárást dolgozott ki („**5D3 antibody shift assay**”), ami alapján az ABCG2 szubsztátjai és inhibitorai elkülöníthetők (Telbisz et al. 2012). **2)** Az 5D3 antitest segítségével rögzítették például az ABCG2 fehérjét a **térszerkezet meghatározásakor** (Manolaridis et al. 2018; Jackson et al. 2018; Taylor et al. 2017) (és itt igazolták a mi korábbi felfedezésünket, amelyben az epitóp elhelyezkedését meghatároztuk, lásd Eredmények fejezet 25. ábra). **3)** Az 5D3 antitest segítségével az **ABCG2 sejten belüli vándorlása** is nyomon követhető

(Bartos and Homolya 2021). **4)** Az 5D3 antitest fontos **diagnosztikus eszközzé** is vált. Sarkadi Balázs kutatócsoportja dolgozott ki egy olyan, az 5D3 antitest felhasználásán alapuló módszert, amelynek segítségével az ABCG2 szintje meghatározható a vörösvértestekben (Kasza et al. 2012). Ezzel a módszerrel a fehérjeexpressziót megváltoztató polimorfizmusok kiszűrhetők, sőt ennek segítségével új ABCG2 változatot is sikerült azonosítaniuk (Zambo et al. 2018). Ennek például a köszvény kialakulásának előrejelzésében van jelentősége (Varady et al. 2013).

5.) Új módszerek az OATP-k vizsgálatában

Csoportunk elsőként vizsgálta mind a 11 humán OATP fehérjét egyazon sejtes rendszerben, amelynek során egy általános (Na-fluoreszcein), és egy, a multispecifikus OATP (1B1, 1B3, 1A2 és 2B1) fehérjékre specifikus fluoreszcens OATP (fluoreszcein-metotrexát) szubsztrátot azonosítottunk (Patik et al. 2015). Ezek segítségével az OATP-k szubsztrát/inhibitor kölcsönhatásai vizsgálhatók, amit később néhány OATP-nél mások is megerősítettek (Atilano-Roque and Joy 2017; Izumi et al. 2016). A továbbiakban dolgoztunk a humán OATP-ket kifejező emlős sejtes modellek (A431, HeLa, MDCKII és HEK-293) létrehozásán is, de nem minden OATP fehérjénél sikerült megfelelő expressziót elérni, és az előző festékeknel kedvezőbb tulajdonságú fluoreszcens indikátorokat kellett keresnünk.

Csoportunk egyik fő eredménye olyan nem sejtporomeabilis fluoreszcens festékek „megtalálása” volt, amelyek az OATP-k érzékeny kimutatására és működésük vizsgálatára alkalmasak. Több viabilitási festéket, szulfopiréneket és szulfurodaminokat azonosítottunk OATP szubsztrátként (Bakos, Nemet, et al. 2020; Patik et al. 2018; Szekely et al. 2020; Ungvari et al. 2021). Az új fluoreszcens festékszubsztrátok között találtunk specifikusakat, amely(eke)t csak néhány OATP ismer fel (Bakos, Nemet, et al. 2020; Patik et al. 2018; Ungvari et al. 2021). Ez jó eszköz lehet az OATP-k funkciójának elkülönítésére nem overexpresszáló rendszerekben, például májsejtekben vagy epiteliális modell sejtvonalakban. Hozzá kell azonban tenni, hogy nem overexpresszáló rendszerekben az új festékszubsztrátokat még nem volt módunk tesztelni. Ez tehát egy fontos további iránya lesz kutatásainknak. Itt elsősorban primer humán májsejt kultúrát lesz érdemes tesztelni, mert a tumor-eredetű vagy immortalizált májsejt vonalakat (HepG2, HepaRG) csökkent OATP transzporter expresszió jellemzi. A rágcéló modellek (például patkány májsejt

kultúra) szintén nem megfelelőek, mert a humán máj-specifikus OATP1B-knek nincs rágcsláló ortológja (Hagenbuch and Meier 2003).

A fluoreszcens festékek között találtunk olyanokat, amelyekkel a májsejtek OATP1B1 fehérjéje és az MRP2 együttesen vizsgálhatók (Szekely et al. 2020). Érdekes módon, korábban a karboxi-dikloro-fluoreszcein (CDCF) festéket OATP1B1 (Izumi et al. 2016) és MRP2 (Heredi-Szabo et al. 2008) szubsztrátként azonosították, és rutinszerűen alkalmazzák hepatocita szendvics kultúrában az epekanalikulusok megjelenítésére, MRP2 vizsgálatára, azonban OATP1B1 és MRP2 együttes vizsgálatában való alkalmasságát nem tesztelték. Így az általunk azonosított festékek az első igazolt kettős, OATP1B1 és MRP2 fluoreszcens próbák. Ezeknek a próbáknak humán májsejt kultúrán való tesztelése is egy fontos továbblépés lesz, amely további terveink között szerepel.

Az új festékszubsztrátok között több festéket, köztük a szulfrodaminokat azonosítottuk a tiroid hormon transzporter OATP1C1 szubsztrátjaként (Bakos, Nemet, et al. 2020). Az OATP1C1 a központi idegrendszer tiroid hormon ellátásában betöltött fontos szerepére nemrégiben derült fény (Stromme et al. 2018), de *in vitro* vizsgálatára a radioaktívan jelzett tiroxinon kívül eddig nem volt eszköz.

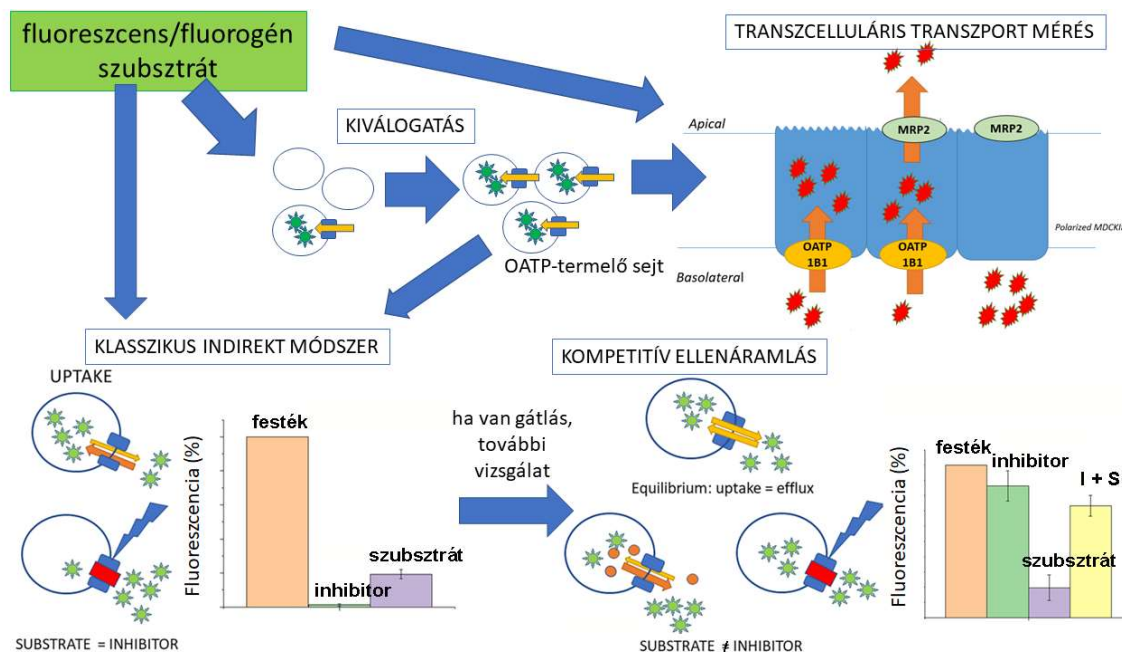
A festékek másik lehetséges alkalmazása az OATP-t termelő sejtek kiválogatása. Ennek segítségével az *in vitro* modellekben magas OATP expressziót lehet elérni, ami közel sem triviális. A magas OATP expressziójú sejtek segítségével nagy érzékenységgű, mikrolemezre adaptált módszert dolgoztunk ki. A kidolgozott módszerek és létrehozott sejtvonalak kapcsán csoportunk több hazai és nemzetközi megkeresést kapott, aminek során részt vettünk új OATP szubsztrátok és inhibitorok azonosításában. Ezek között van egy új, diagnosztikus próba (erlotinib) (Bauer et al. 2018), a táplálékunkban előforduló flavonoidok és metabolitjaik (Mohos, Fliszar-Nyul, Ungvari, Bakos, et al. 2020; Mohos, Fliszar-Nyul, Ungvari, Kuffa, et al. 2020), illetve egy antivirális szer (maraviroc) (Tupova et al. 2020). Létrehoztunk továbbá egy olyan sejt modellt, amiben az OATP2B1 és mCherry fehérjét együttesen fejeztettük ki. Ennek segítségével az FDA által jóváhagyott citosztatikumokat tudtunk tesztelni és olyan, potenciális OATP2B1 szubsztrátokat azonosítottunk, amelyekkel szemben az OATP2B1 érzékenyíti a sejteket (Windt et al. 2019). Ez volt az első vizsgálat, amelyben potenciálisan toxikus OATP szubsztrátok szisztematikus tesztelésére sor került.

Itt nem bemutatott (közlés előtt álló) munkánkban, szintén a festékfelvétel alapú kiválogatás segítségével sikerült olyan sejtvonalakat előállítani, amelyekben az eddig egyetlen, rákspecifikus OATP változatot, OATP1B3-V1 (Thakkar et al. 2013) tudtuk vizsgálni. Az OATP1B3-V1 a csak májban kifejeződő OATP1B3 alternatív transzkripcióval keletkező izoformája, ami egészséges szövetekben nem, de tumorokban (például vastagbél rák, tüdőrák) megjelenik. Szerepét, megfelelő lokalizációját és működését illetően az irodalmi adatok ellentmondásosak (Furihata, Sun, and Chiba 2015; Imai et al. 2013; Thakkar et al. 2013). Saját kutatásunk ezirányban is folytatódik, mind *in vitro*, mind pedig egér xenograftokon végzett kísérletek folyamatban vannak. Az OATP-k, különösen a tumorspecifikus OATP1B3-V1 izoforma felmerül olyan tumor markerként, amely diagnosztikus festéket felhalmozva felhasználható lehet tumorok detektálására. A Gd-EOB-DTPA MRI kontrasztanyag például igazolt OATP1B3-V1 szubsztrát (Imai et al. 2013). Azonban a fluoreszcens próbák, különösen az infravörös festékek tesztelése az OATP1B3-V1 változaton még nem történt meg. Kutatásainkat tehát ilyen irányba is ki fogjuk terjeszteni.

A másik új felfedezésünk az első olyan módszer megalkotása volt, amellyel a máj OATP-i, hasonlóan a P-gp-re széleskörben alkalmazott „calcein assay”-hez, valós időben, a festék kimosása nélkül vizsgálhatók (Ungvari et al. 2021). Habár kimutattuk, hogy az új „add-és-mérd” módszer más, overexpresszáló sejt modelleken is használható (például HEK-293, MDCKII), itt szintén felmerül olyan sejteken történő tesztelése, amelyek az OATP-eket endogénean termelik. Mindenesetre, mivel a festék indikátort ebben a módszerben nem kell a mérés végén eltávolítani, ez utat nyit az automatizálás és miniaturizálás felé. Fontos megjegyezni azonban, hogy a fluoreszcens indikátorral azonosított kölcsönhatást más teszt vegyülettel (Izumi et al. 2013), esetleg fiziológiásan releváns próbával is szükséges lehet megerősíteni. A leggyakrabban alkalmazott *in vitro* OATP próba a radioaktívan jelzett ösztron-3-szulfát, illetve fiziológiás próba lehet a coproporfirin I és III (Shen et al. 2017).

Végezetül, de nem utolsó sorban, a módszert olyan irányba fejlesztettük, amelynek segítségével a szubsztrátok és inhibitorok egyszerűen elkülöníthetők (kompetitív ellenáramlásos módszer, CCF (Ungvari et al. 2021)). Ez alapján javasolunk egy lehetséges kísérleti felállást, amelyben az általunk fejlesztett fluoreszcens módszerek segítségével egy kémiai entitásról (például a gyógyszerfejlesztés korai fázisában) eldönthető, hogy várható-e kölcsönhatása a máj OATP-ivel, és ha igen, az milyen természetű (43. ábra). Mivel további OATP-k, OATP1A2 és OATP1B3 relevánsak gyógyszerkölcsönhatás

szempontjából, folyamatban van olyan irányú kutatásunk, ahol ezen fehérjékre is tervezzük a CCF kidolgozását.



43. ábra: Az OATP-k vizsgálatára létrehozott új módszereink és egy új hatóanyag OATP-vel való kölcsönhatásának lehetséges tesztelési lépései. A fluoreszcens festék(ek) segítségével az OATP-t termelő sejtek kiválogathatók és dúsíthatók. A kettős OATP és MRP2 szubsztrát festékek segítségével az OATP1B1 és az MRP2 működése egy rendszerben vizsgálható. A „klasszikus” módszerrel az OATP-vel kölcsönható vegyületek azonosíthatók, majd a kompetitív ellenáramlásos módszerben a szubsztrátok és a nem transzportálódó inhibitorok elkülöníthetők. I: inhibitor, S: szubsztrát.

Az OATP-kre, habár cserélőként definiálják őket, úgy tekintenek, mint a gyógyszerek és egyéb szubsztrátjaik sejtbeli felvételét előmozdító (uptake) transzporterekre. A mi felfedezésünk, illetve Schaefer és mtsai eredményei (Schaefer, Bock, and Meyer Zu Schwabedissen 2018; Schaefer et al. 2020) alapján az OATP-k képesek két nagyméretű szubsztrát kicserélésére. Felmerül tehát, hogy vajon fiziológias körülmények között is képesek lehetnek-e szubsztrátjaik sejtől kifelé történő transzportjára, és ez hogyan befolyásolhatja például a farmakokinetikát.

A fluoreszcencia-alapú módszerfejlesztésen kívül intenzíven vizsgáltuk az OATP2B1 új típusú (13 α -ösztion alapú) inhibitorait. Eredményeink alapján együttműködő partnerünk (Mernyák Erzsébet és csoportja) különböző ösztion módosulatokat tervezett és szintetizált.

Ezek alapján nanomólos OATP2B1 inhibitorot sikerült fejleszteni (Jojart et al. 2021). Mivel az OATP2B1-specifikus inhibitorok alulreprezentáltak, Az újonnan azonosított ösztrognázis inhibitorok az OATP2B1 gátlószer új csoportját képviselik, amelyek összetett sejt alapú rendszerekben, ahol több OATP is jelen van, lehetnek jó eszközök az OATP2B1 funkciójának elkülönítésére.

Az OATP2B1 szubsztrát (és HSD1 gátló) vegyületek pedig a nemi hormonfüggő tumorok kezelésében jelenthetnek új stratégiát. Kutatásunk egyik tervezett iránya ennek a további vizsgálata, az azonosított, OATP2B1-szelektív anti-ösztrogének hormonfüggő modellsejteken történő vizsgálatával.

VII. A DISSZERTÁCIÓ ALAPJÁT KÉPEZŐ KÖZLEMÉNYEK

A dolgozatomban a PhD fokozatom megszerzése (2003) után született, már megjelent első vagy utolsó szerzős közleményeimet használtam fel.

1. **Özvegy-Laczka C**, Köblös G, Sarkadi B és Váradi A (2005) Single amino acid (482) variants of the ABCG2 multidrug transporter: major differences in transport capacity and substrate recognition. *BBA-Biomembranes* **1668**, 53-63.

IF.: 4,224

Független idéző: 54

2. Telbisz Á, Hegedüs C, Váradi A, Sarkadi B, **Özvegy-Laczka C**. Regulation of the function of the human ABCG2 multidrug transporter by cholesterol and bile acids: effects of mutations in potential substrate and steroid binding sites. *Drug Metab Dispos.* 2014 Apr;42(4):575-85.

IF: 3,252

Független idéző: 26

3. Gál Z, Hegedüs C, Szakács G, Váradi A, Sarkadi B, **Özvegy-Laczka C**. Mutations of the central tyrosines of putative cholesterol recognition amino acid consensus (CRAC) sequences modify folding, activity, and sterol-sensing of the human ABCG2 multidrug transporter. *Biochim Biophys Acta.* 2015 Feb;1848(2):477-87.

IF: 3,687

Független idéző: 12

4. **Özvegy-Laczka C**, Hegedus T, Várady G, Ujhelly O, Schuetz JD, Váradi A, Kéri G, Órfi L, Német K, Sarkadi B High-affinity interaction of tyrosine kinase inhibitors with the ABCG2 multidrug transporter. *Mol Pharmacol.* 2004 Jun;65(6):1485-95.

IF: 5,08

Független idéző: 281

5. **Özvegy-Laczka C**, Cserepes J, Elkind NB és Sarkadi B (2005) Tyrosine kinase inhibitor resistance in cancer: role of ABC multidrug transporters. *Drug Resist Update* **8**, 15-26.

IF.: 6,172

Független idéző: 112

6. **Özvegy-Laczka C***, Várady G, Köblös G, Ujhelly O, Cervenak J, Schuetz JD, Sorrentino BP, Koomen GJ, Váradi A, Németh K és Sarkadi B (2005) Function-dependent conformational changes of the ABCG2 multidrug transporter modify its interaction with a monoclonal antibody on the cell surface. *J Biol Chem* **280**, 4219-27.

IF: 5,854

Független idéző: 52

7. **Özvegy-Laczka C**, Laczkó R, Hegedus C, Litman T, Várady G, Goda K, Hegedus T, Dokholyan NV, Sorrentino BP, Váradi A és Sarkadi B (2008) Interaction with the 5D3 monoclonal antibody is regulated by intramolecular rearrangements but not by covalent dimer formation of the human ABCG2 multidrug transporter. *J Biol Chem* **283**, 26059-70.

IF.: 5,520

Független idéző: 21

8. Patik I, Kovacsics D, Németh O, Gera M, Várady G, Stieger B, Hagenbuch B, Szakács G, **Özvegy-Laczka C**. Functional expression of the 11 human Organic Anion Transporting Polypeptides in insect cells reveals that sodium fluorescein is a general OATP substrate. *Biochem Pharmacol.* 2015 Dec 15;98(4):649-58.

IF: 5,091

Független idéző: 14

9. Patik I, Székely V, Németh O, Szepesi Á, Kucsma N, Várady G, Szakács G, Bakos É, **Özvegy-Laczka C**. Identification of novel cell-impermeant fluorescent substrates for testing the function and drug interaction of Organic Anion-Transporting Polypeptides, OATP1B1/1B3 and 2B1. *Sci Rep.* 2018 8:2630

IF: 4,011

Független idéző: 6

10. Ungvári O, Király L, Bakos É, **Özvegy-Laczka C.** 8-acetoxy-trisulfopyrene as the first activatable fluorogenic probe for add-and-read assessment of Organic anion-transporting polypeptides, OATP1B1, OATP1B3, and OATP2B1. *FASEB J.* 2021 Sep;35(9):e21863.

IF: 5,191

11. Székely V, Patik I, Ungvári O, Telbisz Á, Szakács G, Bakos É, **Özvegy-Laczka C.** Fluorescent probes for the dual investigation of MRP2 and OATP1B1 function and drug interactions. *Eur J Pharm Sci.* 2020 Aug 1;151:105395.

IF: 4,384

Független idéző: 1

12. Bakos É, Német O, Patik I, Kucsma N, Várady G, Szakács G, **Özvegy-Laczka C.** A novel fluorescence-based functional assay for human OATP1A2 and OATP1C1 identifies interaction between third-generation P-gp inhibitors and OATP1A2. *FEBS J.* 2020 Jun;287(12):2468-2485.

IF: 4,392

13. Laczkó-Rigó R, Jójárt R, Mernyák E, Bakos É, Tuerkova A, Zdrzil B, **Özvegy-Laczka C.** Structural dissection of 13-epiestrones based on the interaction with human Organic anion-transporting polypeptide, OATP2B1. *J Steroid Biochem Mol Biol.* 2020 Jun;200:105652.

IF: 3,813

14. Laczkó-Rigó R, Bakos É, Jójárt R, Tömböly C, Mernyák E, **Özvegy-Laczka C.** Selective antiproliferative effect of C-2 halogenated 13 α -estrones on cells expressing Organic anion-transporting polypeptide 2B1 (OATP2B1). *Toxicol Appl Pharmacol.* 2021 Aug 30;429

IF: 4,219

15. Telbisz Á, Ambrus C, Mózner O, Szabó E, Várady G, Bakos É, Sarkadi B, **Özvegy-Laczka C***. Interactions of Potential Anti-COVID-19 Compounds with Multispecific ABC and OATP Drug Transporters. *Pharmaceutics*. 2021 Jan 9;13(1):81

IF: 6,321

Független idéző: 5

16. Kovacsics D, Patik I, **Özvegy-Laczka C**. The role of organic anion transporting polypeptides in drug absorption, distribution, excretion and drug-drug interactions. *Expert Opin Drug Metab Toxicol*. 2017 Apr;13(4):409-424.

IF: 3,151

Független idéző: 25

*: megosztott első vagy utolsó szerző

A dolgozat témájában benyújtott szabadalmak:

1. PCT/HU2020/050014 “Fluorescence method for assessing transport activity of OATPs and MRP2” benyújtás éve: 2020
2. PCT/HU2020/050062 “A REAL-TIME, ADD-AND-READ FLUORESCENCE-BASED ASSAY FOR TESTING FUNCTION AND DRUG INTERACTIONS OF OATP TRANSPORTERS” benyújtás éve: 2020

VIII. A DISSZERTÁCIÓHOZ KAPCSOLÓDÓ TOVÁBBI KÖZLEMÉNYEK

1. Bakos E, Tusnády GE, Német O, Patik I, Magyar Cs, Németh K, Kele P, **Özvegy-Laczka C**. Synergistic transport of a fluorescent coumarin probe marks coumarins as pharmacological modulators of Organic anion-transporting polypeptide, OATP3A1. *Biochemical Pharmacology*, 2020 Dec;182:114250.
2. Tuerkova A, Ungvári O, Laczkó-Rigó R, Mernyák E, Szakács G, **Özvegy-Laczka C**, Zdrzil B.J Data-Driven Ensemble Docking to Map Molecular Interactions of Steroid Analogs with Hepatic Organic Anion Transporting Polypeptides. *Chem Inf Model*. 2021 Jun 28;61(6):3109-3127.
3. Jójárt R, Laczkó-Rigó R, Klement M, Kóhl G, Kecskeméti G, **Özvegy-Laczka C**, Mernyák E. Design, synthesis and biological evaluation of novel estrone phosphonates as high affinity organic anion-transporting polypeptide 2B1 (OATP2B1) inhibitors. *Bioorg Chem*. 2021 Jul;112:104914
4. Mohos V, Fliszár-Nyúl E, Ungvári O, Bakos É, Kuffa K, Bencsik T, Zsidó BZ, Hetényi C, Telbisz Á, **Özvegy-Laczka C**, Poór M. Effects of chrysin and its major conjugated metabolites chrysin-7-sulfate and chrysin-7-glucuronide on cytochrome P450 enzymes, and on OATP, P-gp, BCRP and MRP2 transporters. *Drug Metab Dispos*. 2020 Jul 13: DMD-AR-2020-000085.
5. Tupova L, Hirschmugl B, Pilarova V, Székely V, Bakos É, Sucha S, Novakova L, **Özvegy-Laczka C**, Wadsack C, Ceckova M Interplay of drug transporters P-glycoprotein (MDR1), MRP1, OATP1A2 and OATP1B3 in passage of maraviroc across human placenta. *Biomedicine & Pharmacotherapy* 2020 129:110506
6. Violetta Mohos, Eszter Fliszár-Nyúl, Orsolya Ungvári, Éva Bakos, Katalin Kuffa, Paul W. Needs, Paul A. Kroon, Ágnes Telbisz, **Csilla Özvegy-Laczka** and Miklós Poór. Inhibitory Effects of Quercetin and Its Main Methyl, Sulfate, and Glucuronic Acid Conjugates on Cytochrome P450 Enzymes, and on OATP, BCRP and MRP2 Transporters. *Nutrients* 2020 Jul 31;12(8):2306.

7. Windt T, Tóth S, Patik I, Sessler J, Kucsma N, Szepesi Á, Zdrazil B, **Özvegy-Laczka C**, Szakács G. Identification of anticancer OATP2B1 substrates by an in vitro triple-fluorescence-based cytotoxicity screen. *Arch Toxicol*. 2019 93:953-964
8. Jójárt R, Pécsy S, Keglevich G, Szécsi M, Rigó R, **Özvegy-Laczka C**, Kecskeméti G, Mernyák E. Pd-Catalyzed microwave-assisted synthesis of phosphonated 13 α -estrone as potential OATP2B1, 17 β -HSD1 and/or STS inhibitors. *Beilstein J Org Chem*. 2018 14:2838-2845
9. Bauer M, Matsuda A, Wulkersdorfer B, Philippe C, Traxl A, **Özvegy-Laczka C**, Stanek J, Nics L, Klebermass EM, Poschner S, Jäger W, Patik I, Bakos É, Szakács G, Wadsak W, Hacker M, Zeitlinger M, Langer O. Influence of OATPs on Hepatic Disposition of Erlotinib Measured With Positron Emission Tomography. *Clin Pharmacol Ther*. 2018 104:139-147
10. Rižner TL, Thalhammer T, **Özvegy-Laczka C**. The Importance of Steroid Uptake and Intracrine Action in Endometrial and Ovarian Cancers. *Front Pharmacol*. 2017 Jun 19;8:346.
11. Telbisz Á, Hegedüs C, **Özvegy-Laczka C**, Goda K, Várady G, Takáts Z, Szabó E, Sorrentino BP, Váradi A, Sarkadi B. Antibody binding shift assay for rapid screening of drug interactions with the human ABCG2 multidrug transporter. *Eur J Pharm Sci*. 2012 Jan 23;45(1-2):101-9.
12. Ambrus C, Bakos É, Sarkadi B, **Özvegy-Laczka C**, Telbisz Á. Interactions of anti-COVID-19 drug candidates with hepatic transporters may cause liver toxicity and affect pharmacokinetics. *Sci Rep*. 2021 Sep 8;11(1):17810.

IX. KÖSZÖNETNYILVÁNÍTÁS

Nagy hálával tartozom Váradi Andrásnak (Döcének) és Sarkadi Balázsnak, akik már egyetemi éveim, majd PhD munkám során a témavezetőim voltak, segítettek, irányították a munkámat, és a mai napig a mentoraim. Rengeteg tudást és támogatást kaptam, kapok tőlük. Az általuk megteremtett Biomembrán közösség igazán inspiráló és baráti közeg. Hálás vagyok, hogy a tagja lehetek.

Köszönöm Szakács Gergelynek, hogy tudásával, építő kritikáival és önzetlen támogatásával a PhD éveim kezdete óta segíti munkámat!

Az elért eredmény csapatmunka. Végtelenül hálás vagyok Bakos Évának, aki régi kollégaként és példaképmként, sok év kihagyást követően csatlakozott a munkánkhoz, és adott nagy tudásával lendületet az OATP-s kutatásainknak, inspiráló a vele való szakmai diskurzus.

Köszönettel tartozom korábbi és jelenlegi diákjaimnak, elsősorban Patik Izabelnek, Német Orsinak, Székely Virágnak, Laczkó-Rigó Rékának és Ungvári Orsinak, akik munkájukkal lehetővé tették az eredmények megszületését.

Az ABCG2-es munkákban Telbisz Ágnessel és Várady Györggyel dolgoztunk együtt, és ez az együttműködés azóta is tart, amit ezúton is nagyon köszönök! Az ABCG2-es munkákban sokat segítettek az asszisztensek, Zombori Ilona (Mica), Andrási Zsuzsa, Krizsán Éva, Kis Judit és Bézsényi Gyöngyi. Köszönöm nekik!

Köszönöm az Enzimológiai Intézet kutató közösségének, hogy befogadtak, és a Természettudományi Kutatóközpontnak a kutatásunkhoz biztosított háttérrel!

A munkámat számos ösztöndíj és pályázat támogatta, köztük a Magyar Tudományos Akadémia Bolyai János kutatási ösztöndíja és az OTKA (NKFIH), amit ezúton is köszönök!

Végül, de nem utolsó sorban köszönöm a családomnak, hogy vannak, támogatnak és elviselnek. A nagymamáknak, hogy vigyáztak a gyermekeimre, ha kellett. Négy gyermekem az életem értelme. Ők és a férjem szeretete a biztos háttér és örömforrás, ami átsegített kutatói pályám számos nehéz pillanatán.

Köszönöm mindannyiuknak!

X. IRODALOMJEGYZÉK

- Abe, T., M. Unno, T. Onogawa, T. Tokui, T. N. Kondo, R. Nakagomi, H. Adachi, K. Fujiwara, M. Okabe, T. Suzuki, K. Nunoki, E. Sato, M. Kakyo, T. Nishio, J. Sugita, N. Asano, M. Tanemoto, M. Seki, F. Date, K. Ono, Y. Kondo, K. Shiiba, M. Suzuki, H. Ohtani, T. Shimosegawa, K. Iinuma, H. Nagura, S. Ito, and S. Matsuno. 2001. 'LST-2, a human liver-specific organic anion transporter, determines methotrexate sensitivity in gastrointestinal cancers', *Gastroenterology*, 120: 1689-99.
- Allen, J. D., S. C. Jackson, and A. H. Schinkel. 2002. 'A mutation hot spot in the Bcrp1 (Abcg2) multidrug transporter in mouse cell lines selected for Doxorubicin resistance', *Cancer Res*, 62: 2294-9.
- Allen, J. D., A. van Loevezijn, J. M. Lakhai, M. van der Valk, O. van Tellingen, G. Reid, J. H. Schellens, G. J. Koomen, and A. H. Schinkel. 2002. 'Potent and specific inhibition of the breast cancer resistance protein multidrug transporter in vitro and in mouse intestine by a novel analogue of fumitremorgin C', *Mol Cancer Ther*, 1: 417-25.
- Allikmets, R., L. M. Schriml, A. Hutchinson, V. Romano-Spica, and M. Dean. 1998. 'A human placenta-specific ATP-binding cassette gene (ABCP) on chromosome 4q22 that is involved in multidrug resistance', *Cancer Res*, 58: 5337-9.
- Atilano-Roque, A., and M. S. Joy. 2017. 'Characterization of simvastatin acid uptake by organic anion transporting polypeptide 3A1 (OATP3A1) and influence of drug-drug interaction', *Toxicol In Vitro*, 45: 158-65.
- Bacsa, I., R. Jojart, G. Schneider, J. Wolfling, P. Maroti, B. E. Herman, M. Szecsi, and E. Mernyak. 2015. 'Synthesis of A-ring halogenated 13alpha-estrone derivatives as potential 17beta-HSD1 inhibitors', *Steroids*, 104: 230-6.
- Bakos, E., R. Evers, G. Calenda, G. E. Tusnady, G. Szakacs, A. Varadi, and B. Sarkadi. 2000. 'Characterization of the amino-terminal regions in the human multidrug resistance protein (MRP1)', *J Cell Sci*, 113 Pt 24: 4451-61.
- Bakos, E., O. Nemet, I. Patik, N. Kucsma, G. Varady, G. Szakacs, and C. Ozvegy-Laczka. 2020. 'A novel fluorescence-based functional assay for human OATP1A2 and OATP1C1 identifies interaction between third-generation P-gp inhibitors and OATP1A2', *FEBS J*, 287: 2468-85.
- Bakos, E., G. E. Tusnady, O. Nemet, I. Patik, C. Magyar, K. Nemeth, P. Kele, and C. Ozvegy-Laczka. 2020. 'Synergistic transport of a fluorescent coumarin probe marks coumarins as pharmacological modulators of Organic anion-transporting polypeptide, OATP3A1', *Biochem Pharmacol*, 182: 114250.
- Banerjee, N., C. Allen, and R. Bendayan. 2012. 'Differential role of organic anion-transporting polypeptides in estrone-3-sulphate uptake by breast epithelial cells and breast cancer cells', *J Pharmacol Exp Ther*, 342: 510-9.
- Bartos, Z., and L. Homolya. 2021. 'Identification of Specific Trafficking Defects of Naturally Occurring Variants of the Human ABCG2 Transporter', *Front Cell Dev Biol*, 9: 615729.
- Bauer, M., A. Matsuda, B. Wulkersdorfer, C. Philippe, A. Traxl, C. Ozvegy-Laczka, J. Stanek, L. Nics, E. M. Klebermass, S. Poschner, W. Jager, I. Patik, E. Bakos, G. Szakacs, W. Wadsak, M. Hacker, M. Zeitlinger, and O. Langer. 2018. 'Influence of OATPs on Hepatic Disposition of Erlotinib Measured With Positron Emission Tomography', *Clin Pharmacol Ther*, 104: 139-47.
- Buxhofer-Ausch, V., L. Secky, K. Wlcek, M. Svoboda, V. Kounnis, E. Briasoulis, A. G. Tzakos, W. Jaeger, and T. Thalhammer. 2013. 'Tumor-specific expression of organic anion-transporting polypeptides: transporters as novel targets for cancer therapy', *J Drug Deliv*, 2013: 863539.
- Cesar-Razquin, A., B. Snijder, T. Frappier-Brinton, R. Isserlin, G. Gyimesi, X. Bai, R. A. Reithmeier, D. Hepworth, M. A. Hediger, A. M. Edwards, and G. Superti-Furga. 2015. 'A Call for Systematic Research on Solute Carriers', *Cell*, 162: 478-87.
- Chen, Z. S., R. W. Robey, M. G. Belinsky, I. Shchaveleva, X. Q. Ren, Y. Sugimoto, D. D. Ross, S. E. Bates, and G. D. Kruh. 2003. 'Transport of methotrexate, methotrexate polyglutamates, and 17beta-estradiol

- 17-(beta-D-glucuronide) by ABCG2: effects of acquired mutations at R482 on methotrexate transport', *Cancer Res*, 63: 4048-54.
- Choudhuri, S., and C. D. Klaassen. 2020. 'Elucidation of OATP1B1 and 1B3 transporter function using transgenic rodent models and commonly known single nucleotide polymorphisms', *Toxicol Appl Pharmacol*, 399: 115039.
- Cserepes, J., Z. Szentpetery, L. Seres, C. Ozvegy-Laczkó, T. Langmann, G. Schmitz, H. Glavinas, I. Klein, L. Homolya, A. Varadi, B. Sarkadi, and N. B. Elkind. 2004. 'Functional expression and characterization of the human ABCG1 and ABCG4 proteins: indications for heterodimerization', *Biochem Biophys Res Commun*, 320: 860-7.
- Dano, K. 1973. 'Active outward transport of daunomycin in resistant Ehrlich ascites tumor cells', *Biochim Biophys Acta*, 323: 466-83.
- De Bruyn, T., S. Fattah, B. Stieger, P. Augustijns, and P. Annaert. 2011. 'Sodium fluorescein is a probe substrate for hepatic drug transport mediated by OATP1B1 and OATP1B3', *J Pharm Sci*, 100: 5018-30.
- Dean, M. 2005. 'The genetics of ATP-binding cassette transporters', *Methods Enzymol*, 400: 409-29.
- Dean, M., and R. Allikmets. 1995. 'Evolution of ATP-binding cassette transporter genes', *Curr Opin Genet Dev*, 5: 779-85.
- Diop, N. K., and C. A. Hrycyna. 2005. 'N-Linked glycosylation of the human ABC transporter ABCG2 on asparagine 596 is not essential for expression, transport activity, or trafficking to the plasma membrane', *Biochemistry*, 44: 5420-9.
- Doyle, L. A., W. Yang, L. V. Abruzzo, T. Krogmann, Y. Gao, A. K. Rishi, and D. D. Ross. 1998. 'A multidrug resistance transporter from human MCF-7 breast cancer cells', *Proc Natl Acad Sci U S A*, 95: 15665-70.
- Drozdik, M., C. Groer, J. Penski, J. Lapczuk, M. Ostrowski, Y. Lai, B. Prasad, J. D. Unadkat, W. Siegmund, and S. Oswald. 2014. 'Protein abundance of clinically relevant multidrug transporters along the entire length of the human intestine', *Mol Pharm*, 11: 3547-55.
- Dumitrescu, A. M., X. H. Liao, T. B. Best, K. Brockmann, and S. Refetoff. 2004. 'A novel syndrome combining thyroid and neurological abnormalities is associated with mutations in a monocarboxylate transporter gene', *Am J Hum Genet*, 74: 168-75.
- Elkind, N. B., Z. Szentpetery, A. Apati, C. Ozvegy-Laczkó, G. Varady, O. Ujhelly, K. Szabo, L. Homolya, A. Varadi, L. Buday, G. Keri, K. Nemet, and B. Sarkadi. 2005. 'Multidrug transporter ABCG2 prevents tumor cell death induced by the epidermal growth factor receptor inhibitor Iressa (ZD1839, Gefitinib)', *Cancer Res*, 65: 1770-7.
- Epand, R. M. 2008. 'Proteins and cholesterol-rich domains', *Biochim Biophys Acta*, 1778: 1576-82.
- Fostier, C. R., L. Monlezun, F. Ousalem, S. Singh, J. F. Hunt, and G. Boel. 2021. 'ABC-F translation factors: from antibiotic resistance to immune response', *FEBS Lett*, 595: 675-706.
- Furihata, T., Y. Sun, and K. Chiba. 2015. 'Cancer-type Organic Anion Transporting Polypeptide 1B3: Current Knowledge of the Gene Structure, Expression Profile, Functional Implications and Future Perspectives', *Curr Drug Metab*, 16: 474-85.
- Furukawa, T., K. Wakabayashi, A. Tamura, H. Nakagawa, Y. Morishima, Y. Osawa, and T. Ishikawa. 2009. 'Major SNP (Q141K) variant of human ABC transporter ABCG2 undergoes lysosomal and proteasomal degradations', *Pharm Res*, 26: 469-79.
- Gal, Z., C. Hegedus, G. Szakacs, A. Varadi, B. Sarkadi, and C. Ozvegy-Laczkó. 2015. 'Mutations of the central tyrosines of putative cholesterol recognition amino acid consensus (CRAC) sequences modify folding, activity, and sterol-sensing of the human ABCG2 multidrug transporter', *Biochim Biophys Acta*, 1848: 477-87.
- Gan, B. S., E. Krump, L. D. Shrode, and S. Grinstein. 1998. 'Loading pyranine via purinergic receptors or hypotonic stress for measurement of cytosolic pH by imaging', *Am J Physiol*, 275: C1158-66.
- Gao, B., B. Hagenbuch, G. A. Kullak-Ublick, D. Benke, A. Aguzzi, and P. J. Meier. 2000. 'Organic anion-transporting polypeptides mediate transport of opioid peptides across blood-brain barrier', *J Pharmacol Exp Ther*, 294: 73-9.
- Glavinas, H., O. von Richter, K. Vojnits, D. Mehn, I. Wilhelm, T. Nagy, J. Janossy, I. Krizbai, P. Couraud, and P. Krajcsi. 2011. 'Calcein assay: a high-throughput method to assess P-gp inhibition', *Xenobiotica*, 41: 712-9.
- Gong, I. Y., and R. B. Kim. 2013. 'Impact of genetic variation in OATP transporters to drug disposition and response', *Drug Metab Pharmacokinet*, 28: 4-18.

- Gorczyca, L., and L. M. Aleksunes. 2020. 'Transcription factor-mediated regulation of the BCRP/ABCG2 efflux transporter: a review across tissues and species', *Expert Opin Drug Metab Toxicol*, 16: 239-53.
- Gottesman, M. M., and V. Ling. 2006. 'The molecular basis of multidrug resistance in cancer: the early years of P-glycoprotein research', *FEBS Lett*, 580: 998-1009.
- Group, Search Collaborative, E. Link, S. Parish, J. Armitage, L. Bowman, S. Heath, F. Matsuda, I. Gut, M. Lathrop, and R. Collins. 2008. 'SLCO1B1 variants and statin-induced myopathy--a genomewide study', *N Engl J Med*, 359: 789-99.
- Grube, M., K. Kock, S. Karner, S. Reuther, C. A. Ritter, G. Jedlitschky, and H. K. Kroemer. 2006. 'Modification of OATP2B1-mediated transport by steroid hormones', *Mol Pharmacol*, 70: 1735-41.
- Gui, C., Y. Miao, L. Thompson, B. Wahlgren, M. Mock, B. Stieger, and B. Hagenbuch. 2008. 'Effect of pregnane X receptor ligands on transport mediated by human OATP1B1 and OATP1B3', *Eur J Pharmacol*, 584: 57-65.
- Gui, C., A. Obaidat, R. Chaguturu, and B. Hagenbuch. 2010. 'Development of a cell-based high-throughput assay to screen for inhibitors of organic anion transporting polypeptides 1B1 and 1B3', *Curr Chem Genomics*, 4: 1-8.
- Guragossian, N., B. Belhani, A. Moreno, M. T. Nunes, L. Gonzalez-Lobato, C. Marminon, L. Berthier, A. D. Rocio Andrade Pires, C. Ozvegy-Laczka, B. Sarkadi, R. Terreux, Z. Bouaziz, M. Berredjem, J. Jose, A. Di Pietro, P. Falson, and M. Le Borgne. 2021. 'Uncompetitive nanomolar dimeric indenoindole inhibitors of the human breast cancer resistance pump ABCG2', *Eur J Med Chem*, 211: 113017.
- Hagenbuch, B., and P. J. Meier. 2003. 'The superfamily of organic anion transporting polypeptides', *Biochim Biophys Acta*, 1609: 1-18.
- . 2004. 'Organic anion transporting polypeptides of the OATP/SLC21 family: phylogenetic classification as OATP/SLCO superfamily, new nomenclature and molecular/functional properties', *Pflugers Arch*, 447: 653-65.
- Hagenbuch, B., and B. Stieger. 2013. 'The SLCO (former SLC21) superfamily of transporters', *Mol Aspects Med*, 34: 396-412.
- Hagos, L., and S. Hulsmann. 2016. 'Unspecific labelling of oligodendrocytes by sulforhodamine 101 depends on astrocytic uptake via the thyroid hormone transporter OATP1C1 (SLCO1C1)', *Neurosci Lett*, 631: 13-18.
- Hamada, A., T. Sissung, D. K. Price, R. Danesi, C. H. Chau, N. Sharifi, D. Venzon, K. Maeda, K. Nagao, A. Sparreboom, H. Mitsuya, W. L. Dahut, and W. D. Figg. 2008. 'Effect of SLCO1B3 haplotype on testosterone transport and clinical outcome in caucasian patients with androgen-independent prostatic cancer', *Clin Cancer Res*, 14: 3312-8.
- Hanggi, E., A. F. Grundschober, S. Leuthold, P. J. Meier, and M. V. St-Pierre. 2006. 'Functional analysis of the extracellular cysteine residues in the human organic anion transporting polypeptide, OATP2B1', *Mol Pharmacol*, 70: 806-17.
- Hediger, M. A., B. Clemençon, R. E. Burrier, and E. A. Bruford. 2013. 'The ABCs of membrane transporters in health and disease (SLC series): introduction', *Mol Aspects Med*, 34: 95-107.
- Hegedus, C., C. Ozvegy-Laczka, A. Apati, M. Magocsi, K. Nemet, L. Orfi, G. Keri, M. Katona, Z. Takats, A. Varadi, G. Szakacs, and B. Sarkadi. 2009. 'Interaction of nilotinib, dasatinib and bosutinib with ABCB1 and ABCG2: implications for altered anti-cancer effects and pharmacological properties', *Br J Pharmacol*, 158: 1153-64.
- Hegedus, C., C. Ozvegy-Laczka, G. Szakacs, and B. Sarkadi. 2009. 'Interaction of ABC multidrug transporters with anticancer protein kinase inhibitors: substrates and/or inhibitors?', *Curr Cancer Drug Targets*, 9: 252-72.
- Hegedus, C., A. Telbisz, T. Hegedus, B. Sarkadi, and C. Ozvegy-Laczka. 2015. 'Lipid regulation of the ABCB1 and ABCG2 multidrug transporters', *Adv Cancer Res*, 125: 97-137.
- Hegedus, C., K. Truta-Feles, G. Antalffy, A. Brozik, I. Kasza, K. Nemet, T. I. Orban, C. Ozvegy-Laczka, A. Varadi, and B. Sarkadi. 2012. 'PI3-kinase and mTOR inhibitors differently modulate the function of the ABCG2 multidrug transporter', *Biochem Biophys Res Commun*, 420: 869-74.
- Hegedus, C., K. Truta-Feles, G. Antalffy, G. Varady, K. Nemet, C. Ozvegy-Laczka, G. Keri, L. Orfi, G. Szakacs, J. Settleman, A. Varadi, and B. Sarkadi. 2012. 'Interaction of the EGFR inhibitors gefitinib, vandetanib, pelitinib and neratinib with the ABCG2 multidrug transporter: implications for the emergence and reversal of cancer drug resistance', *Biochem Pharmacol*, 84: 260-7.
- Hegedus, T., L. Orfi, A. Seprodi, A. Varadi, B. Sarkadi, and G. Keri. 2002. 'Interaction of tyrosine kinase inhibitors with the human multidrug transporter proteins, MDR1 and MRP1', *Biochim Biophys Acta*, 1587: 318-25.

- Hegy, Z., and L. Homolya. 2016. 'Functional Cooperativity between ABCG4 and ABCG1 Isoforms', *PLoS One*, 11: e0156516.
- Henriksen, U., J. U. Fog, T. Litman, and U. Gether. 2005. 'Identification of intra- and intermolecular disulfide bridges in the multidrug resistance transporter ABCG2', *J Biol Chem*, 280: 36926-34.
- Heredi-Szabo, K., E. Kis, E. Molnar, A. Gyorfi, and P. Krajcsi. 2008. 'Characterization of 5(6)-carboxy-2,'7'-dichlorofluorescein transport by MRP2 and utilization of this substrate as a fluorescent surrogate for LTC4', *J Biomol Screen*, 13: 295-301.
- Heyes, N., P. Kapoor, and I. D. Kerr. 2018. 'Polymorphisms of the Multidrug Pump ABCG2: A Systematic Review of Their Effect on Protein Expression, Function, and Drug Pharmacokinetics', *Drug Metab Dispos*, 46: 1886-99.
- Hirota, T., Y. Fujita, and I. Ieiri. 2020. 'An updated review of pharmacokinetic drug interactions and pharmacogenetics of statins', *Expert Opin Drug Metab Toxicol*, 16: 809-22.
- Hollo, Z., L. Homolya, C. W. Davis, and B. Sarkadi. 1994. 'Calcein accumulation as a fluorometric functional assay of the multidrug transporter', *Biochim Biophys Acta*, 1191: 384-8.
- Hollo, Z., L. Homolya, T. Hegedus, and B. Sarkadi. 1996. 'Transport properties of the multidrug resistance-associated protein (MRP) in human tumour cells', *FEBS Lett*, 383: 99-104.
- Homolya, L. 2021. 'Medically Important Alterations in Transport Function and Trafficking of ABCG2', *Int J Mol Sci*, 22.
- Honjo, Y., C. A. Hrycyna, Q. W. Yan, W. Y. Medina-Perez, R. W. Robey, A. van de Laar, T. Litman, M. Dean, and S. E. Bates. 2001. 'Acquired mutations in the MXR/BCRP/ABCP gene alter substrate specificity in MXR/BCRP/ABCP-overexpressing cells', *Cancer Res*, 61: 6635-9.
https://www.ema.europa.eu/en/documents/scientific-guideline/guideline-investigation-drug-interactions-revision-1_en.pdf.
<https://www.fda.gov/files/drugs/published/In-Vitro-Metabolism--and-Transporter--Mediated-Drug-Drug-Interaction-Studies-Guidance-for-Industry.pdf>.
- Huber, R. D., B. Gao, M. A. Sidler Pfandler, W. Zhang-Fu, S. Leuthold, B. Hagenbuch, G. Folkers, P. J. Meier, and B. Stieger. 2007. 'Characterization of two splice variants of human organic anion transporting polypeptide 3A1 isolated from human brain', *Am J Physiol Cell Physiol*, 292: C795-806.
- Imai, S., R. Kikuchi, Y. Tsuruya, S. Naoi, S. Nishida, H. Kusuhara, and Y. Sugiyama. 2013. 'Epigenetic regulation of organic anion transporting polypeptide 1B3 in cancer cell lines', *Pharm Res*, 30: 2880-90.
- International Transporter, Consortium, K. M. Giacomini, S. M. Huang, D. J. Tweedie, L. Z. Benet, K. L. Brouwer, X. Chu, A. Dahlin, R. Evers, V. Fischer, K. M. Hillgren, K. A. Hoffmaster, T. Ishikawa, D. Keppler, R. B. Kim, C. A. Lee, M. Niemi, J. W. Polli, Y. Sugiyama, P. W. Swaan, J. A. Ware, S. H. Wright, S. W. Yee, M. J. Zamek-Gliszczynski, and L. Zhang. 2010. 'Membrane transporters in drug development', *Nat Rev Drug Discov*, 9: 215-36.
- Izumi, S., Y. Nozaki, T. Komori, K. Maeda, O. Takenaka, K. Kusano, T. Yoshimura, H. Kusuhara, and Y. Sugiyama. 2013. 'Substrate-dependent inhibition of organic anion transporting polypeptide 1B1: comparative analysis with prototypical probe substrates estradiol-17beta-glucuronide, estrone-3-sulfate, and sulfobromophthalein', *Drug Metab Dispos*, 41: 1859-66.
- Izumi, S., Y. Nozaki, T. Komori, O. Takenaka, K. Maeda, H. Kusuhara, and Y. Sugiyama. 2016. 'Investigation of Fluorescein Derivatives as Substrates of Organic Anion Transporting Polypeptide (OATP) 1B1 To Develop Sensitive Fluorescence-Based OATP1B1 Inhibition Assays', *Mol Pharm*, 13: 438-48.
- Jackson, S. M., I. Manolaridis, J. Kowal, M. Zechner, N. M. I. Taylor, M. Bause, S. Bauer, R. Bartholomaeus, G. Bernhardt, B. Koenig, A. Buschauer, H. Stahlberg, K. H. Altmann, and K. P. Locher. 2018. 'Structural basis of small-molecule inhibition of human multidrug transporter ABCG2', *Nat Struct Mol Biol*, 25: 333-40.
- Jacquemin, E., B. Hagenbuch, B. Stieger, A. W. Wolkoff, and P. J. Meier. 1994. 'Expression cloning of a rat liver Na(+)-independent organic anion transporter', *Proc Natl Acad Sci U S A*, 91: 133-7.
- Jiao, Q., L. Bi, Y. Ren, S. Song, Q. Wang, and Y. S. Wang. 2018. 'Advances in studies of tyrosine kinase inhibitors and their acquired resistance', *Mol Cancer*, 17: 36.
- Jojart, R., R. Laczko-Rigo, M. Klement, G. Kohl, G. Kecskemeti, C. Ozvegy-Laczka, and E. Mernyak. 2021. 'Design, synthesis and biological evaluation of novel estrone phosphonates as high affinity organic anion-transporting polypeptide 2B1 (OATP2B1) inhibitors', *Bioorg Chem*, 112: 104914.
- Jojart, R., S. Pecszy, G. Keglevich, M. Szecsi, R. Rigo, C. Ozvegy-Laczka, G. Kecskemeti, and E. Mernyak. 2018. 'Pd-Catalyzed microwave-assisted synthesis of phosphonated 13alpha-estrones as potential OATP2B1, 17beta-HSD1 and/or STS inhibitors', *Beilstein J Org Chem*, 14: 2838-45.

- Jonker, J. W., M. Buitelaar, E. Wagenaar, M. A. Van Der Valk, G. L. Scheffer, R. J. Scheper, T. Plosch, F. Kuipers, R. P. Elferink, H. Rosing, J. H. Beijnen, and A. H. Schinkel. 2002. 'The breast cancer resistance protein protects against a major chlorophyll-derived dietary phototoxin and protoporphyrin', *Proc Natl Acad Sci U S A*, 99: 15649-54.
- Jonker, J. W., J. W. Smit, R. F. Brinkhuis, M. Maliepaard, J. H. Beijnen, J. H. Schellens, and A. H. Schinkel. 2000. 'Role of breast cancer resistance protein in the bioavailability and fetal penetration of topotecan', *J Natl Cancer Inst*, 92: 1651-6.
- Juliano, R. L., and V. Ling. 1976. 'A surface glycoprotein modulating drug permeability in Chinese hamster ovary cell mutants', *Biochim Biophys Acta*, 455: 152-62.
- Kaehler, M., and I. Cascorbi. 2021. 'Pharmacogenomics of Impaired Tyrosine Kinase Inhibitor Response: Lessons Learned From Chronic Myelogenous Leukemia', *Front Pharmacol*, 12: 696960.
- Kage, K., S. Tsukahara, T. Sugiyama, S. Asada, E. Ishikawa, T. Tsuruo, and Y. Sugimoto. 2002. 'Dominant-negative inhibition of breast cancer resistance protein as drug efflux pump through the inhibition of S-S dependent homodimerization', *Int J Cancer*, 97: 626-30.
- Kanai, N., R. Lu, J. A. Satriano, Y. Bao, A. W. Wolkoff, and V. L. Schuster. 1995. 'Identification and characterization of a prostaglandin transporter', *Science*, 268: 866-9.
- Kasza, I., G. Varady, H. Andrikovics, M. Koszarska, A. Tordai, G. L. Scheffer, A. Nemeth, G. Szakacs, and B. Sarkadi. 2012. 'Expression levels of the ABCG2 multidrug transporter in human erythrocytes correspond to pharmacologically relevant genetic variations', *PLoS One*, 7: e48423.
- Keogh, J., Hagenbuch, B., Caroline Rynn, Bruno Stieger, and Nicholls, G. 1996. 'Membrane Transporters: Fundamentals, Function and Their Role in ADME', *Drug Transporters*, volume 1: Role and Importance in ADME and Drug Development, : 1-56.
- Kerr, I. D., A. J. Haider, and I. C. Gelissen. 2011. 'The ABCG family of membrane-associated transporters: you don't have to be big to be mighty', *Br J Pharmacol*, 164: 1767-79.
- Kerr, I. D., E. Hutchison, L. Gerard, S. M. Aleidi, and I. C. Gelissen. 2021. 'Mammalian ABCG-transporters, sterols and lipids: To bind perchance to transport?', *Biochim Biophys Acta Mol Cell Biol Lipids*, 1866: 158860.
- Khunweeraphong, N., D. Szollosi, T. Stockner, and K. Kuchler. 2019. 'The ABCG2 multidrug transporter is a pump gated by a valve and an extracellular lid', *Nat Commun*, 10: 5433.
- Kindla, J., F. Muller, M. Mieth, M. F. Fromm, and J. Konig. 2011. 'Influence of non-steroidal anti-inflammatory drugs on organic anion transporting polypeptide (OATP) 1B1- and OATP1B3-mediated drug transport', *Drug Metab Dispos*, 39: 1047-53.
- Knauer, M. J., A. J. Girdwood, R. B. Kim, and R. G. Tirona. 2013. 'Transport function and transcriptional regulation of a liver-enriched human organic anion transporting polypeptide 2B1 transcriptional start site variant', *Mol Pharmacol*, 83: 1218-28.
- Kobayashi, D., T. Nozawa, K. Imai, J. Nezu, A. Tsuji, and I. Tamai. 2003. 'Involvement of human organic anion transporting polypeptide OATP-B (SLC21A9) in pH-dependent transport across intestinal apical membrane', *J Pharmacol Exp Ther*, 306: 703-8.
- Koenen, A., K. Kock, M. Keiser, W. Siegmund, H. K. Kroemer, and M. Grube. 2012. 'Steroid hormones specifically modify the activity of organic anion transporting polypeptides', *Eur J Pharm Sci*, 47: 774-80.
- Konig, J., Y. Cui, A. T. Nies, and D. Keppler. 2000. 'A novel human organic anion transporting polypeptide localized to the basolateral hepatocyte membrane', *Am J Physiol Gastrointest Liver Physiol*, 278: G156-64.
- Kovacsics, D., I. Patik, and C. Ozvegy-Laczka. 2017. 'The role of organic anion transporting polypeptides in drug absorption, distribution, excretion and drug-drug interactions', *Expert Opin Drug Metab Toxicol*, 13: 409-24.
- Krishnamurthy, P., D. D. Ross, T. Nakanishi, K. Bailey-Dell, S. Zhou, K. E. Mercer, B. Sarkadi, B. P. Sorrentino, and J. D. Schuetz. 2004. 'The stem cell marker Bcrp/ABCG2 enhances hypoxic cell survival through interactions with heme', *J Biol Chem*, 279: 24218-25.
- Kullak-Ublick, G. A., B. Hagenbuch, B. Stieger, C. D. Scheingart, A. F. Hofmann, A. W. Wolkoff, and P. J. Meier. 1995. 'Molecular and functional characterization of an organic anion transporting polypeptide cloned from human liver', *Gastroenterology*, 109: 1274-82.
- Kullak-Ublick, G. A., M. G. Ismail, B. Stieger, L. Landmann, R. Huber, F. Pizzagalli, K. Fattinger, P. J. Meier, and B. Hagenbuch. 2001. 'Organic anion-transporting polypeptide B (OATP-B) and its functional comparison with three other OATPs of human liver', *Gastroenterology*, 120: 525-33.

- Lacapere, J. J., and V. Papadopoulos. 2003. 'Peripheral-type benzodiazepine receptor: structure and function of a cholesterol-binding protein in steroid and bile acid biosynthesis', *Steroids*, 68: 569-85.
- Laczko-Rigo, R., E. Bakos, R. Jojart, C. Tomboly, E. Mernyak, and C. Ozvegy-Laczka. 2021. 'Selective antiproliferative effect of C-2 halogenated 13 α -estrone on cells expressing Organic anion-transporting polypeptide 2B1 (OATP2B1)', *Toxicol Appl Pharmacol*, 429: 115704.
- Laczko-Rigo, R., R. Jojart, E. Mernyak, E. Bakos, A. Tuerkova, B. Zdrzil, and C. Ozvegy-Laczka. 2020. 'Structural dissection of 13-epiestrones based on the interaction with human Organic anion-transporting polypeptide, OATP2B1', *J Steroid Biochem Mol Biol*, 200: 105652.
- Laszlo, L., B. Sarkadi, and T. Hegedus. 2016. 'Jump into a New Fold-A Homology Based Model for the ABCG2/BCRP Multidrug Transporter', *PLoS One*, 11: e0164426.
- Lavis, L. D., T. Y. Chao, and R. T. Raines. 2011. 'Synthesis and utility of fluorogenic acetoxymethyl ethers', *Chem Sci*, 2: 521-30.
- Lee, C. A., M. A. O'Connor, T. K. Ritchie, A. Galetin, J. A. Cook, I. Ragueneau-Majlessi, H. Ellens, B. Feng, M. E. Taub, M. F. Paine, J. W. Polli, J. A. Ware, and M. J. Zamek-Gliszczynski. 2015. 'Breast cancer resistance protein (ABCG2) in clinical pharmacokinetics and drug interactions: practical recommendations for clinical victim and perpetrator drug-drug interaction study design', *Drug Metab Dispos*, 43: 490-509.
- Lee, H. H., B. F. Leake, R. B. Kim, and R. H. Ho. 2017. 'Contribution of Organic Anion-Transporting Polypeptides 1A/1B to Doxorubicin Uptake and Clearance', *Mol Pharmacol*, 91: 14-24.
- Lee, W., A. Belkhir, A. C. Lockhart, N. Merchant, H. Glaeser, E. I. Harris, M. K. Washington, E. M. Brunt, A. Zaika, R. B. Kim, and W. El-Rifai. 2008. 'Overexpression of OATP1B3 confers apoptotic resistance in colon cancer', *Cancer Res*, 68: 10315-23.
- Lee, W., J. M. Ha, and Y. Sugiyama. 2020. 'Post-translational regulation of the major drug transporters in the families of organic anion transporters and organic anion-transporting polypeptides', *J Biol Chem*, 295: 17349-64.
- Leonhardt, M., M. Keiser, S. Oswald, J. Kuhn, J. Jia, M. Grube, H. K. Kroemer, W. Siegmund, and W. Weitschies. 2010. 'Hepatic uptake of the magnetic resonance imaging contrast agent Gd-EOB-DTPA: role of human organic anion transporters', *Drug Metab Dispos*, 38: 1024-8.
- Letschert, K., H. Faulstich, D. Keller, and D. Keppler. 2006. 'Molecular characterization and inhibition of amanitin uptake into human hepatocytes', *Toxicol Sci*, 91: 140-9.
- Leuthold, S., B. Hagenbuch, N. Mohebbi, C. A. Wagner, P. J. Meier, and B. Stieger. 2009. 'Mechanisms of pH-gradient driven transport mediated by organic anion polypeptide transporters', *Am J Physiol Cell Physiol*, 296: C570-82.
- Li, L., T. K. Lee, P. J. Meier, and N. Ballatori. 1998. 'Identification of glutathione as a driving force and leukotriene C4 as a substrate for oatp1, the hepatic sinusoidal organic solute transporter', *J Biol Chem*, 273: 16184-91.
- Li, Y., J. Lu, and J. W. Paxton. 2012. 'The role of ABC and SLC transporters in the pharmacokinetics of dietary and herbal phytochemicals and their interactions with xenobiotics', *Curr Drug Metab*, 13: 624-39.
- Liu, T., and Q. Li. 2014. 'Organic anion-transporting polypeptides: a novel approach for cancer therapy', *J Drug Target*, 22: 14-22.
- Malagnino, V., J. Hussner, I. Seibert, A. Stolzenburg, C. P. Sager, and H. E. Meyer Zu Schwabedissen. 2018. 'LST-3TM12 is a member of the OATP1B family and a functional transporter', *Biochem Pharmacol*, 148: 75-87.
- Maliepaard, M., G. L. Scheffer, I. F. Faneyte, M. A. van Gastelen, A. C. Pijnenborg, A. H. Schinkel, M. J. van De Vijver, R. J. Scheper, and J. H. Schellens. 2001. 'Subcellular localization and distribution of the breast cancer resistance protein transporter in normal human tissues', *Cancer Res*, 61: 3458-64.
- Manolaridis, I., S. M. Jackson, N. M. I. Taylor, J. Kowal, H. Stahlberg, and K. P. Locher. 2018. 'Cryo-EM structures of a human ABCG2 mutant trapped in ATP-bound and substrate-bound states', *Nature*, 563: 426-30.
- Martinez-Abundis, E., F. Correa, E. Rodriguez, E. Soria-Castro, J. S. Rodriguez-Zavala, D. Pacheco-Alvarez, and C. Zazueta. 2011. 'A CRAC-like motif in BAX sequence: relationship with protein insertion and pore activity in liposomes', *Biochim Biophys Acta*, 1808: 1888-95.
- Matsumoto, J., N. Ariyoshi, M. Sakakibara, T. Nakanishi, Y. Okubo, N. Shiina, K. Fujisaki, T. Nagashima, Y. Nakatani, I. Tamai, H. Yamada, H. Takeda, and I. Ishii. 2015. 'Organic anion transporting polypeptide 2B1 expression correlates with uptake of estrone-3-sulfate and cell proliferation in estrogen receptor-positive breast cancer cells', *Drug Metab Pharmacokinet*, 30: 133-41.

- Meier-Abt, F., Y. Mokrab, and K. Mizuguchi. 2005. 'Organic anion transporting polypeptides of the OATP/SLCO superfamily: identification of new members in nonmammalian species, comparative modeling and a potential transport mode', *J Membr Biol*, 208: 213-27.
- Meyer Zu Schwabedissen, H. E., K. Boettcher, T. Steiner, U. I. Schwarz, M. Keiser, H. K. Kroemer, and W. Siegmund. 2014. 'OATP1B3 is expressed in pancreatic beta-islet cells and enhances the insulinotropic effect of the sulfonylurea derivative glibenclamide', *Diabetes*, 63: 775-84.
- Meyer zu Schwabedissen, H. E., R. G. Tirona, C. S. Yip, R. H. Ho, and R. B. Kim. 2008. 'Interplay between the nuclear receptor pregnane X receptor and the uptake transporter organic anion transporter polypeptide 1A2 selectively enhances estrogen effects in breast cancer', *Cancer Res*, 68: 9338-47.
- Miwa, M., S. Tsukahara, E. Ishikawa, S. Asada, Y. Imai, and Y. Sugimoto. 2003. 'Single amino acid substitutions in the transmembrane domains of breast cancer resistance protein (BCRP) alter cross resistance patterns in transfectants', *Int J Cancer*, 107: 757-63.
- Miyake, K., L. Mickley, T. Litman, Z. Zhan, R. Robey, B. Cristensen, M. Brangi, L. Greenberger, M. Dean, T. Fojo, and S. E. Bates. 1999. 'Molecular cloning of cDNAs which are highly overexpressed in mitoxantrone-resistant cells: demonstration of homology to ABC transport genes', *Cancer Res*, 59: 8-13.
- Mizuarai, S., N. Aozasa, and H. Kotani. 2004. 'Single nucleotide polymorphisms result in impaired membrane localization and reduced atpase activity in multidrug transporter ABCG2', *Int J Cancer*, 109: 238-46.
- Mohos, V., E. Fliszar-Nyul, O. Ungvari, E. Bakos, K. Kuffa, T. Bencsik, B. Z. Zsido, C. Hetenyi, A. Telbisz, C. Ozvegy-Laczka, and M. Poor. 2020. 'Effects of Chrysin and Its Major Conjugated Metabolites Chrysin-7-Sulfate and Chrysin-7-Glucuronide on Cytochrome P450 Enzymes and on OATP, P-gp, BCRP, and MRP2 Transporters', *Drug Metab Dispos*, 48: 1064-73.
- Mohos, V., E. Fliszar-Nyul, O. Ungvari, K. Kuffa, P. W. Needs, P. A. Kroon, A. Telbisz, C. Ozvegy-Laczka, and M. Poor. 2020. 'Inhibitory Effects of Quercetin and Its Main Methyl, Sulfate, and Glucuronic Acid Conjugates on Cytochrome P450 Enzymes, and on OATP, BCRP and MRP2 Transporters', *Nutrients*, 12.
- Morio, H., Y. Sun, M. Harada, H. Ide, O. Shimozaoto, X. Zhou, K. Higashi, R. Yuki, N. Yamaguchi, J. P. Hofbauer, C. Guttman-Gruber, N. Anzai, H. Akita, K. Chiba, and T. Furihata. 2018. 'Cancer-Type OATP1B3 mRNA in Extracellular Vesicles as a Promising Candidate for a Serum-Based Colorectal Cancer Biomarker', *Biol Pharm Bull*, 41: 445-49.
- Morisaki, K., R. W. Robey, C. Ozvegy-Laczka, Y. Honjo, O. Polgar, K. Steadman, B. Sarkadi, and S. E. Bates. 2005. 'Single nucleotide polymorphisms modify the transporter activity of ABCG2', *Cancer Chemother Pharmacol*, 56: 161-72.
- Mozner, O., Z. Bartos, B. Zambo, L. Homolya, T. Hegedus, and B. Sarkadi. 2019. 'Cellular Processing of the ABCG2 Transporter-Potential Effects on Gout and Drug Metabolism', *Cells*, 8.
- Nagy, T., A. Toth, A. Telbisz, B. Sarkadi, H. Tordai, A. Tordai, and T. Hegedus. 2021. 'The transport pathway in the ABCG2 protein and its regulation revealed by molecular dynamics simulations', *Cell Mol Life Sci*, 78: 2329-39.
- Nakanishi, T., and I. Tamai. 2012. 'Genetic polymorphisms of OATP transporters and their impact on intestinal absorption and hepatic disposition of drugs', *Drug Metab Pharmacokinet*, 27: 106-21.
- Namgoong, S., H. S. Cheong, J. O. Kim, L. H. Kim, H. S. Na, I. S. Koh, M. W. Chung, and H. D. Shin. 2015. 'Comparison of genetic variations of the SLCO1B1, SLCO1B3, and SLCO2B1 genes among five ethnic groups', *Environ Toxicol Pharmacol*, 40: 692-7.
- Narita, M., E. Hatano, S. Arizono, A. Miyagawa-Hayashino, H. Isoda, K. Kitamura, K. Taura, K. Yasuchika, T. Nitta, I. Ikai, and S. Uemoto. 2009. 'Expression of OATP1B3 determines uptake of Gd-EOB-DTPA in hepatocellular carcinoma', *J Gastroenterol*, 44: 793-8.
- Navarro-Quiles, C., E. Mateo-Bonmati, and J. L. Micol. 2018. 'ABCE Proteins: From Molecules to Development', *Front Plant Sci*, 9: 1125.
- Niemi, M., M. K. Pasanen, and P. J. Neuvonen. 2011. 'Organic anion transporting polypeptide 1B1: a genetically polymorphic transporter of major importance for hepatic drug uptake', *Pharmacol Rev*, 63: 157-81.
- Nimmerjahn, A., F. Kirchhoff, J. N. Kerr, and F. Helmchen. 2004. 'Sulforhodamine 101 as a specific marker of astroglia in the neocortex in vivo', *Nat Methods*, 1: 31-7.
- Nozawa, T., K. Imai, J. Nezu, A. Tsuji, and I. Tamai. 2004. 'Functional characterization of pH-sensitive organic anion transporting polypeptide OATP-B in human', *J Pharmacol Exp Ther*, 308: 438-45.

- Nozawa, T., M. Suzuki, K. Takahashi, H. Yabuuchi, T. Maeda, A. Tsuji, and I. Tamai. 2004. 'Involvement of estrone-3-sulfate transporters in proliferation of hormone-dependent breast cancer cells', *J Pharmacol Exp Ther*, 311: 1032-7.
- Obaidat, A., M. Roth, and B. Hagenbuch. 2012. 'The expression and function of organic anion transporting polypeptides in normal tissues and in cancer', *Annu Rev Pharmacol Toxicol*, 52: 135-51.
- Omasits, U., C. H. Ahrens, S. Muller, and B. Wollscheid. 2014. 'Protter: interactive protein feature visualization and integration with experimental proteomic data', *Bioinformatics*, 30: 884-6.
- Orlando, B. J., and M. Liao. 2020. 'ABCG2 transports anticancer drugs via a closed-to-open switch', *Nat Commun*, 11: 2264.
- Ozvegy-Laczkó, C., J. Cserepes, N. B. Elkind, and B. Sarkadi. 2005. 'Tyrosine kinase inhibitor resistance in cancer: role of ABC multidrug transporters', *Drug Resist Updat*, 8: 15-26.
- Ozvegy-Laczkó, C., T. Hegedus, G. Varady, O. Ujhelly, J. D. Schuetz, A. Varadi, G. Keri, L. Orfi, K. Nemet, and B. Sarkadi. 2004. 'High-affinity interaction of tyrosine kinase inhibitors with the ABCG2 multidrug transporter', *Mol Pharmacol*, 65: 1485-95.
- Ozvegy-Laczkó, C., G. Koblos, B. Sarkadi, and A. Varadi. 2005. 'Single amino acid (482) variants of the ABCG2 multidrug transporter: major differences in transport capacity and substrate recognition', *Biochim Biophys Acta*, 1668: 53-63.
- Ozvegy-Laczkó, C., R. Laczkó, C. Hegedus, T. Litman, G. Varady, K. Goda, T. Hegedus, N. V. Dokholyan, B. P. Sorrentino, A. Varadi, and B. Sarkadi. 2008. 'Interaction with the 5D3 monoclonal antibody is regulated by intramolecular rearrangements but not by covalent dimer formation of the human ABCG2 multidrug transporter', *J Biol Chem*, 283: 26059-70.
- Ozvegy-Laczkó, C., G. Varady, G. Koblos, O. Ujhelly, J. Cervenak, J. D. Schuetz, B. P. Sorrentino, G. J. Koomen, A. Varadi, K. Nemet, and B. Sarkadi. 2005. 'Function-dependent conformational changes of the ABCG2 multidrug transporter modify its interaction with a monoclonal antibody on the cell surface', *J Biol Chem*, 280: 4219-27.
- Ozvegy, C., T. Litman, G. Szakacs, Z. Nagy, S. Bates, A. Varadi, and B. Sarkadi. 2001. 'Functional characterization of the human multidrug transporter, ABCG2, expressed in insect cells', *Biochem Biophys Res Commun*, 285: 111-7.
- Ozvegy, C., A. Varadi, and B. Sarkadi. 2002. 'Characterization of drug transport, ATP hydrolysis, and nucleotide trapping by the human ABCG2 multidrug transporter. Modulation of substrate specificity by a point mutation', *J Biol Chem*, 277: 47980-90.
- Pal, A., D. Mehn, E. Molnar, S. Gedey, P. Meszaros, T. Nagy, H. Glavinas, T. Janaky, O. von Richter, G. Bathori, L. Szente, and P. Krajcsi. 2007. 'Cholesterol potentiates ABCG2 activity in a heterologous expression system: improved in vitro model to study function of human ABCG2', *J Pharmacol Exp Ther*, 321: 1085-94.
- Palmeira, A., E. Sousa, M. H. Vasconcelos, and M. M. Pinto. 2012. 'Three decades of P-gp inhibitors: skimming through several generations and scaffolds', *Curr Med Chem*, 19: 1946-2025.
- Pan, Q., X. Zhang, L. Zhang, Y. Cheng, N. Zhao, F. Li, X. Zhou, S. Chen, J. Li, S. Xu, D. Huang, Y. Chen, L. Li, H. Wang, W. Chen, S. Y. Cai, J. L. Boyer, and J. Chai. 2018. 'Solute Carrier Organic Anion Transporter Family Member 3A1 Is a Bile Acid Efflux Transporter in Cholestasis', *Gastroenterology*, 155: 1578-92 e16.
- Patik, I., D. Kovacsics, O. Nemet, M. Gera, G. Varady, B. Stieger, B. Hagenbuch, G. Szakacs, and C. Ozvegy-Laczkó. 2015. 'Functional expression of the 11 human Organic Anion Transporting Polypeptides in insect cells reveals that sodium fluorescein is a general OATP substrate', *Biochem Pharmacol*, 98: 649-58.
- Patik, I., V. Szekely, O. Nemet, A. Szepesi, N. Kucsma, G. Varady, G. Szakacs, E. Bakos, and C. Ozvegy-Laczkó. 2018. 'Identification of novel cell-impermeant fluorescent substrates for testing the function and drug interaction of Organic Anion-Transporting Polypeptides, OATP1B1/1B3 and 2B1', *Sci Rep*, 8: 2630.
- Polgar, O., R. W. Robey, and S. E. Bates. 2008. 'ABCG2: structure, function and role in drug response', *Expert Opin Drug Metab Toxicol*, 4: 1-15.
- Pomari, E., A. Nardi, C. Fiore, A. Celegghin, L. Colombo, and L. Dalla Valle. 2009. 'Transcriptional control of human organic anion transporting polypeptide 2B1 gene', *J Steroid Biochem Mol Biol*, 115: 146-52.
- Rizner, T. L., T. Thalhammer, and C. Ozvegy-Laczkó. 2017. 'The Importance of Steroid Uptake and Intracrine Action in Endometrial and Ovarian Cancers', *Front Pharmacol*, 8: 346.
- Robey, R. W., K. M. Pluchino, M. D. Hall, A. T. Fojo, S. E. Bates, and M. M. Gottesman. 2018. 'Revisiting the role of ABC transporters in multidrug-resistant cancer', *Nat Rev Cancer*, 18: 452-64.

- Ronaldson, P. T., and T. P. Davis. 2013. 'Targeted drug delivery to treat pain and cerebral hypoxia', *Pharmacol Rev*, 65: 291-314.
- Roth, M., A. Obaidat, and B. Hagenbuch. 2012. 'OATPs, OATs and OCTs: the organic anion and cation transporters of the SLCO and SLC22A gene superfamilies', *Br J Pharmacol*, 165: 1260-87.
- Rubin, E. H., D. P. de Alwis, I. Pouliquen, L. Green, P. Marder, Y. Lin, R. Musanti, S. L. Grospe, S. L. Smith, D. L. Toppmeyer, J. Much, M. Kane, A. Chaudhary, C. Jordan, M. Burgess, and C. A. Slapak. 2002. 'A phase I trial of a potent P-glycoprotein inhibitor, Zosuquidar.3HCl trihydrochloride (LY335979), administered orally in combination with doxorubicin in patients with advanced malignancies', *Clin Cancer Res*, 8: 3710-7.
- Saison, C., V. Helias, B. A. Ballif, T. Peyrard, H. Puy, T. Miyazaki, S. Perrot, M. Vayssier-Taussat, M. Waldner, P. Y. Le Pennec, J. P. Cartron, and L. Arnaud. 2012. 'Null alleles of ABCG2 encoding the breast cancer resistance protein define the new blood group system Junior', *Nat Genet*, 44: 174-7.
- Saranko, H., H. Tordai, A. Telbisz, C. Ozvegy-Laczka, G. Erdos, B. Sarkadi, and T. Hegedus. 2013. 'Effects of the gout-causing Q141K polymorphism and a CFTR DeltaF508 mimicking mutation on the processing and stability of the ABCG2 protein', *Biochem Biophys Res Commun*, 437: 140-5.
- Sarkadi, B., L. Homolya, and T. Hegedus. 2020. 'The ABCG2/BCRP transporter and its variants - from structure to pathology', *FEBS Lett*, 594: 4012-34.
- Sarkadi, B., L. Homolya, G. Szakacs, and A. Varadi. 2006. 'Human multidrug resistance ABCB and ABCG transporters: participation in a chemoimmunity defense system', *Physiol Rev*, 86: 1179-236.
- Sarkadi, B., E. M. Price, R. C. Boucher, U. A. Germann, and G. A. Scarborough. 1992. 'Expression of the human multidrug resistance cDNA in insect cells generates a high activity drug-stimulated membrane ATPase', *J Biol Chem*, 267: 4854-8.
- Satlin, L. M., V. Amin, and A. W. Wolkoff. 1997. 'Organic anion transporting polypeptide mediates organic anion/HCO₃⁻ exchange', *J Biol Chem*, 272: 26340-5.
- Schafer, A. M., T. Bock, and H. E. Meyer Zu Schwabedissen. 2018. 'Establishment and Validation of Competitive Counterflow as a Method To Detect Substrates of the Organic Anion Transporting Polypeptide 2B1', *Mol Pharm*, 15: 5501-13.
- Schafer, A. M., H. E. Meyer Zu Schwabedissen, S. Bien-Moller, A. Hubeny, S. Vogelgesang, S. Oswald, and M. Grube. 2020. 'OATP1A2 and OATP2B1 Are Interacting with Dopamine-Receptor Agonists and Antagonists', *Mol Pharm*, 17: 1987-95.
- Scharenberg, C. W., M. A. Harkey, and B. Torok-Storb. 2002. 'The ABCG2 transporter is an efficient Hoechst 33342 efflux pump and is preferentially expressed by immature human hematopoietic progenitors', *Blood*, 99: 507-12.
- Schnepf, R., and O. Zolk. 2013. 'Effect of the ATP-binding cassette transporter ABCG2 on pharmacokinetics: experimental findings and clinical implications', *Expert Opin Drug Metab Toxicol*, 9: 287-306.
- Schulte, R. R., and R. H. Ho. 2019. 'Organic Anion Transporting Polypeptides: Emerging Roles in Cancer Pharmacology', *Mol Pharmacol*, 95: 490-506.
- Schwarz, U. I., H. E. Meyer zu Schwabedissen, R. G. Tirona, A. Suzuki, B. F. Leake, Y. Mokrab, K. Mizuguchi, R. H. Ho, and R. B. Kim. 2011. 'Identification of novel functional organic anion-transporting polypeptide 1B3 polymorphisms and assessment of substrate specificity', *Pharmacogenet Genomics*, 21: 103-14.
- Shen, H., W. Chen, D. M. Drexler, S. Mandlekar, V. K. Holenarsipur, E. E. Shields, R. Langish, K. Sidik, J. Gan, W. G. Humphreys, P. Marathe, and Y. Lai. 2017. 'Comparative Evaluation of Plasma Bile Acids, Dehydroepiandrosterone Sulfate, Hexadecanedioate, and Tetradecanedioate with Coproporphyrins I and III as Markers of OATP Inhibition in Healthy Subjects', *Drug Metab Dispos*, 45: 908-19.
- Shimada, H., Y. Nakamura, T. Nakanishi, and I. Tamai. 2015. 'OATP2A1/SLCO2A1-mediated prostaglandin E2 loading into intracellular acidic compartments of macrophages contributes to exocytotic secretion', *Biochem Pharmacol*, 98: 629-38.
- Shirasaka, Y., M. Shichiri, T. Mori, T. Nakanishi, and I. Tamai. 2013. 'Major active components in grapefruit, orange, and apple juices responsible for OATP2B1-mediated drug interactions', *J Pharm Sci*, 102: 3418-26.
- Shitara, Y., M. Hirano, H. Sato, and Y. Sugiyama. 2004. 'Gemfibrozil and its glucuronide inhibit the organic anion transporting polypeptide 2 (OATP2/OATP1B1:SLC21A6)-mediated hepatic uptake and CYP2C8-mediated metabolism of cerivastatin: analysis of the mechanism of the clinically relevant drug-drug interaction between cerivastatin and gemfibrozil', *J Pharmacol Exp Ther*, 311: 228-36.

- Shitara, Y., K. Maeda, K. Ikejiri, K. Yoshida, T. Horie, and Y. Sugiyama. 2013. 'Clinical significance of organic anion transporting polypeptides (OATPs) in drug disposition: their roles in hepatic clearance and intestinal absorption', *Biopharm Drug Dispos*, 34: 45-78.
- Storch, C. H., R. Ehehalt, W. E. Haefeli, and J. Weiss. 2007. 'Localization of the human breast cancer resistance protein (BCRP/ABCG2) in lipid rafts/caveolae and modulation of its activity by cholesterol in vitro', *J Pharmacol Exp Ther*, 323: 257-64.
- Stromme, P., S. Groeneweg, E. C. Lima de Souza, C. Zevenbergen, A. Torgersbraten, A. Holmgren, E. Gurcan, M. E. Meima, R. P. Peeters, W. E. Visser, L. Honeren Johansson, A. Babovic, H. Zetterberg, H. Heuer, E. Frengen, D. Misceo, and T. J. Visser. 2018. 'Mutated Thyroid Hormone Transporter OATP1C1 Associates with Severe Brain Hypometabolism and Juvenile Neurodegeneration', *Thyroid*, 28: 1406-15.
- Szafraniec, M. J., M. Szczygiel, K. Urbanska, and L. Fiedor. 2014. 'Determinants of the activity and substrate recognition of breast cancer resistance protein (ABCG2)', *Drug Metab Rev*, 46: 459-74.
- Szakacs, G., A. Varadi, C. Ozvegy-Laczka, and B. Sarkadi. 2008. 'The role of ABC transporters in drug absorption, distribution, metabolism, excretion and toxicity (ADME-Tox)', *Drug Discov Today*, 13: 379-93.
- Szatmari, I., G. Vamosi, P. Brazda, B. L. Balint, S. Benko, L. Szeles, V. Jeney, C. Ozvegy-Laczka, A. Szanto, E. Barta, J. Balla, B. Sarkadi, and L. Nagy. 2006. 'Peroxisome proliferator-activated receptor gamma-regulated ABCG2 expression confers cytoprotection to human dendritic cells', *J Biol Chem*, 281: 23812-23.
- Szekely, V., I. Patik, O. Ungvari, A. Telbisz, G. Szakacs, E. Bakos, and C. Ozvegy-Laczka. 2020. 'Fluorescent probes for the dual investigation of MRP2 and OATP1B1 function and drug interactions', *Eur J Pharm Sci*, 151: 105395.
- Szente, L., and J. Szejtli. 1999. 'Highly soluble cyclodextrin derivatives: chemistry, properties, and trends in development', *Adv Drug Deliv Rev*, 36: 17-28.
- Tarling, E. J., and P. A. Edwards. 2011. 'ATP binding cassette transporter G1 (ABCG1) is an intracellular sterol transporter', *Proc Natl Acad Sci U S A*, 108: 19719-24.
- Taylor, N. M. I., I. Manolaridis, S. M. Jackson, J. Kowal, H. Stahlberg, and K. P. Locher. 2017. 'Structure of the human multidrug transporter ABCG2', *Nature*, 546: 504-09.
- Telbisz, A., C. Hegedus, C. Ozvegy-Laczka, K. Goda, G. Varady, Z. Takats, E. Szabo, B. P. Sorrentino, A. Varadi, and B. Sarkadi. 2012. 'Antibody binding shift assay for rapid screening of drug interactions with the human ABCG2 multidrug transporter', *Eur J Pharm Sci*, 45: 101-9.
- Telbisz, A., C. Hegedus, A. Varadi, B. Sarkadi, and C. Ozvegy-Laczka. 2014. 'Regulation of the function of the human ABCG2 multidrug transporter by cholesterol and bile acids: effects of mutations in potential substrate and steroid binding sites', *Drug Metab Dispos*, 42: 575-85.
- Telbisz, A., M. Muller, C. Ozvegy-Laczka, L. Homolya, L. Szente, A. Varadi, and B. Sarkadi. 2007. 'Membrane cholesterol selectively modulates the activity of the human ABCG2 multidrug transporter', *Biochim Biophys Acta*, 1768: 2698-713.
- Telbisz, A., C. Ozvegy-Laczka, T. Hegedus, A. Varadi, and B. Sarkadi. 2013. 'Effects of the lipid environment, cholesterol and bile acids on the function of the purified and reconstituted human ABCG2 protein', *Biochem J*, 450: 387-95.
- Thakkar, N., K. Kim, E. R. Jang, S. Han, K. Kim, D. Kim, N. Merchant, A. C. Lockhart, and W. Lee. 2013. 'A cancer-specific variant of the SLCO1B3 gene encodes a novel human organic anion transporting polypeptide 1B3 (OATP1B3) localized mainly in the cytoplasm of colon and pancreatic cancer cells', *Mol Pharm*, 10: 406-16.
- Thomas, C., S. G. Aller, K. Beis, E. P. Carpenter, G. Chang, L. Chen, E. Dassa, M. Dean, F. Duong Van Hoa, D. Ekiert, R. Ford, R. Gaudet, X. Gong, I. B. Holland, Y. Huang, D. K. Kahne, H. Kato, V. Koronakis, C. M. Koth, Y. Lee, O. Lewinson, R. Lill, E. Martinoia, S. Murakami, H. W. Pinkett, B. Poolman, D. Rosenbaum, B. Sarkadi, L. Schmitt, E. Schneider, Y. Shi, S. L. Shyng, D. J. Slotboom, E. Tajkhorshid, D. P. Tieleman, K. Ueda, A. Varadi, P. C. Wen, N. Yan, P. Zhang, H. Zheng, J. Zimmer, and R. Tampe. 2020. 'Structural and functional diversity calls for a new classification of ABC transporters', *FEBS Lett*, 594: 3767-75.
- Tuerkova, A., O. Ungvari, R. Laczko-Rigo, E. Mernyak, G. Szakacs, C. Ozvegy-Laczka, and B. Zdrzil. 2021. 'Data-Driven Ensemble Docking to Map Molecular Interactions of Steroid Analogs with Hepatic Organic Anion Transporting Polypeptides', *J Chem Inf Model*, 61: 3109-27.
- Tupova, L., B. Hirschmugl, S. Sucha, V. Pilarova, V. Szekely, E. Bakos, L. Novakova, C. Ozvegy-Laczka, C. Wadsack, and M. Ceckova. 2020. 'Interplay of drug transporters P-glycoprotein (MDR1), MRP1,

- OATP1A2 and OATP1B3 in passage of maraviroc across human placenta', *Biomed Pharmacother*, 129: 110506.
- Tusnady, G. E., and I. Simon. 2001. 'The HMMTOP transmembrane topology prediction server', *Bioinformatics*, 17: 849-50.
- Ujhelly, O., C. Ozvegy, G. Varady, J. Cervenak, L. Homolya, M. Grez, G. Scheffer, D. Roos, S. E. Bates, A. Varadi, B. Sarkadi, and K. Nemet. 2003. 'Application of a human multidrug transporter (ABCG2) variant as selectable marker in gene transfer to progenitor cells', *Hum Gene Ther*, 14: 403-12.
- Ungvari, O., L. Kiraly, E. Bakos, and C. Ozvegy-Laczka. 2021. '8-acetoxy-trisulfopyrene as the first activatable fluorogenic probe for add-and-read assessment of Organic anion-transporting polypeptides, OATP1B1, OATP1B3, and OATP2B1', *FASEB J*, 35: e21863.
- Urquhart, B. L., and R. B. Kim. 2009. 'Blood-brain barrier transporters and response to CNS-active drugs', *Eur J Clin Pharmacol*, 65: 1063-70.
- van de Steeg, E., V. Stranecky, H. Hartmannova, L. Noskova, M. Hrebicek, E. Wagenaar, A. van Esch, D. R. de Waart, R. P. Oude Elferink, K. E. Kenworthy, E. Sticova, M. al-Edreesi, A. S. Knisely, S. Kmoch, M. Jirsa, and A. H. Schinkel. 2012. 'Complete OATP1B1 and OATP1B3 deficiency causes human Rotor syndrome by interrupting conjugated bilirubin reuptake into the liver', *J Clin Invest*, 122: 519-28.
- van Herwaarden, A. E., E. Wagenaar, G. Merino, J. W. Jonker, H. Rosing, J. H. Beijnen, and A. H. Schinkel. 2007. 'Multidrug transporter ABCG2/breast cancer resistance protein secretes riboflavin (vitamin B2) into milk', *Mol Cell Biol*, 27: 1247-53.
- Varady, G., J. Cserepes, A. Nemeth, E. Szabo, and B. Sarkadi. 2013. 'Cell surface membrane proteins as personalized biomarkers: where we stand and where we are headed', *Biomark Med*, 7: 803-19.
- Velamakanni, S., T. Janvilisri, S. Shahi, and H. W. van Veen. 2008. 'A functional steroid-binding element in an ATP-binding cassette multidrug transporter', *Mol Pharmacol*, 73: 12-7.
- Vlaming, M. L., J. S. Lagas, and A. H. Schinkel. 2009. 'Physiological and pharmacological roles of ABCG2 (BCRP): recent findings in Abcg2 knockout mice', *Adv Drug Deliv Rev*, 61: 14-25.
- Williams, S. P., and P. B. Sigler. 1998. 'Atomic structure of progesterone complexed with its receptor', *Nature*, 393: 392-6.
- Windt, T., S. Toth, I. Patik, J. Sessler, N. Kucsma, A. Szepesi, B. Zdrzil, C. Ozvegy-Laczka, and G. Szakacs. 2019. 'Identification of anticancer OATP2B1 substrates by an in vitro triple-fluorescence-based cytotoxicity screen', *Arch Toxicol*, 93: 953-64.
- Winter, E., F. Lecerf-Schmidt, G. Gozzi, B. Peres, M. Lightbody, C. Gauthier, C. Ozvegy-Laczka, G. Szakacs, B. Sarkadi, T. B. Creczynski-Pasa, A. Boumendjel, and A. Di Pietro. 2013. 'Structure-activity relationships of chromone derivatives toward the mechanism of interaction with and inhibition of breast cancer resistance protein ABCG2', *J Med Chem*, 56: 9849-60.
- Woodward, O. M., A. Kottgen, J. Coresh, E. Boerwinkle, W. B. Guggino, and M. Kottgen. 2009. 'Identification of a urate transporter, ABCG2, with a common functional polymorphism causing gout', *Proc Natl Acad Sci U S A*, 106: 10338-42.
- Woodward, O. M., D. N. Tukaye, J. Cui, P. Greenwell, L. M. Constantoulakis, B. S. Parker, A. Rao, M. Kottgen, P. C. Maloney, and W. B. Guggino. 2013. 'Gout-causing Q141K mutation in ABCG2 leads to instability of the nucleotide-binding domain and can be corrected with small molecules', *Proc Natl Acad Sci U S A*, 110: 5223-8.
- Wright, J. L., E. M. Kwon, E. A. Ostrander, R. B. Montgomery, D. W. Lin, R. Vessella, J. L. Stanford, and E. A. Mostaghel. 2011. 'Expression of SLCO transport genes in castration-resistant prostate cancer and impact of genetic variation in SLCO1B3 and SLCO2B1 on prostate cancer outcomes', *Cancer Epidemiol Biomarkers Prev*, 20: 619-27.
- Wu, M. R., Y. Y. Huang, and J. K. Hsiao. 2019. 'Use of Indocyanine Green (ICG), a Medical Near Infrared Dye, for Enhanced Fluorescent Imaging-Comparison of Organic Anion Transporting Polypeptide 1B3 (OATP1B3) and Sodium-Taurocholate Cotransporting Polypeptide (NTCP) Reporter Genes', *Molecules*, 24.
- Xie, Y., K. Xu, D. E. Linn, X. Yang, Z. Guo, H. Shimelis, T. Nakanishi, D. D. Ross, H. Chen, L. Fazli, M. E. Gleave, and Y. Qiu. 2008. 'The 44-kDa Pim-1 kinase phosphorylates BCRP/ABCG2 and thereby promotes its multimerization and drug-resistant activity in human prostate cancer cells', *J Biol Chem*, 283: 3349-56.
- Yaguchi, Y., M. Tachikawa, Z. Zhang, and T. Terasaki. 2019. 'Organic Anion-Transporting Polypeptide 1a4 (Oatp1a4/Slco1a4) at the Blood-Arachnoid Barrier is the Major Pathway of Sulforhodamine-101 Clearance from Cerebrospinal Fluid of Rats', *Mol Pharm*, 16: 2021-27.

- Yoshida, K., K. Maeda, and Y. Sugiyama. 2013. 'Hepatic and intestinal drug transporters: prediction of pharmacokinetic effects caused by drug-drug interactions and genetic polymorphisms', *Annu Rev Pharmacol Toxicol*, 53: 581-612.
- Zambo, B., Z. Bartos, O. Mozner, E. Szabo, G. Varady, G. Poor, M. Palinkas, H. Andrikovics, T. Hegedus, L. Homolya, and B. Sarkadi. 2018. 'Clinically relevant mutations in the ABCG2 transporter uncovered by genetic analysis linked to erythrocyte membrane protein expression', *Sci Rep*, 8: 7487.
- Zamek-Gliszczyński, M. J., M. E. Taub, P. P. Chothe, X. Chu, K. M. Giacomini, R. B. Kim, A. S. Ray, S. L. Stocker, J. D. Unadkat, M. B. Wittwer, C. Xia, S. W. Yee, L. Zhang, Y. Zhang, and Consortium International Transporter. 2018. 'Transporters in Drug Development: 2018 ITC Recommendations for Transporters of Emerging Clinical Importance', *Clin Pharmacol Ther*, 104: 890-99.
- Zelinski, T., G. Coghlan, X. Q. Liu, and M. E. Reid. 2012. 'ABCG2 null alleles define the Jr(a-) blood group phenotype', *Nat Genet*, 44: 131-2.
- Zhang, J. H., T. D. Chung, and K. R. Oldenburg. 1999. 'A Simple Statistical Parameter for Use in Evaluation and Validation of High Throughput Screening Assays', *J Biomol Screen*, 4: 67-73.
- Zhang, W., J. Mojsilovic-Petrovic, M. F. Andrade, H. Zhang, M. Ball, and D. B. Stanimirovic. 2003. 'The expression and functional characterization of ABCG2 in brain endothelial cells and vessels', *FASEB J*, 17: 2085-7.
- Zhang, Z., W. Xia, J. He, Z. Zhang, Y. Ke, H. Yue, C. Wang, H. Zhang, J. Gu, W. Hu, W. Fu, Y. Hu, M. Li, and Y. Liu. 2012. 'Exome sequencing identifies SLCO2A1 mutations as a cause of primary hypertrophic osteoarthropathy', *Am J Hum Genet*, 90: 125-32.
- Zhou, S., J. D. Schuetz, K. D. Bunting, A. M. Colapietro, J. Sampath, J. J. Morris, I. Lagutina, G. C. Grosveld, M. Osawa, H. Nakauchi, and B. P. Sorrentino. 2001. 'The ABC transporter Bcrp1/ABCG2 is expressed in a wide variety of stem cells and is a molecular determinant of the side-population phenotype', *Nat Med*, 7: 1028-34.
- Zhou, Y., J. Yuan, Z. Li, Z. Wang, D. Cheng, Y. Du, W. Li, Q. Kan, and W. Zhang. 2015. 'Genetic polymorphisms and function of the organic anion-transporting polypeptide 1A2 and its clinical relevance in drug disposition', *Pharmacology*, 95: 201-8.

XI. A DOLGOZAT ALAPJÁT KÉPEZŐ KÖZLEMÉNYEK EREDETI VERZIÓI
(csak az elektronikus verzióban szerepelnek)



Single amino acid (482) variants of the ABCG2 multidrug transporter: major differences in transport capacity and substrate recognition

Csilla Özvegy-Laczka^{a,b}, Gabriella Köblös^b, Balázs Sarkadi^a, András Váradi^{b,*}

^aNational Medical Center, Institute of Haematology and Immunology, Membrane Research Group of the Hungarian Academy of Sciences, Diószegi út 64., H-1113 Budapest, Hungary

^bInstitute of Enzymology, Hungarian Academy of Sciences, Karolina út 29., H-1113 Budapest, Hungary

Received 28 June 2004; received in revised form 19 October 2004; accepted 10 November 2004

Available online 24 November 2004

Abstract

The human ABCG2 protein is an ATP binding cassette half-transporter, which protects our cells and tissues against various xenobiotics, while overexpression of ABCG2 in tumor cells confers multidrug resistance. It has been documented that single amino acid changes at position 482 resulted in altered drug resistance and transport capacity. In this study, we have generated nine Arg-482 mutants (G, I, M, S, T, D, N, K, Y) of ABCG2, and expressed them in insect cells. All ABCG2 variants showed cell surface expression and, in isolated membranes, an ABCG2-specific ATPase activity. When methotrexate accumulation was measured in inside-out membrane vesicles, this transport was supported only by the wild-type ABCG2. In intact cells, mitoxantrone was transported by all ABCG2 variants, except by R482K. Rhodamine 123 was extruded by most of the mutants, except by R482K, Y and by wild-type ABCG2. Hoechst 33342 was pumped out from cells expressing the wild-type and all Arg-482 variants, but not from those expressing R482K and Y. Our study demonstrates that the substrate specificity of the Arg (wild-type) form is unique and that amino acid replacements at position 482 induce major alterations in both the transport activity and substrate specificity of this protein.

© 2004 Elsevier B.V. All rights reserved.

Keywords: Multidrug half-transporter; Single amino acid mutant; Cell surface localization; Membrane ATPase; Vesicular transport; Fluorescent dye extrusion

1. Introduction

The human ABCG2 multidrug transporter (ABCP/BCRP/MXR) is a plasma membrane glycoprotein, which belongs to the ATP binding cassette (ABC) protein family. ABCG2 is a half transporter, possessing only one ATP binding and one transmembrane domain, and most probably acts as a homodimer [1,2]. The ABCG2 protein is present in

several normal tissues [3,4], and its overexpression has also been documented in drug-resistant cell lines and tumors [1].

ABCG2 transports a wide variety of compounds, including cytotoxic agents (mitoxantrone, topotecan, flavopiridol, methotrexate), fluorescent dyes (e.g., Hoechst 33342) and different toxic compounds found in normal food (e.g., 2-amino-1-methyl-6-phenylimidazo[4,5-*b*]pyridine (PhIP) or pheophorbide a) [4–8]. ABCG2 mediates the extrusion of these compounds towards the extracellular space, a process energized by ATP hydrolysis [1]. Transport function and tissue distribution of ABCG2 suggest its role in protection/detoxification against xenobiotics [3,9] and, indeed, ABCG2 has been shown to influence the intestinal topotecan absorption and its secretion into the bile [10,11].

There is little information about the amino acids responsible for the substrate specificity of ABCG2. The transmembrane domain of ABC transporters is thought to be responsible for the recognition of transported substrates. In

Abbreviations: ABC, ATP binding cassette; ABCP, placenta specific ABC transporter; BCRP, breast cancer resistance protein; β -gal., β -galactosidase; Hst, Hoechst 33342; MDR1, human multidrug resistance protein (P-glycoprotein, ABCB1); MRP, human multidrug resistance associated protein, ABCC1; MXR, mitoxantrone resistance protein; MTX, methotrexate; MX, mitoxantrone; R123, rhodamine 123; Sf9 cells, *Spodoptera frugiperda* ovarian cells; SN-38, 7-ethyl-10-hydroxy-camptothecin; TM, transmembrane; wt, wild-type

* Corresponding author. Tel./fax: +36 1 466 5465.

E-mail address: varadi@enzim.hu (A. Váradi).

the case of MDR1, deletion mutants containing only the transmembrane domains still retained their substrate binding capacity [12]. Moreover, different studies have identified amino acids in TM helices 4, 5, 6, 9, 10, 11 and 12 of MDR1, responsible for drug binding and thought to form the drug-binding domain of this protein [12–15]. In colchicine selected cells, mutation of Gly 185 to Val (found in the intracellular loop between TM helices 2 and 3) occurred in the overexpressed MDR1 protein [16]. The G185V mutant conferred altered basal ATPase activity and altered interaction with substrates, as well as with the inhibitor cyclosporin A [17,18]. In case of MRP1, 2 or 3, again amino acids found in the TM region were shown to influence substrate specificity [19–21].

In some drug-selected cell lines overexpressing human ABCG2 (or its mouse ortholog), a single amino acid change at position 482 (predicted to be situated in the third TM helix) occurred [22,23]. The mutants, containing R482G, T or M (R482M or S in the mouse *abcg2*), showed altered substrate specificity [22–24]. Previously, we have shown that the R482G and T mutants have increased ATP hydrolytic activity, therefore they are “gain of function” mutants in this regard [25]. However, the R482G and T mutants were unable to transport methotrexate, which is a substrate of the wtABCG2 [6,26]. A recent study by Miwa et al. [27] analyzed several mutant forms of ABCG2 in conferring resistance to mitoxantrone or SN38.

The aim of the present work was to analyze how different Arg-482 mutants influence the function of human ABCG2. Therefore, we have created seven additional ABCG2-R482 mutants (I, M, S, D, N, K and Y), representing various amino acid properties. We have expressed these mutants in the baculovirus-Sf9 insect cell expression system, which allows the investigation of both the transport and ATP-hydrolytic functions of ABCG2. Moreover, in this heterologous expression system there is no potential endogenous dimerization partner for the human ABCG2, thus the mutant variants function only as uniform homodimers.

The ATP hydrolytic capacity of the mutants was measured in isolated membrane vesicles, and the effect of potential substrates and inhibitors on this activity was determined. We also compared the MgATP-dependent methotrexate transport capacity of wtABCG2 and nine Arg-482 mutants using inside-out membrane vesicles. Additionally, we analyzed the transport of several fluorescent compounds (mitoxantrone, rhodamine 123 and Hoechst 33342) in intact cells expressing these mutants.

2. Materials and methods

2.1. Materials

ATP, methotrexate, mitoxantrone, Na-orthovanadate, prazosin, propidium iodide and rhodamine 123 were purchased from Sigma. Hoechst 33342 was purchased from Molecular

Probes. Ko143 was a generous gift from Dr. G. Koomen (Division of Experimental Therapy, The Netherlands Cancer Institute, and Laboratory of Organic Chemistry, University of Amsterdam, Amsterdam, The Netherlands). [³H]methotrexate was purchased from Moravék Biochemicals.

2.2. Generation of transfer vectors possessing different human ABCG2 cDNAs

pAcUW21-L/ABCG2 (wild-type, R482G, T or K86M/R482G) was constructed as described earlier [25]. In this study, we used the K86M-R482 single mutant, which was generated by cloning the *NotI*–*SpeI* fragment of pAcUW21-L/K86M-R482G [25] into the corresponding site of pAcUW21-L/R482. The seven additional Arg-482 variants were created using ABCG2-R482G cDNA as a template by overlap extension PCR [25,28]. The same outer primer pairs were used and the same cloning strategy was performed as described previously [25]. The two internal complementary primer pairs containing the specific mutation were: 5'-tta tta cca atg atc atg tta cc-3' and 5'-gg taa cat gat cat tgg taa taa-3' (R482I), 5'-tta tca gat cta tta ccc atg-3' and 5'-gg taa cat cat cat ggg taa t-3' (R482M), 5'-ta ccc atg tgc atg tta cca a-3' and 5'-t tgg taa cat cga cat ggg ta-3' (R482S), 5'-cc atg gac atg tta cca tgc att ata-3' and 5'-tat aat cga tgg taa cat gtc cat gg-3' (R482D), 5'-atg tta cca tgc att ata tt acc-3' and 5'-cc atg aat atg tta cca tgc att ata-3' (R482N), 5' -tta tta cct atg aag atg tta-3' cc and 5'-gg taa cat ctt cat agg taa taa-3' (R482K) and 5'-tta tta cct atg tac atg tta cc-3' and 5'-gg taa cat gta cat agg taa taa-3' (R482Y). The mutations were confirmed by sequencing the *PstI*–*MscI* fragments of the constructs.

2.3. Generation of recombinant baculoviruses

Recombinant baculoviruses carrying the different human ABCG2 cDNAs were generated as described [25,29]. ABCG2 protein expression was determined by immunoblotting and immunoflow cytometry (see below).

2.4. Membrane preparation and immunodetection of ABCG2

Virus-infected Sf9 cells were harvested after 72 h of infection. Membranes were isolated by differential centrifugation [30] and stored at –80 °C. The membrane protein concentrations were determined by the modified Lowry method [29]. Immunoblot detection was performed as described in Ref. [25]. The expression level of different ABCG2 mutants was determined by densitometry of the immunoblots (BioRad ChemiDoc).

Immunoflow cytometry was performed by labeling 2–5 × 10⁵ Sf9 cells after 40 h of infection [25] at 37 °C, by using the anti-ABCG2 monoclonal antibody 5D3 (eBioscience), which recognizes a cell-surface epitope of human ABCG2 [4]. The antibody was used in a final concentration of 1 µg/ml, and binding was visualized by the addition of a

second, phycoerythrin-conjugated anti-mouse IgG (Immunotech), in 1 µg/ml final concentration. Flow cytometry determination of the antibody reaction was carried out at 488-nm excitation and 585-nm emission wavelengths using a FACSCalibur cytometer (Becton Dickinson).

2.5. Membrane ATPase measurements

ATPase activity was measured as described in Ref. [25] by determining the liberation of inorganic phosphate from ATP with a colorimetric assay. Normalized ATPase activities (A_n) were determined as follows: $A_n = ((A_x - A_b) \times E_r) + A_b$. A_b : background ATPase activity (8 nmol P_i /min/mg protein) measured in membranes containing β -galactosidase, A_x : activity measured in the case of the ABCG2 mutants, E_r : relative expression level of the mutants compared to the wild-type, determined by densitometry (see above).

2.6. Measurement of [3H]methotrexate transport by ABCG2

Sf9 membrane vesicles (90 µg) containing one of the Arg-482 mutants, wtABCG2 or the K86M mutant were prepared on the same day to ensure the same inside-out vesicle ratio of the different membranes. Membranes were incubated in the presence or absence of 4 mM MgATP (or 4 mM MgATP+1 µM Ko143) in a buffer containing 40 mM 3-(*N*-morpholino) propanesulfonic acid–Tris (pH 7.0), 56 mM KCl, 6 mM $MgCl_2$ and 2 mM dithiothreitol, in a final volume of 140 µl, at 37 °C for 5 min (or as indicated in Fig. 3A). The measurement was started by the addition of 10–3000 µM MTX. The reaction was carried out as described earlier [31].

2.7. Mitoxantrone or rhodamine 123 uptake in intact Sf9 cells

The uptake of mitoxantrone or rhodamine 123 was measured by using intact Sf9 cells overexpressing one of the ABCG2 mutants as described [25]. A FACSCalibur cytometer equipped with 488-nm argon and 635-nm red diode laser, and 530- and 670-nm bandpass filters, was used to determine the cellular fluorescence of rhodamine 123 and mitoxantrone, respectively. A total of 30 000 cells were counted; dead cell exclusion was based on propidium iodide staining.

2.8. Hoechst 33342 dye accumulation assay

Accumulation of Hoechst dye (Hst) was performed by using intact Sf9 cells overexpressing one of the ABCG2 mutants, in a fluorescence spectrophotometer (Perkin Elmer LS 50B) at 350 nm (excitation)/460 nm (emission) as described [25]. The increase in cellular fluorescence due to Hoechst accumulation was determined in the absence (F_0) or presence of 1 µM Ko143 (F_{100}). Transport activity of ABCG2 protein variants was calculated as $((F_{100} - F_0) / F_{100}) \times 100$.

3. Results

3.1. Expression of ABCG2-R482 mutants in Sf9 cells

In the present study, we have generated seven Arg-482 mutants (I, M, S, D, N, K and Y) and expressed them in Sf9 cells using recombinant baculoviruses. Expression of the ABCG2 mutants was detected by immunoblotting, using the BXP-21 monoclonal antibody [3]. Fig. 1A demonstrates that all ABCG2-R482 mutants were successfully expressed in Sf9 cells, although with some variations, at about equal protein levels. The expression levels of the R482I and the R482D variants were usually somewhat lower than those for the other mutants.

To find out whether the mutants were properly expressed and localized in insect cells, we performed flow cytometry by using the 5D3 monoclonal antibody, which recognizes an extracellular epitope and thus detects cell surface expression of ABCG2 [4]. Fig. 1B shows that all ABCG2-R482 mutants were clearly recognized by the 5D3 antibody in intact insect cells, indicating that all of these proteins localize to the plasma membrane. Similar membrane localization was found for the inactive K86M human ABCG2 mutant [25] in the insect cells. In the control Sf9 cells, or in those expressing the MDR1 protein, there was no measurable labeling by the 5D3 antibody.

3.2. ATPase activity measurements in isolated insect cell membranes

We have previously shown that the overexpression of human ABCG2 in insect cells results in high ATPase activity without exogenously added substrates, and this basal activity is approximately three times higher than that of human MDR1 [32]. The high basal ATPase activity of ABCG2 is sensitive to Na-orthovanadate and to specific ABCG2 inhibitors (e.g., Fumitremorgin C and Ko143).

To find out whether the seven newly expressed Arg-482 mutants were active, we determined their ATPase activity by using membrane vesicles prepared from insect cells expressing these proteins. Fig. 2 demonstrates that all seven, new ABCG2-R482 mutants showed a significantly higher, vanadate-sensitive, basal ATPase activity than the K86M mutant. In order to compare the ATP hydrolytic capacity of the mutants with that of wtABCG2, we normalized the ATPase activity of the different Arg-482 mutants to their actual expression levels (determined by densitometry, see Section 2) in each experiment, and the measurements were repeated three times for all variants. The slight variations in the expression levels were most probably due to the differences in actual culturing conditions and/or the differences in the titers of the recombinant baculoviruses.

Comparing the normalized ATPase activities, we have found that the G, S, T and N mutants had higher, the I, M, K and Y had similar, while the D variant had a lower basal ATPase activity than wtABCG2 (see Fig. 2).

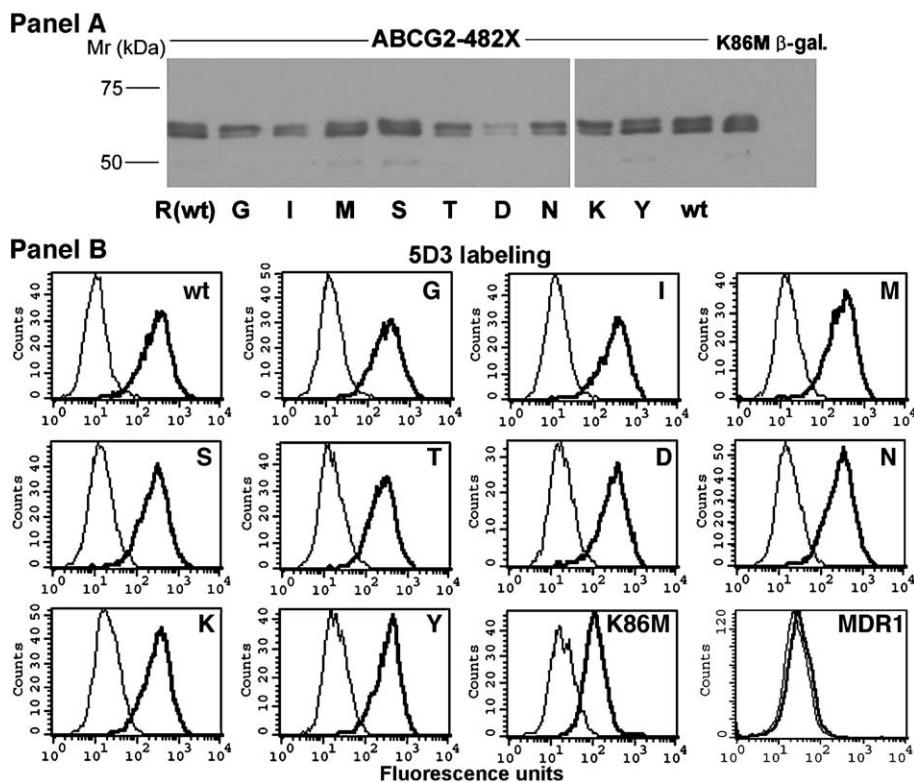


Fig. 1. Expression of ABCG2 482 mutants in insect cells. Panel A: Immunoblot detection of ABCG2 variants, expressed in Sf9 cells. Sf9 membranes were prepared and dissolved in disaggregation buffer. Proteins were separated by SDS-PAGE on 7.5% gels, electrotransferred to PVDF membranes and analyzed by immunodetection with the BXP-21 antibody. The amounts of the total membrane proteins loaded on the gel were 2 μg . Experiments were performed three times, the figure shows the result of one representative experiment. Panel B: Immunodetection of cell surface expression of the ABCG2 mutants. Sf9 cells infected with baculoviruses containing the cDNA of the ABCG2 variants, or MDR1, were collected after 40 h of infection. Labeling was performed with 1 $\mu\text{g}/\text{ml}$ 5D3 antibody (heavy solid line) or 1 $\mu\text{g}/\text{ml}$ isotype control (solid line) and 1 $\mu\text{g}/\text{ml}$ phycoerythrin conjugated anti-mouse IgG. Fluorescence was detected in a FACSCalibur cytometer. Dead cells were excluded based on propidium iodide staining. Experiments were performed twice for each variant, the figure shows one representative experiment.

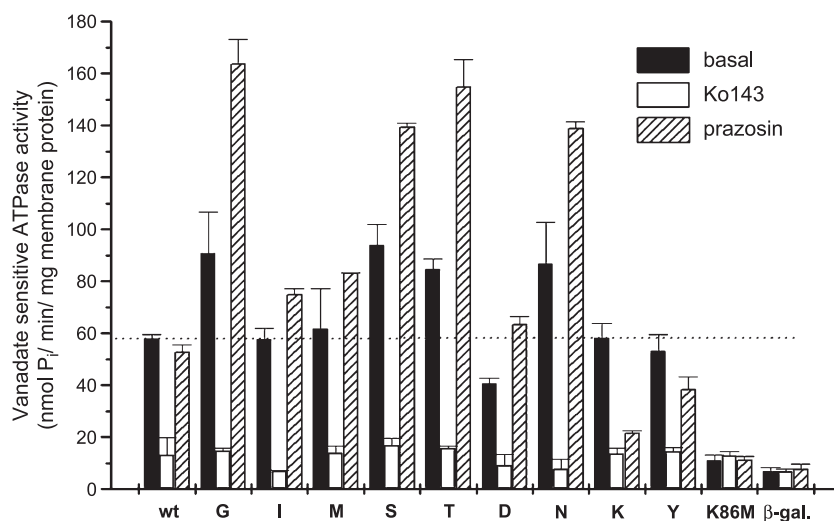


Fig. 2. Vanadate-sensitive ATPase activity measured in membranes of Sf9 cells, expressing the wild-type ABCG2 or its R482 or K86M mutants. ATPase activity of isolated Sf9 membranes was determined by measuring vanadate-sensitive inorganic phosphate liberation, using 3.3 mM MgATP in the absence of added compounds (black columns), with 100 μM prazosin (shaded columns), or with 1 μM Ko143 (blank columns). The data were normalized based on the difference in the expression level of the various ABCG2 forms (see Section 2). Data points represent the mean \pm standard deviation (S.D.) values of at least four measurements, performed with two different membrane preparations.

Ko143 is a specific inhibitor of ABCG2 [33]. When tested in the ATPase assay, this compound was found to inhibit the basal ATPase activity of all Arg-482 mutants (Fig. 2). This observation indicates that all Arg-482 mutants are active, since all show a specific, ABCG2-inhibitor-sensitive ATPase activity. When testing different Ko143 concentrations, we could not detect any major difference between the ABCG2 mutants with respect to their Ko143 sensitivity (i.e., the Ko143 concentrations producing 50% inhibition of the basal ATPase activities

were between 20 and 100 nM for each variant; data not shown).

Prazosin is a substrate of the wtABCG2, R482G and R482T [34], and it stimulates the ATPase activity of R482G and T mutants, but it has no major effect on the ATPase activity of wtABCG2 [25]. When tested in the ATPase assay, prazosin was found to stimulate the activity of the R482I, M, S, D and N mutants by 1.3- to 1.6-fold. In contrast, the basal ATPase activity of R482K and Y mutants was rather inhibited than stimulated by prazosin

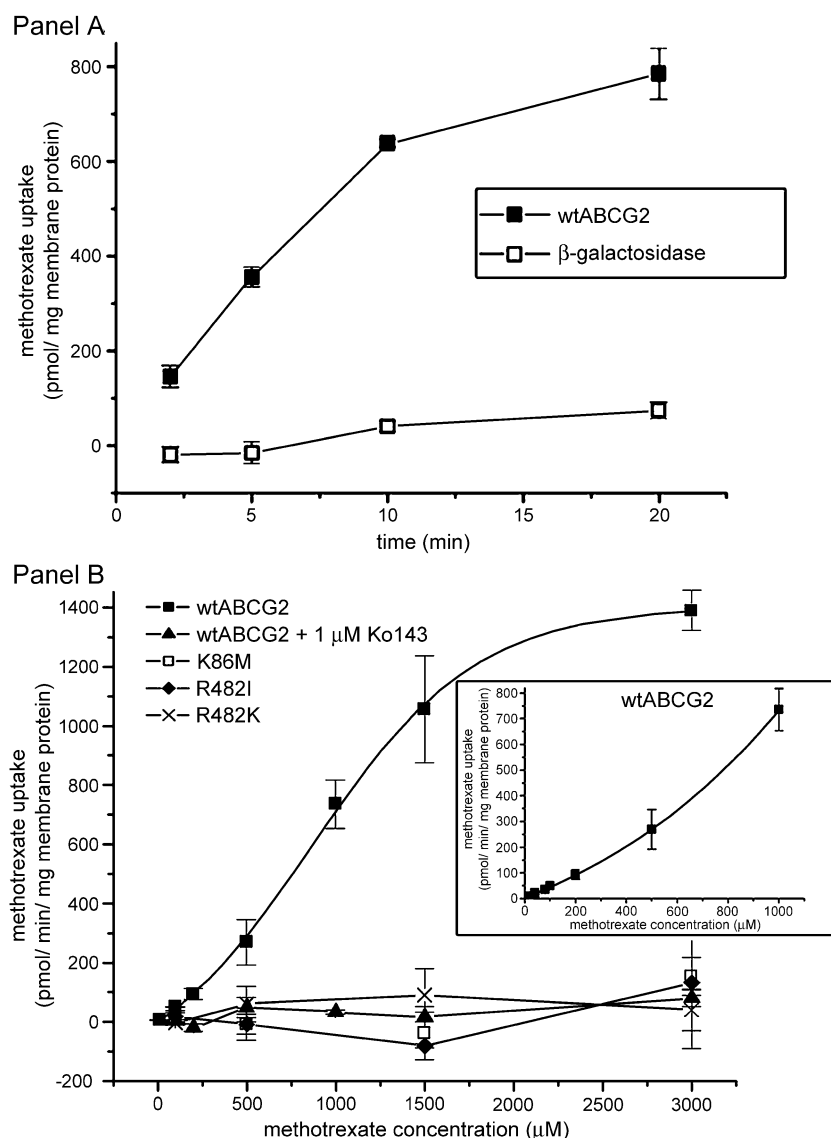


Fig. 3. [3 H]methotrexate transport characteristics of wtABCG2 and its mutant variants. Panel A: Time course of methotrexate transport. Sf9 membrane vesicles (90 μ g) containing wtABCG2 or β -galactosidase were incubated with 100 μ M MTX, containing [3 H]MTX, in the presence or absence of 4 mM MgATP, in a final volume of 150 μ l, at 37 $^{\circ}$ C for different time periods. ATP-dependent transport was calculated by subtracting the values obtained in the absence of ATP from those in the presence of ATP. Panel B: Concentration dependence of MTX uptake by wtABCG2, R482I, R482K and K86M. Sf9 membrane vesicles (90 μ g) containing wtABCG2 (solid square), K86M (open square), R482I (diamond), and R482K (cross) were incubated in the presence or absence of 4 mM MgATP, with (up-triangle) or without 1 μ M Ko143, with different MTX concentrations (10–3000 μ M in a final volume of 150 μ l) at 37 $^{\circ}$ C for 5 min. ATP-dependent [3 H]MTX uptake was calculated by subtracting the values obtained in the absence of ATP from those in the presence of ATP. Inset: Concentration dependence of MTX uptake by wtABCG2 below 1000 μ M. Values shown are means of at least four independent experiments \pm standard deviation (S.D.) values.

(see Fig. 2). In case of the latter two mutants, all ABCG2 substrates tested (e.g., mitoxantrone, rhodamine 123; not shown here) produced an inhibition of the ABCG2-ATPase activity.

3.3. Characterization of [^3H]methotrexate transport by ABCG2 mutants

It has been shown earlier that methotrexate is a transported substrate of the wtABCG2 but not of R482G or T [6,26]. In order to analyze the methotrexate (MTX) transport characteristics of wtABCG2, expressed in Sf9 cells, we determined the time and concentration dependence of [^3H]methotrexate transport in isolated membrane vesicles.

Fig. 3, panel A shows that a significant, MgATP-dependent MTX uptake by the wtABCG2 into membrane vesicles could be observed, which was practically linear for about 5 min. On the other hand, MTX accumulation measured in membranes from cells expressing β -galactosidase (Fig. 3A) or ABCG2-K86M (see below) was very low, and did not increase during this time period.

Fig. 3B documents that, when measuring the MTX concentration dependence of MTX uptake by wtABCG2, this transport followed a sigmoidal curve (see insert in Fig. 3B), with an approximate V_{max} of 1389 ± 69 pmol/min/mg membrane protein. MTX transport by ABCG2 was found to be fully inhibited by Ko143, down to the level of that seen in the presence of the ABCG2-K86M mutant (see Fig. 3B).

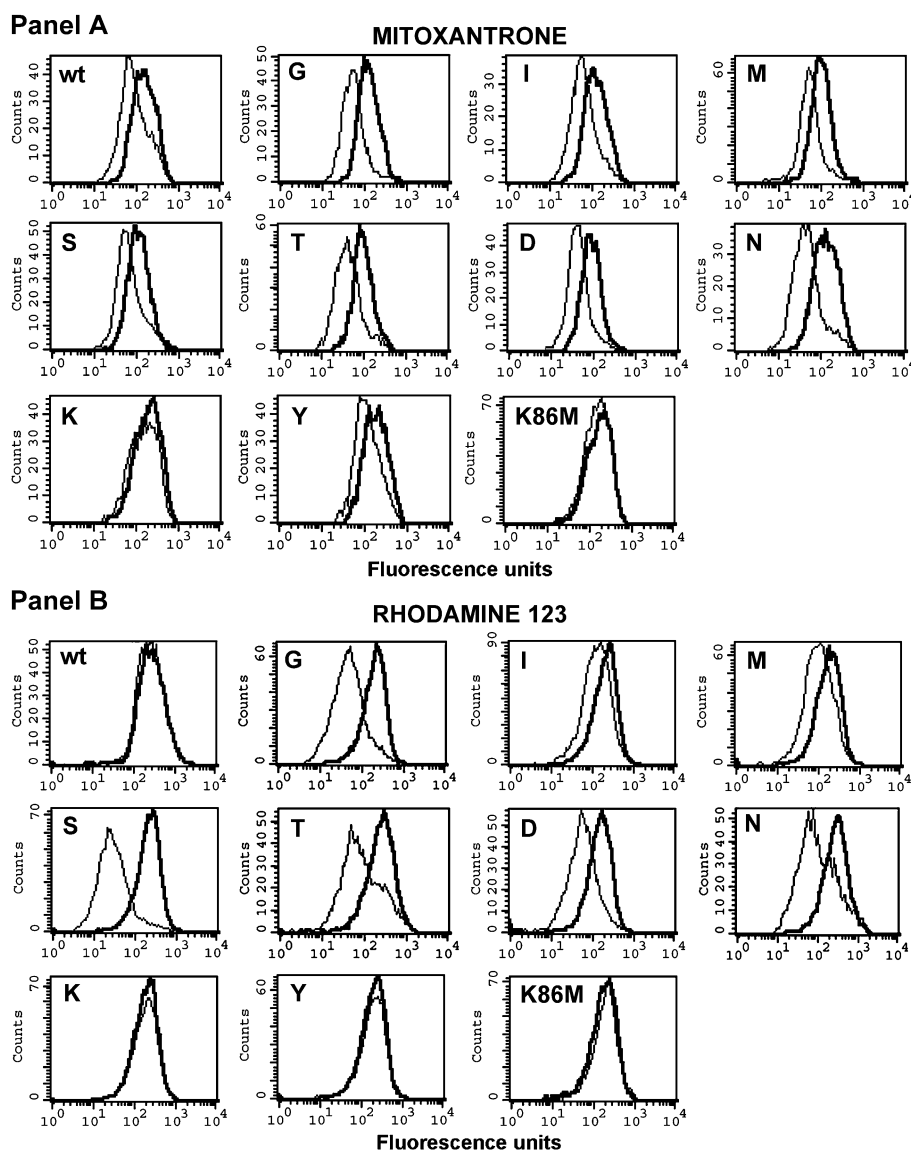


Fig. 4. Mitoxantrone and rhodamine 123 accumulation in Sf9 cells expressing wild-type ABCG2 (Arg-482), the R482X or K86M mutants. Sf9 cells were incubated for 30 min at 37°C with 20 μM MX (panel A) or 2 μM rhodamine 123 (panel B), in the presence (heavy solid line) or in the absence (solid line) of 1 μM Ko143. Flow cytometry was performed as described in Section 2. Dead cells were excluded based on propidium iodide staining. Measurements were repeated at least three times. Figures show the result of one representative experiment.

In order to test whether the various ABCG2-R482 mutants were also able to transport MTX, we measured [^3H]methotrexate accumulation at various MTX concentrations (100–3000 μM) in inside-out Sf9 cell membrane vesicles, for 5 min at 37 °C. We made sure that the different membrane preparations contained similar percent of inside-out vesicles, and that the expression levels of the mutants were comparable with that of the wild-type ABCG2. We found that none of the Arg-482 mutants had any measurable MTX uptake, as compared to the inactive ABCG2-K86M mutant (see Fig. 3B for R482I and for R482K; the data for the other variants are not shown).

These results indicate that wtABCG2, as expressed in insect cells, can transport methotrexate, while the Arg-482 mutants are inactive in this regard. Interestingly, we found that the MTX-transport characteristics of wtABCG2 expressed in insect cells, i.e., the S-shape curve indicating a complex interaction of this transporter with MTX (see Fig. 3B inset), have not been observed in vesicles prepared from mammalian cells [26,35].

3.4. Flow cytometry assay of mitoxantrone and rhodamine 123 extrusion from intact Sf9 cells expressing wtABCG2 and its Arg-482 mutants

It has been documented earlier that mitoxantrone (MX) is a transported substrate both of the wtABCG2 and its R482G or T mutants, while rhodamine 123 (R123) is transported only by the R482G and R482T variants [22,25]. Both MX and R123 are fluorescent, therefore we could directly analyze their accumulation in ABCG2-expressing intact cells, using flow cytometry [22,25].

In order to characterize the transport of MX or R123 by the Arg-482 mutants, we have used intact insect cells expressing one of the nine 482 mutants, the wtABCG2, or the K86M mutant (as a negative control). The transport rate of these fluorescent compounds was determined by flow cytometry, as described in Section 2. The expression level of the ABCG2 variants in each experiment was confirmed by Western blotting.

Fig. 4A shows the accumulation of mitoxantrone in insect cells, expressing one of the ABCG2 variants. We found that cells containing wtABCG2 or R482G, I, M, S, T, D, N, and Y mutants accumulate less mitoxantrone than cells expressing the inactive K86M mutant. However, in each case, when ABCG2 function was blocked by Ko143, MX accumulation increased to the level observed in the ABCG2-K86M expressing cells. These data indicate that most of the ABCG2-R482 mutant variants can actively extrude mitoxantrone, while the R482K mutant is inactive in this regard.

Fig. 4B demonstrates rhodamine 123 accumulation in the ABCG2-expressing insect cells. We found that while the R482K, R482Y, the wtABCG2, and the inactive K86M mutant had no R123 extrusion activity, several ABCG2 variants were highly active in R123 extrusion. R123

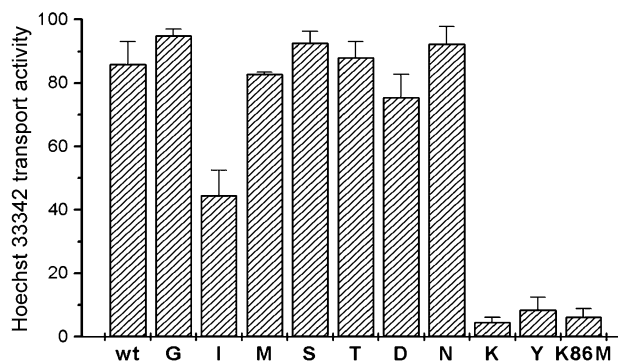


Fig. 5. Hoechst 33342 (Hst) accumulation in Sf9 cells expressing different ABCG2 variants. A total of $2\text{--}5 \times 10^5$ Sf9 cells with different ABCG2 variants were incubated with Hoechst 33342 (2 μM) for 10 min at 37 °C, then 1 μM Ko143 was added. Hoechst fluorescence was measured in a fluorescence spectrophotometer. Transport activity of ABCG2 protein variants was calculated as described in Section 2.

transport by all these active forms was inhibited by Ko143, down to the level of the K86M mutant.

3.5. Measurement of Hoechst 33342 transport by the ABCG2-R482 mutants

It has been shown that Hoechst 33342 is a transported substrate of the wtABCG2 protein, as well as of its R482G and T mutant variants. The transport kinetics of the Hoechst dye can be determined by spectrofluorometry [25] in insect cells, expressing either wtABCG2 or Arg-482 mutants. This assay allows a quantitative comparison of the transport capacities of the various ABCG2 forms.

In order to compare the Hoechst 33342 (Hst) transport capacity of the seven new Arg-482 mutants, we measured Hst transport kinetics in intact insect cells, expressing one of the mutants. The expression levels of the different ABCG2 variants were determined and quantitated by densitometry on Western blots.

Fig. 5 shows the calculated transport activities for the different Arg-482 variants. We found that the R482G, M, S, T, D and N mutants were active in Hoechst transport, and there was no significant difference between the Hst-transport kinetics of these Arg-482 mutants and the wtABCG2. The R482I mutant was also active in this assay, but it had a decreased Hst-transport activity when compared to the wild-type protein, which may be due to a lower expression level of this mutant (not shown). On the other hand, mutants R482K and Y showed no Hst-transport capacity, although their expression levels were similar to that of the wild-type ABCG2 (not shown).

4. Discussion

Human ABCG2 was shown to confer tumor cell resistance to various clinically important compounds, e.g., mitoxantrone, methotrexate, topotecan, SN38, flavopiridol

[1,2]. Understanding the substrate recognition of ABCG2 could promote the development of specific inhibitors and modulators of this protein. Additionally, it could help to predict whether ABCG2 plays a role in the absorption and/or secretion of a given compound with potential pharmacological importance. There is only limited information available about amino acids influencing the substrate specificity of ABCG2.

The aim of this study was to investigate the 482 position of ABCG2, namely how different amino acids at this position influence the activity of the protein. We have generated Arg-482 mutants that represent different amino acid characters (I, D, N, Y), together with the mutant that occurred in the mouse ortholog, *abcg2* (S), and the mutant found both in human ABCG2 and mouse *abcg2* (M). We have also replaced Arg-482 with another positively charged amino acid (K) in order to determine the functional role of a positive charge in this position.

All Arg-482 variants (including R482G, T, wild-type, and K86M, as a negative control) were expressed in insect cells, which produce high levels of ABCG2 and allow the detailed characterization of the function of the protein. Also, there is no potential endogenous dimerization partner for ABCG2 which could significantly alter the observed features of the mutant variants.

Recently, Miwa et al. [27] have published the expression of 15 different Arg-482 mutants (Y, N, C, M, S, T, V, A, G, E, W, D, Q, H and K) in murine fibroblasts, and analyzed these mutants mostly for their drug resistance activities. The present study is a significant extension of these experiments, providing a detailed cell biology and biochemical characterization of the mutant proteins.

In this paper, we show that all Arg-482 mutants expressed in insect cells show cell surface localization (Fig. 1A and B). This finding suggests that Arg-482 has no crucial role in the correct folding and membrane insertion of ABCG2, although ABC proteins may fold differently in different expression systems and at different culturing temperatures [36].

When we studied the ABCG2-specific ATPase activity in isolated membranes, all Arg-482 mutants were found to show a high basal ATPase activity, characteristic for ABCG2, when expressed in insect cells. These ATPase activities were sensitive to Ko143, a specific inhibitor of ABCG2, again confirming the functionality of the mutants (Fig. 2). In addition, the maximum activities of the mutants were quite variable: a three- to fourfold variation in the maximum, Ko143-sensitive ATPase activities was observed.

We have shown previously that the transported substrates could not stimulate the ATPase activity of the wtABCG2, while they stimulated the ATPase activity of the R482G and T mutants (26). In order to find out the effects of substrates in the newly generated Arg-482 mutants, we have examined the effects of various substrates on their ATPase activities. We found that most of the new Arg-482 mutants (I, M, S, D and N) were clearly distinguished from wtABCG2, i.e., their

ATPase activity was stimulated by, e.g., prazosin (Fig. 2). On the other hand, mutants R482K and Y showed inhibition in the presence of prazosin, as well as in the presence of all other potential substrates tested (e.g., mitoxantrone, rhodamine 123; not shown here).

Although these ATPase activities may not directly answer the exact substrate specificities of these ABCG2 variants, they can be highly informative regarding the maximum turnover (transport and ATP hydrolysis) rates, as well as for interactions with wide range of potential substrates. If the basal ATPase activity of ABCG2 is indeed due to the presence of a low affinity endogenous substrate in insect cell membranes, this endogenous substrate differently affects the ATPase activity of the ABCG2 variants examined here. While the wtABCG2, the R482K and R482Y mutants are already fully activated, and prazosin either does not affect or reduces the ATPase activity, the other variants can be further stimulated by exogenously added substrates.

In order to characterize the transport properties, we performed direct transport studies with the expressed ABCG2 variants. Methotrexate uptake was examined in inside-out membrane vesicles, while mitoxantrone, rhodamine 123 and Hoechst 33342 transport was examined in intact Sf9 cells.

When we measured the uptake of [³H]methotrexate into Sf9 vesicles (see Fig. 3), we found a specific, ATP-dependent and Ko143-sensitive transport of MTX in membranes containing wtABCG2. The concentration dependence of MTX uptake by wtABCG2 showed a sigmoidal curve that suggests a complex interaction between ABCG2 and methotrexate. This finding indicates that ABCG2, similarly to other ABC transporters [37], has multiple binding and/or transport sites of MTX, and the endogenous substrates in Sf9 membranes may have a heterotropic effect on MTX transport. As shown in Fig. 3, none of the Arg-482 mutants showed any MTX transport, similarly to the entirely inactive K86M mutant and the R482G or T mutants [6,26].

Methotrexate is an anionic drug, and it is feasible that the positively charged Arg in the wtABCG2 plays a crucial role in the acceptance of this compound at the transport site. However, the 482 Lys mutant, in spite of having the same positive charge, had no methotrexate transport activity, indicating that Arg-482 is absolutely critical in handling of methotrexate by ABCG2.

When measuring the accumulation of mitoxantrone, rhodamine 123 or Hoechst 33342 in intact, ABCG2-expressing Sf9 cells (see Figs. 4 and 5), we found that most of the Arg-482 mutants (R482G, I, M, S, T, D and N) were able to actively extrude these compounds. The exceptions were the R482Y mutant, effective only in mitoxantrone transport, and the R482K mutant, showing no transport activity with any of these substrates.

The above ATPase and transport experiments seem to define two major groups of Arg-482 mutants of ABCG2. One group (G, I, M, S, T, D and N) contains amino acids

with small, hydrophobic, nucleophilic, acidic or amide side chains. These are characterized with high ATPase capacity, mitoxantrone, rhodamine 123 and Hoechst 33342 transport activity, and methotrexate transport inability. The other group of mutants is represented by the aromatic Tyr and the basic Lys. These mutants resemble wtABCG2 regarding the level of their relatively low basal ATPase activity, and the absence of rhodamine 123 transport. On the other hand, they are distinguished from wtABCG2 because of the lack of methotrexate and Hoechst 33342 transport. Actually, the R482K mutant showed no measurable transport activity in any of the assays applied here, while the R482Y was found to be active only in the whole-cell mitoxantrone extrusion assay (see Fig. 4A).

The above data indicate that the substrate specificity of the wild-type, Arg-482 form of ABCG2 is unique, which may have important consequences regarding the interaction of this protein with natural substrates or various toxic agents. This finding may explain why the Arg form of ABCG2 was conserved during evolution, in spite of its relatively lower transport and ATPase capacity.

Arg-482 is found in the third TM helix of ABCG2. It is feasible that some of the Arg-482 mutants alter the substrate specificity of ABCG2 by altering the structure of the transmembrane domain of this protein. However, our cell surface localization data (Fig. 1B) argue against major changes in the membrane topology of the ABCG2 mutants because the conformation sensitive anti-ABCG2 5D3 antibody recognized all mutant variants. Since structural data are only available for certain bacterial ABC transporters [38,39], which are not closely related to ABCG2, we could not perform a detailed homology analysis in this regard.

When comparing our results to those of Miwa et al. [27], expressing Arg-482 mutants of ABCG2 in murine fibroblast cells, we can analyze their drug resistance and our transport biochemistry data in these protein variants. Mutants R482G, M, S, T, D and N were shown to confer higher resistance against mitoxantrone (MX) and doxorubicin than the wtABCG2 [22]. Indeed, these mutants showed well measurable mitoxantrone transport capacities in our assay. We found that the R482Y mutant is a very weak mitoxantrone transporter (see Fig. 4A), and Miwa et al. [27] demonstrated that this mutant confers decreased resistance in murine cells against MX. Only low level of expression of the R482K mutant was achieved in murine cells, nevertheless, the cells were sensitive to MX. We could generate insect cells expressing this mutant in high quantity (see Fig. 1) and found that it possesses no mitoxantrone transport capacity (see Fig. 4A). As a summary, the results obtained in the two entirely different experimental systems are in harmony, and further demonstrate the key role of the side-chain position 482 in substrate handling.

In addition to their relevance of structure-function studies in ABCG2, our studies may have important applications in the field of stem cell-based gene therapy. As shown recently, ABCG2-R482G has been successfully applied as a select-

able marker protein in ex vivo gene transfer experiments. Based on the relatively small cDNA, natural expression in stem cells, and significantly altered transport properties, some of the Arg-482 variants of human ABCG2 may be ideal candidates for providing selective in vitro and in vivo advantages of modified stem cells in medical gene therapy [40].

Acknowledgment

The technical help of Zsuzsanna András, Judit Kis and Györgyi Demeter is gratefully acknowledged. The authors are also grateful to Emese Sinkó for helping with the vesicular transport experiments, to István Simon and Gábor E. Tusnády for useful discussion on the topology/structure of ABCG2, and to Éva Bakos for helpful suggestions in preparing this manuscript. We appreciate the kind gifts, Ko143 obtained from Dr. G. J. Koomen, and the BXP-21 antibody obtained from Drs. George Scheffer and Rik Scheper. This work has been supported by research grants from OTKA and OM, Hungary (T-29921, T-35126, T-31952, T35926, T38337, ETT, NKFP, and OM-1421/1999). Csilla Özvegy-Laczka is a grantee of the Postdoctoral Fellowship (D 45957) of OTKA, Hungary and of the János Bolyai Scholarship of the Hungarian Academy of Sciences. Balázs Sarkadi is a recipient of a Howard Hughes International Scholarship.

References

- [1] J.D. Allen, A.H. Schinkel, Multidrug resistance and pharmacological protection mediated by the breast cancer resistance protein (BCRP/ABCG2), *Mol. Cancer Ther.* 1 (2002) 427–434.
- [2] S.E. Bates, R. Robey, K. Miyake, K. Rao, D.D. Ross, T. Litman, The role of half-transporters in multidrug resistance, *J. Bioenerg. Biomembranes* 33 (2001) 503–511.
- [3] M. Maliepaard, G.L. Scheffer, I.F. Faneyte, M.A. van Gastelen, A.C. Pijnenborg, A.H. Schinkel, M.J. van De Vijver, R.J. Scheper, J.H. Schellens, Subcellular localization and distribution of the breast cancer resistance protein transporter in normal human tissues, *Cancer Res.* 61 (2001) 3458–3464.
- [4] S. Zhou, J.D. Schuetz, K.D. Bunting, A.M. Colapietro, J. Sampath, J.J. Morris, I. Lagutina, G.C. Grosveld, M. Osawa, H. Nakauchi, B.P. Sorrentino, The ABC transporter Bcrp1/ABCG2 is expressed in a wide variety of stem cells and is a molecular determinant of the side-population phenotype, *Nat. Med.* 7 (2001) 1028–1034.
- [5] T. Litman, T.E. Druley, W.D. Stein, S.E. Bates, From MDR to MXR: new understanding of multidrug resistance systems, their properties and clinical significance, *Cell. Mol. Life Sci.* 58 (2001) 931–959.
- [6] E.L. Volk, K.M. Farley, Y. Wu, F. Li, R.W. Robey, E. Schneider, Overexpression of wild-type breast cancer resistance protein mediates methotrexate resistance, *Cancer Res.* 62 (2002) 5035–5040.
- [7] J.W. Jonker, M. Buitelaar, E. Wagenaar, M.A. Van Der Valk, G.L. Scheffer, R.J. Scheper, T. Plosch, F. Kuipers, R.P. Elferink, H. Rosing, J.H. Beijnen, A.H. Schinkel, The breast cancer resistance protein protects against a major chlorophyll-derived dietary phototoxin and protoporphyria, *Proc. Natl. Acad. Sci. U. S. A.* 99 (2002) 15649–15654.

- [8] A.E. van Herwaarden, J.W. Jonker, E. Wagenaar, R.F. Brinkhuis, J.H. Schellens, J.H. Beijnen, A.H. Schinkel, The breast cancer resistance protein (Bcrp1/Abcg2) restricts exposure to the dietary carcinogen 2-amino-1-methyl-6-phenylimidazo[4,5-*b*]pyridine, *Cancer Res.* 63 (2003) 6447–6452.
- [9] G.L. Scheffer, M. Maliepaard, A.C. Pijnenborg, M.A. van Gastelen, M.C. de Jong, A.B. Schroeijers, D.M. van der Kolk, J.D. Allen, D.D. Ross, P. van der Valk, W.S. Dalton, J.H. Schellens, R.J. Scheper, Breast cancer resistance protein is localized at the plasma membrane in mitoxantrone- and topotecan-resistant cell lines, *Cancer Res.* 60 (2000) 2589–2593.
- [10] J.W. Jonker, J.W. Smit, R.F. Brinkhuis, M. Maliepaard, J.H. Beijnen, J.H. Schellens, A.H. Schinkel, Role of breast cancer resistance protein in the bioavailability and fetal penetration of topotecan, *J. Natl. Cancer Inst.* 92 (2000) 1651–1656.
- [11] C.M. Kruijtzter, J.H. Beijnen, H. Rosing, W.W. ten Bokkel Huinink, M. Schot, R.C. Jewell, E.M. Paul, J.H. Schellens, Increased oral bioavailability of topotecan in combination with the breast cancer resistance protein and P-glycoprotein inhibitor GF120918, *J. Clin. Oncol.* 20 (2002) 2943–2950.
- [12] T.W. Loo, D.M. Clarke, The transmembrane domains of the human multidrug resistance P-glycoprotein are sufficient to mediate drug binding and trafficking to the cell surface, *J. Biol. Chem.* 274 (1999) 24759–24765.
- [13] P. Hafkemeyer, S. Dey, S.V. Ambudkar, C.A. Hrycyna, I. Pastan, M.M. Gottesman, Contribution to substrate specificity and transport of nonconserved residues in transmembrane domain 12 of human P-glycoprotein, *Biochemistry (Mosc.)* 37 (1998) 16400–16409.
- [14] K. Ueda, Y. Taguchi, M. Morishima, How does P-glycoprotein recognize its substrates? *Semin. Cancer Biol.* 8 (1997) 151–159.
- [15] Y. Taguchi, K. Kino, M. Morishima, T. Komano, S.E. Kane, K. Ueda, Alteration of substrate specificity by mutations at the His61 position in predicted transmembrane domain 1 of human MDR1/P-glycoprotein, *Biochemistry (Mosc.)* 36 (1997) 8883–8889.
- [16] K.H. Choi, C.J. Chen, M. Kriegler, I.B. Roninson, An altered pattern of cross-resistance in multidrug-resistant human cells results from spontaneous mutations in the *mdr1* (P-glycoprotein) gene, *Cell* 53 (1988) 519–529.
- [17] M. Ramachandra, S.V. Ambudkar, M.M. Gottesman, I. Pastan, C.A. Hrycyna, Functional characterization of a glycine 185-to-valine substitution in human P-glycoprotein by using a vaccinia-based transient expression system, *Mol. Biol. Cell* 7 (1996) 1485–1498.
- [18] C.O. Cardarelli, I. Aksentijevich, I. Pastan, M.M. Gottesman, Differential effects of P-glycoprotein inhibitors on NIH3T3 cells transfected with wild-type (G185) or mutant (V185) multidrug transporters, *Cancer Res.* 55 (1995) 1086–1091.
- [19] D.W. Zhang, H.M. Gu, D. Situ, A. Haimeur, S.P. Cole, R.G. Deeley, Functional importance of polar and charged amino acid residues in transmembrane helix 14 of multidrug resistance protein 1 (MRP1/ABCC1): identification of an aspartate residue critical for conversion from a high to low affinity substrate binding state, *J. Biol. Chem.* 278 (2003) 46052–46063.
- [20] D.W. Zhang, H.M. Gu, M. Vasa, M. Muredda, S.P. Cole, R.G. Deeley, Characterization of the role of polar amino acid residues within predicted transmembrane helix 17 in determining the substrate specificity of multidrug resistance protein 3, *Biochemistry (Mosc.)* 42 (2003) 9989–10000.
- [21] K. Koike, C.J. Oleschuk, A. Haimeur, S.L. Olsen, R.G. Deeley, S.P. Cole, Multiple membrane-associated tryptophan residues contribute to the transport activity and substrate specificity of the human multidrug resistance protein, MRP1, *J. Biol. Chem.* 277 (2002) 49495–49503.
- [22] Y. Honjo, C.A. Hrycyna, Q.W. Yan, W.Y. Medina-Perez, R.W. Robey, A. van de Laar, T. Litman, M. Dean, S.E. Bates, Acquired mutations in the MXR/BCRP/ABCP gene alter substrate specificity in MXR/BCRP/ABCP-overexpressing cells, *Cancer Res.* 61 (2001) 6635–6639.
- [23] J.D. Allen, S.C. Jackson, A.H. Schinkel, A mutation hot spot in the Bcrp1 (Abcg2) multidrug transporter in mouse cell lines selected for doxorubicin resistance, *Cancer Res.* 62 (2002) 2294–2299.
- [24] X. Wang, T. Furukawa, T. Nitanda, M. Okamoto, Y. Sugimoto, S. Akiyama, M. Baba, Breast cancer resistance protein (BCRP/ABCG2) induces cellular resistance to HIV-1 nucleoside reverse transcriptase inhibitors, *Mol. Pharmacol.* 63 (2003) 65–72.
- [25] C. Özvegy, A. Váradi, B. Sarkadi, Characterization of drug transport, ATP hydrolysis, and nucleotide trapping by the human ABCG2 multidrug transporter. Modulation of substrate specificity by a point mutation, *J. Biol. Chem.* 277 (2002) 47980–47990.
- [26] Z.S. Chen, R.W. Robey, M.G. Belinsky, I. Shchavelova, X.Q. Ren, Y. Sugimoto, D.D. Ross, S.E. Bates, G.D. Kruh, Transport of methotrexate, methotrexate polyglutamates, and 17 β -estradiol 17-(β -D-glucuronide) by ABCG2: effects of acquired mutations at R482 on methotrexate transport, *Cancer Res.* 63 (2003) 4048–4054.
- [27] M. Miwa, S. Tsukahara, E. Ishikawa, S. Asada, Y. Imai, Y. Sugimoto, Single amino acid substitutions in the transmembrane domains of breast cancer resistance protein (BCRP) alter cross resistance patterns in transfectants, *Int. J. Cancer* 107 (2003) 757–763.
- [28] G. Szakács, C. Özvegy, É. Bakos, B. Sarkadi, A. Váradi, Role of glycine-534 and glycine-1179 of human multidrug resistance protein (MDR1) in drug-mediated control of ATP hydrolysis, *Biochem. J.* 356 (2001) 71–75.
- [29] M. Müller, É. Bakos, E. Welker, A. Váradi, U.A. Germann, M.M. Gottesman, B.S. Morse, I.B. Roninson, B. Sarkadi, Altered drug-stimulated ATPase activity in mutants of the human multidrug resistance protein, *J. Biol. Chem.* 271 (1996) 1877–1883.
- [30] B. Sarkadi, E.M. Price, R.C. Boucher, U.A. Germann, G.A. Scarborough, Expression of the human multidrug resistance cDNA in insect cells generates a high activity drug-stimulated membrane ATPase, *J. Biol. Chem.* 267 (1992) 4854–4858.
- [31] É. Bakos, R. Evers, G. Szakács, G.E. Tusnády, E. Welker, K. Szabó, M. de Haas, L. van Deemter, P. Borst, A. Váradi, B. Sarkadi, Functional multidrug resistance protein (MRP1) lacking the N-terminal transmembrane domain, *J. Biol. Chem.* 273 (1998) 32167–32175.
- [32] C. Özvegy, T. Litman, G. Szakács, Z. Nagy, S. Bates, A. Váradi, B. Sarkadi, Functional characterization of the human multidrug transporter, ABCG2, expressed in insect cells, *Biochem. Biophys. Res. Commun.* 285 (2001) 111–117.
- [33] J.D. Allen, A. van Loevezijn, J.M. Lakhai, M. van der Valk, O. van Tellingen, G. Reid, J.H. Schellens, G.J. Koomen, A.H. Schinkel, Potent and specific inhibition of the breast cancer resistance protein multidrug transporter in vitro and in mouse intestine by a novel analogue of fumitremorgin C, *Mol. Cancer Ther.* 1 (2002) 417–425.
- [34] R.W. Robey, Y. Honjo, K. Morisaki, T.A. Nadjem, S. Runge, M. Risbood, M.S. Poruchynsky, S.E. Bates, Mutations at amino-acid 482 in the ABCG2 gene affect substrate and antagonist specificity, *Br. J. Cancer* 89 (2003) 1971–1978.
- [35] E.L. Volk, E. Schneider, Wild-type breast cancer resistance protein (BCRP/ABCG2) is a methotrexate polyglutamate transporter, *Cancer Res.* 63 (2003) 5538–5543.
- [36] G.M. Denning, M.P. Anderson, J.F. Amara, J. Marshall, A.E. Smith, M.J. Welsh, Processing of mutant cystic fibrosis transmembrane conductance regulator is temperature-sensitive, *Nature* 358 (1992) 761–764.
- [37] A. Bodó, É. Bakos, F. Szeri, A. Váradi, B. Sarkadi, Differential modulation of the human liver conjugate transporters MRP2 and MRP3 by bile acids and organic anions, *J. Biol. Chem.* 278 (2003) 23529–23537.
- [38] D.R. Stenham, J.D. Campbell, M.S. Sansom, C.F. Higgins, I.D. Kerr, K.J. Linton, An atomic detail model for the human ATP binding cassette transporter P-glycoprotein derived from disulfide cross-linking and homology modeling, *FASEB J.* 17 (2003) 2287–2289.

- [39] J.D. Campbell, K. Koike, C. Moreau, M.S. Sansom, R.G. Deeley, S.P. Cole, Molecular modeling correctly predicts the functional importance of Phe594 in transmembrane helix 11 of the multidrug resistance protein, MRP1 (ABCC1), *J. Biol. Chem.* 279 (2004) 463–468.
- [40] O. Ujhelly, C. Özvegy, G. Várady, J. Cervenak, L. Homolya, M. Grez, G. Scheffler, D. Roos, S.E. Bates, A. Váradi, B. Sarkadi, K. Németh, Application of a human multidrug transporter (ABCG2) variant as selectable marker in gene transfer to progenitor cells, *Hum. Gene Ther.* 14 (2003) 403–412.

Special Section on Transporters in Toxicity and Disease

Regulation of the Function of the Human ABCG2 Multidrug Transporter by Cholesterol and Bile Acids: Effects of Mutations in Potential Substrate and Steroid Binding Sites[§]

Ágnes Telbisz, Csilla Hegedüs, András Váradi, Balázs Sarkadi, and Csilla Özvegy-Laczka

Institute of Molecular Pharmacology, Research Centre for Natural Sciences, Hungarian Academy of Sciences (A.T., B.S.); Molecular Biophysics Research Group, Hungarian Academy of Sciences and Semmelweis University (C.H.); and Institute of Enzymology, Research Centre for Natural Sciences, Hungarian Academy of Sciences (A.V., C.O.-L.), Budapest, Hungary

Received November 1, 2013; accepted January 2, 2014

ABSTRACT

ABCG2 (ATP-binding cassette, subfamily G, member 2) is a plasma membrane glycoprotein that actively extrudes xenobiotics and endobiotics from the cells and causes multidrug resistance in cancer. In the liver, ABCG2 is expressed in the canalicular membrane of hepatocytes and excretes its substrates into the bile. ABCG2 is known to require high membrane cholesterol content for maximal activity, and by examining purified ABCG2 reconstituted in proteoliposomes we have recently shown that cholesterol is an essential activator, while bile acids significantly modify the activity of this protein. In the present work, by using isolated insect cell membrane preparations expressing human ABCG2 and its mutant variants, we have analyzed whether certain regions in this protein are involved in sterol recognition. We found that replacing ABCG2-R482 with large amino acids does not affect cholesterol dependence, but changes to

small amino acids cause altered cholesterol sensitivity. When leucines in the potential steroid-binding element (SBE, aa 555–558) of ABCG2 were replaced by alanines, cholesterol dependence of ABCG2 activity was strongly reduced, although the L558A mutant variant when purified and reconstituted still required cholesterol for full activity. Regarding the effect of bile acids in isolated membranes, we found that these compounds decreased ABCG2-ATPase in the absence of drug substrates, which did not significantly affect substrate-stimulated ATPase activity. These ABCG2 mutant variants also altered bile acid sensitivity, although cholic acid and glycocholate were not transported by the protein. We suggest that the aforementioned two regions in ABCG2 are important for sterol sensing and may represent potential targets for pharmacologic modulation of ABCG2 function.

Introduction

Human ABCG2 (ATP-binding cassette, subfamily G, member 2) is a plasma membrane glycoprotein expressed in many tissues, especially in those with barrier or detoxifying functions (brain endothelium, placenta, gut, liver) (Robey et al., 2009). This protein is an active transporter, working as a homodimer, using the energy of ATP hydrolysis for the extrusion of various compounds across the plasma membrane. ABCG2 is a promiscuous transporter, and its physiologic role is the protection of the body and fetus against exogenous or endogenous toxic compounds.

This work was supported by the Hungarian Research Fund grant [NK 83533], and grants from KMOP-1.1.2-07/1-2008-0003, NKTH-STEMKILL, and NIH-ARD ACHILLES.

dx.doi.org/10.1124/dmd.113.055731.

[§]This article has supplemental material available at dmd.aspetjournals.org.

Among ABCG2 substrates are various anticancer agents, so the protein is one of the key players causing the so-called multidrug resistant phenotype of cancer cells, resulting in the failure of cancer chemotherapy.

ABCG2 has been documented to be located in cholesterol rich microdomains, the so-called rafts, and its direct interaction with caveolin-1, a marker of lipid rafts, has also been demonstrated (Storch et al., 2007). In accordance with this finding, high membrane cholesterol levels were found to significantly improve the function of ABCG2. We and others found that the enrichment of insect membranes with cholesterol greatly increases the ATPase and transport function of ABCG2 (Pal et al., 2007; Telbisz et al., 2007). A dramatic but reversible inhibition of ABCG2 function in mammalian cells upon depletion of cholesterol has also been shown (Storch et al., 2007; Telbisz et al., 2007). It is not known whether cholesterol is only a modulator of ABCG2 function or it is directly transported by the protein. Other members of the ABCG subfamily (ABCG1, ABCG4, and ABCG5/ABCG8) are involved in

ABBREVIATIONS: ABCG2, ATP-binding cassette, subfamily G, member 2; BSEP, bile salt export pump; CA, cholic acid; CHAPS, 3-[(3-cholamidopropyl)dimethylammonio]-1-propanesulfonate; EKI-785, *N*-[4-[(3-bromophenyl)amino]-6-quinazolonyl]-2-butynamide; ESG, estradiol-glucuronide; GC, glycocholic acid; Hst, Hoechst 33342; Ko143, (3S,6S,12aS)-1,2,3,4,6,7,12,12a-octahydro-9-methoxy-6-(2-methylpropyl)-1,4-dioxopyrazino[1',2':1,6]pyrido[3,4-*b*]indole-3-propanoic acid 1,1-dimethylethyl ester; MRP2, multidrug resistance protein 2; MTX, methotrexate; PCR, polymerase chain reaction; RAMEB, randomly methylated β -cyclodextrin; R123, rhodamine 123; SBE, steroid-binding element; SN-38, 7-ethyl-10-hydroxy-camptothecin; TC, taurocholate; UDC, ursodeoxycholic acid; wt, wild type; ZD1839, *N*-(3-chloro-4-fluorophenyl)-7-methoxy-6-(3-morpholin-4-ylpropoxy)quinazolin-4-amine, gefitinib, Iressa.

cholesterol or sitosterol transport (Wang et al., 2008; Kerr et al., 2011).

We and others have recently shown that Arg 482 is important in cholesterol sensing of human ABCG2, as the function of ABCG2 mutants having Gly or Thr at position 482 was only slightly modified by cholesterol. We found that these mutants are fully active in Sf9 membranes with low cholesterol content or in mammalian cells partially depleted of cholesterol. In contrast, the ATPase and transport function of the wild-type ABCG2 greatly increases in insect membranes enriched with cholesterol. Still, in isolated ABCG2 preparations even the R482G mutant required low levels of cholesterol for full function (Telbisz et al., 2013).

Structural analysis of steroid hormone (progesterone, androgen, estrogen, or glucocorticoid) receptors and other steroid-binding proteins such as oxysterol-binding protein-related proteins revealed a complex interaction between the ligand-binding domains and the steroid substrates. A conserved motif of these ligand-binding domains is an L/MxxLxxL sequence or a shorter LxxL, in which the leucines form Van der Waals bonds with the rings of steroid hormones (Williams and Sigler, 1998; Im et al., 2005). In the ABCG8 protein, which is involved in sterol transport by forming a heterodimer with ABCG5, the fifth transmembrane helix contains an MxxLxxL motif; a Gly to Arg mutation at the beginning of this element causes loss of activity and sitosterolemia. Mutations in the LxxL motif in the homologous region of ABCG2, as a putative steroid-binding element (SBE), have been shown to cause failure in the progesterone and estradiol recognition of ABCG2 expressed in *Lactococcus lactis* (Velamakanni et al., 2008). Surprisingly, these mutants were similarly activated by cholesterol as the non-mutant protein.

Bile acids are abundantly formed from cholesterol in hepatocytes, and bile acids and their derivatives are present in all tissue fluids. Due to their enterohepatic circulation, bile acid concentrations are especially high in the intestinal epithelial cells and in hepatocytes. The interaction between ABCG2 and bile acids has been extensively investigated, but these studies have yielded controversial data. Two groups have reported that there is no interaction with ABCG2 or direct transport of taurocholate, tauroolithocholate sulfate, or tauroursodeoxycholic acid by this protein (Suzuki et al., 2003; Vaidya and Gerke, 2006). In contrast, two other laboratories described direct interaction between ABCG2 and bile acids (Imai et al., 2003; Janvilisri et al., 2005). ABCG2-specific extrusion of a fluorescein-conjugated bile acid derivative cholyglycylamidofluorescein and also a low-level transport of cholic acid, glycocholic acid, taurocholic acid, and tauroolithocholic acid-3-sulfate have been suggested (Blazquez et al., 2012).

In our present study, we provide a detailed mutational analysis of the cholesterol-sensing capability of different ABCG2 R482 mutants as well as mutants carrying the L555A, L558A, or L555A/L558A point mutations. In addition, we present a comprehensive characterization of the interaction between ABCG2 and bile acids. We demonstrate the modulatory effects of these mutations on ABCG2 function and their contribution to the cholesterol/bile acid sensing capability of the protein. We also show that as compared with “professional” bile acid transporters ABCG2 has no significant bile acid transport capacity.

Materials and Methods

Unless indicated otherwise, all materials were purchased from Sigma-Aldrich (Budapest, Hungary). Cholesterol-RAMEB (cholesterol-loaded randomly methylated β -cyclodextrin) was kindly provided by CycloLab Ltd. (Budapest, Hungary). The BXP-21 monoclonal antibody (Maliepaard et al., 2001) and Ko143 [(3S,6S,12aS)-1,2,3,4,6,7,12,12a-octahydro-9-methoxy-6-(2-methylpropyl)-1,4-dioxopyrazino[1',2':1,6]pyrido[3,4-b]indole-3-propanoic acid 1,1-dimethylethyl

ester] (Allen et al., 2002) were kind gifts from Drs. George Scheffer and Rik Scheper, and from Dr. G. J. Koomen, respectively.

Expression Vectors. Generation of the baculovirus transfer vector (pAcUW21-L) harboring the cDNA for wild-type (wt) ABCG2 or the R482 and K86M mutants was described previously (Ozvegy et al., 2002; Ozvegy-Laczka et al., 2005). The steroid-binding element mutants were created by site-directed polymerase chain reaction (PCR) mutagenesis using the following complementary primer pairs: L555A: 5' T TCA GGT CTC GCG GTC AAT CT and 5' AG ATT GAC CGC GAG ACC TGA A; L558A: 5' GT CTG TTG GTG AAT GCC ACA ACC ATT and 5' AAT GGT TGT GGC ATT CAC CAA CAG AC; L555/558A: 5' GT CTC GCG GTG AAT GCC ACA ACC ATT and 5' AAT GGT TGT GGC ATT CAC CGC GAG AC. The PCR fragments containing the mutant cDNAs were cloned between the NcoI-SacI sites of the pAcUW21-L/wtABCG2 vector. The base order of the constructs was confirmed by sequencing of the appropriate fragments. The R482G/L555/558A triple mutant was created by replacing the DNA fragment between the PstI-NcoI sites of the pAcUW21-L/R482G with that of derived from the pAcUW21-L/L555/558A vector.

Generation of His₆-Tagged ABCG2 Variants. His₆-ABCG2 was generated as described by Telbisz et al. (2013). The His₆-tagged L558A and L555/558A mutants were created by cloning the PstI-SacI site from pAcUW21-L/ABCG2-L558A or L555/558A into the pAcUW21-L/His₆-ABCG2.

Cell Culturing, Generation of Recombinant Baculoviruses, and Membrane Preparation. We cultured Sf9 cells and generated recombinant baculoviruses as described previously (Bakos et al., 2000; Ozvegy et al., 2001). Membrane preparation was performed as described by Ozvegy et al. (2001). Cholesterol loading of the membrane preparations was achieved by incubation with 2 mM cholesterol-RAMEB on ice for 30 minutes, as published previously (Telbisz et al., 2007).

Immunodetection of ABCG2. We suspended the Sf9 membranes in Laemmli sample buffer containing 2% of the reducing agent β -mercaptoethanol. Western blot analysis was performed as described elsewhere (Ozvegy et al., 2002) by use of the BXP-21 monoclonal antibody in a 2000 \times dilution, and a goat anti-mouse horseradish peroxidase-conjugated secondary antibody (10,000 \times dilution, Jackson ImmunoResearch Laboratories, West Grove, PA).

Solubilization, Purification, and Reconstitution into Proteoliposomes. Solubilization of His₆-tagged wtABCG2 and its SBE mutant variants was performed with 1% (w/v) DDM (dodecyl maltoside), 0.4% *Escherichia coli* lipid extract (100500; Avanti Polar Lipids, Inc., Alabaster, AL), as described (Telbisz et al., 2013). Purification and reconstitution were performed as described in our recent article (Telbisz et al., 2013). Briefly, Ni-NTA (Ni²⁺-nitrilotriacetate; Sigma His-select, H-0537) was used for purification, and the purified ABCG2 protein (wild-type or its SBE mutants) was reconstituted in *E. coli* lipid extract supplemented with 0–0.4 mM cholesterol.

ATPase Activity Measurements. ATPase activity was measured on isolated membranes of Sf9 cells expressing wtABCG2 or its mutant variants by colorimetric detection of inorganic phosphate liberation, as previously described (Ozvegy et al., 2002). Figures represent the mean values of at least two independent experiments with four parallels, measured in two different membrane preparations for each type of ABCG2. ATPase activity of ABCG2 in proteoliposomes was determined as described previously (Telbisz et al., 2013).

Vesicular Uptake Measurements. The Sf9 membrane vesicles were incubated in the presence or absence of 4 mM MgATP (or 4 mM MgATP + 1 μ M Ko143) in a buffer containing 40 mM 3-(*N*-morpholino) propanesulfonic acid-Tris (pH 7.0), 56 mM KCl, 6 mM MgCl₂, and 2 mM dithiothreitol, in a final volume of 140 μ l at 37°C for 5 minutes. The measurement was started by the addition of 100 μ M [³H]methotrexate (Moravek Biochemicals and Radiochemicals, Brea, CA), 25 or 50 μ M [³H]estradiol-glucuronide (Perkin-Elmer Life and Analytical Sciences, Waltham, MA), 100 μ M [³H]glycocholate (PerkinElmer) or 100 μ M [³H]cholic acid (American Radiolabeled Chemicals, Inc., St. Louis, MO). The experiments were performed as described previously (Ozvegy-Laczka et al., 2005).

Cellular Dye Uptake and Calculation of ABCG2 Transport Activity. Measurement of pheophorbide A and rhodamine 123 extrusion by ABCG2 from intact insect cells was described earlier (Ozvegy-Laczka et al., 2008). Geometric mean fluorescence values measured in the absence (M_0) or presence (M_i) of inhibitor were determined, and the activity factor was calculated as follows: $(M_i - M_0)/M_i * 100$.

Measurement of Hoechst 33342 Transport Activity. Hoechst 33342 transport was determined as described in Ozvegy-Laczka et al. (2004). Transport activity was calculated as $((F_{100} - F_0)/F_{100}) * 100$, where F_{100} is fluorescence in the presence of 1 μ M Ko143, and F_0 is fluorescence in the absence of the inhibitor.

Results

Effect of Cholesterol on the Function of ABCG2 R482 Mutant Variants

Effect of Cholesterol on the ATPase Activity of the ABCG2 R482 Mutants. The cholesterol dependence of human ABCG2 in Sf9 cell membranes has been characterized in detail previously (Pal et al., 2007; Telbisz et al., 2007). Briefly, human ABCG2 when expressed in cholesterol “poor” insect cells (5–8 μ g cholesterol/mg membrane protein) has well-measurable ATPase and transport activity. However, increasing the cholesterol content of the insect membranes by cholesterol-loaded randomly methylated β -cyclodextrin (cholesterol-RAMEB) up to 40–60 μ g cholesterol/mg membrane protein results in 4- to 20-fold activation of the transport function of ABCG2. Accordingly, substrate stimulation of the ATPase activity becomes more pronounced in cholesterol-enriched Sf9 membranes (Pal et al., 2007; Telbisz et al., 2007). Moreover, in our recent study we demonstrated that cholesterol is essential for ABCG2 function: purified ABCG2 is only active when the proteoliposomes contain 20–30 mol % cholesterol (Telbisz et al., 2013). Despite the crucial role of cholesterol in ABCG2 function, the cholesterol-sensing sites in ABCG2 are yet to be defined.

The Arg482 residue, residing in or near the third transmembrane helix of ABCG2, has been documented to significantly alter the substrate interactions of the transporter. Several of the R482 variants gain a rhodamine 123 transport function, while all of them lose methotrexate (MTX) transport capacity (Ozvegy et al., 2002; Ozvegy-Laczka et al., 2005). We showed earlier that Arg482 also has a critical role in the cholesterol sensitivity of human ABCG2. In contrast to the wild-type protein, in Sf9 cell membranes increasing the membrane cholesterol levels did not significantly influence the activity of the R482G and R482T mutants (Telbisz et al., 2007), although experiments on purified ABCG2 reconstituted in proteoliposomes revealed that cholesterol is also essential for the function of the R482G variant (Telbisz et al., 2013).

To examine how the characteristics of amino acid 482 influence the cholesterol-sensing capability of ABCG2, we have analyzed seven additional R482 mutants (R482D, I, M, N, S, Y, and K). These ABCG2-R482 variants were expressed in Sf9 insect cells at similar level to the wild-type protein (data not shown); as documented earlier, all these mutants were active, showing a measurable basal ATPase activity that was sensitive to Ko143, a specific inhibitor of ABCG2 (Ozvegy-Laczka et al., 2005). In our present study, the ATPase activity of the mutant variants was measured in “control” (native, cholesterol-poor) and cholesterol-enriched Sf9 membranes. In cholesterol-loaded membranes, the basal ATPase activity of most of these variants increased (see Supplemental Table 1), but the increase in membrane cholesterol levels did not change the relative substrate stimulation of the R482D, G, N, S, and T variants (Fig. 1A). In contrast, in the case of the R482I, K, M, and Y variants, similarly to the wild-type ABCG2, cholesterol enrichment significantly improved the ratio of substrate stimulation, as examined after the addition of prazosin (Fig. 1A). We also observed a similar effect of other substrates (e.g., quercetin) on the ATPase activity of these mutants (data summarized in Supplemental Table 1).

Effect of Cholesterol on the Transport Activity of the ABCG2 R482 Mutants. To find out whether membrane cholesterol has a direct effect on the transport activity of the R482 mutants, we measured the [3 H]methotrexate uptake in Sf9 inside-out membrane vesicles containing different R482 variants either in the presence or absence of excess

cholesterol. As shown in Supplemental Fig. 1A, in contrast to wild-type ABCG2, none of the R482 mutants exhibited significant methotrexate transport, either in the control or in the cholesterol-loaded membrane vesicles. These findings suggest that cholesterol enrichment of the membranes did not alter this particular substrate interaction of the mutant ABCG2 variants.

Intact Sf9 cells, which transiently express ABC transporters, are suitable for fluorescent dye accumulation measurements in which the transport activity of the human ABCG2 can be determined (Ozvegy et al., 2002). In the following experiments, intact Sf9 cells were harvested 24–40 hours after transfection, when approximately 60–70% of the cells are viable; accumulation of different ABCG2 substrates was measured in control or cholesterol-enriched Sf9 cells.

When the Sf9 cells were loaded with cholesterol by incubating them with 2 mM cholesterol-RAMEB, we found that this treatment did not influence cell viability, at least during the period of the transport experiments. The cellular fluorescence of Hoechst 33342 (Hst) and rhodamine 123 (R123) was analyzed by fluorometry and flow cytometry, respectively. The activity factors for the different ABCG2 variants were calculated based on the intracellular fluorescence detected in the presence or absence of the specific inhibitor Ko143. The actual expression levels of the ABCG2 variants were examined by Western blot analysis, and they showed similar expression levels of the transporter (data not shown).

Similar to earlier findings, there was a well-measurable Ko143-sensitive Hst dye transport both in the cells expressing wtABCG2 and in those expressing most R482 mutants, with only very low activity in the case of the R482K and R482Y variants (Fig. 1B). When the cells were loaded with cholesterol, this Hst dye uptake was significantly improved in the wild-type and the R482I and M variants. Moreover, significant Hst transport activity occurred in the case of the R482K and Y variants. In contrast, we did not observe a significant effect of cholesterol on the Hst transport by the R482D, G, N, S, and T variants. Note that these cholesterol-mediated alterations in the Hst transport capacity of ABCG2 correspond to the effect of cholesterol on the ABCG2-ATPase activity.

To examine the potential effects of cholesterol on the substrate specificity of the mutant variants, we also measured ABCG2-dependent R123 extrusion both in the control and cholesterol-loaded Sf9 cells, expressing the human ABCG2 variants (Supplemental Fig. 2B). As noted earlier, the wtABCG2 had no R123 transport activity, whereas several mutant variants acquired such a transport function. Cholesterol loading significantly increased R123 extrusion in cells expressing the R482I and M variants, while there was no measurable effect in the D, G, N, S, or T variants. In the case of the wild-type protein and the R482K and Y variants, there was no detectable R123 extrusion in either the absence or presence of cholesterol.

Effect of Cholesterol on the Function of ABCG2-SBE Mutant Variants

A predicted steroid-binding element (SBE, LxxL) of ABCG2 is located in the potential fifth transmembrane helix of the transporter (see *Introduction*). The motif was reported to alter ABCG2-mediated recognition of progesterone and estradiol, two steroid hormones closely related to cholesterol (Velamakanni et al., 2008). We have generated the Leu to Ala mutations L555A, L558A, and L555A/L558A in this motif. The mutants were expressed in Sf9 cells at equal levels to wtABCG2 (Fig. 2A), and the effect of cholesterol on the ATP hydrolysis and transport activity of the mutants was investigated using membrane vesicles or transporter-expressing intact Sf9 cells.

Effect of Cholesterol on the ATPase Activity of the SBE Mutant ABCG2. As shown in Fig. 2B, the L555A, L558A, and L555A/L558A mutants exhibited a well-measurable vanadate-sensitive ATPase

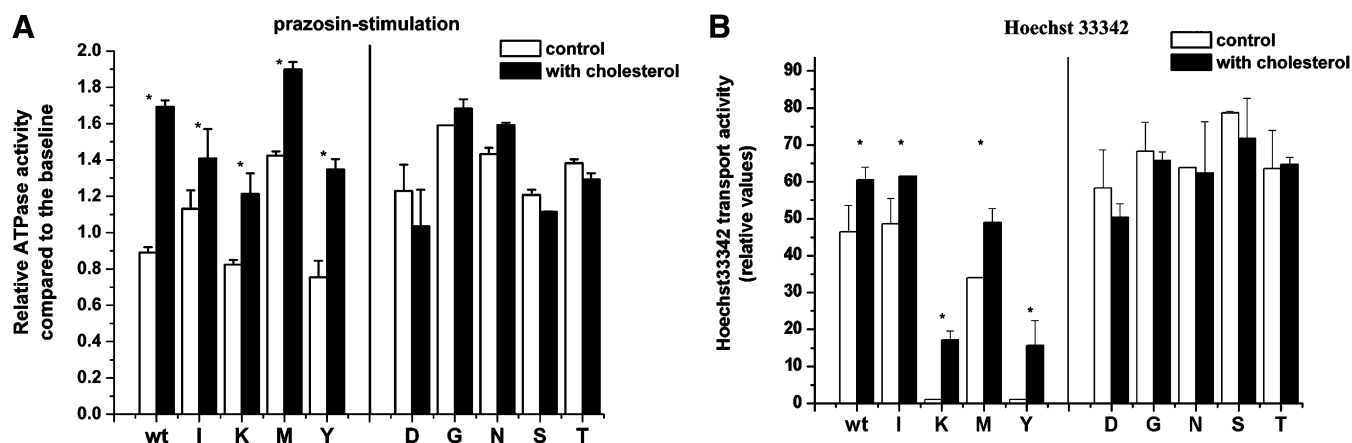


Fig. 1. ATPase and transport activity of the ABCG2-R482 mutants: effect of cholesterol. (A) Vanadate-sensitive ATP hydrolysis of wtABCG2 and its R482 mutant variants was determined in insect cell membranes (open bars) and in insect cell membranes loaded with cholesterol (black columns). The ratio of substrate-stimulated ATPase activity (measured in the presence of 100 μ M prazosin) and baseline ATP hydrolysis (no added substrate) is shown. Columns represent data obtained from two independent experiments with four parallels, bars \pm S.D. values. * $P < 0.05$, Student's t test, significant difference. (B) Hoechst 33342 (1 μ M) uptake was determined in insect cells transfected with baculoviruses encoding different ABCG2-R482 mutants or the wild-type protein. Cellular fluorescence was determined via fluorescence spectrophotometer. Transport activity was calculated as $(F_{100} - F_0)/F_{100} * 100$, where F_{100} is fluorescence in the presence of 1 μ M Ko143, and F_0 is fluorescence in the absence of the inhibitor. * $P < 0.05$, Student's t test, significant difference.

activity. However, given the similar expression levels of the wild-type and the mutant proteins, we found that L555A and L555A/L558A had only about one-third the basal ATPase activity as compared with wtABCG2. Moreover, in the case of the L555A and L555A/L558A mutants, ATPase turnover in the presence of quercetin was also well below of that measured for the wild-type protein or the L558A mutant.

When analyzing the effect of cholesterol loading on the quercetin-stimulated ATP hydrolysis, we found no significant change in ATPase turnover in any of the three SBE mutants (see Fig. 2B).

Next, we studied the effect of numerous wtABCG2 substrates on the ATPase activity of the SBE mutants in both control and cholesterol-enriched Sf9 cell membranes. Several activators of wtABCG2 ATPase (doxorubicin, flavopiridol, SN-38 [7-ethyl-10-hydroxy-camptothecin], and topotecan) did not stimulate ATP hydrolysis of the mutants even in cholesterol-enriched membranes (not shown). However, we found a few substrates (nilotinib, prazosin, quercetin, and EKI-785 (*N*-[4-[(3-bromophenyl)amino]-6-quinazolinyl]-2-butynamide) that enhanced ATP hydrolysis in these mutants as well. To investigate the effect of cholesterol on substrate-stimulated ATPase activity of the SBE mutants, we have measured the effect of these "activators" in membranes loaded with different amounts of cholesterol (by applying 0.025–2 mM cholesterol-RAMEB for cholesterol loading). We found that increasing the cholesterol content of the Sf9 cell membranes did not significantly enhance the substrate stimulation of the ATPase activity in the LxxL mutants. These effects of nilotinib and quercetin in such membrane preparations are shown in Supplemental Fig. 2; prazosin and EKI-785 gave similar results (data not shown).

Effect of Cholesterol on the Transport Activity of the SBE Mutant ABCG2. In these experiments, we examined the effect of cholesterol on the [3 H]methotrexate ([3 H]MTX) and [3 H]estradiol-glucuronide ([3 H]ESG) transport activity of ABCG2 L555A, L558A, and L555A/L558A mutant variants expressed in Sf9 insect cells. As discussed earlier, cholesterol enrichment of the Sf9 inside-out membrane vesicles greatly increases MTX and ESG transport by wtABCG2 (see the previous discussion and Telbisz et al., 2007). To test whether cholesterol has any effect on the transport function of the SBE mutants, Sf9 membrane inside-out vesicles containing the SBE mutants were analyzed for their [3 H]MTX and [3 H]ESG transport activity.

We found that despite their comparable expression level to wtABCG2, the L555A and L555A/L558A mutants did not show any detectable

vesicular transport activity for MTX in either control or cholesterol-rich membranes. Even in the case of the L558A mutant, which showed high ATPase activity, we could detect only very low MTX transport activity, similar to that observed in the R482 mutants (Supplemental Figs. 1A and 3A). When we analyzed [3 H]MTX transport by the L558A mutant in membranes loaded with cholesterol, we found only a nonsignificant increase in this transport activity (Supplemental Fig. 3A). In the ESG vesicular transport experiments, again none of the three mutants showed ABCG2-specific activity, and cholesterol did not improve their ESG transport function (Supplemental Fig. 3B).

To further analyze the effect of cholesterol on the activity of the SBE mutants, we measured the accumulation of different fluorescent ABCG2 substrates in intact Sf9 insect cells. Accumulation of Hoechst 33342 or pheophorbide A was determined by fluorometry or flow cytometry, respectively, in both control cells and cells loaded with 2 mM cholesterol-RAMEB. The actual expression levels of ABCG2 variants were examined in each experiment by Western blot analysis (data not shown). We found that the SBE mutants were able to transport both Hoechst 33342 and pheophorbide A, but in contrast to the wild-type protein, cholesterol did not improve their dye extrusion capacity (Fig. 2, C and D).

Effect of Cholesterol on the Function of Isolated and Reconstituted ABCG2-SBE Mutants

It was shown earlier that an increase in the cholesterol levels of the insect membranes did not significantly modulate the function of the ABCG2 R482G mutant, which would imply its apparent cholesterol insensitivity. However, reconstitution of the purified ABCG2 R482G variant revealed that the presence of cholesterol was also essential for the function of this mutant variant; however, lower cholesterol levels (amounts that are most probably present in native insect membranes) were sufficient to achieve its full activity as compared with wtABCG2 (Telbisz et al., 2013). To analyze the cholesterol sensing of the purified SBE mutants, we have generated N-terminally His₆-tagged versions of the L558A and L555/558A variants. The His₆-L558A and His₆-L555A/L558A ABCG2 mutants were successfully expressed in Sf9 cells, and we also found that tagging did not alter their functionality (data not shown).

The membrane isolation as well as the purification and reconstitution of the L558A variant were successful. However, though

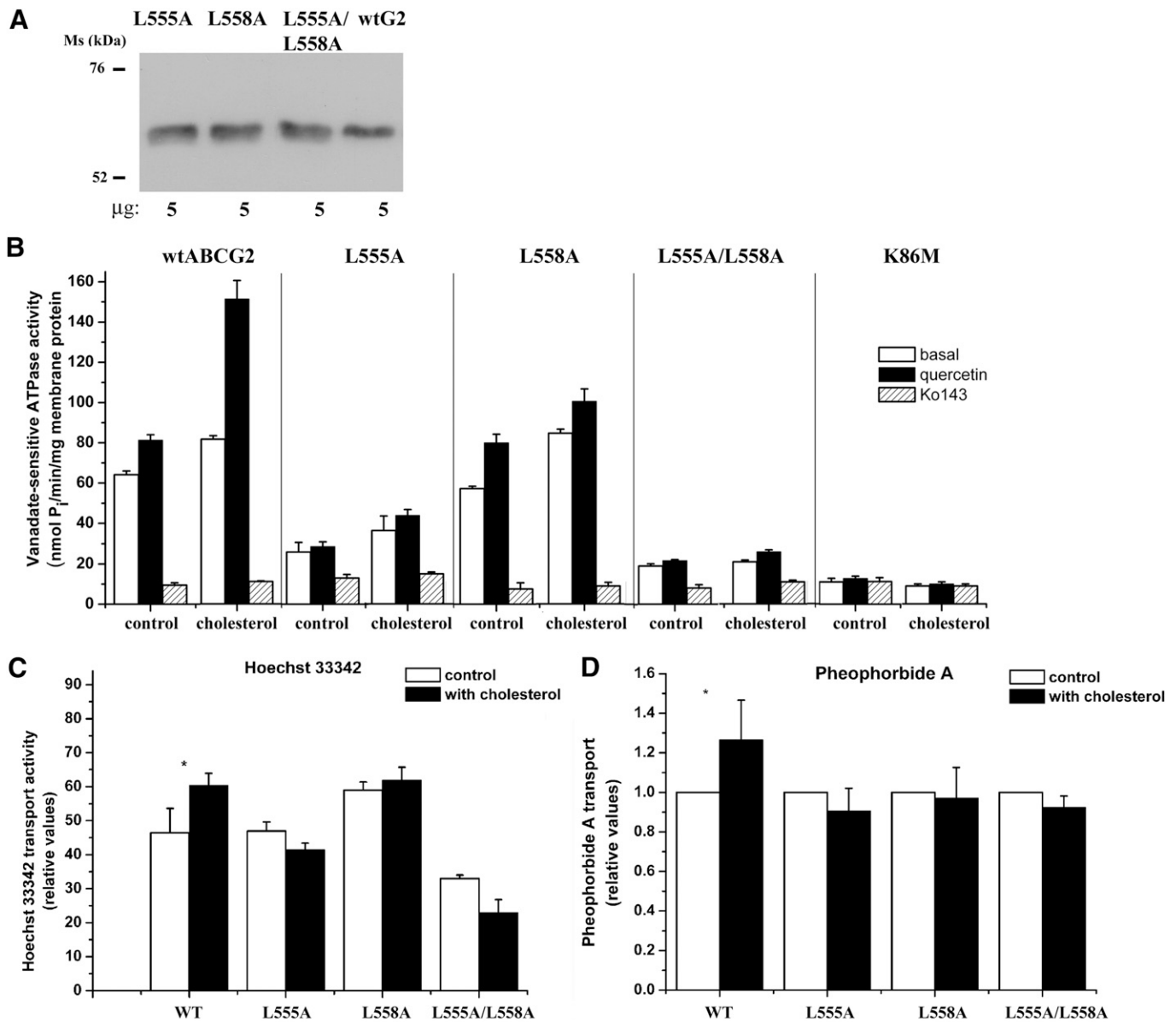


Fig. 2. Expression and ATPase activity of ABCG2 SBE mutants in Sf9 cells. (A) Western blot detection of the SBE mutants in insect membranes using the BXP-21 antibody. Samples were loaded in equal amounts to the gel. (B) ATP hydrolysis of the SBE mutants in control and cholesterol-loaded membranes. ATPase activity was determined in the absence of added substrates (open bars) or in the presence of 1 μ M quercetin (black columns) or 10 μ M Ko143 (striped bars). Data were compiled from two independent experiments with four parallels, and the average \pm S.D. values are indicated. (C and D) Effect of cholesterol on the transport activity of wtABCG2 and the SBE mutant variants in insect cells. Fluorescent dye uptake was determined in insect cells transfected with baculoviruses encoding different ABCG2-SBE mutants or wild-type protein. Cellular fluorescence was determined in a FACsCalibur cytometer (2 μ M pheophorbide A) or in a fluorescence spectrophotometer (1 μ M Hoechst 33342). Transport activity was calculated as described in the experimental procedures or in Fig. 1. For pheophorbide A uptake, data were normalized to the activity measured in the absence of added cholesterol. Average \pm S.D. values of three independent experiments are shown.

the expression level of the His₆-L555A/L558A variant in the Sf9 cells was comparable to that of the other variants, the purification yielded a much lower amount of this mutant (data not shown).

We analyzed the ATPase activity of the purified L558A variant, reconstituted in *E. coli* lipids in the absence and in the presence of cholesterol. Interestingly, this ABCG2 mutant had a negligible ATP hydrolysis in cholesterol-free *E. coli* lipids, similar to the wild type, while increasing cholesterol concentrations greatly accelerated both the basal (Fig. 3A) and the substrate-stimulated (data not shown) ATPase activities, again in harmony with the wild type.

Surprisingly, the L555/558A mutant lost its functionality upon purification. There was no ATPase activity in proteoliposomes, regardless

the amount of cholesterol applied. When we investigated the dimerization state of the double mutant, we found that in contrast to the wild-type protein, the disulphide bridge linked homodimer (corresponding to the physiologic state of ABCG2) could not be detected in the case of the double mutant after purification (Fig. 3B). Therefore, the inactivity of the double mutant can be due to its impaired dimerization capability.

Effect of Bile Acids on the Function of Human Wild-Type ABCG2 Expressed in Sf9 Cell Membranes

Bile acids are continuously present in all tissue fluids, including blood plasma, where after a meal free bile acid levels can reach 100 μ M. Bile acids participate in continuous enterohepatic circulation, and

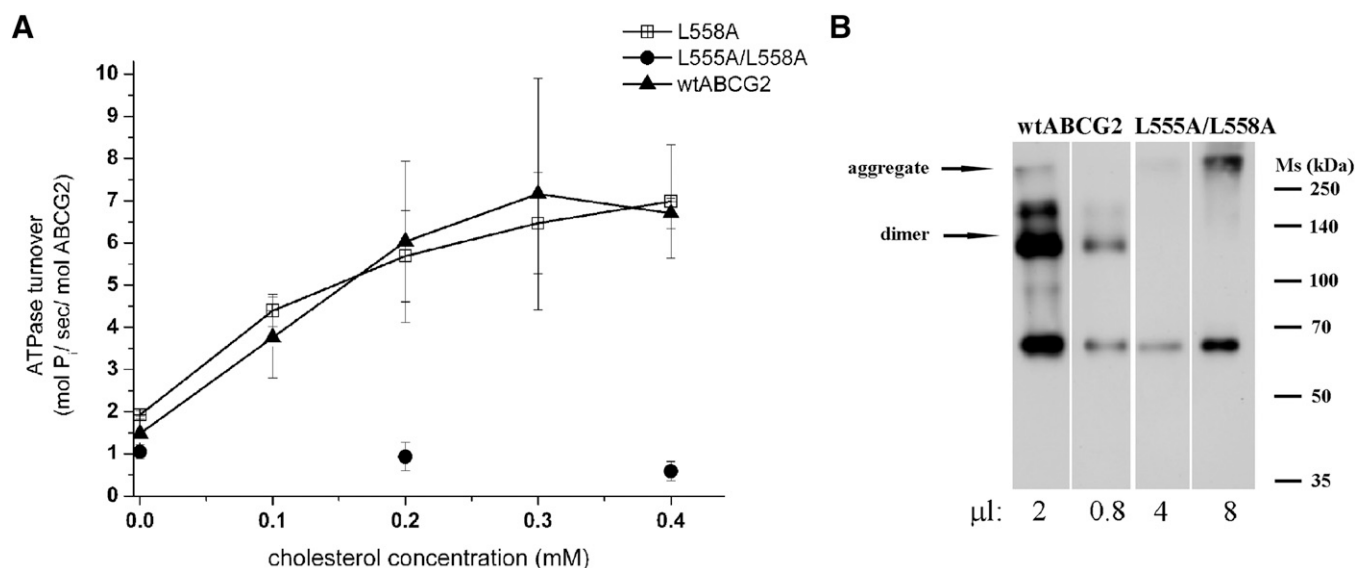


Fig. 3. (A) ATPase activity of purified wtABCG2, ABCG2-L558A, and L555/558A in proteoliposomes. N-terminally His₆-tagged ABCG2 was isolated, purified, and reconstituted in 1 mg/ml *E. coli* lipid extract plus various amounts of cholesterol, as indicated on the x-axis. ATPase activity was measured in the absence of added substrates. Data points show the average of three independent experiments \pm S.D. values. (B) Lack of dimerization of the purified L555/558A mutant. Purified wtABCG2 or L555/558A was treated with 4 mM oxidized dithiothreitol (DTT) for 5 minutes at 37°C, and then dissolved in sample buffer (62.5 μ M Tris HCl pH 6.8, 2% SDS, 10 μ M EDTA-Na pH 6.8, 10% glycerol, 2 M urea, 0.14 mg/ml bromophenol blue). Electrophoresis and Western blotting have been performed as described in *Materials and Methods* section. ABCG2 was detected by the BXP-21 antibody.

their concentrations inside intestinal epithelial cells or in hepatocytes are considerably higher, especially in the bile-secreting canalicular membranes (Li and Chiang, 2012). The critical micelle concentrations of bile acids are in the range of 2–10 mM (Simonović and Momirović, 1997), and hepatic bile acid secretion occurs by the formation of mixed micelles with phospholipids and cholesterol. In the next set of experiments, we determined whether, similar to cholesterol, bile acids modulate the function of ABCG2.

Effect of Bile Acids on the ATPase Activity and Transport Function of Wild-Type ABCG2. To compare the effect of cholesterol and bile acids, we performed studies with these sterols alone or in combination. In the control Sf9 cell membranes, there is no stimulation of ATPase activity with prazosin (a known transported substrate of ABCG2), whereas quercetin (also a transported substrate of the protein) has a measurable stimulatory effect even in these conditions. When the cholesterol content of the membranes is increased, significant activation of ATP hydrolysis by prazosin occurs, and an increase in quercetin-stimulated ATPase activity is also observed (see Fig. 4A). When cholic acid (CA, 1 mM) is added to the control membranes, a significant reduction in the baseline ABCG2-ATPase (measured in the absence of added drug-substrates) and a slight stimulatory effect of prazosin are observed (the effect of quercetin is unaltered; Fig. 4B, left columns). However, the most pronounced effect of CA is observed in cholesterol-loaded membranes (Fig. 4B, right columns): baseline ATPase activity is strongly reduced (almost to the level of Sf9 membranes expressing the inactive ABCG2-K86M mutant; see Fig. 2B), while drug-stimulated ATPase activity is unchanged. Thus, relative drug-stimulated ATPase activity (ATP hydrolysis with drug substrates/basal ATP hydrolysis) is increased up to 6- to 8-fold.

To characterize these phenomena in more detail, we examined the concentration-dependent effects of bile acids on human wtABCG2-ATPase activity in cholesterol-loaded Sf9 cell membranes, closely reflecting the plasma membrane environment of mammalian cells. It has to be emphasized that bile acids were used under their critical micelle concentration values, thus a direct membrane effect was unlikely to occur.

As shown in Fig. 4C, all the investigated bile acids—glycocholate (GC), taurocholate (TC) cholic acid (CA) and ursodeoxycholic acid (UDC) and the synthetic derivative CHAPS (3-[(3-cholamidopropyl) dimethylammonio]-1-propanesulfonate), which has a critical micelle concentration of 6–10 mM—effectively reduced the baseline ATPase activity of wtABCG2, while substrate-stimulated ATPase was unaltered. Due to these effects, the relative drug-stimulated ATPase activity (measured in the presence of quercetin) was increased, and especially UDC produced a high ratio of drug-stimulated and basal ABCG2-ATPase activity (Fig. 4D).

We examined drug-stimulated ATPase activity for several other known ABCG2 substrates and found that bile acids did not increase the V_{max} of ATPase; however, due to the decreased baseline ATP hydrolytic activity, relative drug stimulation was increased. These effects for several substrates are documented in Table 1. It should also be noted that the effect of the ABCG2 inhibitor Ko143 remained unaltered in the presence of bile acids.

In the following experiments, we examined the effect of various bile acids on the transport function of ABCG2 in vesicular uptake assays. In these studies, we used radiolabeled MTX and ESG as established ABCG2 substrates and added various bile acids to the medium. We found that at low concentrations (25–50 μ M) bile acids had no effect on ABCG2-dependent substrate transport, but higher bile acid concentrations (above 250 μ M) inhibited both MTX (data not shown) and ESG transport activity (Supplemental Fig. 4). Because in the vesicular transport measurements we used low substrate concentrations, a high ratio of bile acid/transported substrate may explain these latter results (see *Discussion*).

It had been documented by others that bile acids can stimulate the transport activity of MRP2 (Bodo et al., 2003). This was also observed by us when measuring ATP-dependent ESG transport by MRP2—the addition of 250 μ M cholic acid doubled the ESG transport activity in the case of MRP2, and glycocholate also increased this transport by 25% (Supplemental Fig. 4).

Examination of the Transport of Bile Acids by ABCG2. As described earlier, bile acids decrease the basal ATPase activity of

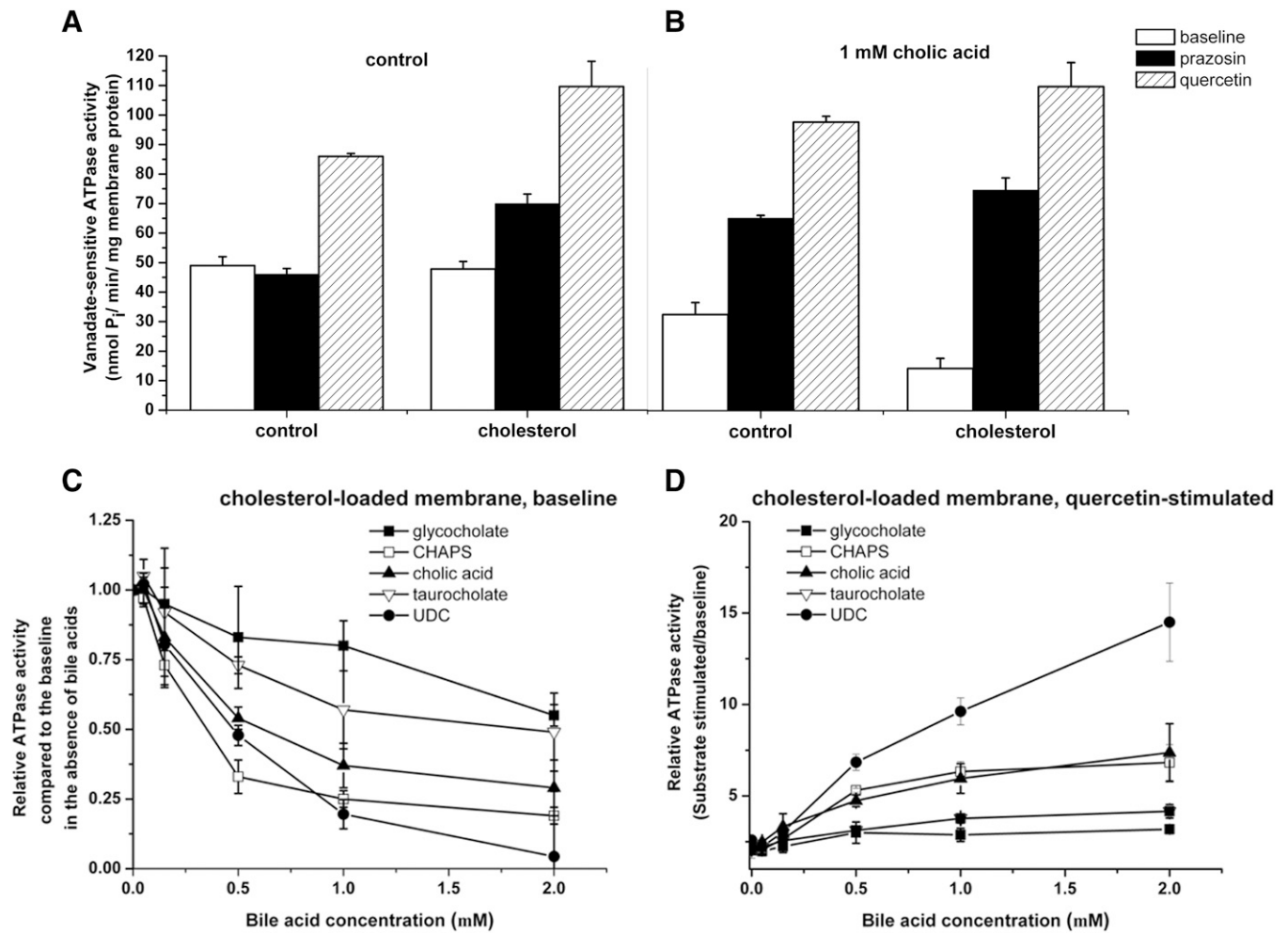


Fig. 4. Effect of bile acids on ABCG2 ATPase function. (A) Vanadate-sensitive ATPase activity in Sf9 membrane vesicles containing wtABCG2 was determined in either the absence (A) or the presence (B) of 1 mM cholic acid both in control and 2 mM cholesterol-RAMEB-treated membranes. Open columns represent baseline ATPase activity (no added compound); black or striped columns show ATP hydrolysis in the presence of 100 μ M prazosin or 5 μ M quercetin, respectively. Average of two independent experiments, each with two parallels \pm S.E. values. (C and D) Relative ATPase activity of wtABCG2 in cholesterol-loaded Sf9 membranes: effect of increasing amounts of bile acids. (C) ATP hydrolysis in cholesterol-loaded ABCG2-containing Sf9 membranes is shown as a relative value compared with the activity measured in the absence of added substrates and bile acids. (D) ATP hydrolysis in the presence of 5 μ M quercetin compared with the baseline ATPase activity (no drug-substrate, no bile acid added). Measurements were performed in quadruplicate; mean \pm S.E. values are shown.

ABCG2. However, this does not necessarily mean that they are not transported molecules (e.g., Hoechst 33342, a known transported ABCG2 substrate, inhibits the ATPase function; Ozvegy et al., 2002). To explore this question, we examined the transport of several bile acids in transporter-expressing inside-out Sf9 membrane vesicles.

ATP-dependent uptake of different radiolabeled bile acids was measured in ABCG2-containing, cholesterol-loaded, inside-out insect membrane vesicles (showing maximum transport activity, such as for ESG). In parallel experiments, we also examined similar bile acid transport by using membrane vesicles containing multidrug resistance protein 2 (MRP2, ABCC2) or BSEP (bile salt export pump, ABCB11), two known bile acid transporters. In all cases, the transport of labeled GC, CA, ESG, or MTX was examined in concentrations already documented to provide well-measurable uptake in the case of these transporters.

As documented in Fig. 5, significant, ATP-dependent, GC uptake was measured in the case of MRP2 and BSEP, whereas ABCG2 showed no transport activity. CA was efficiently transported by BSEP but not by MRP2 or ABCG2. These direct transport measurements also indicate that bile acids in the applied concentrations (100 μ M)

have no pronounced effect on the stability of the inside-out Sf9 membrane vesicles used in these experiments. In the case of ESG, MRP2 had the highest transport activity, and MTX was best transported by ABCG2. These results indicate that ABCG2 is most probably not a professional bile acid transporter.

Effect of Bile Acids on the Function of ABCG2 R482 and SBE Mutants

We documented that mutations in amino acid position 482 and the replacement of leucines to alanines in the potential steroid-binding element (SBE) of ABCG2 strongly influence the cholesterol-sensing capability of the protein. To explore the effect of bile acids, we performed these experiments in cholesterol-loaded Sf9 cell membranes by examining selected representatives of the R482 variants. These were the R482G and R482S variants, which are fully active already at low membrane cholesterol levels, and the R482K and R482I mutants, which show similar cholesterol-sensing capability to the wtABCG2 (see earlier). We also examined the effect of bile acids on the LxxL mutants (see Fig. 6).

TABLE 1

Effect of cholic acid on the stimulation or inhibition of the ABCG2-ATPase in cholesterol-loaded, isolated Sf9 membranes by various ABCG2-interacting compounds.

Compound	Concentration μM	Relative ATPase Activity Compared with Baseline	
		Control	With 1 mM Cholic Acid
ABCG2 substrates			
Quercetin	5	2	5.4
ZD1839	1	1.7	2.7
Nilotinib	0.1	1.6	3.1
Topotecan	100	1	1.7
Flavopiridol	50	0.8	1.8
Sulfasalazine	5	2	2.8
Prazosin	50	1.8	6
ABCG2 inhibitor			
Ko143	1	0.2	0.3

ZD1839, *N*-(3-chloro-4-fluorophenyl)-7-methoxy-6-(3-morpholin-4-ylpropoxy)quinazolin-4-amine, gefitinib, Iressa.

When measuring the effect of bile acids on ABCG2-ATPase activity in isolated Sf9 membranes, we found that, in contrast to the wild-type protein (Figs. 4, C and D, and 6A), in the case of the R482G or S variants low concentrations of CA did not significantly alter ABCG2-ATPase activity; however, when we used higher bile acid concentrations (above 0.5 mM), both baseline and substrate-stimulated ATPase activities decreased (see Fig. 6B for the R482G mutant; R482S is not shown). Thus, relative substrate stimulation was not increased by bile acids in these variants (see also Fig. 6D). In the case of the R482K and I mutants, a variable alteration in the substrate stimulation was observed for different bile acids (Fig. 6D).

Figure 6C shows that CA does not influence ATP hydrolysis of the L555A/L558A mutant—that is, both basal and substrate-stimulated activities remained unaltered. GC and TC also did not influence the activity of the L555A/L558A mutant (data not shown). Similarly, the activity of the L555A was not altered by the presence of bile acids. In the case of the L558A mutant, a similar effect of bile acids was observed as in the case of the R482G variant: CA and TC inhibited both basal and substrate-stimulated ATPase activity (Supplemental Fig. 5), but the relative substrate activation was practically unchanged

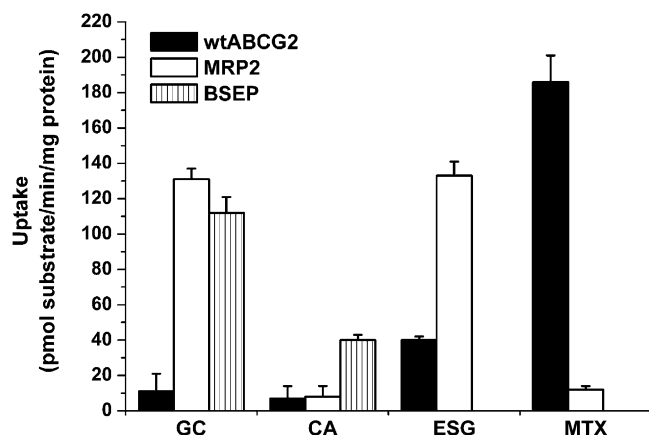


Fig. 5. ATP-dependent uptake of different bile acids and ABCG2-substrates into cholesterol-loaded Sf9 vesicles. Inside-out membrane vesicles containing wtABCG2, MRP2, or BSEP were incubated with [^3H]-labeled glycocholate (GC, 100 μM), cholic acid (CA, 100 μM), methotrexate (MTX, 100 μM), or estradiol-glucuronide (ESG, 50 μM). Mean values of ATP-dependent uptake obtained from at least two independent experiments with four parallels \pm S.D. values are shown.

(Fig. 6D). GC had no effect on either baseline or substrate-stimulated activity of the L558A mutant (Supplemental Fig. 5).

Discussion

Human ABCG2 has an important role in detoxification. Therefore better understanding of the regulation of its function may allow the modulation of ADME-Tox (absorption, distribution, metabolism, excretion and toxicity) properties thus may improve anticancer therapies. Membrane cholesterol has been shown to modulate the activity of ABCG2 (Pal et al., 2007; Storch et al., 2007; Telbisz et al., 2007); however, the protein sites for cholesterol recognition have not yet been identified.

To achieve a better understanding of the interaction between sterols and ABCG2, we generated several mutant variants of the transporter, expressed them in insect cells, and characterized their sterol sensitivity. Previously, Arg482 was found to be critical in cholesterol-sensing of ABCG2 (Telbisz et al., 2007). Here, we investigated R482 mutants with various amino acid side-chain characters. Based on our present results, the cholesterol-sensing capability of these variants could be grouped into two clusters.

Members of the first cluster, also including the wild-type protein (R), contain large (hydrophobic or positively charged) amino acids, represented by R482I, M, K, and Y. The function of these ABCG2 protein variants is highly cholesterol-dependent: they are significantly activated by increased membrane cholesterol levels (Fig. 1, A and B). Interestingly, the activating effect of cholesterol is the most pronounced in the case of the R482K and Y mutants, as these variants are practically unable to transport Hoechst 33342 unless high levels of cholesterol are present in the cell membranes (Fig. 1B).

In contrast, R482 mutants represented by relatively small (polar, uncharged, or negatively charged) amino acids formed another cluster regarding cholesterol sensing. The basal ATP hydrolysis in these variants was slightly accelerated by increased membrane cholesterol levels (Supplemental Table 1), and their substrate stimulation and transport function was practically unaltered by cholesterol loading (Fig. 1).

In earlier studies (Velamakanni et al., 2008), a potential steroid-binding element (SBE, aa 555–558) in ABCG2 was suggested to be responsible for sterol sensing in this transporter. In their study, Velamakanni et al. (2008) found that the ABCG2-L555A/L558A mutant does not have an altered cholesterol sensing, but progesterone and estradiol binding as well as transport were abolished. In our present work, we expressed and analyzed in detail the SBE (or LxxL motif) mutants L555A, L558A, and L555/558A of human ABCG2. We found that the mutants are active, showing a vanadate and Ko143 (an ABCG2-specific inhibitor) sensitive ATPase activity and are able to transport several established wtABCG2 substrates (Fig. 2). Additionally, though the SBE mutants were active, they showed altered substrate specificity, as compared with the wtABCG2 protein (see *Effect of Cholesterol on the Function of ABCG2-SBE Mutant Variants*).

When examining the effect of cholesterol on their function, we found that although a slight increase in the baseline ATP hydrolysis of the L555A and L558A mutants occurred in cholesterol-enriched membranes (fold activation was 1.2 ± 0.1 and 1.5 ± 0.1 , respectively), their relative substrate stimulation (ratio of ATP hydrolysis in the presence and absence of substrates) did not change (Fig. 2B and Supplemental Fig. 2). Accordingly, in direct transport experiments we found that all three SBE mutants were already fully active without excess cholesterol (Fig. 2, C and D). Moreover, the L555A/L558A mutant was absolutely insensitive to cholesterol loading in the ATPase-activity measurements (Fig. 2B). This apparent cholesterol independence of the L555A/L558A

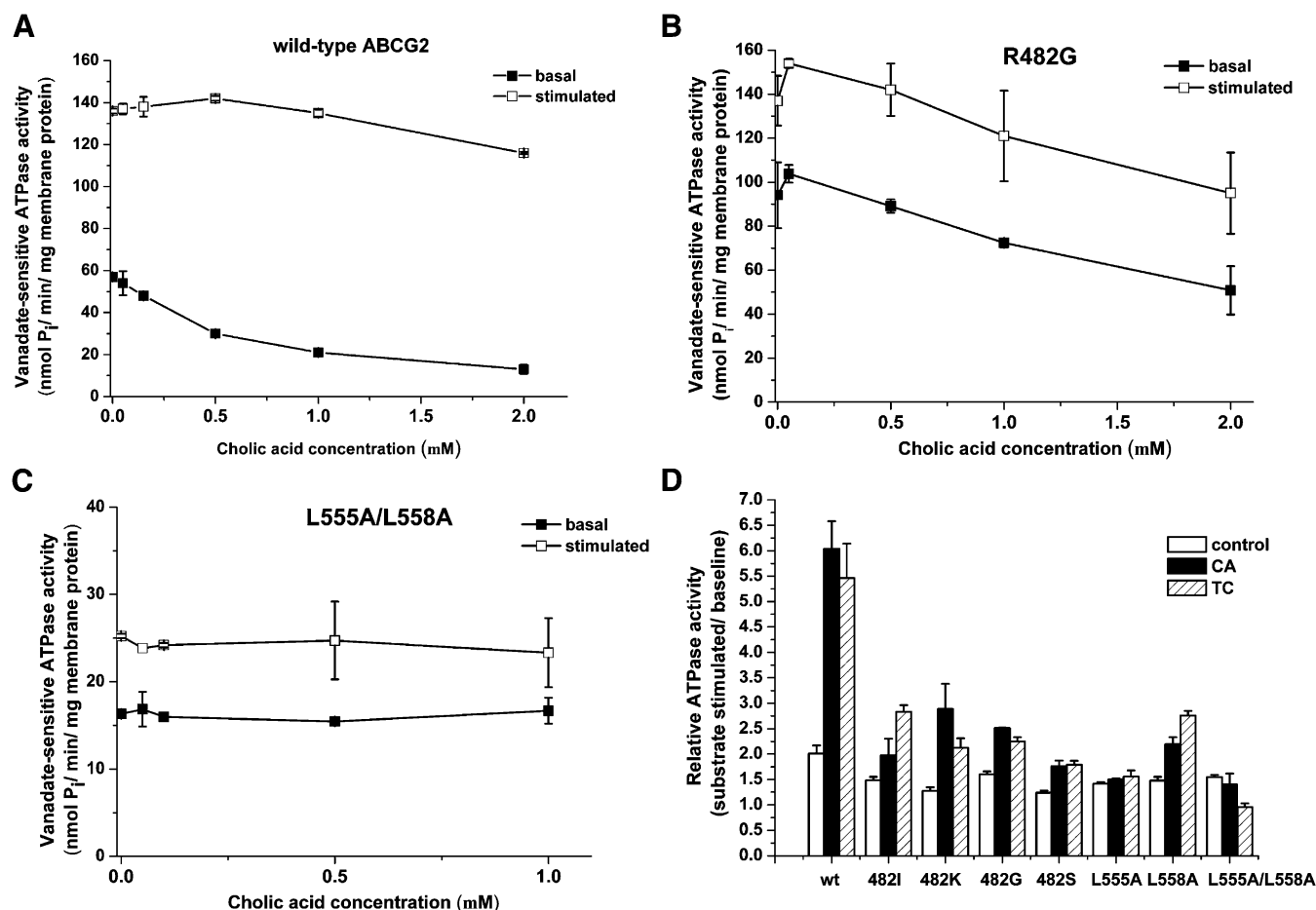


Fig. 6. Effect of bile acids on the ATPase activity of wtABCG2 and its mutant variants. (A–C) Increasing amounts of cholic acid were added to insect cell membranes previously loaded with cholesterol. Basal (■) or substrate-stimulated ATP hydrolysis (□), measured in the presence of 1 μ M quercetin (A and B), or 1 μ M nilotinib (C) was determined. The figure shows the average of at least two independent measurements, four parallels \pm S.E. values. (D) Effect of bile acids on the substrate stimulation of the ATPase activity of wtABCG2 and its mutant variants. Membranes were incubated with or without 1 mM bile acid; the ratio of ATP hydrolysis in the presence of 1 μ M quercetin (wt, R482G, S, K, and I) or 1 μ M nilotinib (SBE mutants) and the baseline ATPase activity were calculated. Columns represent an average of at least four data points, and bars show S.D. values.

mutant contradicted the results described by Velamakanni et al. (2008), which may be due to the fact that they investigated a triple mutant of ABCG2, which had R482G besides the L555A/L558A mutation, whereas we performed our experiments using the wild-type ABCG2 (482R) as a background. As demonstrated elsewhere and in this report as well, the R482G variant is already fully active in cholesterol-deficient Sf9 membranes. To solve this contradiction, we also generated the triple mutant R482G/L555A/L558A of ABCG2 and expressed this protein in insect cells. Still, this variant was also not activated by cholesterol (data not shown).

Because even very low levels of membrane sterols may affect ABCG2 function, we have purified and reconstituted the L558A and L555A/L558A mutants in cholesterol-free liposomes. Surprisingly, we found that the L558A mutant also needs cholesterol for its full activity. Unfortunately, cholesterol sensing of the double mutant could not be defined as it became inactive during purification. In summary, we suggest that the aforementioned two regions, both localized to the transmembrane domain, modulate both cholesterol sensing and substrate recognition of ABCG2.

The effect of sterols has been studied in detail in the case of the ABCB1/MDR1 protein (Garrigues et al., 2002). Increased cholesterol accelerates the basal ATPase activity of this multidrug transporter, while sterols have no major effect on substrate-stimulated ATP hydrolysis. It

has also been shown that membrane cholesterol differentially modulates the effect of MDR1 substrates, depending on the size of these molecules. Kimura et al. (2007a) found that the presence of cholesterol increased the recognition of small-molecular-weight MDR1 substrates (molecular mass below 800 Da) but had no impact on the transport of larger molecules (molecular mass higher than 900 Da), and cholesterol itself was not transported by MDR1. Based on these findings, a review suggested a cholesterol fill-in model (Kimura et al., 2007b)—that is, in the case of larger substrates, the binding pocket of MDR1 is completely filled, and there is no room for cholesterol. However, in the case of smaller substrates, an empty space remains in the binding pocket, which can be filled up with cholesterol.

In the case of wtABCG2, we tested a large number of substrates and found that cholesterol increased the activation in all cases. When analyzing the size of these compounds, we found that all these molecules belong to the “smaller” category, so the effect of cholesterol found in the case of ABCG2 may be in harmony with the cholesterol fill-in model. Larger compounds (e.g., cyclosporin A) mostly behave as inhibitors of ABCG2, so this question is difficult to answer. Based on our current results, we suggest that in the case of ABCG2, larger side chains at position aa 482 and 555 or 558 may keep the gate of the substrate binding pocket clogged, and cholesterol is required to widen the channel for the entry of the substrates.

In the next series of experiments, we investigated the modulatory effect of bile acids on the function of wtABCG2. We found that bile acids and their derivatives, much below their critical micelle concentrations, strongly reduce the basal ABCG2-ATPase activity of the wild-type protein without significantly affecting its substrate-stimulated ATPase (Fig. 4C). Moreover, we observed that when membranes were loaded with cholesterol, CA decreased the baseline ATP hydrolysis down to the background level, that is, to ATP hydrolysis in membranes expressing the inactive mutant ABCG2-K86M (see Fig. 2B). As a consequence, in the presence of bile acids the relative substrate stimulation was greatly increased (Fig. 4D).

A key advantage of the insect cell overexpression system is that isolated membrane preparations contain a much higher level of ABCG2 than membranes isolated from mammalian overexpression systems (Ozvegy et al., 2001), thus providing an efficient tool for examining the modulation of ABCG2 ATPase or transport activity (Hegedus et al., 2009). Based on our present observations, we suggest that to obtain maximum activation with ABCG2 substrates, cholesterol-loaded insect membranes should be used in the presence of bile acids. This provides an improved ATPase assay for testing the potential substrate interactions of ABCG2.

Several studies have already investigated the interaction between the ABCG2 transporter and bile acids, though with contradictory results (see *Introduction*). In our experiments, we could not detect direct transport of the investigated bile acids in membrane vesicles (Fig. 5), but we found an inhibitory effect of higher bile acid concentrations on ABCG2-dependent vesicular uptake (Supplemental Fig. 4). A direct effect of bile acids on membrane vesicle integrity was clearly excluded by the finding that under the same conditions bile acids significantly increased MRP2-dependent vesicular ESG transport (Bodo et al., 2003) (Supplemental Fig. 4), and both MRP2- and BSEP-containing vesicles performed efficient bile acid uptake (Fig. 5).

Our data thus do not support the findings of some earlier reports, but can be explained by the different expression systems and experimental conditions used. Even Blazquez et al. (2012) suggested that because the expression of this protein in the liver is significantly lower than that of the “professional” bile acid transporter BSEP, the role of ABCG2 in this function is questionable (while placental bile acid transport by ABCG2 may be relevant). Accordingly, *Abcg2*^{-/-} mice do not develop the symptoms of cholestasis (Mennone et al., 2010); thus, ABCG2 may have only a moderate effect on bile acid transport. Based on our results, we suggest that although bile acids modulate basal ATP hydrolysis by ABCG2, they are not exported from the cells at a significant rate by this transporter. A low-affinity, low-transport-activity type interaction of ABCG2 with bile acids may explain this phenomenon.

Interestingly, we found that R482 and the L555-L558 positions are also crucial for bile acid recognition of ABCG2 (Fig. 6, B–D; Supplemental Fig. 5). Mutations at these sites removed the major effects of bile acids on basal ATPase activity, thus suggesting a site-specific modulatory effect of bile acids.

Sterols may significantly affect the function of ABCG2, especially in the liver. In hepatocytes, ABCG2 is abundantly expressed and is a key transporter for xenobiotics into the bile. Cholesterol significantly activates the transport function of ABCG2; therefore, an increased cholesterol level may promote enhanced detoxification. Currently we cannot exclude whether cholesterol (albeit with low efficiency) is also a transported substrate of this protein. Our present data reveal that bile acids, although probably not efficiently transported by ABCG2, also significantly modulate its function. In the liver, where a large amount of bile acids is formed from cholesterol, bile acids may cause a reduction in futile ATP consumption by ABCG2, represented as baseline ATPase activity. In addition to the functional regulation,

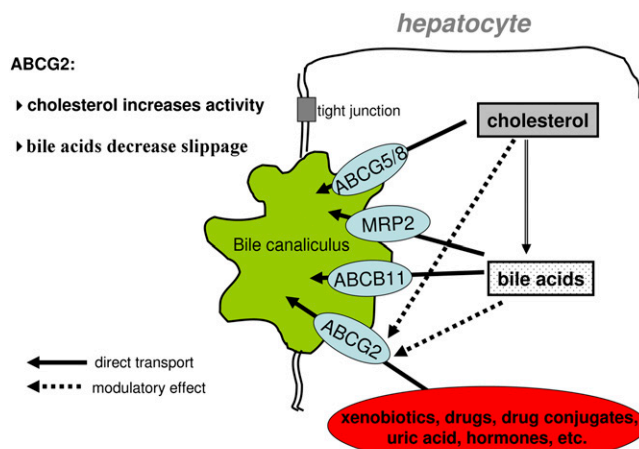


Fig. 7. Schematic representation of a complex regulation of ABCG2 function in hepatocytes.

although not examined in our present report, it should be mentioned that sterols may also modulate ABCG2 transcription and expression levels through interactions with nuclear receptors such as peroxisome proliferator-activated receptor (PPAR γ), pregnane X receptor (PXR), and constitutive androstane receptor (CAR) (Jigorel et al., 2006).

Based on our present results, we suggest a model describing complex posttranslational regulation of ABCG2 function in the liver (Fig. 7). Although cholesterol and bile acids are mostly transported by professional active ABC transporters—that is ABCG5/G8, BSEP, and MRP2—into the bile, the drug-transport function of ABCG2 is significantly modulated by sterols. Based on these findings, we also suggest that the amino acid positions characterized in this study may serve as potential targets for pharmacologic modulation of ABCG2 function.

Acknowledgments

The authors thank Zsuzsanna András, Éva Krizsán, Katalin Mihály, and Györgyi Vermes for their technical help, which was gratefully appreciated, and SOLVO Biotechnology Ltd. for providing BSEP-containing Sf9 membrane vesicles.

Authorship Contributions

Participated in research design: Telbisz, Hegedüs, Özvegy-Laczka, Sarkadi.
Conducted experiments: Telbisz, Hegedüs, Özvegy-Laczka.
Performed data analysis: Telbisz, Hegedüs, Özvegy-Laczka.
Wrote or contributed to the writing of the manuscript: Hegedüs, Özvegy-Laczka, Váradi, Sarkadi.

References

- Allen JD, van Loevezijn A, Lakhai JM, van der Valk M, van Tellingen O, Reid G, Schellens JH, Koomen GJ, and Schinkel AH (2002) Potent and specific inhibition of the breast cancer resistance protein multidrug transporter in vitro and in mouse intestine by a novel analogue of fumitremogin C. *Mol Cancer Ther* 1:417–425.
- Bakos E, Evers R, Sinkó E, Váradi A, Borst P, and Sarkadi B (2000) Interactions of the human multidrug resistance proteins MRP1 and MRP2 with organic anions. *Mol Pharmacol* 57: 760–768.
- Blazquez AG, Briz O, Romero MR, Rosales R, Monte MJ, Vaquero J, Macias RI, Cassio D, and Marin JJ (2012) Characterization of the role of ABCG2 as a bile acid transporter in liver and placenta. *Mol Pharmacol* 81:273–283.
- Bodo A, Bakos E, Szeri F, Váradi A, and Sarkadi B (2003) Differential modulation of the human liver conjugate transporters MRP2 and MRP3 by bile acids and organic anions. *J Biol Chem* 278:23529–23537.
- Garrigues A, Escargueil AE, and Orłowski S (2002) The multidrug transporter, P-glycoprotein, actively mediates cholesterol redistribution in the cell membrane. *Proc Natl Acad Sci USA* 99: 10347–10352.
- Hegedus C, Szakács G, Homolya L, Orbán TI, Telbisz A, Jani M, and Sarkadi B (2009) Ins and outs of the ABCG2 multidrug transporter: an update on in vitro functional assays. *Adv Drug Deliv Rev* 61:47–56.
- Im YJ, Raychaudhuri S, Prinz WA, and Hurley JH (2005) Structural mechanism for sterol sensing and transport by OSBP-related proteins. *Nature* 437:154–158.
- Imai Y, Asada S, Tsukahara S, Ishikawa E, Tsuruo T, and Sugimoto Y (2003) Breast cancer resistance protein exports sulfated estrogens but not free estrogens. *Mol Pharmacol* 64:610–618.

- Janvilisri T, Shahi S, Venter H, Balakrishnan L, and van Veen HW (2005) Arginine-482 is not essential for transport of antibiotics, primary bile acids and unconjugated sterols by the human breast cancer resistance protein (ABCG2). *Biochem J* **385**:419–426.
- Jigorel E, Le Vee M, Boursier-Neyret C, Parmentier Y, and Fardel O (2006) Differential regulation of sinusoidal and canalicular hepatic drug transporter expression by xenobiotics activating drug-sensing receptors in primary human hepatocytes. *Drug Metab Dispos* **34**:1756–1763.
- Kerr ID, Haider AJ, and Gelissen IC (2011) The ABCG family of membrane-associated transporters: you don't have to be big to be mighty. *Br J Pharmacol* **164**:1767–1779.
- Kimura Y, Kioka N, Kato H, Matsuo M, and Ueda K (2007a) Modulation of drug-stimulated ATPase activity of human MDR1/P-glycoprotein by cholesterol. *Biochem J* **401**:597–605.
- Kimura Y, Kodan A, Matsuo M, and Ueda K (2007b) Cholesterol fill-in model: mechanism for substrate recognition by ABC proteins. *J Bioenerg Biomembr* **39**:447–452.
- Li T and Chiang JY (2012) Bile acid signaling in liver metabolism and diseases. *J Lipids* **2012**:754067.
- Maliepaard M, Scheffer GL, Faneyte IF, van Gastelen MA, Pijnenborg AC, Schinkel AH, van De Vijver MJ, Scheper RJ, and Schellens JH (2001) Subcellular localization and distribution of the breast cancer resistance protein transporter in normal human tissues. *Cancer Res* **61**:3458–3464.
- Mennone A, Soroka CJ, Harry KM, and Boyer JL (2010) Role of breast cancer resistance protein in the adaptive response to cholestasis. *Drug Metab Dispos* **38**:1673–1678.
- Ozvegy-Laczka C, Hegedus T, Várady G, Ujhelly O, Schuetz JD, Váradi A, Kéri G, Orfi L, Németh K, and Sarkadi B (2004) High-affinity interaction of tyrosine kinase inhibitors with the ABCG2 multidrug transporter. *Mol Pharmacol* **65**:1485–1495.
- Ozvegy-Laczka C, Köblös G, Sarkadi B, and Váradi A (2005) Single amino acid (482) variants of the ABCG2 multidrug transporter: major differences in transport capacity and substrate recognition. *Biochim Biophys Acta* **1668**:53–63.
- Ozvegy-Laczka C, Laczkó R, Hegedus C, Litman T, Várady G, Goda K, Hegedus T, Dokholyan NV, Sorrentino BP, and Váradi A, et al. (2008) Interaction with the 5D3 monoclonal antibody is regulated by intramolecular rearrangements but not by covalent dimer formation of the human ABCG2 multidrug transporter. *J Biol Chem* **283**:26059–26070.
- Ozvegy C, Litman T, Szakács G, Nagy Z, Bates S, Váradi A, and Sarkadi B (2001) Functional characterization of the human multidrug transporter, ABCG2, expressed in insect cells. *Biochem Biophys Res Commun* **285**:111–117.
- Ozvegy C, Váradi A, and Sarkadi B (2002) Characterization of drug transport, ATP hydrolysis, and nucleotide trapping by the human ABCG2 multidrug transporter. Modulation of substrate specificity by a point mutation. *J Biol Chem* **277**:47980–47990.
- Pál A, Méhn D, Molnár E, Gedey S, Mészáros P, Nagy T, Glavinas H, Janáky T, von Richter O, and Báthori G, et al. (2007) Cholesterol potentiates ABCG2 activity in a heterologous expression system: improved in vitro model to study function of human ABCG2. *J Pharmacol Exp Ther* **321**:1085–1094.
- Robey RW, To KK, Polgar O, Dohse M, Fetsch P, Dean M, and Bates SE (2009) ABCG2: a perspective. *Adv Drug Deliv Rev* **61**:3–13.
- Simonović BR and Momirović M (1997) Determination of critical micelle concentration of bile acid salts by micro-calorimetric titration. *Mikrochim Acta* **127**:101–104 DOI:10.1007/BF01243172.
- Storch CH, Ehehalt R, Haefeli WE, and Weiss J (2007) Localization of the human breast cancer resistance protein (BCRP/ABCG2) in lipid rafts/caveolae and modulation of its activity by cholesterol in vitro. *J Pharmacol Exp Ther* **323**:257–264.
- Suzuki M, Suzuki H, Sugimoto Y, and Sugiyama Y (2003) ABCG2 transports sulfated conjugates of steroids and xenobiotics. *J Biol Chem* **278**:22644–22649.
- Telbisz A, Müller M, Ozvegy-Laczka C, Homolya L, Szente L, Váradi A, and Sarkadi B (2007) Membrane cholesterol selectively modulates the activity of the human ABCG2 multidrug transporter. *Biochim Biophys Acta* **1768**:2698–2713.
- Telbisz A, Ozvegy-Laczka C, Hegedus T, Váradi A, and Sarkadi B (2013) Effects of the lipid environment, cholesterol and bile acids on the function of the purified and reconstituted human ABCG2 protein. *Biochem J* **450**:387–395.
- Vaidya SS and Gerk PM (2006) Lack of interaction between tauroursodeoxycholate and ATP-binding cassette transporter isoform G2 (ABCG2). *Mol Pharm* **3**:303–306.
- Velamakanni S, Janvilisri T, Shahi S, and van Veen HW (2008) A functional steroid-binding element in an ATP-binding cassette multidrug transporter. *Mol Pharmacol* **73**:12–17.
- Wang N, Yvan-Charvet L, Lütjohann D, Mulder M, Vanmierlo T, Kim TW, and Tall AR (2008) ATP-binding cassette transporters G1 and G4 mediate cholesterol and desmosterol efflux to HDL and regulate sterol accumulation in the brain. *FASEB J* **22**:1073–1082.
- Williams SP and Sigler PB (1998) Atomic structure of progesterone complexed with its receptor. *Nature* **393**:392–396.

Address correspondence to: Csilla Özvegy-Laczka, Institute of Enzymology, Research Centre for Natural Sciences, Hungarian Academy of Sciences, Karolina út 29., 1113 Budapest, Hungary. E-mail: laczka.csilla@ttk.mta.hu

Drug Metabolism and Disposition

Regulation of the function of the human ABCG2 multidrug transporter by cholesterol and bile acids: effects of mutations in potential substrate- and steroid-binding sites

Ágnes Telbisz, Csilla Hegedüs, András Váradi, Balázs Sarkadi and Csilla Özvegy-Laczka

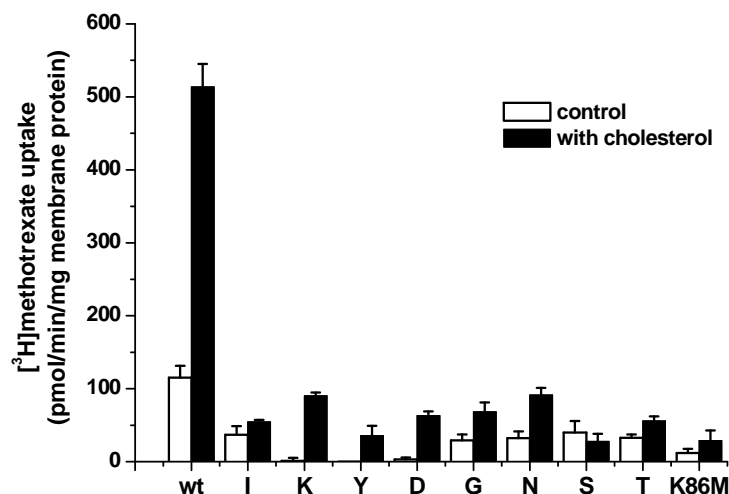
Supplemental Table: Effect of cholesterol loading on substrate stimulated ATPase activity of wtABCG2 and the R482 mutants

	Fold activation in control membranes		Fold activation in cholesterol-loaded membranes		Change in basal activity upon cholesterol loading
	quercetin	prazosin	quercetin	prazosin	
wild-type	1.5	0.9	2.5	1.5	1.3
482I	1.1	1.1	1.5	1.4	1.2
482K	0.6	0.8	1.9	1.2	0.8
482M	1.3	1.4	1.5	1.9	1.7
482Y	1.3	0.8	1.8	1.4	1.0
482D	1.1	1.2	1.2	1.0	1.6
482G	1.6	1.6	1.8	1.7	1.3
482N	1.6	1.4	1.4	1.6	1.8
482S	1.3	1.2	1.1	1.1	1.8
482T	1.3	1.4	1.4	1.3	1.8

Supplemental Figures

Figure 1

A



B

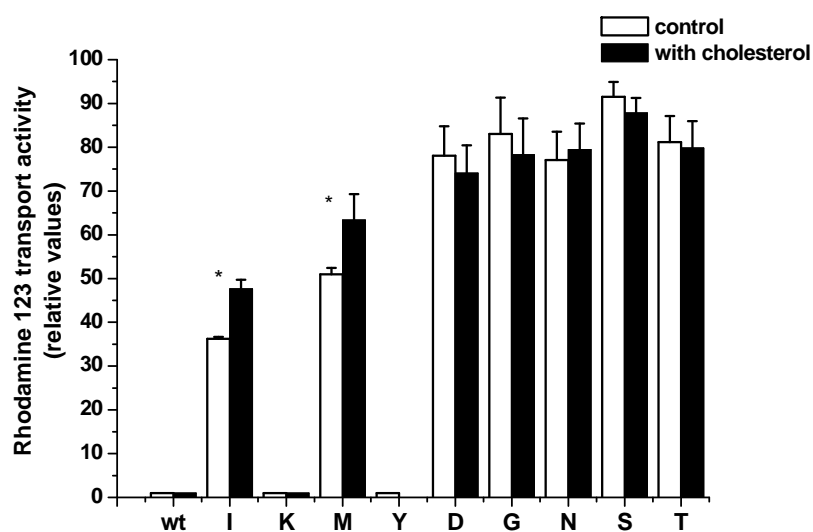
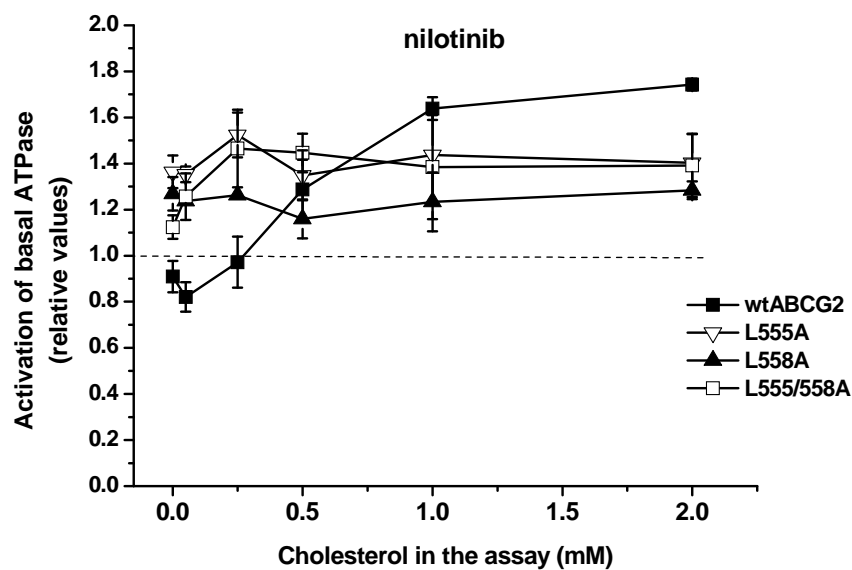


Figure 1: Effect of cholesterol on the transport activity of the R482 mutants. Panel A: [³H]methotrexate uptake was measured in control or cholesterol-loaded insect inside-out membrane vesicles. ATP-dependent uptake is shown. Columns represent mean \pm SD values of data obtained from two independent experiments.

Panel B: Rhodamine 123 (2 μ M) fluorescence was determined in insect cells expressing wtABCG2 or one of the R482 mutants by fluorescent cell sorting. Dead cells were excluded by propidium iodide staining. Transport activity was calculated as described in the Experimental procedures. White columns show transport in control cells, black columns stand for activity in 2 mM cholesterol-loaded cells. Mean \pm SD values are shown. *: Student's t-test, significant difference, $p < 0.05$

Figure 2

A



B

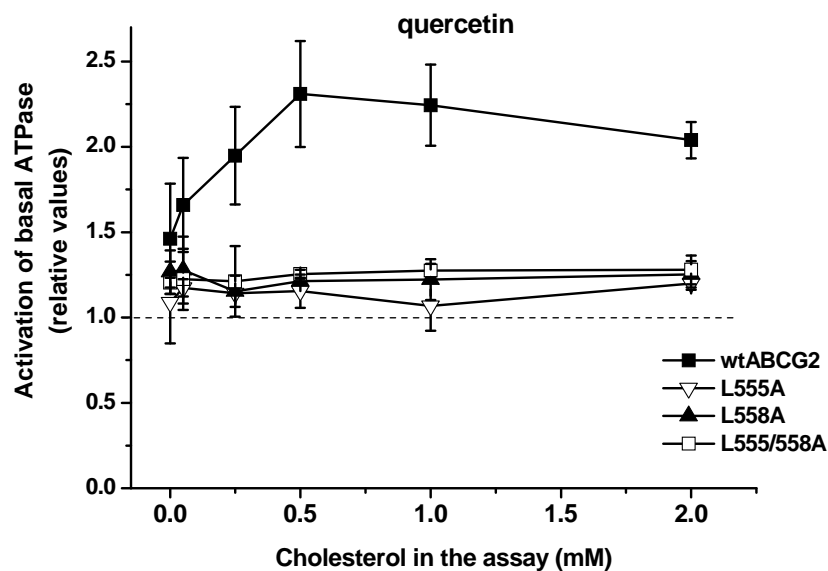
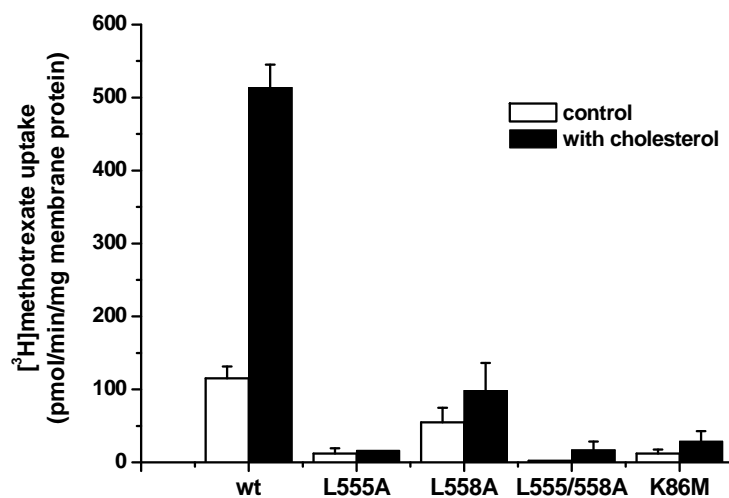


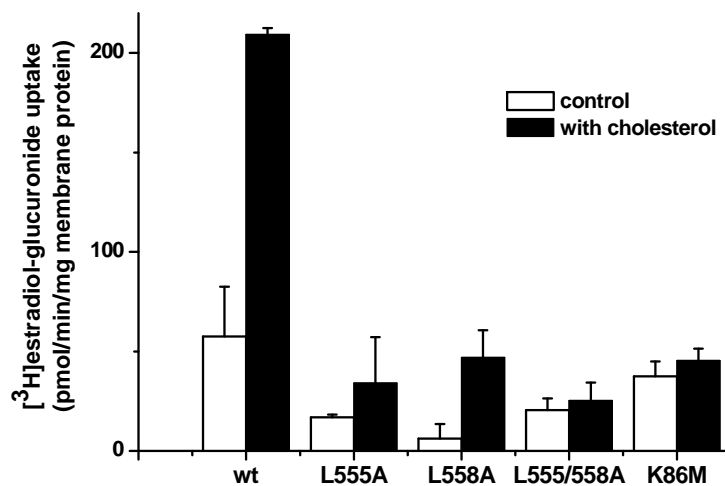
Figure 2: Effect of cholesterol on substrate stimulation of wtABCG2 and SBE mutants. Insect membranes were incubated with different amounts of cholesterol and baseline ATPase activity and that obtained in the presence of 1 μ M nilotinib (Panel A) or 1 μ M quercetin (Panel B) were determined. Substrate stimulation is shown as a ratio of ATP hydrolysis in the presence of substrates and in the absence of added compounds (panels A and B). Experiments were performed in quadruplicates; average \pm SD values are shown.

Figure 3

A



B

**Figure 3: Effect of cholesterol on the transport activity of the SBE mutants.**

ATP-dependent $[^3\text{H}]$ methotrexate (**Panel A**) or $[^3\text{H}]$ estradiol-glucuronide (**Panel B**) uptake was determined in control or cholesterol-loaded insect inside-out membrane vesicles. Mean \pm SD values of two independent experiments are shown.

Figure 4

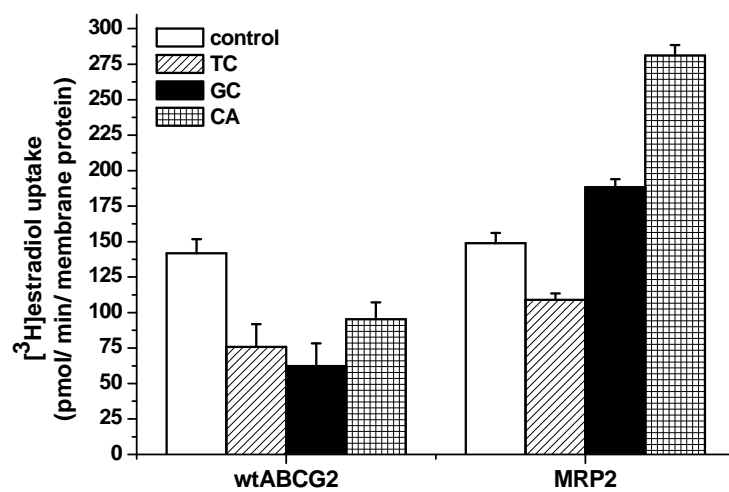


Figure 4: Effect of bile acids on [³H]estradiol-glucuronide uptake. [³H]ESG uptake (25 μ M) was measured in cholesterol-loaded inside out vesicles containing wtABCG2 or MRP2 in the absence (control) or in the presence of 250 μ M bile acids (glycocholate (GC), taurocholate (TC) or cholic acid (CA)). Measurement was done in triplicates, mean \pm SD values are shown.

Figure 5

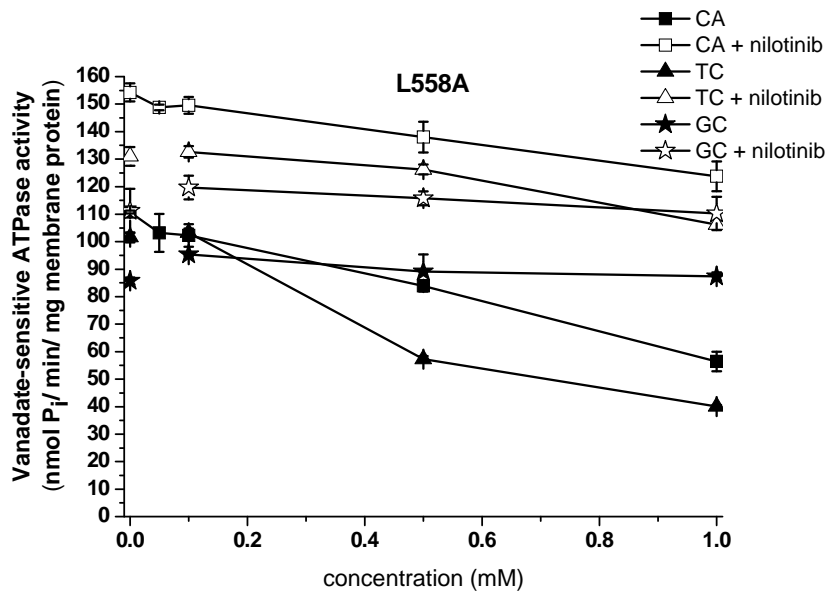


Figure 5: Effect of bile acids on the ATPase activity of the L558A mutant. Cholesterol-loaded Sf9 membranes were incubated with increasing amounts of bile acids (cholic acid, CA, taurocholate, TC or glycocholate, GC) with the addition of 1 μ M nilotinib. Experiments were carried out in duplicates, mean \pm SD values are shown.



Contents lists available at ScienceDirect

Biochimica et Biophysica Acta

journal homepage: www.elsevier.com/locate/bbamem

Mutations of the central tyrosines of putative cholesterol recognition amino acid consensus (CRAC) sequences modify folding, activity, and sterol-sensing of the human ABCG2 multidrug transporter



Zita Gál^a, Csilla Hegedüs^{a,b}, Gergely Szakács^a, András Váradi^a, Balázs Sarkadi^{a,b}, Csilla Özvegy-Laczka^{a,*}

^a Institute of Enzymology, Research Centre for Natural Sciences, Hungarian Academy of Sciences, Magyar tudósok körútja 2., H-1117 Budapest, Hungary

^b Molecular Biophysics Research Group, Hungarian Academy of Sciences and Semmelweis University, Diószegi út 64., H-1113 Budapest, Hungary

ARTICLE INFO

Article history:

Received 4 August 2014

Received in revised form 30 October 2014

Accepted 6 November 2014

Available online 14 November 2014

Keywords:

ABCG2

Multidrug resistance

Cholesterol

Bile acids

Cholesterol recognition amino acid consensus

ABSTRACT

Human ABCG2 is a plasma membrane glycoprotein causing multidrug resistance in cancer. Membrane cholesterol and bile acids are efficient regulators of ABCG2 function, while the molecular nature of the sterol-sensing sites has not been elucidated. The cholesterol recognition amino acid consensus (CRAC, L/V-(X)₍₁₋₅₎-Y-(X)₍₁₋₅₎-R/K) sequence is one of the conserved motifs involved in cholesterol binding in several proteins. We have identified five potential CRAC motifs in the transmembrane domain of the human ABCG2 protein. In order to define their roles in sterol-sensing, the central tyrosines of these CRACs (Y413, 459, 469, 570 and 645) were mutated to S or F and the mutants were expressed both in insect and mammalian cells. We found that mutation in Y459 prevented protein expression; the Y469S and Y645S mutants lost their activity; while the Y570S, Y469F, and Y645F mutants retained function as well as cholesterol and bile acid sensitivity. We found that in the case of the Y413S mutant, drug transport was efficient, while modulation of the ATPase activity by cholesterol and bile acids was significantly altered. We suggest that the Y413 residue within a putative CRAC motif has a role in sterol-sensing and the ATPase/drug transport coupling in the ABCG2 multidrug transporter.

© 2014 Published by Elsevier B.V.

1. Introduction

ABCG2 is a plasma membrane glycoprotein in the ABC (ATP Binding Cassette) family of proteins that are characterized by a unique nucleotide binding/hydrolyzing domain (NBD) and hydrophobic membrane spanning sequences (transmembrane domain, TMD), mediating ATPase activity and the recognition and translocation of transported substrates, respectively. Several ABC transporters, called multidrug resistance (MDR) proteins, extrude various chemically unrelated compounds from the cells by utilizing the energy of ATP hydrolysis. ABCG2 is an MDR half transporter, harboring only a single NBD and a single TMD, and must at least homodimerize to exert its proper transporter function [1–3].

ABCG2 is expressed in many tissues, most abundantly in organs displaying barrier functions (brain, placenta, and intestine) where it

influences the passage of hydrophobic or slightly negatively charged molecules, including numerous drugs and food constituents. Therefore, ABCG2 can significantly influence the ADME-Tox (Absorption, Distribution, Metabolism, Excretion and Toxicity) properties of drugs, especially the absorption from the intestine, penetration to the central nervous system through the blood–brain barrier, or the elimination from the liver or kidney [3–6]. Optimal activity of ABCG2 has been shown to be important in the regulation of serum urate levels, and polymorphic ABCG2 variants with decreased function or expression were shown to be associated with a higher risk of gout [7–9]. Human ABCG2 is expressed in stem cells of various origins, where it provides a protective role under hypoxic conditions [10]. Overexpression of ABCG2 confers multidrug resistance to cancer cells [11–13].

We and others have shown that both the ATPase and the transport activity of ABCG2 are significantly accelerated by cholesterol enrichment of “cholesterol poor” insect cell membranes; whereas cholesterol depletion of mammalian cells results in decreased ABCG2 function [14, 15], implying that cholesterol is a major modulator of ABCG2 function. Subsequent studies have shown that functional reconstitution of purified ABCG2 requires cholesterol, suggesting that cholesterol is in fact essential for ABCG2 activity [16].

The mechanisms by which cholesterol-ABCG2 interactions translate into the observed changes of function, or the site(s) involved in cholesterol-sensing have not been defined. There is no experimental evidence

Abbreviations: CA, cholic acid; CRAC, cholesterol recognition amino acid consensus; DOX, doxorubicin; FBS, fetal bovine serum; FLP, flavopiridol; GC, glycocholate; HRP, horseradish peroxidase; MTX, methotrexate; PBS, phosphate buffered saline; RAMEB, randomly methylated β -cyclodextrin; SN-38, 7-ethyl-10-hydroxycamptothecin; TC, taurocholate; TOP, topotecan

* Corresponding author at: Institute of Enzymology, Research Centre for Natural Sciences, Hungarian Academy of Sciences, Magyar tudósok körútja 2., H-1117 Budapest, Hungary. Tel.: +36 1 3826715; fax: +36 1 3826295.

E-mail address: laczka.csilla@ttk.mta.hu (C. Özvegy-Laczka).

proving direct binding of cholesterol by ABCG2 and it is not known if ABCG2 recognizes cholesterol as a transported substrate, as shown for some related ABCG transporters [17,18]. More probably, cholesterol is an allosteric modulator of the transporter, or may also have an indirect effect through influencing the biophysical properties of the lipid bilayer.

Previous studies have suggested that single amino acids can influence cholesterol-sensing of ABCG2. Mutation of R482 to small amino acids (D, G, N, S, T) was shown to alter the cholesterol sensitivity [19]; mutation of the leucines in the LxxL motif (potential steroid binding element (aa 555–558 [20]) resulted in an apparent cholesterol insensitivity of ABCG2 in Sf9 membranes [19]. While these results may suggest that the mutated amino acids directly participate in cholesterol binding, they are not part of any known motifs that characterize dedicated cholesterol binding regions. Many proteins that interact with cholesterol possess an amino acid consensus sequence termed “CRAC” (cholesterol recognition amino acid consensus) with the pattern (L/V-(X)_(1–5)-Y-(X)_(1–5)-R/K). The CRAC sequence was shown to be an essential determinant of cholesterol recognition in the peripheral-type benzodiazepine receptor, caveolin, the gp41 protein of the HIV virus, or an integral outer mitochondrial membrane translocator protein [21–24]. The length of a CRAC motif varies between 5 and 13 amino acids, however, only the first and last amino acids and the central tyrosine residue are conserved. Various mutational studies of the CRAC motifs of cholesterol binding proteins and cholesterol-regulated ion channels have demonstrated the crucial role of the central tyrosine in cholesterol binding [22,23,25].

Given the modulatory effects of cholesterol on ABCG2 activity, we screened the amino acid sequence of the protein for CRAC motifs. We have identified five putative CRAC sequences, and changed the central tyrosines to define the role of each of these motifs in cholesterol-sensing. Here we show that the CRAC motif containing tyrosine at position 413 in transmembrane helix 1 is involved in sterol-sensing and the modulation of ATPase/transport coupling of the ABCG2 transporter.

2. Experimental procedures

2.1. Materials

Cholesterol-RAMEB (randomly methylated β -cyclodextrin) was a kind gift from Cyclolab Hungary. All other chemicals were purchased from Sigma (Sigma Aldrich, Hungary) unless stated otherwise.

2.2. Plasmid constructs

For the expression of ABCG2 mutants in insect cells, baculovirus plasmids containing the appropriate mutant ABCG2 cDNAs were generated by PCR mutagenesis as described earlier [26]. The list of primers used for mutagenesis is provided in the “Supplementary material”. The PCR products were digested with PstI and NcoI enzymes and were ligated into the corresponding sites of the pAcUW21-L/wtABCG2 plasmid [27]. The base order of the constructs was confirmed by sequencing. The generation of the vector construct with the ABCG2-K86M mutant was described earlier [26].

The plasmids for stable expression in mammalian cell lines were created by the ligation of the appropriate fragments from pAcUW21-L/ABCG2-Tyr mutant between the NotI-BamHI sites of the pSB-CMV-wtABCG2 plasmid [28].

2.3. Cells and cell lines

Sf9 cells (Invitrogen, Life technologies) were grown in TNM-FH insect cell medium complemented with 10% FBS and 100 μ g/ml penicillin/100 U/ml streptomycin at 27 °C. HEK 293 cells were cultured in DMEM medium containing 10% FBS and 100 μ g/ml penicillin/100 U/ml streptomycin and 5 mM glutamine at 37 °C in 5% CO₂.

2.4. Generation of insect cells expressing ABCG2-Tyr mutants

Sf9 cells were co-transfected with 250 ng linearized baculovirus DNA + 250 ng baculovirus plasmid DNA using the BaculoGold transfection kit following the protocol provided by the supplier (BD Biosciences). The presence of the engineered mutations was verified by restriction endonuclease digestion of the PCR-amplified ABCG2 DNA.

2.5. Generation of HEK 293 cells stably overexpressing human ABCG2 and its Tyr mutants

Cells were transfected using 3 μ l Fugene6 reagent (Promega) and 500 ng of the Sleeping Beauty pSB-ABCG2 plasmid DNA and 500 ng plasmid coding a transposase [29]. 48 h post transfection the cells were cultured in 1 μ g/ml puromycin for 14 days. Cells overexpressing the highest amounts of the appropriate ABCG2 variant were sorted based on 5D3 labeling using a FACSAria cell sorter (Becton Dickinson). In cholesterol depletion experiments we used the HEK 293 cell line stably expressing the R482G mutant established earlier [15].

2.6. Membrane preparation

Isolation of membranes from Sf9 cells expressing human ABCG2 or its Tyr mutants and the determination of membrane protein concentrations by the modified Lowry method were performed as described previously [30]. Besides control membranes prepared from untreated Sf9 cells, cholesterol pre-loaded membranes were also generated by co-incubation of the membranes with 0.25, 0.5, 1 or 2 mM cholesterol-RAMEB at 0 °C for 30 min prior to the final ultracentrifugation step of the membrane preparation procedure [15].

2.7. Detection of ABCG2 by Western blotting

Sf9 membranes or intact HEK 293 cells were suspended in sample loading buffer (62.5 μ M Tris HCl pH 6.8, 2% SDS, 10 μ M EDTA-Na pH 6.8, 10% glycerol, 2 M urea, 0.14 mg/ml bromophenol blue, 100 μ M dithiothreitol). Protein samples were separated on 7.5% Laemmli gels. Western blot analysis was performed as described earlier [26], by using the BXP-21 monoclonal antibody in a 2,000 \times dilution, and a goat anti-mouse HRP-conjugated secondary antibody (10,000 \times dilution, Jackson Immunoresearch).

2.8. BXP-21 or 5D3 labeling

5×10^5 HEK 293 cells were incubated in 1 ml HPMI buffer (120 mM NaCl, 5 mM KCl, 400 μ M MgCl₂, 40 μ M CaCl₂, 10 mM Hepes, 10 mM NaHCO₃, 10 mM glucose and 5 mM Na₂HPO₄ pH 7.4), containing 0.5% bovine serum albumin and 1 μ g/ml 5D3 antibody for 30 min at 37 °C in the presence of 1 μ M Ko143. After washing, the cells were further incubated with a secondary, phycoerythrin-conjugated anti-mouse antibody (Molecular Probes, 2 μ g/ml). Fluorescence was analyzed in an Attune focusing flow cytometer (Applied Biosystems).

When Sf9 membranes were labeled with anti-ABCG2 antibodies, 90 μ g membranes were incubated with BXP-21 (100 \times dilution) or 5D3 (final concentration 2 μ g/ml) antibody in a buffer containing 40 mM MOPS-Tris, 50 mM KCl and 500 μ M EGTA-Tris for 30 min at 37 °C, and after washing, with phycoerythrin-conjugated goat anti-mouse antibody (final concentration 1 μ g/ml) for additional 30 min at 37 °C. Fluorescence was analyzed in a FACSCalibur cytometer (BD Biosciences) [15,31].

2.9. ATPase assay

Measurement of ATP hydrolysis was performed as described earlier [27]. The concentrations of test compounds used in the different experiments are indicated in the figure legends. Basal or drug-stimulated

ATPase activities were compared to that measured in the absence of excess cholesterol. For the calculation of the K_A values, the data were fitted with a non-linear dose response curve using the Origin 8.6 software.

2.10. Vesicular uptake assay

The accumulation of 50 μM ^3H -methotrexate in inside-out membrane vesicles was measured for 10 min at 37 °C, and the transport reaction was terminated by rapid filtration [32]. ATP-dependent transport was determined by subtracting the transport measured in the absence of MgATP from that of measured in the presence of 4 mM MgATP.

2.11. Cellular uptake of Hoechst 33342, BODIPY-prazosin, Pheophorbide A and mitoxantrone

Accumulation of 1 μM Hoechst 33342, 20 nM BODIPY-prazosin, 2 μM Pheophorbide A or 5 μM mitoxantrone was measured as described earlier [26]. Briefly, 5×10^5 HEK 293 cells were co-incubated with the given compound at 37 °C for 20 (Hoechst 33342 and BODIPY-prazosin) or 30 (Pheophorbide A and mitoxantrone) min. The reaction was terminated by the addition of ice-cold PBS. After centrifugation at 100 g for 5 min at 4 °C, the cells were suspended in 1 ml PBS containing 1.25 $\mu\text{g}/\text{ml}$ propidium iodide and intracellular fluorescence was measured in an Attune (Hoechst 33342 and BODIPY-prazosin) or a FACSCalibur (Pheophorbide A and mitoxantrone) cytometer. In the case of Hoechst 33342, cellular fluorescence “transport factor” was calculated as follows: $(F_{100} - F_0) / F_{100} \times 100$, where F_0 is the fluorescence (geomean values) of Hoechst 33342 in the absence of an inhibitor; F_{100} is the fluorescence (geomean values) in the presence of 1 μM Ko143.

2.12. Cholesterol depletion

1×10^6 HEK 293 cells were incubated with 0.9 ml 4 mM empty RAMEB diluted in HPMI for 30 min at 37 °C. Then RAMEB was removed by centrifugation at 700 g for 5 min at room temperature, and the transport experiment was performed as described in Section 2.11.

2.13. Determination of doxorubicin efflux

5×10^5 HEK 293 cells were incubated with 5 μM doxorubicin in a final volume of 100 μl for 30 min at 37 °C in the presence or the absence of 1 μM Ko143. After washing the cells with 1 ml HPMI, the cells were further incubated in 100 μl HPMI with or without 1 μM Ko143 for 30 min at 37 °C. The reaction was stopped by washing the cells with 1 ml ice-cold PBS. After centrifugation at 100 g for 5 min at 4 °C, the cells were suspended in 1 ml PBS containing 1.25 $\mu\text{g}/\text{ml}$ propidium iodide and intracellular fluorescence was measured in an Attune flow cytometer at Ex/Em = 488 nm/574 nm.

2.14. Cytotoxicity assay

3×10^3 HEK 293 cells were seeded on flat bottom 96-well plates and were left to adhere. Next day, cells were treated and were further incubated with the indicated drug for 72 h. The supernatant was then removed and 100 μl 5% PrestoBlue (Life Technologies) was added to the cells. After incubation at 37 °C, 5% CO_2 for 1.5 hours, metabolized PrestoBlue was measured in a Perkin Elmer Victor X3 2030 Multilabel Plate Reader at 540 nm excitation and 579 nm emission wavelengths.

2.15. Statistical analysis of data

Statistical significance was assessed using paired Student's t-test.

3. Results

3.1. Identification of potential CRAC motifs

Cholesterol sensor motifs are located in or near the membrane plane; therefore we restricted our analysis to the transmembrane domain of ABCG2. We identified five putative CRAC motifs in ABCG2 (Fig. 1). Alignment of the corresponding regions of the human ABCG proteins revealed that three out of the five identified CRAC motifs are also present in other members of the human ABCG family (see Fig. 1, inset). The putative CRAC motifs identified in the sequence of human ABCG2 are also present in ABCG2 homologs. The 1st CRAC motif (aa 407–418) is conserved amongst mammals (with the exception of rhesus monkey), but is absent in chicken, or lower species. The 2nd and 3rd potential CRAC motifs (aa 454–465 and 466–473, respectively) can be found even in various fish, e.g. Atlantic salmon or Rainbow trout; the 4th and 5th putative CRAC motifs (aa 564–575 and 641–647, respectively) are conserved amongst vertebrates.

3.2. Expression and ATPase activity of ABCG2 CRAC mutants in Sf9 insect cells

To analyze whether the putative CRAC motifs of ABCG2 influence cholesterol-sensing, we mutated the central tyrosines (Y413, 459, 469, 570 and 645) to Ser. The mutant proteins were expressed in Sf9 insect cells for functional measurements. All but one of the ABCG2 mutants were successfully expressed in Sf9 insect cells. Mutation of Y459 to S prevented the expression of the protein, precluding this mutant from further analysis (Fig. 2A).

Transport of substrates by ABCG2 is coupled to the hydrolysis of ATP. Measurement of the ATPase activity of the transporter is a well-established tool for the characterization of the activity of various mutant protein variants as well as for the screening of potential ABCG2-interacting compounds [5]. In order to determine the functionality and the cholesterol dependence of the CRAC mutant ABCG2 proteins, we measured their ATP hydrolytic capacity in isolated Sf9 insect cell membranes. We found that mutation of Tyr to Ser at position 469 or 645 resulted in the loss of ATP hydrolysis (even if the activity is corrected for the lower expression level of the Y469S mutant); while mutations in the other two positions apparently did not alter ABCG2 functionality, as both the Y413S and Y570S mutants showed a high level of ATPase activity, which could be inhibited by a general ATPase inhibitor vanadate or the specific ABCG2 inhibitor Ko143 (Fig. 2B).

In order to test if the inactivity of the Y469S and Y645S mutants was due to a specific loss of Tyr at this position, we also mutated these tyrosines to phenylalanines. We found that the Y469F and Y645F mutants were active (Fig. 2B), indicating the importance of the phenyl ring, but not of a hydroxyl group at these positions for protein function.

3.3. Effects of cholesterol on the ATPase activity of the CRAC mutants

To test whether the CRAC tyrosine mutants are sensitive to the cholesterol content of the membranes, we characterized their ATPase activity in cholesterol-enriched insect cell membranes (Fig. 2C). The cholesterol content of the insect cell membranes is relatively low, as compared to mammalian cells (5–8 μg cholesterol/mg membrane protein vs. 50 μg cholesterol/mg membrane protein in insect and mammalian cells, respectively). Co-incubation with cholesterol-loaded cyclodextrin complexes was shown to be a reliable experimental tool to increase the cholesterol contents of Sf9 membranes by up to 10-fold [15]. Using this approach, we have shown that the ATPase activity, especially the activation of ATP hydrolysis by transported substrates, in the case of the wild-type ABCG2 is greatly enhanced when the Sf9 membranes are enriched in cholesterol (see [15] and Figs. 2C and 3A).

We found that the basal ATPase activity of the Y469F, Y570S and Y645F mutants showed a moderate (approximately 20%, $p < 0.05$)

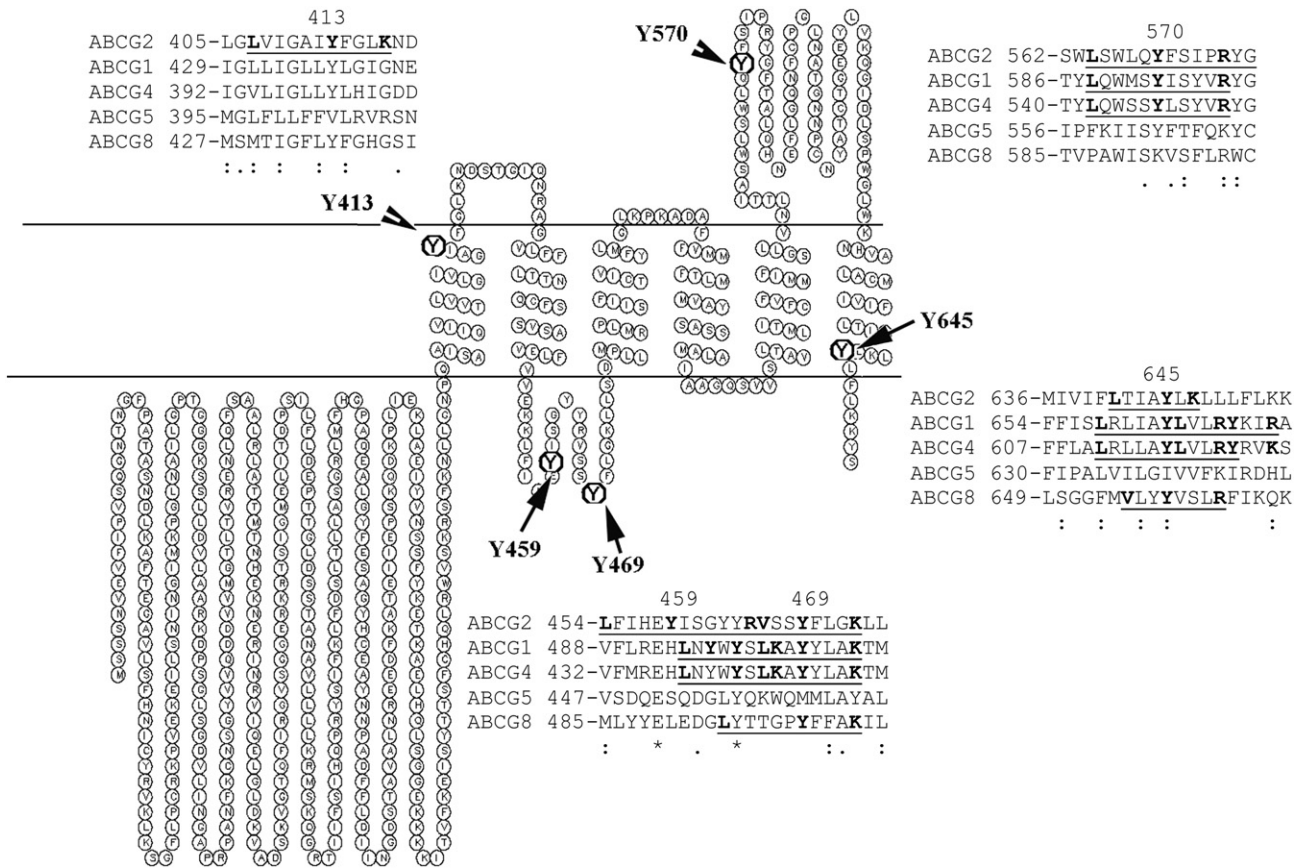


Fig. 1. Topology model of human ABCG2 indicating the positions of tyrosines mutated in this study and also showing sequence alignment of human ABCG proteins. Protein sequences of human ABCG proteins (ABCG2 AAG52982.1, ABCG1 P45844.3, ABCG4 NP_001135977.1, ABCG5 AG40003.1, ABCG8 AAG40004.1) were aligned using Clustalw (<https://www.ebi.ac.uk/Tools/msa/clustalw2/>). Putative CRAC motifs are underlined; the 3 conserved amino acids in CRAC motifs are labeled with bold letters. The 2D structure was drawn by using <http://emboss.bioinformatics.nl/cgi-bin/emboss/topo> based on the topology created by CCTOP (http://htp.enzim.hu/?_=viewer/HTP_002649) [42,43].

increase upon cholesterol addition, while the substrate stimulated ATP hydrolysis of the same mutants was significantly (50–100% increase, $p < 0.01$) accelerated by cholesterol loading (Fig. 2C). Therefore, these CRAC mutants behaved similarly to the wild-type ABCG2 protein. These results argue against a role of tyrosines 469, 570 and 645 in cholesterol-sensing, suggesting that the corresponding regions are not functional CRAC motifs.

Conversely, we found that in the presence of cholesterol, the ATPase activity of ABCG2-Y413S was distinct from that of the wild-type transporter. In the case of Y413S, cholesterol resulted in a major (50 +/- 8%; $p < 0.01$) enhancement of the basal ATP hydrolysis, which could be only slightly stimulated by the addition of prazosin or quercetin (Figs. 2B and C, and 4B).

Next, we investigated whether other compounds which are known substrates of wtABCG2 also differently modify the Y413S-ATPase in the presence of cholesterol (Fig. 3). Again, cholesterol potentiated the drug-stimulated ATPase activity of the wild-type protein (Fig. 3A), as well as the 469F, the 570S and 645F mutants in the presence of several substrates (Supplementary Fig. S1). In contrast, the Y413S mutant had a significantly altered ATPase modulation pattern. Quercetin showed a 30 +/- 6.5% stimulation ($p < 0.01$), whereas doxorubicin, flavopiridol, topotecan and SN-38 resulted in a concentration dependent inhibition (ranging from 26–70%) of the ATPase activity of the protein (Fig. 3B, C, D and not shown).

For a detailed analysis of the effects of cholesterol loading, the basal and drug-stimulated ATPase activities of the wild-type and Y413S ABCG2 mutants were compared at increasing membrane cholesterol concentrations. As shown in Fig. 4A, the baseline ATPase of Y413S is activated by lower cholesterol concentrations than that of

the wild-type protein, with a lower apparent half-maximum cholesterol activation concentration (K_A value of 0.37 +/- 0.27 mM) as compared to the apparent affinity of the wild-type protein for cholesterol (K_A for cholesterol of 0.70 +/- 0.09 mM). In contrast, in the case of the substrate-stimulated ATPase activities, wtABCG2 showed higher sensitivity to cholesterol loading (Fig. 4B): in the presence of quercetin the calculated K_A value for cholesterol activation of the wild-type protein was 0.22 +/- 0.20 mM, while, due to the low level of cholesterol activation a reliable K_A for the Y413S protein could not be determined.

3.4. Altered bile acid sensitivity of the ABCG2-Y413S mutant

The experiments described above showed that both the baseline and the drug-stimulated ATPase activity of the Y413S mutant differ significantly from that of the wild-type protein when excess cholesterol is present. We have recently found that bile acids (steroids formed from cholesterol in the liver) significantly decrease the high basal ATPase activity of wtABCG2, while they do not interfere with the ABCG2-mediated ATP hydrolysis measured in the presence of substrates [16, 19]. This phenomenon results in a significant (up to 5- to 7-fold) increase in the relative, substrate stimulated ATP hydrolysis, depending on the type of the bile acid. In order to find out whether the active ABCG2 CRAC mutants have any alterations in their interactions with bile acids, we measured their ATPase activities in the presence of cholic acid, glycocholate and taurocholate.

We found that the ATPase activities of the 570S, 469F, 645F and wild-type ABCG2 variants were similarly modified by bile acids (data not shown). In contrast, we found major differences in the effects of

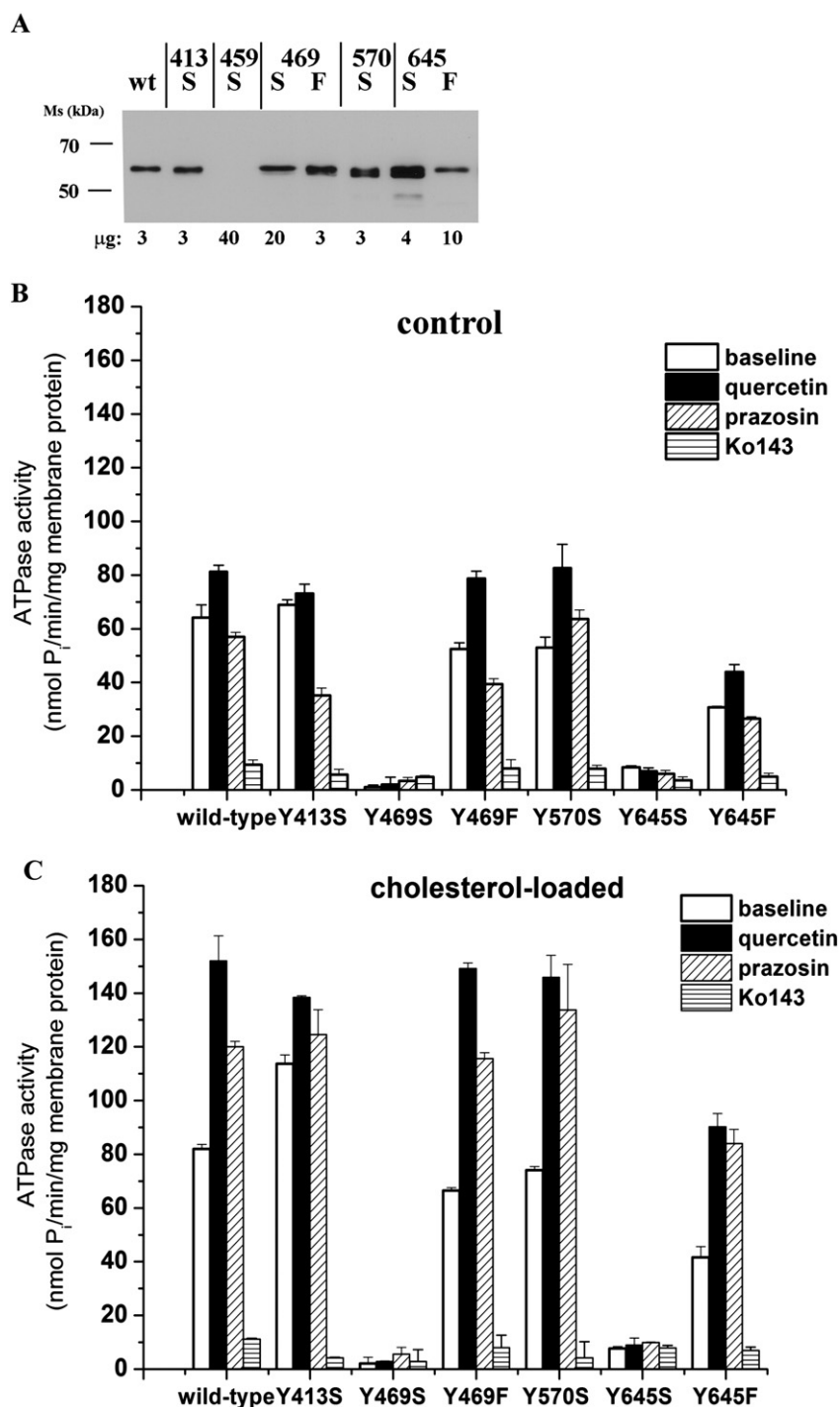


Fig. 2. Expression and ATPase activity of ABCG2 CRAC tyrosine mutants in Sf9 insect cells. Panel A: Expression of CRAC mutants in Sf9 membranes. Sf9 membranes expressing wtABCG2 and its Tyr mutants were subjected to Laemmli gel electrophoresis. ABCG2 was visualized by the BXP-21 antibody. Panels B and C: ATPase activity of ABCG2-CRAC mutants in Sf9 insect membranes. Vanadate-sensitive ATPase activity was measured in non-treated (labeled as control, Panel B) insect membranes or in insect membranes loaded with 2 mM cholesterol-RAMEB (Panel C) during the membrane preparation (see Section 2.6.) in the absence of added compounds (baseline), or in the presence of 1 μ M quercetin, 100 μ M prazosin or 1 μ M Ko143. Bars show the average of at least two independent experiments, each measured in two parallels, \pm S.D. values.

bile acids on the ATPase activity of the Y413S mutant. Though the addition of bile acids decreased the baseline ATPase activity of this ABCG2 mutant (Fig. 5A), bile acids also decreased ATP hydrolysis in the presence of substrates. Therefore the net result of bile acid effects was only a slight increase in the relative substrate stimulation of the Y413S mutant (Fig. 5B–D).

3.5. Effects of cholesterol on the transport activity of the ABCG2 CRAC mutants in Sf9 membranes

In addition to its effect on the ABCG2-ATPase activity, cholesterol has also been shown to significantly enhance the transport capacity of the protein – e.g. methotrexate transport by the wild-type ABCG2 was

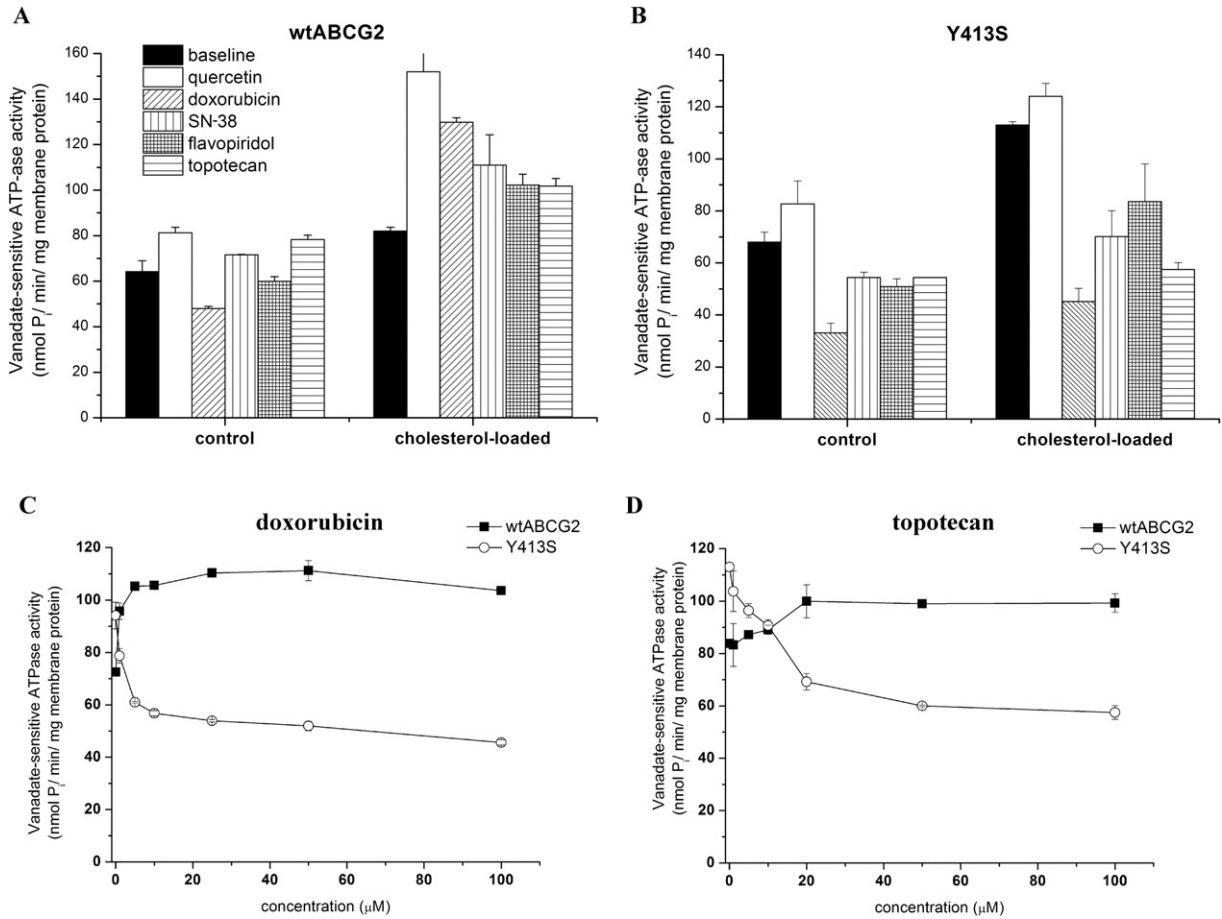


Fig. 3. Effect of known wtABCG2 substrates on the ATPase activity of wtABCG2 and the Y413S mutant. Vanadate-sensitive ATPase activity was determined in 2 mM cholesterol-RAMEB treated membranes in the absence of substrates (baseline) or in the presence of 5 μM quercetin, 50 μM doxorubicin, 20 μM SN-38, 50 μM flavopiridol or 50 μM topotecan (Panels A and B). ATPase activity was also determined in the presence of increasing concentrations of doxorubicin or topotecan (Panels C and D). Figure shows the result of three independent experiments, +/– S.D. values.

about 4-fold activated when the insect cell membrane vesicles were enriched in cholesterol [15]. To further analyze the consequence of the putative CRAC Tyr mutations on the cholesterol-sensing of ABCG2, we measured ³H-methotrexate transport both in control and cholesterol-loaded Sf9 membrane vesicles. As documented in Fig. 6, all the examined ABCG2 mutants, including Y413S, exhibited a methotrexate transport activity that, similarly to the wild-type transporter, was significantly (3- to 4-fold) enhanced by cholesterol loading of the membranes.

3.6. Expression and transport activity of ABCG2 CRAC mutants in HEK 293 cells – effect of cholesterol depletion

According to the presented results the baseline ATPase activity of the ABCG2-Y413S mutant showed a sterol sensitivity that significantly differed from that of the wild-type protein, while in the vesicular transport measurement the effect of cholesterol on this mutant did not differ from that measured for wtABCG2. In order to further characterize the “cholesterol-dependence” of the CRAC mutant ABCG2 proteins, we

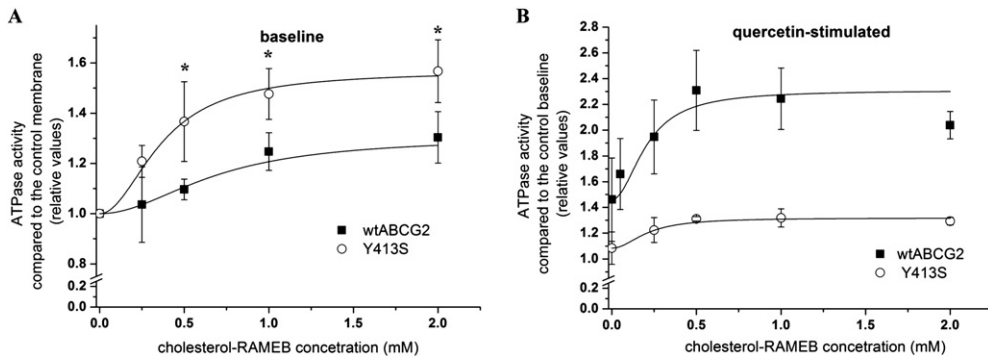


Fig. 4. Effect of cholesterol on the wtABCG2 and Y413S-ATPase. Vanadate-sensitive ATPase activity was determined as described in Section 2.9. Control membranes were co-incubated with 0.25–2 mM cholesterol-RAMEB to achieve various membrane cholesterol levels. ATPase activity was measured in the absence of added substrates (Panel A) or in the presence of 5 μM quercetin (Panel B). The average of four independent experiments +/– S.D. values are shown. *Student’s t-test, significant difference, p < 0.05.

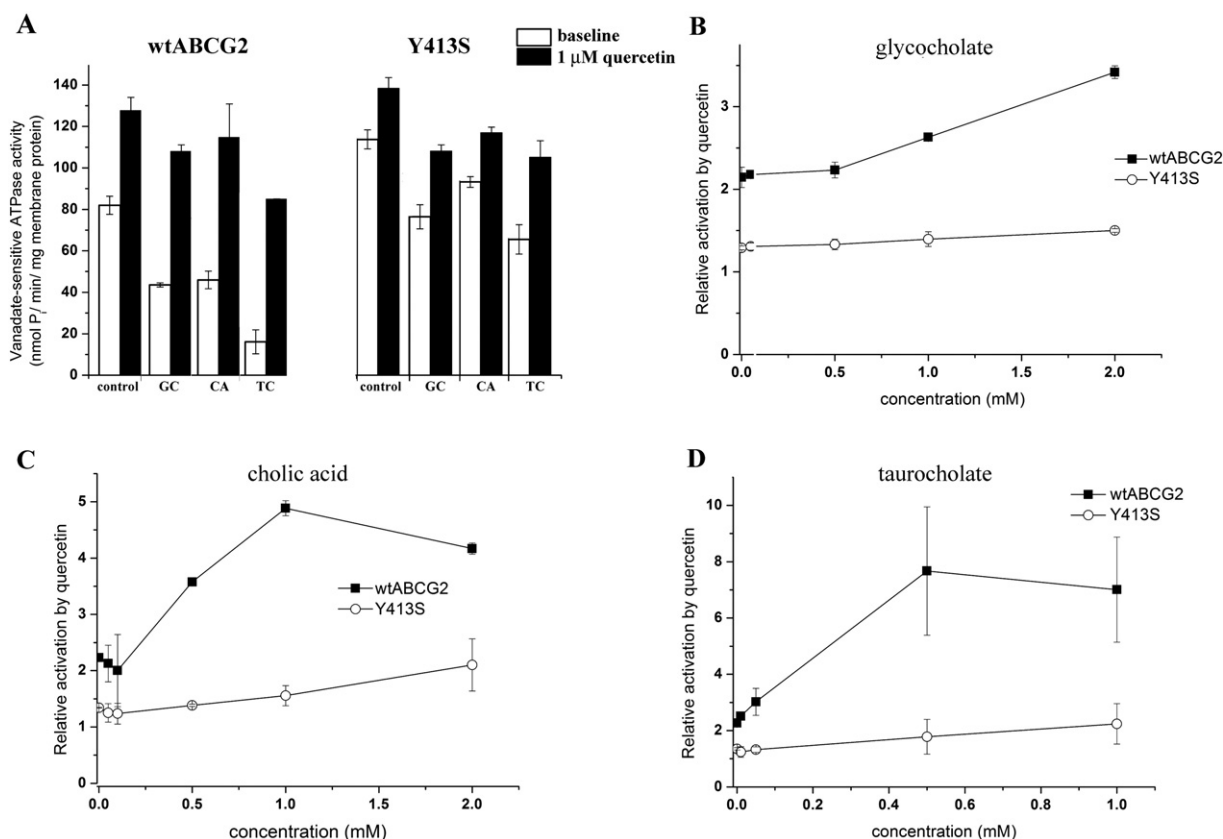


Fig. 5. Effect of bile acids on the wtABCG2 and Y413S-ATPase. ATPase activity was determined in Sf9 membrane vesicles loaded with 2 mM cholesterol-RAMEB. Panel A: Vanadate-sensitive basal (no added substrate) or 1 μ M quercetin-stimulated ATPase activity in the absence or presence of 1 mM glycocholate (GC), 1 mM cholic acid (CA) or taurocholate (TC). Panel B: Relative ATPase activity in the presence of 1 μ M quercetin compared to the baseline is shown against increasing bile acid concentrations. Experiments were performed in quadruplicates, average \pm S.D. values are shown.

generated mammalian HEK 293 cells stably expressing the Y413S, Y469F, Y570S and Y645F mutants. Western blotting confirmed successful expression of these proteins (data not shown). Moreover, labeling with the anti-ABCG2 5D3 antibody, which recognizes an extracellular epitope, indicated proper plasma membrane localization of these mutants (Supplemental Fig. S2).

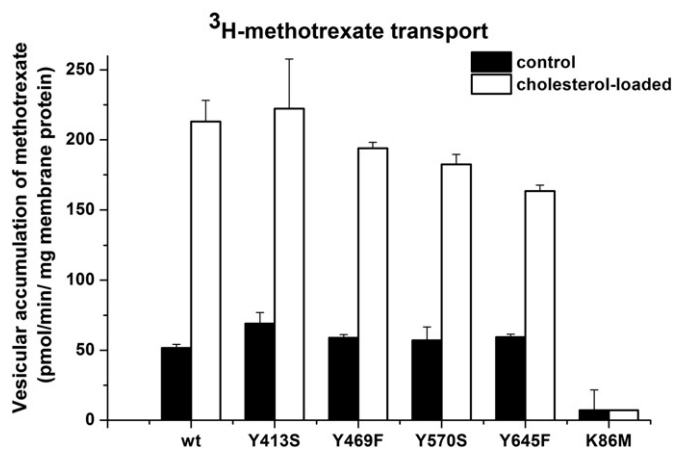


Fig. 6. Transport of ^3H -methotrexate into control and cholesterol-loaded inside-out Sf9 insect membrane vesicles. Intravesicular accumulation of 50 μ M ^3H -methotrexate in Sf9 membrane vesicles with different ABCG2 mutants containing 90 μ g of total membrane protein was measured at 37 $^\circ\text{C}$ for 10 min in the presence or absence of 1 μ M Ko143. For the investigation of the effect of cholesterol, the membranes were loaded with 2 mM cholesterol-RAMEB. Control represents non-loaded membranes. Bars represent average Ko143-dependent transport obtained in two independent experiments, each with two parallels \pm S.D. values.

To characterize the effect of cholesterol on the ABCG2 transport function, we depleted the cholesterol content of the cells by co-incubation with cyclodextrin (RAMEB). This method decreases membrane cholesterol levels by about 25%, and was successfully used in earlier studies to define the effects of various cholesterol levels on ABCG2 function in mammalian cells [15,33]. Previously we have demonstrated that mild cholesterol depletion of HEK 293 cells resulted in a decreased transport function of wtABCG2, while did not alter the localization of ABCG2 or the viability of the cells [15].

For measuring ABCG2 transport activity, intracellular accumulation of Hoechst 33342 was followed in control and cyclodextrin-treated HEK 293 cells, expressing the wild-type and the CRAC mutant ABCG2 proteins. As shown in Fig. 7, all ABCG2 mutants, including Y413S, were able to actively transport Hoechst 33342, and cholesterol depletion significantly decreased the Hoechst 33342 transport activity of all the CRAC mutants similarly to wild-type ABCG2.

3.7. Putative CRAC mutants of ABCG2, including Y413S, effectively transport substrate drugs and protect HEK 293 cells against cytotoxic substrates

The differential effect of the transported substrates on the wild-type and the Y413S ABCG2 ATPase activity may reflect different transport properties. Still, we did not find any alteration of the transport capacity or the cholesterol sensitivity of the Hoechst 33342 transport in the CRAC mutants.

In order to further explore the relationship of altered drug-stimulated ATPase and transport activities, the transport of various fluorescent ABCG2 substrates was compared in HEK 293 cells overexpressing wtABCG2 and the Y413S mutant, respectively. No major difference was found in BODIPY-prazosin, Hoechst 33342, mitoxantrone and Pheophorbide A transport by any of the active mutants analyzed in

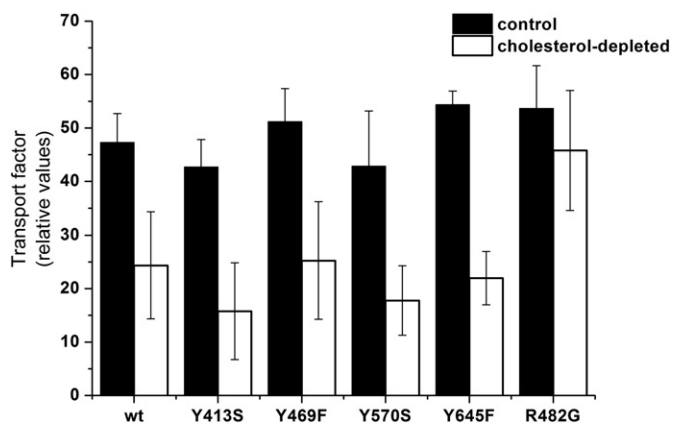


Fig. 7. Hoechst 33342 transport in ABCG2-expressing HEK 293 cells – effect of cholesterol depletion. HEK 293 cells stably expressing wtABCG2 and its mutants were incubated with 2 μ M Hoechst 33342 for 20 min at 37 °C with or without 1 μ M Ko143. After washing, cellular fluorescence of Hoechst 33342 was determined by flow cytometry. Cholesterol depletion was achieved by co-incubation of the membranes with empty cyclodextrin (see 2.12.); control values show results obtained with non-treated cells. Transport factor in living (propidium-iodide negative) cells was calculated as described in Section 2.11. Experiments were performed in quadruplicates; bars show the average of at least three independent measurements \pm S.D. values.

this study (Table 1). Interestingly, in spite of its different behavior in the ATPase assay, the Y413S mutant also did not differ significantly from the wild-type protein, with respect to the transport of the above mentioned substrates.

Among the cytotoxic drugs, the Y413S mutant ABCG2 protein (similarly to the wild-type) was able to transport doxorubicin (Fig. 8A) and provided protection against doxorubicin, SN-38, flavopiridol and topotecan, strongly indicating an active transport of these compounds by this mutant (Fig. 8B and Supplementary Fig. S3).

4. Discussion

Understanding the regulation of the expression and function of ABCG2 may have important implications with regard to the modulation the ADME-Tox parameters of drugs and xenobiotics, in anti-cancer therapies, as well as in the treatment of gout. Cholesterol has been shown to be an essential activator of ABCG2 function [14–16], although the exact nature of the interaction between cholesterol and the transporter has not yet been defined. Also, the molecular determinants of cholesterol-sensing by ABCG2 remain largely unknown [19,20]. Cholesterol recognition amino acid consensus sequence (CRAC) motifs have previously been confirmed to be involved in cholesterol-sensing of various proteins [21–25,34,35]. Site directed mutagenesis studies targeting conserved CRAC amino acids identified a large variety of protein-specific phenotypes. In the case of the HIV gp41 protein, CRAC mutations resulted in reduced cholesterol binding [35]; mutant peripheral-type benzodiazepine receptor variants showed altered cholesterol transport [34], while in ion channels the channel function was retained but regulation by cholesterol was abolished [25,36].

Here, we aimed to determine whether the CRAC motifs identified in the ABCG2 sequence play any role in the sterol-sensing of the human ABCG2 multidrug transporter. We found five putative CRAC sequences

Table 1

All active Tyr mutants are able to transport various known ABCG2 substrates. Ko143-sensitive transport was determined in HEK 293 cells expressing one of the ABCG2 variants.

	BODIPY-prazosin	Pheophorbide A	Hoechst 33342	mitoxantrone
wtABCG2	+	+	+	+
Y413S	+	+	+	+
Y469F	+	+	+	+
Y570S	+	+	+	+
Y645F	+	+	+	+

located in or near the transmembrane helices of ABCG2 (Fig. 1). Based on the previous CRAC mutagenesis studies described above, we expected that mutation of a functional CRAC motif would modify the effect of cholesterol on ABCG2 function. We have approached this question by using a number of specific methods.

ABC transporters couple ATPase and transport activities to promote the transmembrane movement of their substrates. This complex enzymatic activity can be followed in several experimental systems. ABCG2 expressed in Sf9 membranes displays relatively high baseline ATPase activity that can be moderately stimulated by transported compounds. The low intrinsic cholesterol content of the insect cell membrane allows the systematic modulation of membrane cholesterol levels. Using this model system, we and others have shown that the substrate-stimulated ATPase activity of ABCG2 is significantly accelerated by cholesterol [14,15]. Cholesterol makes up to 20% of the total lipids in mammalian cell membranes. Partial cholesterol depletion can be achieved by using “empty” cyclodextrins, which has been shown to result in a decrease of ABCG2 transport activity [15,33]. Using this repertoire of assays we aimed to determine the role of the identified five CRAC motifs in the cholesterol-sensitive functions of ABCG2.

We found that tyrosines of putative CRAC motifs predicted to be located in or near to the intracellular surface of ABCG2 (Fig. 1) are essential for protein expression and/or function. Tyr to Ser mutations at positions 459, 469 and 645 resulted in the loss of protein function, and the Tyr 459 to Ser mutation resulted in a complete loss of ABCG2 expression (Fig. 2). Insect cells are cultured at 27 °C which has been shown to allow the expression of improperly folded proteins [37]. The fact that the Y459S mutant could not be expressed properly in insect cells suggests that the tyrosine at this amino acid position is crucial for the proper folding and processing of the protein and therefore might be an important determinant of ABCG2 structure. Recently, the Y459C heterozygous mutation was reported to occur in patients with renal cancer [38]. Therefore further exploration of the effect of mutations to residue 459 in ABCG2 is warranted.

The Y469S and Y645S mutants could be expressed in comparable amounts to the wild-type protein, however, they were found to be non-functional (Fig. 2). These results may be interpreted in two ways. First, these tyrosines may be important for proper function or, alternatively, these mutants may lose their cholesterol-sensing capability. Interestingly, introduction of a phenyl residue at the same position was found to be compatible with normal ATPase and transport activity, as well as with cholesterol-sensing, indicating that these regions are not functional CRAC motifs. Rather, Y469 and Y645, along with Y459, may be important for proper folding of ABCG2. Our experiments, in which we tested the conformation of the ABCG2 mutants by labeling them with the conformation sensitive anti-ABCG2 5D3 antibody, revealed that the Y469S and Y645S mutants have decreased 5D3 binding capacity (Supplementary Fig. S4). Therefore the loss of the activity of the Y469S and Y645S mutants is most probably due to their improper conformation and not by their altered cholesterol-sensing.

Previously, the Y645F mutation has been found to be functional, although has shown slightly decreased Hoechst 33342 transport capacity [39]. Interestingly, we did not find any major alteration in the substrate recognition by this mutant. Even its Hoechst 33342 transport capacity did not differ significantly from that of the wild-type protein (Fig. 7).

The other two tyrosines (Y413 and Y570) mutated in this study are located in or near the extracellular surface of the transmembrane domain. We found that changing these amino acids is well tolerable for ABCG2, resulting in fully active proteins. The Tyr 570 to Ser mutation did not alter protein expression either in Sf9 or in HEK 293 cells, and substrate recognition and cholesterol-sensing of this mutant was also similar to that of the wild-type transporter (Figs. 2 and 6 and Supplementary Fig. S1).

However, the Y413S mutant exhibited a distinct ATPase activity. This mutant showed a greatly increased baseline ATPase in the presence of low levels of added cholesterol (Fig. 4A), revealing an increased

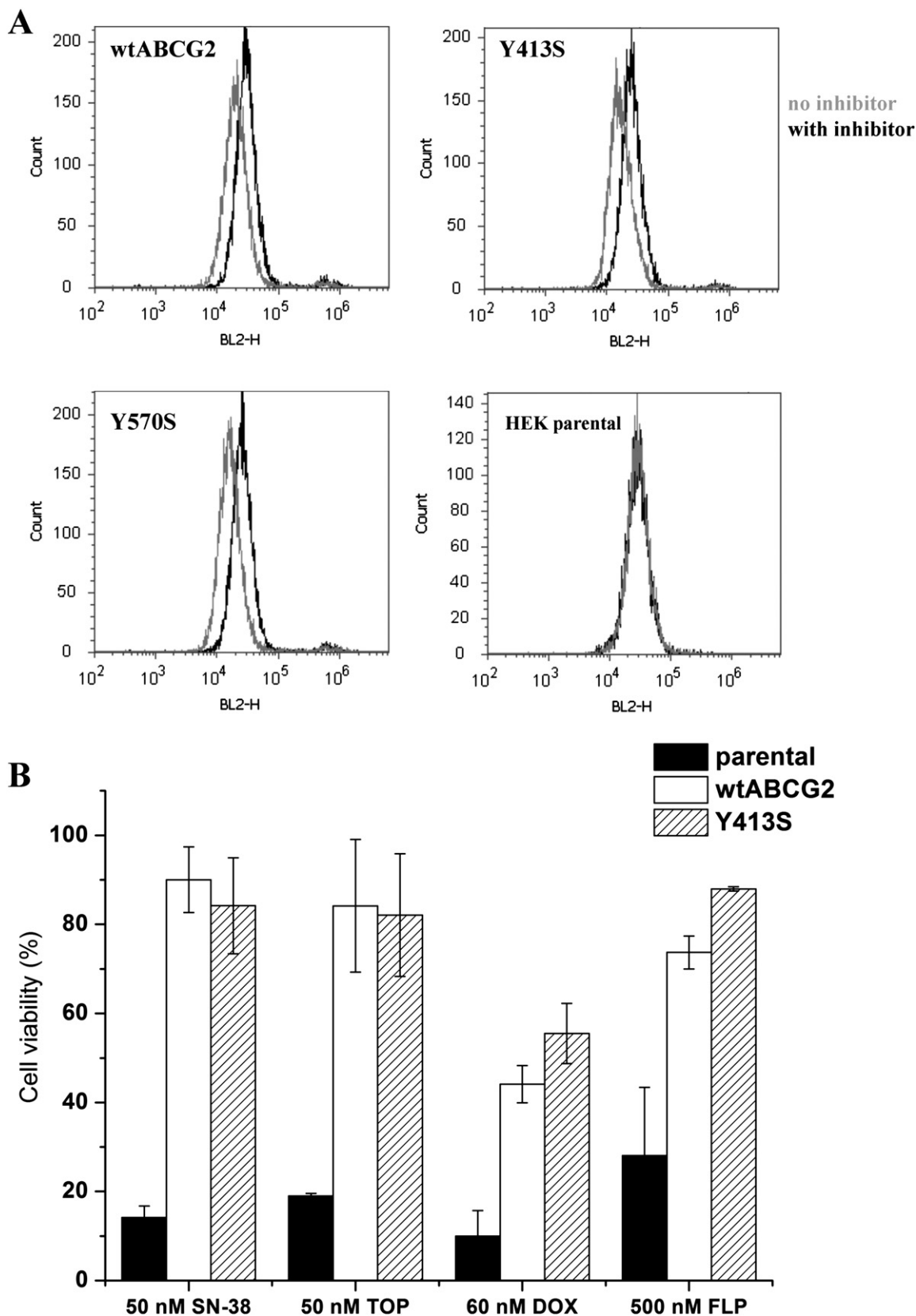


Fig. 8. Panel A: Doxorubicin efflux from HEK 293 cells. Doxorubicin (5 μ M) efflux was measured as described in Section 2.13. Fluorescence of the cells was monitored by flow cytometry. Experiments were performed in duplicates. Figure shows representative graphs. Panel B. Cytotoxicity of ABCG2 substrates in HEK 293 cells. HEK 293 parental cells or stably expressing wtABCG2 or its Y413S mutant were incubated with 50 nM SN-38, 50 nM topotecan (TOP), 60 nM doxorubicin (DOX) or 500 nM flavopiridol (FLP) for 72 hours. Cell viability was determined by PrestoBlue staining. 100% represents cells incubated at the same conditions in the absence of any drugs. Bars show the average of four independent experiments with quadruplicates each, \pm S.D. values.

cholesterol sensitivity, while no further activation of the ABCG2-413S ATPase could be achieved by administration of transported substrates regardless of the cholesterol content of the membrane. Moreover, potential substrates that are known to activate the wild-type ABCG2-ATPase, rather inhibited the ATPase activity of the Y413S mutant (Fig. 3). In addition to this altered cholesterol-sensing, the ATPase activity of the Y413S mutant also showed an altered bile acid sensitivity, as this mutant was less sensitive to bile acids than the wild-type protein (Fig. 5).

The nature of the relatively high baseline ATPase activity of the human ABCG2 transporter is still not clarified. One explanation is an intrinsic, partially uncoupled function of the protein, manifesting in a “futile” ATP hydrolysis, keeping this multidrug transporter alert for rapid export of potentially harmful compounds [40]. Another possibility is the presence of an endogenous transported substrate, potentially cholesterol, triggering ATP hydrolysis without the addition of exogenous compounds. In the case of the Y413S mutant, cholesterol may promote “uncoupling” of the ATP hydrolysis in the ABCG2 protein. Alternatively, if we consider the possibility that cholesterol is transported by ABCG2, the results could be explained by a higher affinity to cholesterol by the ABCG2-Y413S mutant, also observed in the case of the R482G mutant [15]. The cholesterol-dependent increase in the ATPase activity is similar to that observed for several transported substrates. If ABCG2 can transport cholesterol, our data can be interpreted to suggest that the Y413S mutant is a more efficient cholesterol transporter. Unfortunately, experimental verification of cholesterol transport is difficult due to the lack of dedicated assays measuring ABCG2-mediated cholesterol transport. Tarling et al. [41] measured cholesterol efflux to HDL in ABCG1 and ABCG2 overexpressing cells, and found that, in contrast to ABCG1, ABCG2 is not able to transport cholesterol to HDL. Since ABCG2-mediated cholesterol transport has not been experimentally confirmed, we speculate that the “cholesterol-stimulated” ATPase activity of the ABCG2-Y413S mutant is a result of its differential sensitivity to the modulatory effect of cholesterol.

In contrast to these findings related to the ABCG2-ATPase activity, we did not find any significant alteration in the cholesterol sensitivity of the ABCG2-Y413S mediated transport either in insect cell vesicular transport, or mammalian intact cell transport assays. Active substrate transport by the Y413S mutant was clearly activated by cholesterol in both systems, and by all the compounds examined (Figs. 6 and 7). Moreover, the Y413S mutant protected the cells against toxic drugs similarly to the wild-type ABCG2. All these experimental data suggest that although the ABCG2-Y413S mutant has an altered cholesterol interaction, it is rather manifested in a partial uncoupling of the ATPase activity of the transporter in the absence of transported substrates.

5. Conclusions

Our study is the first detailed analysis of potential CRAC motifs within an ABC protein, and here we provide experimental data for various functional consequences of the mutations in these motifs in ABCG2. Surprisingly, none of the functional CRAC mutants analyzed here abolished the cholesterol-sensitivity of the transporter, although mutation of Y413 significantly affected cholesterol and bile acid interactions. These data suggest that Tyr 413 within a putative CRAC motif is most probably part of a sterol-dependent regulatory region of ABCG2 and may regulate the coupling of ATPase to transport activity.

Acknowledgements

We are grateful to Hedvig Tordai for providing us the pSB-CMV-ABCG2 plasmid and to György Várady for helping in cell sorting. The technical help by Zsuzsanna András, Éva Krizsán, Katalin Mihály and Györgyi Vermes is also greatly appreciated. We are also thankful to Drs. George Scheffer and Rik Scheper for providing us the BXP-21

antibody (Department of Pathology, Free University, Medical Center, Amsterdam, the Netherlands).

Funding: This work has been supported by the Hungarian Scientific Research Fund (OTKA) grants [83533, 109423 and 104227], and by NKTH-ANR [10-1-2011-0401] Achilles. G. Sz. was supported by a Momentum Grant of the Hungarian Academy of Sciences.

Appendix A. Supplementary data

Supplementary data to this article can be found online at <http://dx.doi.org/10.1016/j.bbmem.2014.11.006>.

References

- [1] B. Sarkadi, C. Ozvegy-Laczka, K. Nemet, A. Varadi, ABCG2 – a transporter for all seasons, *FEBS Lett.* 567 (2004) 116–120.
- [2] U. Henriksen, J.U. Fog, T. Litman, U. Gether, Identification of intra- and intermolecular disulfide bridges in the multidrug resistance transporter ABCG2, *J. Biol. Chem.* 280 (2005) 36926–36934.
- [3] K. Noguchi, K. Katayama, Y. Sugimoto, Human ABC transporter ABCG2/BCRP expression in chemoresistance: basic and clinical perspectives for molecular cancer therapeutics, *Pharmgenomics Pers. Med.* 7 (2014) 53–64.
- [4] I.D. Kerr, A.J. Haider, I.C. Gelissen, The ABCG family of membrane-associated transporters: you don't have to be big to be mighty, *Br. J. Pharmacol.* 164 (2011) 1767–1779.
- [5] G. Szakacs, A. Varadi, C. Ozvegy-Laczka, B. Sarkadi, The role of ABC transporters in drug absorption, distribution, metabolism, excretion and toxicity (ADME-Tox), *Drug Discov. Today* 13 (2008) 379–393.
- [6] P. Godoy, N.J. Hewitt, U. Albrecht, M.E. Andersen, N. Ansari, S. Bhattacharya, J.G. Bode, J. Bolleyn, C. Borner, J. Bottger, A. Braeuning, R.A. Budinsky, B. Burkhardt, N.R. Cameron, G. Camussi, C.S. Cho, Y.J. Choi, J. Craig Rowlands, U. Dahmen, G. Damm, O. Dirsch, M.T. Donato, J. Dong, S. Dooley, D. Drasdo, R. Eakins, K.S. Ferreira, V. Fonsato, J. Fraczek, R. Gebhardt, A. Gibson, M. Glanemann, C.E. Goldring, M.J. Gomez-Lechon, G.M. Groothuis, L. Gustavsson, C. Guyot, D. Hallifax, S. Hammad, A. Hayward, D. Haussinger, C. Hellerbrand, P. Hewitt, S. Hoehme, H.G. Holzhtuter, J.B. Houston, J. Hrach, K. Ito, H. Jaeschke, V. Keitel, J.M. Kelm, B. Kevin Park, C. Kordes, G.A. Kullak-Ublick, E.L. LeCluyse, P. Lu, J. Luebke-Wheeler, A. Lutz, D.J. Maltman, M. Matz-Soja, P. McMullen, I. Merfort, S. Messner, C. Meyer, J. Mwynyi, D.J. Naisbitt, A.K. Nussler, P. Olinga, F. Pampaloni, J. Pi, L. Pluta, S.A. Przyborski, A. Ramachandran, V. Rogiers, C. Rowe, C. Schelcher, K. Schmich, M. Schwarz, B. Singh, E.H. Stelzer, B. Stieger, R. Stober, Y. Sugiyama, C. Tetta, W.E. Thasler, T. Vanhaecke, M. Vincken, T.S. Weiss, A. Widera, C.G. Woods, J.J. Xu, K.M. Yarborough, J.G. Hengstler, Recent advances in 2D and 3D in vitro systems using primary hepatocytes, alternative hepatocyte sources and non-parenchymal liver cells and their use in investigating mechanisms of hepatotoxicity, cell signaling and ADME, *Arch. Toxicol.* 87 (2013) 1315–1530.
- [7] O.M. Woodward, A. Kottgen, J. Coresh, E. Boerwinkle, W.B. Guggino, M. Kottgen, Identification of a urate transporter, ABCG2, with a common functional polymorphism causing gout, *Proc. Natl. Acad. Sci. U. S. A.* 106 (2009) 10338–10342.
- [8] A. Nakayama, H. Matsuo, T. Takada, K. Ichida, T. Nakamura, Y. Ikebuchi, K. Ito, T. Hosoya, Y. Kanai, H. Suzuki, N. Shinomiya, ABCG2 is a high-capacity urate transporter and its genetic impairment increases serum uric acid levels in humans, *Nucleosides Nucleotides Nucleic Acids* 30 (2011) 1091–1097.
- [9] A. Dehghan, A. Kottgen, Q. Yang, S.J. Hwang, W.L. Kao, F. Rivadeneira, E. Boerwinkle, D. Levy, A. Hofman, B.C. Astor, E.J. Benjamin, C.M. van Duijn, J.C. Witteman, J. Coresh, C.S. Fox, Association of three genetic loci with uric acid concentration and risk of gout: a genome-wide association study, *Lancet* 372 (2008) 1953–1961.
- [10] P. Krishnamurthy, J.D. Schuetz, The ABC transporter Abcg2/Bcrp: role in hypoxia mediated survival, *Biomaterials* 18 (2005) 349–358.
- [11] D. Turk, G. Szakacs, Relevance of multidrug resistance in the age of targeted therapy, *Curr. Opin. Drug Discov. Devel.* 12 (2009) 246–252.
- [12] R.W. Robey, P.R. Massey, L. Amiri-Kordestani, S.E. Bates, ABC transporters: unvalidated therapeutic targets in cancer and the CNS, *Anticancer Agents Med. Chem.* 10 (2010) 625–633.
- [13] K. Natarajan, Y. Xie, M.R. Baer, D.D. Ross, Role of breast cancer resistance protein (BCRP/ABCG2) in cancer drug resistance, *Biochem. Pharmacol.* 83 (2012) 1084–1103.
- [14] A. Pal, D. Mehn, E. Molnar, S. Gedey, P. Meszaros, T. Nagy, H. Glavinas, T. Janaky, O. von Richter, G. Bathori, L. Szente, P. Krajcsi, Cholesterol potentiates ABCG2 activity in a heterologous expression system: improved in vitro model to study function of human ABCG2, *J. Pharmacol. Exp. Ther.* 321 (2007) 1085–1094.
- [15] A. Telbisz, C. Hegedus, A. Varadi, B. Sarkadi, C. Ozvegy-Laczka, Regulation of the Function of the Human ABCG2 Multidrug Transporter by Cholesterol and Bile Acids: Effects of Mutations in Potential Substrate and Steroid Binding Sites, *Drug Metab. Dispos.* 42 (2007) 575–585.
- [16] A. Telbisz, C. Ozvegy-Laczka, T. Hegedus, A. Varadi, B. Sarkadi, Effects of the lipid environment, cholesterol and bile acids on the function of the purified and reconstituted human ABCG2 protein, *Biochem. J.* 450 (2013) 387–395.
- [17] G.A. Graf, L. Yu, W.P. Li, R. Gerard, P.L. Tuma, J.C. Cohen, H.H. Hobbs, ABCG5 and ABCG8 are obligate heterodimers for protein trafficking and biliary cholesterol excretion, *J. Biol. Chem.* 278 (2003) 48275–48282.

- [18] N. Wang, L. Yvan-Charvet, D. Lutjohann, M. Mulder, T. Vanmierlo, T.W. Kim, A.R. Tall, ATP-binding cassette transporters G1 and G4 mediate cholesterol and desmosterol efflux to HDL and regulate sterol accumulation in the brain, *FASEB J.* 22 (2008) 1073–1082.
- [19] A. Telbisz, C. Hegedus, A. Varadi, B. Sarkadi, C. Ozvegy-Laczka, Regulation of the function of the human ABCG2 multidrug transporter by cholesterol and bile acids: effects of mutations in potential substrate and steroid binding sites, *Drug Metab. Dispos.* 42 (2014) 575–585.
- [20] S. Velamakanni, T. Janvilisri, S. Shahi, H.W. van Veen, A functional steroid-binding element in an ATP-binding cassette multidrug transporter, *Mol. Pharmacol.* 73 (2008) 12–17.
- [21] J.J. Lacapere, V. Papadopoulos, Peripheral-type benzodiazepine receptor: structure and function of a cholesterol-binding protein in steroid and bile acid biosynthesis, *Steroids* 68 (2003) 569–585.
- [22] R.M. Epand, Proteins and cholesterol-rich domains, *Biochim. Biophys. Acta* 1778 (2008) 1576–1582.
- [23] R.M. Epand, B.G. Sayer, R.F. Epand, Caveolin scaffolding region and cholesterol-rich domains in membranes, *J. Mol. Biol.* 345 (2005) 339–350.
- [24] A. Midzak, G. Rammouz, V. Papadopoulos, Structure-activity relationship (SAR) analysis of a family of steroids acutely controlling steroidogenesis, *Steroids* 77 (2012) 1327–1334.
- [25] A.K. Singh, J. McMillan, A.N. Bukiya, B. Burton, A.L. Parrill, A.M. Dopico, Multiple cholesterol recognition/interaction amino acid consensus (CRAC) motifs in cytosolic C tail of Slo1 subunit determine cholesterol sensitivity of Ca²⁺ + - and voltage-gated K⁺ (BK) channels, *J. Biol. Chem.* 287 (2012) 20509–20521.
- [26] C. Ozvegy, A. Varadi, B. Sarkadi, Characterization of drug transport, ATP hydrolysis, and nucleotide trapping by the human ABCG2 multidrug transporter. Modulation of substrate specificity by a point mutation, *J. Biol. Chem.* 277 (2002) 47980–47990.
- [27] C. Ozvegy, T. Litman, G. Szakacs, Z. Nagy, S. Bates, A. Varadi, B. Sarkadi, Functional characterization of the human multidrug transporter, ABCG2, expressed in insect cells, *Biochem. Biophys. Res. Commun.* 285 (2001) 111–117.
- [28] H. Saranko, H. Tordai, A. Telbisz, C. Ozvegy-Laczka, G. Erdos, B. Sarkadi, T. Hegedus, Effects of the gout-causing Q141K polymorphism and a CFTR DeltaF508 mimicking mutation on the processing and stability of the ABCG2 protein, *Biochem. Biophys. Res. Commun.* 437 (2013) 140–145.
- [29] O. Kolacsek, V. Krizsik, A. Schamberger, Z. Erdei, A. Apati, G. Varady, L. Mates, Z. Izsvak, Z. Ivics, B. Sarkadi, T.I. Orban, Reliable transgene-independent method for determining Sleeping Beauty transposon copy numbers, *Mob. DNA* 2 (2011) 5.
- [30] E. Bakos, I. Klein, E. Welker, K. Szabo, M. Muller, B. Sarkadi, A. Varadi, Characterization of the human multidrug resistance protein containing mutations in the ATP-binding cassette signature region, *Biochem. J.* 323 (Pt 3) (1997) 777–783.
- [31] M.F. Khan, T.L. Unruh, J.P. Deans, Implementation of a Flow Cytometry Strategy to Isolate and Assess Heterogeneous Membrane Raft Domains, *Flow Cytometry - Recent Perspectives* 2012.
- [32] C. Ozvegy-Laczka, G. Koblos, B. Sarkadi, A. Varadi, Single amino acid (482) variants of the ABCG2 multidrug transporter: major differences in transport capacity and substrate recognition, *Biochim. Biophys. Acta* 1668 (2005) 53–63.
- [33] C.H. Storch, R. Ehehalt, W.E. Haefeli, J. Weiss, Localization of the human breast cancer resistance protein (BCRP/ABCG2) in lipid rafts/caveolae and modulation of its activity by cholesterol in vitro, *J. Pharmacol. Exp. Ther.* 323 (2007) 257–264.
- [34] H. Li, V. Papadopoulos, Peripheral-type benzodiazepine receptor function in cholesterol transport. Identification of a putative cholesterol recognition/interaction amino acid sequence and consensus pattern, *Endocrinology* 139 (1998) 4991–4997.
- [35] R.F. Epand, B.G. Sayer, R.M. Epand, The tryptophan-rich region of HIV gp41 and the promotion of cholesterol-rich domains, *Biochemistry* 44 (2005) 5525–5531.
- [36] S. Oddi, E. Dainese, F. Fezza, M. Lanuti, D. Barcaroli, V. De Laurenzi, D. Centonze, M. Maccarrone, Functional characterization of putative cholesterol binding sequence (CRAC) in human type-1 cannabinoid receptor, *J. Neurochem.* 116 (2011) 858–865.
- [37] G.M. Denning, M.P. Anderson, J.F. Amara, J. Marshall, A.E. Smith, M.J. Welsh, Processing of mutant cystic fibrosis transmembrane conductance regulator is temperature-sensitive, *Nature* 358 (1992) 761–764.
- [38] I. Zoernig, C. Ziegelmeier, B. Lahrman, N. Grabe, D. Jager, N. Halama, Sequence mutations of the substrate binding pocket of stem cell factor and multidrug resistance protein ABCG2 in renal cell cancer: a possible link to treatment resistance, *Oncol. Rep.* 29 (2013) 1697–1700.
- [39] Z. Ni, Z. Bikadi, X. Cai, M.F. Rosenberg, Q. Mao, Transmembrane helices 1 and 6 of the human breast cancer resistance protein (BCRP/ABCG2): identification of polar residues important for drug transport, *Am. J. Physiol. Cell Physiol.* 299 (2010) C1100–C1109.
- [40] B. Sarkadi, L. Homolya, G. Szakacs, A. Varadi, Human multidrug resistance ABCB and ABCG transporters: participation in a chemoinnity defense system, *Physiol. Rev.* 86 (2006) 1179–1236.
- [41] E.J. Tarling, P.A. Edwards, ATP binding cassette transporter G1 (ABCG1) is an intracellular sterol transporter, *Proc. Natl. Acad. Sci. U. S. A.* 108 (2011) 19719–19724.
- [42] G.E. Tusnady, I. Simon, The HMMTOP transmembrane topology prediction server, *Bioinformatics* 17 (2001) 849–850.
- [43] L. Dobson, I. Reményi, G.E. Tusnady, The Human Transmembrane Proteome submitted to, *PLoS One* (2014).

High-Affinity Interaction of Tyrosine Kinase Inhibitors with the ABCG2 Multidrug Transporter

Csilla Özvegy-Laczka, Tamás Hegedűs, György Várady, Olga Ujhelly, John D. Schuetz, András Váradi, György Kéri, László Órfi, Katalin Német, and Balázs Sarkadi

National Medical Center, Institute of Haematology and Immunology, Membrane Research Group of the Hungarian Academy of Sciences (C.Ö.-L., T.H., B.S.) and Department of Experimental Gene Therapy, Budapest, Hungary (G.V., O.U., K.N.); Department of Pharmaceutical Sciences, St. Jude Children's Research Hospital, Memphis, Tennessee (J.D.S.); Institute of Enzymology, Hungarian Academy of Sciences, Budapest, Hungary (C.Ö.-L., A.V.); and Semmelweis University, Department of Medical Chemistry, Peptide Biochemistry Research Group of the Hungarian Academy of Sciences, Budapest, Hungary (G.K., L.Ó.)

Received December 1, 2003; accepted March 3, 2004

This article is available online at <http://molpharm.aspetjournals.org>

ABSTRACT

Tyrosine kinase inhibitors (TKIs) are promising new agents for specific inhibition of malignant cell growth and metastasis formation. Because most of the TKIs have to reach an intracellular target, specific membrane transporters may significantly modulate their effectiveness. In addition, the hydrophobic TKIs may interact with so-called multidrug transporters and thus alter the cellular distribution of unrelated pharmacological agents. In the present work, we show that certain TKIs, already in the clinical phase of drug development, directly interact with the ABCG2 multidrug transporter protein with a high affinity. We found that in several *in vitro* assay systems, STI-571 (Gleevec; imatinib mesylate), ZD1839 (Iressa; gefitinib), and *N*-[4-[(3-bromophenyl)amino]-6-quinazoliny]-2-butyramide (EKI-785) interacted

with ABCG2 at submicromolar concentrations, whereas other multidrug transporters, human multidrug resistance protein (P-glycoprotein, ABCB1) and human multidrug resistance protein 1 (ABCC1), showed much lower reactivity toward these agents. Low concentrations of the TKIs examined selectively modulated ABCG2-ATPase activity, inhibited ABCG2-dependent active drug extrusion, and significantly affected drug resistance patterns in cells expressing ABCG2. Our results indicate that multidrug resistance protein modulation by TKIs may be an important factor in the clinical treatment of cancer patients. These data also raise the possibility that an extrusion of TKIs by multidrug transporters, e.g., ABCG2, may be involved in tumor cell TKI resistance.

In current antitumor drug research, a large variety of TKIs with increasing specificity and selectivity have been developed (Traxler, 2003). STI-571 (Gleevec; imatinib), an inhibitor of Bcr-Abl kinase, has been successfully applied in the treatment of chronic myeloid leukemia and is under clinical studies for cancers involving other deregulated kinases (Joensuu et al., 2001; van Oosterom et al., 2002). A number of epidermal growth factor receptor tyrosine kinase (EGFR-TK) inhibitors have also reached various phases of clinical or preclinical trials, including the compound ZD1839 (Iressa; gefitinib) and the irreversible TKI

EKI-785 (Ranson et al., 2002; Roberts et al., 2002). The therapeutic potential of most TKIs, in addition to specific kinase-inhibitory potential, also depends on their access to intracellular targets.

An emerging question is the possible interaction of TKIs with multidrug resistance ABC transporters. These plasma membrane glycoproteins cause chemotherapy resistance by actively extruding a large variety of therapeutic compounds from the cancer cells. ABC transporters also play important protective functions against toxic compounds, e.g., in the blood-brain barrier, the gut, liver, or kidney. The three major multidrug resistance ABC proteins are MDR1 (P-glycoprotein, ABCB1), MRP1 (multidrug resistance protein 1; ABCC1) and ABCG2 (ABCP/BCRP/MXR) (Litman et al., 2001; Allen and Schinkel,

This work has been supported by research grants from the Hungarian Scientific Research Fund and Ministry of Education, Hungary (T-29921, T-35126, T-31952, T35926, T38337 and D 45957, ETT, NKFP, and OM-1421/1999). B.S. is the recipient of a Howard Hughes International Scholarship.

ABBREVIATIONS: TKI, tyrosine kinase inhibitor; ABC, ATP-binding cassette; ABCP, placenta-specific ABC transporter; ADME-Tox, absorption, tissue distribution, metabolism, and toxicity; BCRP, breast cancer resistance protein; AM, acetoxymethyl ester; MOPS, 3-(*N*-morpholino)propanesulfonic acid; GS, glutathione; MDR1, human multidrug resistance protein (P-glycoprotein, ABCB1); MRP1, human multidrug resistance protein 1 (ABCC1); MXR, mitoxantrone resistance-associated protein; MX, mitoxantrone; NEM, *N*-ethylmaleimide; Sf9 cells, *Spodoptera frugiperda* ovarian cells; TK, tyrosine kinase; C11033, 2-propenamide, *N*-[4-[(3-chloro-4-fluorophenyl)amino]-7-[3-(4-morpholinyl)propoxy]-6-quinazoliny]-, dihydrochloride.

2002; Gottesman et al., 2002). MDR1 and MRP1 can transport a large variety of hydrophobic drugs, and MRP1 can also extrude anionic drugs or drug conjugates. The substrate specificity of ABCG2 partially overlaps with that of MDR1 and MRP1; that is, the transported compounds include mitoxantrone (MX), topotecan, flavopiridol, methotrexate, and Hoechst 33342 (Litman et al., 2001; Zhou et al., 2001; Volk et al., 2002).

The ABCG2 multidrug transporter is present in the placenta, stem cells, liver, small intestine, colon, lung, kidney, adrenal and sweat glands, and endothelia, suggesting its role in the protection/detoxification against xenobiotics (Litman et al., 2001; Maliepaard et al., 2001; Zhou et al., 2001; Cooray et al., 2002). Indeed, ABCG2 was shown to influence the absorption and secretion of topotecan (Jonker et al., 2000). ABCG2 overexpression was documented in several drug-resistant cell lines and tumors, which indicates its importance in the multidrug-resistant phenotype of cancer cells (Doyle et al., 1998; Brangi et al., 1999; Ross et al., 2000; Litman et al., 2001; Diestra et al., 2002).

Modulators of multidrug resistance ABC transporters are regarded as potential clinically applicable agents to inhibit cancer multidrug resistance, as well as to alter the absorption, tissue distribution, metabolism, and toxicity (ADME-Tox) parameters for various pharmacons (Fisher et al., 1996; Bakos et al., 2000). In our previous communication, we documented that several TKIs interacted with the human MDR1 and MRP1, and significantly inhibited their transport activities for other substrate drugs (Hegeudus et al., 2002). This modulatory property may make TKIs ideal compounds for use in combination with other anticancer drugs, allowing an effective penetration of various cytotoxic agents.

In the present work, we have analyzed the interactions of the three major multidrug resistance proteins, ABCG2, MDR1, and MRP1, with three TKIs (STI-571/Gleevec, ZD1839/Iressa, and EKI-785), already in large-scale pre-clinical and clinical trials. In these experiments we have used several enzyme- and cell-based test systems. We measured transport-related ABC-ATPase activity, which is significantly modified by the transported substrates or inhibitors (Sarkadi et al., 1992; Bakos et al., 1998; Ozvegy et al., 2001). Another assay system was to investigate the extrusion of fluorescent dyes from mammalian cells, expressing the respective transporter. In the case of ABCG2, we measured the extrusion of the Hoechst 33342 dye (Ozvegy et al., 2002), whereas for MDR1 and MRP1 function, we analyzed the inhibition of calcein accumulation (Homolya et al., 1993; Hollo et al., 1996). These studies were complemented with direct cell toxicity assays in human cell lines selectively expressing the respective transporter proteins and, by using mitoxantrone as a cytotoxic agent, extruded by all three multidrug transporters (Litman et al., 2001).

Our data indicate that ABCG2 shows a high-affinity interaction with the three TKIs examined, whereas interaction with the MDR1 and MRP1 proteins could only be observed at much higher TKI concentrations. These in vitro data may significantly help the evaluation of the drug resistance-modulatory effects of these TKIs, as well as to predict their ADME-Tox properties.

Materials and Methods

Expression of MDR1, MRP1, and ABCG2 (R482) in Insect Cells

Recombinant baculoviruses containing the respective cDNA were prepared as described previously (Muller et al., 1996; Bakos et al., 1998; Ozvegy et al., 2002). Sf9 (*Spodoptera frugiperda*) cells were cultured and infected with a baculovirus as described by Muller et al. (1996).

Membrane Preparation and Immunoblotting

Virus-infected Sf9 cells were harvested, and their membranes were isolated and stored at -80°C . The membrane protein concentrations were determined, as described by Sarkadi et al. (1992). Immunoblot detection was performed by the specific anti-MDR1 4077, anti-MRP1 R1, or anti-ABCG2 BXP-21 antibodies, respectively. Protein-antibody interaction was determined using the enhanced chemiluminescence technique (Amersham Biosciences UK Ltd., Little Chalfont, Buckinghamshire, UK) as described earlier (Bakos et al., 1998).

Membrane ATPase Measurements

ATPase activity was measured basically as described by Sarkadi et al. (1992), by determining the liberation of inorganic phosphate from ATP with a colorimetric reaction. The incubation media contained 40 mM 4-MOPS-Tris, pH 7.0, 50 mM KCl, 2 to 5 mM dithiothreitol, 0.1 to 0.5 mM EDTA, 4 to 5 mM sodium azide, 1 mM ouabain, 10 to 20 μg of membrane, and 3.3 to 4 mM MgATP. The figures represent the mean values of at least three independent experiments with duplicates.

Multidrug Transporter Assays in Mammalian Cells

For the investigation of the function of MDR1 and MRP1 in mammalian cells, we applied well characterized HL60/PLB cell lines, all closely related derivatives of a human myelomonocytic cell line. The drug-selected HL60-MDR1 and HL60-MRP1 (adriamycin) cells singularly express MDR1 and MRP1, respectively, at constant high levels (Hollo et al., 1996). For the investigation of the function of wild-type (R482) ABCG2 in mammalian cells, we applied retrovirally transduced HL60/PLB cells (PLB-ABCG2), further selected by a low concentration of mitoxantrone, as described by Ujhelly et al. (2003). All these cells were cultured in standard RPMI media supplemented with 10% fetal calf serum and 50 U/ml penicillin and streptomycin. A constant level of multidrug resistance protein expression was periodically monitored by immunoblotting and functional flow cytometry analysis. In the latter case, selective expression of the respective multidrug resistance transporters was examined by selective transporter inhibitors (e.g., MK571 for MRP1; verapamil, as a competitive inhibitor for MDR1; and Ko143 for ABCG2).

Fluorescent Dye Uptake. The calcein assay, used for the quantitative determination of multidrug transporter activity, was performed as described earlier (Homolya et al., 1993). In brief, fluorescence intensities were determined in a fluorescence spectrophotometer (LS 50B; Applied Biosystems, Foster City, CA) after a short in vitro incubation. Cultured and well characterized MDR1- or MRP1-expressing cells were incubated with the nonfluorescent calcein AM, and with the respective concentrations of the compounds to be examined. The increase in cellular fluorescence caused by the liberation of free calcein inside the cells was determined. MDR1- and/or MRP1-interactive compounds inhibit the outward transport of calcein AM, thus significantly increasing the rate of calcein accumulation. The increase in cellular fluorescence was determined in the presence of the compound (F_x), in the presence of 50 μM verapamil (or 10 μM MK571 for MRP1) completely inhibiting the transporter proteins (F_{100}), and in the absence of any inhibitor (F_0). To obtain the respective IC_{50} values for the TKIs, the inhibition values were calculated as $(F_x - F_0)/(F_{100} - F_0) \times 100$ by a computer-based evaluation protocol.

Accumulation of Hoechst 33342 dye was measured in a fluorescence spectrophotometer (LS 50B; Applied Biosystems) at 350 nm (excitation)/460 nm (emission), by using 5×10^5 cells in 2 ml of buffer A (120 mM NaCl, 5 mM KCl, 400 μ M MgCl₂, 40 μ M CaCl₂, 10 mM HEPES, 10 mM NaHCO₃, 10 mM glucose, and 5 mM Na₂HPO₄) solution. This dye becomes fluorescent only in a complex with DNA (Haugland, 1996), and the increase in cellular fluorescence reflects dye influx into the cells. In cells expressing the ABCG2 protein, dye accumulation is much slower than in the control cells (Ozvegy et al., 2002) and can be accelerated by compounds interfering with the ABCG2-dependent Hoechst dye extrusion. The intact control or ABCG2-expressing HL60/PLB cells were preincubated at 37°C in buffer A for 4 min and further incubated with 1 μ M Hoechst dye for 10 min. The compounds examined subsequently were added to the cells and the altered rate of accumulation was measured for another 10 min. For maximum inhibition of the ABCG2 protein, 1 μ M Ko143 was applied in each experiment, and maximum Hoechst dye binding was determined in the presence of digitonin (see Ozvegy et al., 2002 and Fig. 4). The inhibition values were calculated as in the case of calcein measurements. Figures show data compiled from at least four independent measurements.

Cytotoxicity Assays. Cytotoxicity assays were carried out by using the HL60/PLB human myelomonocytic parent and drug-resistant cell lines [HL60-MDR1, HL60-MRP1 (adriamycin), and HL60/PLB-ABCG2; see above]. The assay was performed in 24-well plates, each well containing an initial cell number of 10^5 cells, in a final volume of 1 ml. Cell culturing was performed in the presence of the agents indicated in figure legends for 120 h at 37°C in 5% CO₂, and both living and dead cells (stained by propidium iodide) were counted in a FACSCalibur cytometer (BD Biosciences, San Jose, CA). Figures represent data obtained from at least two independent experiments.

Mitoxantrone Accumulation Assay. HL60-MDR1, HL60-MRP1, HL60/PLB-ABCG2, and parental HL60 cells were suspended in buffer A (see above). Aliquots of the suspension containing 3×10^5 cells were incubated with 0.5 μ M MX with or without the addition of a specific inhibitor of ABCG2, MDR1 or MRP1, or TKIs (EKI-785, ZD1839, STI-571), in concentrations indicated in the figure legends. After an incubation for 60 min at 37°C, the cells were washed and resuspended in ice-cold HPMI. Cellular MX fluorescence was determined at excitation and emission wavelengths of 635 and 661 ± 16 nm, respectively, in a FACSCalibur cytometer as above. Dead cells were excluded based on propidium iodide staining.

TK Inhibitors Investigated in the Present Study

The tyrosine kinase inhibitors used in these experiment were synthesized and characterized in the laboratory of author G. K. Figure 1 shows the structural formulas for the TKIs examined in the present experiments.

Results

ATPase Activity Measurements in Isolated Insect Cell Membranes. We have examined the effects of TKIs on the transport-related, drug-stimulated ATPase activity of the human ABCG2, as well as of MDR1 and MRP1 multidrug transporter proteins, expressed in isolated insect cell (Sf9) membranes. It has been documented that the stimulation of the multidrug transporter ATPase activity and its drug concentration dependence closely correlates with the respective transport activity of these proteins (Sarkadi et al., 1992; Bakos et al., 2000), and transport inhibitors also inhibit the ATPase activity.

The MDR1-ATPase can be stimulated by hydrophobic substrate drugs (Sarkadi et al., 1992; Muller et al., 1996), whereas the MRP1-ATPase is stimulated by various glutathione-conjugates (GS-X), glucuronate-conjugates, and

anionic drugs (Bakos et al., 2000). The basal ATPase activity of ABCG2 is relatively high, with only a small drug-stimulation effect, whereas several transported compounds are inhibitory (Ozvegy et al., 2001, 2002). Therefore, the presence of endogenous (probably lipid-like) substrate of ABCG2 in the membranes has been suggested (Ozvegy et al., 2001, 2002).

In the experiments presented in Fig. 2, we have examined the effects of the three TKIs on the ATPase activity in isolated membranes expressing the human ABCG2 protein. We compared the effects of the TKIs to those of a specific, high-affinity inhibitor of ABCG2, Ko143 (Allen et al., 2002), and verapamil, which is not a substrate of this protein.

As shown in Fig. 2, the vanadate-sensitive ATPase activity of ABCG2-containing isolated Sf9 cell membranes was relatively high, approximately 75 nmol/mg membrane protein/

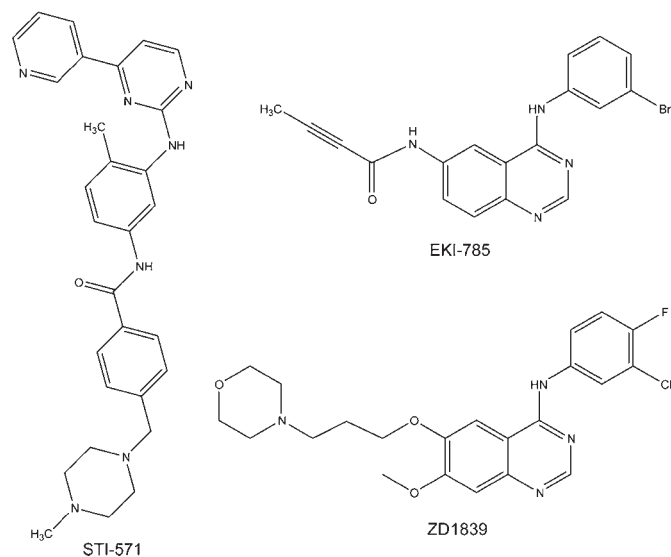


Fig. 1. Chemical formulas of the TKIs (ZD1839, STI-571, and EKI-785) examined in this article.

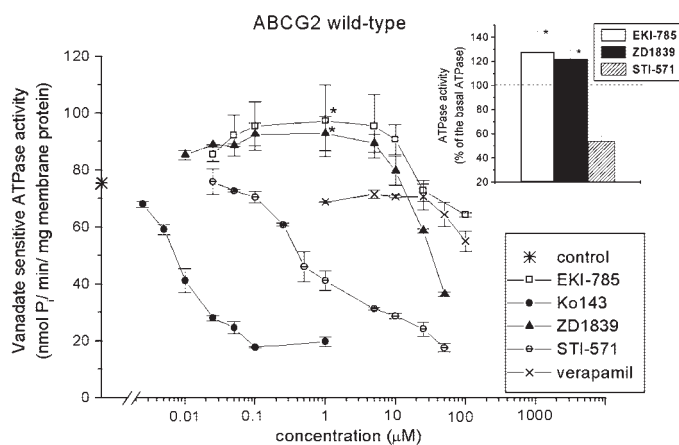


Fig. 2. Concentration dependence of the effects of the TKIs, Ko143, and verapamil, on the human ABCG2-ATPase activity in isolated membrane preparations. Inset, relative effects of the TKIs at 1 μ M concentrations, compared with the basal ATPase activity. Vanadate-sensitive ATPase activity in isolated Sf9 cell membranes, containing human ABCG2, and the drug effects were measured in three independent experiments with duplicates, as described under *Materials and Methods*. Control represents the ATPase activity measured in the absence of added compounds. *, Student's *t* test, $p < 0.05$.

min, largely exceeding that of a control, β -galactosidase-expressing Sf9 cell membrane preparation (about 6–8 nmol/mg membrane protein/min; not shown here). This ATPase was effectively inhibited by nanomolar concentrations (half-maximal inhibition observed at about 8–9 nM) of the specific inhibitor of ABCG2, Ko143 (Allen et al., 2002). In contrast, verapamil, a substrate and/or inhibitor of both MDR1 and MRP1, inhibited the ABCG2-ATPase activity only from the 50 μ M concentration.

The TKIs examined in these experiments had considerably different effects on the ABCG2-ATPase. Low concentrations of EKI-785 and ZD1839 produced a small, but statistically significant ($p < 0.05$) stimulation of the ABCG2 ATPase activity (see Fig. 2 inset for 1 μ M concentrations of each compound). This effect reached its maximum between 0.1 and 1 μ M TKI concentrations, whereas higher EKI-785 or, even more effectively, ZD1839 concentrations were inhibitory. In contrast, STI-571 caused a strong inhibition even at low concentrations, with a half-maximal effect at about 0.5 μ M. These data indicate a high-affinity interaction of ABCG2 with these TKIs, also suggesting that ZD1839 and EKI-785 may be actively transported substrates of this protein. In several cases it has been found that higher substrate concentrations inhibited the ATPase activity of both MDR1 and MRP1 (Sarkadi et al., 1992; Bakos et al., 2000).

Regarding the effects of TKIs on the MDR1 and MRP1 protein, we have already reported that STI-571 stimulated the MDR1-ATPase activity in the micromolar concentration range, whereas EKI-785 had no major effect in this assay. In contrast, both STI-571 and EKI-785 effectively inhibited the verapamil-activated MDR1-ATPase activity at concentrations between 5 and 20 μ M (Hegedus et al., 2002). In the case of the MRP1-ATPase, none of these compounds stimulated this activity. The NEM-GS-stimulated MRP1-ATPase was inhibited by EKI-785 in the micromolar range (50% inhibition at about 10 μ M), whereas STI-571 had a smaller effect and only at higher concentrations (50% inhibition at higher than 100 μ M).

In the following experiments, we have examined the effects of ZD1839 on the ATPase activity of the MDR1 and MRP1 proteins. As documented in Fig. 3A, ZD1839 significantly stimulated the MDR1-ATPase, with a half-maximal effect at about 4 μ M, although this stimulation reached only about 50% of that produced by verapamil, and a relative inhibitory effect was seen above 20 μ M ZD1839 concentrations. ZD1839 had no measurable effect on the ATPase activity of MRP1 in the isolated membranes (Fig. 3A).

To study a potential inhibitory effect of ZD1839 on MDR1 and MRP1, its effect was also measured on the maximally stimulated transporters (Fig. 3B). In the case of the MDR1-ATPase, this maximum stimulation was achieved by 50 μ M verapamil, whereas MRP1-ATPase activity was stimulated by a 6 mM concentration of the glutathione-conjugate, NEM-GS. In these experiments ZD1839 was effective only at concentrations between 10 and 100 μ M, and its inhibitory effect was similar in the case of both MDR1 and MRP1 (Fig. 3B). All these data suggest that the examined TKIs at low micromolar concentrations show a much more pronounced interaction with the ABCG2 protein than with MDR1 or MRP1.

Fluorescent Dye Extrusion Studies. In the following experiments we applied a whole-cell screening system for studying the interactions of TKIs with the multidrug trans-

porter proteins. In this study we used the human HL60/PLB cells, expressing large amounts of the respective multidrug transporters (see *Materials and Methods*).

As described in the literature (Zhou et al., 2001; Ozvegy et al., 2002), in cells expressing the ABCG2 protein, a decreased rate of accumulation of the Hoechst 33342 dye directly reflects the activity of the ABCG2 protein, and ABCG2 inhibition results in a rapid increase in the rate of dye accumulation.

In the present study, we measured the fluorescent dye accumulation directly in intact PLB cells by using a spectrofluorometer. Because Hoechst 33342 becomes fluorescent only in a complex with DNA, the increase in cellular fluorescence directly correlates with dye influx and DNA binding within the cells. As documented in Fig. 4, in ABCG2-expressing cells, the dye accumulation is relatively slow and is accelerated by compounds interfering with the Hoechst dye extrusion activity of ABCG2. The initial rapid dye uptake, as shown in Fig. 4, reflects a rapid Hoechst permeation and DNA-binding in damaged cells, whereas the following slow

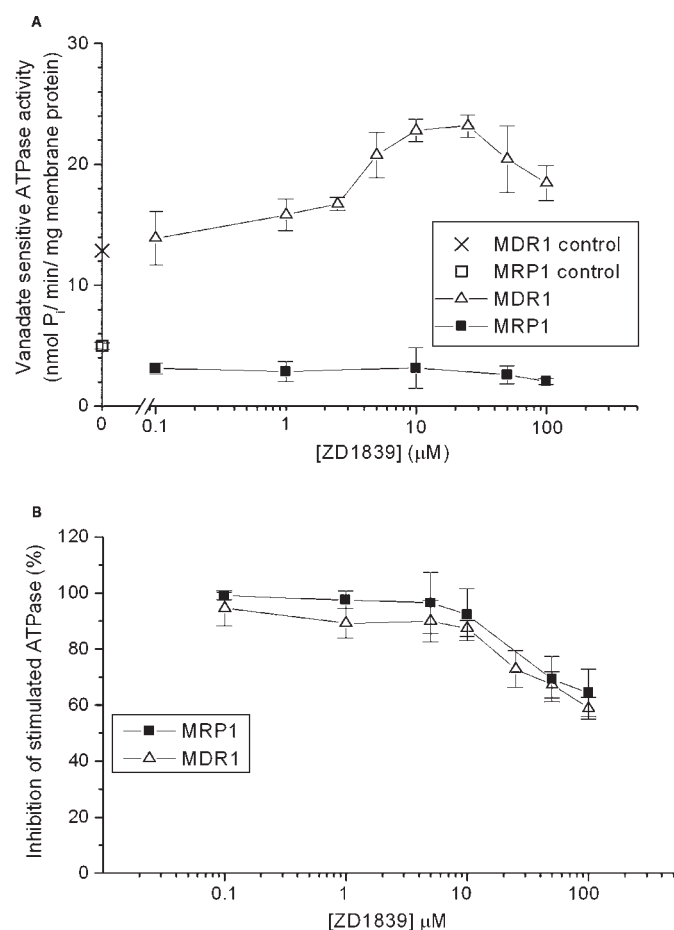


Fig. 3. Effect of ZD1839 on the human MDR1- and MRP1-ATPase activities in isolated membrane preparations. A, modulation of the vanadate-sensitive ATPase activity by ZD1839 in MDR1- or MRP1-expressing isolated Sf9 cell membranes. B, relative inhibition of the maximally stimulated MDR1- and MRP1-ATPase activities by ZD1839. The data are presented as relative values, compared with 100% activation obtained with 50 μ M verapamil in the case of MDR1, and in the presence of 6 mM GS-NEM in the case of MRP1. Controls represent the ATPase activity measured in the absence of added compounds. Vanadate-sensitive ATPase activity in isolated Sf9 cell membranes, containing human MDR1 or MRP1, and the effects of ZD1839 were measured in three independent experiments with duplicates, as described under *Materials and Methods*.

increase of fluorescence reaches a linear phase. This slow, linear phase is absent in the control HL60 or PLB cells (data not shown) and is caused by the function of the overexpressed ABCG2 multidrug transporter in the cell membrane. When a compound interfering with ABCG2-dependent dye extrusion is added to the cells, the rate of Hoechst dye accumulation increases.

For maximum inhibition of the ABCG2 protein, 1 μM Ko143 is applied, whereas the maximum level of cellular Hoechst dye binding is determined by the addition of digitonin. Maximum dye loading achieved in the presence of this membrane-permeabilizing agent is much higher than that reached during the accumulation phase; thus a possible dye saturation effect can be excluded. By using this sensitive assay system, it is possible to analyze ABCG2-Hoechst dye transport inhibition, but the system does not reveal the competitive or noncompetitive nature of such an inhibition (Ozvegy et al., 2002).

As documented in Fig. 5 by the various compounds examined, inhibition of Hoechst dye extrusion could be achieved at concentrations varying by 6 orders of magnitude. The specific ABCG2 inhibitor, Ko143 (Allen et al., 2002), a derivative of the fungal toxin fumitremorgin C, inhibited dye extrusion at low nanomolar concentrations, with a half-maximal effect at about 5 nM. In contrast, verapamil had no significant inhibitory effect up to 10 μM , and half-maximal inhibition of ABCG2 function was achieved at higher than 50 μM verapamil.

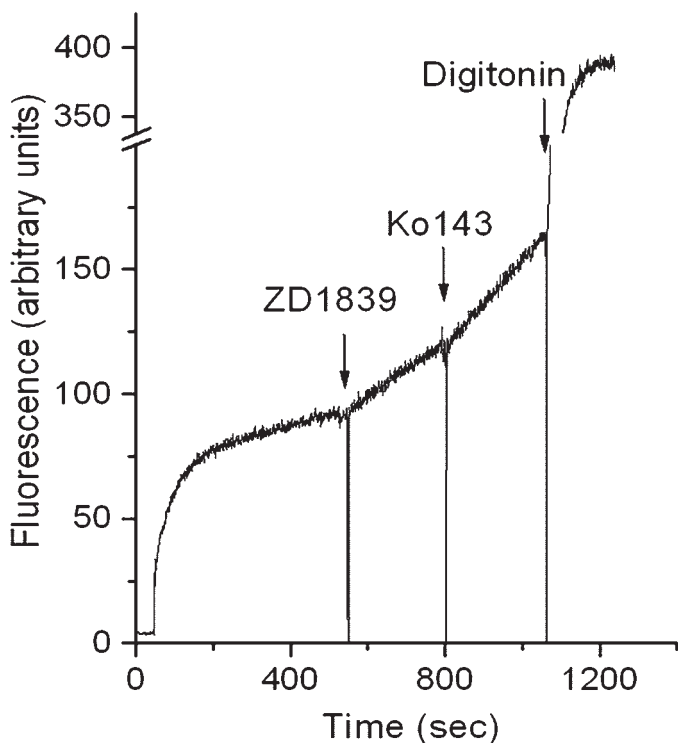


Fig. 4. Measurement of Hoechst dye uptake in a spectrofluorometry assay. Intact PLB-ABCG2 cells were preincubated for 5 min at 37°C and then further incubated at the same temperature under continuous gentle stirring. Hoechst 33342 dye (1 μM) was added at 20 s of the measurement period, and then 0.2 μM ZD1839, 1 μM Ko143, and 10 μM digitonin were added at the times indicated. Fluorescence increase is caused by the binding of Hoechst 33342 to cellular DNA. Maximum dye influx rate was estimated at the fully inhibited transporter, in the presence of Ko143. The figure shows one representative experiment.

The three TKIs examined here had a strong inhibitory effect on ABCG2-dependent dye extrusion at relatively low concentrations. Half-maximal inhibitory effects were observed at about 0.4 μM ZD1839, 0.2 μM EKI-785, and 0.9 μM STI-571. These findings indicate that the TKIs examined bind to ABCG2 and compete with Hoechst at very low concentrations, suggesting a high-affinity interaction of ABCG2 with these TKIs.

In the following experiments, the interaction of the TKIs with MDR1 and MRP1 in intact cells was analyzed by the calcein assay system (Homolya et al., 1993; Hollo et al., 1996). The nonfluorescent, hydrophobic calcein AM rapidly enters into the cells and is cleaved by nonspecific esterases to yield the fluorescent, cell-retained, free calcein. When cells expressing the multidrug transporters MDR1 or MRP1 are incubated with calcein AM, as a result of an active dye extrusion, free calcein accumulation is slow. Agents that interact with the multidrug resistance proteins inhibit dye extrusion and greatly accelerate fluorescent calcein accumulation. The concentration-dependence of this transport inhibition reflects the level of drug interaction with the drug pump proteins (see *Materials and Methods*). Again, competitive or direct inhibition of the transporters cannot be distinguished in this system.

We have already documented (Hegedus et al., 2002) that the TKI inhibitors STI-571 and EKI-785 inhibited calcein AM extrusion by MDR1 at micromolar (half-maximally at about 8–30 μM) concentrations. EKI-785 also inhibited MRP1-dependent transport at micromolar concentrations (5–10 μM), whereas this transport was inhibited only at relatively high concentrations (above 20 μM) by STI-571.

Figure 6 shows the effects of ZD1839 on calcein extrusion from MDR1- and MRP1-expressing HL60 cells, respectively. As shown, calcein AM extrusion by both MDR1 and MRP1 was inhibited by micromolar concentrations of ZD1839, with an approximately half-maximal effect at ZD1839 concentrations of about 4 to 5 μM . The effective concentration of ZD1839 in the calcein assay is slightly different from that measured in the ATPase assay, when inhibition of verapamil- or NEM-GS-activated ATPase activity was measured. The two assays represent the result of the competition between

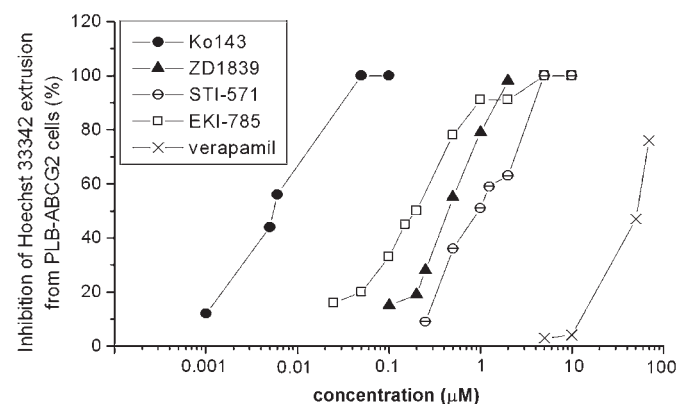


Fig. 5. Inhibition of ABCG2-dependent Hoechst 33342 dye extrusion in PLB-ABCG2 cells by various concentrations of TKIs, Ko143, and verapamil. The relative inhibition of dye extrusion was estimated as described under *Materials and Methods*. Data were compiled from at least four independent measurements for each compound. Error bars did not exceed 5 to 10% of the values.

ZD1839 and calcein AM, or ZD1839 and verapamil or NEMGS, respectively.

Cellular Drug Toxicity Assays. To examine the direct effect of TKIs on cellular drug resistance, we applied the HL60/PLB cell lines expressing the respective multidrug transporters (see above) in a drug cytotoxicity assay. Cells were cultured in standard media on microwell plates in the presence or absence of different TKI concentrations. After 120 h of incubation, the living and dead cells were counted by flow cytometry analysis using propidium iodide staining (see *Materials and Methods*). In the presentation of these experiments we show the relative cell numbers, compared with those found in the absence of TKIs.

As shown in Fig. 7, A, the addition of up to 5 μM ZD1839 to the HL60/PLB cells, either in the case of control cells or those expressing ABCG2, MDR1, or MRP1, had no significant effect on cell growth and survival in this assay. We found a similar lack of effect of STI-571 (up to 5 μM) and EKI-785 (up to 3 μM) on the growth of these cell types. It is noteworthy that cell growth was also not significantly affected by Ko143 (up to 1 μM) and verapamil (up to 10 μM ; except for a slight inhibition of cell growth in the HL60-MDR1 cells) in the cell lines examined (data not shown).

As shown in Fig. 7, B to E, the addition of 25 nM MX caused a complete growth inhibition and cell death in the parental HL60/PLB cells, whereas this MX concentration induced only a small inhibition in cell growth and survival in the ABCG2-, MDR1-, or MRP1-expressing cells (the number of live cells, compared with that in the absence of MX, was 80–90% in the ABCG2-expressing cells, whereas it was 90–100% in the MDR1 and in the MRP1 cells; not shown).

As shown in Fig. 7B, the addition of ZD1839 in the presence of 25 nM MX caused a major inhibition in cell growth in the ABCG2-expressing cells lines, and this inhibitory effect reached 50% at about 0.2 μM ZD1839. In contrast, in the MDR1 cells, a 50% inhibition could be obtained at higher than 10 μM ZD1839 (data not shown), and in the case of MRP1 cells, only a slight inhibition was caused by 10 μM ZD1839 (data not shown). Thus, in accordance with the ATPase and dye extrusion results, ZD1839 was a much more effective chemosensitizing agent in the case of ABCG2 than in the case of MDR1 or MRP1.

Figure 7, C and D, shows the effects of STI-571 and EKI-

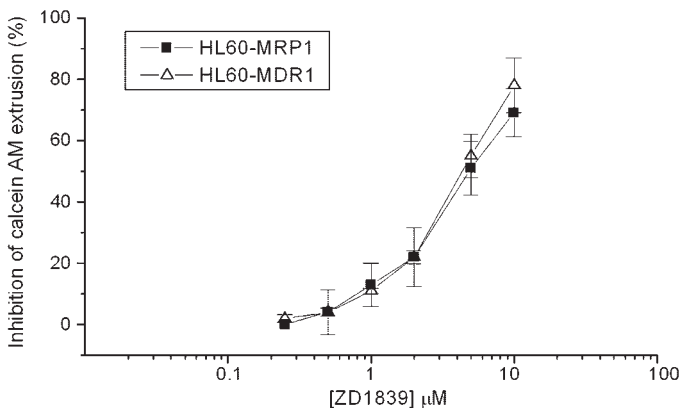


Fig. 6. Inhibition of calcein AM extrusion by the human MDR1 and MRP1 proteins by ZD1839. Calcein AM extrusion was measured in HL60-MDR1 and HL60-MRP1 cells, as described under *Materials and Methods*. Data were compiled from at least four independent measurements for each transporter.

785 in the same cellular toxicity assay system. In the concentration range presented, neither of these TKIs had a measurable effect on the cell growth in the parental or multidrug-resistant HL60/PLB cells. However, a chemosensitizing effect was observed in the ABCG2-expressing cells, in the presence of 25 nM mitoxantrone, by both of these TKIs. As documented, STI-571 caused a half-maximal growth inhibition at 0.2 μM in the ABCG2-expressing cells, whereas at 5 μM STI-571, cell growth was inhibited by about 20% in MDR1-expressing cells and uninhibited in the MRP1-expressing cells. In the case of EKI-785 (Fig. 7D), a similar finding was obtained for the ABCG2-expressing cells (50% inhibition at 0.35 μM). In the case of MDR1-expressing cells, the combination of 0.5 to 1 μM EKI-785 and 25 nM MX actually increased cell growth by approximately 60% and was inhibitory only above 2.5 μM . There was no significant effect of MX + EKI-785 in the MRP1-expressing HL60 cells in this concentration range.

To compare the effect of TKIs to those of Ko143, a specific, high-affinity inhibitor of ABCG2, we have performed similar cell toxicity assays with this compound as well. As documented in Fig. 7E, low concentrations of Ko143 induced a selective toxicity of 25 nM mitoxantrone in the ABCG2-expressing cells. The Ko143 concentration causing 50% growth arrest was about 6 nM, in agreement with the concentration causing 50% inhibition of Hoechst dye extrusion by ABCG2 (see Fig. 5). Again, Ko143 had no significant effect on cell growth of MDR1- or MRP1-expressing cells, even in the presence of 25 nM mitoxantrone (a slight stimulation of the growth of MDR1-expressing cells was observed at 25 nM MX + 10–100 nM Ko143).

As shown in Fig. 7F, similar experiments were carried out using verapamil as a chemosensitizer for MDR1 and (although less effectively) of MRP1; in contrast, verapamil is not an effective modulator of the ABCG2 function (see Figs. 2 and 3). MK571, a specific inhibitor of MRP1, could not be applied in these cytotoxicity assays, because of the rapid loss of MK571 activity under our cell culturing conditions.

As shown, verapamil, up to 10 μM , did not cause a growth inhibition in HL60/PLB cells, including the cell lines expressing the multidrug transporter proteins (data not shown). A slight inhibition of cell growth, approaching a 30% decrease in the HL60-MDR1 cells, was observed with verapamil, which could be caused by the continuous transport of verapamil and a slight ATP-depletion in these cells (data not shown). In contrast to the TKIs or Ko143, verapamil (with 25 nM mitoxantrone) was effective in the growth inhibition of the ABCG2-expressing cells only above 5 to 10 μM concentrations. A strong growth arrest by the combination of verapamil and 25 nM MX was observed in the HL60-MDR1 cells, and a less pronounced effect in the HL60-MRP1 cells (MRP1 has been shown to be less sensitive to verapamil in several studies; see Hollo et al., 1996).

All the cytotoxicity experiments presented in Fig. 7 document the preferential modulation of the ABCG2-dependent MX resistance by Ko143 and by the TKIs, compared with verapamil, whereas the opposite effects were observed in the MDR1- and MRP1-expressing HL60 tumor cells.

Mitoxantrone Transport Experiments. In the cytotoxicity assay, we documented that the TKIs examined greatly increased the cytotoxic effect of mitoxantrone. This is most probably caused by the inhibition of the MX transport activ-

ity of ABCG2, MDR1, or MRP1. Mitoxantrone is a fluorescent compound; therefore, its accumulation in cells can be directly monitored by flow cytometry (Robey et al., 2001). We used the above described HL60/PLB cells, overexpressing ABCG2, MDR1, or MRP1, respectively, to determine mitoxantrone accumulation with or without the addition of TKIs or specific inhibitors (Ko143, verapamil, or MK571), by using a FACS-Calibur cytometer.

Figure 8 shows that after 60 min of incubation with 0.5 μM mitoxantrone, the ABCG2-expressing cells (Fig. 8B) had a much lower level of mitoxantrone accumulation than did the related control cells (Fig. 8A). This decreased accumulation is caused by an active extrusion of mitoxantrone by ABCG2, as indicated by the effect of the ABCG2 inhibitor, Ko143, which increased cellular MX fluorescence up to the level observed in the control cells. The addition of 1 μM ZD1839 (Fig. 8B; and

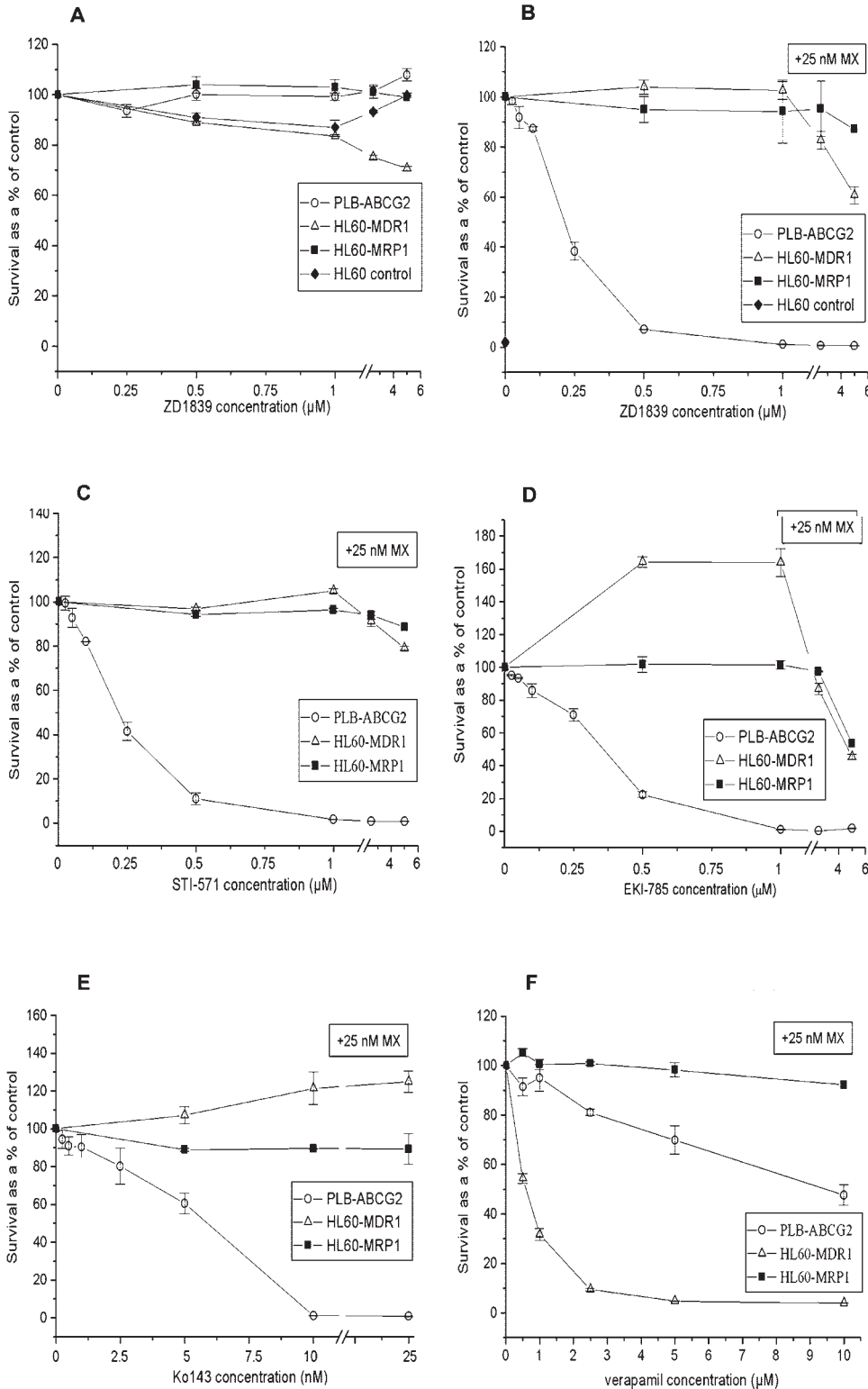


Fig. 7. Combined cellular toxicity assay performed with the TKIs in parental and multidrug-resistant HL60/PLB cell lines. A, effect of ZD1839 on the survival of PLB-ABCG2, HL60-MDR1, HL60-MRP1, and HL60/PLB (control) cells. B, combined effects of various ZD1839 concentrations and 25 nM mitoxantrone (MX) on the survival of HL60/PLB, PLB-ABCG2, HL60-MDR1, and HL60-MRP1 cells. C, combined effects of various STI-571 concentrations and 25 nM mitoxantrone (MX) on the survival of PLB-ABCG2, HL60-MDR1, and HL60-MRP1 cells. D, combined effects of various EKI-785 concentrations and 25 nM mitoxantrone (MX) on the survival of PLB-ABCG2, HL60-MDR1, and HL60-MRP1 cells. E, combined effects of various Ko143 concentrations and 25 nM mitoxantrone (MX) on the survival of PLB-ABCG2, HL60-MDR1, and HL60-MRP1 cells. F, combined effects of various verapamil concentrations and 25 nM mitoxantrone (MX) on the survival of PLB-ABCG2, HL60-MDR1, and HL60-MRP1 cells. Figures represent data obtained from at least two independent experiments.

also of 1 μM EKI-785, or 2 μM STI-571, not shown in the figure) caused a significant increase in MX accumulation in the ABCG2-expressing cells, whereas these TKIs caused no further increase of MX fluorescence in the control cells (Fig. 8A). A significant, concentration-dependent increase in MX accumulation could be observed between 0.2 and 2 μM ZD1839 in these experiments (data not shown). These data strongly suggest that an increased cytotoxicity of MX by the TKIs and Ko143 in the ABCG2-expressing PLB cells was caused by an effective modulation of mitoxantrone extrusion from these cells.

Under the same experimental conditions, the HL60 cells expressing MDR1 (Fig. 8C) or MRP1 (Fig. 8D) showed somewhat greater MX accumulation than did cells with ABCG2, but significantly lower accumulation than did the HL60 control cells. When verapamil (MDR1 cells, Fig. 8C) or MK571 (MRP1 cells, Fig. 8D) was also added, cellular fluorescence of MX increased up to the level observed in the HL60 control cells. Neither verapamil nor MK571 caused an increased MX accumulation in the HL60 control cells. These data indicate that both MDR1 and MRP1 can transport MX, although probably with lower effectiveness than ABCG2.

When the effects of ZD1839, EKI-785, and STI-571 were examined in the MDR1- and MRP1-expressing cells, respectively, we found a much less significant effect of these agents than in the case of ABCG2-expressing cells. In fact, TKI concentrations above 5 to 10 μM were required to obtain any increase in MX accumulation in MDR1- or MRP1-expressing cells. As shown in Fig. 8, C and D, 10 μM ZD1839 caused a detectable increase in MX accumulation both in the MDR1- and MRP1-expressing cells, but this effect was still much less than that observed in the presence of verapamil (MDR1) or MK571 (MRP1). These experimental results are in harmony

with the cytotoxicity assays, indicating a lower-affinity interaction of the TKIs examined with MDR1 or MRP1, compared with that with ABCG2.

Discussion

The application of specific TKIs is a rapidly progressing/expanding area of promising cancer therapy efforts. STI-571 (Gleevec, imatinib), which has been introduced as a selective inhibitor of the tyrosine kinase Abl and its unregulated version (Bcr-Abl), causative in the development of chronic myeloid leukemia, was found to be highly effective in these diseases and rapidly passed clinical trials to reach approved applications. Moreover, because of its inhibitory effect on signaling through platelet-derived growth factor receptor and c-Kit, this compound is also potentially effective in the treatment of cancers involving these deregulated kinases (Heinrich et al., 2000; Joensuu et al., 2001; van Oosterom et al., 2002), and clinical trials have been initiated in these directions.

A number of erythroblastic leukemia viral/EGFR/human estrogen receptor family receptor tyrosine kinase inhibitors have also reached various phases of clinical or preclinical trials, and these include the EGFR inhibitor compound ZD1839 (Iressa, gefitinib) and its relatively close structural relative, the irreversible TK inhibitor EKI-785 (Sweeney et al., 1999; Herbst, 2002; Roberts et al., 2002). The ADME-Tox properties of these TKIs are important points in their clinical application, which should be preferentially addressed during the phase of preclinical studies. All these TKIs are essentially hydrophobic compounds, which have to pass the cell membrane barrier to reach their intracellular target molecules. Therefore, their interactions with membrane transporters may be crucial in effectiveness, as well as in their absorption and tissue distribution.

Large hydrophobic molecules, such as the TKIs, have a potential to interact with the so-called multidrug resistance ABC proteins. These are ATP-dependent primary active transporters, which extrude a large variety of chemically unrelated, large, and at least partially hydrophobic compounds from the cells. When overexpressed in tumor cells, some of these proteins, especially MDR1, MRP1, and ABCG2, cause clinical multidrug resistance in cytotoxic therapy. However, these proteins also play important physiological roles, e.g., in modulating the transport properties and secretory functions of the liver and kidney, or modulating penetration of various compounds in the intestine or the blood-brain barrier. The transported substrates of the three major multidrug transporters are wide and somewhat overlapping; all of them can transport hydrophobic drugs, and MRP1 and ABCG2 may also extrude anionic drugs or drug conjugates (Bakos et al., 2000; Bates et al., 2001; Litman et al., 2001).

ABCG2 is a recently recognized drug transporter, which has been shown to extrude cytotoxic agents, e.g., mitoxantrone, topotecan, flavopiridol, and methotrexate, when overexpressed in various tumor tissues (Maliapaard et al., 1999; Litman et al., 2001; Robey et al., 2001; Volk et al., 2002). ABCG2 is abundantly expressed physiologically in the placenta, stem cells, liver, and intestine. Expression of ABCG2 has also been reported in the lung, kidney, adrenal glands, and endothelia of veins and capillaries (Litman et al., 2001; Maliapaard et al., 2001; Zhou et al., 2001; Cooray et al., 2002).

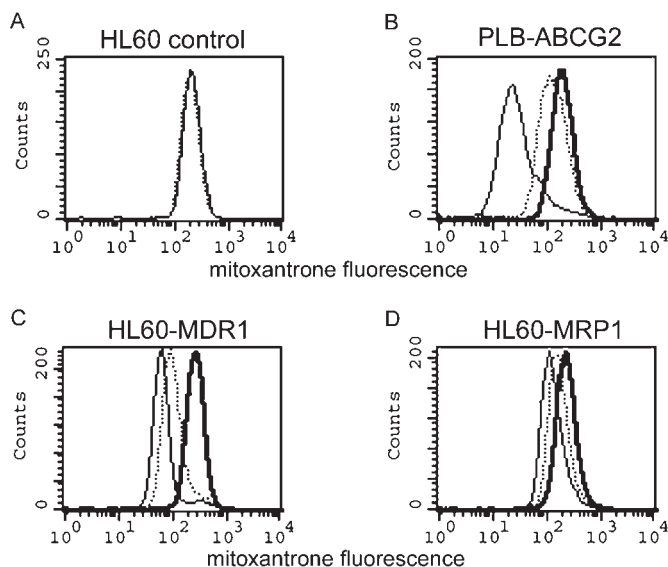


Fig. 8. Effect of TKIs on mitoxantrone accumulation in cells expressing ABCG2, MDR1, and MRP1, respectively. Parental HL60 (control), PLB-ABCG2, HL60-MDR1, and HL60-MRP1 cells were incubated with 0.5 μM MX without (solid line) or with the addition of specific inhibitors (heavy solid line) or ZD1839 (dotted line). A, HL60 control cells with MX and 10 μM ZD1839; B, ABCG2 with 1 μM Ko143 or 1 μM ZD1839; C, MDR1 with 50 μM verapamil or 10 μM ZD1839; D, MRP1 with 10 μM MK571 or 10 μM ZD1839. Cellular MX fluorescence was determined as described under *Materials and Methods*. The assay was repeated three times; the histograms show data from a representative experiment.

In the present experiments we have analyzed the interactions of various TKIs with the three major multidrug resistance transporters, the classical P-glycoprotein (MDR1), with MRP1 and the relatively newly recognized transporter, ABCG2 (ABCP/MXR/BCRP). These proteins are involved in cancer multidrug resistance; thus, the application of TKIs, which have to reach their intracellular targets, may be significantly modified by the presence of these transporter proteins in the cell membrane. On the other hand, the TKI interactions with the respective multidrug transporters may have a significant drug resistance-modulatory effect during combination chemotherapy. We found that in several *in vitro* assay systems, STI-571 (Gleevec), ZD1839 (Iressa), and EKI-785 interacted with ABCG2 at submicromolar concentrations, whereas the other multidrug transporters, MDR1 and MRP1, were much less sensitive to these agents.

When measuring multidrug transporter ATPase activity in isolated membranes, low concentrations of these TKIs selectively modulated ABCG2-ATPase activity. Moreover, in 0.1 to 1 μM concentrations, ZD1839 and EKI-785 significantly stimulated, whereas STI-571 only inhibited, this ATPase activity. The activation of ABCG2-ATPase at low concentrations of ZD1839 and EKI-785, based on earlier studies with other multidrug transporter ATPases, suggests that these agents are actually transported substrates of the ABCG2 multidrug transporter (Sarkadi et al., 1992; Bakos et al., 2000). To support such a transported substrate-like interaction, we have initiated both vesicular and whole-cell transport experiments, although no decisive data is yet available. At higher TKI concentrations, a strong inhibition of the multidrug transporters was observed in each case. Such an effect has already been observed for several substrate drugs for the various multidrug transporters and is probably caused by a less efficient dissociation of these compounds at the off-site of the transporters (Sarkadi et al., 1994).

Membrane ATPase activity of MRP1 was hardly affected by any of the TKIs examined, whereas ZD1839, similar to STI-571 (Hegedus et al., 2002), activated the MDR1 ATPase, but only at 5 to 15 μM concentrations. ZD1839 in concentrations above 10 μM inhibited both maximally stimulated MDR1 and MRP1 ATPase activities. Thus, these ATPase experiments suggested a preferential interaction of all the ZD1839, STI-571, and EKI-785 with the ABCG2 transporter, compared with their interaction with MDR1 or MRP1.

In the following experiments, we have documented that the three TKIs examined preferentially inhibited ABCG2-dependent active fluorescent dye extrusion. For studying the pump activity of MDR1 and MRP1, we used the calcein accumulation assay, whereas for examining the transport function of ABCG2, we used the Hoechst dye extrusion assay. In this latter case, we documented that, by measuring Hoechst dye fluorescence increase in cells in a fluorometry assay, the inhibitory action of various compounds could be successfully estimated. Because the changes in the rate of dye accumulation can be well measured, and the saturation of the dye uptake is only at relatively high values, this assay provides an efficient tool for such drug interaction studies.

The Hoechst 33342 dye is also efficiently extruded by the MDR1 protein, whereas it is not transported by MRP1 (Litman et al., 2001). In experiments not documented here, we have also studied the relative efficiency of ZD1839 to block Hoechst dye extrusion in MDR1- versus ABCG2-expressing

HL60 cells. These experiments indicated that ZD1839 was more effective at much lower concentrations for the ABCG2-dependent Hoechst transport (50% inhibition at about 0.4 μM) than for the Hoechst extrusion caused by MDR1 expression (50% inhibition at about 5 μM ZD1839).

All these dye transport assays emphasize the high-affinity interaction of TKIs with the ABCG2 transporter. However, these assays do not reveal the competitive or noncompetitive nature of these interactions; thus, a potential TKI extrusion by ABCG2 and a direct TKI inhibition of the transporter both appear as inhibition of dye extrusion.

We have also performed detailed drug resistance assays by using cell lines selectively expressing the various multidrug transporters. In cells expressing ABCG2, all three TKIs greatly increased the cytotoxicity of low concentrations (25 nM) of mitoxantrone, which was ineffective in this cell line without these modulating compounds. A selective inhibition of ABCG2 by Ko143 in nanomolar concentrations produced a similar drug sensitivity increase, whereas higher verapamil concentrations had to be applied to modulate MX sensitivity in ABCG2-expressing cells.

Cells expressing MDR1 or MRP1 were also resistant against 25 nM mitoxantrone, and TKIs caused a decrease in this resistance. However, significantly higher concentrations of the TKIs were needed to inhibit the MX resistance in cells expressing these multidrug transporters. When the effective inhibitor verapamil (although more effective for MDR1 than for MRP1) was added, a modulation of MX toxicity that could be well measured was observed. Unfortunately, the effect of the selective MRP1 inhibitor MK571 could not be assessed, because this inhibitor rapidly lost its activity under the cytotoxicity assay conditions (data not shown). In cells expressing MDR1, EKI-785 in low concentrations caused a measurable increase in cell growth. We do not have a ready explanation for this finding, but EKI-785 competition with mitoxantrone may decrease ATP hydrolysis by MDR1, saving cellular ATP, or, alternatively, EKI-785 and mitoxantrone may be cotransported and/or may stimulate the transport of each other. In fact, in MDR1-expressing HL60 cells, the addition of low (1–5 μM) EKI-785 concentrations decreased mitoxantrone accumulation, indicating an increased MX transport activity by MDR1 (data not shown).

To directly examine MX extrusion in cell lines used in the drug resistance assays, we have also determined intracellular mitoxantrone fluorescence by flow cytometry. The findings in these assays closely correlated with those of the cytotoxicity measurements: MX accumulation in PLB-ABCG2 cells was greatly increased by low micromolar concentrations of the TKIs examined. In contrast, in cells expressing MDR1 or MRP1, which also showed a significant MX extrusion, these TKIs were much less effective in increasing MX accumulation.

The various assays in this study investigated different aspects of interactions between ABC multidrug transporters and TKIs. The stimulation or inhibition of the transporter ATPase activity represent direct interactions between TKIs and ABC transporters, whereas the inhibition of a fluorescent dye extrusion or the modulation of mitoxantrone cytotoxicity shows the net result of possible combined cellular interactions. The effective concentrations of TKIs in the three assays were found to be somewhat different, but in the same order of magnitude. Moreover, all the assays supported the

notion that the ABCG2 protein has a higher affinity toward these TKIs than does either MDR1 or MRP1.

Based on these experimental data, we suggest that multidrug resistance protein modulation by TKIs may be an important factor in the clinical treatment of cancer patients. Coadministration of TKIs with cytotoxic agents may prevent ABCG2-dependent cancer multidrug resistance and increase effectiveness for both types of intracellularly effective compounds.

The high-affinity interaction of ZD1839 with ABCG2 and its relatively low-affinity interaction with MDR1 and MRP1 may also modulate absorption and tissue distribution of this compound. In fact, the oral applicability and the intestinal absorption of ZD1839 (Ranson et al., 2002) may be caused by a strong inhibition of the ABCG2 and MDR1 multidrug transporters by high concentrations of ZD1839 at the apical surface of the intestinal epithelial cells, thus allowing a passive permeation of these hydrophobic agents into these cells. Such an effect has already been reported for ABCG2 inhibitors modulating topotecan absorption (Jonker et al., 2000).

In contrast, further cellular or tissue entry of TKIs at the relatively low plasma levels may be adversely affected by these transporters. Moreover, the removal of TKIs by multidrug transporters, e.g., ABCG2, may be involved in tumor cell TKI resistance.

The human estrogen receptor family inhibitor CI1033 has already been shown to increase the cellular accumulation and antiproliferative effectiveness of topotecan in BCRP/ABCG2-expressing tumor cells (Erlichman et al., 2001). According to a recent study with STI-571 (imatinib), the overexpression of MDR1/Pgp induced only a relatively small STI-571 resistance in intact tumor cells (Ferrao et al., 2003; Mahon et al., 2003). These findings are in line with our experiments showing a less efficient STI-571 interaction with MDR1 than with ABCG2.

The present study demonstrates the applicability of relatively simple in vitro assays for demonstrating specific, high-affinity interactions with the multidrug resistance proteins and advocates the use of such assays in further TKI drug development. Further experiments, regarding the direct extrusion of TKIs and, thus, the modulation of their cellular action by the overexpression of the ABCG2 and/or MDR1 proteins are underway in our laboratory.

Acknowledgments

The technical help by Zsuzsanna András, Ilona Zombori, Judit Kis, and Mónika Bátkai is gratefully acknowledged. We appreciate the kind gift of Ko143, obtained from Drs. J. D. Allen and G. J. Koomen.

References

Allen JD and Schinkel AH (2002) Multidrug resistance and pharmacological protection mediated by the breast cancer resistance protein (BCRP/ABCG2). *Mol Cancer Ther* **1**:427–434.

Allen JD, van Loevezijn A, Lakhai JM, van der Valk M, van Tellingen O, Reid G, Schellens JH, Koomen GJ, and Schinkel AH (2002) Potent and specific inhibition of the breast cancer resistance protein multidrug transporter in vitro and in mouse intestine by a novel analogue of fumitremorgin C. *Mol Cancer Ther* **1**:417–425.

Bakos E, Evers R, Sinko E, Varadi A, Borst P, and Sarkadi B (2000) Interactions of the human multidrug resistance proteins MRP1 and MRP2 with organic anions. *Mol Pharmacol* **57**:760–768.

Bakos E, Evers R, Szakacs G, Tusnady GE, Welker E, Szabo K, de Haas M, van Deemter L, Borst P, Varadi A, and Sarkadi B (1998) Functional multidrug resistance protein (MRP1) lacking the N-terminal transmembrane domain. *J Biol Chem* **273**:32167–32175.

Bates SE, Robey R, Miyake K, Rao K, Ross DD, and Litman T (2001) The role of half-transporters in multidrug resistance. *J Bioenerg Biomembr* **33**:503–511.

Brangi M, Litman T, Ciotti M, Nishiyama K, Kohlhagen G, Takimoto C, Robey R, Pommier Y, Fojo T, and Bates SE (1999) Camptothecin resistance: role of the ATP-binding cassette (ABC), mitoxantrone-resistance half-transporter (MXR) and potential for glucuronidation in MXR-expressing cells. *Cancer Res* **59**:5938–5946.

Cooray HC, Blackmore CG, Maskell L, and Barrand MA (2002) Localisation of breast cancer resistance protein in microvessel endothelium of human brain. *Neuroreport* **13**:2059–2063.

Diestra JE, Scheffer GL, Catala I, Maliepaard M, Schellens JH, Scheper RJ, Germa-Lluch JR, and Izquierdo MA (2002) Frequent expression of the multi-drug resistance-associated protein BCRP/MXR/ABCP/ABCG2 in human tumors detected by the BXP-21 monoclonal antibody in paraffin-embedded material. *J Pathol* **198**: 213–219.

Doyle LA, Yang W, Abruzzo LV, Krogmann T, Gao Y, Rishi AK, and Ross DD (1998) A multidrug resistance transporter from human MCF-7 breast cancer cells. *Proc Natl Acad Sci USA* **95**:15665–15670.

Erlichman C, Boerner SA, Hallgren CG, Spieker R, Wang XY, James CD, Scheffer GL, Maliepaard M, Ross DD, Bible KC, et al. (2001) The HER tyrosine kinase inhibitor CI1033 enhances cytotoxicity of 7-ethyl-10-hydroxycamptothecin and topotecan by inhibiting breast cancer resistance protein-mediated drug efflux. *Cancer Res* **61**:739–748.

Ferrao PT, Frost MJ, Siah SP, and Ashman LK (2003) Overexpression of P-glycoprotein in K562 cells does not confer resistance to the growth inhibitory effects of Imatinib (STI571) in vitro. *Blood* **102**:4499–4503.

Fisher GA, Lum BL, Hausdorff J, and Sikic BI (1996) Pharmacological considerations in the modulation of multidrug resistance. *Eur J Cancer* **32A**:1082–1088.

Gottesman MM, Fojo T, and Bates SE (2002) Multidrug resistance in cancer: role of ATP-dependent transporters. *Nat Rev Cancer* **2**:48–58.

Haugland RP (2002) Nucleic acid detection and genomics technology, in *Handbook of Fluorescent Probes and Research Products*, 9th ed. (Gregory J and Spence MITZ eds) pp 280, Molecular Probes, Eugene, OR.

Hegedus T, Orfi L, Seprodi A, Varadi A, Sarkadi B, and Keri G (2002) Interaction of tyrosine kinase inhibitors with the human multidrug transporter proteins, MDR1 and MRP1. *Biochim Biophys Acta* **1587**:318–325.

Heinrich MC, Griffith DJ, Druker BJ, Wait CL, Ott KA, and Zigler AJ (2000) Inhibition of c-kit receptor tyrosine kinase activity by STI 571, a selective tyrosine kinase inhibitor. *Blood* **96**:925–932.

Herbst RS (2002) ZD1839: targeting the epidermal growth factor receptor in cancer therapy. *Expert Opin Investig Drugs* **11**:837–849.

Hollo Z, Homolya L, Hegedus T, and Sarkadi B (1996) Transport properties of the multidrug resistance-associated protein (MRP) in human tumour cells. *FEBS Lett* **383**:99–104.

Homolya L, Hollo Z, Germann UA, Pastan I, Gottesman MM, and Sarkadi B (1993) Fluorescent cellular indicators are extruded by the multidrug resistance protein. *J Biol Chem* **268**:21493–21496.

Joensuu H, Roberts PJ, Sarlomo-Rikala M, Andersson LC, Tervahartiala P, Tuveson D, Silberman S, Capdeville R, Dimitrijevic S, Druker B, et al. (2001) Effect of the tyrosine kinase inhibitor STI571 in a patient with a metastatic gastrointestinal stromal tumor. *N Engl J Med* **344**:1052–1056.

Jonker JW, Smit JW, Brinkhuis RF, Maliepaard M, Beijnen JH, Schellens JH, and Schinkel AH (2000) Role of breast cancer resistance protein in the bioavailability and fetal penetration of topotecan. *J Natl Cancer Inst* **92**:1651–1656.

Litman T, Druley TE, Stein WD, and Bates SE (2001) From MDR to MXR: new understanding of multidrug resistance systems, their properties and clinical significance. *Cell Mol Life Sci* **58**:931–959.

Mahon FX, Belloc F, Lagarde V, Chollet C, Moreau-Gaudry F, Reiffers J, Goldman JM, and Melo JV (2003) MDR1 gene overexpression confers resistance to imatinib mesylate in leukemia cell line models. *Blood* **101**:2368–2373.

Maliepaard M, Scheffer GL, Faneyte IF, van Gastelen MA, Pijnenborg AC, Schinkel AH, van De Vijver MJ, Scheper RJ, and Schellens JH (2001) Subcellular localization and distribution of the breast cancer resistance protein transporter in normal human tissues. *Cancer Res* **61**:3458–3464.

Maliepaard M, van Gastelen MA, de Jong LA, Pluim D, van Waardenburg RC, Ruevekamp-Helmers MC, Floot BG, and Schellens JH (1999) Overexpression of the BCRP/MXR/ABCP gene in a topotecan-selected ovarian tumor cell line. *Cancer Res* **59**:4559–4563.

Muller M, Bakos E, Welker E, Varadi A, Germann UA, Gottesman MM, Morse BS, Roninson IB, and Sarkadi B (1996) Altered drug-stimulated ATPase activity in mutants of the human multidrug resistance protein. *J Biol Chem* **271**:1877–1883.

Ozvegy C, Litman T, Szakacs G, Nagy Z, Bates S, Varadi A, and Sarkadi B (2001) Functional characterization of the human multidrug transporter, ABCG2, expressed in insect cells. *Biochem Biophys Res Commun* **285**:111–117.

Ozvegy C, Varadi A, and Sarkadi B (2002) Characterization of drug transport, ATP hydrolysis and nucleotide trapping by the human ABCG2 multidrug transporter. Modulation of substrate specificity by a point mutation. *J Biol Chem* **277**:47980–47990.

Ranson M, Hammond LA, Ferry D, Kris M, Tullio A, Murray PI, Miller V, Averbuch S, Ochs J, Morris C, et al. (2002) ZD1839, a selective oral epidermal growth factor receptor-tyrosine kinase inhibitor, is well tolerated and active in patients with solid, malignant tumors: results of a phase I trial. *J Clin Oncol* **20**:2240–2250.

Roberts RB, Min L, Washington MK, Olsen SJ, Settle SH, Coffey RJ, and Threadgill DW (2002) Importance of epidermal growth factor receptor signaling in establishment of adenomas and maintenance of carcinomas during intestinal tumorigenesis. *Proc Natl Acad Sci USA* **99**:1521–1526.

Robey RW, Medina-Perez WY, Nishiyama K, Lahusen T, Miyake K, Litman T, Senderowicz AM, Ross DD, and Bates SE (2001) Overexpression of the ATP-binding cassette half-transporter, ABCG2 (Mxr/BCrp/ABCP1), in flavopiridol-resistant human breast cancer cells. *Clin Cancer Res* **7**:145–152.

Ross DD, Karp JE, Chen TT, and Doyle LA (2000) Expression of breast cancer resistance protein in blast cells from patients with acute leukemia. *Blood* **96**:365–368.

- Sarkadi B, Muller M, Homolya L, Hollo Z, Seprodi J, Germann UA, Gottesman MM, Price EM, and Boucher RC (1994) Interaction of bioactive hydrophobic peptides with the human multidrug transporter. *FASEB J* **8**:766–770.
- Sarkadi B, Price EM, Boucher RC, Germann UA, and Scarborough GA (1992) Expression of the human multidrug resistance cDNA in insect cells generates a high activity drug-stimulated membrane ATPase. *J Biol Chem* **267**:4854–4858.
- Sweeney WE, Futey L, Frost P, and Avner ED (1999) In vitro modulation of cyst formation by a novel tyrosine kinase inhibitor. *Kidney Int* **56**:406–413.
- Traxler P (2003) Tyrosine kinases as targets in cancer therapy—successes and failures. *Expert Opin Ther Targets* **7**:215–234.
- Ujhelly O, Ozvegy C, Varady G, Cervenak J, Homolya L, Grez M, Scheffer G, Roos D, Bates SE, Varadi A, et al. (2003) Application of a human multidrug transporter (ABCG2) variant as selectable marker in gene transfer to progenitor cells. *Hum Gene Ther* **14**:403–412.
- van Oosterom AT, Judson IR, Verweij J, Stroobants S, Dumez H, Donato di Paola E, Scot R, Van Glabbeke M, Dimitrijevic S, and Nielsen OS (2002) Update of phase I study of imatinib (STI571) in advanced soft tissue sarcomas and gastrointestinal stromal tumors: a report of the EORTC Soft Tissue and Bone Sarcoma Group. *Eur J Cancer* **38** (Suppl 5):S83–S87.
- Volk EL, Farley KM, Wu Y, Li F, Robey RW, and Schneider E (2002) Overexpression of wild-type breast cancer resistance protein mediates methotrexate resistance. *Cancer Res* **62**:5035–5040.
- Zhou S, Schuetz JD, Bunting KD, Colapietro AM, Sampath J, Morris JJ, Lagutina I, Grosveld GC, Osawa M, Nakauchi H, and Sorrentino BP (2001) The ABC transporter Bcrp1/ABCG2 is expressed in a wide variety of stem cells and is a molecular determinant of the side-population phenotype. *Nat Med* **7**:1028–1034.

Address correspondence to: Dr. Balázs Sarkadi, National Medical Center, Institute of Hematology and Immunology, 1113 Budapest, Diószegi u. 64, Hungary. E-mail: sarkadi@biomembrane.hu



Tyrosine kinase inhibitor resistance in cancer: role of ABC multidrug transporters

Csilla Özvegy-Laczka^a, Judit Cserepes^{a,b}, N. Barry Elkind^a, Balázs Sarkadi^{a,*}

^a National Medical Center, Institute of Haematology and Immunology, Membrane Research Group of the Hungarian Academy of Sciences, Diószegi u. 64, H-1113 Budapest, Hungary

^b Institute of Enzymology, Hungarian Academy of Sciences, H-1113 Budapest, Hungary

Received 5 January 2005; accepted 20 January 2005

Abstract

Recent antitumor drug research has seen the development of a large variety of tyrosine kinase inhibitors (TKIs) with increasing specificity and selectivity. These are highly promising agents for specific inhibition of malignant cell growth and metastasis. However, their therapeutic potential also depends on access to their intracellular targets, which may be significantly affected by certain ABC membrane transporters. It has been recently shown that several human multidrug transporter ABC proteins interact with specific TKIs, and the ABCG2 transporter has an especially high affinity for some of these kinase inhibitors. These results indicate that multidrug resistance protein modulation by TKIs may be an important factor in the treatment of cancer patients; moreover, the extrusion of TKIs by multidrug transporters may result in tumor cell TKI resistance. Interaction with multidrug resistance ABC transporters may also significantly modify the pharmacokinetics and toxicity of TKIs in patients.

© 2005 Published by Elsevier Ltd.

Keywords: ABCG2; Multidrug transporter; Xenobiotic transport; Cancer drug resistance; Polymorphic variants

1. Introduction

The tyrosine kinase (TK) signaling pathways regulate diverse physiological responses, including proliferation, differentiation, cell motility, and survival. However, these pathways are also utilized to promote tumor growth in a variety of cancers (Fig. 1). Much effort has been expended

to develop specific TK inhibitors in order to prevent cancer. The two most promising therapeutic approaches make use of monoclonal antibodies and small molecule inhibitors that specifically target the tyrosine kinase enzymatic activity (Rowinsky, 2003; Vlahovic and Crawford, 2003).

Several small molecule TK inhibitors (TKIs) have been already introduced into clinical practice with significant effects in overcoming certain malignancies (Table 1). However, as usually found for anticancer agents, a variety of resistance phenotypes have been observed.

In the present review we summarize recent information concerning resistance to TKI-based drugs with respect to the function and overexpression of ABC multidrug transporters. The information presented may help in determining the proper dosing of TKIs in order to obtain optimum cellular kinase modulation, as well as to consider the possible effects of ABC multidrug transporters in the absorption, distribution, metabolism, and toxicity (ADME-Tox) of the TKIs, even before entering clinical development.

Abbreviations: ABC transporters, ATP-binding cassette transporters; ABCP, placenta-specific ABC protein; ADME-Tox, absorption, distribution, metabolism, and toxicity; AML, acute myeloid leukemia; BCRP, breast cancer resistance protein; FDA, Food and Drug Administration; GIST, gastrointestinal stromal tumors; MDR1, human multidrug resistance protein (P-glycoprotein, ABCB1); MRP1, human multidrug resistance-associated protein 1, ABCC1; MXR, mitoxantrone resistance protein; NSCLC, non-small cell lung cancer; SCF, stem cell factor; Sf9 cells, *Spodoptera frugiperda* ovarian cells; TK, tyrosine kinase; TKI, tyrosine kinase inhibitor; SM-TKI, small molecule tyrosine kinase inhibitor; RTKI, receptor tyrosine kinase inhibitor

* Corresponding author. Tel.: +36 1 372 4353; fax: +36 1 372 4353.

E-mail address: sarkadi@biomembrane.hu (B. Sarkadi).

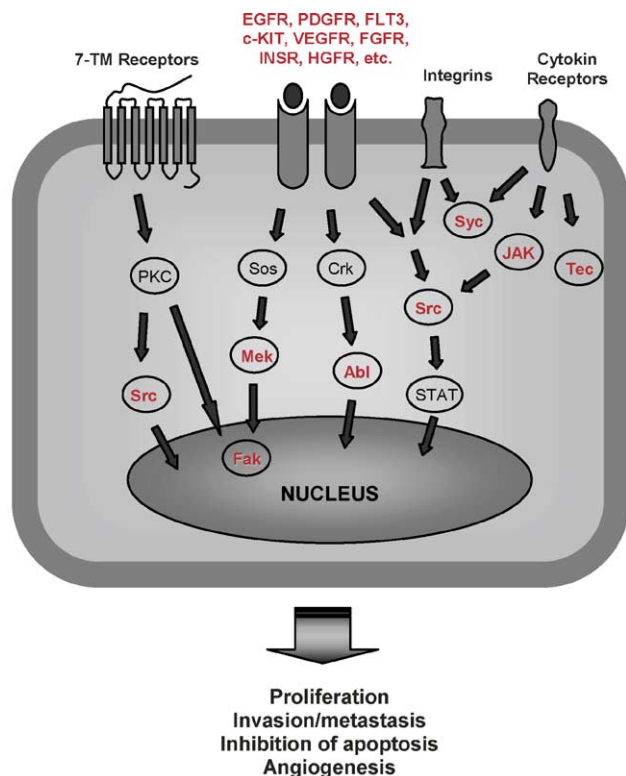


Fig. 1. Signaling pathways involving TKs in cancer cells. Protein tyrosine kinases are marked with red color.

2. Tyrosine kinase inhibitors in cancer treatment

Protein tyrosine kinases form a large and diverse multi-gene family. The members of this family are involved in regulating cell-to-cell signaling, growth, differentiation, motility, changes in cell shape, and adhesion. Deregulation of tyrosine kinase activity has been demonstrated to play a significant role in disease development, including congenital syndromes, diabetes and cancer. In fact, about one third of oncogenes involved in most forms of human malignancies are derived from tyrosine kinases (Robinson et al., 2000). Over the past decades, intensive studies of this protein family have revealed new insights into structure, function and regulation. Moreover, a rationally targeted inhibition of specific TKs has emerged as a promising strategy for cancer treatment (Gschwind et al., 2004; Vlahovic and Crawford, 2003).

Currently about 90 human TKs have been identified, which can be divided into two major groups based on their structure and localization. About two thirds of the known TKs are transmembrane receptors, while the other major group contains intracellular tyrosine kinases (Robinson et al., 2000).

2.1. Receptor tyrosine kinases and their inhibitors

The human receptor tyrosine kinases (RTKs) can be grouped into numerous subfamilies, based on their ki-

nase domain sequences. These families, among others, include the epidermal growth factor receptor (EGFR/ErbB), platelet-derived growth factor receptor (PDGFR), vascular endothelial growth factor receptor (VEGFR), fibroblast growth factor receptor (FGFR), and the hepatocyte growth factor receptor (MET) subfamilies.

The proteins have a conserved modular structure: they consist of an extracellular ligand binding domain, a membrane-spanning domain and an intracellular tyrosine kinase domain. The binding of the corresponding growth factor to the extracellular domain causes receptor dimerization and subsequent activation of the tyrosine kinase domain. In most cases, this leads to autophosphorylation of certain intracellular tyrosine residues within the receptor protein. These residues serve as docking sites for intracellular SH₂ domain-containing signal transducer proteins. At the same time, receptor-dependent phosphorylation of different cytoplasmic signaling molecules may also occur, resulting in the activation of signal transduction cascades. These signals induce proliferation, differentiation, cell survival and other important physiological responses (Gschwind et al., 2004). Constitutive activation of RTKs which leads to malignant transformation may occur by several mechanisms; that is, by the overexpression of the wild-type receptor or its growth factor ligand, ligand-independent constitutive receptor activation, failure of the inactivation mechanisms, or trans-activation through receptor dimerization (Gschwind et al., 2004; Vlahovic and Crawford, 2003).

A variety of approaches for inhibiting the action of RTKs or their stimulatory ligands have been investigated leading to the development of small molecule (SM) TKIs that prevent autophosphorylation and thus the propagation of downstream intracellular signals, monoclonal antibodies (mAbs) that block ligand binding, and antisense oligonucleotides or ribozymes that block receptor translation (Gschwind et al., 2004; Noble et al., 2004).

Since ABC transporters especially modify the effects of small molecule TKIs, we will discuss here only RTK-targeting anticancer strategies involving the application of these agents. SM-TKIs in most cases compete with ATP binding to the tyrosine kinase domain and thereby abrogate the catalytic activity of the receptor (Vlahovic and Crawford, 2003). Their most important mechanisms of action in cancers are arrest/inhibition of cell cycle, angiogenesis, tumor cell invasion and metastasis as well as induction of apoptosis. Furthermore, according to several studies, the combination of SM-TKIs with chemotherapy or radiation therapy enhanced the effects of these conventional methods. In the following section, we summarize the most relevant RTKs involved in malignancies and clinically targeted by SM-TK inhibitors.

2.1.1. EGF receptor

The EGF receptor is a member of the Erb subfamily, and its abnormally elevated activity was detected in a great

variety of solid tumors, including non-small cell lung cancer (NSCLC), colorectal adenocarcinoma, squamous cell carcinoma of the head and neck, glioblastoma, ovarian, breast, and prostate carcinoma. In these tumors the overexpression of the EGFR or its ligand activator (e.g., TNF), activating mutations, and activation of different signaling pathways have been described. HER2, a possible heterodimerization partner of EGFR, was found to be upregulated in breast cancer and the formation of EGFR/HER2 heterodimer results in the most active form of EGFR (Ciardiello and Tortora, 2003; Rowinsky, 2003). Considering the wide-spread contribution of epidermal growth factor receptors in tumorigenesis, these receptors turned out to be promising targets for rationally targeted therapies (Grandis and Sok, 2004; Gschwind et al., 2004; Vlahovic and Crawford, 2003).

A large number of small molecule anti-EGFR TKIs have been developed by pharmaceutical companies and academic laboratories, and several of these have already reached clinical trials (see Table 1) (Ciardiello and Tortora, 2002; Gschwind et al., 2004; Rowinsky, 2003). A prominent representative of these TKIs is ZD1839 (Iressa; Gefinitib, AstraZeneca), which is a small, orally active molecule that is a selective and reversible inhibitor of the EGFR tyrosine kinase while having much lower activity against related receptor tyrosine kinases, such as HER2. ZD1839 completely

abrogates EGFR signal transduction pathways (Anderson et al., 2001; Arteaga and Johnson, 2001; Barker et al., 2001; Herbst, 2004).

Preclinical studies showed that Iressa has a significant growth inhibitory effect in human cancer cell lines expressing EGFR, including NSCLC, breast, ovarian, prostate, colon, or epidermoid cancers. Iressa treatment was effective as a single agent, as well as in combination with chemotherapy or radiation therapy. In vitro and in vivo experiments demonstrated that the antitumor effect of Iressa was also mediated by the inhibition of tumor angiogenesis (Blackledge and Averbuch, 2004; Cohen et al., 2004).

Phase I and Phase II trials suggested that Iressa has an acceptable tolerability profile and promising antitumor activity in a variety of tumor types, particularly NSCLC. The most frequent adverse effects were mild acneiform skin rash and diarrhea. The combination studies were promising in patients with advanced NSCLC or colorectal carcinoma, when Iressa was co-administrated with gemcitabine/cisplatin or carboplatine/paclitaxel. Phase II and Phase III trials were conducted in patients with advanced NSCLC after first- or second-line chemotherapy and in patients with chemotherapy-naïve NSCLC, respectively. The results of these trials have clearly demonstrated that Iressa has a significant antitumor activity in patients with

Table 1
Rationally targeted inhibitors of TKs as anticancer drugs in clinical development (for details see the online link: <http://www.cancer.gov/clinicaltrials>)

Agent	Target TK	Tumor types	Development phase
ZD1839 (Iressa/gefitinib)	EGFR	NSCLC, head and neck, breast, colorectal, breast	Approved (NSCLC) Ph III (head and neck) Ph II (breast, colorectal, prostate, oesophageal, renal, glioblastoma)
OSI-774 (Tarceva/erlotinib)	EGFR	NSCLC, pancreas, head and neck, glioblastoma, ovarian, breast	Ph III (NSCLC, pancreas) Ph II (head and neck, breast, ovarian)
CI1033	pan-Erb	Solid tumors (e.g., NSCLC)	Ph II
PKI166	EGFR	Solid tumors	Ph I (clinical trials stopped recently)
EKB-569	EGFR	Solid tumors (e.g., colorectal, NSCLC)	Ph II
SU5416	VEGFR1–2, FLT3, c-KIT	AML, colorectal	Ph III (colorectal), Ph II (AML)
SU11248	VEGFR1–2, PDGF α and β , FLT3, c-KIT	AML	Ph I (AML)
PTK787	VEGFR2	Colorectal cancer	Ph III (clinical trials recently discontinued)
STI571	PDGF α and β c-KIT	Dermatofibrosarcoma Gastrointestinal stromal tumor	Ph II Approved
	ABL	CML, ALL	Approved (CML), Ph III (ALL)

advanced NSCLC. However, these trials also showed that in NSCLC the addition of Iressa to the conventional chemotherapy did not enhance the clinical benefit of chemotherapy alone. On the basis of these clinical trials performed in 2003, the FDA approved an application of Iressa as monotherapy for patients with advanced NSCLC that had failed both platinum-based and docetaxel chemotherapy (Cohen et al., 2004; Giaccone, 2004; Herbst et al., 2004b).

Interestingly, no clear association between EGFR expression levels and response to the Iressa-treatment has been revealed, and preclinical studies suggested a complex relationship between the expression level of EGFR and the efficacy of the EGFR-targeted TKIs (Campiglio et al., 2004; Parra et al., 2004). Moreover, Iressa was also found to be effective in tumor cells with low levels of EGFR, suggesting that the levels of the phosphorylated, activated EGFR are more informative in this regard than total EGFR levels (Ciardiello and Tortora, 2003).

HER2, which belongs to the ErbB family of RTKs, provides a possible heterodimerization partner to EGFR (Chen et al., 2003). Indeed, although Iressa is a poor inhibitor of HER2 itself, the antiproliferative effect of Iressa correlated with the expression level of HER2 (Ciardiello and Tortora, 2003). The signals induced by HER2-containing heterodimers may have the strongest biological activity and HER2 expression in tumors (breast, ovarian) is associated with poor prognosis in vivo. Several studies have demonstrated that tumor cell lines expressing both EGFR and HER2 are particularly sensitive to Iressa (Campiglio et al., 2004), and in this case Iressa also inhibited the phosphorylation of HER2 and the activation of receptor-dependent signaling pathways (Anido et al., 2003).

Recent reports showed that somatic mutations in the EGFR gene in patients with NSCLC greatly increased the tumor-responsiveness to Iressa treatment. These studies described mutations around the region encoding the ATP-binding pocket of the receptor tyrosine kinase domain (Lynch et al., 2004; Paez et al., 2004; Pao et al., 2004). Ninety-three percent of the Iressa-responder patients had EGFR mutations, while none of the non-responders had such mutations (Arteaga, 2004). In vitro experiments proved that these mutations resulted in enhanced tyrosine kinase activity in response to EGF (Lynch et al., 2004), or the mutants had altered substrate specificity, as compared to the wild-type protein (Pao et al., 2004).

Another promising anti-EGFR TKI is Tarceva (OSI774; Erlotinib, Genentech, Inc.). This compound, like Iressa, is a small molecule, orally bioavailable, specific and reversible EGFR inhibitor. Its anticancer effects were demonstrated in case of head-and-neck cancer, NSCLC, and ovarian and breast cancer cells (Herbst, 2004; Langer, 2004). Phase II trials in NSCLC patients demonstrated significant antitumor activity of Tarceva and several Phase III trials have also been started (Langer, 2004). When used as a monotherapy agent in patients with stage III/IV NSCLC, Tarceva was shown to prolong survival. However, similarly to Iressa, Tarceva did

not increase patient survival when used in combination with carboplatin and paclitaxel or with cisplatin and gemcitabine therapies (Herbst et al., 2004a). The reason for failure of Tarceva (and Iressa) in combination with conventional chemotherapy in Phase III trials is still unknown.

According to recent reports in the literature, several anti-EGFR TKIs, such as CI1033, EKB-569, and PKI166, are in the pipeline to reach a clinical phase of application (see Table 1) (Blackledge and Averbuch, 2004; Bonomi, 2003; Janmaat and Giaccone, 2003).

2.1.2. The VEGF receptor family

Members of the VEGFR family play a key role in tumor growth and metastasis and their activation promotes angiogenesis. The first VEGFR-targeted agent, SU5416, proved to be an effective inhibitor of VEGFR1–3, as well as PDGFR β , FLT3, CSF-1R, and it had an encouraging anti-angiogenic and anti-tumor activity in animal models. However, this compound was not orally bioavailable, which, together with thromboembolic side effects, resulted in the cessation of the related trials. SU11248, a more effective inhibitor of RTKs, showed a promising antitumor effect, and entered Phase I clinical trials for acute leukemia. PTK787, a more selective inhibitor of VEGFR2, showed most encouraging inhibitory effects on tumor growth. After promising Phase I and Phase II results, Phase III trials are currently in progress for metastatic colorectal cancer. On the basis of these observations, new rationally designed VEGFR2-specific inhibitors, like AAL993, are now emerging (Dreves, 2003; Manley et al., 2004; Verheul and Pinedo, 2003).

2.1.3. PDGF receptor

PDGF receptor (PDGFR) deregulation was found in several human tumor types, including dermatofibrosarcoma, glioblastoma, myeloproliferative disorders, NSCLC, etc. The compound STI571 (Imatinib mesylate, Gleevec; Novartis), a synthetic TKI developed against the BCR-ABL, approved for the therapy of CML (see below), showed a significant inhibitory effect also on different PDGFRs, such as PDGFR α and β , and c-KIT (see Table 1) (Fletcher, 2004; Savage and Antman, 2002). Promising results for STI571 treatment have been reported in cases of dermatofibrosarcoma pubertans (McArthur, 2004; Sjoblom et al., 2001). The receptor for stem cell factor (SCF), c-KIT TK, was reported to be important in the development of gastrointestinal stromal tumors (GIST), as mutations of c-KIT lead to ligand-independent constitutive activation (de Silva and Reid, 2003). Gleevec is now considered to be the drug of choice for metastatic and inoperable GIST (Duensing et al., 2004; Logrono et al., 2004; Sawaki and Yamao, 2004). A further member of the PDGFR family, the FLT3 receptor protein, is also involved in tumorigenesis by different mutations. In patients with acute myeloid leukemia (AML) mutations causing constitutively active FLT3 receptor were reported. Therefore, drugs that inhibit the function of FLT3 mutants may be effective in the treatment of AML (see

Table 1) (O'Farrell et al., 2003; Smith et al., 2004; Stone et al., 2005).

2.2. Non-receptor tyrosine kinases

Non-receptor tyrosine kinases are found in the cytoplasm and the nucleus, and they transduce extracellular signals to downstream intermediates in pathways that regulate cellular growth, activation and differentiation. The activation of many cytoplasmic TKs is directly linked to membrane receptor activation by extracellular signals. Other non-receptor TKs are activated by cellular adhesion or intracellular signals without a direct connection to membrane receptors (Vlahovic and Crawford, 2003). Dysregulation of cytoplasmic TK activity has been revealed in the pathogenesis of many human cancers; the most clinically relevant being the non-receptor TK, BCR-ABL. This protein is derived from a translocation event of chromosomes 9 and 22 (Philadelphia chromosome, Ph), resulting in a fusion of the *c-abl* and the breakpoint cluster region (*bcr*) genes. The encoded fusion protein, BCR-ABL, is a constitutively active form of the Abl TK, that drives uncontrolled growth of cells (Deininger and Druker, 2003; Melo et al., 2003; Vlahovic and Crawford, 2003).

STI571 (Imatinib mesylate, Gleevec), a rationally designed anticancer TKI, has been shown to be an effective inhibitor of BCR-ABL protein (see Table 1) (Deininger, 2004; Roskoski, 2003). It blocks the growth of BCR-ABL transformed leukemic cells and induces apoptosis. The effectiveness of Gleevec resulted in a rapid path into the clinic; it was approved in 2001 for treatment of Ph+ CML patients. In early stages of the disease, this compound is very effective in inhibiting progression of CML and Ph+ adult ALL. However, most patients with advanced CML relapse with a Gleevec-resistant tumor variant (Deininger and Druker, 2003; Melo et al., 2003; Noble et al., 2004; O'Dwyer et al., 2003; Vlahovic and Crawford, 2003).

The Src family of kinases was described to be involved in various types of cancers including colon, breast and leukemia. Recently, a correlation of increased expression or activity of Src with the stage and metastatic potential of some neoplasia has been reported (Tsygankov and Shore, 2004; Warmuth et al., 2003). AZD0530 (AstraZeneca), a src inhibitor, is in phase I clinical testing.

Recently, the involvement of Jak kinase in acute lymphoid leukemia has also been described (Luo and Laaja, 2004; Steelman et al., 2004).

3. Tumor resistance to TKIs

Much of TKI drug development is in a relatively early phase, thus clinical resistance mechanisms could not have been explored in detail. Several cellular mechanisms were suggested to affect TKI tumor response, ranging from the amplification of the target receptor expression, impaired binding of TKIs as a consequence of receptor mutations,

and a decreased TKI uptake into the tumor cells. Other resistance mechanisms may include the use of alternative pathways of cell activation or a constitutive activation of downstream signaling effectors (Kim and Toge, 2004). Iressa and Gleevec are two clinically effective agents where we have more detailed information regarding tumor resistance. We will discuss resistance against these compounds caused by multidrug resistance ABC transporters. For Tarceva, another clinically relevant TKI, there are no data available yet about its interaction with ABC transporters.

As mentioned above, the tumor response to Iressa was increased by somatic mutations in the receptor gene. These mutations significantly enhanced tyrosine kinase activity in response to EGF, or altered the substrate specificity of the protein (Lynch et al., 2004; Paez et al., 2004; Pao et al., 2004), for a review see (Arteaga, 2004). Thus low-level Iressa sensitivity, which clinically may appear as a relative resistance, may appear in tumors with wild-type EGFR. Iressa resistance was reported to be caused by an EGFR-independent constitutive Akt activation even in EGFR-overexpressing breast cancer cells. In this case the loss of PTEN may have lead to an unregulated high activity of PI3K/Akt pathway and a consequent Iressa resistance, which could be reversed by the recovery of the PTEN function (She et al., 2003).

In the case of Gleevec, several mechanisms of resistance have been reported (Daub et al., 2004; Weisberg and Griffin, 2003). The most common causes are mutations in the kinase domain or the overamplification of the *bcr-abl* gene (Nimmanapalli and Bhalla, 2002; Shah and Sawyers, 2003). In most cases mutations appear in the tyrosine kinase region, obstructing the appropriate binding of Gleevec to the kinase pocket (Melo et al., 2003; Nardi et al., 2004). Another resistance mechanism observed was the compensation of the inhibited BCR-ABL signaling by other kinase pathways, such as the Src-family member Lyn kinase (Dai et al., 2004), or extracellular sequestration of Gleevec by $\alpha 1$ acid glycoprotein (Gambacorti-Passerini et al., 2003).

4. The ABC multidrug transporters in cancer drug resistance

The ABC family is one of the largest groups of transmembrane proteins consisting of 49 human members. A common, characteristic feature of ABC proteins is the specific ABC (ATP-Binding Cassette) domain that is responsible for ATP binding and hydrolysis. ABC proteins are present in all living species and can function both as receptors, channels, and transporters (Ueda et al., 1999). For receptors and channels, ATP binding and/or hydrolysis has a regulatory function, while in case of active ABC transporters ATP hydrolysis is necessary to provide energy for the transport process.

Within the group of ABC proteins are the multidrug transporters, so named because they extrude a large number of structurally diverse compounds from cells. These are often overexpressed in cancer cells where they confer cross-

resistance against various cytotoxic compounds (Gottesman et al., 1996; Higgins, 1992).

There are numerous ABC transporters suspected to confer cancer drug resistance. They include the multidrug resistance protein or P-glycoprotein (MDR1, Pgp, ABCB1); the multidrug resistance-associated proteins MRP1, 2, 3, 4 and 5 (ABCC1, 2, 3, 4 and 5, respectively); sister of Pgp or bile salt-exporter protein (SPGP, BSEP, ABCB11); ABCA2 and ABCG2 (ABCP/MXR/BCRP). However, as only three of these, MDR1, MRP1 and ABCG2, are thought to be clinically relevant in anticancer multidrug resistance, we discuss only these regarding their interactions with TKIs.

MDR1 is a 170-kDa membrane glycoprotein, expressed in the apical membranes of epithelial cells of the gastrointestinal tract, renal proximal tubules, the canalicular surface of hepatocytes, in the endothelium of blood–brain and blood–testis barrier and in adrenal glands. Its physiological role lies most probably in the protection of the body from xenobiotics. MDR1 is a transporter for large, hydrophobic, either uncharged or slightly positively charged molecules (Bates, 2003).

MRP1 is a 190-kDa membrane glycoprotein, present in many tissues, and localized to the basolateral membrane in polarized cells. MRP1 transports hydrophobic drugs, drug conjugates, and also extrudes various organic anions (Deeley and Cole, 2003). Overexpression of MDR1 and MRP1 in both hematological malignancies and in solid tumors has been demonstrated. However, data about their role as prognostic factors of the outcome of chemotherapy are still contradictory (Leonard et al., 2003).

ABCG2 is a more recently discovered 70-kDa plasma membrane glycoprotein. It is called an ABC half-transporter which must homo-dimerize for its active transport function (Doyle and Ross, 2003). ABCG2 is present in many tissues, including stem cells, placental syncytiotrophoblast cells, epithelial cells of the intestine and colon, liver canaliculi, gallbladder epithelium, side population stem cells in the lung, endothelia of veins and capillaries, the blood–brain and blood–testis barrier (Cooray et al., 2002; Maliepaard et al., 2001; Zhou et al., 2001). ABCG2 is located in the apical membrane in polarized cells (Dietrich et al., 2003).

Physiologically, ABCG2 was demonstrated to protect the body from various food breakdown products (Jonker et al., 2002) or heme metabolites (Krishnamurthy et al., 2004). Studies, carried out by using *abcg2* knock-out mice and inhibitors have indicated that this protein has an important function in preventing the absorption of toxic compounds from the gut, increase their hepatobiliary clearance, and protect the maternal–fetus and blood–brain barriers (Jonker et al., 2000; Mizuno et al., 2004; van Herwaarden et al., 2003).

The presence of ABCG2 was detected in various drug-selected tumor cell lines arising from diverse tissue types, e.g., lung, breast, colon, ovarian and gastric carcinomas, fibrosarcomas and myelomas (Allen and Schinkel, 2002). ABCG2 was shown to confer in vitro resistance against various cytotoxic compounds used in the treatment of

cancer patients; for example mitoxantrone, flavopiridol, methotrexate, topotecan, irinotecan, and SN-38 (Brangi et al., 1999; Jonker et al., 2000; Miyake et al., 1999; Robey et al., 2001; Volk et al., 2000).

In vivo studies of patients undergoing chemotherapy revealed that ABCG2 was overexpressed in several tumors, including non-small cell lung cancer, oral squamous cell carcinoma, osteosarcoma, hepatic metastases, non-seminoma, seminoma and testicular lymphoma samples and in acute lymphoblastic leukemia (Bart et al., 2004; Candeil et al., 2004; Chano et al., 2004; Friedrich et al., 2004; Hirschmann-Jax et al., 2004; Kawabata et al., 2003). In most of these cases, ABCG2 overexpression correlated with lower response rate to chemotherapy, increased drug resistance and shorter patient survival (Candeil et al., 2004; Friedrich et al., 2004; Kawabata et al., 2003).

In the case of acute myeloid leukemia (AML) ABCG2 expression did not correlate with the outcome of the disease (Galimberti et al., 2004; van der Pol et al., 2003), and did not show an upregulation upon relapse (van der Kolk et al., 2002). However, ABCG2 expression was increased in a refractory state (van den Heuvel-Eibrink et al., 2002), and ABCG2 mRNA levels correlated with flavopiridol resistance (Nakanishi et al., 2003; van den Heuvel-Eibrink et al., 2002). Interestingly, several groups found that ABCG2 was expressed only in subpopulations of AML samples (Abbott et al., 2002; Suvannasankha et al., 2004). Such subpopulations, with high ABCG2 levels and characteristic stem cell phenotype, were also found in neuroblastoma, Ewing sarcoma, teratocarcinoma, breast cancer, small-cell lung cancer, and glioblastoma samples (Hirschmann-Jax et al., 2004). These stem cells may survive chemotherapy and contribute to relapses.

5. Interactions of TKIs with ABC multidrug transporters—special role of ABCG2

The effectiveness of specific tyrosine kinase inhibitors, as discussed above, can be decreased due to mutations occurring in their target molecules, amplification of the target gene, or due to the activity of ABC transporters that can prevent TKIs from reaching their intracellular targets through drug extrusion.

5.1. TKI resistance mediated by MDR1 or MRP1

It was first shown by Mahon et al. that a possible mechanism of BCR-ABL-positive cells to overcome the apoptotic effect of Gleevec is the overexpression of MDR1 (Mahon et al., 2000). In our work, the interaction of MDR1 and MRP1 with several tyrosine kinase inhibitors, including STI571 (Gleevec, Imatinib mesylate), an EGFR-specific tyrosine kinase inhibitor, EKI-785, and some other rationally designed small molecule TKIs, were studied. Several TKIs tested in this study, especially Gleevec, modulated the ATPase and

transport activities of MDR1 at low micromolar concentrations, while the ATPase and transport activities of MRP1 were only affected by higher TKI concentrations (Hegedus et al., 2002).

It has been documented that MDR1-overexpressing BCR-ABL-positive K562 cells survived up to 1 μM Gleevec concentrations, while upon the addition of MDR1 modulators Gleevec was effective at lower concentrations (Mahon et al., 2003). In the MDR1-expressing cells, higher Gleevec concentrations were required to decrease tyrosine phosphorylation, of the bcr-abl kinase indicating that Gleevec could not reach its intracellular target. A similar MDR1-mediated Gleevec resistance was found in a CML cell line expressing MDR1. Moreover, CML cells from patients with low MDR1 levels showed a Gleevec resistance reversible by PSC833, a cyclosporin analog MDR1 inhibitor (Mahon et al., 2003).

Recent studies confirmed that MDR1 prevents the effect of Gleevec in BCR-ABL-positive K562 cells, while Gleevec also enhanced the cytotoxic effects of MDR1 substrate agents (Mukai et al., 2003). Additionally, high concentrations (200 μM) of Gleevec efficiently prevented the binding of an MDR1 substrate to the protein. The same study indicated that Gleevec is a poor substrate for MRP1; even at hundreds of micromolar concentrations, Gleevec had no effect on MRP1-related drug resistance, substrate binding, or LTC4 transport. Recently, Thomas et al. demonstrated that the MDR1-mediated basolateral to apical transport of Gleevec in MDCK cells was prevented by the inhibitor PSC833 (Thomas et al., 2004). It should be mentioned that in contrast to the above reports, Ferrao et al. found that K562 cells overexpressing MDR1 were not significantly resistant to Gleevec, nor did MDR1 prevent the inhibitory effect of Gleevec on protein phosphorylation (Ferrao et al., 2003).

In our recent studies, we examined the interaction of Iressa (ZD1839, Gefitinib) with MDR1 and MRP1 by using various in vitro assay systems (Ozvegy-Laczka et al., 2004). We found that Iressa is most probably a transported substrate of MDR1, while this compound only inhibited MRP1. It is important to emphasize that the Iressa concentrations at which interactions with MDR1 were demonstrated were relatively high (1–10 μM), therefore it is not likely that MDR1 may cause resistance against Iressa during cancer therapy. Still, MDR1 may modulate the absorption or metabolism of Iressa, where this agent is present at higher concentrations. A recent study (Yanase et al., 2004) that supports our findings, demonstrated that MDR1, but not MRP1 could protect the EGFR-dependent A431 cells against the action of Iressa, and Iressa inhibited MDR1-mediated etoposide and vincristine resistance.

5.2. TKI resistance mediated by ABCG2

It has been first shown in cell lines overexpressing ABCG2 (Erlichman et al., 2001) that an experimental TKI agent, CI1033, enhanced the cytotoxic ef-

fect of SN-38 and topotecan, by increasing the accumulation of these ABCG2 substrates. Moreover, CI1033 was directly extruded by ABCG2. Thus, ABCG2 may play a role in clinical CI1033 resistance, and CI1033 can modulate the effectiveness/toxicity of ABCG2 substrate drugs.

In our recent study we have tested the in vitro interaction between Gleevec (STI571), EKI-785 and Iressa (ZD1839, Gefitinib) with the ABCG2 protein (Ozvegy-Laczka et al., 2004). We found that at lower concentrations both EKI-985 and Iressa stimulated the ATPase activity of ABCG2, while above 10 μM they were inhibitory to ATP hydrolysis. We also showed that all three TKIs inhibited the transport function and cell protecting activity of ABCG2. Our results suggest that at lower concentrations, EKI-985 and Iressa are transported substrates of ABCG2, while in the case of Gleevec the nature of interaction could not be determined. Our study also indicated that ABCG2 has a significantly higher affinity for these TKIs than MDR1 or MRP1.

Regarding the interaction of Gleevec with ABCG2, two recent studies were published with contradictory findings. Houghton et al. showed that in Saos2 osteosarcoma cells expressing ABCG2, Gleevec, in submicromolar concentrations, reversed SN-38 and topotecan resistance (Houghton et al., 2004). However, they found that the sensitivity to Gleevec, or the accumulation and efflux of labeled Gleevec, were not modulated by ABCG2 expression in these cells. Therefore, they concluded that Gleevec is a high affinity inhibitor of ABCG2 but not a transported substrate of the protein. In contrast, by using labeled Gleevec and ABCG2-expressing MCF-7 or HEK cell lines, Burger et al. found that the accumulation of Gleevec was significantly lower in ABCG2-expressing cell lines than in the parental counterparts (Burger et al., 2004). Moreover, when the specific ABCG2 inhibitor, Ko143, was added, Gleevec accumulation in ABCG2-expressing cell lines reached the same high level as in parental cells. The discrepancy between the two studies may stem from the fact that Houghton et al. performed their transport experiments at unfavorable temperature and other conditions, thus probably missing the transport of Gleevec by ABCG2.

For the analysis of the interactions of Iressa with ABCG2, several studies were performed recently. Stewart et al. examined the effect of Iressa in combination with irinotecan on the growth of tumor xenografts (Stewart et al., 2004). They found that Iressa had no effect on xenografts that had no EGFR expression, while this TKI still increased the antitumor activity of the ABCG2 substrate, irinotecan. Iressa could also reverse ABCG2-mediated resistance to SN-38 in ABCG2-expressing Saos2 cells. These data suggested that Iressa inhibited the function of ABCG2. Stewart et al. also demonstrated that Iressa can increase the plasma concentration of irinotecan and SN-38 in mice, therefore the co-administration of Iressa and cytotoxic compounds may significantly increase the effectiveness of anticancer agents.

When measuring the accumulation and efflux of labeled Iressa in control and ABCG2-expressing Saos2 cells, respectively, Stewart et al. found no difference in these parameters, suggesting that Iressa is not a transported substrate for ABCG2 (Stewart et al., 2004). However, these experiments were also carried out at unfavorable transport conditions (see above).

Two recent studies examined the interactions of Iressa with ABCG2 in a pharmacologically relevant model system; that is, by using the EGFR signaling-dependent A431 tumor cells. These cells stop proliferating and show mostly apoptotic cell death upon inhibition of the EGFR signaling pathway. Yanase et al. (2004) reported that in transfected A431 cells, ABCG2 provided a resistance against Iressa. In this study they also demonstrated that Iressa reversed ABCG2-mediated SN-38 or vincristine resistance and inhibited topotecan and estrone 3-sulfate transport by ABCG2. Moreover, in mice Iressa increased irinotecan resistance *in vivo*.

In our recent findings (Elkind et al., 2005), we investigated the nature of the interaction between ABCG2 and Iressa in an A431 tumor cell system. We created wild-type and inactive mutant ABCG2-expressing, EGFR signaling-dependent A431 cells, and examined whether ABCG2 prevented the apoptotic effect of Iressa caused by inhibition of EGFR phosphorylation. We found that wtABCG2 protected the A431 cell from Iressa, while this protection was absent in the presence of the selective ABCG2 inhibitor, Ko143, or in cells expressing an inactive ABCG2 mutant. It was also demonstrated that ABCG2 function prevented EGFR dephosphorylation and the extracellular appearance of phosphatidyl serine, a marker for early apoptosis.

All these experimental data strongly suggest that Iressa interacts with ABCG2 at low, pharmacologically relevant concentrations, and that ABCG2 can actively extrude Iressa. These data also indicate that expression level and functionality of ABC multidrug transporters, especially that of ABCG2, may significantly alter the ADME-Tox parameters for TKIs.

There are several naturally occurring ABCG2 polymorphic variants with suggested differences in their activities and substrate-recognition (Backstrom et al., 2003; de Jong et al., 2004; Honjo et al., 2002; Iida et al., 2002; Imai et al., 2002; Itoda et al., 2003; Sparreboom et al., 2003; Kobayashi et al., 2005; Mizuarai et al., 2004; Zamber et al., 2003). Of special interest is the ABCG2 variant Q141K (glutamine to lysine replacement). It has a high allele frequency of 35% in the Japanese population and this was demonstrated to cause reduced ABCG2 expression and decreased transport activity (Imai et al., 2002; Mizuarai et al., 2004; Morisaki et al., *in press*). Interestingly, when Iressa was introduced in Japan, a number of patients died due to inappropriate dosing or unexpected toxicity (Dancey and Freidlin, 2003; Inoue et al., 2003). We suggest that patients harboring this ABCG2 variant may be more sensitive to Iressa, and this sensitivity may be relevant in this clinical finding.

6. Conclusions and future perspectives

Upregulation or aberrant activity of receptor tyrosine kinases can lead to tumor formation. Several specific tyrosine kinase inhibitors, like Gleevec, Iressa and Tarceva, have been successfully used in cancer treatment. However, there are subsets of tumors that do not respond to TKI treatment. This resistance may be due to the drug extrusion activity of multidrug resistance ABC transporters, especially of ABCG2. The multidrug transporters are present in many of our tissues with barrier functions, and may modulate the absorption of orally administered cytotoxic compounds.

Based on the ability of MDR1 and ABCG2 to extrude TKIs, it is possible that multidrug transporters affect the absorption, distribution, cellular levels and effectiveness of these TKIs. Many specific TKIs, though effectively inhibiting TK activity *in vitro*, fail in *in vivo* experiments or clinical studies. It is likely that multidrug transporters are responsible for some of this lowered TKI efficacy *in vivo*. Therefore, some of the *in vitro* assays discussed above should be included during the preclinical testing of newly developed TKIs.

Some of the results discussed suggest that there may be a narrow concentration range in which multidrug resistance proteins can transport the TKIs, while above these concentrations, TKIs inhibit the function of these proteins (Elkind et al., 2005; Ozvegy-Laczka et al., 2004). Therefore, it is possible that high-affinity transporters like ABCG2 may not influence the intestinal absorption of Iressa (for example) present at this site in high concentrations but may play a role in cellular extrusion of drug in the tumor where the local concentration of the drug is lower. On the other hand, MDR1, although having a much lower affinity to TKIs, still may modulate TKI absorption at various tissue barriers.

As shown above, TKIs can inhibit the transport of cytotoxic compounds by multidrug transporters, especially by ABCG2, thus circumventing transporter-mediated multidrug resistance. Therefore, the co-administration of TKIs and cytotoxic agents may enhance the effectiveness of anticancer therapies. On the other hand, a co-administration of TKIs and other cytotoxic compounds may lead to an increased toxicity.

It is important to note that ABCG2 has several polymorphic variants with altered substrate-specificities and activities. Further studies are required to determine whether there is any difference between the affinities of these polymorphic ABCG2 variants to TKIs when functioning as variant homodimers and wild-type:variant heterodimers, and if there is any clinical relevance of ABCG2 polymorphisms in response to TKI treatment.

Acknowledgments

This work has been supported by research grants from OTKA, ETT and OM, Hungary (T35126, T31952, T35926,

T38337, ETT, and NKFP). Csilla Özvegy-Laczka is a grantee of the Postdoctoral Fellowship (D 45957) of OTKA, Hungary and the János Bolyai Scholarship of the Hungarian Academy of Sciences. Balázs Sarkadi is a recipient of a Howard Hughes International Scholarship.

References

- Abbott, B.L., Colapietro, A.M., Barnes, Y., Marini, F., Andreeff, M., Sorrentino, B.P., 2002. Low levels of ABCG2 expression in adult AML blast samples. *Blood* 100, 4594–4601.
- Allen, J.D., Schinkel, A.H., 2002. Multidrug resistance and pharmacological protection mediated by the breast cancer resistance protein (BCRP/ABCG2). *Mol. Cancer Ther.* 1, 427–434.
- Anderson, N.G., Ahmad, T., Chan, K., Dobson, R., Bundred, N.J., 2001. ZD1839 (Iressa), a novel epidermal growth factor receptor (EGFR) tyrosine kinase inhibitor, potentially inhibits the growth of EGFR-positive cancer cell lines with or without erbB2 overexpression. *Int. J. Cancer* 94, 774–782.
- Anido, J., Matar, P., Albanell, J., Guzman, M., Rojo, F., Arribas, J., Averbuch, S., Baselga, J., 2003. ZD1839, a specific epidermal growth factor receptor (EGFR) tyrosine kinase inhibitor, induces the formation of inactive EGFR/HER2 and EGFR/HER3 heterodimers and prevents heregulin signaling in HER2-overexpressing breast cancer cells. *Clin. Cancer Res.* 9, 1274–1283.
- Arteaga, C.L., 2004. Selecting the right patient for tumor therapy. *Nat. Med.* 10, 577–578.
- Arteaga, C.L., Johnson, D.H., 2001. Tyrosine kinase inhibitors-ZD1839 (Iressa). *Curr. Opin. Oncol.* 13, 491–498.
- Backstrom, G., Taipalensuu, J., Melhus, H., Brandstrom, H., Svensson, A.C., Artursson, P., Kindmark, A., 2003. Genetic variation in the ATP-binding cassette transporter gene ABCG2 (BCRP) in a Swedish population. *Eur. J. Pharm. Sci.* 18, 359–364.
- Barker, A.J., Gibson, K.H., Grundy, W., Godfrey, A.A., Barlow, J.J., Healy, M.P., Woodburn, J.R., Ashton, S.E., Curry, B.J., Scarlett, L., Henthorn, L., Richards, L., 2001. Studies leading to the identification of ZD1839 (IRESSA): an orally active, selective epidermal growth factor receptor tyrosine kinase inhibitor targeted to the treatment of cancer. *Bioorg. Med. Chem. Lett.* 11, 1911–1914.
- Bart, J., Hollema, H., Groen, H.J., de Vries, E.G., Hendrikse, N.H., Sleijfer, D.T., Wegman, T.D., Vaalburg, W., van der Graaf, W.T., 2004. The distribution of drug-efflux pumps, P-gp, BCRP, MRP1 and MRP2, in the normal blood–testis barrier and in primary testicular tumours. *Eur. J. Cancer* 40, 2064–2070.
- Bates, S.E., 2003. Solving the problem of multidrug resistance: ABC transporters in clinical oncology. In: Holland, I.B., Cole, S.P., Kuchler, K., Higgins, C.F. (Eds.), *ABC Proteins from Bacteria to Man*. Academic Press, London, pp. 359–392.
- Blackledge, G., Averbuch, S., 2004. Gefitinib ('Iressa', ZD1839) and new epidermal growth factor receptor inhibitors. *Br. J. Cancer* 90, 566–572.
- Bonomi, P., 2003. Clinical studies with non-Iressa EGFR tyrosine kinase inhibitors. *Lung Cancer* 41 (Suppl. 1), S43–S48.
- Brangi, M., Litman, T., Ciotti, M., Nishiyama, K., Kohlhagen, G., Takimoto, C., Robey, R., Pommier, Y., Fojo, T., Bates, S.E., 1999. Camptothecin resistance: role of the ATP-binding cassette (ABC), mitoxantrone-resistance half-transporter (MXR), and potential for glucuronidation in MXR-expressing cells. *Cancer Res.* 59, 5938–5946.
- Burger, H., van Tol, H., Boersma, A.W., Brok, M., Wiemer, E.A., Stoter, G., Nooter, K., 2004. Imatinib mesylate (STI571) is a substrate for the breast cancer resistance protein (BCRP)/ABCG2 drug pump. *Blood* 104, 2940–2942.
- Campiglio, M., Locatelli, A., Olgiati, C., Normanno, N., Somenzi, G., Viganò, L., Fumagalli, M., Menard, S., Gianni, L., 2004. Inhibition of proliferation and induction of apoptosis in breast cancer cells by the epidermal growth factor receptor (EGFR) tyrosine kinase inhibitor ZD1839 ('Iressa') is independent of EGFR expression level. *J. Cell. Physiol.* 198, 259–268.
- Candeil, L., Gourdiere, I., Peyron, D., Vezzio, N., Copois, V., Bibeau, F., Orsetti, B., Scheffer, G.L., Ychou, M., Khan, Q.A., Pommier, Y., Pau, B., Martineau, P., Del Rio, M., 2004. ABCG2 overexpression in colon cancer cells resistant to SN38 and in irinotecan-treated metastases. *Int. J. Cancer* 109, 848–854.
- Chano, T., Mori, K., Scotlandi, K., Benini, S., Lapucci, C., Manara, M.C., Serra, M., Picci, P., Okabe, H., Baldini, N., 2004. Differentially expressed genes in multidrug resistant variants of U-2 OS human osteosarcoma cells. *Oncol. Rep.* 11, 1257–1263.
- Chen, J.S., Lan, K., Hung, M.C., 2003. Strategies to target HER2/neu overexpression for cancer therapy. *Drug Resist. Update* 6, 129–136.
- Ciardello, F., Tortora, G., 2002. Anti-epidermal growth factor receptor drugs in cancer therapy. *Expert. Opin. Investig. Drugs* 11, 755–768.
- Ciardello, F., Tortora, G., 2003. Epidermal growth factor receptor (EGFR) as a target in cancer therapy: understanding the role of receptor expression and other molecular determinants that could influence the response to anti-EGFR drugs. *Eur. J. Cancer* 39, 1348–1354.
- Cohen, M.H., Williams, G.A., Sridhara, R., Chen, G., McGuinn Jr., W.D., Morse, D., Abraham, S., Rahman, A., Liang, C., Lostritto, R., Baird, A., Pazdur, R., 2004. United States Food and Drug Administration Drug Approval summary: Gefitinib (ZD1839; Iressa) tablets. *Clin. Cancer Res.* 10, 1212–1218.
- Cooray, H.C., Blackmore, C.G., Maskell, L., Barrand, M.A., 2002. Localisation of breast cancer resistance protein in microvessel endothelium of human brain. *Neuroreport* 13, 2059–2063.
- Dai, Y., Rahmani, M., Corey, S.J., Dent, P., Grant, S., 2004. A Bcr/Abl-independent, Lyn-dependent form of imatinib mesylate (STI-571) resistance is associated with altered expression of Bcl-2. *J. Biol. Chem.* 279, 34227–34239.
- Dancey, J.E., Freidlin, B., 2003. Targeting epidermal growth factor receptor—are we missing the mark? *Lancet* 362, 62–64.
- Daub, H., Specht, K., Ullrich, A., 2004. Strategies to overcome resistance to targeted protein kinase inhibitors. *Nat. Rev. Drug Discov.* 3, 1001–1010.
- de Jong, F.A., Marsh, S., Mathijssen, R.H., King, C., Verweij, J., Sparreboom, A., McLeod, H.L., 2004. ABCG2 pharmacogenetics: ethnic differences in allele frequency and assessment of influence on irinotecan disposition. *Clin. Cancer Res.* 10, 5889–5894.
- de Silva, C.M., Reid, R., 2003. Gastrointestinal stromal tumors (GIST): C-kit mutations, CD117 expression, differential diagnosis and targeted cancer therapy with Imatinib. *Pathol. Oncol. Res.* 9, 13–19.
- Deeley, R.G., Cole, S.P., 2003. Multidrug Resistance Protein 1 (ABCC1). In: Holland, I.B., Cole, S.P., Kuchler, K., Higgins, C.F. (Eds.), *ABC Proteins from Bacteria to Man*. Academic Press, London, pp. 393–422.
- Deininger, M.W., 2004. Basic science going clinical: molecularly targeted therapy of chronic myelogenous leukemia. *J. Cancer Res. Clin. Oncol.* 130, 59–72.
- Deininger, M.W., Druker, B.J., 2003. Specific targeted therapy of chronic myelogenous leukemia with imatinib. *Pharmacol. Rev.* 55, 401–423.
- Dietrich, C.G., Geier, A., Oude Elferink, R.P., 2003. ABC of oral bioavailability: transporters as gatekeepers in the gut. *Gut* 52, 1788–1795.
- Doyle, L.A., Ross, D.D., 2003. Multidrug resistance mediated by the breast cancer resistance protein BCRP (ABCG2). *Oncogene* 22, 7340–7358.
- Dreves, J., 2003. PTK/ZK (Novartis). *IDrugs* 6, 787–794.
- Duensing, A., Heinrich, M.C., Fletcher, C.D., Fletcher, J.A., 2004. Biology of gastrointestinal stromal tumors: KIT mutations and beyond. *Cancer Invest.* 22, 106–116.
- Elkind, N., Szentpetery, Z., Apati, A., Özvegy-Laczka, C., Varady, G., Ujhelyi, O., Szabo, K., Homolya, L., Varadi, A., Buday, L., Keri, G., Nemet, K., Sarkadi, B., 2005. The multidrug transporter ABCG2

- prevents tumor cell death induced by the EGF receptor inhibitor Iressa (ZD1839, Gefitinib). *Cancer Res.* 65.
- Erllichman, C., Boerner, S.A., Hallgren, C.G., Spieker, R., Wang, X.Y., James, C.D., Scheffer, G.L., Maliepaard, M., Ross, D.D., Bible, K.C., Kaufmann, S.H., 2001. The HER tyrosine kinase inhibitor CI1033 enhances cytotoxicity of 7-ethyl-10-hydroxycamptothecin and topotecan by inhibiting breast cancer resistance protein-mediated drug efflux. *Cancer Res.* 61, 739–748.
- Ferrao, P.T., Frost, M.J., Siah, S.P., Ashman, L.K., 2003. Overexpression of P-glycoprotein in K562 cells does not confer resistance to the growth inhibitory effects of imatinib (STI571) in vitro. *Blood* 102, 4499–4503.
- Fletcher, J.A., 2004. Role of KIT and platelet-derived growth factor receptors as oncoproteins. *Semin. Oncol.* 31, 4–11.
- Friedrich, R.E., Punke, C., Reymann, A., 2004. Expression of multi-drug resistance genes (mdr1, mrp1, bcrp) in primary oral squamous cell carcinoma. *In Vivo* 18, 133–147.
- Galimberti, S., Guerrini, F., Palumbo, G.A., Consoli, U., Fazzi, R., Morabito, F., Santini, V., Petrini, M., 2004. Evaluation of BCRP and MDR-1 co-expression by quantitative molecular assessment in AML patients. *Leukoc. Res.* 28, 367–372.
- Gambacorti-Passerini, C., Zucchetti, M., Russo, D., Frapolli, R., Verga, M., Bungaro, S., Tornaghi, L., Rossi, F., Pioltelli, P., Pogliani, E., Alberti, D., Corneo, G., D'Incalci, M., 2003. Alpha1 acid glycoprotein binds to imatinib (STI571) and substantially alters its pharmacokinetics in chronic myeloid leukemia patients. *Clin. Cancer Res.* 9, 625–632.
- Giaccone, G., 2004. The role of gefitinib in lung cancer treatment. *Clin. Cancer Res.* 10, 4233s–4237s.
- Gottesman, M.M., Pastan, I., Ambudkar, S.V., 1996. P-glycoprotein and multidrug resistance. *Curr. Opin. Genet. Dev.* 6, 610–617.
- Grandis, J.R., Sok, J.C., 2004. Signaling through the epidermal growth factor receptor during the development of malignancy. *Pharmacol. Ther.* 102, 37–46.
- Gschwind, A., Fischer, O.M., Ullrich, A., 2004. The discovery of receptor tyrosine kinases: targets for cancer therapy. *Nat. Rev. Cancer* 4, 361–370.
- Hegedus, T., Orfi, L., Seprodi, A., Varadi, A., Sarkadi, B., Keri, G., 2002. Interaction of tyrosine kinase inhibitors with the human multidrug transporter proteins, MDR1 and MRP1. *Biochim. Biophys. Acta* 1587, 318–325.
- Herbst, R.S., 2004. Review of epidermal growth factor receptor biology. *Int. J. Radiat. Oncol. Biol. Phys.* 59, 21–26.
- Herbst, R.S., Fukuoka, M., Baselga, J., 2004a. Gefitinib—a novel targeted approach to treating cancer. *Nat. Rev. Cancer* 4, 956–965.
- Herbst, R.S., Giaccone, G., Schiller, J.H., Natale, R.B., Miller, V., Manegold, C., Scagliotti, G., Rosell, R., Oliff, I., Reeves, J.A., Wolf, M.K., Krebs, A.D., Averbuch, S.D., Ochs, J.S., Grous, J., Fandi, A., Johnson, D.H., 2004b. Gefitinib in combination with paclitaxel and carboplatin in advanced non-small-cell lung cancer: a phase III trial—INTACT 2. *J. Clin. Oncol.* 22, 785–794.
- Higgins, C.F., 1992. ABC transporters: from microorganisms to man. *Annu. Rev. Cell Biol.* 8, 67–113.
- Hirschmann-Jax, C., Foster, A.E., Wulf, G.G., Nuchtern, J.G., Jax, T.W., Gobel, U., Goodell, M.A., Brenner, M.K., 2004. A distinct “side population” of cells with high drug efflux capacity in human tumor cells. *Proc. Natl. Acad. Sci. U.S.A.* 101, 14228–14233.
- Honjo, Y., Morisaki, K., Huff, L.M., Robey, R.W., Hung, J., Dean, M., Bates, S.E., 2002. Single-nucleotide polymorphism (SNP) analysis in the ABC half-transporter ABCG2 (MXR/BCRP/ABCP1). *Cancer Biol. Ther.* 1, 696–702.
- Houghton, P.J., Germain, G.S., Harwood, F.C., Schuetz, J.D., Stewart, C.F., Buchdunger, E., Traxler, P., 2004. Imatinib mesylate is a potent inhibitor of the ABCG2 (BCRP) transporter and reverses resistance to topotecan and SN-38 in vitro. *Cancer Res.* 64, 2333–2337.
- Iida, A., Saito, S., Sekine, A., Mishima, C., Kitamura, Y., Kondo, K., Harigae, S., Osawa, S., Nakamura, Y., 2002. Catalog of 605 single-nucleotide polymorphisms (SNPs) among 13 genes encoding human ATP-binding cassette transporters: ABCA4, ABCA7, ABCA8, ABCD1, ABCD3, ABCD4, ABCE1, ABCF1, ABCG1, ABCG2, ABCG4, ABCG5, and ABCG8. *J. Hum. Genet.* 47, 285–310.
- Imai, Y., Nakane, M., Kage, K., Tsukahara, S., Ishikawa, E., Tsuruo, T., Miki, Y., Sugimoto, Y., 2002. C421A polymorphism in the human breast cancer resistance protein gene is associated with low expression of Q141K protein and low-level drug resistance. *Mol. Cancer Ther.* 1, 611–616.
- Inoue, A., Saijo, Y., Maemondo, M., Gomi, K., Tokue, Y., Kimura, Y., Ebina, M., Kikuchi, T., Moriya, T., Nukiwa, T., 2003. Severe acute interstitial pneumonia and gefitinib. *Lancet* 361, 137–139.
- Itoda, M., Saito, Y., Shirao, K., Minami, H., Ohtsu, A., Yoshida, T., Saijo, N., Suzuki, H., Sugiyama, Y., Ozawa, S., Sawada, J., 2003. Eight single nucleotide polymorphisms in ABCG2/BCRP in Japanese cancer patients administered irinotecan. *Drug Metab. Pharmacokin.* 18, 212–217.
- Janmaat, M.L., Giaccone, G., 2003. Small-molecule epidermal growth factor receptor tyrosine kinase inhibitors. *Oncologist* 8, 576–586.
- Jonker, J.W., Buitelaar, M., Wagenaar, E., Van Der Valk, M.A., Scheffer, G.L., Scheper, R.J., Plosch, T., Kuipers, F., Elferink, R.P., Rosing, H., Beijnen, J.H., Schinkel, A.H., 2002. The breast cancer resistance protein protects against a major chlorophyll-derived dietary phototoxin and protoporphyria. *Proc. Natl. Acad. Sci. U.S.A.* 99, 15649–15654.
- Jonker, J.W., Smit, J.W., Brinkhuis, R.F., Maliepaard, M., Beijnen, J.H., Schellens, J.H., Schinkel, A.H., 2000. Role of breast cancer resistance protein in the bioavailability and fetal penetration of topotecan. *J. Natl. Cancer Inst.* 92, 1651–1656.
- Kawabata, S., Oka, M., Soda, H., Shiozawa, K., Nakatomi, K., Tsurutani, J., Nakamura, Y., Doi, S., Kitazaki, T., Sugahara, K., Yamada, Y., Kamihira, S., Kohno, S., 2003. Expression and functional analyses of breast cancer resistance protein in lung cancer. *Clin. Cancer Res.* 9, 3052–3057.
- Kim, R., Toge, T., 2004. Changes in therapy for solid tumors: potential for overcoming drug resistance in vivo with molecular targeting agents. *Surg. Today* 34, 293–303.
- Kobayashi, D., Ieiri, I., Hirota, T., Takane, H., Maegawa, S., Kigawa, J., Suzuki, H., Nanba, E., Oshimura, M., Terakawa, N., Otsubo, K., Mine, K., Sugiyama, Y., 2005. Functional assessment of abcg2 (bcrp) gene polymorphisms to protein expression in human placenta. *Drug Metab. Dispos.* 33, 94–101.
- Krishnamurthy, P., Ross, D.D., Nakanishi, T., Bailey-Dell, K., Zhou, S., Mercer, K.E., Sarkadi, B., Sorrentino, B.P., Schuetz, J.D., 2004. The stem cell marker Bcrp/ABCG2 enhances hypoxic cell survival through interactions with heme. *J. Biol. Chem.* 279, 24218–24225.
- Langer, C.J., 2004. Emerging role of epidermal growth factor receptor inhibition in therapy for advanced malignancy: focus on NSCLC. *Int. J. Radiat. Oncol. Biol. Phys.* 58, 991–1002.
- Leonard, G.D., Fojo, T., Bates, S.E., 2003. The role of ABC transporters in clinical practice. *Oncologist* 8, 411–424.
- Logrono, R., Jones, D.V., Faruqi, S., Bhutani, M.S., 2004. Recent advances in cell biology, diagnosis, and therapy of gastrointestinal stromal tumor (GIST). *Cancer Biol. Ther.* 3, 251–258.
- Luo, C., Laaja, P., 2004. Inhibitors of JAKs/STATs and the kinases: a possible new cluster of drugs. *Drug Discov. Today* 9, 268–275.
- Lynch, T.J., Bell, D.W., Sordella, R., Gurubhagavatula, S., Okimoto, R.A., Brannigan, B.W., Harris, P.L., Haserlat, S.M., Supko, J.G., Haluska, F.G., Louis, D.N., Christiani, D.C., Settleman, J., Haber, D.A., 2004. Activating mutations in the epidermal growth factor receptor underlying responsiveness of non-small-cell lung cancer to gefitinib. *N. Engl. J. Med.* 350, 2129–2139.
- Mahon, F.X., Belloc, F., Lagarde, V., Chollet, C., Moreau-Gaudry, F., Reiffers, J., Goldman, J.M., Melo, J.V., 2003. MDR1 gene overex-

- pression confers resistance to imatinib mesylate in leukemia cell line models. *Blood* 101, 2368–2373.
- Mahon, F.X., Deininger, M.W., Schultheis, B., Chabrol, J., Reiffers, J., Goldman, J.M., Melo, J.V., 2000. Selection and characterization of BCR-ABL positive cell lines with differential sensitivity to the tyrosine kinase inhibitor STI571: diverse mechanisms of resistance. *Blood* 96, 1070–1079.
- Maliepaard, M., Scheffer, G.L., Faneyte, I.F., van Gastelen, M.A., Pijnenborg, A.C., Schinkel, A.H., van De Vijver, M.J., Scheper, R.J., Schellens, J.H., 2001. Subcellular localization and distribution of the breast cancer resistance protein transporter in normal human tissues. *Cancer Res.* 61, 3458–3464.
- Manley, P.W., Bold, G., Bruggen, J., Fendrich, G., Furet, P., Mestan, J., Schnell, C., Stolz, B., Meyer, T., Meyhack, B., Stark, W., Strauss, A., Wood, J., 2004. Advances in the structural biology, design and clinical development of VEGF-R kinase inhibitors for the treatment of angiogenesis. *Biochim. Biophys. Acta* 1697, 17–27.
- McArthur, G., 2004. Molecularly targeted treatment for dermatofibrosarcoma protuberans. *Semin. Oncol.* 31, 30–36.
- Melo, J.V., Hughes, T.P., Apperley, J.F., 2003. Chronic myeloid leukemia. *Hematology (Am. Soc. Hematol. Educ. Program)*, 132–152.
- Miyake, K., Mickley, L., Litman, T., Zhan, Z., Robey, R., Cristensen, B., Brangi, M., Greenberger, L., Dean, M., Fojo, T., Bates, S.E., 1999. Molecular cloning of cDNAs which are highly overexpressed in mitoxantrone-resistant cells: demonstration of homology to ABC transport genes. *Cancer Res.* 59, 8–13.
- Mizuarai, S., Aozasa, N., Kotani, H., 2004. Single nucleotide polymorphisms result in impaired membrane localization and reduced ATPase activity in multidrug transporter ABCG2. *Int. J. Cancer* 109, 238–246.
- Mizuno, N., Suzuki, M., Kusuhara, H., Suzuki, H., Takeuchi, K., Niwa, T., Jonker, J.W., Sugiyama, Y., 2004. Impaired renal excretion of 6-hydroxy-5,7-dimethyl-2-methylamino-4-(3-pyridylmethyl) benzothiazole (E3040) sulfate in breast cancer resistance protein (BCRP1/ABCG2) knockout mice. *Drug Metab. Dispos.* 32, 898–901.
- Morisaki, K., Robey, R., Ozvegy-Laczka, C., Honjo, Y., Polgar, O., Steadman, K., Sarkadi, B., Bates, S., in press. Single nucleotide polymorphisms modify the transporter activity of ABCG2. *Cancer Chemother. Pharmacol.*
- Mukai, M., Che, X.F., Furukawa, T., Sumizawa, T., Aoki, S., Ren, X.Q., Haraguchi, M., Sugimoto, Y., Kobayashi, M., Takamatsu, H., Akiyama, S., 2003. Reversal of the resistance to STI571 in human chronic myelogenous leukemia K562 cells. *Cancer Sci.* 94, 557–563.
- Nakanishi, T., Karp, J.E., Tan, M., Doyle, L.A., Peters, T., Yang, W., Wei, D., Ross, D.D., 2003. Quantitative analysis of breast cancer resistance protein and cellular resistance to flavopiridol in acute leukemia patients. *Clin. Cancer Res.* 9, 3320–3328.
- Nardi, V., Azam, M., Daley, G.Q., 2004. Mechanisms and implications of imatinib resistance mutations in BCR-ABL. *Curr. Opin. Hematol.* 11, 35–43.
- Nimmanapalli, R., Bhalla, K., 2002. Mechanisms of resistance to imatinib mesylate in Bcr-Abl-positive leukemias. *Curr. Opin. Oncol.* 14, 616–620.
- Noble, M.E., Endicott, J.A., Johnson, L.N., 2004. Protein kinase inhibitors: insights into drug design from structure. *Science* 303, 1800–1805.
- O'Dwyer, M.E., Mauro, M.J., Druker, B.J., 2003. STI571 as a targeted therapy for CML. *Cancer Invest.* 21, 429–438.
- O'Farrell, A.M., Abrams, T.J., Yuen, H.A., Ngai, T.J., Louie, S.G., Yee, K.W., Wong, L.M., Hong, W., Lee, L.B., Town, A., Smolich, B.D., Manning, W.C., Murray, L.J., Heinrich, M.C., Cherrington, J.M., 2003. SU11248 is a novel FLT3 tyrosine kinase inhibitor with potent activity in vitro and in vivo. *Blood* 101, 3597–3605.
- Ozvegy-Laczka, C., Hegedus, T., Varady, G., Ujhelly, O., Schuetz, J.D., Varadi, A., Keri, G., Orfi, L., Nemet, K., Sarkadi, B., 2004. High-affinity interaction of tyrosine kinase inhibitors with the ABCG2 multidrug transporter. *Mol. Pharmacol.* 65, 1485–1495.
- Paez, J.G., Janne, P.A., Lee, J.C., Tracy, S., Greulich, H., Gabriel, S., Herman, P., Kaye, F.J., Lindeman, N., Boggon, T.J., Naoki, K., Sasaki, H., Fujii, Y., Eck, M.J., Sellers, W.R., Johnson, B.E., Meyerson, M., 2004. EGFR mutations in lung cancer: correlation with clinical response to gefitinib therapy. *Science* 304, 1497–1500.
- Pao, W., Miller, V., Zakowski, M., Doherty, J., Politi, K., Sarkaria, I., Singh, B., Heelan, R., Rusch, V., Fulton, L., Mardis, E., Kupfer, D., Wilson, R., Kris, M., Varmus, H., 2004. EGF receptor gene mutations are common in lung cancers from “never smokers” and are associated with sensitivity of tumors to gefitinib and erlotinib. *Proc. Natl. Acad. Sci. U.S.A.* 101, 13306–13311.
- Parra, H.S., Cavina, R., Latteri, F., Zucali, P.A., Campagnoli, E., Morengi, E., Grimaldi, G.C., Roncalli, M., Santoro, A., 2004. Analysis of epidermal growth factor receptor expression as a predictive factor for response to gefitinib (‘Iressa’, ZD1839) in non-small-cell lung cancer. *Br. J. Cancer* 91, 208–212.
- Robey, R.W., Medina-Perez, W.Y., Nishiyama, K., Lahusen, T., Miyake, K., Litman, T., Senderowicz, A.M., Ross, D.D., Bates, S.E., 2001. Overexpression of the ATP-binding cassette half-transporter, ABCG2 (Mxr/BCRP/ABCP1), in flavopiridol-resistant human breast cancer cells. *Clin. Cancer Res.* 7, 145–152.
- Robinson, D.R., Wu, Y.M., Lin, S.F., 2000. The protein tyrosine kinase family of the human genome. *Oncogene* 19, 5548–5557.
- Roskoski Jr., R., 2003. STI-571: an anticancer protein-tyrosine kinase inhibitor. *Biochem. Biophys. Res. Commun.* 309, 709–717.
- Rowinsky, E.K., 2003. Signal events: cell signal transduction and its inhibition in cancer. *Oncologist* 8 (Suppl. 3), 5–17.
- Savage, D.G., Antman, K.H., 2002. Imatinib mesylate—a new oral targeted therapy. *N. Engl. J. Med.* 346, 683–693.
- Sawaki, A., Yamao, K., 2004. Imatinib mesylate acts in metastatic or unresectable gastrointestinal stromal tumor by targeting KIT receptors—a review. *Cancer Chemother. Pharmacol.* 54 (Suppl. 1), S44–S49.
- Shah, N.P., Sawyers, C.L., 2003. Mechanisms of resistance to STI571 in Philadelphia chromosome-associated leukemias. *Oncogene* 22, 7389–7395.
- She, Q.B., Solit, D., Basso, A., Moasser, M.M., 2003. Resistance to gefitinib in PTEN-null HER-overexpressing tumor cells can be overcome through restoration of PTEN function or pharmacologic modulation of constitutive phosphatidylinositol 3'-kinase/Akt pathway signaling. *Clin. Cancer Res.* 9, 4340–4346.
- Sjoblom, T., Shimizu, A., O'Brien, K.P., Pietras, K., Dal Cin, P., Buchdunger, E., Dumanski, J.P., Ostman, A., Heldin, C.H., 2001. Growth inhibition of dermatofibrosarcoma protuberans tumors by the platelet-derived growth factor receptor antagonist STI571 through induction of apoptosis. *Cancer Res.* 61, 5778–5783.
- Smith, B.D., Levis, M., Beran, M., Giles, F., Kantarjian, H., Berg, K., Murphy, K.M., Dausies, T., Allebach, J., Small, D., 2004. Single-agent CEP-701, a novel FLT3 inhibitor, shows biologic and clinical activity in patients with relapsed or refractory acute myeloid leukemia. *Blood* 103, 3669–3676.
- Sparreboom, A., Danesi, R., Ando, Y., Chan, J., Figg, W.D., 2003. Pharmacogenomics of ABC transporters and its role in cancer chemotherapy. *Drug Resist. Update* 6, 71–84.
- Stelman, L.S., Pohnert, S.C., Shelton, J.G., Franklin, R.A., Bertrand, F.E., McCubrey, J.A., 2004. JAK/STAT, Raf/MEK/ERK, PI3K/Akt and BCR-ABL in cell cycle progression and leukemogenesis. *Leukemia* 18, 189–218.
- Stewart, C.F., Leggas, M., Schuetz, J.D., Panetta, J.C., Cheshire, P.J., Peterson, J., Daw, N., Jenkins III, J.J., Gilbertson, R., Germain, G.S., Harwood, F.C., Houghton, P.J., 2004. Gefitinib enhances the antitumor activity and oral bioavailability of irinotecan in mice. *Cancer Res.* 64, 7491–7499.
- Stone, R.M., Deangelo, D.J., Klimek, V., Galinsky, I., Estey, E., Nimer, S.D., Grandin, W., Lebowitz, D., Wang, Y., Cohen, P., Fox, E.A., Neuberg, D., Clark, J., Gilliland, D.G., Griffin, J.D., 2005. Patients with acute myeloid leukemia and an activating mutation in FLT3

- respond to a small-molecule FLT3 tyrosine kinase inhibitor, PKC412. *Blood* 105, 54–60.
- Suvannasankha, A., Minderman, H., O'Loughlin, K.L., Nakanishi, T., Greco, W.R., Ross, D.D., Baer, M.R., 2004. Breast cancer resistance protein (BCRP/MXR/ABCG2) in acute myeloid leukemia: discordance between expression and function. *Leukemia* 18, 1252–1257.
- Thomas, J., Wang, L., Clark, R.E., Pirmohamed, M., 2004. Active transport of imatinib into and out of cells: implications for drug resistance. *Blood* 104, 3739–3745.
- Tsygankov, A.Y., Shore, S.K., 2004. Src: regulation, role in human carcinogenesis and pharmacological inhibitors. *Curr. Pharm. Des.* 10, 1745–1756.
- Ueda, K., Matsuo, M., Tanabe, K., Morita, K., Kioka, N., Amachi, T., 1999. Comparative aspects of the function and mechanism of SUR1 and MDR1 proteins. *Biochim. Biophys. Acta* 1461, 305–313.
- van den Heuvel-Eibrink, M.M., Wiemer, E.A., Prins, A., Meijerink, J.P., Vossebeld, P.J., van der Holt, B., Pieters, R., Sonneveld, P., 2002. Increased expression of the breast cancer resistance protein (BCRP) in relapsed or refractory acute myeloid leukemia (AML). *Leukemia* 16, 833–839.
- van der Kolk, D.M., Vellenga, E., Scheffer, G.L., Muller, M., Bates, S.E., Scheper, R.J., de Vries, E.G., 2002. Expression and activity of breast cancer resistance protein (BCRP) in de novo and relapsed acute myeloid leukemia. *Blood* 99, 3763–3770.
- van der Pol, M.A., Broxterman, H.J., Pater, J.M., Feller, N., van der Maas, M., Weijers, G.W., Scheffer, G.L., Allen, J.D., Scheper, R.J., van Loevezijn, A., Ossenkoppele, G.J., Schuurhuis, G.J., 2003. Function of the ABC transporters, P-glycoprotein, multidrug resistance protein and breast cancer resistance protein, in minimal residual disease in acute myeloid leukemia. *Haematologica* 88, 134–147.
- van Herwaarden, A.E., Jonker, J.W., Wagenaar, E., Brinkhuis, R.F., Schellens, J.H., Beijnen, J.H., Schinkel, A.H., 2003. The breast cancer resistance protein (Bcrp1/Abcg2) restricts exposure to the dietary carcinogen 2-amino-1-methyl-6-phenylimidazo[4,5-b]pyridine. *Cancer Res.* 63, 6447–6452.
- Verheul, H.M., Pinedo, H.M., 2003. Vascular endothelial growth factor and its inhibitors. *Drugs Today (Barc)* 39 (Suppl. C), 81–93.
- Vlahovic, G., Crawford, J., 2003. Activation of tyrosine kinases in cancer. *Oncologist* 8, 531–538.
- Volk, E.L., Rohde, K., Rhee, M., McGuire, J.J., Doyle, L.A., Ross, D.D., Schneider, E., 2000. Methotrexate cross-resistance in a mitoxantrone-selected multidrug-resistant MCF7 breast cancer cell line is attributable to enhanced energy-dependent drug efflux. *Cancer Res.* 60, 3514–3521.
- Warmuth, M., Damoiseaux, R., Liu, Y., Fabbro, D., Gray, N., 2003. SRC family kinases: potential targets for the treatment of human cancer and leukemia. *Curr. Pharm. Des.* 9, 2043–2059.
- Weisberg, E., Griffin, J.D., 2003. Resistance to imatinib (Gleevec): update on clinical mechanisms. *Drug Resist. Update* 6, 231–238.
- Yanase, K., Tsukahara, S., Asada, S., Ishikawa, E., Imai, Y., Sugimoto, Y., 2004. Gefitinib reverses breast cancer resistance protein-mediated drug resistance. *Mol. Cancer Ther.* 3, 1119–1125.
- Zamber, C.P., Lamba, J.K., Yasuda, K., Farnum, J., Thummel, K., Schuetz, J.D., Schuetz, E.G., 2003. Natural allelic variants of breast cancer resistance protein (BCRP) and their relationship to BCRP expression in human intestine. *Pharmacogenetics* 13, 19–28.
- Zhou, S., Schuetz, J.D., Bunting, K.D., Colapietro, A.M., Sampath, J., Morris, J.J., Lagutina, I., Grosveld, G.C., Osawa, M., Nakauchi, H., Sorrentino, B.P., 2001. The ABC transporter Bcrp1/ABCG2 is expressed in a wide variety of stem cells and is a molecular determinant of the side-population phenotype. *Nat. Med.* 7, 1028–1034.

Function-dependent Conformational Changes of the ABCG2 Multidrug Transporter Modify Its Interaction with a Monoclonal Antibody on the Cell Surface*

Received for publication, October 4, 2004, and in revised form, November 19, 2004
Published, JBC Papers in Press, November 22, 2004, DOI 10.1074/jbc.M411338200

Csilla Özvegy-Laczka^{‡§¶}, György Várady^{¶**} Gabriella Köblös[§], Olga Ujhelly^{**}, Judit Cervenak^{**}, John D. Schuetz^{‡‡}, Brian P. Sorrentino^{‡‡}, Gerrit-Jan Koomen^{§§}, András Váradi[§], Katalin Németh^{**}, and Balázs Sarkadi^{‡¶¶}

From the [‡]National Medical Center, Institute of Haematology and Immunology, Membrane Research Group and Hungarian Academy of Sciences, 1113 Budapest, Hungary, [§]Institute of Enzymology, Hungarian Academy of Sciences, 1113 Budapest, Hungary, ^{**}National Medical Center, Institute of Haematology and Immunology, Experimental Gene Therapy Unit, 1113 Budapest, Hungary, ^{‡‡}Department of Pharmaceutical Sciences and Department of Hematology, St. Jude Children's Research Hospital, Memphis, Tennessee 38105, and ^{§§}Laboratory of Organic Chemistry, Institute of Molecular Chemistry, University of Amsterdam, 1100 DE Amsterdam, The Netherlands

The human ABCG2 protein is an important primary active transporter for hydrophobic compounds in several cell types, and its overexpression causes multidrug resistance in tumors. A monoclonal antibody (5D3) recognizes this protein on the cell surface. In ABCG2-expressing cells 5D3 antibody showed a saturable labeling and inhibited ABCG2 transport and ATPase function. However, at low antibody concentrations 5D3 binding to intact cells depended on the actual conformation of the ABCG2 protein. ATP depletion or the addition of the ABCG2 inhibitor Ko143 significantly increased, whereas the vanadate-induced arrest of ABCG2 strongly decreased 5D3 binding. The binding of the 5D3 antibody to a non-functional ABCG2 catalytic center mutant (K86M) in intact cells was not affected by the addition of vanadate but still increased with the addition of Ko143. In isolated membrane fragments the ligand modulation of 5D3 binding to ABCG2 could be analyzed in detail. In this case 5D3 binding was maximum in the presence of ATP, ADP, or Ko143, whereas the non-hydrolysable ATP analog, adenosine 5'-(β,γ -imido)triphosphate (AMP-PNP), and nucleotide trapping by vanadate decreased antibody binding. In membranes expressing the ABCG2-K86M mutant, ATP, ADP, and AMP-PNP decreased, whereas Ko143 increased 5D3 binding. Based on these data we suggest that the 5D3 antibody can be used as a sensitive tool to reveal intramolecular changes, reflecting ATP binding, the formation of a catalytic intermediate, or substrate inhibition within the transport cycle of the ABCG2 protein.

The ABCG2¹ (MXR/BCRP/ABCP) protein causes multidrug resistance in cancer cells and may have an important function

* This work has been supported by OTKA Research Grants T-29921, T-35126, T-31952 and Grants NKFP 1/024/2001 and OM-2568/1999, Hungary. The costs of publication of this article were defrayed in part by the payment of page charges. This article must therefore be hereby marked "advertisement" in accordance with 18 U.S.C. Section 1734 solely to indicate this fact.

[¶] These authors contributed equally.

^{¶¶} Supported by OTKA, Hungary Postdoctoral Fellowship D45957 and the János Bolyai Scholarship of the Hungarian Academy of Sciences.

^{¶¶¶} Recipient of a Howard Hughes International Scholarship. To whom correspondence should be addressed: National Medical Center, Institute of Haematology and Immunology, 1113 Budapest, Diószegi u. 64, Hungary. Tel.: and Fax: 36-1-372-4353; E-mail: sarkadi@biomembrane.hu.

¹ The abbreviations used are: ABCG2, human MXR/BCRP/ABCP

in physiological protection of various tissues against toxic agents. ABCG2 was first cloned from the placenta, where it is most abundantly expressed (1). The overexpression of ABCG2 was observed in certain drug-resistant cell lines and tumors, providing a special multidrug-resistant phenotype in these cancer cells (2–5). The ABCG2 protein is a so-called ABC half-transporter, which has only one nucleotide binding (ABC) and one transmembrane domain and most probably works as a homodimer in the plasma membrane (6–11).

The overexpression of ABCG2 was documented in several human tumors, which indicates its possible importance in the multidrug-resistant phenotype of various cancer cells (12–15). The substrate specificity of ABCG2 partially overlaps with the other major multidrug resistance ABC transporters, MDR1 and human multidrug resistance protein 1 (MRP1); the compounds transported by ABCG2 are also large, hydrophobic molecules, including mitoxantrone, topotecan, flavopiridol, methotrexate, and Hoechst 33342 (13, 16, 17).

ABCG2 was found to be physiologically expressed in the liver, small intestine, colon, lung, kidney, adrenal, and sweat glands and in the endothelia of veins and capillaries. The functional characteristics and the tissue distribution of ABCG2 suggest a major role in the tissue protection against xenobiotics (4, 13, 18). High level expression of the ABCG2 protein and its fluorescent dye extrusion function has been suggested for the identification of bone marrow stem cells (17). Moreover, this so called "side population" of progenitor cells, actively extruding the fluorescent Hoechst 33342 dye, seems to contain pluripotent stem cells in a variety of tissue sources (17, 19–21).

The proper detection of the ABCG2 protein would be of major importance in cancer diagnostics as well as in stem cell research and stem cell-based therapeutic developments. The recent development of a monoclonal antibody specifically reacting with the human ABCG2 protein on the cell surface (17) has been a major breakthrough in this regard. This antibody was prepared by immunizing mice with intact mouse fibroblasts expressing the human ABCG2. The antibody, named 5D3, was

multidrug transporter; ABC transporters, ATP binding cassette transporters; AMP-PNP, adenosine 5'-(β,γ -imido)triphosphate; GAM-PE, goat anti-mouse phycoerythrin-conjugated secondary antibody; mAb, monoclonal antibody; MDR1, human multidrug resistance protein (P-glycoprotein, ABCB1); MX, mitoxantrone; PFA, paraformaldehyde; Sf9 cells, *Spodoptera frugiperda* ovarian cells; V_i, sodium orthovanadate; HEK cells, human embryonic kidney cells; WT, wild-type; MOPS, 4-morpholinepropanesulfonic acid.

reported to inhibit the Hoechst 33342 dye transport function of ABCG2 in intact cells (22) and was made commercially available (eBioscience). Similar antibodies have already been prepared against the human MDR1 multidrug transporter (23, 24). In the case of MDR1, several of the mAbs reacting with extracellular epitopes were found to inhibit the transport function of the protein, and the reactivity of one of these antibodies, UIC2, was reported to depend on the conformation of the MDR1 protein (23, 25–27).

In the present experiments we have studied the interaction of the anti-ABCG2 monoclonal antibody 5D3 in various cell types expressing the human ABCG2 protein and examined the effects of ABCG2 protein modulators on this interaction. We have also compared these effects to those of cell fixation and/or permeabilization and correlated ABCG2 protein detection with another monoclonal antibody, raised against an intracellular epitope of human ABCG2, BXP-21 (28). We also show here that 5D3 binding to ABCG2 in isolated membrane fragments can be analyzed, which allows a detailed investigation of the ligand modulation of antibody binding.

We found that the interaction of 5D3 with ABCG2 was strongly dependent on the modulation of the multidrug transporter protein; thus, 5D3 binding to an extracellular ABCG2 epitope was conformation-sensitive. Based on these data and on previous results for the interaction of human MDR1 protein with conformation-sensitive antibodies, we suggest a model for the transport cycle dependence of 5D3 antibody interaction with the ABCG2 protein. Our data indicate that this conformation-sensitive antibody interaction can be applied for studying the molecular mechanism and the detection of ligand interactions of ABCG2.

EXPERIMENTAL PROCEDURES

Materials—Mitoxantrone, sodium orthovanadate, propidium iodide, AMP, ADP, AMP-PNP, and ATP were purchased from Sigma. Hoechst 33342 was purchased from Molecular Probes. BXP-21 antibody was obtained from Drs. George Scheffer and Rik Scheper (Department of Pathology, Free University, Medical Center, Amsterdam, The Netherlands).

Cell Lines and Retroviral Transduction—Retrovirus-producing cells and HEK 293T cells were obtained from the American Type Culture Collection (Manassas, VA). The human PLB985 (PLB) cells were kindly provided by Dr. M. Dinauer (Department of Microbiology and Immunology, Indiana University School of Medicine, Indianapolis, IN), and the MCF-7 parental cells and the MCF-7/MX cells were gifts of Dr. Susan E. Bates (Cancer Therapeutics Branch, Center for Cancer Research, NCI, National Institutes of Health, Bethesda, MD). PG13 (29) was obtained from the American Type Culture Collection. The construction of the ABCG2 retroviral vectors and cell transduction methods were described in detail in Ujhelly *et al.* (30). Transduced cells in some cases were selected by stepwise increases in mitoxantrone or flavopiridol concentrations or single-cell-cloned for the desired level of protein expression. Sf9 cells expressing the ABCG2 protein or its K86M variant were prepared as described previously (31). In the present study we used the K86M variant introduced into the wild-type (R482) ABCG2 by cloning the NotI-SpeI fragment of pAcUW21-L/K86M-R482G (31) into the corresponding site of the pAcUW21-L/R482 vector.

Immunodetection of ABCG2—For immunoblotting, washed cells were suspended in the presence of 2 mM diisopropyl fluorophosphate in 2× Laemmli buffer and sonicated for 3 × 5 s at 4 °C. Sf9 membranes were also suspended in Laemmli buffer. The proteins separated on 7.5% SDS-polyacrylamide gels were electroblotted onto polyvinylidene difluoride membranes, and immuno-detection was performed by using the monoclonal antibody BXP-21 (500× dilution) and a horseradish peroxidase-conjugated goat anti-mouse IgG (5000× dilution, Jackson ImmunoResearch). An enhanced chemiluminescence (ECL) technique was applied to detect horseradish peroxidase activity on the blots.

For measuring ABCG2 expression by flow cytometry (BD Biosciences FACSCalibur) 5D3 primary antibody (purified anti-human ABCG2, clone 5D3, eBioscience catalog number 14-8888) or BXP-21 antibody and phycoerythrin-labeled anti-mouse secondary antibody (GAM-PE, Beckman Coulter) were used. 5D3 binding in intact cells was examined by suspending the cells in phenol red-free Hanks' balanced salt solution with additional pH stabilization by 20 mM phosphate buffer. Aliquots of

the suspension containing 3×10^5 cells were incubated with 500× diluted 5D3 primary antibody (1 μg/ml), 100× diluted BXP-21 antibody, or mouse IgG2b (1 μg/ml, as isotype control) in 50 μl of buffer for 45 min at 37 °C (all labeling experiments were carried out in shaker water bath). After washing the cells with Hanks' solution containing 0.5% bovine serum albumin, the cells were labeled by 200× diluted goat anti-mouse phycoerythrin-conjugated secondary antibody (GAM-PE, 3 μg/ml), in 50 μl of buffer for 30 min at 37 °C. After washing, the cells were resuspended in Hanks' medium, and 5D3 binding was determined at 488-nm excitation and 585/42-nm emission (FL2) wavelengths. When the labeling was carried out with paraformaldehyde (PFA)-prefixed cells, the cells were incubated in 200 μl of phosphate-buffered saline solution containing 1% paraformaldehyde for 10 min at 37 °C before the above-mentioned labeling procedure.

For obtaining PFA-fixed and -permeabilized cells, the cells were incubated in 200 μl of phosphate-buffered saline solution containing 4% paraformaldehyde and 0.05% Triton X-100 for 10 min at 37 °C. The same 0.05% Triton X-100 was present during all steps of the labeling procedure. When labeling was carried out in the presence of modifying agents (5 μM Ko143, 10 mM sodium orthovanadate, 50 μM flavopiridol, or 5 μM mitoxantrone), the cells were preincubated with these agents for 10 min at 37 °C before labeling, and the agents were present during antibody labeling. When applicable, ATP depletion of the cells was carried out before the labeling procedure by washing the cells twice in sugar-free Hanks' medium and 30 min of incubation at 37 °C in Hanks' medium containing 50 mM 2-deoxy-D-glucose and 15 mM sodium azide. During cell labeling and washing the media contained the same ATP-depleting agents.

Isolated membrane fragments from Sf9 cells (45 μg) were labeled with 1 μg/ml 5D3 (or mouse IgG2b as isotype control) in the 100-μl final volume of assay mix (40 mM MOPS-Tris, pH 7.0, 5 mM sodium azide, 50 mM KCl, 2 mM dithiothreitol, and 500 μM EGTA-Tris, pH 7.0) for 30 min at 37 °C. The membranes were then washed with 500 μl of assay mix and pelleted at $10,000 \times g$ for 4 min. The pellet was suspended in assay mix containing 1 μg/ml GAM-PE and incubated at 37 °C for 30 min. The membranes were then washed and centrifuged ($10,000 \times g$ for 4 min). Finally, the pellet was suspended in 200 μl of assay mix, and the fluorescence was detected in a fluorescence plate reader (Fluoroskan II, Labsystems) at 485 nm (excitation)/590 nm (emission). When the effects of different agents were investigated the membranes were preincubated in assay mix containing 2 mM sodium orthovanadate, 1 μM Ko143, 10 mM MgAMP, MgADP, MgAMP-PNP, MgATP, or 10 mM AMP, ADP, AMP-PNP, ATP plus 2 mM EDTA, or the combination of these agents (as described in Fig. 7, panels C and D) for 5 min at 37 °C before the addition of the 5D3 antibody. The relative level of 5D3 binding was calculated as $(F_x - F_{IT})/(F_0 - F_{IT}) \times 100$, where F_x is fluorescence measured in the presence of 5D3 and the investigated compound, F_{IT} is fluorescence measured in the presence of mouse IgG2b (isotype control), and F_0 is fluorescence measured in the presence of 5D3 alone.

Cellular Mitoxantrone Uptake—The drug extrusion function of ABCG2 in intact cells was evaluated by the mitoxantrone (MX) uptake assay of Robey *et al.* (32) as modified by Ujhelly *et al.* (30). After 5D3 labeling at 37 °C for 30 min and washing (as described for immunolabeling), the cells were suspended in phenol red-free Hanks' balanced salt solution containing 5 μM MX or 5 μM MX plus 5 μM Ko143 (in some experiments 10 mM sodium orthovanadate or 50 μM flavopiridol) and incubated at 37 °C for 30 min. After washing, MX fluorescence was analyzed by flow cytometry (FACSCalibur, BD Biosciences) at 635 nm excitation and 661/16 nm emission wavelengths (FL4). Dead cells were excluded based on propidium iodide (5 μg/ml) staining.

Measurement of Hoechst 33342 Transport Activity—Accumulation of Hoechst dye was performed by using intact PLB-ABCG2 (R482), PLB-MDR1, or parental PLB cells (30) in a fluorescence spectrophotometer (PerkinElmer Life Sciences LS 50B) at 350 nm (excitation)/460 nm (emission). The cells (3×10^5) were incubated with or without 12 μg of 5D3 antibody in a 100 μl final volume of the transport buffer (120 mM NaCl, 5 mM KCl, 400 μM MgCl₂, 40 μM CaCl₂, 10 mM HEPES, 10 mM NaHCO₃, 10 mM glucose, and 5 mM Na₂HPO₄) at 37 °C for 30 min. Hoechst transport was then determined on 5D3 labeled or non-labeled cells, as described (33).

ATPase Activity Measurement—Sf9 membranes containing human ABCG2, MDR1, or ABCG2-K86M were harvested, and their membranes were isolated and stored at –80 °C according to Sarkadi *et al.* (34, 35). ATPase activity was measured as described previously by determining the liberation of inorganic phosphate from ATP with a colorimetric reaction (11). When the effect of antibody binding was investigated, membranes were preincubated with anti-ABCG2 5D3 monoclonal antibody (eBioscience) or mouse IgG2b (isotype control,

Sigma) in 20 or 160 $\mu\text{g}/\text{mg}$ membrane concentration for 30 min at 37 °C and then washed twice in ice-cold buffer (40 mM MOPS-Tris, pH 7.0, 50 mM KCl, 2 mM dithiothreitol, and 0.5 mM EDTA) before the ATPase activity measurement. The figures represent the mean values of at least three independent experiments with duplicates.

RESULTS

Antibody Detection of ABCG2—For the immuno-detection of the human ABCG2 protein in various cell types we used two monoclonal antibodies. The BXP-21 antibody was generated against an N-terminal intracellular epitope (amino acids 271–396; see Maliepaard *et al.* (28)), whereas mAb 5D3 was produced by immunizing mice with intact mouse fibroblasts expressing the human ABCG2 protein (17). As documented earlier, BXP-21 recognizes the ABCG2 protein both in immunoblots and in permeabilized cells (28). In contrast, the 5D3 antibody could be used to recognize human ABCG2 on the surface of intact cells (17) but not on immunoblots (see below).

Fig. 1 shows immunoblot detection of the human ABCG2 protein in the various cells used in the present study by mAb BXP-21. *Panel A* shows expression of human, wild-type ABCG2, or the K86M-ABCG2 variant in isolated membranes of Sf9 insect cells (11).

Panel B shows BXP-21 immunoreactions with cell lysates of PLB cells, engineered to express the wild-type ABCG2 or its

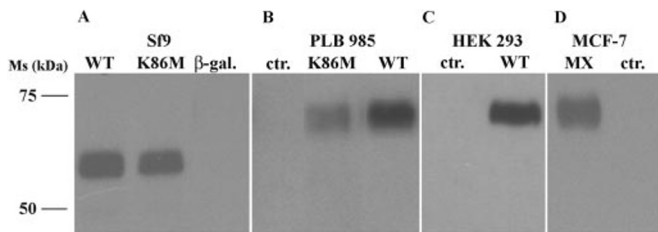


FIG. 1. Immunoblot detection of human ABCG2 by monoclonal antibody, BXP-21. Sf9 membranes containing WT ABCG2, ABCG2-K86M, or β -galactosidase (β -gal, *panel A*) and cell lysates from PLB (*panel B*), HEK 293 (*panel C*), and MCF-7/MX (*panel D*) cells expressing WT ABCG2 (or ABCG2-K86M) or parental cells (*ctr.*) were subjected to Laemmli gel electrophoresis and electroblotting. The amount of protein samples loaded on the gel was 2 μg for Sf9 membranes, HEK and MCF-7 cells, and 40 μg for PLB cells lysates. ABCG2 was detected by the BXP-21 monoclonal antibody. Experiments were performed three times, the figure shows the result of one representative experiment. *Ms*, molecular mass standards.

K86M mutant variant. The expression level of the K86M variant of ABCG2 was about one-third the expression obtained for the wild-type protein (these cells could not be selected by mitoxantrone; see “Experimental Procedures” and Ozvegy *et al.* (31)).

Fig. 1, *panel C*, documents the retrovirally evoked expression of human ABCG2 in HEK 293T cells, and *panel D* demonstrates the overexpression of ABCG2 in the mitoxantrone-selected MCF-7 cell derivative (MCF-7/MX), as detected by the BXP-21 antibody. It should be noted that, in accordance with previous results, we did not find any immuno-reactivity of the 5D3 antibody with ABCG2 on immunoblots.

Fig. 2 demonstrates the detection of ABCG2 in the parental and the ABCG2-expressing PLB cells, respectively, by flow cytometry and using the BXP-21 and the 5D3 monoclonal antibodies. In these experiments each antibody was used in a concentration of 0.2 $\mu\text{g}/10^6$ cells.

We found that in the parental PLBs the 5D3 antibody showed no immunoreactivity even if the cells were fixed by PFA or fixed and permeabilized by PFA plus Triton X-100 treatment (Fig. 2, *panel A*). When parental PLB cells were labeled with the BXP-21 antibody (Fig. 2, *panel B*), there was some background labeling observed as compared with the isotype control. However, in these parental cells BXP-21 labeling did not increase upon treatment with PFA or PFA plus Triton X-100.

As shown in Fig. 2, *panel D*, in the case of the ABCG2-expressing PLB cells, there was no reaction with the BXP-21 mAb unless the cells were both fixed and Triton-permeabilized. In this latter case a significant, ABCG2-dependent labeling of the cells by BXP-21 was found. In contrast, the 5D3 antibody showed a well visible immunoreactivity with the native ABCG2-expressing PLBs (Fig. 2, *panel C*). This reactivity was increased by PFA fixation, whereas a further permeabilization with Triton X-100 had no effect on 5D3 binding.

It has to be noted that a similar shift in 5D3 reactivity was found upon PFA fixation and independent of membrane permeabilization in all ABCG2-expressing cell types studied, including Sf9 insect cells (not shown here). The 5D3 labeling in this latter cell line indicates that the level or even the absence of *N*-glycosylation does not influence the interaction of 5D3 antibody with ABCG2.

Inhibition of ABCG2 Function by the 5D3 Antibody—The

FIG. 2. Flow cytometry detection of ABCG2 in the parental PLB (*panels A and B*) and the ABCG2-expressing PLB cells (*panels C and D*) by the 5D3 and the BXP-21 monoclonal antibodies. Effect of fixation by PFA and permeabilization by PFA plus Triton X-100. PLB cells were treated with 1% PFA (*dashed line*) or 4% PFA plus 0.05% Triton X-100 (*heavy solid line*) before 5D3 (*left panels*) or BXP-21 (*right panels*) labeling. Non-treated PLB cells (*native, solid line*) were also labeled with one of the monoclonal antibodies or isotype control (*IT, dotted line*). Fluorescence of phycoerythrin-conjugated secondary antibody was analyzed by flow cytometry (FACSCalibur, BD Biosciences). The figure shows the result of one representative experiment.

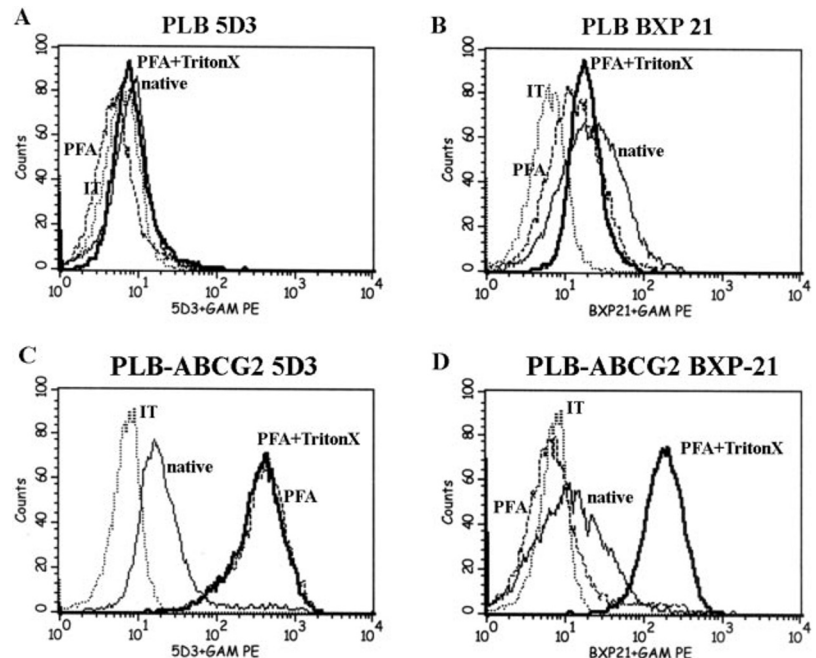
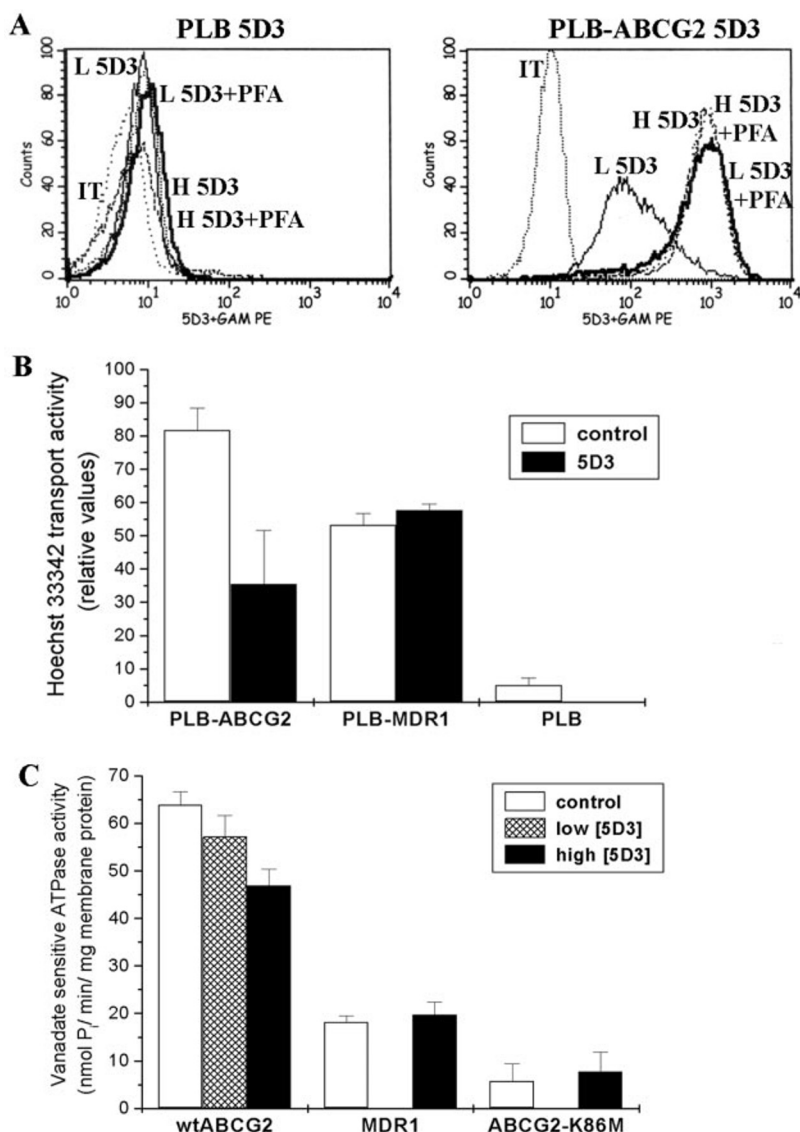


FIG. 3. Effect of 5D3 antibody concentration on the labeling (panel A) or function of ABCG2 (panels B and C). Panel A, labeling of PLB cells by 5D3. PLB parental (left) or WT ABCG2-expressing (right) cells were incubated with different concentrations of the 5D3 antibody: 0.2 $\mu\text{g}/10^6$ cells (L 5D3, solid line) or 10 $\mu\text{g}/10^6$ cells (H 5D3, dotted line) or isotype control (IT, dotted line). Cells fixed with 1% PFA were also labeled with 0.2 μg (L 5D3 + PFA, heavy solid line) or 10 μg (H 5D3 + PFA, dashed line)/ 10^6 cells 5D3 concentrations. Fluorescence of phycoerythrin-conjugated secondary antibody was analyzed by flow cytometry (FACSCalibur, BD Biosciences). Panel B, inhibition of the Hoechst 33342 dye transport by the 5D3 antibody in PLB cells. 3×10^5 PLB cells expressing WT ABCG2 or MDR1 and control cells were incubated with (5D3, black columns) or without (control, white columns) 12 μg of 5D3, and then Hoechst transport activity was measured in a fluorescence spectrophotometer (PerkinElmer Life Sciences LS 50B) at 350 nm (excitation)/460 nm (emission). Hoechst transport was determined as described under "Experimental Procedures." Panel C, inhibition of the ABCG2-ATPase activity in isolated Sf9 cell membranes by the 5D3 antibody. Sf9 membranes containing WT ABCG2, ABCG2-K86M, or MDR1 were incubated with 20 (low 5D3, hatched columns) or 160 μg (high 5D3, black columns)/mg membrane concentration of 5D3 antibody. ATPase activity was determined in 5D3-labeled or -non-labeled (control, white columns) membranes by measuring vanadate-sensitive inorganic phosphate liberation by colorimetric detection of inorganic phosphate liberation. Data points represent the mean \pm S.D. values of at least four measurements.



data presented in Fig. 2 were obtained with relatively low concentrations of the 5D3 antibody (0.2 $\mu\text{g}/10^6$ cells). By increasing the antibody concentration up to 10 $\mu\text{g}/10^6$ cells, a saturable level of ABCG2 labeling could be achieved that was not significantly modified by PFA fixation (Fig. 3A).

To investigate the effect of 5D3 on the ABCG2 function, we preincubated the PLB-ABCG2 cells with the 5D3 antibody (40 $\mu\text{g}/10^6$ cells) and then measured Hoechst 33342 dye extrusion. As shown in Fig. 3B, at high 5D3 concentrations (40 $\mu\text{g}/10^6$ cells), a significant ($p = 0.002$), about 65% inhibition of dye transport, was observed. In contrast, 5D3 did not inhibit the Hoechst dye transport measured in MDR1-expressing PLBs. In addition, the anti-MDR1 inhibitory monoclonal antibody, UIC2, inhibited Hoechst 33342 extrusion in the MDR1-expressing cells but did not modify the transport activity in the PLB-ABCG2 cells (not shown).

To further explore the ABCG2 inhibitory potential and selectivity of the 5D3 antibody, we have performed direct ABCG2-ATPase measurements in isolated Sf9 cell membranes (Fig. 3C). In these experiments we preincubated the isolated membranes for 30 min at 37 °C with two different 5D3 concentrations (20 and 160 μg of 5D3/mg of membrane protein, respectively) in the absence of ATP to assure maximum 5D3 labeling of ABCG2 (see below). We found that the application of the lower, 20 $\mu\text{g}/\text{mg}$ membrane 5D3 concentration, although at

least 20 times greater than that used in the whole-cell experiments, did not significantly affect the ABCG2-ATPase ($p = 0.1$). However, when the ATPase activity was measured after labeling with 160 μg of 5D3/mg of membrane protein, a significant ($p = 0.007$), about 30% decrease in the vanadate-sensitive ATPase activity of ABCG2 was observed. No inhibition was seen in the presence of similar concentrations of an isotype control antibody. There was no effect of 5D3 antibody on the ATPase activity of MDR1 or ABCG2-K86M membranes. All these data indicate that the 5D3 antibody, when applied in high concentrations, specifically inhibits the transport and ATPase function of the ABCG2 protein.

Effects of ABCG2 Inhibitors on 5D3 Reactivity and Mitochondrion Transport by ABCG2 in Intact Cells—In the following experiments we have studied the effects of a specific ABCG2 inhibitor, Ko143 (36), and the general ABC transporter inhibitor, sodium orthovanadate (V_i) on the binding of 5D3 antibody in intact cells by flow cytometry. The 5D3-labeling conditions were as described for Fig. 2; that is, relatively low antibody concentrations were applied. In the same cells we have also measured MX accumulation by using a different fluorescence detection channel (see "Experimental Procedures").

As shown in Fig. 4, panel A, in the parental PLB cells 5D3 reactivity was negligible and unchanged by the addition of

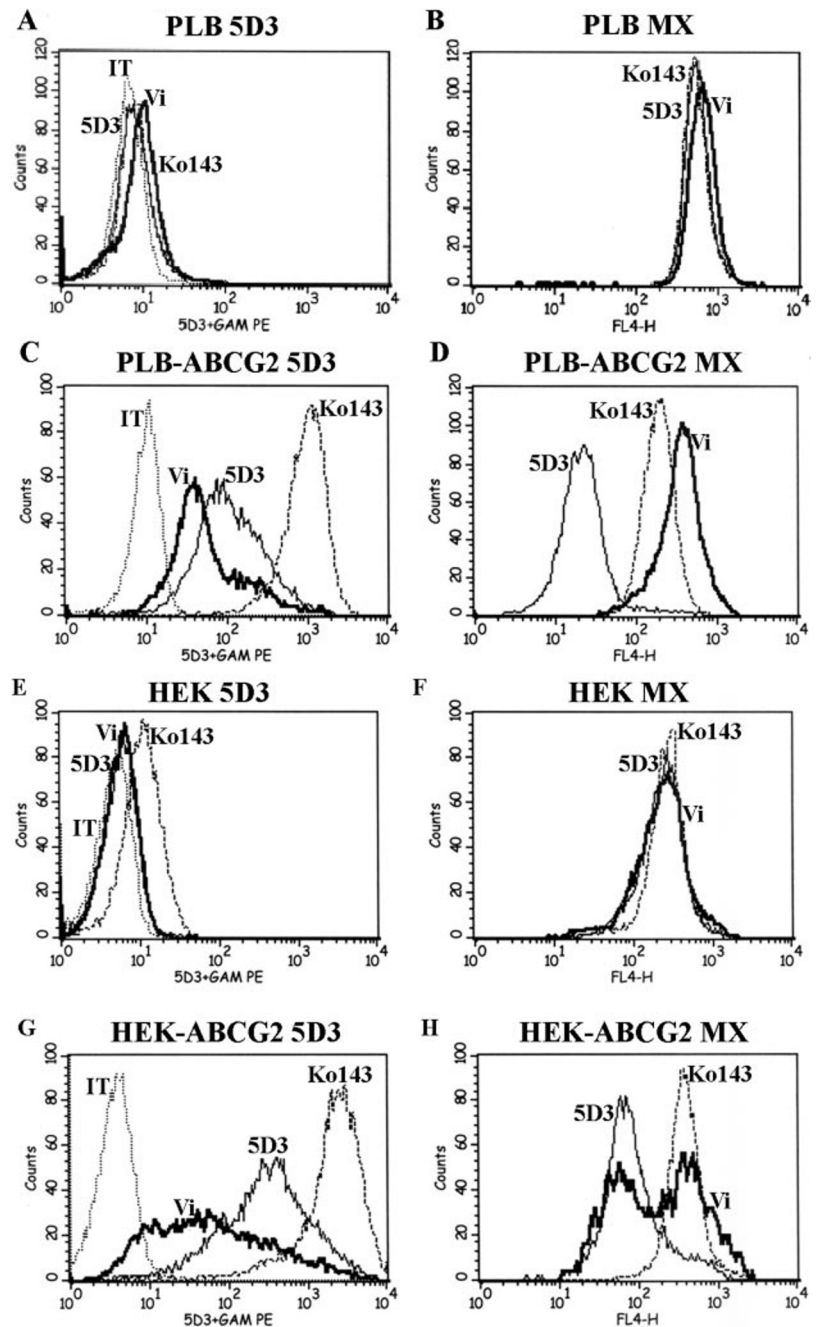


FIG. 4. Flow cytometry detection of 5D3 mAb binding and MX extrusion by ABCG2 in intact cells. Effects of Ko143 and sodium orthovanadate. *Panels A and B* show parental PLB cells, and *panels C and D* represent ABCG2-expressing PLBs. *Panels E and F* show parental HEK 293 cells, and *G and H* show HEK 293 cells expressing ABCG2. Cells were incubated with $0.2 \mu\text{g}$ of 5D3 antibody/ 10^6 cells without (5D3, *solid line*) or with the addition of $5 \mu\text{M}$ Ko143 (*dashed line*) or 2 mM sodium orthovanadate (V_i , *heavy solid line*). IT means isotype control (*dotted line*). MX accumulation was measured on 5D3-labeled cells in the absence (5D3, *solid line*) or presence of $5 \mu\text{M}$ Ko143 (*dashed line*) or 2 mM sodium orthovanadate (*heavy solid line*). Experiments were performed three times. The figure shows the result of one representative experiment.

Ko143 or sodium orthovanadate (V_i). MX accumulation in the same cells reached a high level and was unaffected by the presence of Ko143 or V_i (Fig. 4, *panel B*).

In the ABCG2-expressing PLBs we found a low, but measurable 5D3 reactivity (Fig. 4, *panel C*) that was greatly increased by Ko143 while slightly reduced by the addition of sodium orthovanadate. In the parallel MX uptake experiments (*panel D*), in the ABCG2-expressing PLBs MX accumulation was reduced, as compared with that found in the parental cells. ABCG2 inhibition by both Ko143 and V_i significantly increased intracellular MX levels, similar to that seen in cells not expressing ABCG2. Cell labeling with 5D3 at these low antibody concentrations did not cause any change in MX uptake.

According to these results both Ko143 and V_i blocked the ABCG2 transporter function, but Ko143 increased, whereas V_i decreased 5D3 binding on the cell surface. On the other hand, 5D3 labeling at this lower antibody concentration did not inhibit MX transport activity of ABCG2 (see "Discussion").

When we analyzed 5D3 binding and MX uptake in other ABCG2-expressing mammalian cell types, we found a similar modulation of 5D3 binding and MX transport by these inhibitors. The data presented in Fig. 4, *panel G*, document that in ABCG2-transduced HEK 293T cells 5D3 binding was decreased by V_i treatment and increased by Ko143. As shown in *panel H*, MX transport in these cells was inhibited by both inhibitors (interestingly, vanadate preincubation could not block MX extrusion in all HEK cells; a variable population of transporting cells was still observed in these experiments). Parental HEK cells did not show a significant ABCG2 expression or MX transport activity (*panels E and F*).

We obtained essentially similar data in the MCF-7/MX cells and the PLBs expressing the gain-of-function R482G mutant of ABCG2 (not shown). As a summary, the addition of Ko143 and V_i treatment blocked ABCG2 function in all these cell types, and Ko143 significantly increased, whereas sodium orthovanadate decreased 5D3 binding to the ABCG2 protein.

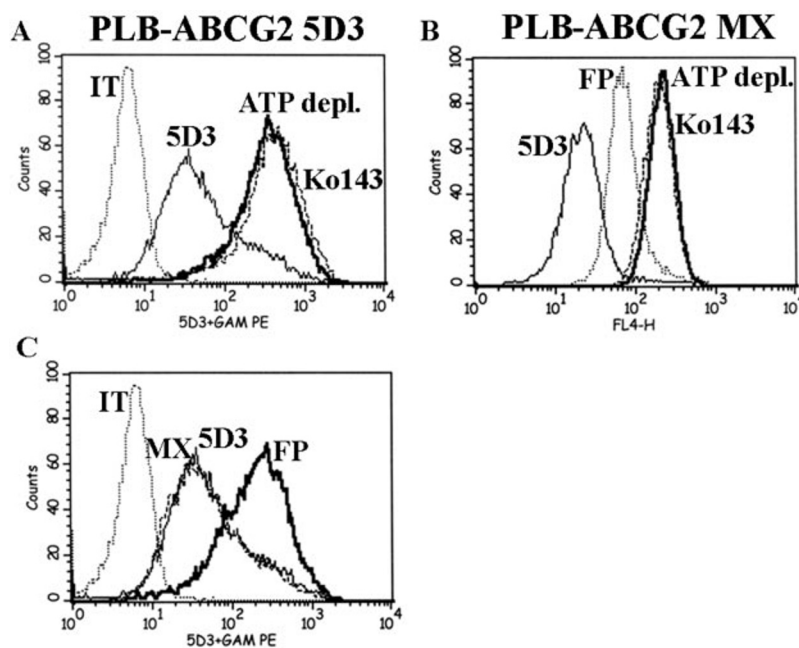


FIG. 5. Effects of ATP depletion and transported substrates on 5D3 binding (panels A and C) and MX extrusion (panel B) in ABCG2-expressing intact PLB cells. PLB-ABCG2 cells were incubated in medium containing 50 mM 2-deoxy-D-glucose and 15 mM sodium azide (ATP depl., heavy solid line), 5 μ M Ko143 (dashed line), 50 μ M flavopiridol (FP, heavy solid line on panel C or dotted line on panel B), or 5 μ M MX (dashed line) during the 5D3 labeling (panels A and C) or MX accumulation assay (panel B). IT means isotype control. Experiments were performed three times. The figure shows the result of one representative experiment.

Effect of ATP Depletion and Transported Substrates on 5D3 Reactivity and Mitoxantrone Transport by ABCG2 in Intact Cells—In the following experiments we have studied the effect of ATP depletion and various transported substrates on 5D3 binding and MX extrusion by ABCG2 in intact PLB cells. For achieving an efficient ATP depletion of the ABCG2-expressing PLBs, we used a 30-min pretreatment at 37 °C with a combination of sodium azide and 2-deoxy-D-glucose (see “Experimental Procedures”). As documented earlier in many hematopoietic cell lines, this treatment reduces the ATP level below 5% of the original levels and results in the accumulation of both ADP and AMP in the cells.

As shown in Fig. 5, this ATP depletion strongly inhibited the ABCG2 transport function; that is, eliminated the ABCG2-dependent MX extrusion in these cells (panel B). Interestingly, ATP depletion significantly increased 5D3 binding, thus transforming the ABCG2 protein in a conformation optimal for 5D3 labeling (panel A).

We have examined the effects of various agents on 5D3 binding, which were demonstrated transported substrates of the ABCG2 protein. The co-incubation of the ABCG2 cells with mitoxantrone (2–5 μ M) did not influence 5D3 labeling (see Fig. 5, panel C). We also found no appreciable effect on 5D3 binding by the addition of other substrates, prazosin (10–50 μ M) or ZD1839 (0.1–1 μ M) (not shown) (5, 32, 33). Flavopiridol, another transported substrate of ABCG2 (37), in low (1–5 μ M) concentrations had no effect on 5D3 antibody labeling, whereas in concentrations above 50 μ M this agent significantly increased 5D3 labeling and interfered with MX extrusion (Fig. 5, panels B and C). This is in line with the ABCG2-ATPase measurements, where high flavopiridol concentrations were inhibitory and, thus, could act similarly to Ko143 (data not shown in detail).

Effects of Substrates, Inhibitors, and ATP Depletion on 5D3 Reactivity in the Mutant, Non-functional K86M-ABCG2, Expressed in Intact Cells—In the next set of experiments we studied intact mammalian cells expressing a non-functional mutant (K86M) variant of ABCG2. This mutation in the highly conserved Walker A motif does not affect ATP binding by ABCG2 but impairs its drug transport and ATPase activity as well as the formation of a vanadate-induced trapped nucleotide (31). As shown in Fig. 6, panels A and B, this K86M-ABCG2

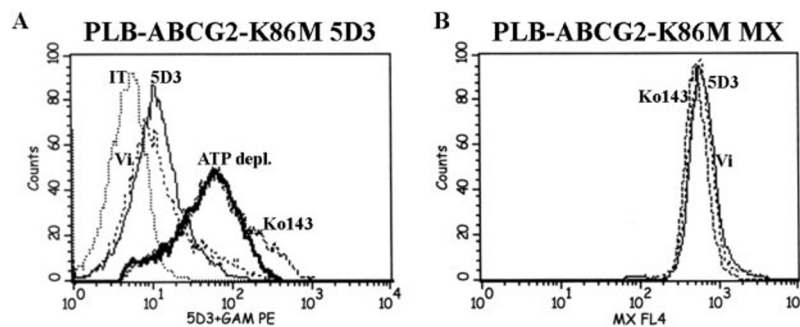
had no MX extrusion function but showed a well measurable 5D3 binding on the cell surface.

In these studies we found that the 5D3 binding of the K86M mutant ABCG2 was significantly increased by PFA fixation, ATP depletion, or Ko143 treatment. Still, the relative increase in 5D3 binding due to these effects was much smaller than in the case of the WT ABCG2, and 5D3 binding was unaffected by pretreatment with sodium orthovanadate (Fig. 6, panel A). Thus, the non-functional K86M variant of ABCG2 showed a relatively high 5D3 binding in its native state, but in the case of ATP removal and Ko143 treatment, similar conformational changes were detected by 5D3 in this mutant variant as in the wild-type protein. The lack of the formation of a transition-state intermediate in the K86M-ABCG2 correlated with the absence of an effect of sodium orthovanadate.

Effects of Nucleotides and Transport Inhibitors on 5D3 Reactivity of ABCG2 in Isolated Membrane Fragments—In the following experiments we examined the effects of various nucleotides and transport inhibitors on 5D3 binding by human ABCG2 and its mutant (K86M) variant in isolated insect cell membrane fragments. In these membrane preparations ABCG2 expression reaches a high level (up to 5% of the membrane proteins) in a fully active form, as reflected by the ABCG2-ATPase activity (11, 31). A large fraction of the isolated membrane fragments are accessible both from the cytoplasmic and the external cell surface, as tested by the trypsin sensitivity of open fragments (38) and simultaneous staining of the membrane fragments with two antibodies (polyclonal Ab 405 and mAb 5D3), which recognize an intracellular (5) and an extracellular epitope of ABCG2, respectively (not shown here). Therefore, this assay system allows a direct estimation of the effects of cytoplasmic ligands on the cell surface interaction of ABCG2 with the 5D3 antibody. As shown in Fig. 7, panel A, 5D3 binding to isolated Sf9 cell membranes containing the human ABCG2 protein reached a high level, significantly exceeding that seen in the control, MDR1-containing membranes, or the labeling obtained with an isotype control antibody.

Fig. 7, B and C, documents the effects of various ligands on 5D3 binding to wild-type (panel B) or K86M (panel C) ABCG2 in isolated membranes. In the case of the wild-type ABCG2 (panel B), the addition of MgAMP, MgADP, or MgATP did not significantly modulate the level of 5D3 labeling, whereas

FIG. 6. Flow cytometry detection of the K86M-ABCG2 protein. 5D3 mAb binding (panel A) and MX extrusion (panel B) in K86M mutant ABCG2-expressing intact PLB cells is shown. Effects of Ko143, ATP-depletion, and sodium orthovanadate are shown. Cells were incubated with 0.2 μ g of 5D3 antibody/ 10^6 cells without (5D3, solid line) or with the addition of 5 μ M Ko143 (dashed line), 2 mM sodium orthovanadate (Vi, dashed line), or 50 mM 2-deoxy-D-glucose and 15 mM sodium azide (ATP depl., heavy solid line). IT means isotype control.



MgAMP-PNP, a non-hydrolysable ATP analog, greatly reduced 5D3 binding. The addition of sodium orthovanadate was ineffective in the presence of MgAMP but produced a major decrease in 5D3 binding together with MgATP. When the cells were preincubated with the transport inhibitor Ko143 either in the presence of MgATP or MgAMP-PNP, a maximum level of 5D3 binding to ABCG2 was observed. Ko143 preincubation produced a maximum 5D3 binding even in the presence of MgATP plus vanadate. An interesting finding in these experiments was that if Ko143 was added after a preincubation with MgAMP-PNP, the reduction in 5D3 binding by this nucleotide could not be reversed by Ko143 (data not shown).

These data indicate that in the case of a functional ABCG2, 5D3 labeling has a relatively high level either in a nucleotide-free or in a nucleotide-liganded, flexible state of the transporter. However, when the transport cycle is blocked by a non-hydrolysable ATP analog or by the inhibition of ATP hydrolysis by sodium orthovanadate, a strong reduction in 5D3 binding occurs. Arresting the ABCG2 transport cycle by Ko143, however, produces a high 5D3 binding, and this effect is not reversed the nucleotides and/or vanadate. Still, a low 5D3 binding conformation first fixed by MgAMP-PNP cannot be changed to a high binding form by a later addition of Ko143.

Fig. 7, panel C, shows 5D3 binding in isolated membranes containing the K86M, non-functional mutant ABCG2 protein. In this case MgAMP had no effect, whereas MgATP, MgADP, and MgAMP-PNP significantly reduced 5D3 labeling. Sodium orthovanadate did not modify 5D3 binding, as compared with that seen with the respective nucleotides (MgAMP or MgATP). The addition of Ko143, again even in the presence of MgATP, MgADP, or MgAMP-PNP, produced maximum 5D3 binding.

These data can be interpreted to mean that although MgAMP does not show binding to the protein, MgATP, MgADP, and MgAMP-PNP are bound to K86M-ABCG2, and in the absence of a full catalytic cycle, they fix the transporter in a nucleotide-bound, reduced 5D3 binding state. This fixation does not require the presence of vanadate. These findings are in agreement with the unchanged ATP binding but the lack of vanadate-dependent nucleotide trapping in the case of this mutant protein (31). Interestingly, Ko143 can still stabilize the K86M-ABCG2 variant in a high 5D3 binding state.

In experiments not documented here in detail, we have performed 5D3 binding to ABCG2 in isolated Sf9 membranes at 4 °C to investigate labeling at non-hydrolytic conditions. We found that 5D3 binding at 4 °C was somewhat reduced ($75 \pm 1.4\%$ of that measured at 37 °C), and the addition of nucleotides or inhibitors (Ko143 or V_i) did not cause a measurable change in 5D3 binding.

We have also investigated 5D3 binding to ABCG2 in isolated Sf9 membranes upon the addition of AMP, ADP, AMP-PNP, and ATP, but in the absence of Mg^{2+} ions (that is, in the presence of excess EDTA) at 37 °C. Interestingly, we found that in the absence of Mg^{2+} , ADP, AMP-PNP, and ATP (but not AMP) significantly decreased 5D3 binding to the ABCG2 protein. These

effects were similar both in the wild-type ABCG2 and the K86M mutant variant (not documented in detail). These data indicate that the binding of ADP, ATP, or AMP-PNP to ABCG2 (causing low 5D3 reactivity) occurs even in the absence of Mg^{2+} , but no further steps of the catalytic cycle are performed.

DISCUSSION

In the present experiments we have studied the interaction of the 5D3 monoclonal antibody, prepared against a cell surface epitope of human ABCG2, with this multidrug transporter both in intact cells and in isolated membranes. We found that in intact cells 5D3 recognition of the ABCG2 protein occurred at an external epitope. The specific antibody binding was significantly increased by fixation of the intact cells by PFA, but this interaction did not require membrane permeabilization (Fig. 2, panel C). In contrast, the interaction of BXP-21 (an antibody raised against an intracellular epitope) with ABCG2 entirely depended on permeabilization of the cell membranes, making the intracellular epitopes accessible for this antibody (Fig. 2, panel D).

In accordance with data in the literature regarding 5D3 effect on ABCG2-induced drug resistance (22), we found that the 5D3 antibody significantly inhibited both the dye transport and the ATPase activity of the ABCG2 protein (Fig. 3, panels B and C). Still, the inhibition of the transport or ATPase activity of ABCG2 found here was incomplete even at very high 5D3 concentrations (see Figs. 3, B and C). This finding is most probably due to the steric and mechanical constraints in such antibody-transporter interactions. A similarly selective but only partial functional inhibition has been reported for several anti-MDR1 antibodies, e.g. MRK16 or UIC2, reacting with cell surface epitopes of the MDR1 multidrug transporter (23, 24).

In this study we found that at low 5D3 concentrations the actual conformation of the ABCG2 protein significantly modified 5D3 binding to the extracellular epitope. In intact cells ABCG2 interaction with 5D3 was greatly increased by the inhibition of ABCG2 function with a specific, high affinity inhibitor, Ko143 (see Fig. 4, panels C and G) or by cellular ATP depletion (Fig. 5, panel A). Similarly, an increase in 5D3 reactivity was observed in the presence of high, inhibitory concentrations of a drug substrate of ABCG2, flavopiridol (Fig. 5C) (37).

In contrast, a reduction in 5D3 binding was observed when the cells were preincubated with sodium orthovanadate, a transition state inhibitor of ABC transporters, including ABCG2 (31, 39–41). In this case, within the nucleotide binding domain of the protein, vanadate anions replace phosphate after ATP hydrolysis, and the transport cycle of ABCG2 is arrested in a transition state. This can be experimentally followed by measuring the vanadate-dependent trapping of MgADP within the protein, which becomes incapable for further ATPase or transport activity (39–41). In the present experiments the arrest of the ABCG2 transport cycle by Ko143 by the removal of the energy donor substrate, ATP, as well as by sodium orthovanadate was documented by the lack of active MX extrusion in the

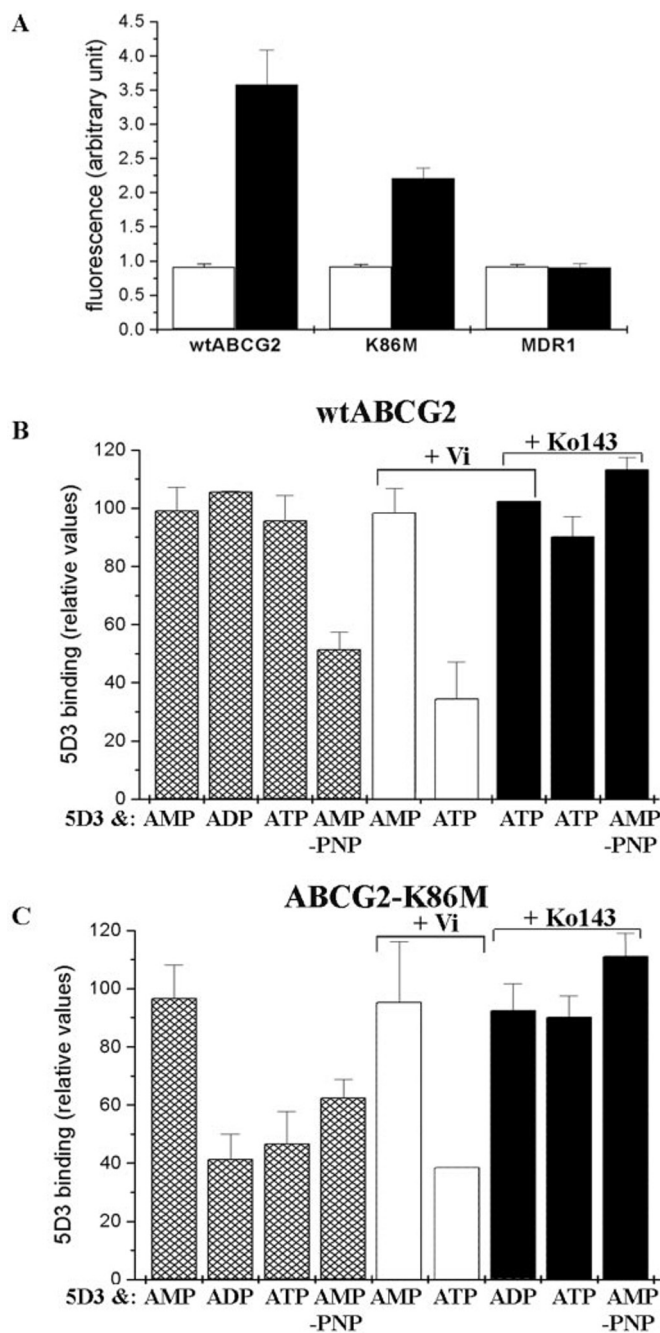


FIG. 7. Detection of 5D3 mAb binding to ABCG2 in isolated Sf9 membrane fragments. Effects of nucleotides, Ko143, and sodium orthovanadate. *Panel A*, comparison of 5D3 and isotype control (IT) antibody binding to isolated Sf9 cell membranes. Isolated membrane fragments (45 μ g) from Sf9 cells containing WT ABCG2, ABCG2-K86M, or MDR1 were labeled with 1 μ g/ml 5D3 (black columns) or 1 μ g/ml mouse IgG2b as isotype control (white columns). Fluorescence was detected in a fluorescence plate reader (Fluoroskan II, Labsystems) at 485 nm (excitation)/590 nm (emission). *Panel B*, 5D3 binding to membranes containing wild-type ABCG2. *Panel C*, 5D3 binding to membranes containing K86M mutant ABCG2. Sf9 membranes containing wild-type ABCG2 (*panel B*) or K86M mutant ABCG2 (*panels C*) were incubated with 5D3 antibody in the presence of 10 mM MgAMP, MgADP, MgATP, MgAMP-PNP, MgAMP plus 2 mM vanadate, MgATP plus 2 mM vanadate, MgATP plus 2 mM vanadate plus 1 μ M Ko143, MgADP plus 1 μ M Ko143, MgATP plus 1 μ M Ko143, or 10 mM MgAMP-PNP plus 1 μ M Ko143. When Ko143 was present the membranes were preincubated with this inhibitor for 5 min before the addition of other reagents. 5D3 binding is shown in the percent fluorescence measured in the presence of 5D3 alone (see "Experimental Procedures"). Values shown are the means of at least four independent experiments \pm S.D. values.

same cells (Fig. 4, *panels D* and *H*, and Fig. 5, *panel B*). In these experiments the addition of low concentrations of transported substrates did not significantly modify cell surface 5D3 binding to ABCG2 (Fig. 5, *panel C*).

According to these data, 5D3 interaction with ABCG2 in intact cells depends on the actual conformation within the transport cycle of this multidrug resistance protein. 5D3 binding is relatively low in the case of the actively functioning protein or in its stabilized transition state. In contrast, 5D3 binding is greatly increased when ABCG2 conformation is stabilized in other specific conformations (by Ko143 or ATP depletion). In unpublished experiments we found that Ko143 inhibition of ABCG2 was reversible by repeated washings. Also, ABCG2-ATPase inhibition achieved by low (10 nM) Ko143 concentration could be removed by the addition of increasing concentrations of transported substrates, *e.g.* prazosin. These results indicate that Ko143 probably inhibits ABCG2 by interacting with its substrate binding site.

When examining the binding of the 5D3 antibody in intact cells to a non-functional ABCG2 catalytic center mutant (K86M-ABCG2), we found that 5D3 binding to this mutant protein was also efficient. In the case of this mutant ABCG2, 5D3 binding was not affected by the addition of transported substrates or vanadate, whereas it was increased by ATP depletion or by the addition of Ko143 (Fig. 6). These data are in line with the impaired catalytic cycle and transition state-forming ability of this mutant, with unchanged ATP binding (31) and probably with conserved drug/inhibitor binding properties.

To further explore the mechanistic details of the ABCG2 catalytic cycle, we have performed a detailed analysis of 5D3 binding to ABCG2 in isolated membrane fragments, accessible from both sides of the membrane (see Fig. 7, *panel B*). It is important to note that the experiments carried out with isolated membranes exclude the possibility that the changes in 5D3-ABCG2 interactions might be due to variable cell surface expression of the multidrug resistance protein in intact cells. They also allow the study of the interaction of non cell-permeating ligands with cytoplasmic domains of the transporter.

In these experiments we observed that the non-hydrolysable ATP analog, AMP-PNP, strongly reduced 5D3 binding to ABCG2. MgAMP, MgADP, or MgATP had no major effect, but MgATP plus sodium orthovanadate induced a major decrease in 5D3 binding. Preincubation with the inhibitor molecule, Ko143, maximized 5D3 binding under all conditions.

In the K86M-ABCG2 variant the addition of MgATP, MgADP, and MgAMP-PNP all caused a major reduction of 5D3 binding, which was not further modulated by sodium orthovanadate. These results coincide with the conserved ATP binding but impaired catalytic intermediate formation by this mutant protein. In the case of this non-functional mutant we still found an increased 5D3 binding upon preincubation with Ko143 even if MgATP, MgADP, or MgAMP-PNP was added thereafter to the media (see Fig. 7, *panel C*). These results suggest a preserved substrate/inhibitor binding site in this mutant protein.

Interestingly, in Sf9 membranes containing either wild-type ABCG2 or its K86M mutant in the absence of Mg²⁺ (that is, in the presence of EDTA), ATP, ADP, and AMP-PNP caused a decrease in 5D3 binding (not shown in detail). These data may indicate that at these high nucleotide concentrations (10 mM), ABCG2 binds nucleotides even in the absence of Mg²⁺, although further ATP hydrolysis is absent.

When trying to investigate the possible effects of transported substrates (*e.g.* prazosin, flavopiridol, or mitoxantrone) on 5D3 binding by ABCG2 in isolated Sf9 cell membrane fragments, we could not detect any major changes evoked by relevant substrate concentrations. This is similar to the lack on ATPase

stimulation by substrates in this system and most probably due to the presence of endogenous substrates of ABCG2 in the Sf9 membranes (31).

These data collectively indicate that the binding of the 5D3 monoclonal antibody closely reflects the changes in the drug and ATP binding as well as the catalytic state of the ABCG2 transporter. This is most probably due to the variable appearance of a conformational epitope within the ABCG2 protein on the cell surface. This study is the first demonstration of such a conformation sensitivity of an antibody binding to the ABCG2 protein, although a conformation-dependent binding of some extracellular antibodies, e.g. MRK16 or UIC2, to another multidrug transporter, the MDR1 protein, has already been documented (23, 24). The determination of the actual epitope structure involved in 5D3 binding should require a detailed molecular mapping of potentially cell-surface domains of ABCG2.

As a summary, the various steps within the catalytic cycle of the ABCG2 multidrug resistance transporter can be visualized through changes in 5D3 binding. A low level 5D3 binding was observed when the non-hydrolysable ATP analog, MgAMP-PNP, or the addition of ATP or ADP without Mg²⁺ ions stabilized the protein in a prehydrolytic state (42, 43). The formation of a catalytic intermediate, reflected by nucleotide trapping in the presence of vanadate anions (40, 41), also coincided with a low 5D3 reactivity of ABCG2. In contrast, transport inhibition by Ko143 or by high concentrations of flavopiridol as well as by ATP depletion stabilized the protein in a conformation with high 5D3 binding capacity.

Based on these data we suggest that the 5D3-reactive form of ABCG2 is a stabilized "substrate off-site" conformation of the transporter. It has to be noted that the ABCG2 protein is an ABC half-transporter, and its function requires homodimerization (6–8,11). Conformational changes detected through a complex extracellular epitope of a membrane protein can be due to a function-dependent rearrangement of the transmembrane helices, triggering the movements of the extracellular loops, or to the surface-exposure of membrane-embedded short segments (for MDR1 see Rosenberg *et al.* (44)). ABCG2 acts as a homodimer, and one additional possible explanation for the conformational changes described in the present study is the function-dependent re-orientation of the monomers within the dimer or facilitation of the dimer formation. However, further experiments are needed to elucidate the dependence of 5D3 binding on the molecular interactions between the dimerizing ABCG2 molecules.

Based on this study we suggest that the 5D3 antibody can be used to reveal major intramolecular changes in the ABCG2 protein during its catalytic/transport cycle. Examining 5D3 binding to various mutant, polymorphic, or stabilized forms of ABCG2 may further help structure-function relationship studies. Moreover, based on the present data, optimum conditions can be selected for the investigation of ABCG2 expression and function by 5D3 binding in intact cell preparations, thus employing this antibody for a sensitive clinical laboratory detection of ABCG2 expression and function.

Acknowledgments—The technical help by Zsuzsanna András, Judit Kis, Mónika Bátkai, Margit Bakki, and Katalin Kelemen is gratefully acknowledged.

REFERENCES

- Allikmets, R., Schriml, L. M., Hutchinson, A., Romano-Spica, V., and Dean, M. (1998) *Cancer Res.* **58**, 5337–5339
- Doyle, L. A., Yang, W., Abruzzo, L. V., Krogmann, T., Gao, Y., Rishi, A. K., and Ross, D. D. (1998) *Proc. Natl. Acad. Sci. U. S. A.* **95**, 15665–15670
- Allen, J. D., Brinkhuis, R. F., Wijnholds, J., and Schinkel, A. H. (1999) *Cancer Res.* **59**, 4237–4241
- Maliepaard, M., van Gastelen, M. A., de Jong, L. A., Pluim, D., van Waardenburg, R. C., Ruevekamp-Helmers, M. C., Floot, B. G., and Schellens, J. H. (1999) *Cancer Res.* **59**, 4559–4563
- Litman, T., Brangi, M., Hudson, E., Fetsch, P., Abati, A., Ross, D. D., Miyake, K., Resau, J. H., and Bates, S. E. (2000) *J. Cell Sci.* **113**, 2011–2021
- Miyake, K., Mickley, L., Litman, T., Zhan, Z., Robey, R., Cristensen, B., Brangi, M., Greenberger, L., Dean, M., Fojo, T., and Bates, S. E. (1999) *Cancer Res.* **59**, 8–13
- Knutsen, T., Rao, V. K., Ried, T., Mickley, L., Schneider, E., Miyake, K., Ghadimi, B. M., Padilla-Nash, H., Pack, S., Greenberger, L., Cowan, K., Dean, M., Fojo, T., and Bates, S. (2000) *Genes Chromosomes Cancer* **27**, 110–116
- Kage, K., Tsukahara, S., Sugiyama, T., Asada, S., Ishikawa, E., Tsuruo, T., and Sugimoto, Y. (2002) *Int. J. Cancer* **97**, 626–630
- Rocchi, E., Khodjakov, A., Volk, E. L., Yang, C. H., Litman, T., Bates, S. E., and Schneider, E. (2000) *Biochem. Biophys. Res. Commun.* **271**, 42–46
- Scheffer, G. L., Maliepaard, M., Pijnenborg, A. C., van Gastelen, M. A., de Jong, M. C., Schroeijs, A. B., van der Kolk, D. M., Allen, J. D., Ross, D. D., van der Valk, P., Dalton, W. S., Schellens, J. H., and Scheper, R. J. (2000) *Cancer Res.* **60**, 2589–2593
- Ozvegy, C., Litman, T., Szakacs, G., Nagy, Z., Bates, S., Varadi, A., and Sarkadi, B. (2001) *Biochem. Biophys. Res. Commun.* **285**, 111–117
- Ross, D. D., Karp, J. E., Chen, T. T., and Doyle, L. A. (2000) *Blood* **96**, 365–368
- Litman, T., Druley, T. E., Stein, W. D., and Bates, S. E. (2001) *Cell. Mol. Life Sci.* **58**, 931–959
- Bates, S. E., Robey, R., Miyake, K., Rao, K., Ross, D. D., and Litman, T. (2001) *J. Bioenerg. Biomembr.* **33**, 503–511
- Diestra, J. E., Scheffer, G. L., Catala, I., Maliepaard, M., Schellens, J. H., Scheper, R. J., Germa-Lluch, J. R., and Izquierdo, M. A. (2002) *J. Pathol.* **198**, 213–219
- Volk, E. L., Farley, K. M., Wu, Y., Li, F., Robey, R. W., and Schneider, E. (2002) *Cancer Res.* **62**, 5035–5040
- Zhou, S., Schuetz, J. D., Bunting, K. D., Colapietro, A. M., Sampath, J., Morris, J. J., Lagutina, I., Grosveld, G. C., Osawa, M., Nakauchi, H., and Sorrentino, B. P. (2001) *Nat. Med.* **7**, 1028–1034
- Cooray, H. C., Blackmore, C. G., Maskell, L., and Barrand, M. A. (2002) *Neuroreport* **13**, 2059–2063
- Scharenberg, C. W., Harkey, M. A., and Torok-Storb, B. (2002) *Blood* **99**, 507–512
- Kim, M., Turnquist, H., Jackson, J., Sgagias, M., Yan, Y., Gong, M., Dean, M., Sharp, J. G., and Cowan, K. (2002) *Clin. Cancer Res.* **8**, 22–28
- Lechner, A., Leech, C. A., Abraham, E. J., Nolan, A. L., and Habener, J. F. (2002) *Biochem. Biophys. Res. Commun.* **293**, 670–674
- Abbott, B. L., Colapietro, A. M., Barnes, Y., Marini, F., Andreeff, M., and Sorrentino, B. P. (2002) *Blood* **100**, 4594–4601
- Mechetner, E. B., and Roninson, I. B. (1992) *Proc. Natl. Acad. Sci. U. S. A.* **89**, 5824–5828
- Hamada, H., and Tsuruo, T. (1986) *Proc. Natl. Acad. Sci. U. S. A.* **83**, 7785–7789
- Mechetner, E. B., Schott, B., Morse, B. S., Stein, W. D., Druley, T., Davis, K. A., Tsuruo, T., and Roninson, I. B. (1997) *Proc. Natl. Acad. Sci. U. S. A.* **94**, 12908–12913
- Goda, K., Nagy, H., Bene, L., Balazs, M., Arceci, R., Mechetner, E., and Szabo, G. (2000) *Cancer Detect. Prev.* **24**, 415–421
- Nagy, H., Goda, K., Arceci, R., Cianfriglia, M., Mechetner, E., and Szabo, G., Jr. (2001) *Eur. J. Biochem.* **268**, 2416–2420
- Maliepaard, M., Scheffer, G. L., Faneyte, I. F., van Gastelen, M. A., Pijnenborg, A. C., Schinkel, A. H., van De Vijver, M. J., Scheper, R. J., and Schellens, J. H. (2001) *Cancer Res.* **61**, 3458–3464
- Miller, A. D., Garcia, J. V., von Suhr, N., Lynch, C. M., Wilson, C., and Eiden, M. V. (1991) *J. Virol.* **65**, 2220–2224
- Ujhelly, O., Ozvegy, C., Varady, G., Cervenak, J., Homolya, L., Grez, M., Scheffer, G., Roos, D., Bates, S. E., Varadi, A., Sarkadi, B., and Nemet, K. (2003) *Hum. Gene Ther.* **14**, 403–412
- Ozvegy, C., Varadi, A., and Sarkadi, B. (2002) *J. Biol. Chem.* **277**, 47980–47990
- Robey, R. W., Honjo, Y., van de Laar, A., Miyake, K., Regis, J. T., Litman, T., and Bates, S. E. (2001) *Biochim. Biophys. Acta* **1512**, 171–182
- Ozvegy-Laczka, C., Hegedus, T., Varady, G., Ujhelly, O., Schuetz, J. D., Varadi, A., Keri, G., Orfi, L., Nemet, K., and Sarkadi, B. (2004) *Mol. Pharmacol.* **65**, 1485–1495
- Sarkadi, B., Price, E. M., Boucher, R. C., Germann, U. A., and Scarborough, G. A. (1992) *J. Biol. Chem.* **267**, 4854–4858
- Sarkadi, B., Bauzon, D., Huckle, W. R., Earp, H. S., Berry, A., Suchindran, H., Price, E. M., Olson, J. C., Boucher, R. C., and Scarborough, G. A. (1992) *J. Biol. Chem.* **267**, 2087–2095
- Allen, J. D., van Loevezijn, A., Lakhai, J. M., van der Valk, M., van Tellingen, O., Reid, G., Schellens, J. H., Koomen, G. J., and Schinkel, A. H. (2002) *Mol. Cancer Ther.* **1**, 417–425
- Robey, R. W., Medina-Perez, W. Y., Nishiyama, K., Lahusen, T., Miyake, K., Litman, T., Senderowicz, A. M., Ross, D. D., and Bates, S. E. (2001) *Clin. Cancer Res.* **7**, 145–152
- Sinko, E., Ilias, A., Ujhelly, O., Homolya, L., Scheffer, G. L., Bergen, A. A., Sarkadi, B., and Varadi, A. (2003) *Biochem. Biophys. Res. Commun.* **308**, 263–269
- Urbatsch, I. L., Sankaran, B., Weber, J., and Senior, A. E. (1995) *J. Biol. Chem.* **270**, 19383–19390
- Taguchi, Y., Yoshida, A., Takada, Y., Komano, T., and Ueda, K. (1997) *FEBS Lett.* **401**, 11–14
- Szabo, K., Welker, E., Bakos, Muller, M., Roninson, I., Varadi, A., and Sarkadi, B. (1998) *J. Biol. Chem.* **273**, 10132–10138
- Hou, Y. X., Cui, L., Riordan, J. R., and Chang, X. B. (2002) *J. Biol. Chem.* **277**, 5110–5119
- Sauna, Z. E., and Ambudkar, S. V. (2001) *J. Biol. Chem.* **276**, 11653–11661
- Rosenberg, M. F., Kamis, A. B., Callaghan, R., Higgins, C. F., and Ford, R. C. (2003) *J. Biol. Chem.* **278**, 8294–8299

Interaction with the 5D3 Monoclonal Antibody Is Regulated by Intramolecular Rearrangements but Not by Covalent Dimer Formation of the Human ABCG2 Multidrug Transporter*

Received for publication, April 28, 2008, and in revised form, July 16, 2008. Published, JBC Papers in Press, July 21, 2008, DOI 10.1074/jbc.M803230200

Csilla Özvegy-Laczka^{†1}, Rozália Laczkó[‡], Csilla Hegedűs[‡], Thomas Litman[§], György Várady[‡], Katalin Goda[¶], Tamás Hegedűs^{||}, Nikolay V. Dokholyan^{**}, Brian P. Sorrentino⁺⁺, András Váradi^{§§}, and Balázs Sarkadi^{‡2}

From the [†]Membrane Research Group of the Hungarian Academy of Sciences, Semmelweis University and National Blood Center, 1113 Budapest, Hungary, [§]Bioinformatics Centre, University of Copenhagen, DK-2100 Copenhagen, Denmark, [¶]Medical and Health Science Center, Department of Biophysics and Cell Biology, University of Debrecen, Nagyerdei Square 98, 4012 Debrecen, Hungary, ^{||}Department of Biochemistry and Biophysics, Cystic Fibrosis Treatment and Research Center, University of North Carolina, Chapel Hill, North Carolina 27599, ^{**}Department of Biochemistry and Biophysics, School of Medicine, University of North Carolina, Chapel Hill, North Carolina 27599, ⁺⁺Division of Experimental Hematology, Department of Hematology/Oncology, St. Jude Children's Research Hospital, Memphis, Tennessee 38105, and ^{§§}Institute of Enzymology, Hungarian Academy of Sciences, 1113 Budapest, Hungary

Human ABCG2 is a plasma membrane glycoprotein working as a homodimer or homo-oligomer. The protein plays an important role in the protection/detoxification of various tissues and may also be responsible for the multidrug-resistant phenotype of cancer cells. In our previous study we found that the 5D3 monoclonal antibody shows a function-dependent reactivity to an extracellular epitope of the ABCG2 transporter. In the current experiments we have further characterized the 5D3-ABCG2 interaction. The effect of chemical cross-linking and the modulation of extracellular S–S bridges on the transporter function and 5D3 reactivity of ABCG2 were investigated in depth. We found that several protein cross-linkers greatly increased 5D3 labeling in ABCG2 expressing HEK cells; however, there was no correlation between covalent dimer formation, the inhibition of transport activity, and the increase in 5D3 binding. Dithiothreitol treatment, which reduced the extracellular S–S bridge-forming cysteines of ABCG2, had no effect on transport function but caused a significant decrease in 5D3 binding. When analyzing ABCG2 mutants carrying Cys-to-Ala changes in the extracellular loop, we found that the mutant C603A (lacking the intermolecular S–S bond) showed comparable transport activity and 5D3 reactivity to the wild-type ABCG2. However, disruption of the intramolecular S–S bridge (in C592A, C608A, or C592A/C608A mutants) in this loop abolished 5D3 binding, whereas the function of the protein was preserved. Based on these results and *ab initio* folding simulations,

we propose a model for the large extracellular loop of the ABCG2 protein.

Human ABCG2 (also called as MXR/BCRP/ABCP) is a plasma membrane glycoprotein that belongs to the large family of ATP-binding cassette (ABC)³ proteins. ABCG2 mediates the energy-dependent transport of various compounds out of the cell. The protein is abundantly expressed in the intestine, the blood-brain barrier, and the placenta, influencing the absorption and fetal penetration of many toxic agents and food constituents (1). ABCG2 is also present in the liver where it is supposed to have an important role in the excretion of toxic metabolites into the bile (2, 3). ABCG2 is a marker protein of stem cells (4), where its physiological role is not yet clearly understood. It has been documented that ABCG2 expression is up-regulated under hypoxic conditions and that the protein can bind and/or transport porphyrins (5, 6); therefore it may play an important role in the protection of stem cells under hypoxic conditions. Overexpression of ABCG2 has been demonstrated in various tumor cells as well (1), where the transporter may be responsible for the emergence of a multidrug-resistant tumor phenotype that often leads to the failure of chemotherapy treatment in cancer patients.

Because ABCG2 is a half-transporter, bearing only one of each of the characteristic ABC family domains (the ATP-binding domain and transmembrane domain), ABCG2 has to form a

* This work was supported by grants from the Hungarian Scientific Research Fund (OTKA) (AT 048986 and NK72057) National Research and Development Programmes (NKFP), FP6-INHER, FP6-MEMTRANS, NEDO, and National Health Council (ETT). The costs of publication of this article were defrayed in part by the payment of page charges. This article must therefore be hereby marked "advertisement" in accordance with 18 U.S.C. Section 1734 solely to indicate this fact.

¹ Recipient of Postdoctoral Fellowship PD45957 from OTKA (Hungary) and the János Bolyai Scholarship of the Hungarian Academy of Sciences.

² To whom correspondence should be addressed: Membrane Research Group of the Hungarian Academy of Sciences, Semmelweis University and National Blood Center, 1113 Budapest, Dioszegi u. 64, Hungary. Tel/Fax: 361-372-4353; E-mail: sarkadi@biomembrane.hu.

³ The abbreviations used are: ABC, ATP-binding cassette; AMP-PNP, adenosine 5'-(β,γ -imidotriphosphate); BM[PEO]₃, 1,8-bis-maleimidotriethylene glycol; BMPH, *N*-[β -maleimidopropionic acid]hydrazide, trifluoroacetic acid salt; DMD, discrete molecular dynamics; DPBS, Dulbecco's modified phosphate-buffered saline; DTT, dithiothreitol; ECL3, third extracellular loop of ABCG2; EDC, [1-ethyl-3-(3-dimethylaminopropyl)carbodiimide hydrochloride]; FTC, fumitremorgin C; HEK, human embryonic kidney; MX, mitoxantrone; MXR, mitoxantrone resistance protein; PFA, paraformaldehyde; PMPI, *N*-(*p*-maleimidophenyl)isocyanate; sulfo-EGS, ethylene glycol bis(sulfosuccinimidyl succinate); sulfo-MBS, *m*-maleimidobenzoyl-*N*-hydroxysuccinimide ester.

homodimer or homo-oligomer to become functionally active (7, 8). The ABCG2 homodimer is covalently linked via a disulfide bond formed by cysteines at position 603, localized in the large ~55-amino acid-long third extracellular loop (ECL3) of the protein (9, 10). Interestingly, mutation of Cys-603 to Ala, Gly, or Ser does not remarkably influence the expression and functionality of the transporter (9–11). In ECL3, ABCG2 has two other cysteines at positions 592 and 608. These two residues are indicated as forming an intramolecular disulfide bridge that influences plasma membrane targeting and substrate specificity of the transporter (10–13).

Being a stem cell marker protein and one of the most important ABC multidrug transporters, a sensitive method for the detection of ABCG2 expression is of great interest. There are several methods for detecting ABCG2 expression in various cell types (14); however, only a limited number of these use intact cells, which is essential when enrichment and further culturing of ABCG2-expressing cells (e.g. stem cells) is required. One such example is the flow cytometric application of the 5D3 antibody, which allows the easy detection and sorting of ABCG2-expressing intact cells.

The 5D3 monoclonal antibody was generated by immunizing mice with murine cells expressing human ABCG2 (4). This antibody recognizes a yet undefined, extracellular epitope of ABCG2. Previously, we have shown that 5D3 binding strongly depends on the conformation of ABCG2 (15). Namely, inhibition of protein function by the specific inhibitor Ko143 or by using an ABCG2 substrate flavopiridol at a high, inhibitory concentration, as well as ATP depletion of the cells, greatly increases 5D3 binding, called a “5D3 shift” (15). On the other hand, mimicking the ATP-bound state by using a non-hydrolyzable ATP analog, AMP-PNP, or by arresting ABCG2 by sodium orthovanadate significantly reduces 5D3 binding (15). We and others have also demonstrated that 5D3 can inhibit the function of ABCG2 (15, 16). Not only is the 5D3 antibody a good candidate for the detection of ABCG2 in flow cytometry-based assays, but this antibody-protein interaction may also facilitate structural studies at a molecular level, such as in the crystallization of ABCG2. However, because 5D3 reactivity is sensitive to conformational changes of ABCG2, proper assay conditions must be determined and accurately controlled.

The aim of the present study was to further characterize the conditions influencing 5D3 binding to ABCG2. We have analyzed in detail how covalent cross-linkings of two ABCG2 proteins influence 5D3 binding and attempted to unravel the role of the intra- and intermolecular disulfide bonds in 5D3 epitope formation. We found several protein cross-linkers that significantly increased 5D3 binding to ABCG2, resulting in a covalent ABCG2 dimer formation and/or inhibition of transport function. However, we also found a cross-linker that caused a 5D3 shift without covalent cross-linking of the two ABCG2 proteins or without the inhibition of ABCG2 function. When administered dithiothreitol (DTT) to intact cells to reduce extracellular cysteines, we found that this treatment abolished 5D3 binding without any effect on the transport function. Characterization of 5D3 binding to ABCG2 proteins bearing mutations in extracellular cysteines revealed that the intermolecular S–S bond has only a minor effect on 5D3 binding, but disruption

of the intramolecular S–S bridge has a dramatic effect on antibody recognition. Based on these data, we suggest that the epitope of 5D3 is located in the third, large extracellular loop of ABCG2. Additionally, we have generated a model showing the conformation of the third extracellular loop and revealing how conformational changes mediated by the disruption of the extracellular S–S bonds may influence 5D3 epitope formation.

EXPERIMENTAL PROCEDURES

Materials

Protein cross-linkers BM[PEO]₃, BMPH, EDC, PMPI, sulfo-EGS, and sulfo-MBS were purchased from Pierce. BXP-21 monoclonal antibody (3) and Ko143 (17) were kind gifts from Drs. George Scheffer and Rik Scheper and from Dr. G. J. Koomen, respectively.

Expression Vectors, Cell Lines, and Cell Culturing

pCIN4 bicistronic mammalian expression vectors containing the cDNAs of ABCG2-R482G, or additional Cys to Ala mutations, were generated as described previously (10). HEK293 cell lines expressing various ABCG2 mutants were generated by transfection of the cells using the FuGENE® 6 (Roche Applied Science). Stable cell lines were obtained by maintaining the cells in Dulbecco's modified Eagle's medium supplemented with 10% fetal calf serum, 50 units/ml penicillin, 50 units/ml streptomycin, 5 mmol/liter glutamine, and 0.5 mg/ml G418 (Invitrogen) at 37 °C in 5% CO₂. To obtain a cell line showing higher ABCG2-C592A/C608A expression, HEK-C592A/C608A cells were sorted based on rhodamine123 extrusion capacity in a FACSAria flow cytometer. The sorted HEK-C592A/C608A cell line was used throughout this study. Generation of HEK293, A431, or PLB985 cells expressing wild-type ABCG2 was described previously (15, 18, 19).

Generation of 5D3-Alexa647, 5D3-Fab and 5D3-Fab-Alexa647

The 5D3 monoclonal antibody was purified from the supernatant of a hybridoma using affinity chromatography. Fab fragments of the antibody were prepared by papain digestion and separated from Fc fragments and the whole antibody on protein A-Sepharose column as described previously (20). Fab fragments and the monoclonal antibody preparations were more than 97% pure as determined by SDS-PAGE. The antibody and the Fab fragments were labeled with Alexa647 succinimidyl ester (Molecular Probes, Invitrogen) and separated from the unconjugated dye by gel filtration on a Sephadex G-50 column (21). The dye-to-protein labeling ratio was 3.28 and 0.98 for the antibody and Fab preparations, respectively.

Immunodetection of ABCG2

Western Blotting—HEK cells were suspended in a Laemmli buffer containing 2% of the reducing agent β-mercaptoethanol or without it, as indicated in Fig. 1A. Western blot analysis was performed as described previously (22) by using the BXP-21 monoclonal antibody in a 500× dilution and a goat anti-mouse horseradish peroxidase-conjugated secondary antibody (5000× dilution, Jackson ImmunoResearch).

Flow Cytometry—5D3 binding in intact cells was examined by suspending HEK cells in HPMI buffer (120 mM NaCl, 5 mM

KCl, 400 μM MgCl_2 , 40 μM CaCl_2 , 10 mM HEPES, 10 mM NaHCO_3 , 10 mM glucose, and 5 mM Na_2HPO_4) containing 0.05% bovine serum albumin (Sigma). Aliquots of the cell suspension (5×10^5 cells in 100 μl) were incubated with Alexa647-conjugated 5D3 antibody (2 $\mu\text{g}/\text{ml}$ final concentration) for 45 min at 37 °C. 5D3-Alexa647 binding was determined in a FACSCalibur cytometer at 635 nm excitation and 661/16 nm emission (FL4) wavelengths. When indirect labeling was performed, cells were incubated with unlabeled 5D3 and mouse IgG2b as an isotype control (both used in 1 $\mu\text{g}/\text{ml}$ final concentration) for 30 min at 37 °C. After washing, the phycoerythrin-conjugated goat anti-mouse secondary antibody (GAM-PE, Beckman Coulter) was used, and its fluorescence was determined at 488-nm excitation and 585/42-nm emission (FL2) wavelengths. Labeling with 5D3-Fab was carried out the same way as with the whole 5D3 antibody. When labeling was carried out in the presence of an ABCG2 inhibitor (1 μM Ko143 or 5 μM FTC), the cells were preincubated with these agents for 10 min at 37 °C before labeling, and the inhibitors were present throughout the antibody labeling procedure.

Confocal Microscopy

HEK cells were seeded onto 8-well Nunc Lab-Tek II chambered coverglass (Nalge Nunc International) at 3×10^4 /well cell density, and grown for 48 h in Dulbecco's modified Eagle's medium containing 10% fetal calf serum. For cell surface labeling, the cells were gently washed with Dulbecco's modified phosphate-buffered saline (DPBS), fixed with 1% paraformaldehyde in DPBS for 15 min at room temperature, and then blocked for 1 h at room temperature in DPBS containing 0.5% bovine serum albumin. The samples were then incubated for 1 h at room temperature with the 5D3 antibody conjugated with allophycocyanin (R&D Systems), diluted 5 \times in DPBS containing 0.5% bovine serum albumin, and finally washed with DPBS.

For immunostaining of permeabilized cells, samples were gently washed and then fixed with 4% paraformaldehyde in DPBS for 15 min at room temperature. After a few washes with DPBS, the cells were further fixed and permeabilized in pre-chilled methanol for 5 min at -20 °C. Following further washing steps, the cells were blocked for 1 h at room temperature in DPBS containing 2% bovine serum albumin, 1% fish gelatin, 0.1% Triton-X 100, and 5% goat serum (blocking buffer). The samples were then incubated for 1 h at room temperature with BXP-21 antibody diluted 100 \times in blocking buffer. After washing with DPBS, the cells were incubated for 1 h at room temperature with Alexa Fluor 488-conjugated goat anti-mouse IgG (H+L) (Molecular Probes) diluted 250 \times in blocking buffer. As isotype controls, allophycocyanin-conjugated mouse IgG2b (eBioscience) (5 $\mu\text{g}/\text{ml}$) and mouse IgG2a (Dako) (2.5 $\mu\text{g}/\text{ml}$) plus Alexa Fluor 488-conjugated goat anti-mouse IgG (1:250) were used. The stained samples were studied with an Olympus FV500-IX confocal laser scanning microscope using an Olympus PLAPO 60 \times (1.4) oil immersion objective (Olympus Europa GmbH) at room temperature. Green and deep red fluorescence was acquired above 505 and 650 nm, using excitation at 488 and 633 nm, respectively.

Cellular Dye Uptake and Calculation of ABCG2 Transport Activity

For measurement of ABCG2 activity, 5×10^5 HEK cells were suspended in 100 μl of HPMI buffer containing 2 μM rhodamine123, 5 μM mitoxantrone (MX) or 1 μM pheophorbide A in the presence or absence of 5 μM FTC for 30 min at 37 °C. Cells were then washed and resuspended in ice-cold phosphate-buffered saline, and fluorescence was determined in a FACSCalibur cytometer. Dead cells in the rhodamine123 uptake experiments were excluded based on TOPRO-3 staining (Molecular Probes) and in MX and pheophorbide A transport experiments by propidium iodide (Sigma) staining. Mean fluorescence values measured in the absence (M_0) and the presence of inhibitor (M_i) were determined and activity was calculated as follows: $(M_i - M_0)/M_i$.

Measurement of Hoechst 33342 Transport Activity

Hoechst 33342 transport was determined as described previously (23). The effect of 5D3 (12 μg in 100 μl for 3×10^5 cells) on Hoechst 33342 transport was measured as described previously (15). The effect of 5D3-Fab on Hoechst 33342 uptake was determined in the same way, except that 24 or 48 μg of 5D3-Fab was used in 100 μl for 3×10^5 cells.

Treatment of ABCG2 with Cross-linkers or Dithiothreitol— 5×10^5 HEK cells were suspended in 100 μl of phosphate-buffered saline containing paraformaldehyde (PFA) (0.001–1%), BM[PEO]₃ (0.5 mM), BMPH (1 mM), PMPI (1 mM), EDC (2 mM), sulfo-EGS (2 mM), sulfo-MBS (2 mM), or dithiothreitol (1–50 mM), and incubated at 37 °C for 10 min. After washing with 1 ml of HPMI containing 0.05% bovine serum albumin, 5D3 labeling or functional analysis of ABCG2 was performed as described above. Alternatively, cells were suspended in SDS-sample loading buffer and analyzed by Western blotting (see above). In some experiments PFA fixation and DTT treatment were used in combination. In these cases, cells were fixed first with PFA (or treated with DTT) as described above, washed with 1 ml of HPMI, and then treated with DTT (or fixed with PFA), washed again with 1 ml of HPMI-0.05% bovine serum albumin, and finally labeled with 5D3.

Ab Initio Folding Simulations and Three-dimensional Characterization of the ECL3 of ABCG2

The folding simulations of the third extracellular loop of ABCG2 were performed as described previously (24). Briefly, a linear ECL3 peptide (residues 563–618) was used to generate a large, diverse pool of structures using a dynamic sampling algorithm, discrete molecular dynamics (DMD) (25–28). The search for low energy conformers was performed by replica exchange (28, 29) DMD simulations (26–29) in two steps. In the first round, accessible conformers of ECL3 were sampled within a higher temperature range (0.5 – $0.78 \epsilon/k_b$), and a preliminary decoy set composed of structures with low potential energy values (lower than -261ϵ) was constructed. Then each decoy in the preliminary set was subjected to a second round of replica exchange DMD, with exchange temperatures in a lower range (0.3 – $0.58 \epsilon/k_b$). The final decoy set consisted of 101 low energy structures (lower than -338ϵ), which were relaxed in a final step of equilibrium simulation at low temperature (0.2

ϵ/k_b). The distance between the two ends of the ECL3 was set between 9 and 12 Å, based on existing ABC protein crystal structures (30). The S–S distance between Cys-592 and Cys-608 were set to maintain the disulfide bond.

To characterize the major conformations accessed by ECL3, decoys were grouped into clusters using the *k*-means algorithm⁸⁸ (MatLab, MathWorks, Inc.) applying $C\alpha$ root-mean-square deviation as the similarity metric between two structures. We selected a single, representative ECL3 structure for presentation (Fig. 8), which was obtained from the most populated cluster having the glycosylation site and cysteine 603 (responsible for intermolecular dimer interaction) on the surface of the structure.

RESULTS

Effect of Paraformaldehyde Fixation on ABCG2 Protein 5D3 Antibody Interaction—5D3 is a conformation-sensitive monoclonal antibody that recognizes a yet undefined extracellular epitope of the human ABC half-transporter, ABCG2. PFA generally used cross-linking fixative. Previously, we had found that in a PLB985 cell line expressing ABCG2, PFA fixation (1% final concentration) as well as inhibition of the function of wild-type ABCG2, *e.g.* by Ko143 or FTC, results in a significant increase in 5D3 labeling (5D3 shift (15)). We found that PFA also increased 5D3 binding in other ABCG2-expressing human cell lines (A431 and HEK). When we analyzed PFA-fixed samples by Western blotting, using the anti-ABCG2 antibody BXP-21 generated against an intracellular epitope of ABCG2, we found that in PFA-fixed cells two higher molecular mass forms of ABCG2 appeared (Fig. 1A, lane 3). These bands have ~200–250-kDa relative molecular weight that, despite an unusually slow mobility, has been suggested to correspond to the dimeric form of the protein. When the ABCG2 homodimer is linked by a disulfide bridge (8–12, 31), the covalent ABCG2 dimer can be also detected under nonreducing conditions by Western blotting (see Fig. 1A, lane 2).

When we analyzed HEK-ABCG2 cells not treated with any cross-linkers but suspended in a nonreducing buffer (without β -mercaptoethanol), we found the same slower mobility bands as in PFA-fixed samples (Fig. 1A, lane 2). These data suggest that the higher apparent molecular mass forms observed in PFA-treated samples are most probably covalently cross-linked ABCG2 dimers (see more on cross-linkers below).

To analyze whether there is a correlation between covalent dimer formation upon PFA fixation and increased 5D3 binding, and whether PFA cross-linking inhibits ABCG2 function, we treated intact HEK cells expressing ABCG2 (R482G) with increasing concentrations of PFA and analyzed 5D3 binding, ABCG2 function, and covalent dimer formation. Throughout this study we used both the wild-type and the R482G mutant variant of ABCG2 in HEK cells, because the background of the cysteine mutations was this latter variant (10). The R482G mutant also allowed the measurement of transport activity followed by rhodamine123 extrusion, characteristic of the mutant protein. In all functional experiments the R482G protein variant showed the same behavior regarding 5D3 binding as the wild-type ABCG2, that is PFA or Ko143 caused a significant 5D3 shift (Fig. 1B).

When analyzing the effect of increasing amounts of PFA, we found that 5D3 labeling showed a saturating curve. We could already detect a slight increase in 5D3 binding at 0.05% PFA concentration as compared with the untreated cells, and 5D3 labeling reached its maximum when cells were fixed with 0.5–1% PFA (Fig. 1C). Increased antibody binding caused by PFA fixation was specific, as there was no 5D3 labeling in control cells transfected with an empty vector (and having no ABCG2 expression), and the fluorescence in cells incubated with an isotype control mAb did not increase upon PFA fixation (Fig. 1C).

To examine whether fixation-mediated increase in 5D3 labeling of ABCG2 positively correlates with the inhibition of the protein transport function, we also analyzed the effect of PFA on the transport function of ABCG2. Fig. 1C also shows rhodamine123 transport activity (activity factor) of the HEK-ABCG2-R482G cells treated with increasing concentrations of PFA. We found that ABCG2 gradually lost its activity upon PFA fixation, but functional inactivation was observed only in cells fixed with 0.5% or more PFA. Notably, there was already an about 80% increase in 5D3 labeling in the 0.1% PFA-fixed samples, whereas rhodamine123 extrusion was hardly inhibited (less than 20%) at this PFA concentration. When we analyzed PFA-fixed cells by Western blotting (Fig. 1D), we found that the relative amount of covalently linked ABCG2 dimer greatly increased in cells fixed with 0.5% or more PFA; thus, covalent cross-linking seemed to correlate with the inhibited transport function but not with the 5D3 shift.

Effect of Various Protein Cross-linkers on ABCG2 Protein 5D3 Antibody Interaction—To further investigate whether there is a correlation between covalent cross-linking of the ABCG2 monomers and an increased 5D3 binding, we treated ABCG2 expressing cells with different specific protein cross-linkers and analyzed them for 5D3 binding, functionality and dimer formation. We chose several non-cell-permeable protein cross-linkers, reacting with different amino acid side chains on the cell surface (Table 1). As Fig. 2 shows, we found several protein cross-linkers (BM[PEO]₃, BMPH, sulfo-MBS, and PMPI) that increased 5D3 binding up to the level observed in FTC or PFA treated cells, whereas they did not affect the labeling of control cells or the fluorescence measured with the isotype antibody control (not shown).

To examine whether the observed increase in 5D3 binding in these protein cross-linker treated samples was due to the inhibition of the function of ABCG2, we analyzed rhodamine123 uptake in these cells (Fig. 2A, right panel). We found that EDC, sulfo-EGS, sulfo-MBS, and PMPI did not inhibit the transport function of ABCG2, whereas the others abolished rhodamine123 extrusion. We also analyzed protein cross-linker treated cells for covalent ABCG2 dimer formation by Western blotting and found that BMPH and EDC, two compounds that caused a 5D3 shift, did not result in a covalently linked ABCG2 (Fig. 2B). The experiments shown in Fig. 2 were performed in HEK-ABCG2-R482G cells, but experiments repeated in both PLB985 and A431 cells, expressing the wild-type ABCG2 protein, provided the same results (data not shown).

In summary, we found that the effect of cross-linkers was highly variable as to function, 5D3 labeling, and covalent dimer

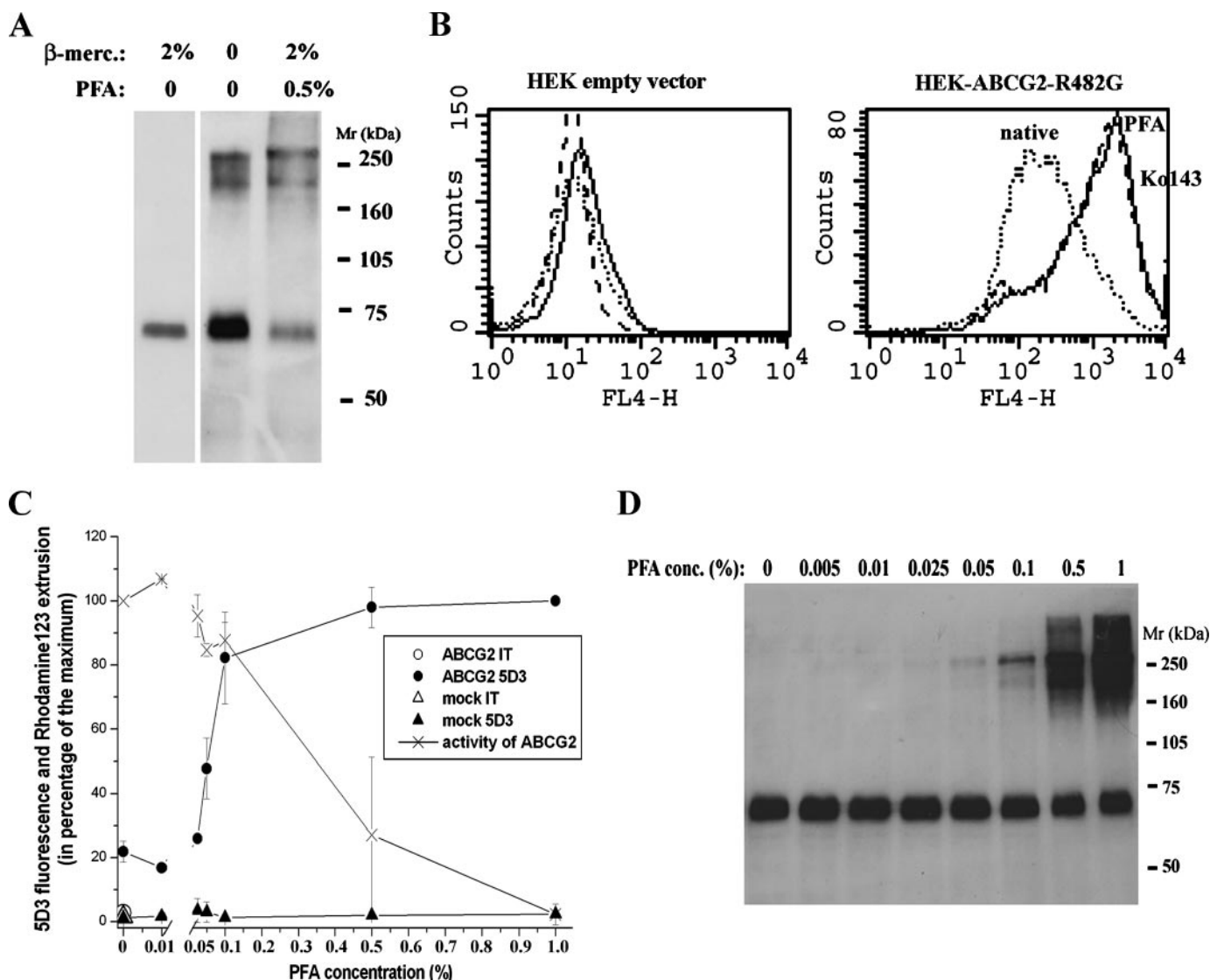


FIGURE 1. *A*, effect of PFA fixation on covalent ABCG2 dimer formation. HEK-ABCG2-R482G cells were lysed, dissolved in disaggregation buffer containing the reducing agent β -mercaptoethanol or without it (as indicated on the figure), and subjected to 7.5% SDS-PAGE. ABCG2 in cells fixed with 0.5% PFA prior to cell lysis is also shown. 15 μ g of protein was loaded into each lane. ABCG2 was detected by the BXP-21 antibody. *B*, effect of PFA fixation on 5D3 labeling of ABCG2. HEK293 cells transfected with empty pCIN4 or pCIN4-ABCG2(R482G) were labeled with Alexa647-conjugated 5D3. Fluorescence was detected using a FACSCalibur cytometer. The solid line represents 5D3 binding of 0.5% PFA-treated and the dotted line for nontreated (native) cells. The dashed line represents labeling of cells in the presence of the specific ABCG2 inhibitor, Ko143. *C*, 5D3 labeling and activity of ABCG2 in cells treated with increasing concentrations of PFA. Mock or pCIN4-ABCG2(R482G)-transfected HEK293 cells were fixed with increasing concentrations of PFA, washed, and then labeled with 5D3 antibody or mouse IgG2b (isotype control (IT)). Fluorescence of goat anti-mouse phycoerythrin-conjugated secondary antibody was detected in a FACSCalibur cytometer. Fluorescence values are shown as the percentage of maximum labeling obtained in ABCG2-expressing cells fixed with 1% PFA and labeled with 5D3. Rhodamine123 uptake is shown in the presence of increasing concentrations of PFA. HEK-ABCG2 cells were fixed with increasing concentrations of PFA, washed, and then incubated with 2 μ M rhodamine123 or 2 μ M rhodamine123 + 1 μ M Ko143. Rhodamine123 fluorescence in living cells was detected in a FACSCalibur cytometer. Rhodamine123 extrusion activity of ABCG2 is shown as the percentage of maximum activity. Activities were calculated as follows: $(M_i - M_0)/M_i$, where M_i is the mean rhodamine123 fluorescence in the presence of Ko143 and M_0 is the mean fluorescence without Ko143. Shown is the average of two independent experiments. *D*, Western blot analysis of ABCG2 in HEK cells treated with increasing concentrations of PFA. HEK-ABCG2 cells were fixed with increasing concentrations of PFA or without it (first lane), washed, and then suspended in disaggregation buffer. Samples (each containing 15 μ g of protein) were then subjected to 7.5% Laemmli gel electrophoresis and electroblotting. ABCG2 was visualized by the BXP-21 antibody.

formation (see Table 1). These results suggest that covalent cross-linking of two (or more) ABCG2s is neither sufficient nor necessary for an increased 5D3 binding and/or for transport inhibition. From these data it seems likely that fixation of the epitope on a monomeric ABCG2 protein, even without the inhibition of transport function, may be responsible for an increased 5D3 binding.

Effect of DTT Treatment on 5D3 Binding—ABCG2 has three cysteines localized on the cell surface in the large third extra-

cellular loop of the protein. It has been suggested that Cys-603 is responsible for intermolecular S–S bond formation, whereas the other two cysteines, Cys-592 and Cys-608, form an intramolecular S–S bridge (9–12). To find out whether the extracellular S–S bonds formed by cysteines are important for 5D3 recognition, we treated HEK-ABCG2 cells with the reducing agent DTT, which has a slow or insignificant cellular permeation. We found that treatment with 10 mM DTT caused a significant decrease in 5D3 binding in native (nonfixed) cells;

TABLE 1
Effects of protein cross-linkers on 5D3 binding, transport activity, and covalent dimer formation of ABCG2

Cross-linker	Side chains cross-linked	Spacer arm length	Increased 5D3 binding	Inhibition of transport function	Cross-linked ABCG2 on Western blot
		Å			
BM[PEO] ₃	SH ₂ -H ₂	14.7	Yes	Yes	Yes
BMPH	CH ₃ -SH ₂	8.1	Yes	Yes	No
EDC	COOH-NH ₂	0	Yes	No	No
Sulfo-EGS	NH ₂ -NH ₂	16.1	No	No	Yes
Sulfo-MBS	NH ₂ -SH ₂	9.9	Yes	No	Yes
PMP1	SH ₂ -OH	8.7	Yes	No	Yes

this low 5D3 binding persisted even if the cells were fixed by PFA after the DTT treatment (Fig. 3B). DTT treatment had no effect on the negligible 5D3 labeling of HEK cells transfected with the empty vector (Fig. 3A), nor did it affect the fluorescence of HEK-ABCG2 cells incubated with an isotype control antibody. In parallel experiments we analyzed the effect of DTT on the function of ABCG2 and found that even in cells treated with 10–50 mM DTT, ABCG2 was fully active (data not shown). This latter finding is in harmony with the results of Mitomo *et al.* (31), who demonstrated that β -mercaptoethanol, another reducing agent, does not influence the functionality of ABCG2.

We also examined the expression level and dimerization of ABCG2 in DTT-treated samples by Western blotting. We found that 10 mM DTT treatment resulted in the complete loss of ABCG2 dimer formation observed in samples dissolved in loading buffer without the reducing agent β -mercaptoethanol. However, DTT had no effect on the covalent cross-linking of ABCG2s by PFA (not shown). These results suggested that intact S–S bridges in the ABCG2 protein on the cell surface may play an important role in the 5D3 epitope formation.

Expression, Function, and 5D3 Binding of ABCG2 Variants Carrying Cys-to-Ala Mutations in the Third Extracellular Loop—To investigate whether DTT treatment causes a decrease in 5D3 binding due to the reduction of the intramolecular or intermolecular S–S bonds, or which of these bonds are important for 5D3 epitope formation, we expressed ABCG2 mutants having single Cys-to-Ala changes or the combination of these mutations in HEK cells.

Fig. 4A shows that all Cys-to-Ala mutants (except for C603A/C608A that was expressed in very low amount and exclusively in an underglycosylated form) could be detected by Western blotting, using the ABCG2-specific BXP-21 antibody. The mutants C592A and C603A showed expression levels comparable to that of the wild-type ABCG2, whereas the amount of double mutant C592A/C608A or the triple Ala mutant proteins was about 50% of that seen for the wild-type ABCG2.

To analyze whether the ABCG2 cysteine mutants were functional, we performed fluorescent dye uptake experiments by flow cytometry and fluorometry (Fig. 4B). We analyzed the transport of four different fluorescent ABCG2 substrate compounds, MX, pheophorbide A, Hoechst 33342, and rhodamine123 (rhodamine123 is transported only by the R482G ABCG2 mutant). We found that all of the expressed cysteine mutants were functional, bearing dye extrusion capacity, but there was a significant variation in their transport activities relative to the different transported compounds.

Hoechst 33342 and pheophorbide A were transported by all of the mutants (except for C603A/C608A); however, the mitox-

antrone transport capacity of the mutants, lacking the intramolecular or both disulfide bonds, was significantly weaker than that of the R482G or C603A variants. There was also a difference in rhodamine123 uptake, with the C592A and C592A/C603A mutants showing practically no transport activity (Fig. 4B). These data are in harmony with the findings of Henriksen *et al.* (10), who report that some of the Cys-to-Ala mutants have altered substrate specificity.

When cells expressing the different Cys-to-Ala mutants were labeled with the 5D3 antibody, we found that only the C603A variant had a clearly detectable 5D3 labeling and the C592A/C608A mutant showed some weak 5D3 binding capacity (Fig. 5A, upper panel). Similar to that seen in the case of the wild-type ABCG2, PFA fixation (Fig. 5A, lower panel) or Ko143 treatment (not shown) of the cells expressing the C603A mutant and the double mutant C592A/C608A resulted in an increased 5D3 binding. However, the other mutant variants did not show any labeling, even in PFA-fixed or Ko143-inhibited samples.

To rule out the possibility that low protein expression level or protein dislocalization was responsible for the absence of labeling of most of the mutants, and to test whether they could reach the plasma membrane (necessary for recognition by 5D3 antibody), we analyzed ABCG2 immunofluorescence by confocal microscopy.

Fig. 5B shows that all mutants could be detected by the BXP-21 antibody, recognizing an intracellular epitope of ABCG2, and all of them were present in the plasma membrane (except for the hardly expressed C603A/C608A double mutant, which was found, for the most part, intracellularly). However, 5D3 labeling analyzed by confocal microscopy gave the same result as the flow cytometry measurements, that is, only the cells expressing the wild-type ABCG2, C603A, and the C592A/C608A variants (the latter one seen only at increased detector voltage) could bind the 5D3 antibody.

It has been shown that the 5D3 antibody inhibits the transport function of ABCG2 (as judged in a sensitive Hoechst 33342 assay), although this inhibition is only partial and requires high concentrations of the antibody (15). To analyze a potential correlation between 5D3 binding and transport inhibition, we added high concentrations of 5D3 to the HEK cells and then analyzed ABCG2-specific Hoechst 33342 transport activity. We found that, in contrast to a 30–40% inhibition found in the case of the wild-type ABCG2, 5D3 did not influence the Hoechst 33342 transport activity of the C592A/C608A and C592A/C603A/C608A mutants (data not shown). All of these data strongly suggest that the ABCG2 mutant proteins lacking the cysteines required for intramolecular S–S bridge forma-

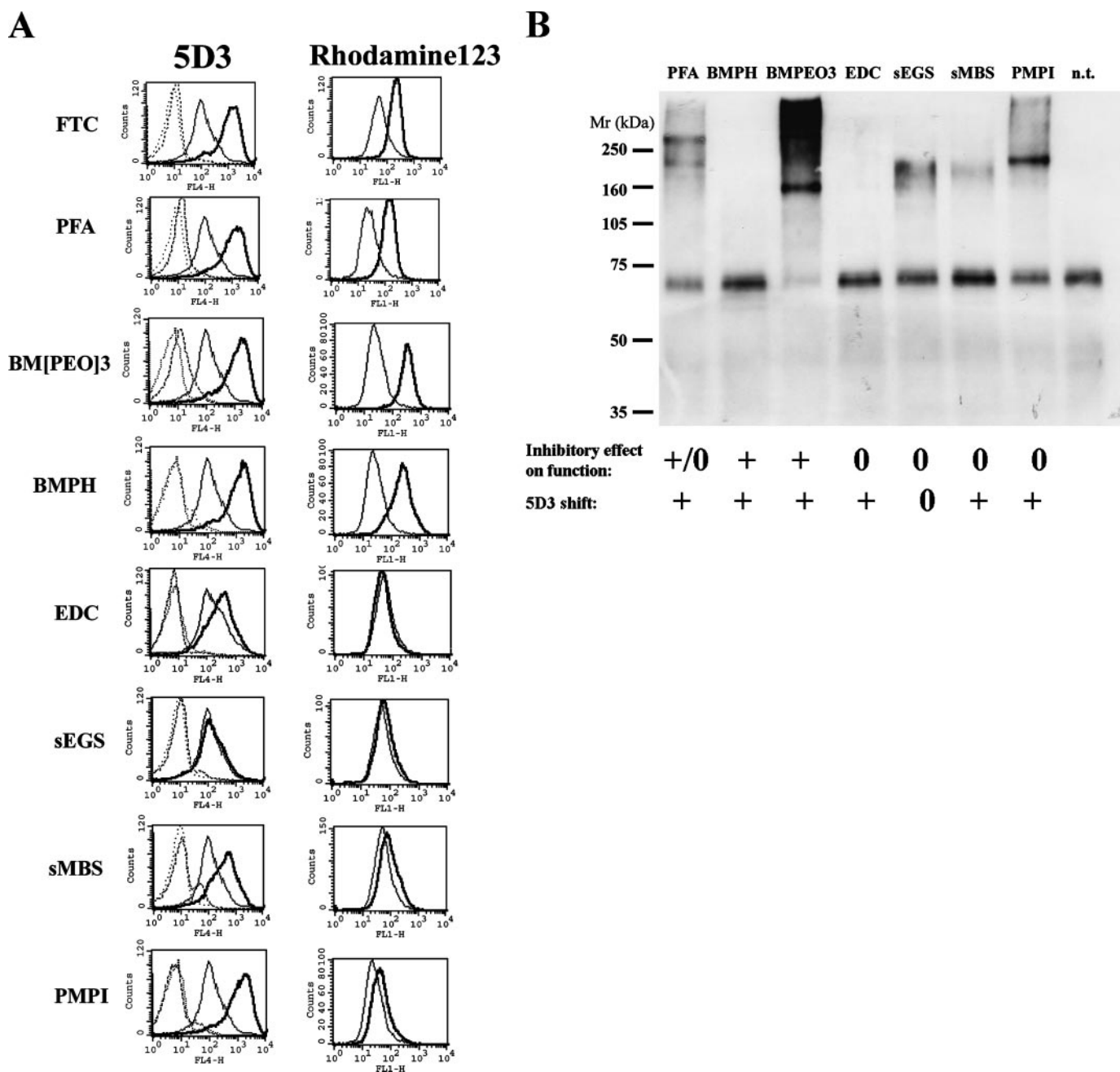


FIGURE 2. *A*, effect of protein cross-linkers on 5D3 labeling and function of ABCG2. HEK-ABCG2-R482G cells were incubated with different protein cross-linkers, washed, and then labeled with 5D3-Alexa647 (*left panel*) or incubated with 2 μ M rhodamine123 (*right panel*) in the presence or absence of the inhibitor Ko143. Fluorescence was determined by flow cytometry. *Left panel*, dotted lines represent labeling of mock-transfected native cells, and dashed lines stand for mock-transfected cells treated with cross-linker (or FTC). The solid lines represent 5D3 labeling of native, and heavy solid lines show cross-linker (or FTC)-treated ABCG2-expressing cells. *Right panel*, rhodamine123 uptake of cross-linker (or FTC) nontreated HEK-ABCG2 cells (solid line) or cross-linker (or FTC)-treated HEK-ABCG2 cells (heavy solid line). Only living cells are shown in the *right panel*. *B*, Western blot analysis of the effect of protein cross-linkers on ABCG2. HEK-ABCG2 cells were incubated with different protein cross-linkers, washed, and then suspended in Laemmli buffer. Proteins were separated by 7.5% SDS-PAGE. After electroblotting, ABCG2 was detected by using the BXP-21 antibody. Each lane represents 15 μ g of protein (+/0, in the case of PFA, its inhibitory effect depends on the concentration used; see Fig. 1C). sEGS, sulfo-EGS; sMBS, sulfo-MBS.

tion are expressed in comparable amounts, reach the cell surface, and work as active transporters in a manner similar to the wild-type ABCG2, but these variants (except for the C592A/C608A mutant showing weak 5D3 binding) are unable to bind the 5D3 antibody.

Effect of DTT on 5D3 Labeling of the Cys-to-Ala Mutants—To test whether decreased 5D3 binding in ABCG2-expressing cells treated with DTT was due to the reduction of the extracellular

cysteines, we also examined the effect of DTT on 5D3 labeling of the mutants C603A and C592A/C608A in native or PFA-fixed cells. Fig. 6, *A* and *B*, shows that DTT is still effective in the reduction of 5D3 binding in the case of the C603A mutant but has practically no effect on 5D3 labeling of the C592A/C608A mutant. When we analyzed 5D3 fluorescence in ABCG2-expressing HEK cells treated with increasing concentrations of DTT, we found that DTT treatment caused a gradual decrease

in 5D3 binding that reached its minimum (almost the fluorescence of the background) at 10–50 mM DTT in ABCG2 and C603A-expressing cells, whereas DTT had no effect on labeling of the C592A/C608A double mutant (Fig. 6C). These experiments suggest that the intramolecular and not the intermolecular S–S bonds are important in 5D3 epitope formation.

Experiments with 5D3-Fab—To analyze whether the 5D3 shift is caused by the stabilization of the epitopes in a dimer form of ABCG2, and thus an intact, bivalent 5D3 is required for

labeling, we incubated HEK-ABCG2 cells with the Alexa647-conjugated Fab fragment of 5D3. We found a lower affinity but specific binding of 5D3 Fab to ABCG2 that was greatly increased by PFA fixation or by Ko143. DTT treatment also reduced Fab binding (Fig. 7). These experiments also suggest that 5D3 binding to ABCG2 depends on the conformation of an epitope found on a monomeric ABCG2.

DISCUSSION

ABCG2 is a marker protein of the side population of stem cells and is also important in tumor cells where it can mediate the emergence of a multidrug-resistant phenotype. On one hand, a sensitive method for the detection of low amounts of ABCG2 may allow the enrichment and selection of ABCG2-expressing cells, such as stem cells. On the other hand, monitoring the presence of ABCG2 in tumor samples from patients can help to find the most effective chemotherapy treatment using non-ABCG2 substrate drugs. The conformation-sensitive antibody 5D3 is a good candidate for the detection of ABCG2 for the above mentioned purposes. However, to establish a reliable method it is essential to find the optimum conditions to be able to detect even low amounts of endogenous ABCG2. In our previous paper we showed that 5D3 binding depends on the actual conformation of ABCG2 (15). We could define two ABCG2 conformations based on the 5D3 binding capacity. The high affinity form was observed in ABCG2 inhibited by the specific inhibitor Ko143 in ATP-depleted cells or after fixation of the cells with PFA, whereas stabilization of ABCG2 in a vanadate-trapped form resulted in decreased 5D3 binding, representing a low affinity form.

In this study we have further analyzed how alterations in ABCG2 structure, covalent cross-linking, or changes in the S–S

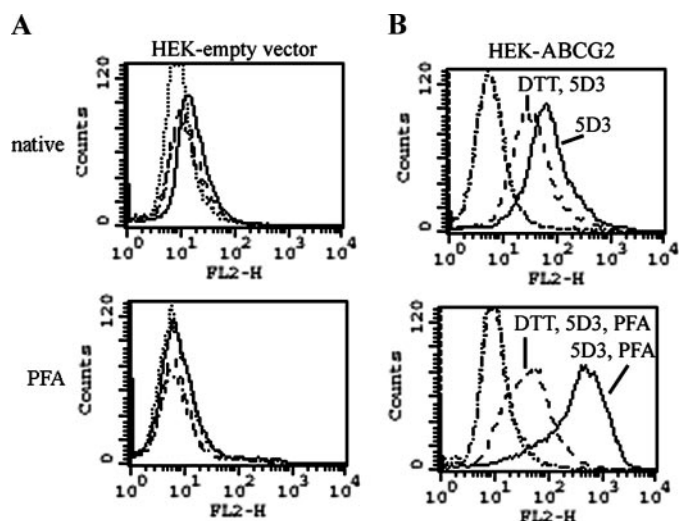


FIGURE 3. Effect of DTT treatment on 5D3 binding. HEK293 cells transfected with empty pCIN4 (A) or pCIN4-ABCG2(R482G) (B) were incubated with or without 10 mM DTT, washed, and then labeled with 5D3 or mouse IgG2b and goat anti-mouse phycoerythrin-conjugated secondary antibody. The upper panels represent labeling of PFA nontreated cells (native), and the lower panels show labeling of cells that were fixed with 1% PFA after DTT treatment. Dotted lines, isotype control; dot-dash-dotted lines, isotype control of DTT-treated cells; solid lines, 5D3; dashed lines, 5D3 labeling of DTT-treated cells.

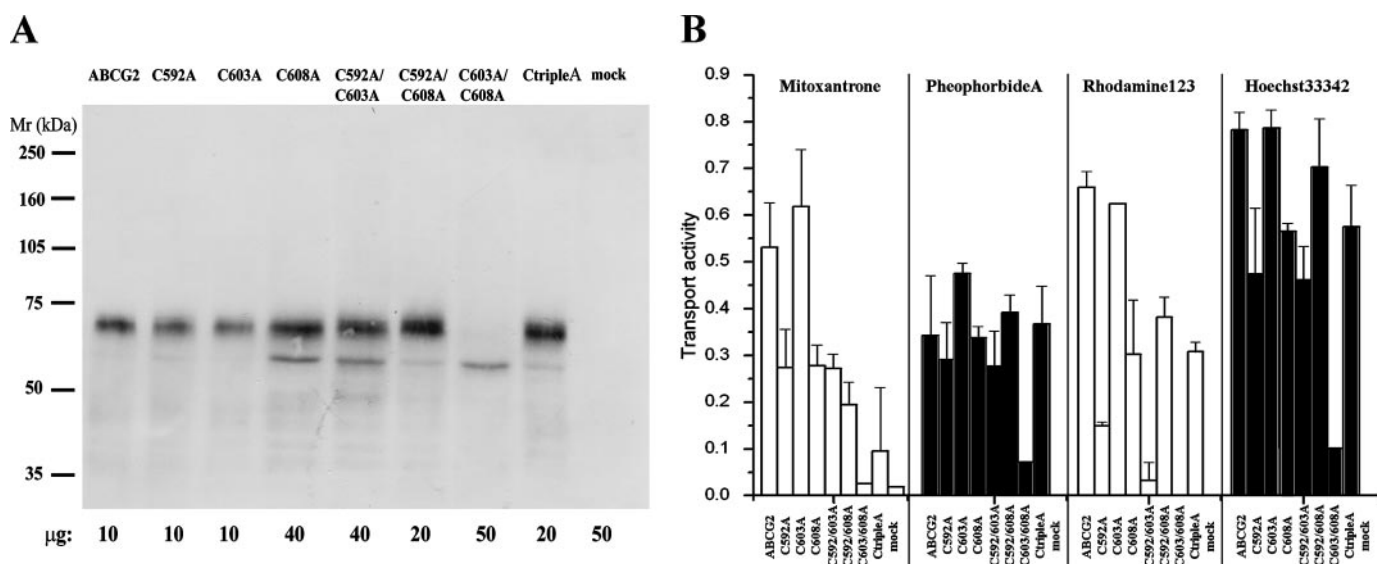


FIGURE 4. A, expression of various ABCG2 mutants carrying Cys-to-Ala changes. HEK cells were transfected with pCIN4 vectors encoding different Cys-to-Ala ABCG2 mutants or R482G (indicated as ABCG2). Cells were lysed, dissolved in disaggregation buffer, and subjected to 7.5% SDS-PAGE. ABCG2 was detected by the BXP-21 antibody. To demonstrate differences in the expression level of the mutants, various amounts of samples were loaded onto the gel as indicated in the figure. **B**, mitoxantrone, pheophorbide A, rhodamine 123, and Hoechst 33342 transport activity of Cys-to-Ala mutants. HEK cells expressing different ABCG2 mutants or R482G (indicated as ABCG2) were incubated with 5 μ M mitoxantrone, 1 μ M pheophorbide A, 2 μ M rhodamine 123, or 1 μ M Hoechst 33342 in the absence or presence of 1 μ M Ko143. Fluorescence of mitoxantrone, pheophorbide A, and rhodamine 123 was detected in a FACScalibur cytometer, and activity factors were calculated from mean fluorescence values as described under “Experimental Procedures.” Fluorescence due to Hoechst 33342 accumulation was determined in a spectrofluorimeter. The transport rate was determined as described under “Experimental Procedures.” Shown are the average transport activities obtained from two independent experiments.

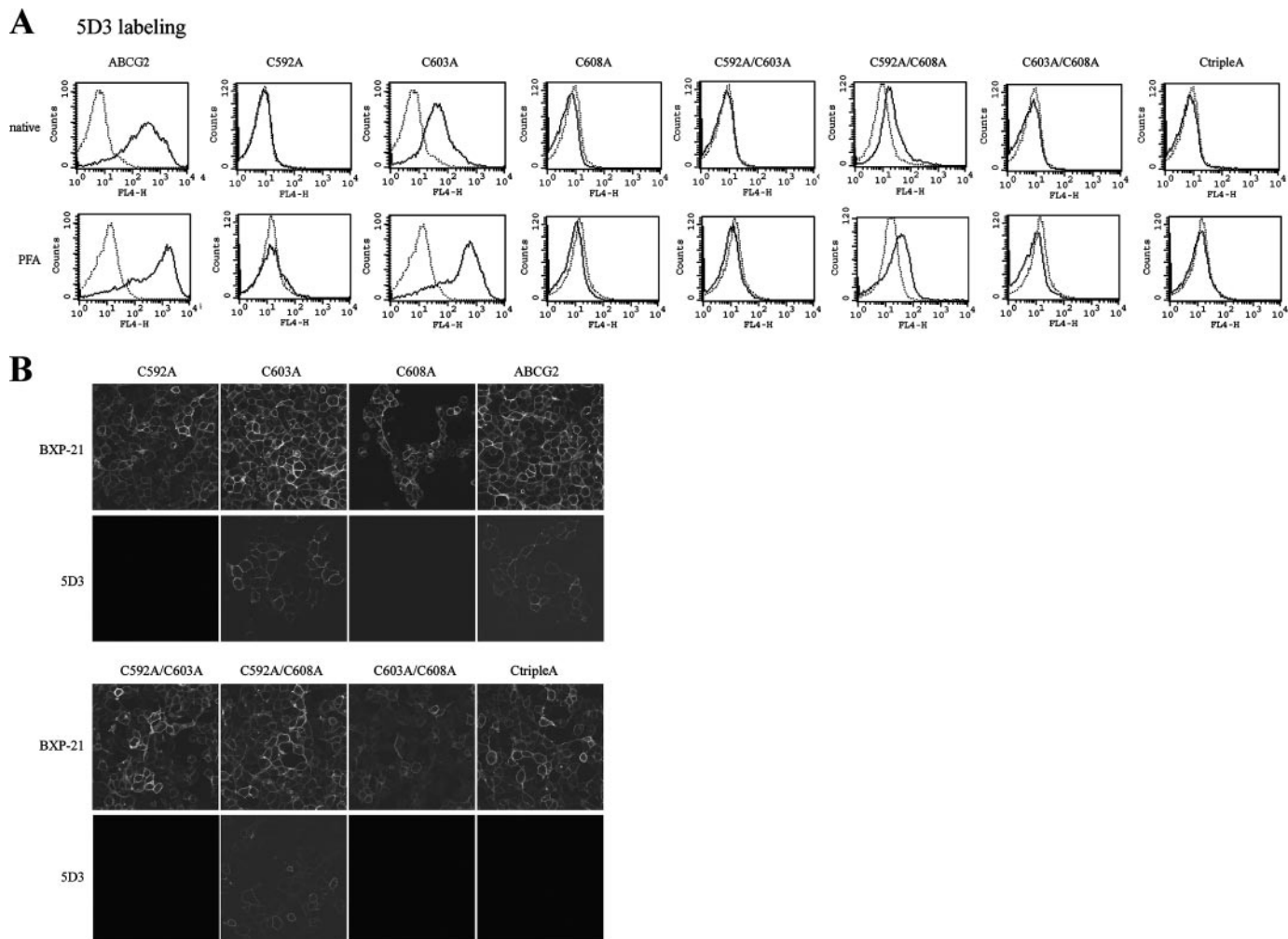


FIGURE 5. *A*, 5D3 labeling of HEK cells expressing different Cys-to-Ala mutants of ABCG2. Native (*upper panel*) or 1% PFA-treated (*lower panel*) cells were labeled with 5D3-Alexa647. 5D3 fluorescence was detected by flow cytometry. Then *solid lines* represent 5D3-Alexa647 labeling of cells expressing different ABCG2 mutants, as indicated *above* the panels, and the *dotted lines* represent 5D3-Alexa647 labeling of cells transfected with empty vector. *B*, localization of the ABCG2 Cys-to-Ala mutants. HEK cells expressing different ABCG2 mutants (as indicated *above* the panels) were fixed in 4% paraformaldehyde, permeabilized in prechilled methanol, and then incubated with the BXP-21 antibody and Alexa Fluor 488-conjugated goat anti-mouse IgG. To label the cell surface epitope of ABCG2, a direct immunofluorescent reaction was performed. The cells were fixed with 1% paraformaldehyde and then incubated with allophycocyanin-conjugated 5D3. The stained slides were analyzed using an Olympus FV500-IX confocal laser scanning microscope. Fluorescence was acquired using the same equipment settings, except the slide representing 5D3 labeling of C592A/C608A was taken at an increased detector voltage.

bonds on the external regions of ABCG2 influence 5D3 binding. When analyzing the effects of PFA fixation in HEK-ABCG2 cells, we found that although at higher concentrations PFA abolishes ABCG2 function and results in the formation of an ABCG2 dimer, at lower concentrations, which already cause a 5D3 shift, PFA is neither inhibitory on function nor does it cross-link ABCG2 dimers (Fig. 1, *C* and *D*). When we analyzed the effects of specific protein cross-linkers on 5D3 binding to ABCG2, we found that some of these agents increased 5D3 binding while causing a variable loss in transport function or covalent dimer formation.

In fact, EDC resulted in a 5D3 shift without the inhibition of ABCG2 function or covalent formation of an ABCG2 dimer (see Fig. 2, *A* and *B*). Thus, there was no general correlation between the 5D3 shift and the inhibition of the function or cross-linking of ABCG2 dimers. Experiments performed with the Fab fragment of 5D3 (see Fig. 7), having only one binding region, also suggested that the epitope is most probably located on an ABCG2 monomer.

The ABCG2 homodimer is linked via a disulfide bond mediated by Cys-603, found in the third extracellular loop of the protein. Additionally, there are two other cysteines (Cys-592 and Cys-608) in the third extracellular loop of ABCG2, suggested to form an intramolecular S–S bridge. When we treated intact HEK-ABCG2 cells with the nonpermeable reducing agent DTT, we found a significant decrease in 5D3 binding with no effect on the ABCG2 transport function (see Figs. 3 and 6), indicating a dramatic effect of the disruption of the extracellular S–S bonds on the 5D3 epitope formation. To find out which disulfide bridge is important for epitope formation, we analyzed different Cys-to-Ala mutants lacking the intermolecular (C603A), the intramolecular (C592A, C608A, C592A/C608A), or both kinds of (C592A/C603A, C603A/C608A, or C592A/C603A/C608A) S–S bonds.

We found that the C603A mutant behaves similarly to ABCG2 having intact S–S bridges. The C603A mutant, which can be expressed in an amount comparable to ABCG2, is found in the plasma membrane (Figs. 4*A* and 5*B*). This mutant is fully

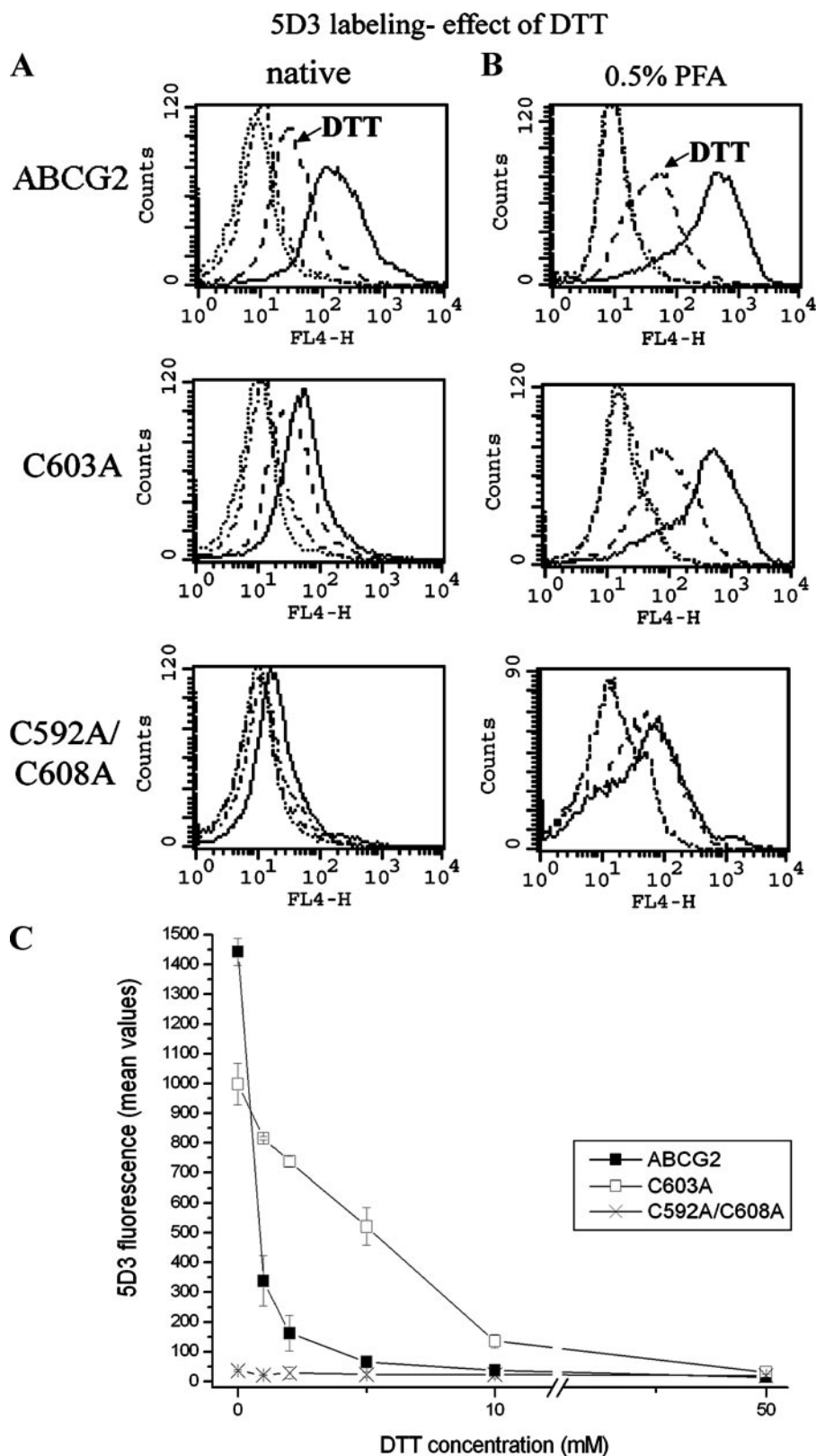


FIGURE 6. *A* and *B*, effect of DTT on labeling of the Cys-to-Ala mutants. HEK293 cells expressing different ABCG2 mutants were treated with 10 mM DTT, washed, and then labeled with 5D3-Alexa647 (*A*). *B* shows the labeling of samples fixed with 0.5% PFA prior to antibody labeling. Fluorescence was determined in a FACSCalibur cytometer. *Dotted lines*, mock-transfected HEK; *dot-dash-dotted lines*, DTT-treated, mock-transfected HEK cells; *solid lines*, HEK cells expressing different ABCG2 mutants; *dashed lines*, HEK cells expressing different ABCG2 mutants treated with DTT. *C*, HEK cells expressing different ABCG2 mutants were treated with increasing concentrations of DTT, fixed with 0.5% PFA, and labeled with 5D3-Alexa647. 5D3 fluorescence was determined by flow cytometry. Mean values obtained from at least in two independent experiments are shown.

active and has the same substrate specificity as ABCG2 (Fig. 4*B*). Cys-603 has a clearly detectable 5D3 binding that can be increased by inhibition of ABCG2 function by Ko143 or treatment with protein cross-linkers. DTT treatment also decreased 5D3 binding of this mutant (Fig. 6), suggesting that this cysteine is not important for the observed effect of S-S bridge reduction.

The single mutants, lacking the intramolecular S-S bond, *i.e.* C592A, C608A, as well as the C592A/C603A/C608A variant, had clearly detectable expression levels, were present in the plasma membrane, and were functional for active transport with somewhat altered substrate specificities (Figs. 4 and 5). However, these mutants did not show any specific 5D3 binding either in a PFA-fixed or in a Ko143-inhibited form, and moreover, 5D3 did not inhibit their function. These experiments suggest that the intramolecular S-S bridge in the third extracellular loop of ABCG2 has a crucial, either direct or indirect (*e.g.* stabilizing the proper conformation), role in the formation of the 5D3 epitope as well as in the substrate specificity of the transporter.

The role of the intramolecular S-S bond in 5D3 epitope formation has already been suggested (9, 10). Kage *et al.* (9) analyzed 5D3 labeling in intact cells expressing various Cys-to-Ser mutants by flow cytometry. They found that C592S and C608S had impaired 5D3 binding; however, these two mutants showed very low expression levels in this study (9). In our experiments we were able to express C592A and C608A mutants in comparable levels to the wild-type ABCG2. Moreover, we demonstrated that even though these mutants were functional and properly localized to the plasma membrane, they could not be labeled with 5D3 even in the presence of an inhibitor or PFA.

Henriksen *et al.* (10) also suggested the role of the intramolecular S-S bridge of ABCG2 in 5D3 bind-

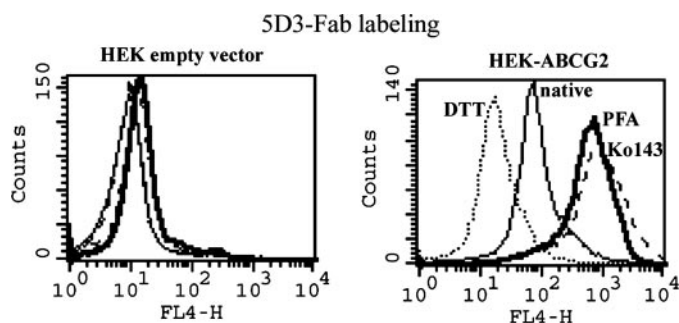


FIGURE 7. Direct labeling of HEK cells by Alexa647-conjugated 5D3-Fab. HEK293 cells transfected with the pCIN4 vector or pCIN4 containing the cDNA of ABCG2(R482G) were incubated with 2 $\mu\text{g}/\text{ml}$ 5D3-Fab-Alexa647. Fluorescence was determined by flow cytometry. The *dotted lines* represent labeling of 10 mM DTT-treated cells; *solid lines* stand for native cells incubated only with 5D3-Fab, *heavy solid lines* show labeling of 0.5% PFA-fixed cells, and *dashed lines* indicate fluorescence in the presence of the inhibitor Ko143.

ing; they detected no 5D3 labeling by confocal microscopy for C592A, C608A, and the C592A/C608A double mutant. In harmony with this study, we could not detect any labeling for the single Cys-to-Ala mutants. However, in our hands the C592A/C608A double mutant showed a weak 5D3 binding both in flow cytometry and confocal microscopy, and the 5D3 shift upon PFA or Ko143 treatment could also be observed (Fig. 5). DTT had no effect on the 5D3 labeling of the C592A/C608A variant (Fig. 6), and the excess amount of 5D3 did not inhibit the function of this mutant.

The single Cys-592 or Cys-608 mutants showed an increased cytoplasmic accumulation (9, 10, 13), whereas the simultaneous removal of cysteines 592 and 608 promoted protein stability and proper targeting (10). Thus such a double mutation may allow the development of a favorable conformation within the ABCG2 protein, allowing some 5D3 labeling.

Based on these data we suggest that protein cross-linking most probably stabilizes the epitope of 5D3 present within a single ABCG2 protein. The effect of DTT treatment on 5D3 labeling together with experiments on the extracellular Cys-to-Ala mutants revealed that the third extracellular loop, and especially the intramolecular S–S bond within this region, has a crucial role in 5D3 epitope formation and probably in the substrate interactions of ABCG2.

To visualize the possible molecular arrangement of the third extracellular loop (ECL3) of the ABCG2 protein, we performed a molecular dynamic simulation of the folding of this relatively large protein sequence. Currently, there are no atomic structures available for eukaryotic ABC transporters, and molecular modeling is usually guided by the recently solved structures of bacterial transporters. Although a recent communication offers a homology model for ABCG2 (30), it does not include ECL3, as this loop shows no homology to any ABC protein sequences with a known structure. Data for other ABC transporters, however, suggest that the adjacent transmembrane regions of these proteins are found near each other, within a distance of 9–12 Å. Therefore in our simulation algorithm, we fixed the N- and C-terminal regions of the ECL3 at this distance at the membrane surface. We have also included the information that the cysteines forming intramolecular S–S bonds (Cys-592 and Cys-608), as well as a cysteine involved in the intermo-

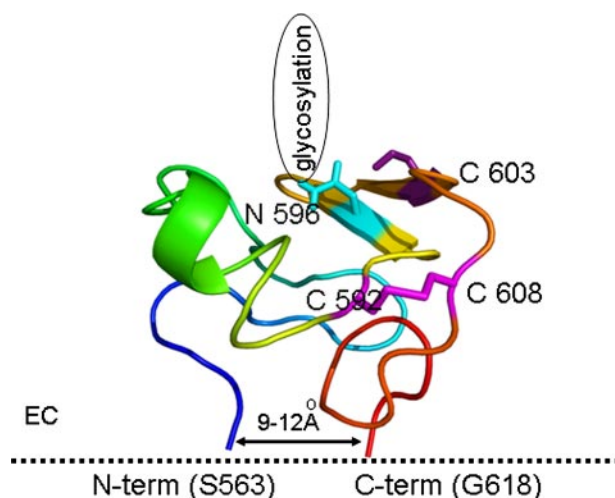


FIGURE 8. Model of the third extracellular loop of ABCG2 (amino acids 563–618) obtained by *ab initio* folding employing discrete molecular dynamics. The structure is colored *blue to red* from the N to the C terminus. Cysteines involved in intramolecular and intermolecular interactions are represented with *sticks* and are colored *magenta*. The glycosylation site (Asn-596) is represented by a *blue stick*.

lecular S–S bridge formation, are most probably located on the surface of this loop. It is interesting to note, that many of the ABCG-type proteins have this large, conserved, extracellular region, with similar arrangements of cysteines and potential glycosylation sites (11).

The conformation obtained, as seen in Fig. 8, corresponds to these requirements and suggests the presence of a stabilized antiparallel loop with β -sheets in the region of the three cysteines, surrounding the glycosylation site. When either Cys-592 or Cys-608 was replaced by alanines in the *in silico* model, the structure of the antiparallel loop collapsed and the folding lost its conserved characteristics (data not shown). The combination of the experimental and the simulation results suggest a well defined structure in this area of ECL3, which may be important in mediating ABCG2 interaction with the plasma membrane or other proteins. Moreover, the conformation of this loop seems to modulate the substrate and antibody binding to this membrane transporter.

Acknowledgments—We greatly appreciate the technical help of Éva Krizsán, Zsuzsanna András, and Judit Kis. We appreciate the kind gifts of Ko143 from Drs. J. D. Allen and G. J. Koomen and anti-ABCG2 BXP-21 antibody obtained from Drs. George Scheffer and Rik Scheper.

REFERENCES

- Sarkadi, B., Homolya, L., Szakacs, G., and Varadi, A. (2006) *Physiol. Rev.* **86**, 1179–1236
- Chandra, P., and Brouwer, K. L. (2004) *Pharm. Res. (N. Y.)* **21**, 719–735
- Maliepaard, M., Scheffer, G. L., Faneyte, I. F., van Gastelen, M. A., Pijnenborg, A. C., Schinkel, A. H., van De Vijver, M. J., Scheper, R. J., and Schellens, J. H. (2001) *Cancer Res.* **61**, 3458–3464
- Zhou, S., Schuetz, J. D., Bunting, K. D., Colapietro, A. M., Sampath, J., Morris, J. J., Lagutina, I., Grosveld, G. C., Osawa, M., Nakauchi, H., and Sorrentino, B. P. (2001) *Nat. Med.* **7**, 1028–1034
- Krishnamurthy, P., Ross, D. D., Nakanishi, T., Bailey-Dell, K., Zhou, S., Mercer, K. E., Sarkadi, B., Sorrentino, B. P., and Schuetz, J. D. (2004) *J. Biol. Chem.* **279**, 24218–24225
- Krishnamurthy, P., and Schuetz, J. D. (2005) *Biometals* **18**, 349–358

7. Ozvegy, C., Litman, T., Szakacs, G., Nagy, Z., Bates, S., Varadi, A., and Sarkadi, B. (2001) *Biochem. Biophys. Res. Commun.* **285**, 111–117
8. Kage, K., Tsukahara, S., Sugiyama, T., Asada, S., Ishikawa, E., Tsuruo, T., and Sugimoto, Y. (2002) *Int. J. Cancer* **97**, 626–630
9. Kage, K., Fujita, T., and Sugimoto, Y. (2005) *Cancer Sci.* **96**, 866–872
10. Henriksen, U., Fog, J. U., Litman, T., and Gether, U. (2005) *J. Biol. Chem.* **280**, 36926–36934
11. Wakabayashi, K., Nakagawa, H., Adachi, T., Kii, I., Kobatake, E., Kudo, A., and Ishikawa, T. (2006) *J. Exp. Ther. Oncol.* **5**, 205–222
12. Takada, T., Suzuki, H., and Sugiyama, Y. (2005) *Pharm. Res. (N. Y.)* **22**, 458–464
13. Wakabayashi, K., Nakagawa, H., Tamura, A., Koshihara, S., Hoshijima, K., Komada, M., and Ishikawa, T. (2007) *J. Biol. Chem.* **282**, 27841–27846
14. Robey, R. W., Polgar, O., Deeken, J., To, K. W., and Bates, S. E. (2007) *Cancer Metastasis Rev.* **26**, 39–57
15. Ozvegy-Laczka, C., Varady, G., Koblos, G., Ujhelly, O., Cervenak, J., Schuetz, J. D., Sorrentino, B. P., Koomen, G. J., Varadi, A., Nemet, K., and Sarkadi, B. (2005) *J. Biol. Chem.* **280**, 4219–4227
16. Abbott, B. L., Colapietro, A. M., Barnes, Y., Marini, F., Andreeff, M., and Sorrentino, B. P. (2002) *Blood* **100**, 4594–4601
17. Allen, J. D., van Loevezijn, A., Lakhai, J. M., van der Valk, M., van Tellingen, O., Reid, G., Schellens, J. H., Koomen, G. J., and Schinkel, A. H. (2002) *Mol. Cancer Ther.* **1**, 417–425
18. Robey, R. W., Honjo, Y., Morisaki, K., Nadjem, T. A., Runge, S., Risbood, M., Poruchynsky, M. S., and Bates, S. E. (2003) *Br. J. Cancer* **89**, 1971–1978
19. Elkind, N. B., Szentpetery, Z., Apati, A., Ozvegy-Laczka, C., Varady, G., Ujhelly, O., Szabo, K., Homolya, L., Varadi, A., Buday, L., Keri, G., Nemet, K., and Sarkadi, B. (2005) *Cancer Res.* **65**, 1770–1777
20. Szollosi, J., Horejsi, V., Bene, L., Angelisova, P., and Damjanovich, S. (1996) *J. Immunol.* **157**, 2939–2946
21. Spack, E. G., Jr., Packard, B., Wier, M. L., and Edidin, M. (1986) *Anal. Biochem.* **158**, 233–237
22. Ozvegy, C., Varadi, A., and Sarkadi, B. (2002) *J. Biol. Chem.* **277**, 47980–47990
23. Ozvegy-Laczka, C., Hegedus, T., Varady, G., Ujhelly, O., Schuetz, J. D., Varadi, A., Keri, G., Orfi, L., Nemet, K., and Sarkadi, B. (2004) *Mol. Pharmacol.* **65**, 1485–1495
24. Hegedus, T., Serohijos, A. W., Dokholyan, N. V., He, L., and Riordan, J. R. (2008) *J. Mol. Biol.* **378**, 1052–1063
25. Dokholyan, N. V., Buldyrev, S. V., Stanley, H. E., and Shakhnovich, E. I. (1998) *Folding Des.* **3**, 577–587
26. Ding, F., and Dokholyan, N. V. (2005) *Trends Biotechnol.* **23**, 450–455
27. Ding, F., and Dokholyan, N. V. (2006) *PLoS Comput. Biol.* **2**, e85
28. Sugita, Y., and Okamoto, Y. (1999) *Chem. Phys. Lett.* **314**, 141–151
29. Ding, F., Tsao, D., Nie, H., and Dokholyan, N. V. (2008) *Structure (Lond.)* **16**, 1010–1018
30. Hazai, E., and Bikadi, Z. (2007) *J. Struct. Biol.* **162**, 63–74
31. Mitomo, H., Kato, R., Ito, A., Kasamatsu, S., Ikegami, Y., Kii, I., Kudo, A., Kobatake, E., Sumino, Y., and Ishikawa, T. (2003) *Biochem. J.* **373**, 767–774



Functional expression of the 11 human Organic Anion Transporting Polypeptides in insect cells reveals that sodium fluorescein is a general OATP substrate



Izabel Patik^a, Daniella Kovacsics^a, Orsolya Németh^a, Melinda Gera^a, György Várady^b, Bruno Stieger^c, Bruno Hagenbuch^d, Gergely Szakács^a, Csilla Özvegy-Laczka^{a,*}

^a Momentum Membrane Protein Research Group, Institute of Enzymology, Research Centre for Natural Sciences, Hungarian Academy of Sciences, Magyar tudósok krt. 2, H-1117 Budapest, Hungary

^b Laboratory of Molecular Cell Biology, Institute of Enzymology, Research Centre for Natural Sciences, Hungarian Academy of Sciences, Magyar tudósok krt. 2, H-1117 Budapest, Hungary

^c Department of Clinical Pharmacology and Toxicology, University Hospital, 8091 Zurich, Switzerland

^d Department of Pharmacology, Toxicology and Therapeutics, The University of Kansas Medical Center, Kansas City, KA 66160, USA

ARTICLE INFO

Article history:

Received 3 August 2015

Accepted 17 September 2015

Available online 28 September 2015

Chemical compounds studied in this article:

Sodium fluorescein (PubChem CID: 16850)

Fluorescein-methotrexate (PubChem CID: 86761749)

Imatinib (PubChem CID: 5291)

Estradiol 17-β-D-glucuronide (PubChem CID: 66424)

Ursolic acid (PubChem CID: 64945)

Cyclosporin A (PubChem CID: 5284373)

Prostaglandin E₂ (PubChem CID: 5280360)

Glycocholate (PubChem CID: 5460316)

Taurocholate (PubChem CID: 6675)

Keywords:

Organic Anion Transporting Polypeptide

Fluorescent assay

New substrates

Drug screening

ABSTRACT

Organic Anion Transporting Polypeptides (OATPs), encoded by genes of the Solute Carrier Organic Anion (SLCO) family, are transmembrane proteins involved in the uptake of various compounds of endogenous or exogenous origin. In addition to their physiological roles, OATPs influence the pharmacokinetics and drug–drug interactions of several clinically relevant compounds. To examine the function and molecular interactions of human OATPs, including several poorly characterized family members, we expressed all 11 human OATPs at high levels in the baculovirus-Sf9 cell system. We measured the temperature- and inhibitor-sensitive cellular accumulation of sodium fluorescein and fluorescein-methotrexate, two fluorescent substrates of the OATPs, OATP1B1 and 1B3. OATP1B1 and 1B3 were functional in Sf9 cells, showing rapid uptake ($t_{1/2}(\text{fluorescein-methotrexate})$ 2.64 and 4.16 min, and $t_{1/2}(\text{fluorescein})$ 6.71 and 5.58 min for OATP1B1 and 1B3, respectively) and high-affinity transport ($K_m(\text{fluorescein-methotrexate})$ 0.23 and 0.53 μM, and $K_m(\text{fluorescein})$ 25.73 and 38.55 μM for OATP1B1 and 1B3, respectively) of both substrates. We found that sodium fluorescein is a general substrate of all human OATPs: 1A2, 1B1, 1B3, 1C1, 2A1, 2B1, 3A1, 4A1, 4C1, 5A1 and 6A1, while fluorescein-methotrexate is only transported by 1B1, 1B3, 1A2 and 2B1. Acidic extracellular pH greatly facilitated fluorescein uptake by all OATPs, and new molecular interactions were detected (between OATP2B1 and Imatinib, OATP3A1, 5A1 and 6A1 and estradiol 17-β-D-glucuronide, and OATP1C1 and 4C1 and prostaglandin E₂). These studies demonstrate, for the first time, that the insect cell system is suitable for the functional analysis of the entire human OATP family, and for drug–OATP interaction screening.

© 2015 Elsevier Inc. All rights reserved.

1. Introduction

The role of uptake transporters in drug pharmacokinetics is being increasingly recognized. One group of uptake transporters

gaining recognition for their relevance to the absorption and toxicity of clinically relevant drugs are the Organic Anion Transporting Polypeptides (OATPs) [1,2]. OATPs are plasma membrane proteins that mediate sodium and ATP-independent transport of

Abbreviations: CA, cholic acid; CsA, cyclosporin A; EG, estradiol 17-β-D-glucuronide; HEPES, 4-(2-hydroxyethyl)-1-piperazineethanesulfonic acid; MES, 4-morpholineethanesulfonic acid; Na-Fluo, Na-fluorescein; Fl-MTX, fluorescein-methotrexate; GC, glycocholate; MTX, methotrexate; PGE₂, prostaglandin E₂; PVDF, polyvinylidene fluoride; Rif, rifampicin; Sf9, *Spodoptera frugiperda* insect cells; TC, taurocholate; UA, ursolic acid.

* Corresponding author.

E-mail address: laczka.csilla@ttk.mta.hu (C. Özvegy-Laczka).

<http://dx.doi.org/10.1016/j.bcp.2015.09.015>

0006-2952/© 2015 Elsevier Inc. All rights reserved.

large (over 300 Da), charged or amphipathic compounds into cells [3–5]. The 11 known OATPs are encoded by genes of the Solute Carrier Organic Anion (SLCO) family.

Based on their substrate specificity, OATPs can be divided into two groups. OATP1A2, 1B1, 1B3 and 2B1 transport a wide range of compounds, from bile acids and hormones, to various therapeutics including statins, antiviral agents and antibiotics. Conversely, OATP3A1, 1C1, 2A1, 4A1, 4C1 and 5A1 have been documented to transport only a few compounds [4,6,7]. Currently, there is no published information on the function or substrate specificity of OATP6A1, primarily due to the lack of convenient expression systems and functional assays.

OATP1B1 and 1B3 are important in the hepatic re-uptake of bile acids, bilirubin and in the hepatic clearance of several drugs [2]. Mutations in *SLCO1B1* and *1B3* result in Rotor syndrome, a benign disorder characterized by increased serum bilirubin levels. The role of the 1A/1B family of OATPs in the hepatic disposition of bile salts, bilirubin and therapeutic drugs was demonstrated via knock out [8] and transgenic mouse models [9]. Deletion of the mouse orthologue of OATP1C1 results in mild, brain-specific hypothyroidism confirming the function of this protein in thyroid transport [10]. The physiological relevance of the remaining OATPs remains to be elucidated.

Several single nucleotide polymorphisms (SNPs) in OATP-encoding genes have been linked to altered drug pharmacokinetics, suggesting that these transporters play an important role in the uptake and elimination of drugs [11]. Population studies and in vitro experiments demonstrate that SNPs in OATP1A2, 1B1, 1B3 and 2B1 affect the uptake of hormones and antihistamines, as well as cholesterol-lowering and anticancer drugs [11]. OATPs also show altered expression in various cancer cells. Liver-specific OATP1B1 and 1B3 were down-regulated in liver cancers, and highly upregulated in tumors of the ovarian gland (1B1), colon (1B1 and 1B3), breast (1B3), prostate (1B3) and lung (1B3) [1]. Similarly, OATP6A1, normally restricted to the testes, was found in cancerous tissues of the bladder, brain and lung [1]. The potential diagnostic and therapeutic value of the cancer-specific localization of OATPs is currently under intense investigation.

Despite the clear clinical relevance, the substrate recognition patterns of only four members of the OATP family, 1A2, 1B1, 1B3 and 2B1 have been thoroughly investigated. The bottleneck in establishing the substrate/inhibitor profile of OATPs is the scarcity and high cost of radioactively labeled substrates. Mass spectrometry (MS) may be an alternative to assays based on radiolabeled substrates [12]. However, MS is more time-consuming and requires high protein expression levels to obtain an acceptable signal to noise ratio. Contrary to these methods, the measurement of fluorescent substrates is sensitive, safe, relatively inexpensive and amenable to automatized detection.

Sodium fluorescein (Na-Fluo) and fluorescein-methotrexate (FI-MTX) have been shown to be suitable for the screening of potential OATP1B1/1B3-interacting compounds [13,14]. Additionally, Fluo-3, indocyanine green and fluorescent bile acids have been shown to be readily transported by OATP1B1 and 1B3 [15–17]. However, fluorescent assays for the remaining members of the OATP family have not yet been described, and for 6A1, there are no known substrates.

In this study, our aim was to develop a comprehensive, fluorescence-based functional assay to analyze the function of all known human OATPs. We expressed these proteins in the baculovirus-insect cell expression system and developed a functional assay measuring the cellular uptake of Na-Fluo and FI-MTX. We show that Na-Fluo is transported by all 11 human OATPs, and, under optimal assay conditions, 1A2 and 2B1 are able to mediate the uptake of fluorescein-methotrexate. Our insect cell-based method provides the first fluorescent assay for the

functional investigation of all human OATPs, which will facilitate further screening of potential OATP substrates and structure–function relationship analyses.

2. Materials and methods

2.1. Materials

Cholic acid (CA), glycocholic acid (GC), propidium iodide, prostaglandin E₂ (PGE₂), rifampicin (Rif), sodium fluorescein salt (Na-Fluo), taurocholic acid (TC) and ursolic acid (UA) were purchased from Sigma–Aldrich (Budapest, Hungary). Fluorescein-methotrexate (FI-MTX) was obtained from Biotium, Inc. (Hayward, CA, US). Restriction endonucleases were from New England Biolabs, Ltd. (Ipswich, MA, US).

2.2. Plasmid constructs

To generate the expression plasmids for human OATPs, we first engineered unique restriction sites that allowed for cloning of all human OATPs into the baculovirus transfer vector pAcUW21 (BD Biosciences, San Jose, CA, US). The modified plasmid, termed pAcUW-L2, was constructed by inserting the oligonucleotide linkers, 5'-GGCCGTGAATTCGGTACCTCGAGCTCGCGGCCGCT-3' and 5'-GATCAGCGCCGCGAGCTCGAGGTACCGAATTCAC-3', between the BamHI and NotI sites of pAcUW21-L/ABCG2, a vector generated previously in our lab [18]. Full-length cDNA sequences encoding human OATPs were then introduced into pAcUW-L2 using the appropriate restriction sites.

OATP1A2, 1B3, 1C1, 2A1, 2B1, 4A1, 5A1 and 6A1 were obtained from the Harvard PlasmID Repository (Harvard Medical School, Boston, MA, US), and the cloning of OATP1B1 (Gene ID: AB026257), 3A1 variant 1 (AB031050) and 4C1 (353189) was performed using the previously constructed vector, pSPORT1 [19,20]. OATP1B1 and 3A1 transfer vectors were constructed by isolating the corresponding full-length OATP cDNA from pSPORT1, and then subcloning into the pAcUW21-L2 plasmid between the KpnI and NotI restriction endonuclease sites. Sequence analysis revealed that the OATP1B1 cDNA encodes a polymorphism (N130D, rs2306283), therefore, we reverted the sequence to wild-type (Q9Y6L6.2) using site-directed mutagenesis. The primers used in the mutagenesis reaction were: 1B1-N130N for 5'-ACTAATATCAATTCATCAGAAAATTCACAA-3', 1B1-N130N rev 5'-TGTTGAATTTCTGATGAATTGATATTAGT-3'. To generate the OATP6A1 construct, the corresponding cDNA was removed from a pBluescriptR vector (BC034976, HsCD00333181) using NotI and BamHI restriction enzymes, and subcloned into pAcUW21-L/ABCG2. Sequencing revealed that the vector HsCD00333181 contains a shorter isoform of 6A1, which is missing amino acids 206–267, compared to the canonical sequence (Q86UG4-1). The cDNA corresponding to the missing region was synthesized by ShineGene Molecular Bio-Technologies, Inc. (Shanghai, China), and subcloned into the pAcUW-21-L/OATP6A1 isoform 2 vector between the NdeI and SpeI sites. The open reading frames of 1A2 (BC042452, HsCD00333163), 1B3 (BC141525, HsCD00348132), 1C1 (BC022461, HsCD00332885), 2A1 (BC041140, HsCD00338568), 2B1 (BC041095.1, HsCD00378878), 4A1 (BC015727, HsCD00334491), 4C1 and 5A1 (BC137424, HsCD00342690) were amplified by HF PCR (Phusion[®] High-Fidelity PCR Kit, NEB, Ipswich, MA, US) following the manufacturer's instructions and using the following primers:

1A2	for	5'-GGAAGATCTGCGCCGCGCCACCATGGGAGAACTGAGAA-3'
	rev	5'-ATTGAGCTCCTGCAGTTACAATTTAGTTTCAAT-3'
1B3	for	5'-GTAATGCGGCCGCAACTCGAGGCCACCATGGACCAACATCAACAT-3'
	rev	5'-GTACATGCGGCCGCACTGCAGTTAGTTGGCAGCAGCAIT-3'
1C1	for	5'-TGTTTAACTCTAGAGCCACCATGGACACTTCATCCAAAGAA-3'
	rev	5'-TAACTGCAGGCGCCGCTTCTAAAGTTGAGTTTCCTTG-3'

2A1 for	5'-GTAATGCGGCCGCAAGAATTCGCCACCATGGGGCTCTGCCCA-3'
rev	5'-GTACATGCGGCCGCTAAGCTTTTCAGATGAGGCCTGCCG-3'
2B1 for	5'-GTAATGCGGCCGCAAGAATTCGCCACCATGGGACCCAGGATAGG-3'
rev	5'-GTACATGCGGCCGCTAAGCTTTTCACACTCGGAATCCTC-3'
4A1 for	5'-GGAAGATCTGATATCGCCACCATGCCCTGCATCAGCTG-3'
rev	5'-ATTGAGCTCAAGCTTTTCAGACGCTGCTCTGGAG-3'
4C1 for	5'-GGAAGATCTGCGGCCGCGCCACATGAAGAGCGCCAAAGGT-3'
rev	5'-ATTGAGCTCAAGCTTTTCACCTTCTTTACTAT-3'
5A1 for	5'-TGTTTAACTCTAGAGCCACCATGGACGAAGGCACTGGACTGC-3'
rev	5'-TAACCTGCAGGAGCGGCCCTTCTTCCATTTTCAAGCTTCAGGAG-3'

The amplified fragments were digested using the appropriate restriction enzymes (1A2, 4A1 and 4C1: BglII and SacI, 1B3: XhoI and NotI, 2A1 and 2B1: EcoRI and NotI, and 1C1 and 5A1: PmeI and NotI) and subcloned into the pAcUW21-L2 plasmid. Because sequencing of the OATP4A1 construct revealed that the purchased cDNA contains a known SNP of OATP4A1 (232G > A (V78I), rs1047099), the canonical sequence (Q96BD0-1) was generated via QuickChange mutagenesis using the following primers: 5'AGGTGCGGTACGTCTCGG 3' (4A1 for and 5'CCGAGACGTACCGCACCT 3' (4A1 reverse). The DNA sequences for all constructs were verified by sequencing analyses.

2.3. Maintenance of Sf9 cell cultures and generation of recombinant baculoviruses

Sf9 (*Spodoptera frugiperda*) cells were grown in suspension culture using TNM-FH insect medium (Sigma–Aldrich, Budapest, Hungary) supplemented with 10% fetal calf serum, 100 units/ml penicillin and 100 µg/ml streptomycin, at 27 °C. Recombinant baculoviruses, carrying the different human OATP cDNA sequences, were generated using the BaculoGold Transfection Kit (BD Biosciences, San Jose, CA, US) according to the manufacturer's instructions. After several rounds of amplification, the virus stocks were stored at 4 °C. Transport experiments were performed using the virus stocks that resulted in the highest OATP expression levels (as determined by Western blot).

2.4. Immunodetection of OATPs

Whole cell lysates of Sf9 cells (5–10 µg) were separated on 7.5% Laemmli SDS-PAGE gels and transferred onto PVDF membranes. Immunoblotting was performed as described in Ref. [18]. Membranes were incubated overnight with polyclonal antibodies. The antibodies used for the detection of OATP1A2, 1B1, 1B3, 1C1, 2B1, 3A1_v1 and 4A1 were previously described [19]. Antibodies against OATP2A1 (HPA013742), 4C1 (HPA036516), 5A1 (HPA025062) and 6A1 (HPA054126) were purchased from Atlas Antibodies (Stockholm, Sweden). The following antibody dilutions were used: 1/250 for 5A1, 1/500 for 1A2, 1B1, 2A1, 4C1 and 6A1, and 1/1000 for 1B3, 1C1, 2B1, 3A1_v1 and 4A1. After

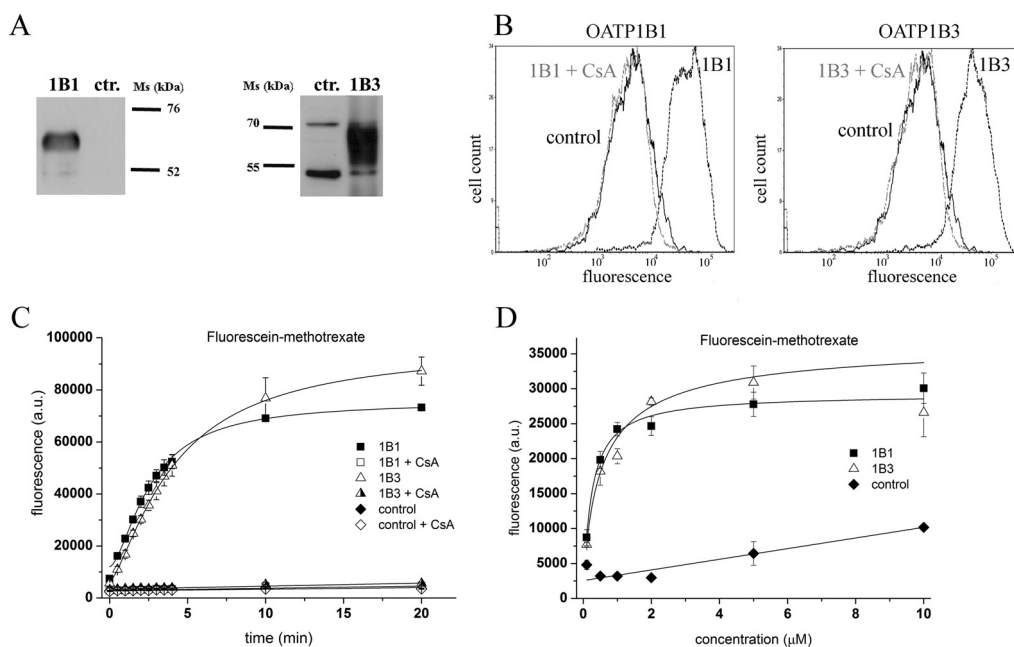


Fig. 1. Overexpression of human OATP1B1 and 1B3 results in increased FI-MTX accumulation within insect cells. (A) Western blot detection of human OATP1B1 and 1B3 expressed in Sf9 insect cells. Total cell lysates (5 µg) were separated on 7.5% SDS gels and the proteins were transferred to PVDF membranes. Anti-OATP1B1 and anti-1B3 polyclonal antibodies [19] (500× and 1000× dilutions, respectively) and 10,000× diluted HRP-conjugated anti-rabbit polyclonal antibodies were used to detect protein expression. Control (ctr.) refers to Sf9 cells overexpressing an unrelated protein (see Section 2). The figure shows a representative experiment. (B) Flow cytometry detection of FI-MTX accumulation in Sf9 cells overexpressing an unrelated protein (control), OATP1B1 or 1B3. Cells were incubated with 1 µM FI-MTX in the presence (gray line) or absence (dashed line) of 20 µM cyclosporin A for 10 min at 37 °C, pH 7.4 (see Section 2). The figure shows a representative experiment. (C) 1 µM FI-MTX uptake determined by flow cytometry at different time points in the presence or absence of 20 µM cyclosporin A (CsA). The data points represent the average geommean ±SD fluorescence values obtained in three independent experiments. (D) Accumulation (2 min) of various concentrations of FI-MTX in insect cells was determined by flow cytometry. Average geommean ±SD values of three independent experiments are shown.

washing, PVDF membranes were incubated with 10,000–20,000x diluted, HRP-conjugated anti-rabbit secondary antibodies (Jackson ImmunoResearch, Suffolk, UK). Luminescence was detected using the Luminor Enhancer Solution kit by Thermo Scientific (Waltham, MA, US).

2.5. Cellular dye uptake and calculation of OATP transport activity

The accumulation of fluorescent molecules was measured as previously described [18], with some minor modifications. Specifically, OATP-transduced Sf9 cells were collected 40 h post infection, washed once and suspended to $2\text{--}5 \times 10^5$ cells/reaction in one of the following buffers: Buffer pH 7.4–8.4: 125 mM NaCl, 4.8 mM KCl, 1.2 mM CaCl_2 , 1.2 mM KH_2PO_4 , 12 mM MgSO_4 , 25 mM HEPES, and 5.6 mM glucose, with the pH adjusted to 8.4 or 7.4 using 10 N NaOH or 10 N HCl, respectively. Buffer pH 4.5–7.4: 125 mM NaCl, 4.8 mM KCl, 1.2 mM CaCl_2 , 1.2 mM KH_2PO_4 , 12 mM MgSO_4 , 25 mM MES, and 5.6 mM glucose, with the pH adjusted to 7.4, 6.5, 5.5 or 4.5 using 10 N NaOH or 1 M HEPES.

Cells ($2\text{--}5 \times 10^5$ /reaction) were pre-incubated in the presence or absence of inhibitors for 5 min at 37 °C. The reaction was initiated with the addition of two times concentrated Fl-MTX or Na-Fluo to a final concentration of 1 μM except for the measurement of concentration dependence. Uptake was stopped after 10 min (unless stated otherwise) of incubation at 37 °C by adding 1 ml of ice-cold phosphate-buffered saline. The cells were kept on ice until flow cytometry analysis. The cellular fluorescence of 10,000 live cells was determined using an Attune[®] Acoustic Focusing Cytometer (Applied Biosystems, Life Technologies, Carlsbad, CA, US) at an excitation wavelength of 488 nm and an emission wavelength of 530/30 nm. Dead cells labeled with propidium iodide (1 $\mu\text{g}/\text{ml}$) were excluded. In control experiments, the levels of fluorescent substrates were analyzed in Sf9 cells expressing a *Drosophila melanogaster* telomerase subunit (the

plasmid encoding this nuclear protein was a generous gift from Dr. Imre Boros at the Biological Research Center in Szeged, Hungary). Activity data were calculated by subtracting the background levels of fluorescence as measured in control cells. Functional data for each OATP represent the mean of at least 3 independent experiments performed on different days.

2.6. Data analysis

Kinetic parameters of dye uptake were calculated using non-linear curve fitting (Hill fit) and Origin 8.6 software. A Student's *t*-test was used to calculate any statistical significance. The *p* value for statistical significance was set at 0.05 (*), 0.01 (**) or 0.001 (***)

3. Results

3.1. Transient expression of human OATP1B1 and OATP1B3 results in increased fluorescein-methotrexate and Na-fluorescein uptake in Sf9 cells

The baculovirus Sf9 (*S. frugiperda*) insect cell expression system is a well-established tool to express membrane proteins. This system has two main advantages over other expression systems. Protein expression levels in Sf9 cells are much higher than those achieved in mammalian cell lines, and, unlike in yeast or bacterial systems, the proper routing of heterologous proteins is unaffected [21–23]. Interestingly, with the exception of OATP2B1, the applicability of this system for the analysis of human OATPs has not yet been described [24].

First, we expressed the two best characterized members of the OATP family, OATP1B1 and 1B3, in Sf9 cells. The immunoblot in Fig. 1A shows that the heterologous proteins were efficiently expressed in the baculovirus-infected insect cells. The functionality of OATP1B1 and 1B3 in this system was tested by measuring the

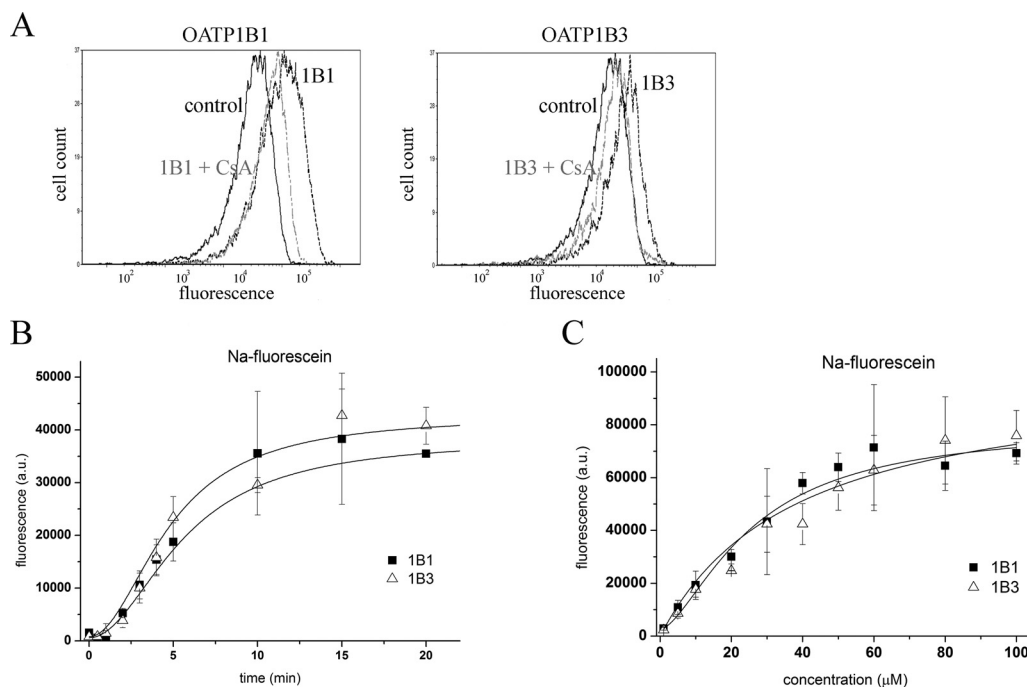


Fig. 2. Na-fluorescein uptake in Sf9 cells overexpressing human OATP1B1 or 1B3. (A) Histograms show the fluorescence of 1 μM Na-Fluo in Sf9 cells expressing an unrelated protein (control), OATP1B1 or OATP1B3 in the presence or absence of 20 μM cyclosporin A (CsA). The result of 1 representative experiment is shown. (B) 1 μM Na-Fluo accumulation was measured for 0.5–20 min at 37 °C and pH 7.4. Geomean fluorescence in 1B1 or 1B3-overexpressing insect cells (minus background fluorescence measured in unrelated virus-infected cells) was determined by flow cytometry. Data points represent the average of three independent experiments \pm SD values. (C) Accumulation of various concentrations (see axis *x*) of Na-Fluo after incubation for 4 min at 37 °C and pH 7.4 as measured by flow cytometry. Geomean values of three independent experiments \pm SD values are shown.

cellular accumulation of two well-described substrates. The baculovirus-insect cell system is a transient expression system, where virus infection results in the lysis of cells. However, we have previously demonstrated that at 36–40 h post-infection, the levels of the heterologously-expressed protein are at near maximum, while 25–30% of the cells still have intact plasma membranes [18]. Dead cells may be readily excluded from the analysis based on propidium-iodide positivity, and the uptake of FI-MTX or Na-Fluo can be selectively measured within intact cells that express high levels of the heterologously-expressed protein.

As shown in Fig. 1B, Sf9 cells transduced with OATP1B1 and 1B3 cDNA exhibit increased accumulation of FI-MTX compared to control cells infected with a recombinant virus containing the cDNA of an unrelated protein. The observed transport was rapid, showing saturation kinetics with the following $t_{1/2}$ values: 2.64 ± 0.53 and 4.16 ± 0.28 min for 1B1 and 1B3, respectively. OATP1B1- and 1B3-mediated uptake was absent at 4 °C (not shown) and in the presence of a known inhibitor, cyclosporin A [25]. The K_m values of $0.23 \pm 0.04 \mu\text{M}$ and $0.53 \pm 0.40 \mu\text{M}$ for 1B1 and 1B3, respectively, were lower than those observed in mammalian cells [14] (Fig. 1, Panels C and D).

The transport of another well-known fluorescent substrate, Na-Fluo, in OATP1B1 or 1B3 overexpressing Sf9 cells (Fig. 2A) was similar to that observed for FI-MTX, showing a rapid uptake ($t_{1/2}$ 6.71 ± 2.33 and 5.58 ± 0.11 for 1B1 and 1B3, respectively) and K_m values of $25.73 \pm 4.68 \mu\text{M}$ and $38.55 \pm 15.00 \mu\text{M}$ for 1B1 and 1B3, respectively (Fig. 2B and C). These results correspond to those obtained in mammalian cells [13].

To further characterize OATP1B1/1B3-mediated transport, we examined the effect of estradiol 17- β -D-glucuronide, various bile acids and other previously identified OATP1B1/1B3-interacting compounds on the uptake of FI-MTX or Na-Fluo (Fig. 3). We observed a significant inhibitory effect on OATP1B1/1B3-mediated transport of the majority of these compounds (but not in control cells), confirming that the observed uptake in insect cells was due to the activity of the overexpressed human proteins. However, the inhibitory potential of the tested compounds differed for the two substrates used, which may be due to potential differences in compound-specific binding sites.

3.2. Functional expression of the entire human OATP family in Sf9 insect cells reveals that fluorescein is a pan-OATP substrate

After confirming that the insect cell system is suitable for the functional expression of OATP1B1 and 1B3, we generated Sf9 cells

overexpressing the remaining 9 human OATPs: 1A2, 1C1, 2A1, 2B1, 3A1, 4A1, 4C1, 5A1 and 6A1. The expression levels of all proteins were determined via Western blotting (Fig. 4A). Specific bands corresponding to the core-glycosylated proteins were detected in each case [26].

Using transport conditions that were optimized for OATP1B1 and 1B3 (10 min incubation at 37 °C, pH 7.4, using 1 μM of substrate), we measured Na-Fluo and FI-MTX uptake in insect cells that expressed individual members of the entire human OATP family. As shown in Fig. 4B, all members of the human OATP family are able to transport fluorescein. In contrast, FI-MTX was only transported by OATP1B1 and 1B3 (Fig. 4C).

3.3. Effect of pH on Na-fluorescein and FI-MTX transport

The above described experiments were performed at pH 7.4. However, previous studies demonstrated that acidic extracellular pH increases the transport of various compounds by the majority of OATPs [27]. As Sf9 cells are grown at pH 6.2, it was possible that the use of a neutral transport buffer precluded the formation of the inwardly directed H^+ gradient necessary for optimal transport by pH-sensitive OATPs. To address this issue and to investigate how the extracellular milieu may influence OATP transport in insect cells, we tested the effect of various buffers, ranging from pH 4.5 to pH 8.5, on OATP1B1/1B3-mediated uptake. Using pH-adjusted buffers, we demonstrate that OATP1B1 and 1B3 are able to transport FI-MTX over a wide pH range, although maximal activity is observed at a neutral pH (Fig. 5A). Interestingly, however, Na-Fluo transport was significantly enhanced in an acidic extracellular environment, suggesting that the transport of Na-Fluo may be triggered by a proton gradient (Fig. 5B). The emission intensity of fluorescein decreases at acidic pH values ([28], and data not shown). Therefore, the elevated Na-Fluo signal observed under acidic pH conditions likely reflects increased Na-Fluo uptake and not a non-specific increase in substrate fluorescence.

Because the transport of Na-Fluo by OATP1B1 and 1B3 was significantly enhanced under acidic assay conditions, we examined the effect of acidic pH on the transport activity of the entire human OATP panel. Investigation of OATP1B1/1B3-mediated transport revealed that the optimal pH range for FI-MTX transport in Sf9 cells is 6.5–7.4, while that of Na-Fluo is 4.5–5.5. To achieve maximal activity under physiologically relevant conditions, we tested FI-MTX and Na-Fluo uptake by all human OATPs at pH 6.5 and 5.5, respectively. Consistent with the results observed for OATP1B1 and 1B3, acidification of the extracellular milieu resulted in increased

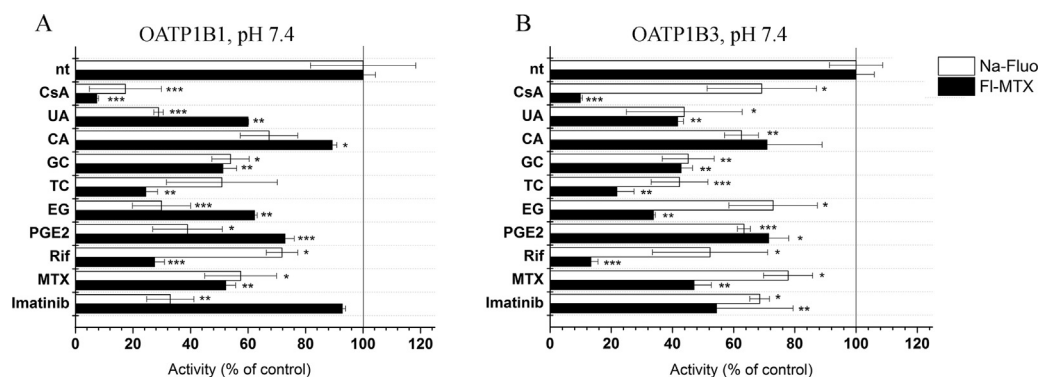


Fig. 3. Effect of various OATP-interacting compounds on the uptake of FI-MTX or Na-Fluo. Accumulation of 1 μM FI-MTX or 1 μM Na-Fluo at 37 °C for 10 min at pH 7.4 was measured in the absence (nt) or presence of various compounds. Activity is determined by comparing the percentage of fluorescence compared to control, non-treated cells. Bars represent the average values of at least three independent experiments (\pm SD). nt: non-treated control, CsA: 20 μM cyclosporin A, UA: 20 μM ursolic acid, CA: 150 μM cholic acid, GC: 150 μM glycocholate, TC: 150 μM taurocholate, EG: 50 μM estradiol 17- β -D-glucuronide, PGE2: 5 μM prostaglandin E₂, Rif: 10 μM rifampicin, and MTX: 10 μM methotrexate. Significantly different from the non-treated control: * $p < 0.05$, ** $p < 0.01$, *** $p < 0.001$.

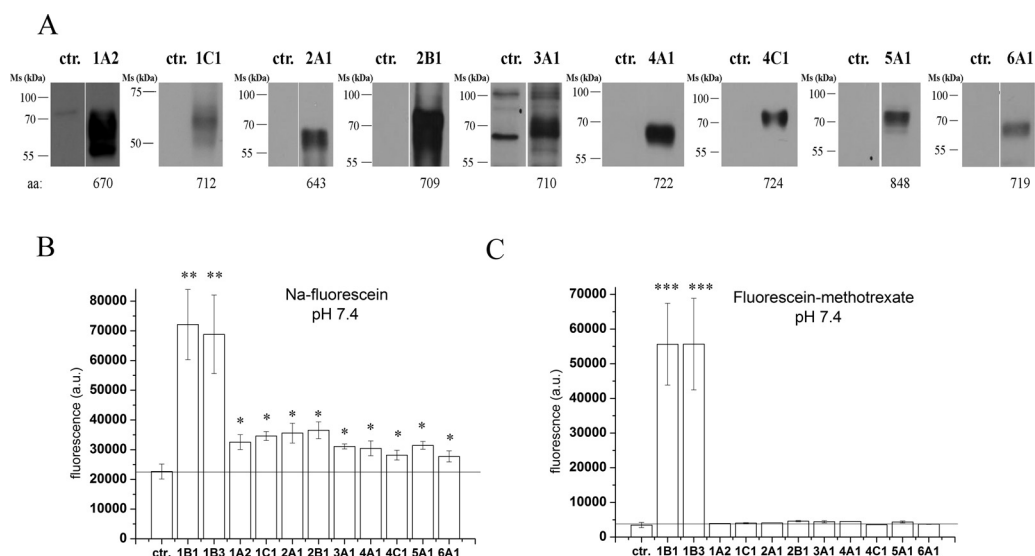


Fig. 4. Overexpression and functional characterization of the entire human OATP panel in insect cells. (A) Western blot detection of various human OATPs overexpressed in insect cells. Total cell lysates (5 μ g for 1C1, 2B1, 4A1, 4C1 and 10 μ g for 1A2, 1B1, 1B3, 2A1, 3A1, 5A1 and 6A1) were loaded on 7.5% Laemmli gels. After transferring onto PVDF membranes, the proteins were labeled with the specific antibodies (see Section 2). Control (ctr.) represents Sf9 cells expressing an unrelated protein. (B and C) Sf9 cells overexpressing the given OATP (see axis x) or an unrelated protein (ctr.) were incubated with 1 μ M Na-Fluo (B) or 1 μ M FI-MTX (C) at 37 °C for 10 min at pH 7.4. Intracellular fluorescence was determined by flow cytometry. Graphs show geomean fluorescence, bars represent the average of three independent experiments \pm SD values. Significantly different from the control: * p < 0.05, ** p < 0.01, *** p < 0.001.

Na-fluorescein transport by all human OATPs despite the increased background fluorescence (Fig. 6A). In contrast, an acidic environment only activated FI-MTX transport for OATP1A2 and 2B1, as the remaining OATPs were inactive (Fig. 6B).

3.4. Effect of inhibitors

To determine whether the insect cell-based Na-Fluo or FI-MTX assay is suitable for testing substrates/inhibitors of all human OATPs, we repeated the assays in the presence of several previously described OATP-interacting compounds. Fig. 7 shows that despite lower baseline transport rates, the transport of FI-MTX by OATP1A2 and 2B1 was inhibited by CsA, ursolic acid, bile acids, PGE₂, MTX and Imatinib. The optimized assay conditions allowed for the identification of several novel OATP-interacting compounds. We demonstrate that ursolic acid, a pentacyclic triterpenoid found in fruit rind influences the activity of OATP1A2. Further, we find that estradiol 17- β -D-glucuronide, glycocholate and Imatinib modulate the function of OATP2B1.

Similar results were obtained using the Na-Fluo uptake assay (Fig. 8). We found that the transport activity for each human OATP

was influenced by at least one test compound. Cyclosporin A inhibited the uptake mediated by OATP1B3, 1A2, 2A1 and 2B1, prostaglandin E₂ decreased the transport by OATP1A2, 1C1, 2A1, 2B1 and 4C1, and ursolic acid by OATP2A1. Interestingly, estradiol 17- β -D-glucuronide and ursolic acid induced the Na-Fluo transport activity of several OATPs, suggesting that Na-Fluo transport may be allosterically activated by these compounds.

4. Discussion

Members of the OATP family are major determinants of the uptake and elimination of drugs [2,29]. Administration of drugs or food components that are either substrates or inhibitors of OATPs may result in adverse drug toxicity [29]. Therefore, the investigation of a potential interaction between OATPs with known pharmacological relevance (OATP1B1 and 1B3) and a new molecular entity is recommended by the International Transporter Consortium [30], the US Food and Drug Administration and by the European Medicines Agency. In addition to OATP1B1 and 1B3, OATP1A2 and 2B1 are also known to transport a wide variety of substrates. Since these transporters are expressed at high levels in

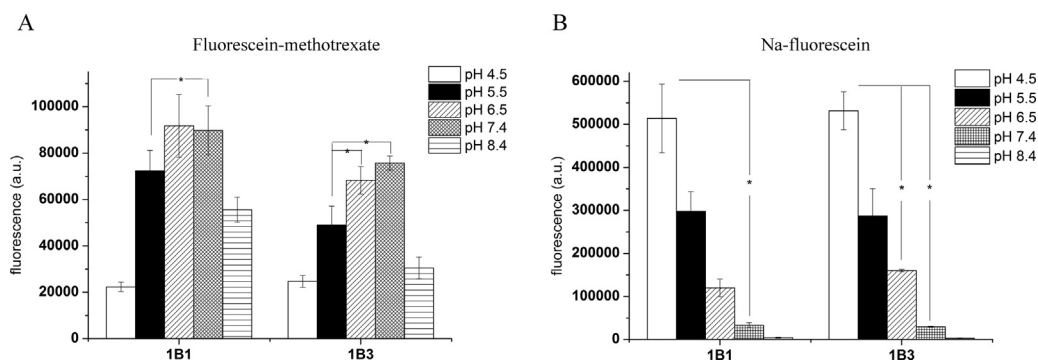


Fig. 5. Uptake of FI-MTX and Na-Fluo using different buffers. Insect cells overexpressing OATP1B1 or 1B3 were incubated with 1 μ M FI-MTX (panel A) or 1 μ M Na-Fluo (panel B) in various buffers with a pH range from 4.5 to 8.5 (see Section 2) for 10 min at 37 °C. Values represent geomean fluorescence minus the background fluorescence detected in control cells. Data were obtained from three independent flow cytometry experiments. Bars show \pm SD values. Student's *t*-test, significant difference: * p < 0.05.

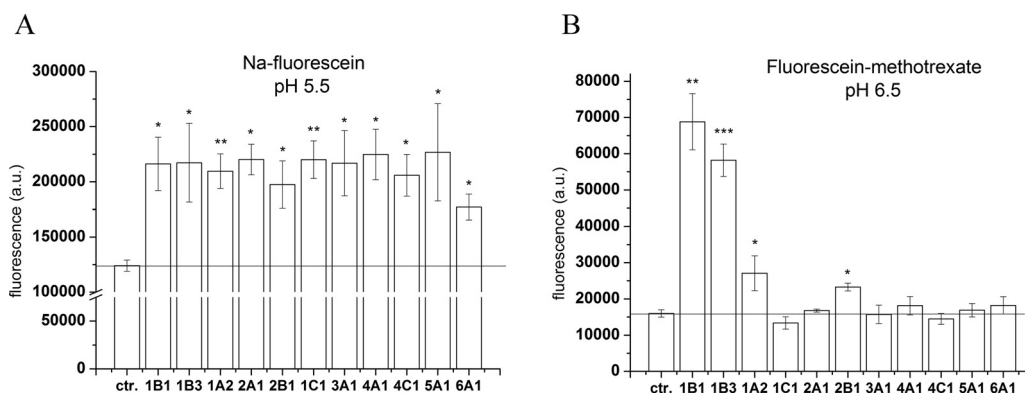


Fig. 6. Na-Fluo or FI-MTX uptake at acidic pH in Sf9 cells overexpressing the entire human OATP panel. Sf9 cells overexpressing OATPs (see axis x) were incubated with 1 μ M Na-Fluo (A) or 1 μ M FI-MTX (B) for 10 min at 37 °C in buffer pH 5.5 (panel A) or pH 6.5 (panel B). Columns show geomean fluorescence. Bars represent an average of three independent experiments \pm SD values. Significantly different from the control: * p < 0.05, ** p < 0.01, *** p < 0.001.

the intestine (2B1), liver (2B1) and the blood–brain barrier (1A2, 2B1), they should also be considered as important determinants of drug pharmacokinetics. Additionally, several OATPs show cancer-specific expression and therefore may be exploited in targeted drug delivery [1,31]. Clearly, information on the substrate specificity and the role in ADME-T (Absorption, Distribution, Metabolism, Excretion and Toxicity) for all of the human OATPs is needed.

Given the absence of suitable functional assays, most members of the human OATP family remain poorly characterized. The major impediment to the investigation of OATP function is the limited availability of radioactively- or fluorescently-labeled substrates and

OATP-specific inhibitors. Functional studies are also hindered by the limited number of cellular models with well-characterized transporter expression. To address these issues, we established an insect cell-based fluorescent transport assay for the investigation of the entire human OATP family. The main advantage of this approach compared to mammalian expression systems is the high level of protein expression, and therefore, the lack of a significant background transport activity. However, to date, only OATP2B1 was studied in insect cells. Tschantz et al. demonstrated functional expression of OATP2B1 in Sf9 insect cells, with saturable uptake of [³H]estrone-3-sulphate [24]. In this study, we focused on the narrow window of time when the cells express high levels of the transporter,

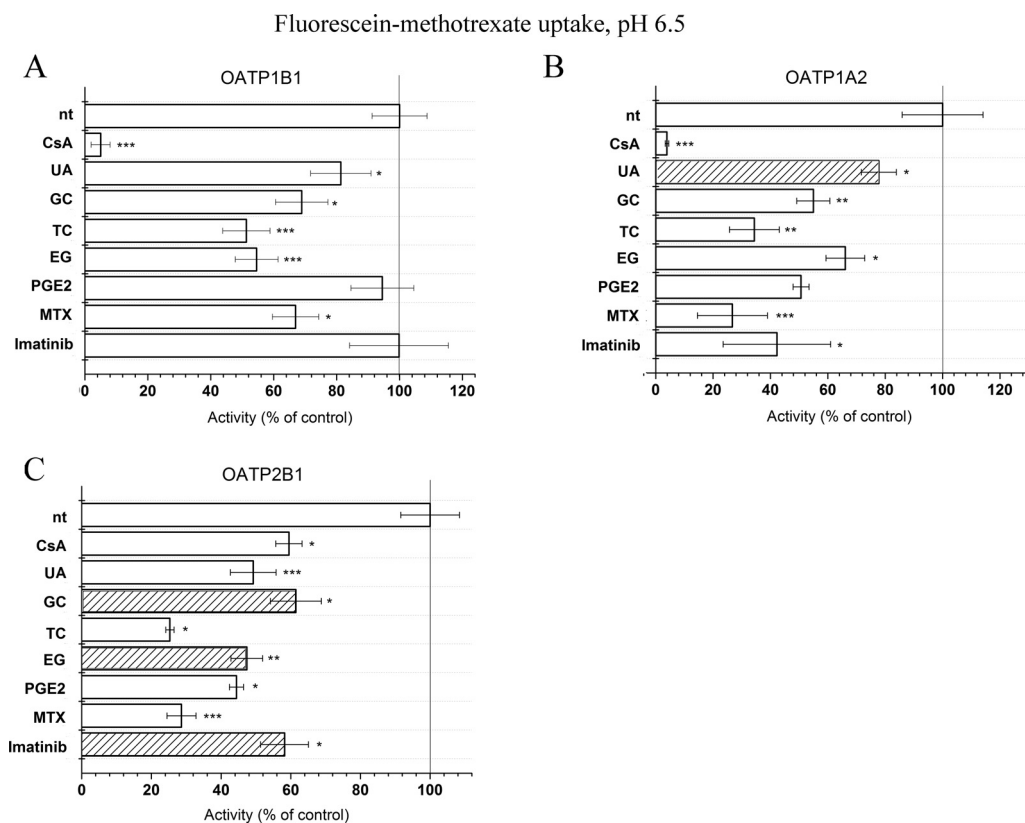


Fig. 7. Effect of various compounds on the accumulation of FI-MTX in insect cells overexpressing OATP1B1, 1A2 or 2B1. Cells were incubated with 1 μ M FI-MTX at pH 6.5 for 10 min in the presence or absence of various compounds. Columns represent activity as a percentage of non-treated (control) fluorescence measured without the added inhibitors/substrates. Measurements were repeated at least four times, columns show average \pm SD values. Striped bars indicate newly identified interactions. * p < 0.05, ** p < 0.01 and *** p < 0.001 indicate significant difference from the non-treated control.

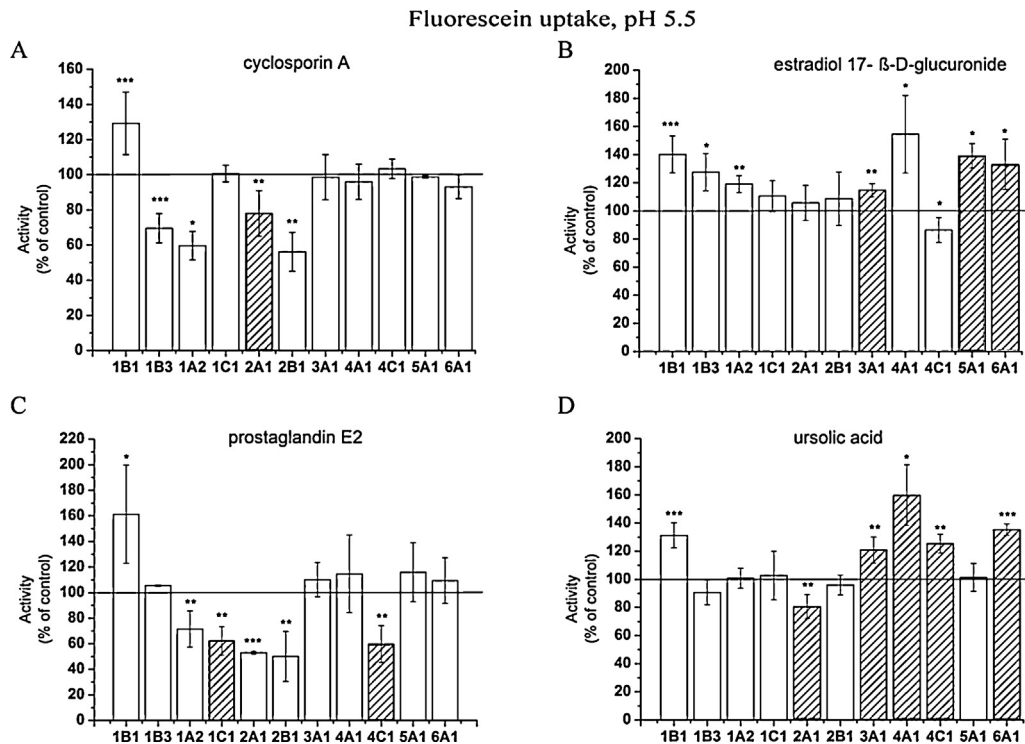


Fig. 8. Effect of various compounds on the accumulation of Na-Fluo in insect cells overexpressing the entire OATP panel (A–D). Cells were incubated with 1 μ M Na-Fluo at pH 5.5 for 10 min in the presence of 20 μ M cyclosporin A, 50 μ M estradiol 17- β -D-glucuronide, 5 μ M prostaglandin E₂ or 20 μ M ursolic acid. Columns represent activity as a percentage of the non-treated (control) fluorescence measured without the added inhibitors/substrates. Columns show average \pm SD values, $n=4$. Striped columns indicate new interactions. Significance was determined by Student's *t*-test. * $p < 0.05$, ** $p < 0.01$, *** $p < 0.001$.

but are still viable. This setup enabled the measurement of OATP-mediated intracellular accumulation of fluorescent substrates in intact cells. Assays using fluorescent compounds are exceptionally suited for the measurement of transport activity given the relative low cost of test substrates, the sensitivity of the transport assay and the potential for application in a high-throughput setup. However, fluorescent substrate-based transport assays were available previously only for OATP1B1 and 1B3 [13–17,32].

Proteins overexpressed in the insect cell system are core-glycosylated [26] and several studies indicated that the lack of *N*-glycosylation impairs OATP function [24,33–35]. To assess the functionality of OATPs expressed in Sf9 cells, we first tested two well-characterized OATPs, OATP1B1 and 1B3, for their ability to transport known substrates. We found that OATP1B1 and 1B3 mediate a rapid, saturable, temperature- and inhibitor-sensitive uptake of Na-Fluo and FI-MTX (Figs. 1 and 2) similar to that observed in mammalian cells [13,14]. Moreover, we demonstrated that known OATP1B-interacting compounds inhibit the uptake activity of both transporters, although the degree of inhibition differed for each substrate (Fig. 3). The molecular mechanism underlying this substrate-dependent inhibition, a well-documented characteristic of OATP1B transporters, is likely due to the difference in affinity of the binding site for the individual substrates [14]. Our data suggest that several assays, using a variety of substrates, will be required to evaluate the pharmacological relevance of OATP–drug interactions. It has also to be noted that our results do not reveal the mechanism of inhibition, as compounds interacting with the transport of the fluorescent test substrate may be competitive or noncompetitive inhibitors.

Several laboratories have found that the acidic extracellular milieu stimulates OATP-mediated transport [27,36–42]. In the human body, acidic environments may be found under both physiological (in the intestine and kidney) and pathological conditions (in tumors, during inflammation or liver disease).

Therefore, a pH-dependent activation of OATP function may provide tissue-specific or local regulation of these proteins [43]. When we investigated the pH dependence of OATP1B1/1B3-mediated transport (Fig. 5), we found that FI-MTX transport is maximal at near neutral pH, while Na-Fluo uptake is significantly increased in an acidic environment. The other OATPs had low level Na-Fluo transport at pH 7.4 (Fig. 4B) even when higher substrate concentrations (5–10 μ M) and a longer incubation time (30 min) were used (data not shown). Lowering the pH to 5.5, however, resulted in a significant increase in Na-Fluo transport by all OATPs (Fig. 6A), demonstrating that Na-Fluo is a general, pH-induced OATP substrate. The precise mechanism by which the acidic milieu triggers OATP transport is not fully understood. A low extracellular pH (low $[H]^+_{EC}$) may result in the protonation of the transporter, i.e., on a pH-sensitive histidine (His) residue located in the third transmembrane domain region [27], or it may alter the charge of the transported molecule. Leuthold and colleagues demonstrated that OATP1C1, lacking the pH sensor His, is not activated by an acidic extracellular milieu [27]. Although we found that OATP1C1-mediated transport was activated by low $[H]^+_{EC}$, this discrepancy may be due to the different substrates that were used.

The Na-Fluo assay is the first transport assay suitable for the characterization of the entire human OATP family. Using a slightly acidified transport buffer (pH 6.5), we identified FI-MTX as a new substrate of OATP1A2 and 2B1 (Fig. 6B), suggesting that FI-MTX can also be used to test substrate interactions for these transporters (Fig. 7). The identification of physiological substrates is of particular importance for poorly characterized members of the OATP family, including OATP5A1, which has only been documented to transport quercetin [6], and OATP6A1, whose function and physiological substrates remain unknown. The relevance of a functional assay encompassing the entire human OATP family is that it may serve as a tool for the identification of new molecular interactions. To test if our assay is able to identify new substrates

and inhibitors, we tested and confirmed previously documented interactions of OATP1A2, 1B1, 1B3 and 2B1 with bile acids, cyclosporin A, PGE2 and methotrexate (Figs. 3, 7 and 8). Furthermore, we identified novel interacting compounds: UA for 1A2, 2A1, 3A1, 4A1, 4C1 and 6A1, cyclosporin A for 2A1, EG for 3A1, 5A1 and 6A1, and PGE2 for 1C1 and 4C1 (Figs. 7 and 8). These data indicate a potential role for new members of the family (OATP3A1, 5A1 and 6A1) in hormone transport. Given that OATP5A1 and 6A1 expression levels are elevated in various cancers [1,44], these findings may have significant implications regarding the survival of hormone-dependent tumors. The results from our fluorescent assay analysis revealed novel interacting compounds (estradiol 17- β -D-glucuronide, glycocholate and Imatinib), even for the relatively well-characterized 2B1 (Fig. 7). The interaction between OATP2B1 and Imatinib, a Bcr-Abl inhibitor used in the treatment of chronic myeloid leukemia, supports the notion that SNPs in *SLCO2B1* may influence Imatinib pharmacokinetics resulting in inter-individual differences in therapy response [45].

Our assay also revealed unexpected interactions. In contrast to De Bruyn et al., we found significant Na-Fluo transport mediated by OATP2B1 at pH 7.4 [13]. In the case of OATP1B1, Na-Fluo transport at pH 5.5 was activated, rather than inhibited, by cyclosporin A, EG, PGE2 and UA. This activating effect appeared to be pH-specific, as these compounds inhibited Na-Fluo uptake at pH 7.4 (Fig. 3). In experiments not documented here, we found a similar, pH-dependent activation of Fl-MTX transport by several known interacting compounds. A similar activating effect was found by EG and UA, which enhanced the Na-Fluo transport activity of 3A1, 5A1 6A1, and 3A1, 4A1, 4C1 and 6A1, respectively (Fig. 8). These data suggest that transport activity is allosterically modulated, a mechanism previously documented for OATP1B3 and 2B1 [14,46,47]. Alternatively, a co-transport mechanism, with one substrate stimulating the uptake of the other, is also feasible, although, this would need to be confirmed by measuring the transport of labeled EG, PGE2 or UA, in the presence of Na-Fluo.

In summary, we established a novel functional assay for the investigation of the entire human OATP family. We demonstrate that the insect cell-based assay provides a useful tool for the systemic, comparative study of the function of each OATP. Functional characterization of the OATPs offers a chance for the discovery of inhibitors or activators that could lead to the identification of physiological substrates, the investigation of the role of SNPs in substrate recognition, and paves the way for a vesicle-based high-throughput screening assay.

Conflict of interest

The authors declare that they have no conflict of interest.

Funding

This research has been supported by the Hungarian Research Fund (OTKA K-109423), the Momentum Program of the Hungarian Academy of Sciences, the TTK_All grant of the Research Centre for Natural Sciences, Hungarian Academy of Sciences (0611-15405) and by the János Bolyai Research Scholarship of the Hungarian Academy of Sciences (Cs. Ö-L.). Csilla Özvegy-Laczka is a recipient of a fellowship by the MedInProt program. BS is supported by grant # 310030_144195 from the Swiss National Science foundation. BH is funded by National Institutes of Health grant GM077336.

Author contributions

Participated in research design and data analysis: I. P., D. K., Cs. Ö-L.

Performed experiments: I. P., D. K., O. N., Gy. V., M. G., Cs. Ö-L.
Cloned the cDNA constructs for OATP1B1, 3A1 and 4C1 and developed the antibodies against OATP1A2, 1B1, 1B3, 1C1, 2B1, 3A1_v1 and 4A1: B. S., B. H.

Wrote the manuscript: D. K., I. P., G. Sz. and Cs. Ö-L.

Acknowledgements


We are grateful to Nóra Kucsma for her technical help and to Balázs Sarkadi and András Váradi for scientific discussions.

References

- [1] V. Buxhofer-Ausch, L. Secky, K. Wlcek, M. Svoboda, V. Kounnis, E. Briasoulis, et al., Tumor-specific expression of organic anion-transporting polypeptides: transporters as novel targets for cancer therapy, *J. Drug Deliv.* 2013 (2013) 863539.
- [2] Y. Zhang, A. Hays, A. Noblett, M. Thapa, D.H. Hua, B. Hagenbuch, Transport by OATP1B1 and OATP1B3 enhances the cytotoxicity of epigallocatechin 3-O-gallate and several quercetin derivatives, *J. Nat. Prod.* 76 (2013) 368–373.
- [3] B. Hagenbuch, B. Stieger, The SLCO (former SLC21) superfamily of transporters, *Mol. Aspects Med.* 34 (2013) 396–412.
- [4] M. Roth, A. Obaidat, B. Hagenbuch, OATPs, OATs and OCTs: the organic anion and cation transporters of the SLCO and SLC22A gene superfamilies, *Br. J. Pharmacol.* 165 (2012) 1260–1287.
- [5] X. Bossuyt, M. Muller, B. Hagenbuch, P.J. Meier, Polyspecific drug and steroid clearance by an organic anion transporter of mammalian liver, *J. Pharmacol. Exp. Ther.* 276 (1996) 891–896.
- [6] H. Glaeser, K. Bujok, I. Schmidt, M.F. Fromm, K. Mandery, Organic anion transporting polypeptides and organic cation transporter 1 contribute to the cellular uptake of the flavonoid quercetin, *Naunyn-Schmiedeberg's Arch. Pharmacol.* 387 (2014) 883–891.
- [7] U. Olszewski-Hamilton, M. Svoboda, T. Thalhammer, V. Buxhofer-Ausch, K. Geissler, G. Hamilton, Organic anion transporting polypeptide 5A1 (OATP5A1) in small cell lung cancer (SCLC) cells: possible involvement in chemoresistance to satraplatin, *Biomarkers Cancer* 3 (2011) 31–40.
- [8] E. van de Steeg, E. Wagenaar, C.M. van der Kruijssen, J.E. Burggraaff, D.R. de Waart, R.P. Elferink, et al., Organic anion transporting polypeptide 1a/1b-knockout mice provide insights into hepatic handling of bilirubin, bile acids, and drugs, *J. Clin. Invest.* 120 (2010) 2942–2952.
- [9] E. van de Steeg, K. der, C.M. ruijssen, E. Wagenaar, J.E. Burggraaff, E. Mesman, K. E. Kenworthy, et al., Methotrexate pharmacokinetics in transgenic mice with liver-specific expression of human organic anion-transporting polypeptide 1B1 (SLCO1B1), *Drug Metab. Dispos.* 37 (2009) 277–281.
- [10] S. Mayerl, T.J. Visser, V.M. Darras, S. Horn, H. Heuer, Impact of Oatp1c1 deficiency on thyroid hormone metabolism and action in the mouse brain, *Endocrinology* 153 (2012) 1528–1537.
- [11] J.D. Clarke, N.J. Cherrington, Genetics or environment in drug transport: the case of organic anion transporting polypeptides and adverse drug reactions, *Expert Opin. Drug Metab. Toxicol.* 8 (2012) 349–360.
- [12] E. Gozalpour, R. Greupink, H.M. Wortelboer, A. Bilos, M. Schreurs, F.G. Russel, et al., Interaction of digitalis-like compounds with liver uptake transporters NTCP, OATP1B1, and OATP1B3, *Mol. Pharm.* 11 (2014) 1844–1855.
- [13] T. De Bruyn, S. Fattah, B. Stieger, P. Augustijns, P. Annaert, Sodium fluorescein is a probe substrate for hepatic drug transport mediated by OATP1B1 and OATP1B3, *J. Pharm. Sci.* 100 (2011) 5018–5030.
- [14] C. Gui, A. Obaidat, R. Chaguturu, B. Hagenbuch, Development of a cell-based high-throughput assay to screen for inhibitors of organic anion transporting polypeptides 1B1 and 1B3, *Curr. Chem. Genomics* 4 (2010) 1–8.
- [15] C. Baldes, P. Koenig, D. Neumann, H.P. Lenhof, O. Kohlbacher, C.M. Lehr, Development of a fluorescence-based assay for screening of modulators of human organic anion transporter 1B3 (OATP1B3), *Eur. J. Pharm. Biopharm.* 62 (2006) 39–43.
- [16] W. de Graaf, S. Hausler, M. Heger, T.M. van Ginhoven, G. van Cappellen, R.J. Bennink, et al., Transporters involved in the hepatic uptake of (99m)Tc-mebrofenin and indocyanine green, *J. Hepatol.* 54 (2011) 738–745.
- [17] H. Yamaguchi, M. Okada, S. Akitaya, H. Ohara, T. Mikkaichi, H. Ishikawa, et al., Transport of fluorescent chenodeoxycholic acid via the human organic anion transporters OATP1B1 and OATP1B3, *J. Lipid Res.* 47 (2006) 1196–1202.
- [18] C. Ozvegy, A. Varadi, B. Sarkadi, Characterization of drug transport, ATP hydrolysis, and nucleotide trapping by the human ABCG2 multidrug transporter. Modulation of substrate specificity by a point mutation, *J. Biol. Chem.* 277 (2002) 47980–47990.
- [19] R.D. Huber, B. Gao, P. Sidler, M.A. fandler, W. Zhang-Fu, S. Leuthold, B. Hagenbuch, et al., Characterization of two splice variants of human organic anion transporting polypeptide 3A1 isolated from human brain, *Am. J. Physiol. Cell Physiol.* 292 (2007) C795–C806.
- [20] G.A. Kullak-Ublick, M.G. Ismail, B. Stieger, L. Landmann, R. Huber, F. Pizzagalli, et al., Organic anion-transporting polypeptide B (OATP-B) and its functional comparison with three other OATPs of human liver, *Gastroenterology* 120 (2001) 525–533.

- [21] B. Sarkadi, E.M. Price, R.C. Boucher, U.A. Germann, G.A. Scarborough, Expression of the human multidrug resistance cDNA in insect cells generates a high activity drug-stimulated membrane ATPase, *J. Biol. Chem.* 267 (1992) 4854–4858.
- [22] E. Bakos, T. Hegedus, Z. Hollo, E. Welker, G.E. Tusnady, G.J. Zaman, et al., Membrane topology and glycosylation of the human multidrug resistance-associated protein, *J. Biol. Chem.* 271 (1996) 12322–12326.
- [23] C. Ozvegy, T. Litman, G. Szakacs, Z. Nagy, S. Bates, A. Varadi, et al., Functional characterization of the human multidrug transporter, ABCG2, expressed in insect cells, *Biochem. Biophys. Res. Commun.* 285 (2001) 111–117.
- [24] W.R. Tschantz, N.D. Pfeifer, C.L. Meade, L. Wang, A. Lanzetti, A.V. Kamath, et al., Expression, purification and characterization of the human membrane transporter protein OATP2B1 from Sf9 insect cells, *Protein Expression Purif.* 57 (2008) 163–171.
- [25] Y. Shitara, T. Itoh, H. Sato, A.P. Li, Y. Sugiyama, Inhibition of transporter-mediated hepatic uptake as a mechanism for drug–drug interaction between cerivastatin and cyclosporin A, *J. Pharmacol. Exp. Ther.* 304 (2003) 610–616.
- [26] A. Contreras-Gomez, A. Sanchez-Miron, F. Garcia-Camacho, E. Molina-Grima, Y. Chisti, Protein production using the baculovirus-insect cell expression system, *Biotechnol. Prog.* 30 (2014) 1–18.
- [27] S. Leuthold, B. Hagenbuch, N. Mohebbi, C.A. Wagner, P.J. Meier, B. Stieger, Mechanisms of pH-gradient driven transport mediated by organic anion polypeptide transporters, *Am. J. Physiol. Cell Physiol.* 296 (2009) C570–C582.
- [28] R. Sjöback, J. Nygren, M. Kubista, Absorption and fluorescence properties of fluorescein, *Spectrochim. Acta Part A* 51 (1995) L7–21.
- [29] K. Maeda, Organic anion transporting polypeptide (OATP) 1B1 and OATP1B3 as important regulators of the pharmacokinetics of substrate drugs, *Biol. Pharm. Bull.* 38 (2015) 155–168.
- [30] K.M. Giacomini, S.M. Huang, D.J. Tweedie, L.Z. Benet, K.L. Brouwer, X. Chu, et al., Membrane transporters in drug development, *Nat. Rev. Drug Discov.* 9 (2010) 215–236.
- [31] T. Liu, Q. Li, Organic anion-transporting polypeptides: a novel approach for cancer therapy, *J. Drug Target.* 22 (2014) 14–22.
- [32] H. Yamaguchi, M. Kobayashi, M. Okada, T. Takeuchi, M. Unno, T. Abe, et al., Rapid screening of antineoplastic candidates for the human organic anion transporter OATP1B3 substrates using fluorescent probes, *Cancer Lett.* 260 (2008) 163–169.
- [33] T.K. Lee, A.S. Koh, Z. Cui, R.H. Pierce, N. Ballatori, *N*-glycosylation controls functional activity of Oatp1, an organic anion transporter, *Am. J. Physiol. Gastrointest. Liver Physiol.* 285 (2003) G371–G381.
- [34] W. Lee, H. Glaeser, L.H. Smith, R.L. Roberts, G.W. Moeckel, G. Gervasini, et al., Polymorphisms in human organic anion-transporting polypeptide 1A2 (OATP1A2): implications for altered drug disposition and central nervous system drug entry, *J. Biol. Chem.* 280 (2005) 9610–9617.
- [35] P. Wang, S. Hata, Y. Xiao, J.W. Murray, A.W. Wolkoff, Topological assessment of oatp1a1: a 12-transmembrane domain integral membrane protein with three N-linked carbohydrate chains, *Am. J. Physiol. Gastrointest. Liver Physiol.* 294 (2008) G1052–G1059.
- [36] D. Kobayashi, T. Nozawa, K. Imai, J. Nezu, A. Tsuji, I. Tamai, Involvement of human organic anion transporting polypeptide OATP-B (SLC21A9) in pH-dependent transport across intestinal apical membrane, *J. Pharmacol. Exp. Ther.* 306 (2003) 703–708.
- [37] T. Nozawa, K. Imai, J. Nezu, A. Tsuji, I. Tamai, Functional characterization of pH-sensitive organic anion transporting polypeptide OATP-B in human, *J. Pharmacol. Exp. Ther.* 308 (2004) 438–445.
- [38] Y. Sai, Y. Kaneko, S. Ito, K. Mitsuoka, Y. Kato, I. Tamai, et al., Predominant contribution of organic anion transporting polypeptide OATP-B (OATP2B1) to apical uptake of estrone-3-sulfate by human intestinal Caco-2 cells, *Drug Metab. Dispos.* 34 (2006) 1423–1431.
- [39] L.M. Satlin, V. Amin, A.W. Wolkoff, Organic anion transporting polypeptide mediates organic anion/HCO₃⁻ exchange, *J. Biol. Chem.* 272 (1997) 26340–26345.
- [40] N. Kanai, R. Lu, Y. Bao, A.W. Wolkoff, V.L. Schuster, Transient expression of oatp organic anion transporter in mammalian cells: identification of candidate substrates, *Am. J. Physiol.* 270 (1996) F319–25.
- [41] J.J. Marin, D. Mangas, M.C. Martinez-Diez, M.Y. El-Mir, O. Briz, M.A. Serrano, Sensitivity of bile acid transport by organic anion-transporting polypeptides to intracellular pH, *Biochim. Biophys. Acta* 1611 (2003) 249–257.
- [42] T. Nishimura, Y. Kubo, Y. Kato, Y. Sai, T. Ogihara, A. Tsuji, Characterization of the uptake mechanism for a novel loop diuretic, M17055, in Caco-2 cells: involvement of organic anion transporting polypeptide (OATP)-B, *Pharm. Res.* 24 (2007) 90–98.
- [43] P. Martinez-Becerra, O. Briz, M.R. Romero, R.I. Macias, M.J. Perez, C. Sancho-Mateo, et al., Further characterization of the electrogenicity and pH sensitivity of the human organic anion-transporting polypeptides OATP1B1 and OATP1B3, *Mol. Pharmacol.* 79 (2011) 596–607.
- [44] S. Brenner, L. Klameth, J. Riha, M. Scholm, G. Hamilton, E. Bajna, et al., Specific expression of OATPs in primary small cell lung cancer (SCLC) cells as novel biomarkers for diagnosis and therapy, *Cancer Lett.* 356 (2015) 517–524.
- [45] I.Y. Gong, R.B. Kim, Impact of genetic variation in OATP transporters to drug disposition and response, *Drug Metab. Pharmacokinet.* 28 (2013) 4–18.
- [46] C. Gui, Y. Miao, L. Thompson, B. Wahlgren, M. Mock, B. Stieger, et al., Effect of pregnane X receptor ligands on transport mediated by human OATP1B1 and OATP1B3, *Eur. J. Pharmacol.* 584 (2008) 57–65.
- [47] M. Grube, K. Kock, S. Karner, S. Reuther, C.A. Ritter, G. Jedlitschky, et al., Modification of OATP2B1-mediated transport by steroid hormones, *Mol. Pharmacol.* 70 (2006) 1735–1741.

SCIENTIFIC REPORTS



OPEN

Identification of novel cell-impermeant fluorescent substrates for testing the function and drug interaction of Organic Anion-Transporting Polypeptides, OATP1B1/1B3 and 2B1

Izabel Patik¹, Virág Székely¹, Orsolya Német¹, Áron Szepesi², Nóra Kucsma¹, György Várady², Gergely Szakács^{1,3}, Éva Bakos¹ & Csilla Özvegy-Laczka¹

Organic Anion-Transporting Polypeptides are multispecific membrane proteins that regulate the passage of crucial endobiotics and drugs across pharmacological barriers. OATP1B1 and OATP1B3 have been described to play a major role in the hepatic uptake of statins, antivirals and various chemotherapeutics; whereas the pharmacological role of the ubiquitously expressed OATP2B1 is less well characterized. According to current industry standards, *in vitro* testing for susceptibility to OATP1B1 and 1B3 mediated transport is recommended for drug candidates that are eliminated in part via the liver. Here we show that human OATP1B1, 1B3 and 2B1 transport a series of commercially available viability dyes that are generally believed to be impermeable to intact cells. We demonstrate that the intracellular accumulation of Zombie Violet, Live/Dead Green, Cascade Blue and Alexa Fluor 405 is specifically increased by OATPs. Inhibition of Cascade Blue or Alexa Fluor 405 uptake by known OATP substrates/inhibitors yielded IC₅₀ values in agreement with gold-standard radioligand assays. The fluorescence-based assays described in this study provide a new tool for testing OATP1B/2B1 drug interactions.

Human Organic Anion-Transporting Polypeptides (OATPs) encoded by the SLCO genes mediate the cellular uptake of large organic, amphipathic molecules^{1,2}. At least four members of the family, OATP1A2, 1B1, 1B3 and 2B1 are multispecific transporters that, besides the transport of endogenous substrates (bilirubin, bile acids and hormones), also promote the cellular uptake of pharmacologically relevant molecules. OATP1B1 and 1B3 are almost exclusively expressed in the sinusoidal membranes of hepatocytes where they regulate the hepatic uptake of bile acids and bilirubin. Simultaneous mutations in the SLCO1B1 and 1B3 genes result in Rotor syndrome, characterized by increased serum bilirubin levels³. Additionally, OATP1B1 and 1B3 are key determinants of the hepatic clearance of widely prescribed medications (e.g. statins, antivirals) and also of chemotherapeutics including docetaxel, irinotecan and cisplatin^{4,5}. Altered function of OATP1B1 and 1B3 due to single nucleotide polymorphisms (SNPs), drug-drug or drug-food interactions or disease conditions influences the *in vivo* efficacy of drugs^{6,7}. Co-administration of OATP1B substrate drugs may cause unexpected toxicity with fatal consequences. For example, statin-induced myopathy was shown to be linked to the inhibition of transporter-mediated hepatic uptake of statins by the co-administered gemfibrozil or Cyclosporin A^{8,9}. Inhibition of OATP1B function

¹Membrane protein research group, Institute of Enzymology, Research Centre for Natural Sciences, Hungarian Academy of Sciences, Magyar tudósok krt. 2, Budapest, H-1117, Hungary. ²Laboratory of Molecular Cell Biology, Institute of Enzymology, Research Centre for Natural Sciences, Hungarian Academy of Sciences, Magyar tudósok krt. 2, Budapest, H-1117, Hungary. ³Institute of Cancer Research, Medical University of Vienna, Borschkegasse 8A, Vienna, 1090, Austria. Correspondence and requests for materials should be addressed to C.Ö.-L. (email: laczka.csilla@ttk.mta.hu)

may also result in elevated bilirubin levels^{10,11}. OATP1B expression is often reduced in liver diseases including non-alcoholic fatty liver disease, hepatocellular carcinoma, inflammatory cholestasis, primary biliary cirrhosis or chronic hepatitis¹². OATP2B1 is also expressed in the liver¹³, though its contribution to the hepatic clearance of exogenous compounds is unclear. OATP2B1 was shown to influence the intestinal absorption of orally administered drugs such as celiprolol, fexofenadine and montelukast^{5,14}. Additionally, OATP2B1 is expressed in skeletal muscle and in the heart, mediating the muscular uptake and myotoxicity of statins¹⁵. OATP1A2, the fourth multispecific member of the OATP family, has a largely overlapping expression pattern with OATP2B1, e.g. in the intestine and the blood-brain-barrier^{5,16}. Additionally, OATP1A2 is present in the liver, however in contrast to OATP1Bs and 2B1, 1A2 is found in cholangiocytes¹⁷. Therefore, although OATP1A2 transports a plethora of clinically applied drugs, it is not directly involved in hepatic drug uptake, but rather in the reabsorption of drugs from the bile. Based on pre-clinical and clinical data, OATP2B1 and 1A2 are key determinants of the intestinal uptake of numerous drugs, including various statins, fexofenadine, sulfasalazine and telmisartan¹⁸.

Recent guidelines issued by the US Food and Drug Administration (FDA) and the European Medicines Agency (EMA) require testing the interaction of new molecular entities with OATP1B1 and 1B3^{19,20}, and OATP2B1 and OATP1A2 are emerging candidates according to the International Transporter Consortium²⁰. Recommended functional assays typically measure the effect of the investigated compounds on the OATP-mediated uptake of radioactively labelled compounds⁷. Typical test substrates of OATP1B and 2B1 include radioactively labelled estrone-3-sulphate, estradiol-glucuronide, bromosulphophthalein, a statin or cholecystokinin-8 (1B3)⁷. Recently, several clinically applied drug substrates of OATP1B1 (various statins, fexofenadine, or bosentan) measured by HPLC-MS (high-performance liquid chromatography with tandem mass spectrometry) have been shown to be applicable as test substrates to predict DDI²¹. Whereas these indirect assays provide a reliable and sensitive measurement of OATP function, radioactive compounds and MS are usually not compatible with large scale screening efforts. Lately, ³H-Rosuvastatin and DHEAS have been demonstrated as *in vivo* substrates of OATP1Bs in cynomolgus monkey^{22,23}, and erlotinib as a potential probe substrate for OATP2B1 applicable in humans²⁴.

Fluorescence-based detection technologies are frequently applied in biological testing, due to their unique advantages in setting up homogeneous, sensitive assays in miniaturized formats²⁵. A common feature of drug transporters is their wide substrate specificity that also encompasses fluorescent molecules. Indeed, fluorescent molecules have been successfully used in *in vitro* and *in vivo* transporter assays²⁶. Calcein-AM, originally developed as a viability dye, was discovered to be a high affinity substrate of several pharmacologically relevant ABC transporters^{27–29}. Similarly, Hoechst 33342 and DyeCycle Violet, two nucleotide/DNA binding dyes, are ABCG2 and ABCB1 substrates that can be used to characterize transporter function^{30,31}. Screening assays based on the OATP1B1/3-mediated uptake of fluorescein, fluorescein-methotrexate or various fluorescein derivatives have also been developed^{32–34}. The applicability of fluorophores in transporter-based assays depends on several sources of potential artefacts, including non-specific protein binding, sequestration within the cell, or quenching by pH or intracellular ions. Unlike fluorescein or fluorescein-methotrexate, an ideal OATP test substrate should be membrane impermeable, and its fluorescence should be independent of the intracellular milieu.

Our aim in this study was to expand the scope of currently available fluorescent indicators of hepatic OATPs, 1B1, 1B3 and 2B1. In particular, we wanted to identify a pH-independent fluorophore with low cell permeability, to ensure a high signal to noise ratio and to allow transport measurements at acidic pH levels needed for the optimal activity of OATPs³⁵. Using cell lines engineered to overexpress human OATP1B1, 1B3, or 2B1, we identify a series of commercially available cell impermeable dyes as high affinity OATP substrates. We show that a transport assay based on the uptake of the best-performing fluorophores is amenable to semi high-throughput screening for OATP drug interactions.

Results

Zombie Violet is a novel substrate of human OATPs, 1B1, 1B3 and 2B1. In an effort to identify new fluorescent substrate candidates of hepatic OATPs, we searched the literature for dyes showing low membrane permeability and pH independent fluorescence. Based on these characteristics we focused on commercially available viability dyes, because these fluorescent molecules do not stain living cells, and therefore are expected to show low passive permeability. Recently, we have shown that the OATP-mediated transport of fluorescent compounds can be quantitatively monitored in insect cells³⁶. Therefore, first we used this expression system to test the contribution of OATP1B1 to the cellular uptake of Zombie Violet[™] (ZV, BioLegend), an amine-reactive fluorescent dye used for the labelling of dead cells. To discern staining due to cell death, we counterstained the cells with propidium iodide (PI). Whereas in control cells staining with ZV was always accompanied by PI-positivity (indicating a loss of membrane integrity), cells expressing the human OATP1B1 transporter were distinctly ZV-positive and PI-negative, indicating that ZV cannot penetrate living cells unless OATP1B1 is present in the plasma membrane (Fig. 1a). Detailed transport measurements confirmed that the accumulation of ZV is due to OATP1B1-mediated uptake, showing saturable (Fig. 1b) and inhibitor-sensitive uptake (Supplementary Figure 1a).

Next, we screened ZV against the other, multispecific human OATPs of the liver, 1B3 and 2B1 (Fig. 1c). We found that, albeit to a lesser extent, ZV is also transported by OATP1B3 and 2B1. ZV transport was sensitive to pH (Fig. 1d), with highest uptake at pH 5.5; and also to inhibitors (Supplementary Figure 1b), indicating that ZV is a bona fide OATP1B and 2B1 substrate. Additionally, we found that Live/Dead Green (LDG, Life Technologies), also designed to label dead cells, is another substrate of these three OATPs, while in the case of Zombie Green (a viability dye from the Zombie[™] family), there was no OATP-mediated transport (Fig. 1c).

Establishment of A431 cells with robust OATP1B1, 1B3 or 2B1 expression using viability dye-based cell sorting. While the Sf9 system has several advantages, the transient nature of OATP expression is not compatible with high-throughput screening (HTS). In order to build a stable model system and to test

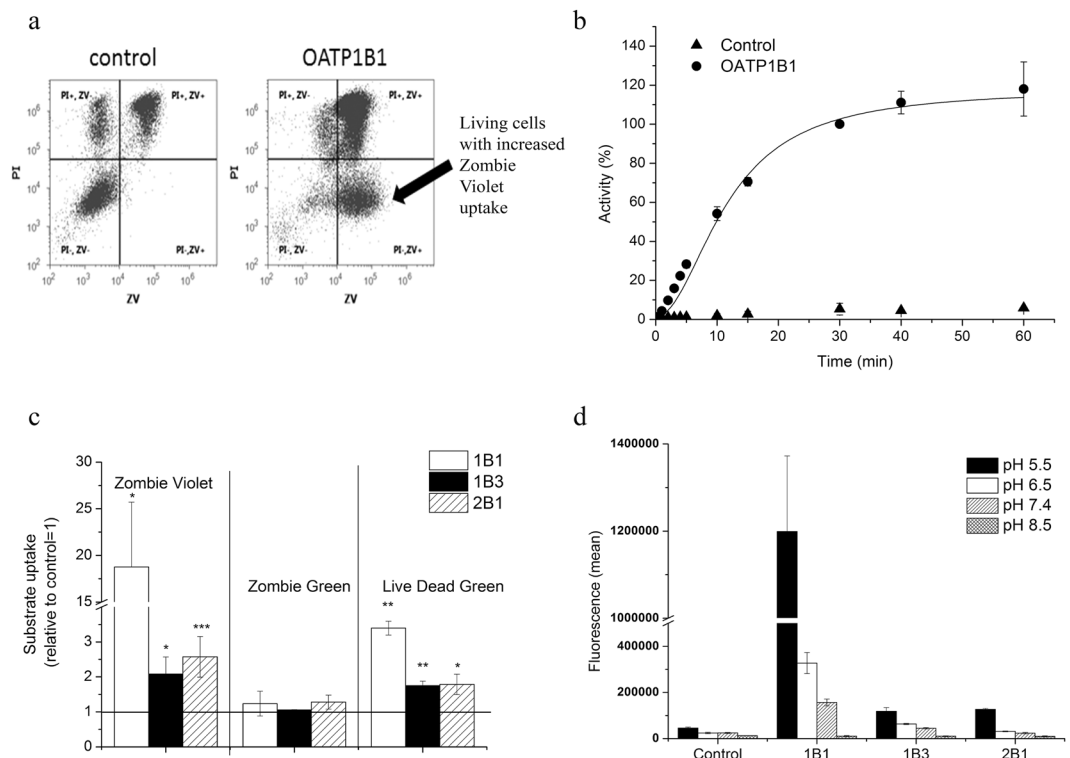


Figure 1. Uptake of viability dyes in Sf9 cells measured by flow cytometry. **(a)** Uptake of ZV (0.2 μ l in 100 μ l) was measured at 37 $^{\circ}$ C in pH 5.5 uptake buffer for 15 minutes. Dead cells were identified based on PI staining. Experiments were repeated at least three times, the result of one representative experiment is shown. **(b)** Kinetics of OATP1B1-mediated ZV uptake. Uptake rates were normalized to the fluorescence values measured for OATP1B1 incubated with 2 μ l ZV for 30 minutes. **(c)** ZV and LDG uptake in Sf9 cells. Dye (0.2 μ l in 100 μ l) uptake was measured after 30 minutes of incubation. Statistical analysis was performed by Student's t-test. * $p < 0.05$, *** $p < 0.001$. **(d)** pH dependent uptake of ZV in Sf9 cells. Uptake of 0.2 μ l ZV in 100 μ l at 37 $^{\circ}$ C was measured in buffers with different pH for 10 minutes. **(b,c and d)** data represent the average of three independent experiments \pm SD values.

whether OATP1B and 2B1-mediated viability dye uptake can also be observed in human cells, we generated A431 (human epidermoid carcinoma) cell lines overexpressing OATP1B1, 1B3 or 2B1. The A431 cell line was chosen based on its good adherence necessary for transport measurements in 96 well plates. OATP2B1 was readily overexpressed in A431 cells, whereas expression levels of OATP1B1 and 1B3 remained very low despite repeated rounds of puromycin selection or lentiviral transduction (Fig. 2a shows OATP protein levels in A431 cells in comparison to the levels achieved in insect cells). Consequently, transport of a common OATP1B and 2B1 substrate, fluorescein-methotrexate showed weak OATP1B activity compared to OATP2B1 (Fig. 2b). Similarly, convincing ZV and LDG uptake could only be observed in A431-OATP2B1 cells (Fig. 2b).

Substrate uptake is proportional to OATP expression/function, and we sought to determine whether subpopulations with increased OATP expression could be identified based on substrate accumulation. Since LDG is well tolerated (see Supplementary Figure 2), we sorted highly fluorescent LDG-positive A431-OATP1B1, 1B3 and 2B1 cells, which were further propagated in cell culture. Stunningly, the sorted cells showed significant OATP expression and function (Fig. 2c,d), indicating that preferential uptake of LDG allowed the function-based sorting of cells with high OATP expression. High expression levels were maintained for at least 2 months (cca. 20 passages) without the need of further sorting or selection.

A set of commercially available fluorophores as OATP1B and 2B1 substrates. In addition to ZV and LDG, a large panel of spectrally diverse dyes aimed for the detection of dead cells is available commercially (Table 1). In order to find out whether these fluorescent dyes are also recognized by OATP1B1, 1B3 and 2B1, we monitored their uptake in 96 well plates using the sorted A431 cells. In addition to the viability dyes, we tested the transport of two other cell-impermeant fluorescent compounds, Cascade Blue hydrazide (CB) and Alexa Fluor 405 succinimidyl ester (AF405), intended for use in cell permeability assays and the fluorescent labelling of proteins, respectively. As shown in Fig. 3, we found a robust fluorescent signal in OATP-expressing cells with several dyes. Moreover, in the case of ZV, LDG, CB and AF405 the signal intensity highly exceeded that of Fl-MTX, indicating that the newly identified dyes may be better suited for fluorescence-based studies assaying OATP function. On the other hand, Zombie Green, Live/Dead Red, Live/Dead Aqua, Live/Dead Yellow, Live/Dead Far-red and Live/Dead near-IR were not transported by the investigated OATPs (Table 1).

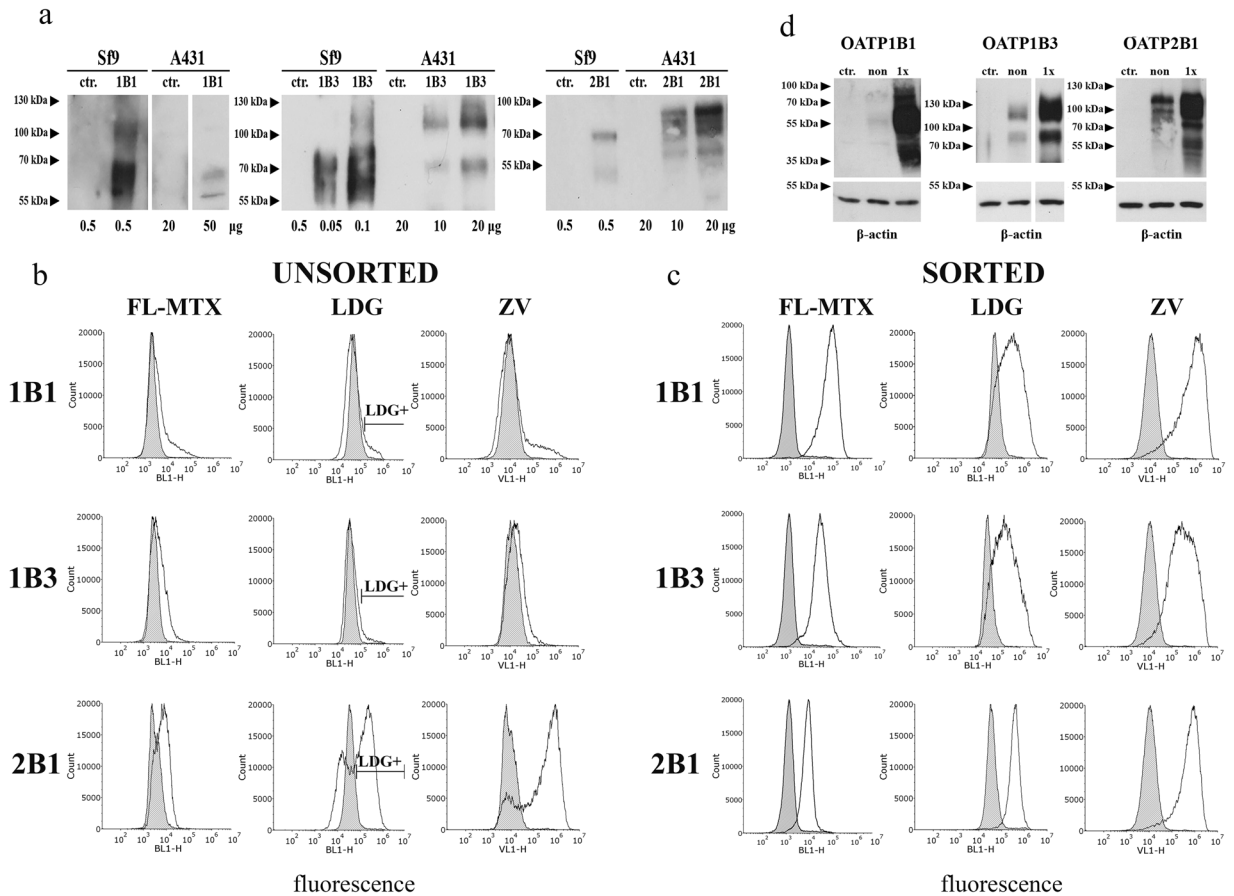


Figure 2. Low level of OATP1B expression in A431 cells. **(a)** Western blot detection of human OATPs expressed in insect and A431 cells. Total cell lysates were analysed by Western blot. Control (ctr.) represents Sf9 cells expressing an unrelated protein or mock transfected A431 cells. Multiple migratory bands most probably represent differently glycosylated forms of OATPs. Figure for OATP1B1 was sliced from the same blot, same exposure time. Full-length blots are presented in Supplementary Figure 7. **(b)** FL-MTX, LDG and ZV uptake in A431 cells. Representative histograms show the uptake of 1 µM FL-MTX or 0.4 µM LDG or ZV into A431 cells before and after sorting. Cells with the highest LDG fluorescence were sorted, and after recovery, the cells were again measured for LDG uptake (panel c). Mock transfected control cells are indicated by filled histograms. Cells were incubated with the substrates for 15 minutes (FL-MTX) or 30 minutes (ZV, LDG) at 37 °C in uptake buffer (pH 5.5) in final volume of 100 µl. Living (PI-negative) cells are shown. **(d)** LDG sorting results in increased expression of OATP1B1, 1B3 and 2B1. OATP expression was determined using whole cell lysates (20 µg each) by Western blot. A431 mock transfected cell lysates were used as control. β-actin served as an internal control. Experiments were repeated at least twice. One representative blot is shown. Ctr.: mock-transfected, non: non-sorted, sort: sorted. Multiple migratory bands most probably represent differentially glycosylated forms of OATPs. Full-length blots with different exposition times are presented in Supplementary Figure 7.

Functional assay adapted to microplates. In order to find optimal conditions for measuring the uptake of the newly identified OATP1B and 2B1 substrates and to choose the best dye that could be applied in a semi high-throughput set up, we characterized the kinetics of uptake by A431-OATP1B1, 1B3 and 2B1 cells seeded in 96-well plates. We found rapid ($t_{1/2}$ values around 10–15 minutes, Supplementary Figure 3b) uptake of the newly identified fluorescent dye substrates, and most importantly we also observed that incubation/reaction time could be prolonged up to 60 minutes without significant “leakage” of the dyes into control cells. The optimum condition for OATP1B and 2B1-mediated uptake for all the tested dyes was found to be at pH 5.5 (Fig. 1d, and Supplementary Figure 4).

Structural information was available for AF405 (Tris(N,N-diethylethanaminium) 8-[2-(4-((2,5-dioxopyrrolidin-1-yl)oxy)carbonyl)piperidin-1-yl)-2-oxoethoxy]pyrene-1,3,6-trisulfonate) and CB ((3,6,8-trisulfo-1-pyrenyl)oxy]-1-hydrazide), which were further characterized to determine the kinetic parameters of transport (see Supplementary Figure 3 for detailed characterization of ZV, LDV and LDG transport). In comparison to FL-MTX, AF405 and CB proved to be lower affinity substrates, whereas the V_{max} of 1B1/2B1-mediated CB transport was 2–4 fold higher. 1B3 showed weak CB transport, but AF405 proved to be an excellent substrate with cca. 3-fold higher V_{max} value as compared to FL-MTX (Fig. 4). In experiments performed at ideal conditions for each dye, we found that the maximum signal (OATP vs. vector control) can be achieved

Distributor	Dye	Ex/Em optimum (nm)	Transported by OATPs in A431 cells
BioLegend	Zombie Green	488/515	—
	Zombie Violet	405/423	1B1, 1B3, 2B1
Thermo Fisher (Life Technologies)	Live/Dead Blue	350/450	very weak 1B1, 1B3, 2B1
	Live/Dead Aqua	367/526	—
	Live/Dead Violet	416/451	1B1, 1B3, 2B1
	Live/Dead Yellow	400/575	—
	Live/Dead Green	495/520	1B1, 1B3, 2B1
	Live/Dead Red	595/615	—
	Live/Dead Far-red	650/665	—
	Live/Dead near-IR	750/775	—
	Alexa Fluor 405 NHS Ester	401/421	1B1, 1B3, 2B1
	Cascade Blue Hydrazide	400/419	1B1, 1B3, 2B1

Table 1. List of the fluorescent dyes tested in the current study. All dyes were tested for transport by OATP1B1, 1B3 and 2B1 expressed in A431 cells in 96-well plates using an Enspire fluorescent plate reader. Transport was tested in at least two independent experiments using triplicates. “—” indicates lack of OATP-mediated uptake.

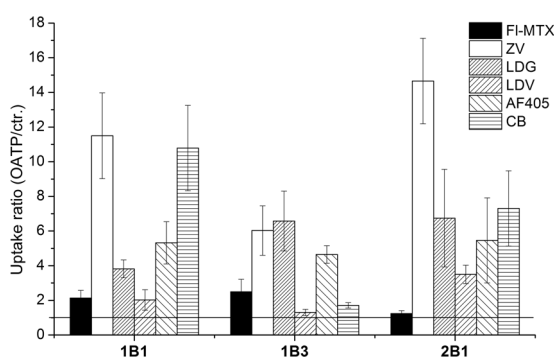


Figure 3. Screening identifies additional fluorescent OATP substrates. Transport was determined in A431 cells expressing OATP1B1, 1B3 or 2B1 seeded in 96-well plates. The cells were incubated with 1 μ l ZV, LDV, LDG, 1 μ M (or 4 μ M for OATP2B1) FI-MTX or 20 μ M CB and AF405 for 30 minutes at 37°C in buffer with pH 5.5, in final reaction volume of 100 μ l. Fluorescence was determined using an Enspire fluorescent plate reader. Activity was calculated by dividing fluorescence measured in A431-OATP cells with that measured in A431 mock transfected cells. Average of at least three independent measurements with triplicates \pm SD values are shown.

with ZV for all three OATPs. CB is as good a substrate for OATP1B1 and 2B1 as ZV. In the case of OATP1B3 the highest signal was achieved with ZV, LDG and AF405 (activity ratios are summarized in Table 2). Importantly, the transport of all novel fluorescent dyes could be inhibited by known inhibitors.

Inhibition assay using Cascade Blue or Alexa Fluor 405 to probe substrates. Next, we tested the applicability of the best performing substrates, CB for OATP1B1 and 2B1, and AF405 for OATP1B3 to detect OATP drug interactions. We measured the inhibitory effect of four well-known OATP1B and 2B1 interacting compounds (Cyclosporin A (CsA), bromosulphophthalein (BSP), taurocholate (TC) and estrone-3-sulphate (ES)). All four compounds inhibited CB or AF405 uptake in a concentration dependent manner (Fig. 5). Moreover, the IC_{50} values obtained in the fluorescence-based assays (Table 3) showed perfect agreement with results obtained using radioactive substrates, and pilot screens yielded a z-factor above 0.5, suggesting that the new, fluorescence-based assays are amenable to HTS detecting OATP1B/2B1 drug interactions (Table 2)³⁷.

Discussion

Testing the interaction between a new molecular entity and OATP1Bs is required at early stages of drug development. Several fluorescent OATP1B substrates have already been identified. These substrates are either molecules with intrinsic fluorescence, mainly fluorescein and its derivatives^{33,34}, or OATP substrates tagged with a fluorophore, such as Oregon green/Flutax-2 (1B3³²), chenodeoxycholy-(N ϵ -1 nitrobenz-2-oxa-1,3-2 diazole)-lysine (CDCA-NBD)³⁸, cholyl-glycylamido-fluorescein (CGamF)³⁹, cholyl-L-lysyl fluorescein (CLF)⁴⁰, fluorescein-methotrexate (FI-MTX)³² and 8-fluorescein-cAMP (8-FcA)⁴¹. Whereas methods based on the uptake of fluorescein and fluorescein-methotrexate have been adapted to semi high-throughput (HT) format^{32,33}, due to reliability, sensitivity and availability issues, most of these probes are not ideal for large scale OATP drug interaction screens³⁴. For example, Gui *et al.* found that due to its lower transport capacity by OATP1B1, FI-MTX is not suitable for HT OATP1B1 drug interaction screening³². Moreover, in the case of OATP2B1, an

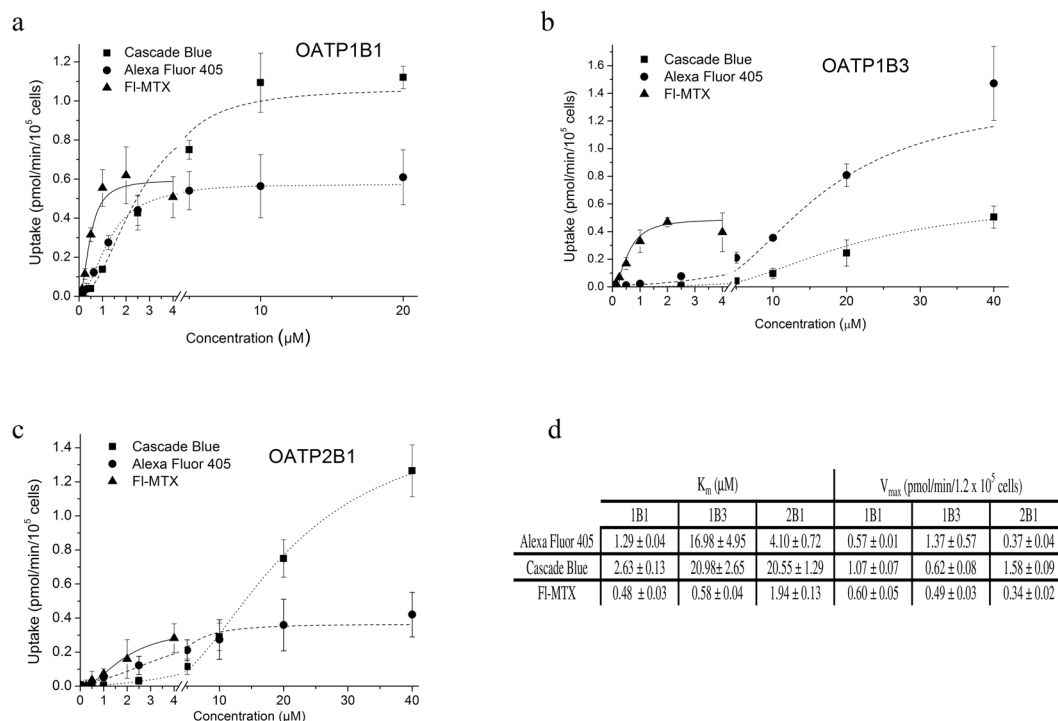


Figure 4. Kinetics of uptake of CB, AF405 and FI-MTX in A431 cells overexpressing OATP1B1, 1B3 or 2B1. Transport was measured in 96-well plates. Cells were incubated with increasing concentrations of FI-MTX, CB or AF405 in the linear phase of uptake (2.5 minutes for FI-MTX, 10 minutes (1B1, 2B1) or 15 minutes (1B3) for CB, and 15 minutes for AF405). Transport capacity was calculated based on calibration with known amounts of the dye. Uptake in A431-OATP cells without background signal (fluorescence in A431-mock cells) is shown. Data points indicate average \pm SD values obtained in three independent experiments.

	Transport ratio compared to control			z-factor		
	1B1	1B3	2B1	1B1	1B3	2B1
FI-MTX	2.14 ± 0.44	2.49 ± 0.72	1.24 ± 0.16	0.59	0.77	-1.80
Zombie Violet	11.05 ± 2.47	6.03 ± 1.43	14.65 ± 2.47	0.61	0.61	0.71
Live/Dead Violet	2.03 ± 0.59	1.33 ± 0.21	3.50 ± 0.53	0.55	-0.42	0.79
Live/Dead Green	3.82 ± 0.51	6.58 ± 1.73	6.74 ± 2.82	0.84	0.76	0.62
Cascade Blue	10.79 ± 2.46	1.71 ± 0.16	7.31 ± 2.17	0.73	0.26	0.66
Alexa Fluor 405	5.32 ± 1.22	4.65 ± 0.51	5.46 ± 2.46	0.59	0.64	0.57

Table 2. Transport ratio and z-factor determined in A431-OATP cells. A431 cells (seeded in 96-well plates) were incubated with the dyes at pH 5.5 for 30 minutes in order to reach maximum fluorescence signal. Data were calculated from at least 3 independent measurements. Dyes were applied in the following concentrations/amounts: FI-MTX 1 μM (1B1 and 1B3) and 4 μM (2B1); ZV, LDV and LDG 1-1 μl ; CB and AF405 10 μM (1B1 and 2B1) and 20 μM (1B3). A z-factor above 0.5 is defined as an excellent assay³⁷. Dyes defined as best candidates for HTS are indicated in bold.

emerging candidate in pharmacokinetic studies, no such fluorescence-based large scale screening method has been reported.

Here our aim was to identify novel fluorescent OATP1B1, 1B3 and 2B1 substrates. We tested commercially available fluorescent molecules showing low passive cellular uptake, high fluorescence quantum yield and pH insensitivity. These characteristics are required to achieve high signal to noise ratio, and maximal OATP activity, since OATP2B1 functions (almost) exclusively at acidic extracellular pH^{36,42}. Based on these criteria, we chose two sets of compounds. First, we tested fluorescent viability dyes (Zombie dyes and the Live/Dead viability dye panel) developed to enter only dead cells. Secondly, we selected CB, a commercially available fluorescent dye used to investigate membrane permeability.

We found that in OATP1B or 2B1 expressing live insect cells a typical transporter mediated uptake of ZV can be observed (Fig. 1). Moreover, a robust OATP-mediated ZV uptake was also confirmed in A431 cells engineered to overexpress the OATP transporters (Figs 2 and 3). ZV was designed to label cells with compromised membranes. Indeed, in control Sf9 and A431 cells ZV fluorescence correlated with propidium iodide staining (Fig. 1a

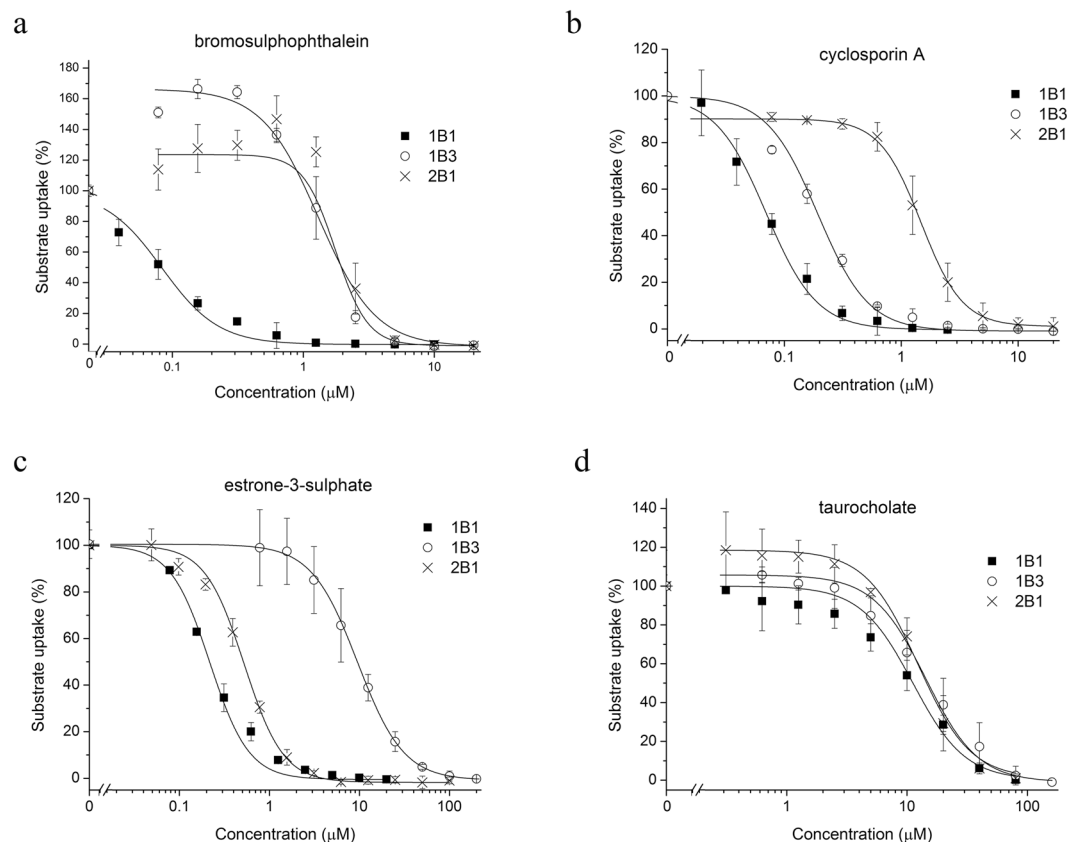


Figure 5. Inhibition of CB and AF405 uptake in A431-OATP cells. Transport of CB (2 μM for OATP1B1 and 10 μM for OATP2B1) and AF405 (5 μM , OATP1B3) was measured for 30 minutes in the absence or presence of the investigated compounds. Transport was determined by subtracting fluorescence in A431-mock cells. Transport measured in cells with the dye alone was set to 100% and the effect of the compounds was compared to this value. Experiments were performed in triplicates with three parallels in each biological replicate. Average \pm SD values are shown.

	OATP1B1		OATP1B3		OATP2B1	
	This study	Literature data	This study	Literature data	This study	Literature data
BSP	0.08 \pm 0.10	0.1 ^{34,41,45}	0.9 \pm 0.31	0.4 ⁵⁵ , 0.5 ⁴¹	1.26 \pm 0.56	1.2 ⁴⁶
CsA	0.07 \pm 0.04	0.1 ^{34,45} 0.2 ⁴¹ , 1.3 ⁴⁴	0.18 \pm 0.05	0.2 ⁴¹ , 1.2 ⁴⁴	1.45 \pm 0.11	36 ⁴⁴
EIS	0.22 \pm 0.004	0.05 ^{34,41}	9.5 \pm 0.13	20 ⁴¹	0.56 \pm 0.05	
TC	11.2 \pm 0.22	9 ³⁴ , 19 ⁴⁵	14.3 \pm 0.32	18 ^{*56}	12.3 \pm 0.15	9 ⁴⁶

Table 3. Comparison of IC_{50} values with literature data. IC_{50} (μM) values were determined using 2 or 10 μM CB (OATP1B1 or 2B1) or 5 μM AF405 (OATP1B3). For detailed description see Fig. 5. Literature data show IC_{50} values obtained in assays using EG, ES, 8-FcA or DCF as probe substrates. When transport inhibition data were not available, K_m values obtained in direct transport experiments are shown, indicated by *.

and Supplementary Figure 5). However, our results demonstrate that the expression of OATPs results in the staining of living (propidium iodide negative) cells, warranting caution in the interpretation of results obtained with ZV as a viability dye.

Using the Sf9 expression system we identified another viability dye, Live/Dead Green as an OATP1B and 2B1 substrate (Fig. 1c). However, further large scale screens required a well-adherent cell line with stable OATP expression. Therefore we generated A431 cells with OATP1B1, 1B3 or 2B1 overexpression. Although A431 is not routinely used in pharmacological applications, due to its well-adherence it is well suited to microplate based assays⁴³. Unexpectedly, only very low levels of OATP1B1 and 1B3 expression could be achieved in this cell line (Fig. 2a) and also in HEK293 or MDCKII cells. Enrichment of OATP1B expressing living cells based on antibody labelling is not feasible due to the lack of an anti-OATP antibody recognizing an extracellular epitope. Therefore we sorted cells based on increased fluorescence associated with OATP1B/2B1 mediated LDG uptake, which led to the enrichment of OATP1B and 2B1 positive cells characterized by elevated OATP expression and function

(Fig. 2c,d). The application of a fluorescent dye to enrich OATP-expressing cells is a unique (and to our knowledge the first) tool that allows the generation of cells with high OATP levels.

To validate the reliability of the A431 model, we also tested the uptake of the newly identified fluorescent substrates in HEK293 and MDCKII cells that are routinely used in transporter interaction studies. Results obtained in HEK and MDCKII cells overexpressing OATP1B1, 1B3 or 2B1 (Supplementary Figure 6) were fully consistent with those obtained in A431 cells, supporting the conclusion that the novel fluorescent dye substrates can be applied to characterize OATP1B/2B1 function.

Consistently with studies showing that an acidic extracellular milieu can significantly stimulate OATP-mediated transport^{35,42}, we observed transport of the new fluorescent substrates almost exclusively at pH 6.5–5.5. Whether this is due to chemical changes in the fluorescent molecules at lower pH or an indication of proton counter transport, needs further investigation. Importantly, inhibition constants obtained with the novel assays at acidic pH are in full harmony with data obtained at neutral pH^{34,41,44}, indicating that the established assay conditions are suited for OATP drug interaction screens.

Although the exact transport kinetics (K_m and V_{max} values) for ZV, LDV and LDG could not be defined (the molecular formula of these dyes could not be obtained from the suppliers due to proprietary concerns), we were able to determine and compare transport kinetics of CB and AF405 with that of Fl-MTX. Fl-MTX is a well-established substrate of OATP1B1 and 1B3³², and we have demonstrated previously that Fl-MTX is also transported by OATP2B1 when an acidic extracellular environment is generated³⁶. In A431 cells we could confirm the OATP2B1-mediated uptake of Fl-MTX, however compared to OATP1Bs, Fl-MTX was found to be a poor substrate of OATP2B1 (Figs 2 and 3). In the case of the novel dye substrates, we found that CB is preferentially transported by OATP1B1 and 2B1 as compared to Fl-MTX, while OATP1B3 shows preferential transport of AF405 as compared to CB and Fl-MTX (Figs 3 and 4 and Table 2).

Besides the hepatic OATP1Bs and 2B1, OATP1A2 is also an important drug transporter. However, in our pilot experiments, we found no detectable transport of Zombie Violet, Cascade Blue or Alexa Fluor 405 by this transporter.

Highly fluorescent dyes with low cell permeability and elevated transport by OATPs are ideal candidates for the development of a sensitive functional assay. Our results demonstrate that the novel OATP1B and 2B1 substrates and the established A431 model cells can be used to measure OATP function in a low to medium throughput format. The z-factor for the novel substrates also suggests that ZV, LDV (1B1, 2B1), LDG, CB (1B1, 2B1) and AF405 may be applied in large scale drug screening studies (Table 2). Experiments using CB or AF405 as probe substrates demonstrate that these dyes are suitable to detect OATP substrate/inhibitor interactions (Fig. 5). The IC_{50} values obtained in our assay are in good agreement with those measured with widely accepted test substrates (estrone-3-sulphate or estradiol-glucuronide) (Table 3). It is well known that OATP1Bs and 2B1 have more than one substrate binding site. The IC_{50} values measured for OATP1B1-mediated CB uptake are in harmony with those obtained with dichlorofluorescein and tritiated estradiol-glucuronide^{34,44,45}. Therefore the CB assay may be a good alternative to test OATP1B1 drug interactions as a substitute to estradiol-glucuronide. Similarly, the AF405 and CB assay for OATP1B3 and 2B1, respectively resulted in IC_{50} values similar to that obtained in assays using tritiated estradiol-glucuronide (1B3)⁴⁴, or estrone-3-sulphate (2B1)^{44,46} as probe substrates. These results again clearly argue that CB and AF405 are good alternatives to these radioactive assays. Interestingly, BSP at low concentrations activated CB or AF405 uptake by OATP2B1 or 1B3, respectively. Such an activation by BSP has not yet been documented, however the stimulatory effect of one compound to the transport of another is a well-known phenomenon (summarized in⁴⁷). In the case of OATP1B3, progesterone was shown to stimulate Fl-MTX³² and epigallocatechin gallate estrone-3-sulphate uptake⁴⁸. Progesterone has also an activating effect on OATP2B1-mediated estrone-3-sulphate and dehydroepiandrosterone sulphate uptake⁴⁹, and prostaglandin A1, testosterone and fendilin on estrone-3-sulphate uptake^{44,50}. One possible explanation may be a co-transport of the two molecules, however reciprocal transport has not yet been confirmed in any of these cases, and also needs further investigation for the fluorescent dyes and BSP.

In conclusion, we show here that several fluorescent viability dyes and two sulfonypyrenes (CB and AF405) are high capacity substrates of the multispecific OATP1B and 2B1 transporters. The fluorescence-based transport assay measuring the uptake of the best-performing substrates, CB and AF405 open the way to the development of sensitive high-throughput assays for the detection of OATP1B/2B1 drug interactions.

Materials and Methods

Materials. Zombie dyes (Violet, Green) were purchased from BioLegend® (San Diego, CA, US). LIVE/DEAD® Fixable Cell Stain Dye panel, Cascade Blue hydrazide, Alexa Fluor 405 succinimidyl ester were bought from Thermo Fischer Scientific (Waltham, MA, US), and fluorescein-methotrexate triammonium salt from Biotium (Hayward, CA, US). Restriction endonucleases were from New England Biolabs Ltd. (Ipswich, MA, US). All other materials, if not indicated otherwise, were purchased from Sigma Aldrich, Merck (Budapest, HU).

Generation of plasmid constructs. Generation of baculovirus vectors (pAcUW21-L/OATP and pAcUW21-control) was described earlier³⁶. OATP2B1 expressing cells were generated by transposase mediated genomic insertion of the OATP2B1 cDNA (BC041095.1, HsCD00378878). Briefly, OATP2B1 cDNA was amplified (Phusion1 High-Fidelity PCR Kit, NEB, Ipswich, MA, US) from the vector obtained from Harvard PlasmID Repository (Harvard Medical School, Boston, MA, US) by using the following primers: forward 5': GTAAT GCGGCCGC AA GAATTC GCCACCATGGG ACCCAGGATAGG and reverse 5' GTACAT GCGGCCGC T AAGCTT TCACACTCGGGAATCCTC. The PCR fragment was cloned between the NotI-HindIII sites of the pSB-CMV vector⁵¹.

OATP1B1 and 1B3 overexpressing cells were generated by lentivirus transduction. The lentivirus based pRRL-CMV-MCS-IRES-ΔCD4 vector was generated by replacing the sequence of GFP with a multicloning

site of the pRRLSIN.cPPT.PGK-GFP.WPRE (Addgene #12252) plasmid (Didier Trono, Lausanne, Switzerland). An IRES was cloned between the PmlI and XbaI sites of the MCS (forward: 5'-ACACGTGTCCGGACTAGTCCACCTTGCC TTACACATGAAGAG, reverse: 5'-ATCTAGAATGATCAGCCATATTATCATCGTGTGTTTTTCAAAG). The plasmid also contains a truncated CD4 receptor enabling monitoring of the virus transfection. Truncated CD4 cDNA was PCR amplified by the following primers (based on⁵²: 5'-GATTCTAGAGCCACCATGAACCGGGGAGTCCCTTTTAGGC and 5'-GTAGTCGACTTAGCGCCTTCGGTGCCGGCAC from the pCMV-SPORT6-CD4 (Harvard Plasmid Repository). After digestion with XbaI-SalI enzymes, the PCR fragment was cloned to the corresponding sites of the pRRL-CMV-MCS-IRES vector.

The open reading frames OATP1B1 (Gene ID: AB026257) and OATP1B3 (BC141525, HsCD00348132) were amplified by HF PCR (Phusion1 High-Fidelity PCR Kit, NEB, Ipswich, MA, US) from the pAcUW-21-L/OATP1B1-wt vector and from the plasmid obtained from Harvard PlasmID, respectively, using the following primers:

OATP1B1: forward 5' TATTATTTCGAAGCCACCATGGACCAAAATCAACAT, reverse 5' CATGTAAC TAGTTTAAACAATGTGTTTCACTATCT.

OATP1B3: forward 5' ACTAGTTTAAACGCCACCATGGACCAACATCAACAT and reverse 5' GTACATGCG GCCGCACTGCAGTTAGTTGGCAGCAGCATTTGTC. After digestion with BstBI and SpeI (OATP1B1) or PmeI-PstI (OATP1B3) enzymes the PCR fragments were cloned to the corresponding sites of the pRRL-CMV-MCS-IRES- Δ CD4 vector.

The base order of the cDNAs in the final vector constructs was verified by sequencing. Empty vectors without the OATP cDNAs, pSB-CMV and pRRLdCD4 were used as negative controls (indicated on the Figures as mock).

Expression in insect cells. Transient expression of human OATP1B1, 1B3 and 2B1 in Sf9 (Spodoptera frugiperda) cells was achieved as described earlier³⁶. For transport measurements, Sf9 cells after 36–40 hours post infection were used.

Generation of cell lines. A431 cells (ATCC) were transfected with 1 μ g plasmid DNA (OATP2B1) + 100 ng plasmid containing the transposase^{51,53} using Fugene HD reagent (Promega, Madison, WI, US) according to the protocol of the supplier. Puromycin (1 μ g/ml) selection was started 48 h later. After 2 weeks of puromycin selection the cells were grown in DMEM (Gibco, Thermo Fischer Scientific (Waltham, MA, US)) supplemented with 10% fetal calf serum, 2 mM L-glutamine, 100 U/ml penicillin, and 100 μ g/ml streptomycin at 37 °C with 5% CO₂ and 95% humidity, without puromycin.

OATP1B1 and 1B3 overexpression in A431 cells was achieved by recombinant lentiviruses as described in⁵⁴. HEK 293 T human embryonic kidney cells (1.8 \times 10⁶ cells on a Petri dish (6 cm in diameter)) were transfected with (6 μ g) pRRL-CMV-MCS-IRES- Δ CD4/OATP1B1 or OATP1B3, 2.2 μ g pMDG and 4 μ g psPax2 vectors⁵⁴ using CaPO₄ precipitation. The supernatant, containing lentiviral particles was collected 72 h after the transfection. Transduction of target A431 cells was carried out on 6 well plates. The multiplicity of infection was approximately 1.

Determination of dye uptake. *Flow cytometry.* In order to determine the uptake of the fluorescent molecules in Sf9 cells, recombinant baculovirus infected cells were collected 36–40 hours post infection. After washing in the appropriate buffer (usually uptake buffer pH 5.5, see below) 5 \times 10⁵ cells were incubated at 37 °C with the appropriate amount of dyes (the exact concentrations/amounts are indicated in the Figure legends) in a final volume of 100 μ l. Transport experiments were carried out in the uptake buffer (125 mM NaCl, 4.8 mM KCl, 1.2 mM CaCl₂, 1.2 mM KH₂PO₄, 12 mM MgSO₄, 25 mM MES, and 5.6 mM glucose, with the pH adjusted to 8.5, 7.4, 6.5 or 5.5 using 10 N NaOH or 1 M HEPES). Incubation time was between 1–60 minutes. The reaction was stopped by the addition of 1 ml ice-cold phosphate-buffered saline (PBS). The cells were kept on ice until flow cytometry analysis. The cellular fluorescence of min. 20,000 live cells was determined using an Attune Acoustic Focusing Cytometer (Applied Biosystems, Life Technologies, Carlsbad, CA, US). Dead cells labelled with propidium iodide (PI, 1 μ g/ml) were excluded. Functional data for each OATP represent the mean of at least 3 independent experiments performed on different days. In the case of A431 cells, cells were collected after trypsinization (0.1% trypsin) and the uptake experiments were performed in the same way as described for insect cells (see above). Data presented on Figures were generated by the FCS Express software.

Microplate-based assay. For the microplate-based assay, OATP-expressing A431 cells were seeded (6 \times 10⁴ cells in 200 μ l final volume/well) onto 96-well plates and cultured for 16–24 h at 37 °C, 5% CO₂. Next day, the supernatant was removed and the cells were washed 3-times with 200 μ l of PBS. When inhibitors were tested, the cells were pre-incubated in the presence of inhibitors (solved in DMSO) for 5 min at 37 °C (usually in 50 μ l volume). The amount of DMSO was kept below 0.5% throughout the study. This amount of the solvent did not influence the fluorescence of the dyes. The reaction was started with the addition of 50 μ l fluorescent dye (1–40 μ M final concentration or 0.05 μ l–1.2 μ l in final volume of 100 μ l) and the plate was incubated at 37 °C for 2–30 minutes. The reaction was stopped by the addition of 200 μ l ice-cold PBS. The supernatant was rapidly removed, and the cells were washed 3-times with 200 μ l ice-cold PBS. Finally, 200 μ l PBS was added to the cells and fluorescence was measured at room temperature using an Enspire fluorescent plate reader (Perkin Elmer) at wavelengths indicated in Table 1.

Cell sorting. Function-based sorting was carried out based on the Live/Dead Green uptake of A431 cells expressing OATP1B1, 1B3 or 2B1. 2–4 \times 10⁶ cells were incubated with 0.8–1.2 μ l Live/Dead Green in 100 μ l of transport buffer (sterile filtered), pH 5.5 at 37 °C for 30 minutes. The reaction was stopped by the addition of 1 ml

DMEM and the cells were centrifuged at 300 g for 4 minutes. The cell pellet was suspended in 500 µl DMEM. Cellular fluorescence was analysed using a BD FACSAria III Cell sorter (BD Biosciences, San Jose, CA, US). Cells with the highest fluorescence (see the applied gate (“LDG+”) on Fig. 2) were collected and cultured for further analysis. Cells kept in culture for maximum 20 passages were used for the experiments.

Western blot. Whole cell lysates of Sf9 or A431 cells (10–50 µg) were separated on 7.5% Laemmli SDS-PAGE gels and transferred onto PVDF membranes. Immunoblotting was performed as described in³⁶. Membranes were incubated overnight with OATP-specific antibodies or anti-β-actin antibody (A1978, Sigma). The antibodies used for the detection of OATP1B1 and 2B1 were kind gifts from Dr. Bruno Stieger (Department of Clinical Pharmacology and Toxicology, University Hospital, 8091 Zurich, Switzerland)⁵⁵. The antibody raised against OATP1B3 (AMAb91231) was purchased from Atlas Antibodies (Stockholm, Sweden). Secondary antibodies used were 10,000–20,000x diluted, HRP-conjugated anti-rabbit or anti-mouse antibodies (Jackson ImmunoResearch, Suffolk, UK). Luminescence was detected using the Luminor Enhancer Solution kit by Thermo Scientific (Waltham, MA, US).

Toxicity measurements. 5×10^3 A431 cells were seeded onto 96-well plates in a final volume of 100 µl DMEM. The next day a transport assay was performed at sterile conditions using 0.4 or 1.6 µl Live/Dead Green or Zombie Violet, respectively/ 5×10^5 cells in a 100 µl final volume. After 30 minutes, the cells were washed twice with PBS. Finally, 200 µl DMEM was added and the cells were cultured for 144 hours. Viability of the cells was determined using the PrestoBlue (Thermo Fischer Scientific) assay. Briefly, the medium was removed, and 100 µl 5% PrestoBlue in PBS was added to the cells. After incubation for 60 minutes at 37 °C, absorbance was detected at 583 nm with an Enspire fluorimeter (Perkin Elmer). Cells incubated with the buffer alone served as control. Background signal was calculated by absorbance measured in empty wells filled with 5% PrestoBlue.

Data analysis and statistics. Z-factor was calculated as follows: $1 - ((3 \times SD_{\text{negative control}} + 3 \times SD_{\text{positive control}}) / (\text{Mean}_{\text{positive}} - \text{Mean}_{\text{negative}}))$ based on³⁷. Kinetic parameters of dye uptake or inhibition were analysed by Hill fit using the Origin 8.6 software. Statistical significance was calculated by Student's t-test. The p value for statistical significance was set at 0.05 (*), 0.01 (**), or 0.001 (***)

Data availability. The datasets generated during the current study are available from the corresponding author.

References

1. Roth, M., Obaidat, A. & Hagenbuch, B. OATPs, OATs and OCTs: the organic anion and cation transporters of the SLCO and SLC22A gene superfamilies. *British journal of pharmacology* **165**, 1260–1287, <https://doi.org/10.1111/j.1476-5381.2011.01724.x> (2012).
2. Hagenbuch, B. & Stieger, B. The SLCO (former SLC21) superfamily of transporters. *Molecular aspects of medicine* **34**, 396–412, <https://doi.org/10.1016/j.mam.2012.10.009> (2013).
3. van de Steeg, E. *et al.* Complete OATP1B1 and OATP1B3 deficiency causes human Rotor syndrome by interrupting conjugated bilirubin reuptake into the liver. *The Journal of clinical investigation* **122**, 519–528, <https://doi.org/10.1172/JCI59526> (2012).
4. Durmus, S., van Hoppe, S. & Schinkel, A. H. The impact of Organic Anion-Transporting Polypeptides (OATPs) on disposition and toxicity of antitumor drugs: Insights from knockout and humanized mice. *Drug resistance updates: reviews and commentaries in antimicrobial and anticancer chemotherapy* **27**, 72–88, <https://doi.org/10.1016/j.drug.2016.06.005> (2016).
5. Shitara, Y. *et al.* Clinical significance of organic anion transporting polypeptides (OATPs) in drug disposition: their roles in hepatic clearance and intestinal absorption. *Biopharmaceutics & drug disposition* **34**, 45–78, <https://doi.org/10.1002/bdd.1823> (2013).
6. Maeda, K. Organic anion transporting polypeptide (OATP)1B1 and OATP1B3 as important regulators of the pharmacokinetics of substrate drugs. *Biological & pharmaceutical bulletin* **38**, 155–168, <https://doi.org/10.1248/bpb.b14-00767> (2015).
7. Giacomini, K. M. *et al.* Membrane transporters in drug development. *Nat Rev Drug Discov* **9**, 215–236, <https://doi.org/10.1038/nrd3028> (2010).
8. Shitara, Y., Itoh, T., Sato, H., Li, A. P. & Sugiyama, Y. Inhibition of transporter-mediated hepatic uptake as a mechanism for drug-drug interaction between cerivastatin and cyclosporin A. *J Pharmacol Exp Ther* **304**, 610–616, <https://doi.org/10.1124/jpet.102.041921> (2003).
9. Elsbly, R., Hilgendorf, C. & Fenner, K. Understanding the critical disposition pathways of statins to assess drug-drug interaction risk during drug development: it's not just about OATP1B1. *Clin Pharmacol Ther* **92**, 584–598, <https://doi.org/10.1038/clpt.2012.163> (2012).
10. Campbell, S. D., de Morais, S. M. & Xu, J. J. Inhibition of human organic anion transporting polypeptide OATP 1B1 as a mechanism of drug-induced hyperbilirubinemia. *Chemico-biological interactions* **150**, 179–187, <https://doi.org/10.1016/j.cbi.2004.08.008> (2004).
11. Keppler, D. The roles of MRP2, MRP3, OATP1B1, and OATP1B3 in conjugated hyperbilirubinemia. *Drug Metab Dispos* **42**, 561–565, <https://doi.org/10.1124/dmd.113.055772> (2014).
12. Zollner, G. *et al.* Hepatobiliary transporter expression in percutaneous liver biopsies of patients with cholestatic liver diseases. *Hepatology* **33**, 633–646, <https://doi.org/10.1053/jhep.2001.22646> (2001).
13. Tamai, I. *et al.* Molecular identification and characterization of novel members of the human organic anion transporter (OATP) family. *Biochem Biophys Res Commun* **273**, 251–260, <https://doi.org/10.1006/bbrc.2000.2922> (2000).
14. Gong, I. Y. & Kim, R. B. Impact of genetic variation in OATP transporters to drug disposition and response. *Drug Metab Pharmacokinet* **28**, 4–18, doi:DN/JST.JSTAGE/dmpk/DMPK-12-RV-099 (2013).
15. Knauer, M. J. *et al.* Human skeletal muscle drug transporters determine local exposure and toxicity of statins. *Circulation research* **106**, 297–306, <https://doi.org/10.1161/CIRCRESAHA.109.203596> (2010).
16. Gao, B., Vavricka, S. R., Meier, P. J. & Stieger, B. Differential cellular expression of organic anion transporting peptides OATP1A2 and OATP2B1 in the human retina and brain: implications for carrier-mediated transport of neuropeptides and neurosteroids in the CNS. *Pflugers Archiv: European journal of physiology* **467**, 1481–1493, <https://doi.org/10.1007/s00424-014-1596-x> (2015).
17. Lee, W. *et al.* Polymorphisms in human organic anion-transporting polypeptide 1A2 (OATP1A2): implications for altered drug disposition and central nervous system drug entry. *J Biol Chem* **280**, 9610–9617, <https://doi.org/10.1074/jbc.M411092200> (2005).

18. Yu, J., Zhou, Z., Tay-Sontheimer, J., Levy, R. H. & Ragueneau-Majlessi, I. Intestinal Drug Interactions Mediated by OATPs: A Systematic Review of Preclinical and Clinical Findings. *Journal of pharmaceutical sciences* **106**, 2312–2325, <https://doi.org/10.1016/j.xphs.2017.04.004> (2017).
19. U.S. Food and Drug Administration. Drug Development and Drug Interactions: Table of Substrates, Inhibitors and Inducers. <http://www.fda.gov/Drugs/DevelopmentApprovalProcess/DevelopmentResources/DrugInteractionsLabeling/ucm093664.htm#major> (2017).
20. Huang, S. M., Zhang, L. & Giacomini, K. M. The International Transporter Consortium: a collaborative group of scientists from academia, industry, and the FDA. *Clin Pharmacol Ther* **87**, 32–36, <https://doi.org/10.1038/clpt.2009.236> (2010).
21. Izumi, S. *et al.* Investigation of the impact of substrate selection on *in vitro* organic anion transporting polypeptide 1B1 inhibition profiles for the prediction of drug-drug interactions. *Drug Metab Dispos* **43**, 235–247, <https://doi.org/10.1124/dmd.114.059105> (2015).
22. Shen, H. *et al.* Evaluation of rosuvastatin as an organic anion transporting polypeptide (OATP) probe substrate: *in vitro* transport and *in vivo* disposition in cynomolgus monkeys. *J Pharmacol Exp Ther* **353**, 380–391, <https://doi.org/10.1124/jpet.114.221804> (2015).
23. Watanabe, T., Kusuhara, H., Maeda, K., Shitara, Y. & Sugiyama, Y. Physiologically based pharmacokinetic modeling to predict transporter-mediated clearance and distribution of pravastatin in humans. *J Pharmacol Exp Ther* **328**, 652–662, <https://doi.org/10.1124/jpet.108.146647> (2009).
24. Bauer, M. *et al.* Influence of OATPs on Hepatic Disposition of Erlotinib Measured With Positron Emission Tomography. *Clin Pharmacol Ther*, <https://doi.org/10.1002/cpt.888> (2017).
25. Gribbon, P. & Sewing, A. Fluorescence readouts in HTS: no gain without pain? *Drug discovery today* **8**, 1035–1043 (2003).
26. He, X., Gao, J., Gambhir, S. S. & Cheng, Z. Near-infrared fluorescent nanoprobe for cancer molecular imaging: status and challenges. *Trends in molecular medicine* **16**, 574–583, <https://doi.org/10.1016/j.molmed.2010.08.006> (2010).
27. Evers, R. *et al.* Inhibitory effect of the reversal agents V-104, GF120918 and Pluronic L61 on MDR1 Pgp-, MRP1- and MRP2-mediated transport. *British journal of cancer* **83**, 366–374, <https://doi.org/10.1054/bjoc.2000.1260> (2000).
28. Hollo, Z., Homolya, L., Hegedus, T. & Sarkadi, B. Transport properties of the multidrug resistance-associated protein (MRP) in human tumour cells. *FEBS letters* **383**, 99–104 (1996).
29. Homolya, L. *et al.* Fluorescent cellular indicators are extruded by the multidrug resistance protein. *J Biol Chem* **268**, 21493–21496 (1993).
30. Scharenberg, C. W., Harkey, M. A. & Torok-Storb, B. The ABCG2 transporter is an efficient Hoechst 33342 efflux pump and is preferentially expressed by immature human hematopoietic progenitors. *Blood* **99**, 507–512 (2002).
31. Nerada, Z. *et al.* Application of fluorescent dye substrates for functional characterization of ABC multidrug transporters at a single cell level. *Cytometry. Part A: the journal of the International Society for Analytical Cytology* **89**, 826–834, <https://doi.org/10.1002/cyto.a.22931> (2016).
32. Gui, C., Obaidat, A., Chagaturu, R. & Hagenbuch, B. Development of a cell-based high-throughput assay to screen for inhibitors of organic anion transporting polypeptides 1B1 and 1B3. *Current chemical genomics* **4**, 1–8, <https://doi.org/10.2174/1875397301004010001> (2010).
33. De Bruyn, T., Fattah, S., Stieger, B., Augustijns, P. & Annaert, P. Sodium fluorescein is a probe substrate for hepatic drug transport mediated by OATP1B1 and OATP1B3. *Journal of pharmaceutical sciences* **100**, 5018–5030, <https://doi.org/10.1002/jps.22694> (2011).
34. Izumi, S. *et al.* Investigation of Fluorescein Derivatives as Substrates of Organic Anion Transporting Polypeptide (OATP) 1B1 To Develop Sensitive Fluorescence-Based OATP1B1 Inhibition Assays. *Molecular pharmaceutics* **13**, 438–448, <https://doi.org/10.1021/acs.molpharmaceut.5b00664> (2016).
35. Leuthold, S. *et al.* Mechanisms of pH-gradient driven transport mediated by organic anion polypeptide transporters. *Am J Physiol Cell Physiol* **296**, C570–582, <https://doi.org/10.1152/ajpcell.00436.2008> (2009).
36. Patik, I. *et al.* Functional expression of the 11 human Organic Anion Transporting Polypeptides in insect cells reveals that sodium fluorescein is a general OATP substrate. *Biochem Pharmacol* **98**, 649–658, <https://doi.org/10.1016/j.bcp.2015.09.015> (2015).
37. Zhang, J. H., Chung, T. D. & Oldenburg, K. R. A Simple Statistical Parameter for Use in Evaluation and Validation of High Throughput Screening Assays. *Journal of biomolecular screening* **4**, 67–73, <https://doi.org/10.1177/108705719900400206> (1999).
38. Yamaguchi, H. *et al.* Transport of fluorescent chenodeoxycholic acid via the human organic anion transporters OATP1B1 and OATP1B3. *Journal of lipid research* **47**, 1196–1202, <https://doi.org/10.1194/jlr.M500532-JLR200> (2006).
39. Annaert, P., Ye, Z. W., Stieger, B. & Augustijns, P. Interaction of HIV protease inhibitors with OATP1B1, 1B3, and 2B1. *Xenobiotica; the fate of foreign compounds in biological systems* **40**, 163–176, <https://doi.org/10.3109/00498250903509375> (2010).
40. de Waart, D. R. *et al.* Hepatic transport mechanisms of cholyl-L-lysyl-fluorescein. *J Pharmacol Exp Ther* **334**, 78–86, <https://doi.org/10.1124/jpet.110.166991> (2010).
41. Bednarczyk, D. Fluorescence-based assays for the assessment of drug interaction with the human transporters OATP1B1 and OATP1B3. *Analytical biochemistry* **405**, 50–58, <https://doi.org/10.1016/j.ab.2010.06.012> (2010).
42. Kobayashi, D. *et al.* Involvement of human organic anion transporting polypeptide OATP-B (SLC21A9) in pH-dependent transport across intestinal apical membrane. *J Pharmacol Exp Ther* **306**, 703–708, <https://doi.org/10.1124/jpet.103.051300> (2003).
43. Usuda, J. *et al.* Breast cancer resistant protein (BCRP) is a molecular determinant of the outcome of photodynamic therapy (PDT) for centrally located early lung cancer. *Lung cancer* **67**, 198–204, <https://doi.org/10.1016/j.lungcan.2009.04.002> (2010).
44. Karlgren, M. *et al.* Classification of inhibitors of hepatic organic anion transporting polypeptides (OATPs): influence of protein expression on drug-drug interactions. *Journal of medicinal chemistry* **55**, 4740–4763, <https://doi.org/10.1021/jm300212s> (2012).
45. Izumi, S. *et al.* Substrate-dependent inhibition of organic anion transporting polypeptide 1B1: comparative analysis with prototypical probe substrates estradiol-17 β -glucuronide, estrone-3-sulfate, and sulfobromophthalein. *Drug Metab Dispos* **41**, 1859–1866, <https://doi.org/10.1124/dmd.113.052290> (2013).
46. Shirasaka, Y., Mori, T., Shichiri, M., Nakanishi, T. & Tamai, I. Functional pleiotropy of organic anion transporting polypeptide OATP2B1 due to multiple binding sites. *Drug Metab Pharmacokinetic* **27**, 360–364 (2012).
47. Stieger, B. & Hagenbuch, B. Organic anion-transporting polypeptides. *Current topics in membranes* **73**, 205–232, <https://doi.org/10.1016/B978-0-12-800223-0.00005-0> (2014).
48. Roth, M., Timmermann, B. N. & Hagenbuch, B. Interactions of green tea catechins with organic anion-transporting polypeptides. *Drug Metab Dispos* **39**, 920–926, <https://doi.org/10.1124/dmd.110.036640> (2011).
49. Grube, M. *et al.* Modification of OATP2B1-mediated transport by steroid hormones. *Mol Pharmacol* **70**, 1735–1741, <https://doi.org/10.1124/mol.106.026450> (2006).
50. Pizzagalli, F. *et al.* Identification of steroid sulfate transport processes in the human mammary gland. *The Journal of clinical endocrinology and metabolism* **88**, 3902–3912, <https://doi.org/10.1210/jc.2003-030174> (2003).
51. Gal, Z. *et al.* Mutations of the central tyrosines of putative cholesterol recognition amino acid consensus (CRAC) sequences modify folding, activity, and sterol-sensing of the human ABCG2 multidrug transporter. *Biochim Biophys Acta* **1848**, 477–487, <https://doi.org/10.1016/j.bbame.2014.11.006> (2015).
52. Liu, X. *et al.* Generation of mammalian cells stably expressing multiple genes at predetermined levels. *Analytical biochemistry* **280**, 20–28, <https://doi.org/10.1006/abio.2000.4478> (2000).
53. Kolacsek, O. *et al.* Reliable transgene-independent method for determining Sleeping Beauty transposon copy numbers. *Mobile DNA* **2**, 5, <https://doi.org/10.1186/1759-8753-2-5> (2011).

54. Tatrai, P. *et al.* Combined introduction of Bmi-1 and hTERT immortalizes human adipose tissue-derived stromal cells with low risk of transformation. *Biochem Biophys Res Commun* **422**, 28–35, <https://doi.org/10.1016/j.bbrc.2012.04.088> (2012).
55. Kullak-Ublick, G. A. *et al.* Organic anion-transporting polypeptide B (OATP-B) and its functional comparison with three other OATPs of human liver. *Gastroenterology* **120**, 525–533 (2001).
56. De Bruyn, T. *et al.* Confocal imaging with a fluorescent bile acid analogue closely mimicking hepatic taurocholate disposition. *Journal of pharmaceutical sciences* **103**, 1872–1881, <https://doi.org/10.1002/jps.23933> (2014).

Acknowledgements

We greatly appreciate the help of Dr. Bruno Stieger (Department of Clinical Pharmacology and Toxicology, University Hospital, 8091 Zurich, Switzerland) for providing the antibodies against OATPs. This work was supported by the National Research, Development and Innovation Office (OTKA, grant number K 109423) and the Austrian Research Fund (FWF, grant number P 29712). É. B. and C. Ö-L. are recipients of the János Bolyai Fellowship of the Hungarian Academy of Sciences. C. Ö-L. was funded by the MedInProt program, G.S. was supported by the Momentum program of the Hungarian Academy of Sciences.

Author Contributions

Participated in research design: Szakács, Bakos, Özvegy-Laczka. Conducted experiments: Patik, Székely, Német, Bakos. Contributed new reagents or analytic tools: Szepesi, Várady, Kucsma. Performed data analysis: Patik, Özvegy-Laczka. Wrote or contributed to the writing of the manuscript: Szakács, Özvegy-Laczka.

Additional Information

Supplementary information accompanies this paper at <https://doi.org/10.1038/s41598-018-20815-1>.

Competing Interests: The authors declare no competing interests.

Publisher's note: Springer Nature remains neutral with regard to jurisdictional claims in published maps and institutional affiliations.



Open Access This article is licensed under a Creative Commons Attribution 4.0 International License, which permits use, sharing, adaptation, distribution and reproduction in any medium or format, as long as you give appropriate credit to the original author(s) and the source, provide a link to the Creative Commons license, and indicate if changes were made. The images or other third party material in this article are included in the article's Creative Commons license, unless indicated otherwise in a credit line to the material. If material is not included in the article's Creative Commons license and your intended use is not permitted by statutory regulation or exceeds the permitted use, you will need to obtain permission directly from the copyright holder. To view a copy of this license, visit <http://creativecommons.org/licenses/by/4.0/>.

© The Author(s) 2018

RESEARCH ARTICLE

8-acetoxy-trisulfopyrene as the first activatable fluorogenic probe for add-and-read assessment of Organic anion-transporting polypeptides, OATP1B1, OATP1B3, and OATP2B1

Orsolya Ungvári | Laura Király | Éva Bakos | Csilla Özvegy-Laczka 

Institute of Enzymology, RCNS, Eötvös Loránd Research Network, Budapest, Hungary

Correspondence

Csilla Özvegy-Laczka, Institute of Enzymology, RCNS, Eötvös Loránd Research Network, Magyar tudósok krt. 2., H-1117 Budapest, Hungary.
Email: laczka.csilla@ttk.hu

Funding information

National Research Development and Innovation Office, Grant/Award Number: FK 128751

Abstract

Organic anion-transporting polypeptides, OATP1B1, OATP1B3, and OATP2B1 are multispecific membrane proteins mediating the hepatocellular uptake of structurally diverse endo- and exogenous compounds, including various kinds of drugs. Co-administration of OATP1B/2B1 substrates may lead to altered pharmacokinetics or even toxicity. Therefore, the study of the interaction with these OATPs is essential in drug development and is recommended by international regulatory agencies, the FDA, EMA, and PMDA. In general, radiolabeled indicators are used to measure drug interactions of OATPs, and, lately, fluorescent probes are also gaining wider application in OATP tests. However, all of the currently available methods (either radioactive or fluorescence-based) comprise multiple steps, including the removal of the indicator in the end of the experiment. Hence, they are not ideally suited for high-throughput screening. In the current study, in order to find an indicator allowing real-time assessment of hepatic OATP function, we searched for an activatable fluorogenic OATP substrate. Here, we show that 8-acetoxypyrene-1,3,6-trisulfonate (Ace), a fluorogenic derivative of the hepatic OATP substrate pyranine (8-hydroxypyrene-1,3,6-trisulfonate) enters the cells via OATP1B1/3 or OATP2B1 function. In living cells, Ace is then converted into highly fluorescent pyranine, allowing “no-wash” measurement of OATP function and drug interactions. Furthermore, we demonstrate that Ace can be used in an indirect assay termed as competitive counterflow suitable to distinguish between transported substrates and inhibitors of OATP1B1. The fluorescence-based methods described here are unique and open the way toward high-throughput screening of interactions between new molecular entities and OATPs.

Abbreviations: ABC, ATP Binding Cassette; Ace, 8-acetoxypyrene-1,3,6-trisulfonate; BSP, bromosulfophthalein; CAM, calcein acetoxy-methylester; CCF, competitive counterflow; CsA, cyclosporine A; E1S, estrone-3-sulfate; EMA, the European Medicines Agency; FDA, the US Food and Drug Administration; HTS, high-throughput screening; NME, new molecular entity; OATP, Organic anion-transporting polypeptide; PFA, paraformaldehyde; PMDA, Pharmaceuticals and Medical Devices Agency, Japan.

This is an open access article under the terms of the Creative Commons Attribution-NonCommercial-NoDerivs License, which permits use and distribution in any medium, provided the original work is properly cited, the use is non-commercial and no modifications or adaptations are made.

© 2021 The Authors. *The FASEB Journal* published by Wiley Periodicals LLC on behalf of Federation of American Societies for Experimental Biology

KEYWORDS

activatable fluorogenic substrate, competitive counterflow, drug interaction, hepatic OATP

1 | INTRODUCTION

Cellular entry of most drugs is governed by Solute Carriers (SLC) of which Organic anion-transporting polypeptides (OATPs) have a renowned role.^{1,2} OATPs (encoded by the SLCO genes) are exchangers of organic solutes that mediate the cellular uptake of bile salts, bilirubin, thyroid, and sex hormones.³ In addition, multispecific members of the OATP family, OATPs, 1A2, 1B1, 1B3, and 2B1 also facilitate cellular entry of various clinically applied drugs, including statins, antivirals, anti-hypertensives and chemotherapeutic agents, as well as certain food components.^{3,4} Of the multispecific OATPs particularly OATP1B1 and OATP1B3 have been extensively investigated, since they are key uptake transporters involved in hepatic detoxification.^{5,6} On the other hand, OATP1A2 and OATP2B1 are gaining increasing interest, since they promote intestinal absorption, hepatic elimination or blood to brain entry of drugs.^{3,7,8} Consequently, inhibition of OATP function due to mutations or by the co-administration of their substrates/inhibitors may lead to altered pharmacokinetics and unexpected side effects.^{9–11} Hence, according to international regulations (released by FDA, the US Food and Drug Administration; EMA, the European Medicines Agency; or PMDA, Pharmaceuticals and Medical Devices Agency, Japan), these OATPs, especially OATP1B1/3 should be investigated during drug development that requires sensitive and reliable assays.

Radioactively labeled substrates, such as bromosulfophthalein, leukotriene C₄, dehydroepiandrosterone sulfate (DHEAS), estrone-3-sulfate (E1S), or estradiol-17 β -D-glucuronide have been repeatedly used in such assays.^{12–15} However, in general, a limitation of the radioligand-based transport assays is the cost associated with the radiolabeling of the substrates. In addition, LC-MS (liquid chromatography-mass spectrometry) is also a frequently applied method to assess OATP function and OATP drug interactions.^{16,17} Fluorescence-based methods offer a cost-effective alternative, and it was shown by various laboratories that fluorescent probe substrates provide an effective and sensitive means to investigate OATP function and drug-transporter interactions.^{18–21} However, all the probes (either radioactive or fluorescent) identified so far require the removal of the probe after the transport reaction in order to get rid of the excess substrate that was not transported into the cells by OATPs. Therefore, the previously developed methods for OATPs are not ideally suited for a high-throughput screen (HTS). A fluorogenic indicator/

probe having two distinguishable forms, one outside and one inside the cell would spare the final washing step and hence simplify the transporter assay. As an example, the most frequently used activatable fluorogenic probe of transporters is the ABC (ATP Binding Cassette) transporter P-glycoprotein substrate calcein acetoxymethyl ester (Calcein-AM, CAM).²² CAM is a membrane permeable non-fluorescent compound rapidly entering the cells by passive diffusion and becoming fluorescent when cleaved by esterases. However, CAM and/or calcein is recognized and extruded from the cells by ABC transporters' ABCB1 (P-gp, P-glycoprotein) and ABCC1/2 (MRP1/2, multidrug resistance associated protein 1/2) function,^{22,23} and hence allows the investigation of these transporters in a high-throughput set up.^{24,25} Although MRP2 and OATPs, 1B1/3 and 2B1 possess numerous common substrates, CAM is not suited for the measurement of OATP function owing to its high-rate passive cellular uptake.

Previously, we identified various cell impermeable sulfonated pyrene-based dyes, pyranine (8-hydroxy pyrene-1,3,6-trisulfonate), Cascade Blue hydrazide (3,6,8-trisulfo-1-pyrenyl)oxy-, 1-hydrazide, trisodium salt), and Alexa Fluor 405 (succinimidooxycarbonylpiperidino)ethoxy]pyrene-1,3,6-trisulfonic acid) as substrates of OATPs, 1B1/3 and 2B1.^{19,26} Here, we looked for further pyrene analogs, with special interest in 8-acetoxypyrene-1,3,6-trisulfonate as potential substrate(s) of multippecific OATPs. 8-acetoxypyrene-1,3,6-trisulfonate, which we further term as Ace, is a fluorogenic compound that similar to CAM becomes fluorescent upon entering a cell and cleaved by intracellular esterases. However, in contrast to CAM, Ace is cell impermeable,²⁷ therefore represents a promising candidate indicator of OATP function.

Besides the determination of the interaction between a new molecular entity (NME) with OATPs, it is often required to ascertain whether the investigated NME can be enriched in the cells by OATP function. However, the indirect assays used for transporter (OATP) investigations do not necessarily distinguish between inhibitors and transported substrates. Recently, an indirect assay, termed as competitive counterflow (CCF) was developed for OATPs, 2B1 and 1A2.^{28,29} The novelty of this method compared to previous indirect assays is that CCF can discriminate substrates and non-transported inhibitors. However, the method developed by Schaefer and colleagues applies a radioactive indicator, and a CCF (either radioactive or fluorescence-based) is not yet available for the major hepatic OATP, 1B1.

Therefore, in the current study besides aiming to find an activatable fluorogenic probe for hepatic OATPs, we also investigated the applicability of Ace to be used in a CCF assay.

2 | MATERIALS AND METHODS

2.1 | Materials

Pyranine, pyrene, 1-pyrenesulfonic acid, 6,8-dihydroxy-1,3-pyrenedisulfonic acid, 1,3,6,8-pyrenetetrasulfonic acid, and all other materials, if not indicated otherwise were purchased from Sigma, Merck (St. Louis, MO, US). 8-acetoxy-1, 3, 6 pyrenetrisulfonic acid was bought from VWR International (Radnor, PA, US).

2.2 | Cell lines

A431 (ATCC), HEK-293 (ATCC), or MDCKII (ATCC) cells overexpressing OATPs, 1A2, 1B1/3 or 2B1, or mock transfected controls were generated previously as described in Refs. 19,26,30. Cell lines were cultured in DMEM (Gibco, Thermo Fischer Scientific, Waltham, MA, US) supplemented with 10% fetal calf serum, 100 U/ml penicillin, and 100 μ g/ml streptomycin at 37°C, 5% CO₂. Cells were used up to 20 passages.

2.3 | Measurement of dye uptake in a “classical” mode

A431 or MDCKII cells (8×10^4 /well) were seeded on 96-well plates (Eppendorf AG, Hamburg, Germany) in 200 μ l DMEM one day prior to the transport measurement. Next day the medium was removed, and the cells were washed three times at room temperature with 1 \times Phosphate Buffered Saline (PBS). The cells were preincubated with 50 μ l uptake buffer (125 mM NaCl, 4.8 mM KCl, 1.2 mM CaCl₂, 1.2 mM KH₂PO₄, 12 mM MgSO₄, 25 mM MES, and 5.6 mM glucose, with the pH adjusted to 5.5 using 1 M HEPES and 10 N NaOH, pH 5.5 or pH 7.4) at 37°C. The reaction was started by the addition of 50 μ l uptake buffer containing pyranine, pyrene, 1-pyrenesulfonic acid, 6,8-dihydroxy-1,3-pyrenedisulfonic acid, 1,3,6,8-pyrenetetrasulfonic acid, or 8-acetoxypyrene-1, 3, 6-trisulfonate in a final concentration of 20 μ M. After 30 min of incubation at 37°C the reaction was stopped by removing the supernatant and washing the cells three times with ice-cold 1 \times PBS. Finally, 200 μ l 1 \times PBS was added to each well and the fluorescence was determined using an Enspire plate

reader. Ex/Em wavelengths were the following: pyranine: 460/510 nm, pyrene: 365/476 nm, 1-pyrenesulfonic acid: 347/378 nm, 6,8-dihydroxy-1,3-pyrenedisulfonic acid: 460/510 nm, 1,3,6,8-pyrenetetrasulfonic acid: 353/406 nm, and 8-acetoxy-1, 3, 6 pyrenetrisulfonic acid: 460/510 nm. Bottom reading was applied with two horizontal (X) and two vertical (Y) points, measurement height was 3 mm with 200 flashes.

Transport activity was determined as the difference between fluorescence in mock transfected controls and in OATP expressing cells. Where applicable transport was calculated based on a calibration curve.

2.3.1 | Inhibitor tests in a “classical” uptake assay

When the effect of inhibitors was tested, the transport measurement on A431-OATP cells seeded on 96-well plates was started with a 5 min preincubation at 37°C in 50 μ l uptake buffer pH 5.5 containing increasing concentrations of the tested compounds (BSP: bromosulphophthalein, CsA: cyclosporine A, benzbromarone or E1S: estrone-3 sulfate) or 0.5% PFA (paraformaldehyde) as a reference inhibitor. Transport reaction was started with the addition of the dye substrate in 50 μ l 5–20 μ M final concentration as indicated on Figure 4 legend. After 15 min (OATP1B1 and OATP2B1) or 30 min (OATP1B3) incubation at 37°C the supernatant was removed, and each well was washed three times with PBS. Fluorescence was detected as described above. Inhibition was calculated by comparing fluorescence in the presence of the investigated inhibitor to the fluorescence with the dye alone (set as 100%).

All experiments were repeated in at least three biological replicates derived from different cell passages.

2.4 | Dye uptake in “no-wash” mode

A431 cells overexpressing OATPs or mock control were prepared as described at 2.3.

After 5 min of incubation at 37°C with 50 μ l uptake buffer pH 5.5 or pH 7.4 with or without increasing concentrations of the OATP-interacting compounds (BSP, CsA, E1S) and after another 10 (OATP1B1/2B1) or 20 (OATP1B3) min incubation with the 8-acetoxypyrene-1, 3, 6-trisulfonate the fluorescence was measured without removing the supernatant in an Enspire fluorescent plate reader at Ex/Em 460/510 nm wavelength. Bottom reading was applied with two horizontal (X) and two vertical (Y) points, measurement height was 3 mm with 200 flashes.

2.5 | Counterflow assay

A431 cells expressing OATP1B1, OATP1B3, or OATP2B1 and mock transfected control were seeded on 96-well plates in 200 μ l DMEM 16–24 h prior to the measurement. Next day, the medium was removed and the cells were washed three times with 1 \times PBS at room temperature. The cells were loaded with 5 μ M (OATP1B1/2B1) or 20 μ M (OATP1B3) 8-acetoxypyrene-1,3,6-trisulfonate in a final volume of 100 μ l, pH 5.5 uptake buffer by incubation at 37°C for 15 min (OATP1B1), 30 min (OATP1B3), or 10 min (OATP2B1). According to our measurements, dye uptake reaches its equilibrium (influx and efflux rate of the dye and its metabolite are equal) at 15 min (OATP1B1) or 10 min (OATP2B1) and stays stable for further 20 min. However, as it can be seen on Figure 5, in the case of OATP1B3, dye uptake did not reach a steady state. In order to control loading of the cells, fluorescence was measured after 10 or 15 min of incubation at Ex/Em 460/510 nm in an Enspire fluorescence plate reader.

In the counterflow phase of the experiment, the supernatant was removed and 5 μ M (OATP1B1/2B1) or 20 μ M (OATP1B3) 8-acetoxypyrene-1,3,6-trisulfonate in 100 μ l, pH 5.5 with or without the tested compounds, BSP, benzbromarone, CsA or E1S in increasing concentrations or 0.5% PFA was added. The plates were incubated for 20 min at 37°C. To stop the reaction the supernatant was removed, and the cells were washed with 200 μ l ice-cold PBS three times. Finally, PBS was removed and 200 μ l 0.1 N NaOH was added to each well to equalize the pH. After further 20 min incubation at room temperature fluorescence was measured at Ex/Em 460/510 nm. The level of intracellular dye was calculated by comparison of fluorescence to the control samples incubated with Ace alone (set as 100%). Experiments were repeated in at least three biological replicates. Average \pm SD values are shown.

2.6 | Efflux assay

Efflux was performed the same way as the counterflow with the exception that in the second phase of the experiment (after preloading the cells to equilibrium) A431-OATP1B1, OATP1B3, or OATP2B1 (or mock control) cells were incubated in uptake buffer (20 min) with or without the presence of the investigated compounds (increasing concentrations of benzbromarone, BSP, CsA, E1S or 0.5% PFA). Fluorescence was measured at Ex/Em 460/510 nm. The level of intracellular dye was calculated by comparison of fluorescence to the preloaded control samples incubated with Ace alone, set as 100%. Experiments were repeated in at least three biological replicates. Average \pm SD values are shown.

2.7 | Data analysis and statistics

All experiments were performed in at least three biological replicates. Average \pm SD values are shown. IC₅₀ values were calculated by Hill1 fit using Origin software (version 2018, OriginLab Corporation, Northampton, MA, US).

z -factor was calculated as follows:
 $1 - ((3 \times SD_{\text{negative control}} + 3 \times SD_{\text{positive control}}) / (I_{\text{Mean positive control}} - \text{Mean}_{\text{negative control}}))$.³¹

3 | RESULTS

3.1 | Mono-, di-, and/or trisulfoxyrenes are substrates of multispecific OATPs

Previously, we found that various sulfoxyrenes, encompassing pyranine (8-hydroxyxyrene, 1,3,6-trisulfonate, HPTS, Solvent Green 7), Cascade Blue hydrazide, and Alexa Fluor 405 are transported substrates of OATPs, 1B1, 1B3, and 2B1, and are applicable to search for molecules interacting with these transporters.^{19,26,32} In order to test, whether additional sulfoxyrenes are also transported by these multispecific OATPs, and to determine which moieties in the sulfoxyrene structure are important determinants in the recognition by OATPs, further pyrene-based dyes (Figure 1) were tested. Since the list of commercially available pyrene-based compounds is inexhaustible, we chose compounds with only minor modifications compared to pyranine. We were especially interested in the role of the sulfonate moiety, since sulfonated compounds are enriched among compounds interacting with hepatic OATPs.³³ The other criterion was intrinsic or activatable (Ace) fluorescence of the compounds in order to ensure direct transport measurements.

In these tests A431 cell lines overexpressing human OATP1A2, OATP1B1, OATP1B3, or OATP2B1, and their mock transfected controls^{19,30} were applied. Potential OATP-mediated cellular uptake of the dyes was followed based on the measurement of intracellular fluorescence. Uptake was investigated both at pH 5.5 and pH 7.4, since pH-dependence of OATP-mediated uptake can vary based on the transported substrate.^{30,34,35} Expression and function of OATPs was continuously monitored by measuring the transport of known substrates, pyranine (OATPs, 1B1, 1B3, and 2B1) or sulforhodamine 101 (SR101, OATP1A2).^{26,34} Figure 2 shows that pyrene and 1,3,6,8-pyrenetetrasulfonic acid were not transported by any of the OATPs investigated (OATP1B1, OATP1B3, OATP2B1, or OATP1A2). 1-pyrenesulfonic acid was exclusively transported by OATP1A2 making it a potential specific probe to

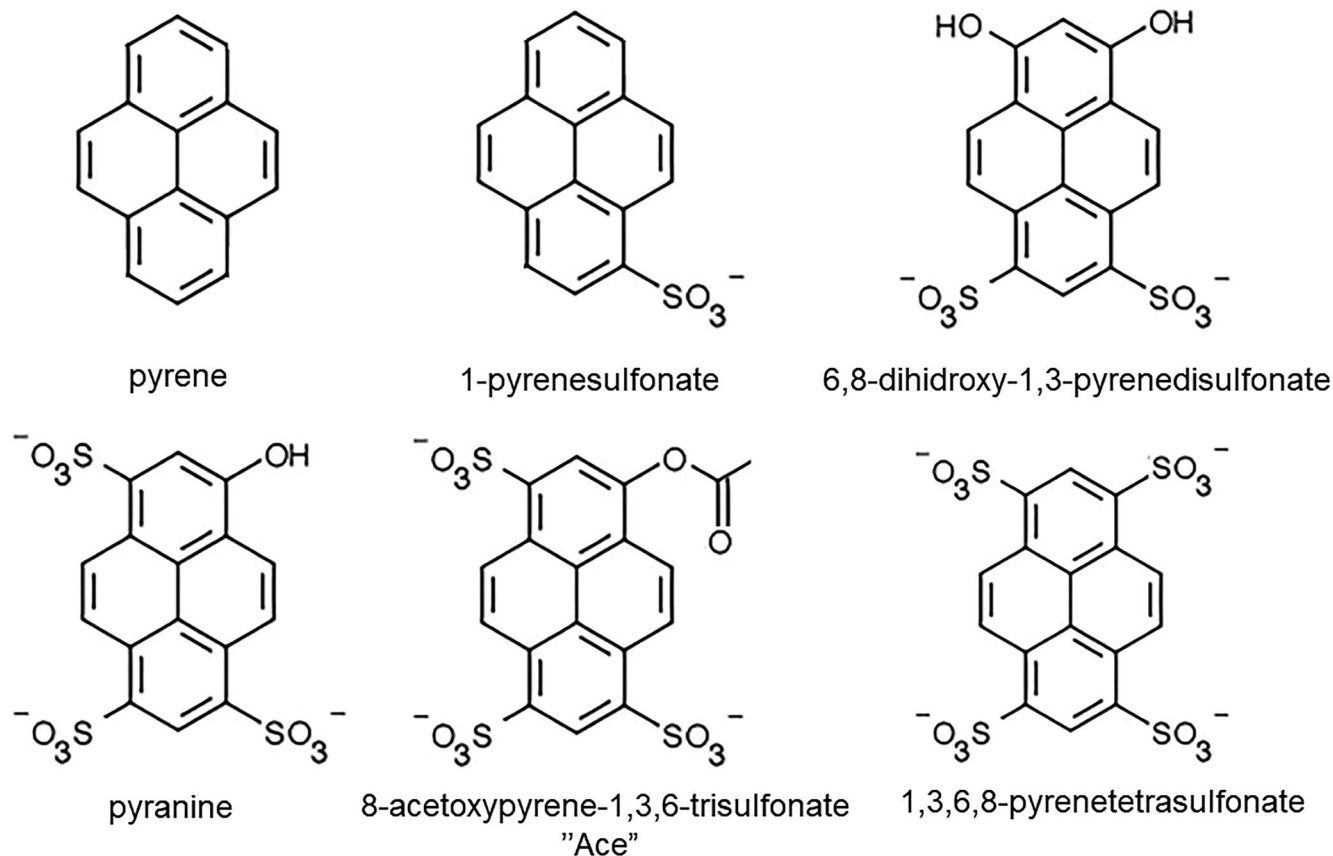


FIGURE 1 Structure of the dyes tested

distinguish OATP1A2 function. However, compared to the previously identified fluorescent OATP1A2 substrate, SR101 (a 17-fold uptake measured on the same cell line, see Figure S1), uptake of 1-pyrenesulfonic acid was negligible (3-fold uptake). 6,8-dihydroxy-1,3-pyrenedisulfonic acid was transported by all four multispecific OATPs, while pyranine and 8-acetoxy-1,3,6-pyrenetrisulfonic acid (further termed as Ace) were transported only by OATPs, 1B1, 1B3, and 2B1. OATP-specific uptake of all of the positive hit dyes was also confirmed by inhibition of their uptake by BSP a well-documented general OATP inhibitor (Figures 3 and 4 or Figure S1).

Concerning pH sensitivity, dye uptake by OATPs, 1A2 and 2B1 showed strong pH-dependence with significantly higher uptake observed in buffer pH 5.5 compared to pH 7.4 (Figure 2). In the case of OATP1B1, transport was also higher at pH_{EC} 5.5 compared to pH_{EC} 7.4, with the exception of 6,8-dihydroxy-1,3-pyrenedisulfonic acid of which OATP1B1-mediated transport was similar at both pH. Transport of pyranine and Ace by OATP1B3 was independent of pH_{EC} (at least at the conditions tested here), while uptake of 6,8-dihydroxy-1,3-pyrenedisulfonic acid was higher at pH_{EC} 7.4 compared to pH_{EC} 5.5 (Figure 2).

3.2 | Real time detection of OATP-function and drug interactions based on measuring cellular uptake of 8-acetoxypyrene-1,3,6-trisulfonate (Ace)

Ace is a fluorogenic compound converted to fluorescent pyranine by (intracellular) esterases (<https://www.sigmaaldrich.com/catalog/product/sigma/a3332?lang=hu®ion=HU>). Accordingly, as it is shown on Figure 3A (and Figure S2), in a cell/enzyme free environment Ace has negligible fluorescence compared to pyranine. Moreover, there is a 20-fold increase of fluorescence (Ex/Em: 460/510) of both Ace and pyranine at $\text{pH} > 7$ compared to pH 5.5 (see Ref. 36 and Figure S2) hence pyranine is used as a pH indicator. Therefore, we hypothesized that extracellular Ace (added in a buffer with pH 5.5) and its intracellular metabolite pyranine (neutral pH inside the cell) can be distinguished by measuring fluorescence, and hence OATP1B1/2B1 function in living cells can be monitored without the need to remove excess Ace in the end of the transport measurement. Indeed, in real-time experiments (Ace continuously present throughout the measurement) we detected a dramatic, concentration-dependent increase of fluorescence in OATP1B1/2B1 overexpressing cells and a modest but still well-detectable

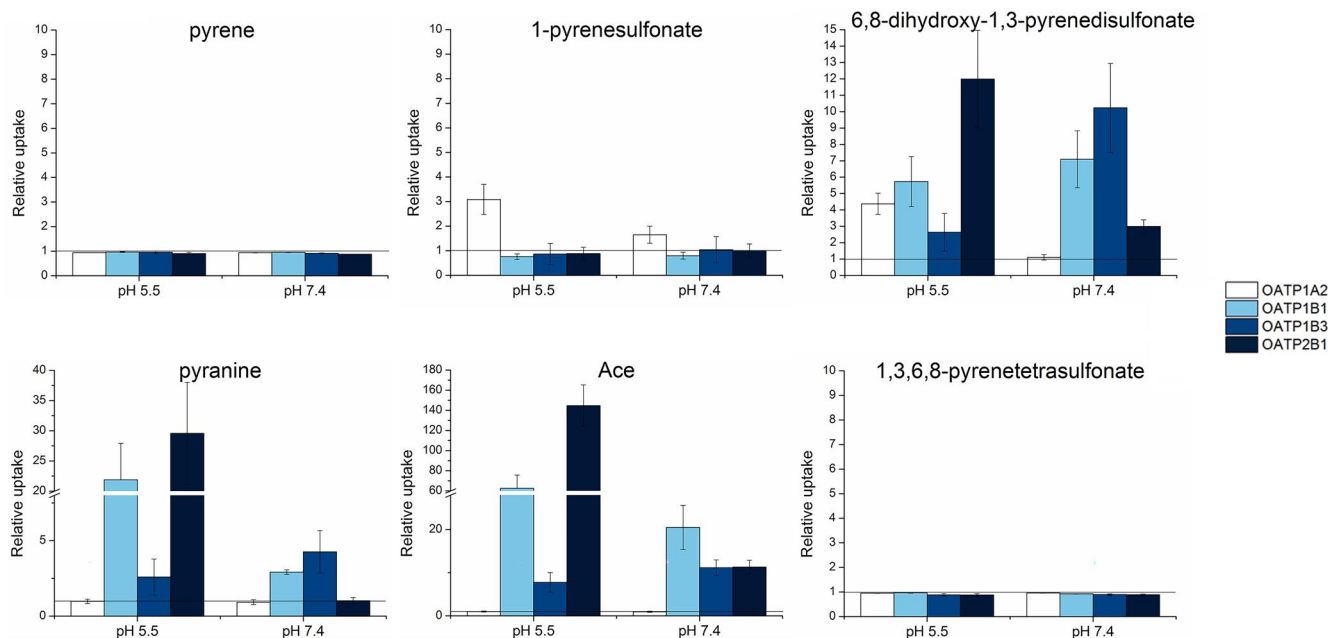


FIGURE 2 Dye uptake in A431 cells expressing human OATPs. A431 cells seeded on 96-well plates were incubated with 20 μ M dye for 30 min at pH 5.5 or pH 7.4. Cellular fluorescence was measured in an Enspire fluorescence plate reader. Relative uptake was determined by dividing fluorescence in OATP-expressing cells with that measured in A431 mock cells (relative uptake 1 meaning no OATP-specific transport). Experiments were performed in three independent measurements with three replicates in each individual experiment, average \pm SD are shown

rise of fluorescence in A431-OATP1B3 cells compared to Ace in a cell-free environment (Figure 3A,B–E). Moreover, in mock transfected control cells, practically no fluorescence was detected up to 30 min. To further prove OATP-mediated Ace uptake, we demonstrate that Ace uptake could be completely blocked by the addition of the known OATP interacting molecule, bromosulphophthalein (BSP) (Figure 3C–E). All these indicate that Ace can potentially be used to measure OATP1B/2B1 substrate/inhibitor interactions without the need to remove the dye in the end of the experiments and hence allowing real-time monitoring of OATP1B/2B1 function.

Interestingly, and emphasizing the need for using an acidic buffer in real-time Ace uptake measurements, we found that although Ace is also transported by OATP1Bs and OATP2B1 at pH 7.4 (see Figure 2 showing Ace transport in a “classical” uptake assay), this condition is not ideally suited for real-time transport measurements. Figure 3F–H shows that when Ace uptake is performed at pH 7.4 fluorescence also increases in A431 mock control cells, and hence transport (though negligible compared to that measured at pH 5.5) could only be detected for OATP1B1.

In order to validate the real-time uptake assay based on the accumulation of Ace (at pH 5.5), we performed detailed transport inhibition experiments using three well-described OATP interacting molecules, BSP, CsA, and E1S. Inhibition of the transport of pyranine and Ace were measured in a “classical” uptake assay (removing excess

dye in the end of the experiment) and Ace uptake was also monitored in a “no-wash” mode. The inhibition data obtained in these three different assays (pyranine, Ace in “classical” and “no-wash” set up) are shown on Figure 4 and IC_{50} values are summarized on Table 1.

Based on the inhibition obtained with pyranine and Ace at two different conditions, and compared to literature data (Table 1), we conclude that these dyes are equally reliable OATP1B and OATP2B1 probes. Although in the case of OATP1B1, pyranine and Ace uptake were less sensitive to inhibition by E1S compared to literature data. In addition, IC_{50} values for BSP and E1S were slightly increased when Ace was used as an OATP1B1 or OATP2B1 probe compared to data obtained with pyranine. These differences may be explained by slightly different binding sites involved in the interaction with the hydroxyl or acetoxy group of pyranine or Ace. Still, our results indicate that Ace is a reliable probe, and the real-time assay based on Ace uptake is the first “no-wash” assay for OATP1B1, OATP1B3, and OATP2B1.

3.3 | A competitive counterflow assay (CCF) based on the OATP1B1/2B1-mediated transport of Ace

Indirect assays can provide a cost-effective means of determining OATP inhibitors. Recently, an indirect method

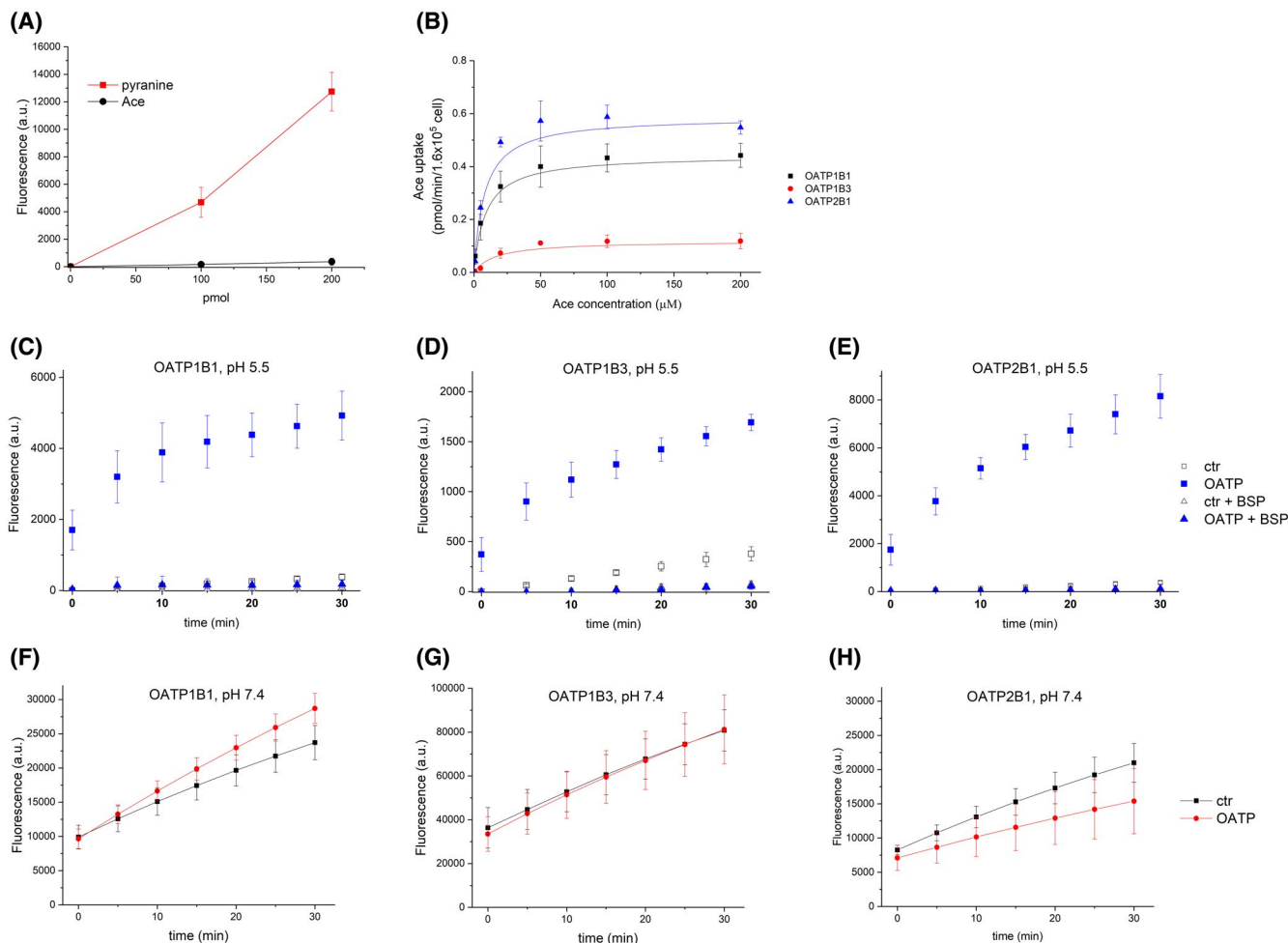


FIGURE 3 Real time measurement of Ace accumulation in A431 cells overexpressing OATP1B1, OATP1B3, or OATP2B1. (A) Fluorescence of Ace and pyranine in a cell free milieu. Fluorescence of 100 and 200 pmol pyranine or Ace in buffer pH 5.5 was measured in an Enspire fluorescence plate reader. (B) Concentration-dependent uptake of Ace in A431-OATP cells. A431 cells were incubated with 5–200 μM Ace in buffer pH 5.5 at 37°C for 15 min, after which fluorescence was measured without washing the cells at Ex/Em: 460/510 nm. (C–E) Ace accumulation in A431-OATP cells at pH 5.5 with or without 10 μM bromosulphophtalein (BSP) or (F–H) pH 7.4. Cell were incubated with 5 μM (OATP1B1, OATP2B1) or 20 μM (OATP1B3) Ace in buffer pH 5.5 or pH 7.4 at 37°C. Fluorescence was continuously monitored without washing (and removing excess Ace) at Ex/Em: 460/510 nm. Data points show average \pm SD obtained from at least three biological replicates

discriminating non-transported inhibitors and transported substrates of OCT2³⁷ has been developed. Later this method was successfully applied for OATPs, 1A2 and 2B1 as well.^{28,29} The basis of the method termed as competitive counterflow (CCF)³⁷ is that OCT2, and also OATPs, work as exchangers, therefore two of their substrates can be swapped. CCF comprises of two consecutive steps. First, cells are preloaded with the indicator substrate (radioactive E1S was used in the case of OATPs, 1A2 and 2B1) until an equilibrium is reached. Then the indicator substrate is quickly removed, and in the second step the cells are further exposed to the same amount of the indicator together with or without the compound of interest. If the indicator and the tested compound share the same transport mechanism, then the tested compound

added in high enough amounts (10-fold of the IC₅₀) will be transported into the cells resulting in a net efflux and a decrease in the signal of the indicator. On the other hand, non-transported inhibitors will block the efflux and there will be no change in the signal in the CCF.

Since Ace performed well in our experiments, we tested its applicability in a CCF mode. In these experiments, cells were first preloaded with Ace until equilibrium, and then Ace or Ace together with a known OATP1B/2B1 substrate, E1S³⁸ was added to the cells and the potential exchange was monitored based on cellular fluorescence. Figure 5 shows that in the case of OATP1B1 and OATP2B1, the fluorescent signal remained unaltered when the cells were exposed to Ace alone, and co-administration of E1S resulted in a significant (>50%), time-dependent decrease

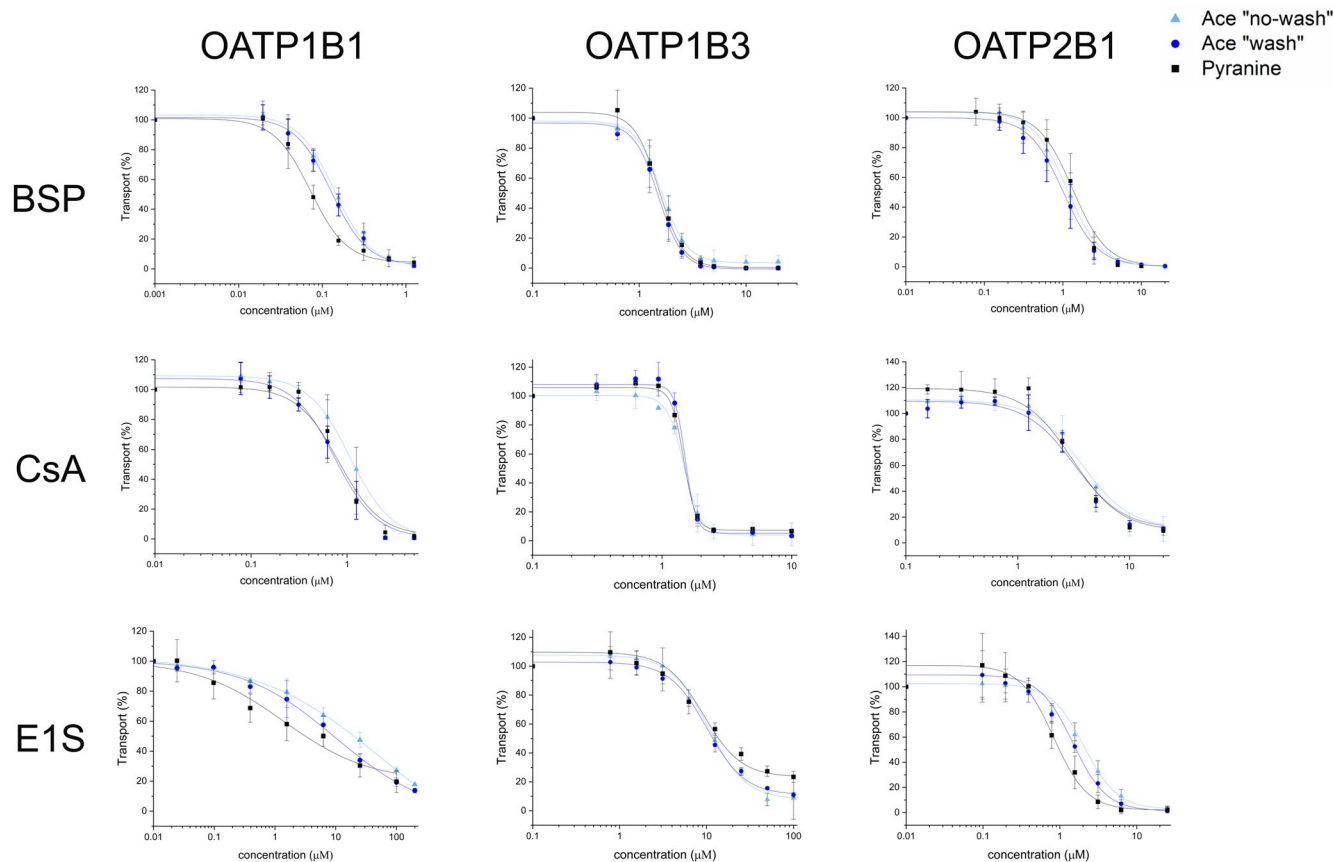


FIGURE 4 Comparison of the pyranine- and Ace-based assays. A431 cell overexpressing OATP1B1, OATP1B3, or OATP2B1, or mock controls were incubated with 10 μM (or 20 μM , OATP1B3 and OATP2B1) pyranine or 5 μM (OATP1B1, OATP2B1) or 20 μM (OATP1B3) Ace at 37°C for 10–15 min or (20–30 min, OATP1B3) in the presence of BSP, CsA, or E1S on microplates. Fluorescence at Ex/Em: 460/510 nm was measured in an Enspire fluorescence plate reader before (Ace “no-wash”) or after (pyranine and Ace “wash”) removing excess dye. Experiments were performed in three biological replicates, average \pm SD are shown

in fluorescence. All of these indicated that Ace (or more precisely its intracellularly formed metabolite pyranine) can be exchanged to the OATP1B1/2B1 substrate E1S. As a further proof, we also investigated dye efflux. In these experiments, after equilibrium, Ace was removed, and the cells were further incubated in a dye-free transport buffer with or without E1S. Figure 5 shows that pyranine was efficiently exported from the cells and this process was not inhibited by the presence of the substrate E1S. In the case of OATP1B3, the fluorescent signal increased continuously throughout the CCF phase, indicating that transport did not reach its equilibrium even after 60 min of incubation (or due to yet undefined factors), therefore Ace cannot be applied to study OATP1B3 in the CCF. Also, efflux was significantly lower in the case of OATP1B3 compared to OATPs, 1B1 or 2B1.

After these “proof-of-concept” experiments, we performed testing of additional known OATP-interacting molecules, CsA, BSP, and benzbromarone in a wide concentration range parallel in uptake, efflux, and CCF for OATP1B1. Complete blockage of OATP1B1 function was

reached by fixing the cells with 0.5% PFA. Since fluorescence excitation of Ace and pyranine is pH sensitive, in the end of these experiments the supernatant was removed, and the cells were treated with 0.1 N NaOH to guarantee that any potential alterations in the intracellular pH do not interfere with the observed signal. Figure 6 shows, that as expected, all of the documented OATP-interacting molecules inhibited Ace uptake. Reported substrates, BSP and E1S resulted in a concentration-dependent decrease of the signal in the CCF mode, while did not interfere with efflux even at the highest concentrations tested. However, blocking OATP1B1 function by PFA fixation inhibited efflux both in the CCF and efflux set-up, regardless of the presence of E1S or BSP. CsA and benzbromarone are known inhibitors of OATP1B1 function,^{11,39} however, their direct, OATP-mediated transport has not yet been investigated. Here, we found that CsA resulted in a concentration dependent decrease of the signal in the CCF assay and did not inhibit efflux, indicating that it may be a competitive inhibitor (substrate). On the other hand, benzbromarone inhibited both uptake and efflux in a

TABLE 1 Comparison of the inhibition data obtained with various assays

		IC ₅₀ ± SD values (μM)			
		BSP	CsA	E1S	z-factor
OATP1B1	Pyranine	0.07 ± 0.006	0.86 ± 0.015	4.44 ± 0.20	0.58
	Ace “no-wash”	0.14 ± 0.008	1.0 ± 0.078	11.44 ± 2.61	0.63
	Ace “wash”	0.13 ± 0.007	0.86 ± 0.015	9.13 ± 2.28	0.75
	Literature data	0.1	0.1–1.0	0.05–0.22	n.a.
	Relative IC ₅₀ values	0.54	1.00	0.48	
OATP1B3	Pyranine	1.53 ± 0.045	1.47 ± 0.037	9.81 ± 1.22	0.7
	Ace “no-wash”	1.62 ± 0.028	1.47 ± 0.029	10.00 ± 0.24	0.3
	Ace “wash”	1.51 ± 0.041	1.51 ± 0.055	10.06 ± 0.46	0.74
	Literature data	0.4	0.2–1.2	9.5–20	n.a.
	Relative IC ₅₀ values	0.99	0.97	0.98	
OATP2B1	Pyranine	1.35 ± 0.065	3.12 ± 0.16	0.85 ± 0.07	0.64
	Ace “no-wash”	1.05 ± 0.064	3.93 ± 0.073	1.64 ± 0.29	0.68
	Ace “wash”	0.93 ± 0.091	3.24 ± 0.12	1.40 ± 0.056	0.79
	Literature data	1.2	1.45–36	0.5	n.a.
	Relative IC ₅₀ values	1.45	0.96	0.61	

Note: Inhibition of pyranine or Ace was determined in A431-OATP or mock control cells as described at Figure 4. When applying Ace, fluorescence was determined both before (“no-wash”) and after (“wash”) removing excess dye in the end of the experiment. IC₅₀ values were calculated by Hill1 fit using Origin software (version 2018, OriginLab Corporation, Northampton, MA, US). z-factor was calculated as according to Ref. 31. n = 3, average ± SD are shown. Literature data can be found in Refs. 19,39,50,51. Relative IC₅₀ values stand for the comparison of inhibition obtained with pyranine and Ace (IC₅₀ pyranine/IC₅₀ Ace).

concentration-dependent manner, while did not influence the signal in the CCF. Hence, benzbromarone is a non-transported OATP1B1 inhibitor.

4 | DISCUSSION

According to the regulations by FDA, EMA, and PMDA, NMEs supposed to be eliminated from the human body through hepatic clearance should be investigated for interaction with certain liver transporters, including OATP1B1 and OATP1B3.^{40–43} In addition, there is increasing evidence that OATP1A2 and OATP2B1 are also important determinants of pharmacokinetics and should be considered for investigation during drug development.^{44,45} Consequently, numerous radioligand- and fluorescence-based methods have been developed to investigate these multispecific OATPs.^{12–15,18–21} However, neither of these probes allow a simple, add-and-read method for OATP drug interaction tests because at the end of the assay the removal of the probe is required.

Fluorogenic probes of transporters having two distinguishable, extracellular and intracellular forms are ideally suited for a real-time, “no-wash” assessment of

transporter function. As an example, fluorogenic CAM was developed into a sensitive and widely applied probe allowing real-time and no-wash investigation of the ABC drug transporters, P-glycoprotein, and MRP1/2.^{24,25} Acetoxy modification of fluorophores masks fluorescence and issues in fluorogenic compounds.⁴⁶ Therefore, in search of a “no-wash” probe we looked for an acetoxy analog of a known OATP substrate, pyranine. Pyranine, a trisulfopyrene dye is a recently identified cell impermeable and highly fluorescent probe of OATPs, 1B1/3 and 2B1.²⁶ Moreover, we found previously that Cascade Blue hydrazide and Alexa Fluor 405 differing from pyranine only at the modification on the 8th carbon (C-8) of the pyrene structure, are also transported substrates OATP1B1.¹⁹ Therefore, we hypothesized that Ace, differing from pyranine only in a C-8 acetoxy modification (Figure 1), will not disrupt recognition by OATPs, 1B1/3 and 2B1. Indeed, we found a well-detectable transport of Ace in A431 cells expressing OATP1B1/3 or OATP2B1 (Figure 2), but not that in A431-OATP1A2 cells. Moreover, based on their affinity, pyranine (as determined earlier in Ref. 26) and Ace are equally good substrates of these OATPs (the affinity of hepatic OATPs toward these two compounds is the following: OATP1B1

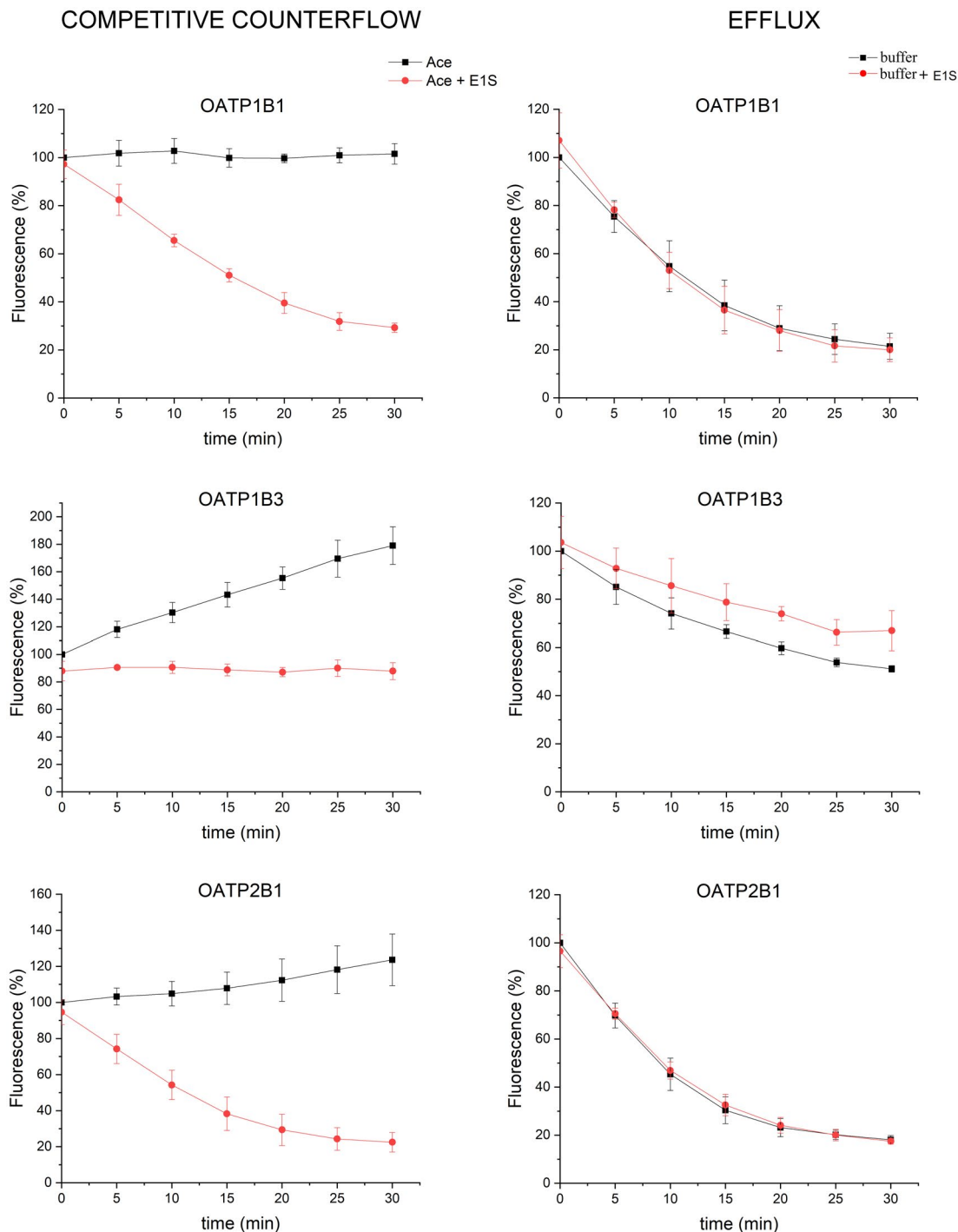


FIGURE 5 Ace is a suitable probe to be applied in a competitive counterflow (CCF) or efflux assay. A431-OATP1B1, OATP1B3, or OATP2B1 cells were loaded with 5 μ M (or 20 μ M, OATP1B3) Ace 100 μ l/well for 10 min (OATP2B1), 15 min (OATP1B1), or 30 min (OATP1B3) and after removing the supernatant the cells were further incubated with 5 μ M (or 20 μ M, OATP1B3) Ace 100 μ l/well or buffer with or without 50 μ M E1S. Fluorescence (Ex/Em: 460/510 nm) was continuously monitored (without washing the cells) in an EnSpire plate reader. Experiments were repeated in three biological replicates, average \pm SD are shown

Km pyranine: 27.8 μ M, Km Ace: 17.6 μ M; OATP1B3 Km pyranine: 92.2 μ M, Km Ace: 61.4 μ M; OATP2B1 Km pyranine: 65.6 μ M, Km Ace: 17.1 μ M). Importantly, we also confirmed OATP1B1-mediated uptake of Ace in HEK-293 and MDCKII cells (Figure S3).

By analyzing a set of pyrene-based dyes we found specific and general substrates (Figure 2) of multispecific OATPs, though further structure-activity studies with a larger set of pyrene derivatives would be needed to define molecular determinants important for transporter interaction.

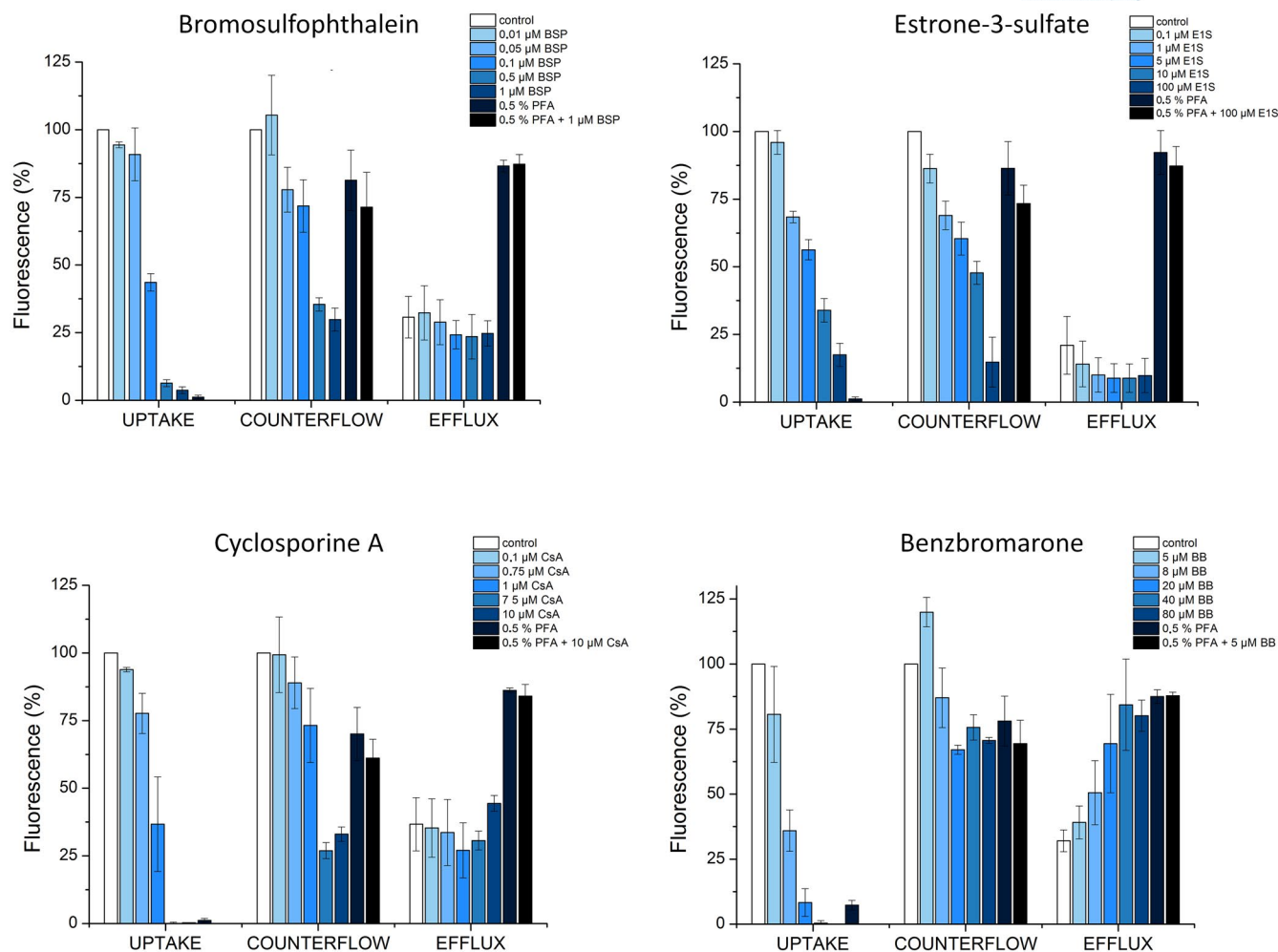


FIGURE 6 Uptake, CCF, and efflux. *Uptake* was performed as described at Figure 4. In the *CCF*, A431-OATP1B1 cells were preloaded with 5 μM Ace for 15 min until dye uptake reached equilibrium, then Ace was removed and 5 μM Ace with or without the investigated compound was added for further 20 min incubation. After 20 min, excess dye was removed and 0.1 N NaOH was added to the wells and fluorescence was measured at Ex/Em: 460/510 nm. *Efflux* was performed the same way as CCF, with the exception that Ace was present only in the “preloading” phase. Average obtained in three independent experiments ± SD are shown

By further analysis of Ace uptake, we demonstrate that owing to its low passive uptake (Figure 3 and Ref. 27), activatable fluorescence and high affinity uptake by OATPs, Ace (at least when applied in an acidic buffer) can be used in an add-and-read assay to monitor the function of OATPs, 1B1/3 and 2B1 (Figure 3). Moreover, Ace can be applied in a “no-wash” set up to assess OATP substrate/inhibitor interactions and provides a similarly reliable method as the pyranine- (Figure 4) or previously validated radioligand-based assays (Table 1). However, as the signal of the Ace-based assay is dependent on esterase cleavage, as an additional control, permeabilization of the cells, for example, by saponin (not shown here) may be needed in order to rule out potential artifacts caused by the inhibition of esterase function by the tested compound. Moreover, since Ace can be used without the removal of the indicator, it can be applied on non-adherent or freshly seeded model

cells (see Figure S3B showing real-time Ace uptake in HEK-293-OATP1B1 cells) in a microplate-based assay allowing high-throughput screening. However, it needs further investigations to decipher whether Ace is suitable to monitor low levels of endogenous OATP (e.g., in human hepatocytes or enterocytes). Regarding the limitations of the Ace-based assay, efflux of the dye (or its metabolite pyranine) by efflux transporters can be another drawback. However, in our cellular model we did not observe any non-OATP-specific efflux of pyranine (Figure 6). On the other hand, dual, fluorescent substrates of ABCs and OATPs can be used to monitor simultaneously, in one assay ABC and OATP function.^{12,26} In experiments not shown here we found that Ace, similarly to pyranine²⁶ can also be applied to test OATP1B1 and MRP2 function that may have further applications, for example, in plated hepatocytes. Finally, it has to be noted that cell permeable compounds that

are able to quench fluorescence of pyranine can potentially result in false positive hits. Hence, artifacts arising from quenchers should be excluded by determining pyranine fluorescence without or with the inhibitor. In case any quenching is observed, these inhibitors should be investigated in an assay using different substrates or methods, for example, radiolabeled estrone-3-sulfate or LC-MS can be applied.

Indirect assays based on the uptake of an indicator OATP substrate are routinely used by researchers and by pharmaceutical industry to identify potential OATP interacting molecules. The major advantage of the indirect assays is that they allow the investigation of a large set of NMEs without the need for optimization of transport conditions or detection methods for every single compound. However, one of the drawbacks of these fluorescence- or radioligand-based indirect assays is that they cannot distinguish between a transported substrate and a non-transported inhibitor, or at least not in a single assay. Therefore when, for example, the potential liver toxicity of an OATP substrate has to be determined additional measurements are required. To identify transported substrates would also be crucial in the development of physiologically based pharmacokinetic models.⁴⁷ However not all of the tested inhibitors are available in a radioactive form, and custom-made radioligand synthesis would be even more expensive. Furthermore, determination of uptake by HPLC and/or LC-MS/MS is not realistic when large compound libraries have to be tested.

Filling this hiatus, recently, an indirect assay, termed as CCF was developed for OATP1A2 and OATP2B1.^{28,29} CCF is based on the activity of SLCs as exchangers,^{37,48} namely at equilibrium, addition of a second substrate will trigger the uphill transport of the indicator while non-transported inhibitors will block this process. Therefore, the indirect method termed as competitive counterflow (CCF) can discriminate transported substrates and non-transported inhibitors. However, a CCF either radioactive or fluorescent has not yet been available for OATP1B1.

Here, by monitoring both CCF and efflux, we showed that E1S, a well-documented substrate of OATP1B1 results in an exchange for the fluorescent dye in agreement with the CCF concept (Figure 5). Based on our experiments, Ace can also be potentially used in a CCF and efflux mode to look for OATP2B1 substrates (Figure 5). On the other hand, Ace uptake seemingly did not reach its equilibrium in OATP1B3-overexpressing cells, therefore for the latter, CCF could not be established yet.

As a further proof of the CCF and efflux assay, additional OATP1B1 interacting molecules were tested in a wide concentration range. We found that transported substrates E1S and BSP resulted in a concentration-dependent decrease in the signal in the CCF. In harmony with the results of

Harper and colleagues,³⁷ we found that competing substrates should be added in excess to trigger exchange. On the other hand, substrates did not inhibit efflux even at concentrations 10-fold of their IC_{50} values (Figure 6).

In the CCF or efflux mode, pH sensitivity of pyranine can be a drawback, since any alterations in the intracellular pH caused by the investigated compounds may also alter pyranine fluorescence, and hence issue in artifacts. Therefore, we propose that CCF should be performed by removing access pyranine in the end of the experiment and setting the pH by an acid or base.

To our surprise CsA, a generally considered inhibitor of OATP1B1 also induced efflux in the CCF mode (Figure 6). All this can be interpreted by the OATP1B1-mediated transport of CsA and its exchange to the dye. In their study, Schaefer and colleagues also identified CsA as a transported substrate of OATP2B1,²⁸ and CsA is a documented ABCB1 (P-glycoprotein) substrate.⁴⁹ Moreover, we found that CsA, similar to the well-documented substrates E1S and BSP, increased the K_m of pyranine uptake with only modest decrease of the V_{max} of transport (Figure S4). Therefore, based on these we confirm that CsA is a competitive inhibitor and a possible transported substrate of OATP1B1, though direct transport measurements with (radiolabeled) CsA would be needed to clarify definitely this issue. Searching literature data, we realized that it is not straightforward to find proven non-transported inhibitors of OATP1B1, which is not surprising if we consider that most of these data derive from indirect assays not aimed to investigate the transported nature of the compound. Therefore, as a reference inhibitor we choose formaldehyde fixation of the cells. Added in the appropriate amount (0.5%), formaldehyde will fix the cells and “freeze” OATP function inhibiting both uptake and efflux without the permeabilization of the cells (Figure 6). Indeed, PFA inhibited uptake and efflux, but did not result in a decrease of the signal in the CCF. Based on the data obtained with formaldehyde, we identify benzbromarone as a non-transported OATP1B1 inhibitor.

In summary, here we describe the establishment of two novel, fluorescence-based methods based on the application of the activatable fluorogenic probe Ace. We propose that real-time Ace uptake can be applied as the first step to screen NME-OATP interaction and to determine IC_{50} values of inhibitor NMEs. Next, in CCF, and applying the NME in 10-times of its IC_{50} , transported substrates and non-transported inhibitors of at least OATP1B1 can be distinguished.

ACKNOWLEDGMENTS

This work was supported by the National Research Development and Innovation Office (NKFIH, OTKA FK 128751).

DISCLOSURES

The authors declare no conflict of interest.

AUTHOR CONTRIBUTIONS

Éva Bakos and Csilla Özvegy-Laczka designed the research, Orsolya Ungvári and Laura Király performed the research, Orsolya Ungvári and Laura Király analyzed the data, Éva Bakos, Orsolya Ungvári, and Csilla Özvegy-Laczka wrote the paper.

ORCID

Csilla Özvegy-Laczka  <https://orcid.org/0000-0002-9721-6339>

REFERENCES

- Giacomini KM, Huang SM. Transporters in drug development and clinical pharmacology. *Clin Pharmacol Ther.* 2013;94:3-9.
- Giacomini KM, Huang SM, Tweedie DJ, et al. Membrane transporters in drug development. *Nat Rev Drug Discov.* 2010;9:215-236.
- Hagenbuch B, Stieger B. The SLCO (former SLC21) superfamily of transporters. *Mol Aspects Med.* 2013;34:396-412.
- Roth M, Obaidat A, Hagenbuch B. OATPs, OATs and OCTs: the organic anion and cation transporters of the SLCO and SLC22A gene superfamilies. *Br J Pharmacol.* 2012;165:1260-1287.
- Kullak-Ublick GA, Ismail MG, Stieger B, et al. Organic anion-transporting polypeptide B (OATP-B) and its functional comparison with three other OATPs of human liver. *Gastroenterology.* 2001;120:525-533.
- Konig J, Cui Y, Nies AT, Keppler D. Localization and genomic organization of a new hepatocellular organic anion transporting polypeptide. *J Biol Chem.* 2000;275:23161-23168.
- Shitara Y, Maeda K, Ikejiri K, Yoshida K, Horie T, Sugiyama Y. Clinical significance of organic anion transporting polypeptides (OATPs) in drug disposition: their roles in hepatic clearance and intestinal absorption. *Biopharm Drug Dispos.* 2013;34:45-78.
- Urquhart BL, Kim RB. Blood-brain barrier transporters and response to CNS-active drugs. *Eur J Clin Pharmacol.* 2009;65:1063-1070.
- Shitara Y. Clinical importance of OATP1B1 and OATP1B3 in drug-drug interactions. *Drug Metab Pharmacokinet.* 2011;26:220-227.
- Link E, Parish S, Armitage J, et al. SLCO1B1 variants and statin-induced myopathy—a genomewide study. *N Engl J Med.* 2008;359:789-799.
- Shitara Y, Itoh T, Sato H, Li AP, Sugiyama Y. Inhibition of transporter-mediated hepatic uptake as a mechanism for drug-drug interaction between cerivastatin and cyclosporin A. *J Pharmacol Exp Ther.* 2003;304:610-616.
- Cui Y, Konig J, Keppler D. Vectorial transport by double-transfected cells expressing the human uptake transporter SLC21A8 and the apical export pump ABC2. *Mol Pharmacol.* 2001;60:934-943.
- Hirouchi M, Kusuhara H, Onuki R, Ogilvie BW, Parkinson A, Sugiyama Y. Construction of triple-transfected cells [organic anion-transporting polypeptide (OATP) 1B1/multidrug resistance-associated protein (MRP) 2/MRP3 and OATP1B1/MRP2/MRP4] for analysis of the sinusoidal function of MRP3 and MRP4. *Drug Metab Dispos.* 2009;37:2103-2111.
- Liu L, Cui Y, Chung AY, et al. Vectorial transport of enalapril by Oatp1a1/Mrp2 and OATP1B1 and OATP1B3/MRP2 in rat and human livers. *J Pharmacol Exp Ther.* 2006;318:395-402.
- Matsushima S, Maeda K, Kondo C, et al. Identification of the hepatic efflux transporters of organic anions using double-transfected Madin-Darby canine kidney II cells expressing human organic anion-transporting polypeptide 1B1 (OATP1B1)/multidrug resistance-associated protein 2, OATP1B1/multidrug resistance 1, and OATP1B1/breast cancer resistance protein. *J Pharmacol Exp Ther.* 2005;314:1059-1067.
- Santockyte R, Kandoussi H, Chen W, et al. LC-MS/MS bioanalysis of plasma 1, 14-tetradecanedioic acid and 1, 16-hexadecanedioic acid as candidate biomarkers for organic anion-transporting polypeptide mediated drug-drug interactions. *Bioanalysis.* 2018;10:1473-1485.
- Yang J, Wang Z, Liu S, Wang W, Zhang H, Gui C. Functional characterization reveals the significance of rare coding variations in human organic anion transporting polypeptide 2B1 (SLCO2B1). *Mol Pharm.* 2020;17:3966-3978.
- Izumi S, Nozaki Y, Komori T, et al. Investigation of fluorescein derivatives as substrates of organic anion transporting polypeptide (OATP) 1B1 to develop sensitive fluorescence-based OATP1B1 inhibition assays. *Mol Pharm.* 2016;13:438-448.
- Patik I, Szekely V, Nemet O, et al. Identification of novel cell-impermeant fluorescent substrates for testing the function and drug interaction of organic anion-transporting polypeptides, OATP1B1/1B3 and 2B1. *Sci Rep.* 2018;8:2630.
- De Bruyn T, Fattah S, Stieger B, Augustijns P, Annaert P. Sodium fluorescein is a probe substrate for hepatic drug transport mediated by OATP1B1 and OATP1B3. *J Pharm Sci.* 2011;100:5018-5030.
- Gui C, Obaidat A, Chaguturu R, Hagenbuch B. Development of a cell-based high-throughput assay to screen for inhibitors of organic anion transporting polypeptides 1B1 and 1B3. *Curr Chem Genomics.* 2010;4:1-8.
- Hollo Z, Homolya L, Davis CW, Sarkadi B. Calcein accumulation as a fluorometric functional assay of the multidrug transporter. *Biochim Biophys Acta.* 1994;1191:384-388.
- Hollo Z, Homolya L, Hegedus T, Sarkadi B. Transport properties of the multidrug resistance-associated protein (MRP) in human tumour cells. *FEBS Lett.* 1996;383:99-104.
- Ansbro MR, Shukla S, Ambudkar SV, Yuspa SH, Li L. Screening compounds with a novel high-throughput ABCB1-mediated efflux assay identifies drugs with known therapeutic targets at risk for multidrug resistance interference. *PLoS ONE.* 2013;8:e60334.
- Peterson BG, Tan KW, Osa-Andrews B, Iram SH. High-content screening of clinically tested anticancer drugs identifies novel inhibitors of human MRP1 (ABCC1). *Pharmacol Res.* 2017;119:313-326.
- Szekely V, Patik I, Ungvari O, et al. Fluorescent probes for the dual investigation of MRP2 and OATP1B1 function and drug interactions. *Eur J Pharm Sci.* 2020;151:105395.
- Langton MJ, Keymeulen F, Ciaccia M, Williams NH, Hunter CA. Controlled membrane translocation provides a mechanism for signal transduction and amplification. *Nat Chem.* 2017;9:426-430.
- Schafer AM, Bock T, Meyer zu Schwabedissen HE. Establishment and validation of competitive counterflow as a

- method to detect substrates of the organic anion transporting polypeptide 2B1. *Mol Pharm.* 2018;15:5501-5513.
29. Schäfer AM, Meyer zu Schwabedissen HE, Bien-Möller S, et al. OATP1A2 and OATP2B1 are interacting with dopamine-receptor agonists and antagonists. *Mol Pharm.* 2020;17:1987-1995.
 30. Bakos E, Nemet O, Patik I, et al. A novel fluorescence-based functional assay for human OATP1A2 and OATP1C1 identifies interaction between third generation P-gp inhibitors and OATP1A2. *FEBS J.* 2020;287(12):2468-2485.
 31. Zhang JH, Chung TD, Oldenburg KR. A simple statistical parameter for use in evaluation and validation of high throughput screening assays. *J Biomol Screen.* 1999;4:67-73.
 32. Telbisz A, Ambrus C, Mozner O, et al. Interactions of potential anti-COVID-19 compounds with multispecific ABC and OATP drug transporters. *Pharmaceutics.* 2021;13(1):81-99.
 33. Pottel J, Armstrong D, Zou L, et al. The activities of drug inactive ingredients on biological targets. *Science.* 2020;369:403-413.
 34. Bakos E, Tusnady GE, Nemet O, et al. Synergistic transport of a fluorescent coumarin probe marks coumarins as pharmacological modulators of Organic anion-transporting polypeptide, OATP3A1. *Biochem Pharmacol.* 2020;182:114250.
 35. Kawasaki T, Shiozaki Y, Nomura N, Kawai K, Uwai Y, Nabekura T. Investigation of fluorescent substrates and substrate-dependent interactions of a drug transporter organic anion transporting polypeptide 2B1 (OATP2B1). *Pharm Res.* 2020;37:115.
 36. Gan BS, Krump E, Shrode LD, Grinstein S. Loading pyranine via purinergic receptors or hypotonic stress for measurement of cytosolic pH by imaging. *Am J Physiol.* 1998;275:C1158-C1166.
 37. Harper JN, Wright SH. Multiple mechanisms of ligand interaction with the human organic cation transporter, OCT2. *Am J Physiol Renal Physiol.* 2013;304:F56-F67.
 38. Obaidat A, Roth M, Hagenbuch B. The expression and function of organic anion transporting polypeptides in normal tissues and in cancer. *Annu Rev Pharmacol Toxicol.* 2012;52:135-151.
 39. Karlgren M, Vildhede A, Norinder U, et al. Classification of inhibitors of hepatic organic anion transporting polypeptides (OATPs): influence of protein expression on drug-drug interactions. *J Med Chem.* 2012;55:4740-4763.
 40. Giacomini KM, Balimane PV, Cho SK, et al. International transporter consortium commentary on clinically important transporter polymorphisms. *Clin Pharmacol Ther.* 2013;94:23-26.
 41. Nagai N. Drug interaction studies on new drug applications: current situations and regulatory views in Japan. *Drug Metab Pharmacokinet.* 2010;25:3-15.
 42. <https://www.fda.gov/files/drugs/published/In-Vitro-Metabolism--and-Transporter--Mediated-Drug-Drug-Interaction-Studies-Guidance-for-Industry.pdf>
 43. https://www.ema.europa.eu/en/documents/scientific-guide-line/guideline-investigation-drug-interactions-revision-1_en.pdf
 44. Huang SM, Zhang L, Giacomini KM. The International Transporter Consortium: a collaborative group of scientists from academia, industry, and the FDA. *Clin Pharmacol Ther.* 2010;87:32-36.
 45. Zamek-Gliszczynski MJ, Taub ME, Chothe PP, et al. Transporters in drug development: 2018 ITC recommendations for transporters of emerging clinical importance. *Clin Pharmacol Ther.* 2018;104:890-899.
 46. Lavis LD, Chao TY, Raines RT. Synthesis and utility of fluorogenic acetoxyethyl ethers. *Chem Sci.* 2011;2:521-530.
 47. Jones HM, Chen Y, Gibson C, et al. Physiologically based pharmacokinetic modeling in drug discovery and development: a pharmaceutical industry perspective. *Clin Pharmacol Ther.* 2015;97:247-262.
 48. Rosenberg T, Wilbrandt W. Uphill transport induced by counterflow. *J Gen Physiol.* 1957;41:289-296.
 49. Saeki T, Ueda K, Tanigawara Y, Hori R, Komano T. Human P-glycoprotein transports cyclosporin A and FK506. *J Biol Chem.* 1993;268:6077-6080.
 50. Bednarczyk D. Fluorescence-based assays for the assessment of drug interaction with the human transporters OATP1B1 and OATP1B3. *Anal Biochem.* 2010;405:50-58.
 51. Izumi S, Nozaki Y, Komori T, et al. Substrate-dependent inhibition of organic anion transporting polypeptide 1B1: comparative analysis with prototypical probe substrates estradiol-17beta-glucuronide, estrone-3-sulfate, and sulfobromophthalein. *Drug Metab Dispos.* 2013;41:1859-1866.

SUPPORTING INFORMATION

Additional supporting information may be found online in the Supporting Information section.

How to cite this article: Ungvári O, Király L, Bakos É, Özvegy-Laczka C. 8-acetoxy-trisulfoxyrene as the first activatable fluorogenic probe for add-and-read assessment of Organic anion-transporting polypeptides, OATP1B1, OATP1B3, and OATP2B1. *FASEB J.* 2021;35:e21863. <https://doi.org/10.1096/fj.20210648R>



Contents lists available at ScienceDirect

European Journal of Pharmaceutical Sciences

journal homepage: www.elsevier.com/locate/ejps

Fluorescent probes for the dual investigation of MRP2 and OATP1B1 function and drug interactions



Virág Székely^{a,b}, Izabel Patik^a, Orsolya Ungvári^a, Ágnes Telbisz^c, Gergely Szakács^{a,d}, Éva Bakos^a, Csilla Özvegy-Laczka^{a,*}

^a Membrane protein research group, Institute of Enzymology, Research Centre for Natural Sciences, H-1117 Budapest, Hungary

^b Doctoral School of Molecular Medicine, Semmelweis University, H-1085 Budapest, Hungary

^c Biomembrane research group, Institute of Enzymology, RCNS, H-1117 Budapest, Hungary

^d Institute of Cancer Research, Medical University Vienna, Borschkegasse 8a, 1090 Wien, Austria

ARTICLE INFO

Keywords:

OATP
MRP2
ABCG2
Fluorescent dye
Transcellular assay
Drug interaction

ABSTRACT

Detoxification in hepatocytes is a strictly controlled process, in which the governed action of membrane transporters involved in the uptake and efflux of potentially dangerous molecules has a crucial role. Major transporters of hepatic clearance belong to the ABC (ATP Binding Cassette) and Solute Carrier (SLC) protein families. Organic anion-transporting polypeptide OATP1B1 (encoded by the *SLCO1B1* gene) is exclusively expressed in the sinusoidal membrane of hepatocytes, where it mediates the cellular uptake of bile acids, bilirubin, and also that of various drugs. The removal of toxic molecules from hepatocytes to the bile is accomplished by several ABC transporters, including P-glycoprotein (ABCB1), MRP2 (ABCC2) and BCRP (ABCG2). Owing to their pharmacological relevance, monitoring drug interaction with OATP1B1/3 and ABC proteins is recommended. Our aim was to assess the interaction of recently identified fluorescent OATP substrates (various dyes used in cell viability assays, pyranine, Cascade Blue hydrazide (CB) and sulforhodamine 101 (SR101)) (Bakos et al., 2019; Patik et al., 2018) with MRP2 and ABCG2 in order to find fluorescent probes for the simultaneous characterization of both uptake and efflux processes. Transport by MRP2 and ABCG2 was investigated in inside-out membrane vesicles (IOVs) allowing a fast screen of the transport of membrane impermeable substrates by efflux transporters. Next, transcellular transport of shared OATP and ABC transporter substrate dyes was evaluated in MDCKII cells co-expressing OATP1B1 and MRP2 or ABCG2. Our results indicate that pyranine is a general substrate of OATP1B1, OATP1B3 and OATP2B1, and we find that the dye Live/Dead Violet and CB are good tools to investigate ABCG2 function in IOVs. Besides their suitability for MRP2 functional tests in the IOV setup, pyranine, CB and SR101 are the first dual probes that can be used to simultaneously measure OATP1B1 and MRP2 function in polarized cells by a fluorescent method.

1. Introduction

The liver has a central role in the defense of the body against harmful compounds. Membrane transporters expressed in hepatocytes are key players in the elimination of potentially toxic compounds of endogenous or exogenous origin (Jetter and Kullak-Ublick, 2019). Na⁺- and ATP-independent uptake of bile acids, bilirubin, steroid hormones and several drugs from the blood into the liver is mediated by members of the Organic anion-transporting polypeptides family, OATP1B1, OATP1B3 and OATP2B1 (Dawson et al., 2009; Hagenbuch and Stieger, 2013). Conversely, following metabolism by hepatic enzymes,

modified compounds are effluxed from hepatocytes into the bile or back to the blood stream by the action of ABC (ATP Binding Cassette) transporters including P-glycoprotein (ABCB1), MRPs (ABCC family) and BCRP (ABCG2) (Kock and Brouwer, 2012). Coordinated action of hepatic OATPs and ABCs ensures efficient hepatobiliary elimination of their shared substrates.

OATP1B1, encoded by the *SLCO1B1* gene is exclusively expressed in the sinusoidal membrane of hepatocytes (Konig et al., 2000), and is the most abundant OATP of the human liver (Badee et al., 2015; Kimoto et al., 2012; Prasad et al., 2014). OATP1B1 is an organic anion exchanger that mediates the cellular uptake of bile acids, bilirubin,

Abbreviations: CaAM, calcein acetoxy-methyl ester; CB, Cascade Blue hydrazide; DDI, drug-drug interaction; FMTX, fluorescein-methotrexate; IOV, inside-out membrane vesicles; LDV, Live/Dead Violet; LDG, Live/Dead Green; LY, Lucifer Yellow; SR101, sulforhodamine 101

* Corresponding author.

E-mail address: laczka.csilla@ttk.mta.hu (C. Özvegy-Laczka).

<https://doi.org/10.1016/j.ejps.2020.105395>

Received 6 December 2019; Received in revised form 27 April 2020; Accepted 25 May 2020

Available online 29 May 2020

0928-0987/ © 2020 The Author(s). Published by Elsevier B.V. This is an open access article under the CC BY-NC-ND license

(<http://creativecommons.org/licenses/by-nc-nd/4.0/>).

thyroid and sex hormones, and also that of numerous clinically applied drugs (Roth et al., 2012). OATP1B1 is a site of drug-drug interactions (DDIs), inhibition of its function results e.g. in statin-induced myopathy (Link et al., 2008; Shitara, 2011; Shitara et al., 2003).

MRP2 (ABCC2) is expressed in the canalicular membrane of hepatocytes (Jedlitschky et al., 2006) where it mediates the active efflux of conjugated and unconjugated organic anions (e.g. bilirubin and steroid conjugates), and also the co-transport of uncharged molecules with glutathione into the bile (Konig et al., 1999). Mutations in OATP1B (SLCO1B) or MRP2 (ABCC2) genes both lead to increased serum bilirubin levels respectively termed as Rotor or Dubin Johnson syndrome, indicating that bilirubin elimination through the liver requires the function of OATP1B1/3 and MRP2 (van de Steeg et al., 2012) (Konig et al., 1999). Besides its endogenous substrates, MRP2 also recognizes various drugs (Jedlitschky et al., 2006). Hence, by mediating the extrusion of metabolites from hepatocytes into the bile, MRP2 plays a key role in the terminal phase of detoxification (Zhou et al., 2008).

Similarly to MRP2, BCRP (ABCG2) is also expressed in the canalicular membrane of hepatocytes (Horsey et al., 2016; Maliepaard et al., 2001) and is involved in the hepatobiliary excretion of various organic compounds (Hirano et al., 2005; Lee et al., 2015; Patel et al., 2016). ABCG2 is a genuine multidrug transporter, recognizing a plethora of chemically diverse molecules that includes chemotherapeutics, statins, anti-HIV drugs and antibiotics (Doyle et al., 1998; Horsey et al., 2016). Given its wide substrate recognition pattern, ABCG2 is also a site of DDI (Lee et al., 2015; Mao and Unadkat, 2015). ABCG2 transports several endogenous substrates such as urate, haem and estrogen conjugates (estradiol-glucuronide and estrone sulfate) (Heyes et al., 2018). The most common ABCG2 polymorphism c.421C>A (p.141Q>K, rs2231142) is associated with gout, due to the mislocalization of the protein (Matsuo et al., 2009; Woodward et al., 2009). Significantly, SNPs in ABCG2 have been correlated with the altered pharmacokinetics of statins and sulfasalazin (Giacomini and Huang, 2013; Heyes et al., 2018). Thus, MRP2, ABCG2 and OATP1B1 have overlapping substrate specificities. They are important determinants of hepatobiliary excretion of various drugs, including chemotherapeutics, statins and anti-HIV agents (Giacomini et al., 2010; Hooijberg et al., 1999; Kitamura et al., 2008; Liu et al., 2010; Roth et al., 2012). Therefore co-administration of their substrates can lead to serious side effects, underlying the relevance of these transporters as sites of DDIs. Hence, according to the recommendations of the US Food and Drug Administration (FDA) and the European Medicines Agency (EMA), interactions with OATP1B1/3 and ABCG2 (and also potentially with MRP2) should be assayed during drug development. FDA and EMA regulations require the use of sensitive and reliable functional assays for the evaluation of transporter drug interactions (Giacomini et al., 2013).

Radioactively labeled substrates, such as bromosulphophthalein, leukotriene C₄, dehydroepiandrosterone sulfate (DHEAS), estrone-3-sulfate (E1S) or estradiol-17 β -D-glucuronide (E217G) have been repeatedly used for the characterization of OATP and ABC transporter function and for the study of DDIs (Cui et al., 2001; Hirouchi et al., 2009; Liu et al., 2006; Matsushima et al., 2005). In general, a limitation of the radioligand transport assays is the cost associated with the radiolabeling of the substrates. Fluorescence assays offer a cost effective alternative, and it was shown that fluorescent probe substrates provide an effective and sensitive means to investigate transporter function and drug-transporter interactions (Szakacs et al., 2008). Since the discovery of Calcein-AM to probe P-glycoprotein and MRP function more than two decades ago (Hollo et al., 1994), the list of fluorescent MRP2 substrates has expanded (Cantz et al., 2000; Notenboom et al., 2005; Prevoo et al., 2011; Siissalo et al., 2009). Similarly, fluorescent dye substrates of ABCG2 (Hoechst, DyeCycle Violet) have long been used to investigate its function or drug interactions (Mathew et al., 2009; Ozvegy et al., 2002). Whereas the study of the efflux function of ABC transporters requires the use of dyes that can accumulate in the cells (high passive uptake) (Szakacs et al., 2008), ideal test substrates

measuring OATP function are cell impermeable (Bednarczyk, 2010; Gui et al., 2010; Kovacsics et al., 2017; Patik et al., 2018; Yamaguchi et al., 2006).

To date, fluorescent probes allowing the simultaneous investigation of OATP1B1 and the hepatic ABC transporters have not been identified. The goal of the current work was to analyze the interaction of fluorescent OATP1B1 substrates with MRP2 and ABCG2 in order to find dual OATP ABC transporter probes. Our earlier work has identified Zombie Violet (ZV), Live/Dead Violet (LDV), Live/Dead Green (LDG), Cascade Blue hydrazide (CB), Alexa Fluor 405 (AF405) (Patik et al., 2018), and recently SR101 (sulforhodamine 101) (Bakos et al., 2019) as novel fluorescent substrates of OATP1Bs. We have also shown that CB and AF405 can be applied as probes in OATP1B1/3 or OATP2B1 drug interaction tests (Patik et al., 2018). Since these OATP probes are cell-impermeant, their transport by ABCG2 or MRP2 cannot be directly investigated in cellular assays. However, transporter-mediated accumulation of the same dyes can be measured in inside-out vesicles (IOVs). Because of the reverse orientation of the membrane lipid bilayer and the efflux transporters, ATP-dependent uptake of a substrate into IOVs corresponds to cellular efflux, allowing the measurement of the transport of cell impermeable dyes by ABC efflux transporters. Using this experimental setup, we show that several cell-impermeable fluorescent substrates are indeed transported by MRP2 and ABCG2. Theoretically, cellular efflux may be measured if the accumulation of the cell impermeable dyes was facilitated by uptake transporters. Using double-transfected, polarized MDCKII cells overexpressing OATP1B1 and MRP2 or ABCG2, we identify dual OATP1B1 and MRP2 fluorescent probes, setting the stage for a fluorescence-based assay development measuring vectorial transport mediated by these transporters.

2. Materials and methods

2.1. Materials

Zombie Violet was purchased from BioLegend® (San Diego, CA, US). LIVE/DEAD® Fixable Cell Stain Dyes (Violet and Green), fluorescein-methotrexate and Cascade Blue hydrazide were purchased from Thermo Fisher Scientific (Waltham, MA, US). All other materials, if not indicated otherwise, were from Sigma Aldrich, Merck (Budapest, HU).

2.2. Generation of cell lines and cell culturing

A431 cells expressing OATPs 1B1, 1B3 or 2B1 and their mock transfected counterparts were generated previously as described in Patik et al. (2018). The MDCKII-MRP2 cell line was generated previously (Bakos et al., 2000). In order to generate MDCKII cells expressing ABCG2, MDCKII parental cells were transfected with 1 μ g plasmid DNA (pSB-CMV-ABCG2, allowing transposon mediated genomic insertion of ABCG2 cDNA (Saranko et al., 2013)) and 100 ng plasmid containing the 100x Sleeping Beauty transposase using Lipofectamine 2000® reagent (Thermo Fisher Scientific) according to the recommendation of the manufacturer. After 48 hours the transfection medium was removed and the cells were selected in puromycin (1 μ g/ml) for two weeks. Transfected cells were sorted based on labeling by the anti-ABCG2 monoclonal antibody 5D3 (Bioscience), which binds to a surface epitope (Ozvegy et al., 2002). Cells showing 5D3 positivity were sorted using a BD FACSAria III Cell Sorter (BD Biosciences, San Jose, CA, US).

OATP1B1 expression in MDCKII, MDCKII-MRP2 or MDCKII-ABCG2 cells was achieved by recombinant lentiviruses as described earlier (Patik et al., 2018). Briefly, MDCKII parental, MDCKII-MRP2 and MDCKII-ABCG2 cells were transfected with the pRRL-CMV-OATP1B1-MCS-IRES- Δ CD4 vector. In order to generate mock transfected control cells for transport experiments, MDCKII cells were transfected with the pRRL-EF1- Δ CD4 vector. Transduced cells were sorted based on their CD4 positivity using a BD FACSAria III Cell Sorter (BD Biosciences, San

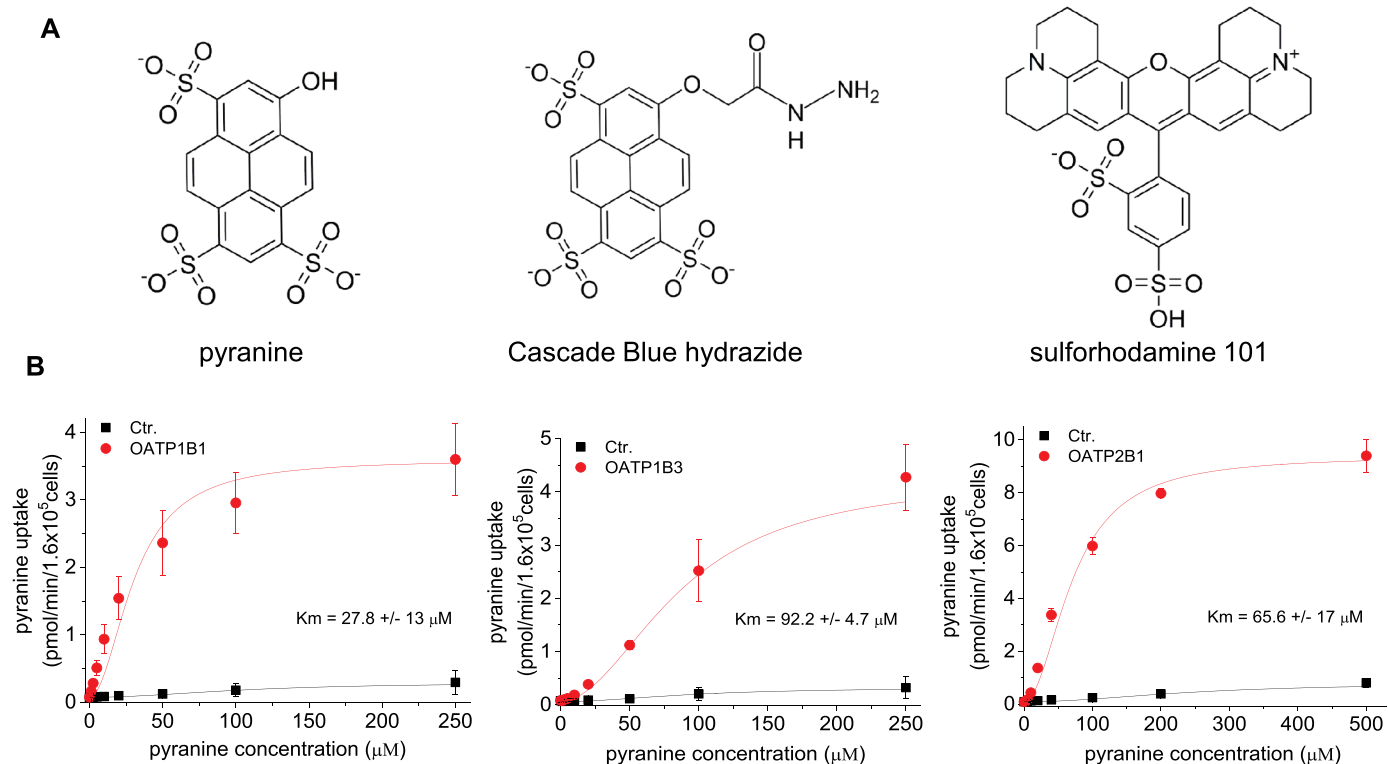


Fig. 1. A) Structure of the dyes tested in the current study. B) Pyranine is a novel substrate of OATP1B1, OATP1B3 and OATP2B1. Concentration dependent uptake of pyranine was measured in A431 cells overexpressing OATP1B1, OATP1B3 or OATP2B1, or mock transfected controls (Ctr.) seeded onto 96-well plates at 37°C in the linear phase of transport, at 10 (OATP1B1) or 15 (OATP1B3 and OATP2B1) minutes at pH 5.5. Fluorescence was determined using an Enspire plate reader (Ex/Em: 403/517 nm). Transport kinetics was determined by subtracting fluorescence measured in mock transfected cells. Average \pm SD values of at least 3 independent measurements are shown.

Jose, CA, US). OATP1B1 overexpressing cells were sorted based on their increased Live/Dead Green uptake, as described earlier (Patik et al., 2018).

A431 and MDCKII cells were grown in DMEM (Gibco, Thermo Fisher Scientific (Waltham, MA, US)) completed with 10 % fetal bovine serum, 2 mM L-glutamine, 100 U/ml penicillin, and 100 μ g/ml streptomycin at 37°C, 5% CO₂, under sterile conditions.

2.3. Western blot

MDCKII cell lysates were separated on 7.5% Laemmli SDS-PAGE gels and transferred onto PVDF membranes. Immunoblotting was performed as described (Sarkadi et al., 1992). Membranes were incubated overnight with anti-OATP1B1, anti-MRP2 (M₂-I-4 / M₂-III-6 monoclonal antibody) (Bakos et al., 2000) or anti-ABCG2 (BXP-21, Maliepaard et al., 2001) antibodies or anti- β -actin antibody (A1978, Sigma). The antibody used for the detection of OATP1B1 was a kind gift from Dr. Bruno Stieger (Department of Clinical Pharmacology and Toxicology, University Hospital, 8091 Zurich, Switzerland) (Kullak-Ublick et al., 2001). Secondary antibodies were HRP-conjugated anti-rabbit (OATP1B1) or anti-mouse (MRP2, ABCG2, β -actin) antibodies (Jackson ImmunoResearch, Suffolk, UK) in a dilution of 20,000x. Luminescence was detected using the Luminor Enhancer Solution kit by Thermo Scientific (Waltham, MA, US).

2.4. MRP2 and ABCG2 expression in insect cells and inside-out membrane vesicle preparation

Recombinant baculovirus containing the ABCG2/MRP2 cDNA (Bakos et al., 2000), ABCG2 cDNA (Ozvegy et al., 2002) or the cDNA of an unrelated protein (Patik et al., 2015) were used to achieve transient expression in *Sf9* insect cells. Culturing and infection of *Sf9* cells was

performed as described earlier (Sarkadi et al., 1992). Virus-infected *Sf9* cells were harvested after 72 hours. Following washing with Tris-mannitol buffer (50 mM Tris, pH 7.0, with HCl, 300 mM mannitol and 0.5 mM phenylmethylsulfonyl fluoride), cells were lysed and homogenized in TMEP (50 mM Tris, pH 7.0, with HCl, 50 mM mannitol, 2 mM EGTA, 10 μ g/ml leupeptin, 8 μ g/ml aprotinin, 0.5 mM phenylmethylsulfonyl fluoride, and 2 mM dithiothreitol) using glass tissue grinder tubes. Undisrupted cells were removed by centrifugation for 10 min at 500 g. Finally, the supernatant containing the membranes was centrifuged for 1 h at 100 000 g, and the pellet was resuspended in TMEP (with freshly appended 0.5 mM phenylmethylsulfonyl fluoride) at concentration of 5-10 mg/ml. Membranes were stored at -80°C in aliquots. (Bakos et al., 2000; Sarkadi et al., 1992). In the case of ABCG2 cholesterol enriched membranes IOVs were prepared in order to achieve maximal ABCG2 activity (Telbisz et al., 2007). Cholesterol loading was performed by incubation of the membranes (containing ABCG2 or their controls) with TMEP containing 2 mM Cholesterol-RAMEB (Cyclolab, Hungary) on ice for 30 minutes, prior to the final centrifugation step (Telbisz et al., 2007).

2.5. Transport measurements in inside-out vesicles

Membrane vesicles (50 μ g/tube) were incubated in transport buffer (Bakos et al., 2000) with 4 mM MgATP or 4 mM MgAMP and with the fluorescent dyes 1 μ M sulforhodamine 101 (SR101)/fluorescein-methotrexate (FMTX), 5 μ M pyranine/Cascade Blue (CB), 10 μ M Lucifer Yellow (LY) or 0.2 μ l/tube ZV/LDV/LDG for 10 (ZV/LDV/LDG/FMTX/SR101/LY) / 20 (pyranine) / 30 (CB) minutes in 150 μ l final volume at 37°C. These experimental conditions were evaluated by measuring time- and concentration dependent transport of the fluorescent dyes in preliminary experiments. For each compound, time and concentration values yielding the highest signal/noise ratio measured were chosen.

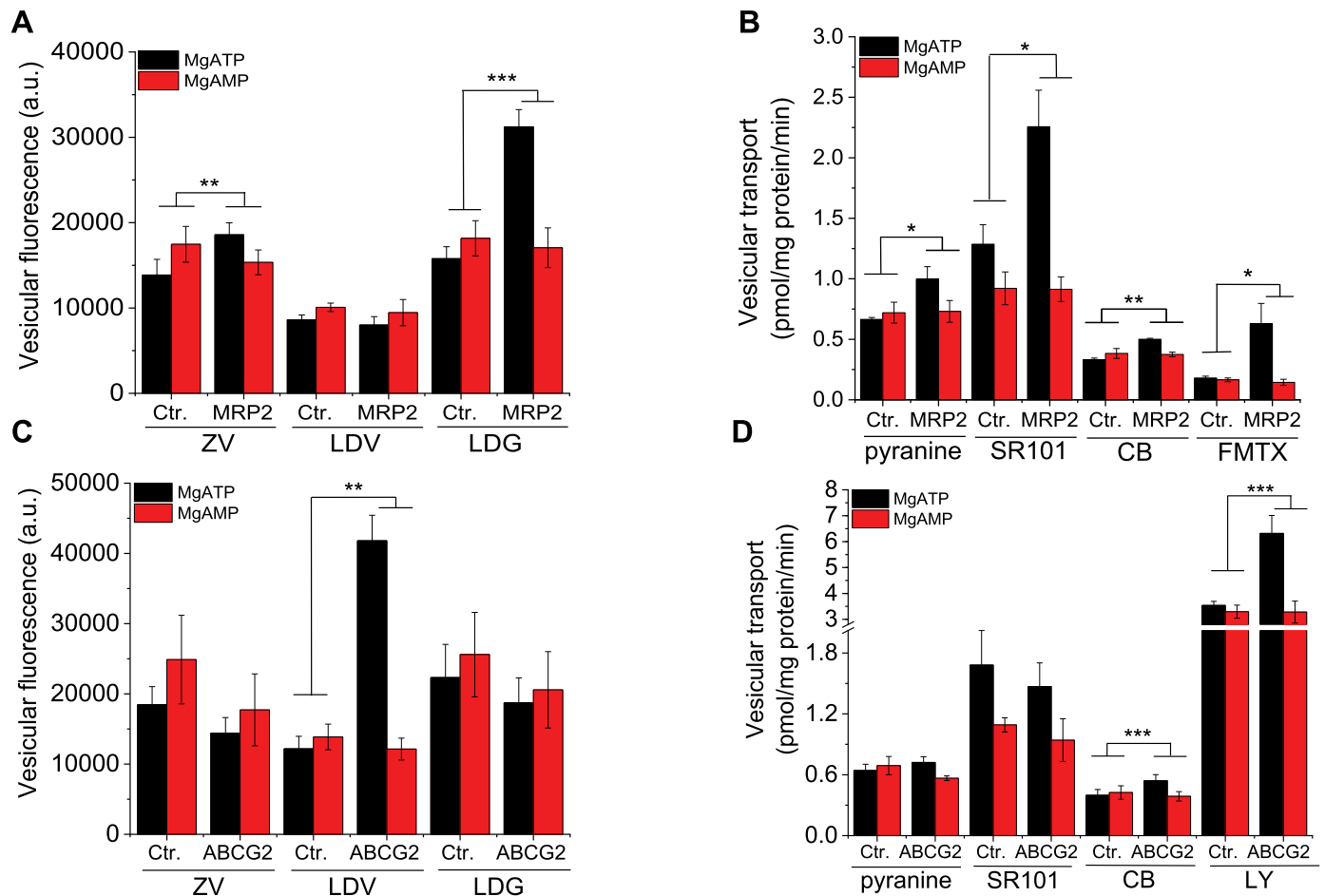


Fig. 2. Fluorescent dye transport measurements in inside-out membrane vesicles. Uptake of the fluorescent dyes, ZV, LDV and LDG (0.2 μ l/sample), 5 μ M pyranine, 1 μ M SR101, 1 μ M FMTX or 10 μ M LY in MRP2- (panels A, B) or ABCG2- (panels C, D) containing or control membrane vesicles (50 μ g) was measured for 30 minutes (CB), 20 minutes (pyranine) or 10 minutes (ZV, LDV, LDG, SR101, FMTX, LY) in the presence of 4 mM MgATP or 4 mM MgAMP at 37°C. Experiments were repeated 3-times. Average of at least 3 independent replicates \pm SD are shown. Statistical significance was calculated between ATP-dependent signals. Delta values generated by subtracting signals with MgAMP from that measured with MgATP were compared for statistical significance by Student's t-test, *: $p < 0.05$, **: $p < 0.01$, ***: $p < 0.001$.

When inhibition was investigated, the vesicles were pre-incubated with 1 μ M Ko143, a known ABCG2 inhibitor (Allen et al., 2002) prior to the addition of the fluorescent dyes. Reaction was stopped by the addition of 550 μ l ice cold transport buffer and by placing the samples on ice. Eppendorf tubes were centrifuged for 5 min at 22000 g. Supernatant was eliminated and the pellet was suspended in 200 μ l RT (room temperature) 1 x Phosphate Buffered Saline (PBS). The suspensions were pipetted onto 96 well plates and fluorescence intensity was measured in an Enspire Fluorescent plate reader (Perkin Elmer) at the following wavelengths: 405/423 nm (ZV), 416/451 nm (LDV), 495/520 nm (LDG), 403/517 nm (pyranine), 400/419 nm (CB), 586/605 nm (SR101), 428/540 nm (LY), 497/516 nm (FMTX). Transport activity in the case of CB, pyranine, LY, SR101 and FMTX was determined based on a calibration curve.

2.6. Transport measurements in MDCKII cells by flow cytometry

MDCKII cells were collected following trypsinization (0.2% trypsin) in complete DMEM. After washing in 1 ml uptake buffer (125 mM NaCl, 4.8 mM KCl, 1.2 mM CaCl₂, 1.2 mM KH₂PO₄, 12 mM MgSO₄, 25 mM MES, and 5.6 mM glucose, with the pH adjusted to 5.5/7.4 using 1 M HEPES and 10 N NaOH for OATP/ABC function, respectively), 5×10^5 cells were incubated at 37°C for 10 min (calcein-AM (CaAM)) / 30 min (CB, DCV (DyeCycle Violet)) in 100 μ l fluorescent dye (final concentrations: 0.5 μ M CaAM, 1-1 μ M CB or DCV) diluted in the

appropriate buffer. CB/CaAM/DCV were used as substrates of OATP1B1/MRP2/ABCG2 for validating functionality. The reaction was stopped by the addition of 700 μ l ice-cold 1 x PBS, and the samples were kept on ice until the flow cytometry analysis. Cellular fluorescence was determined of at least 20,000 living cells from each sample using an Attune Acoustic Focusing Cytometer (Applied Biosystems, Life Technologies, Carlsbad, CA, US).

2.7. OATP-mediated transport of pyranine using a microplate-based transport assay

Uptake of pyranine in A431 cells overexpressing OATPs 1B1, 1B3 or 2B1 was measured as described previously (Patik et al., 2018). Briefly, A431 cells (8×10^4 /well) were seeded on 96-well plates in 200 μ l DMEM one day prior to the transport measurement. Next day the medium was removed, and the cells were washed three times at room temperature with 1 x Phosphate Buffered Saline (PBS). The cells were pre-incubated with 50 μ l uptake buffer (see above) at 37°C. The reaction was started by the addition of 50 μ l uptake buffer containing increasing concentrations of pyranine. Cells were then incubated at 37°C for 10 minutes (OATP1B1) or 15 minutes (OATP1B3 and OATP2B1). The applied incubation time was evaluated during previous unpublished data. The reaction was stopped by removing the supernatant and washing the cells three times with ice-cold 1 x PBS. Wells were loaded with 200 μ l ice-cold 1 x PBS and fluorescence was determined

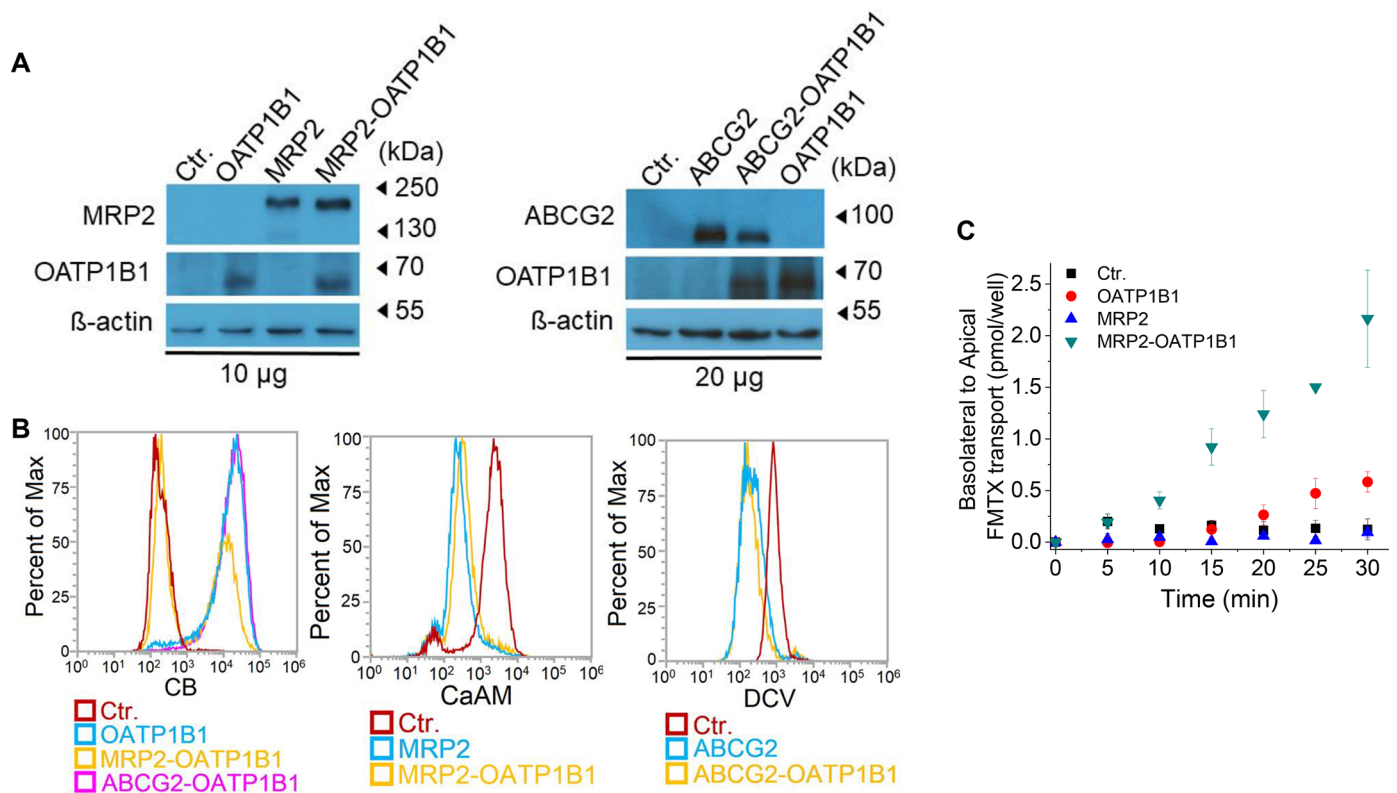


Fig. 3. Expression and function of OATP1B1, MRP2 or ABCG2 in the MDCKII cell lines. 3A: 10 or 20 μ g of total cell lysates were analyzed for transporter expression by Western blot. Signals of OATP1B1/MRP2/ABCG2/ β -actin were visualized by the antibodies raised against these proteins. Transporter expression is equally present for OATP1B1/MRP2/ABCG2 among the appropriate cell lines. β -actin signals verified the equal amount of proteins in the samples tested. Experiments were repeated at least 3-times. The result of one representative experiment is shown. 3B: Transporter function of OATP1B1, MRP2 or ABCG2 in MDCKII cell lines. Functionality of the transporters OATP1B1, MRP2 or ABCG2 was determined based on the transport of CB, CaAM or DCV substrates, respectively. 5×10^5 MDCKII cells were incubated at 37°C for 10 min (CaAM)/30 min (CB, DCV) in 100 μ l fluorescent dye (final concentrations: 0.5 μ M CaAM, 1-1 μ M CB or DCV) diluted in the appropriate buffer (pH 5.5/7.4 for OATP/ABC function). Cellular fluorescence was determined of at least 20,000 living cells from each sample using an Attune Acoustic Focusing Cytometer (Applied Biosystems, Life Technologies, Carlsbad, CA, US). Transport measurements were repeated at least 3-times. One representative experiment is shown. 3C: Transcellular transport of fluorescein-methotrexate: Basolateral to apical transcellular transport of FMTX (1 μ M) in MDCKII-OATP1B1, MDCKII-MRP2, MDCKII-MRP2-OATP1B1 or control (Ctr., mock transfected) cells grown on transwell inserts for 4 days prior to the experiment was followed for 30 minutes at 37°C. Average of 3 independent measurements \pm SD are shown.

using an Enspire plate reader Ex/Em: 403/517 nm. OATP-dependent transport was determined by extracting fluorescence measured in mock transfected cells. Transport activity was calculated based on a calibration curve. Experiments were repeated in 3 biological replicates.

2.8. Transcellular transport measurements

For transcellular transport experiments, OATP1B1 and/or MRP2 or ABCG2 overexpressing MDCKII cells (9×10^4 cells/insert) were grown on Tissue culture plate inserts (6.5 mm diameter, 0.4 μ m pore size, VWR Ltd., Hungary) for four days. The cells were seeded in 300 μ l complete DMEM onto the insert membranes and 1 ml media was added to the wells around the inserts in 24 well plates. The transport measurement was started by the removal of the medium from the transwell inserts and by washing the cells two times with 300 μ l pH 7.4 uptake buffer (see above). The wells were washed three times with 1 ml pH 5.5 uptake buffer (see above). After washing, 300 μ l pH 7.4 buffer was pipetted into the inserts containing the cells and 1 ml pH 5.5 buffer into the wells and a 10 min pre-incubation period at 37°C was applied. The reaction was started by the addition of 1 ml uptake buffer pH 5.5 (ensuring higher OATP1B1 transport (Patik et al., 2018)) containing pyranine, CB, SR101, or FMTX (final concentrations 5-5 μ M and 1-1 μ M respectively) to the wells, and the tissue culture plates were further incubated at 37°C. When inhibitors were tested, 10 μ M cyclosporin A (CsA) or 40 μ M benzbramarone was added to the lower or upper

compartment, respectively. To determine transport, 30 μ l samples from the upper compartment were collected every 5 minutes and pipetted into 70 μ l 1 x PBS for fluorescence measurements. In the case of MDCKII-ABCG2-OATP1B1 cells, CB transport was determined at the following time points: 0, 15 and 30 minutes. The fluorescence intensity of the samples was determined using an Enspire plate reader (Perkin Elmer) at the following wavelengths: 403/517 nm (pyranine), 400/419 nm (CB), 586/605 nm (SR101), or 497/516 nm (FMTX).

In order to evaluate the transport in the opposite direction (A-B), transport reaction was started from the apical side by adding the substrates at the same concentration as applied before but in 300 μ l pH 7.4 buffer. Samples were collected from the wells (B side) to a 96 well plate, 100 μ l at each time points until 25 minutes and fluorescence intensity was determined as described before.

For evaluating intracellular accumulation of pyranine, transport reaction in B-A direction was stopped after 30 minutes by removing the solutions from the wells and inserts and washing the cells three times with cold 1 x PBS on ice. Transwell inserts were then cut out and placed into 200 μ l 1% Triton-PBS in Eppendorf tubes. Inserts were incubated at RT for 75 minutes, and then cell lysates were pipetted onto 96 well plates. Fluorescence intensity was determined using an Enspire plate reader as described above, Ex/Em: 403/517. In order to define the amount of the dyes in the samples, a calibration curve was generated by determining the fluorescence of increasing amounts of the given dye dissolved in 200 μ l 1 x PBS. We found that fluoresce of the dyes

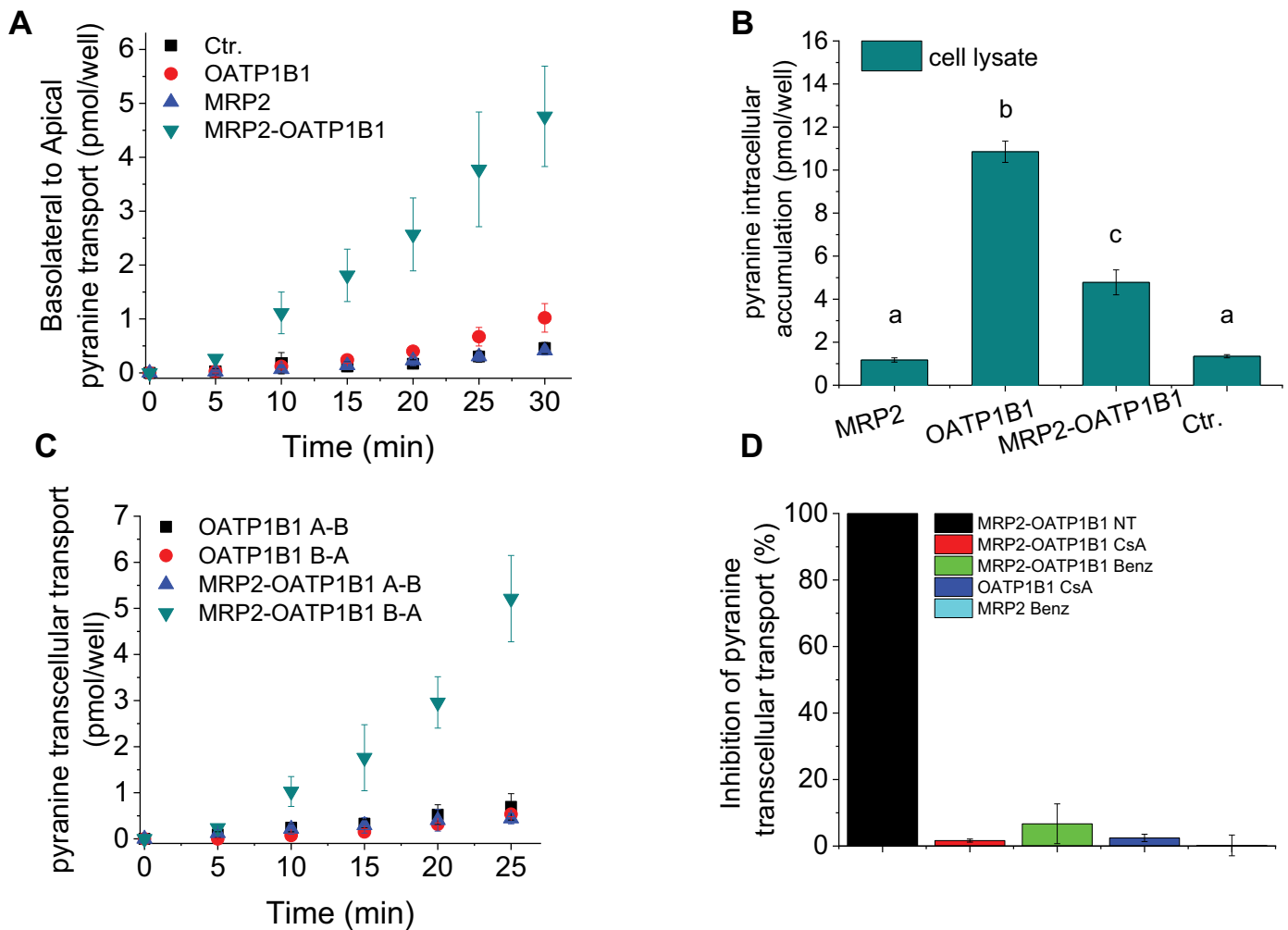


Fig. 4. Transcellular transport of pyranine. 4A: Basolateral to apical transport of pyranine (5 μ M) in MDCKII-OATP1B1, MDCKII-MRP2, MDCKII-MRP2-OATP1B1 or control (Ctr., mock transfected) cells grown on transwell inserts for 4 days prior to the experiment was followed for 30 minutes at 37°C. Average of 5 independent measurements \pm SD are shown. 4B: Intracellular levels of pyranine were determined in MDCKII cells after 30 minutes of incubation with 5 μ M pyranine administered from the basolateral side of the transwells. Average of 3 independent measurements \pm SD are shown. Statistical analysis for multi comparison was evaluated by Tukey-Kramer HSD (Honest Significant Differences) procedure, as a post-hoc test, after rejecting H_0 in One-Way ANOVA ($\alpha=0,05$). Means \pm SD marked with the same letter ("a" for Ctr. and MRP2) were not significantly different ($p > 0,05$, Tukey-Kramer HSD test) from each other unlike "b" and "c" which mean significant difference. 4C: Lack of apical to basolateral transport of pyranine. Experiments were performed with pyranine (5 μ M) added either to the apical or the basolateral compartment and samples were taken from the basolateral (A-B) or the apical compartment (B-A), respectively until 25 minutes. Average of 3 independent measurements \pm SD are shown. 4D: Inhibition of pyranine transcellular transport by cyclosporin A (CsA) or benzbromarone (Benz). Transcellular (B-A) transport of 5 μ M pyranine can be inhibited by known OATP1B1 and MRP2 inhibitors, CsA and Benz. Vectorial transport was measured as described at Fig. 4A, except that 10 μ M CsA or 40 μ M benzbromarone was added to the basolateral or apical compartment, respectively prior to the addition of pyranine (5 μ M). Fluorescence of pyranine was measured using an Enspire plate reader at Ex/Em 403/517 nm. Data obtained from 3 independent experiments \pm SD values are presented as a percent of transport measured in MDCKII-MRP2-OATP1B1 cells without any inhibitor (NT).

(pyranine, CB and SR101) diluted in PBS or accumulated in cells remained stable even after 90 minutes of incubation at room temperature (data not shown).

2.9. Data analysis and statistics

Kinetic parameters shown in Fig. 1B of dye uptake were analyzed by Hill1 fit using the OriginPro 8 software (GraphPad, La Jolla, CA, USA). Statistical significance was calculated by Student's t-test between ATP-dependent signals. Delta values were generated by subtraction of MgAMP or MgAMP + Ko signals from MgATP or MgATP + Ko signals, respectively. These delta values were compared for statistical significance by Student's t-test, *: $p < 0,05$, **: $p < 0,01$, ***: $p < 0,001$ (Figs. 2, 6).

Statistical analysis of the samples shown in Fig. 4B for multi comparison was evaluated by Tukey-Kramer HSD (Honest Significant

Differences) procedure, as a post-hoc test, after rejecting H_0 in One-Way ANOVA ($\alpha=0,05$). Samples marked with the same letter ("a" for MRP2 and Ctr.) were not significantly different from each other.

3. Results

3.1. Pyranine is a novel substrate of hepatic OATPs, 1B1, 1B3 and 2B1

To expand the scope of fluorescent OATP substrates, we evaluated the interaction of pyranine (HPTS, Solvent Green 7, trisodium 8-hydroxypyrene-1,3,6-trisulfonate), a pH indicator closely related to Cascade Blue hydrazide (CB) (Avnir and Barenholz, 2005; Clement and Gould, 1981; Gan et al., 1998) (Fig. 1) with OATP1B1, OATP1B3 and OATP2B1. Measurements were carried out using A431 cells over-expressing OATP1B1, OATP1B3 or OATP2B1. Whereas pyranine does not accumulate in control, mock transfected A431 cells (Fig. 1B), we

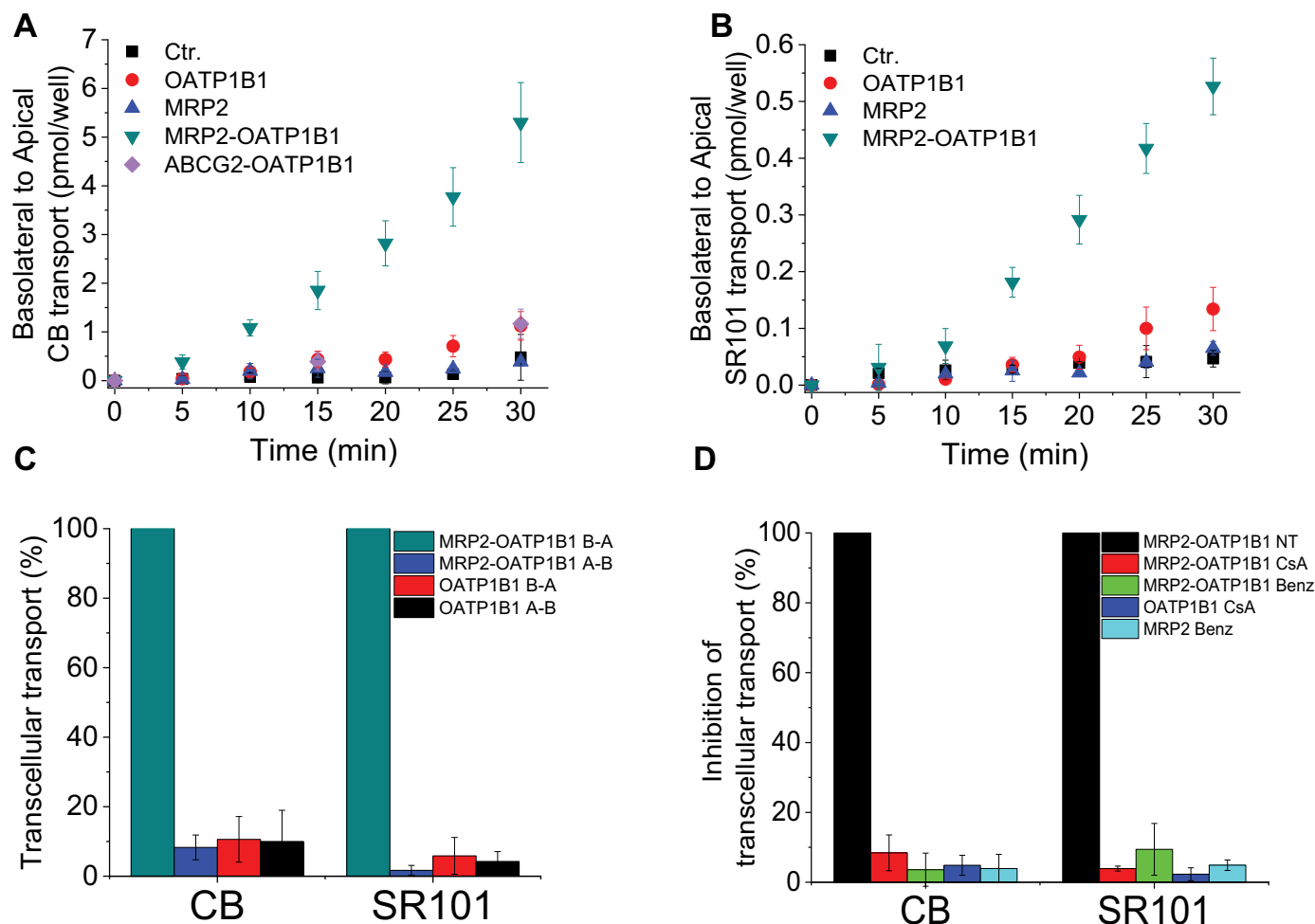


Fig. 5. Transcellular transport of Cascade Blue hydrazide or sulforhodamine 101. Basolateral to apical transport of CB (5 μ M, panel A) or SR101 (1 μ M, panel B) in MDCKII-OATP1B1, MDCKII-MRP2, MDCKII-MRP2-OATP1B1, MDCKII-ABCG2-OATP1B1 (panel A) or control (Ctr., mock transfected) cells grown on transwell inserts for 4 days prior to the measurement was followed for 30 minutes at 37°C. Average of 4 independent measurements \pm SD are shown for MDCKII-OATP1B1, MDCKII-MRP2, MDCKII-MRP2-OATP1B1 and Ctr. cells on panel A, and average of 3 independent measurements \pm SD are shown for MDCKII-ABCG2-OATP1B1 cells (panel A) and on panel B. 5C: Lack of apical to basolateral (A-B) transport of the fluorescent dyes. Experiment was performed on MDCKII cells grown on transwell inserts for 4 days prior to the measurement. CB (5 μ M) or SR101 (1 μ M) were added to the apical (A-B transport) or basolateral (B-A transport) compartment and after 25 minutes of incubation at 37°C samples were taken from the basolateral (A-B transport) or apical (B-A transport) compartment, and fluorescence was determined. Data are shown as a percent of B-A transport measured in MDCKII-MRP2-OATP1B1 cells. Average of 3 independent measurements \pm SD are shown. 5D: Inhibition of CB or SR101 transcellular transport. Transcellular (B-A) transport of 5 μ M CB or 1 μ M SR101 can be inhibited by known OATP1B1 and MRP2 inhibitors, cyclosporin A (CsA) and benzbromarone (Benz). Vectorial transport was measured as described at Fig. 4A, except that 10 μ M CsA or 40 μ M benzbromarone was added to the basolateral or apical compartment, respectively prior to the addition of the dyes 5 μ M CB or 1 μ M SR101. Data represent average \pm SD values of 3 independent experiments and are presented as a percent compared to the B-A transport measured in MDCKII-MRP2-OATP1B1 cells (NT).

found a typical OATP-mediated uptake in A431 cells expressing a hepatic OATP (Fig. 1B) revealing that pyranine is a common substrate of these uptake transporters.

3.2. Identification of novel common fluorescent substrates of OATP1B1, MRP2 and ABCG2

Hepatic OATPs and MRP2 or ABCG2 have an overlapping substrate recognition profile (Giacomini et al., 2010). To characterize the susceptibility of fluorescent OATP probes to MRP2 or ABCG2 mediated transport, we used inside-out membrane vesicles prepared from *Sf9* (*Spodoptera frugiperda*) cells overexpressing either MRP2 or ABCG2 (Fig. 2). IOVs allow the investigation of the transport of membrane impermeable substrates by efflux transporters that otherwise, in the lack of passive uptake, could not be investigated in cell-based assays with single transfectants. IOVs prepared from mock transfected *Sf9* cells, as well as transport in the presence of MgAMP served as negative controls for transport experiments. On the other hand, Lucifer Yellow

(LY) and fluorescein-methotrexate (FMTX), documented substrates of ABCG2 or MRP2 (Deng et al., 2016; Notenboom et al., 2005; Prevoe et al., 2011; Sjostedt et al., 2017), respectively, were used as positive controls. As shown in Fig. 2A and B, ATP-dependent transport by MRP2 was observed for FMTX, ZV, LDG, CB, SR101 and pyranine, while LDV was not transported. Although uptake of the known substrate LY indicated functionality of ABCG2, transport of ZV, LDG, pyranine or SR101 by ABCG2 was not detected. On the other hand, we observed significant transport of LDV and a weak transport of CB by ABCG2. A weak ATP-dependent transport of SR101 was also present in control vesicles (Fig. 2B and D). To reveal the nature of the SR101 uptake observed in control vesicles, transport was measured using EDTA as a Mg²⁺ chelator or Na-orthovanadate as a general ATP-ase inhibitor. These experiments showed a Mg²⁺-dependent and Na-orthovanadate sensitive transport of SR101, confirming the involvement of a yet undefined insect transporter in SR101 transport (Supplementary Figure S1).

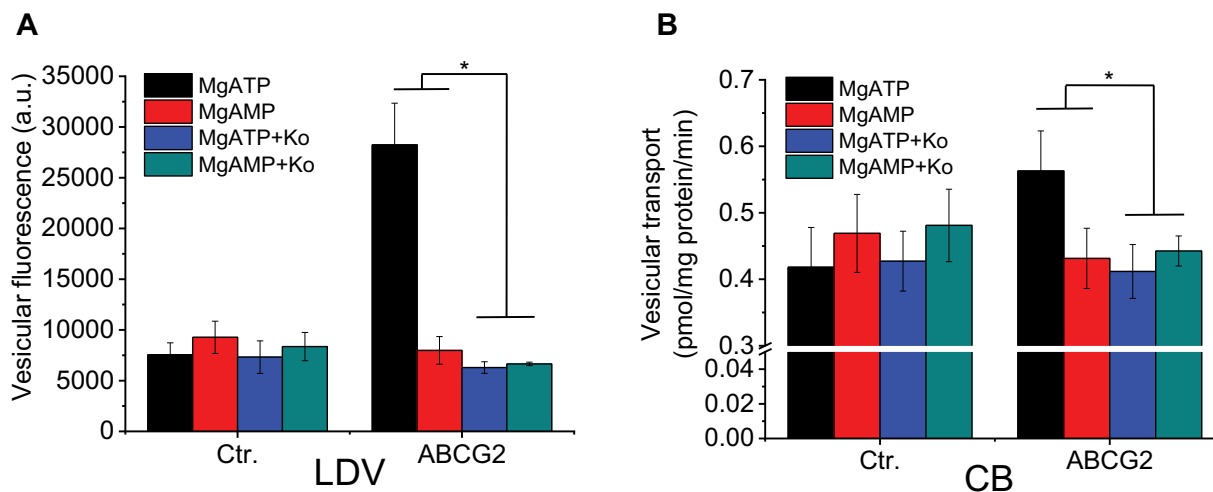


Fig. 6. Inhibition of LDV (panel A) or CB (panel B) uptake in IOVs containing ABCG2. Membrane vesicles (50 μ g) were incubated in the presence or absence of 1 μ M Ko143 for 5 minutes at 37°C. Transport reaction was started by the addition of 0.2 μ l LDV/tube or 5 μ M CB. Fluorescence after 10 minutes (LDV) or 30 minutes (CB) of incubation was determined using an Enspire plate reader. Experiments were repeated 3-times. Average \pm SD values are shown. Statistical significance was calculated between ATP-dependent signals. Delta values generated by subtracting MgAMP or MgAMP + Ko signal from the signal of MgATP or MgATP + Ko, respectively were compared for statistical significance by Student's t-test, *: $p < 0.05$.

3.3. Transcellular transport of pyranine, a novel common substrate of OATP1B1 and MRP2

In order to test whether the newly identified dual fluorescent substrates can indeed be applied for the simultaneous investigation of OATP1B1 and MRP2 function, we examined their transport in double transfected polarized MDCKII cells. Since the structure of ZV, LDG and LDV is unknown, these dyes were excluded from further experiments. First, stable MDCKII cell lines co-expressing these transporters, termed as MDCKII-MRP2-OATP1B1 or MDCKII-ABCG2-OATP1B1 were engineered (see 2.2.). Cell lines containing solely OATP1B1, MRP2, ABCG2 or mock transfected cells (MDCKII-1B1, MDCKII-MRP2, MDCKII-ABCG2 or MDCKII-Ctr.) served as controls. Expression was confirmed by Western blot analysis (Fig. 3A), and functionality of the transporters was verified by transport assays using known OATP1B1, MRP2 or ABCG2 substrates, CB, CaAM and DCV, respectively (Fig. 3B).

For transcellular transport measurements, MDCKII cells were grown on transwell inserts for 4 days to reach a polarized state, when OATP1B1 is localized to the basolateral membrane, and MRP2 or ABCG2 are found apically (Cui et al., 2001; Matsushima et al., 2005). First, FMTX, a previously identified substrate of OATP1B1 (Gui et al., 2010) and MRP2 (Notenboom et al., 2005; Prevoe et al., 2011) was used for the setup of the transcellular transport measurement. As shown on Fig. 3C, a time-dependent transcellular basolateral to apical (B-A) transport of FMTX could be observed in MRP2-OATP1B1 double transfectants that was not present in the control, single transfected MDCKII-1B1, MDCKII-MRP2 or MDCKII-Ctr. (mock) cells. Next, transcellular transport of pyranine was determined. As shown on Fig. 4A, a time-dependent B-A transport of pyranine could be observed in MRP2-OATP1B1 double transfectants, and there was no B-A transport in single or mock transfected cells. When intracellular accumulation of pyranine was measured, we found that pyranine cannot enter the cells without the function of OATP1B1, hence it cannot be detected in control or MRP2 single transfected cells (Fig. 4B). To exclude leakage of the cell monolayer, concurrent pyranine transport in the apical to basolateral (A-B) direction was investigated. Transport of pyranine in both directions was measured on the MRP2-OATP1B1 double and OATP1B1 single transfectant cells (Fig. 4C). We found negligible transcellular transport from the apical to the basal compartment in both cell lines. These results indicate that the B to A directed transport is indeed derived from the interaction of the dye with the OATP1B1 and MRP2

transporters. Finally, in order to verify that the increasing fluorescent pyranine signal at the A side of double transfected cells is a result of the concerted action of OATP1B1 and MRP2, the experiments were repeated in the presence of transporter inhibitors (Fig. 4D). Double transfected cells treated with either cyclosporin A at the basal side or benzbromarone at the apical side showed no detectable transcellular transport. To control these experiments, OATP1B1 and MRP2 single transfected cells were also treated with cyclosporin A or benzbromarone, at the basal or apical side, respectively. Taken together, the results were consistent with the transcellular transport of pyranine in double transfectants as a result of OATP1B1-mediated uptake and MRP2-mediated efflux.

3.4. Identification of Cascade Blue hydrazide and sulforhodamine 101 as dual OATP1B1 and MRP2 probes in transwell measurements

Based on the experiments evaluated in the Sf9 IOV assay, SR101 is another potential common substrate of OATP1B1 and MRP2, and a weak accumulation of CB in IOVs with MRP2 or ABCG2 was also detected. Therefore, in order to test their applicability as fluorescent probes in vectorial transport measurements, their transcellular transport was investigated in transwell transport assays (Fig. 5). When following time dependent accumulation of CB or SR101 in the apical compartment of the transwells, vectorial transport in MRP2-OATP1B1 double transfected cells was detected for both substrates (Fig. 5A-B). Interestingly, although we detected ABCG2-mediated transport of CB in IOVs, transcellular transport activity in ABCG2-OATP1B1 cells could not be observed (Fig. 5A). Transcellular transport of CB and SR101 in the A-B direction was negligible (Fig. 5C), and inhibitory measurements performed with these dyes also confirmed OATP1B1- and MRP2-mediated transport of CB and SR101 (Fig. 5D).

4. Discussion

Concerted action of hepatic uptake (OATP) and efflux transporters (ABCC2 and ABCG2) is crucial in pharmacokinetics and in the disposition of therapeutic drugs and endogenous substances. Consequently, simultaneous administration of transporter substrates can lead to altered pharmacokinetics and undesired side effects. Therefore, international regulations require the evaluation of OATP1B1/3 and ABCG2 (and also potentially MRP2) during early

phases of drug development.

Polarized cell lines engineered to overexpress both uptake and efflux transporters are an accepted *in vitro* model of transepithelial transport measurements. MDCKII cells co-expressing OATP1B and MRP2 or OATP1B and ABCG2 have been used in numerous studies for the measurement of vectorial transport of common OATP and ABC transporter substrates (Cui et al., 2001; Fahrmayr et al., 2012; Matsushima et al., 2005). Double-transfected cell lines allow the identification of dual substrates (especially when the test compound cannot enter the cells without the contribution of an uptake transporter) and also the determination of the involvement of transporters in the transcellular transport (Matsushima, 2005; Sasaki, 2002). MDCKII cells co-expressing OATP and ABC transporters are also used to investigate DDIs mediated by these transporters (Cui et al., 2001; Fahrmayr et al., 2012; Liu et al., 2006; Matsushima et al., 2005).

Considering their overlapping substrate specificities, OATP1Bs, MRP2 and ABCG2 may also share common fluorescent substrates. Indeed, several mutual fluorescent probes were reported (e.g. FMTX Gui et al., 2010; Notenboom et al., 2005), cholyl-lysyl-fluorescein (Barber et al., 2015; de Waart et al., 2010) or carboxy-dichloro-fluorescein derivatives (Heredi-Szabo et al., 2008)). Although separate studies have identified common fluorescent substrates of MRP2 and OATP1Bs, these were not tested in double transfectants for vectorial transport. The only exception is Fluo-3 that has been used in transcellular transport experiments to investigate MRP2 and OATP1B3 function (Cui et al., 2001). However, Fluo-3 is not transported by the major hepatic OATP, OATP1B1 (Izumi et al., 2016), and application of fluorescent probes for dual investigation of ABCG2 and OATP1B function have not yet been documented. One crucial difference between an ideal probe substrate of uptake or efflux transporters is membrane permeability. Uptake transporters require substrates with low membrane permeability, while optimal efflux transporter substrates have high levels of passive uptake (at least in measurements performed on intact cells) (Bednarczyk, 2010; Gui et al., 2010; Kovacsics et al., 2017; Patik et al., 2018; Szakacs et al., 2008; Yamaguchi et al., 2006). However, shared substrates of uptake and efflux transporters can be identified using double transfected polarized cells, or in transport experiments using IOVs. IOVs allow the measurement of intravesicular accumulation of cell impermeable dyes by inversely oriented efflux transporters, and represent a faster and cheaper screening method compared to the transcellular transport assay. Hence, in our current work, the initial transport screens of the previously identified cell impermeable fluorescent OATP probes, and the novel dye substrate pyranine (Fig. 1B), were performed on IOVs containing MRP2 or ABCG2. First, in order to find an alternative for CB, we tested pyranine for transport by hepatic OATPs (Fig. 1B). We found that although pyranine is a lower affinity substrate compared to CB (pyranine K_m values for OATP1B1, OATP1B3 and OATP2B1 were 27.8, 92.2 and 65.6 μM , respectively, vs. CB K_m values were 2.6, 21 and 21 μM (Patik, 2018)), its transport by all three OATPs is about 3-times higher than that of CB. Therefore, we conclude that pyranine can be an excellent tool to investigate hepatic OATP function.

The IOV-based transport screen identified the hitherto undescribed transport of ZV, LDG, pyranine, SR101 and CB by MRP2, and LDV and CB transport by ABCG2 (Fig. 2). Interestingly, SR101 has been previously identified as a transported substrate of an MRP-like fish and rat transporter (Miller et al., 2002, 2000). However, direct interaction of this dye with human MRP2 has not yet been documented. After the IOV screen, the novel substrates were tested in OATP1B1-MRP2 double transfected MDCKII cells for basolateral to apical transport, which confirmed pyranine, CB and SR101 as dual probes of OATP1B1 and MRP2 (Figs. 4 and 5). In these experiments fluorescein-methotrexate, a previously identified substrate of both OATP1B1 and MRP2 served as positive control (Gui et al., 2010; Notenboom et al., 2005). Vectorial transport could be inhibited by known OATP MRP2 inhibitors, indicating that these fluorescent probes can be used for assessing drug

interactions with OATP1B or MRP2.

Although CB transport was very low in MRP2 and ABCG2 containing IOVs, we still detected significant transport of this dye in double transfected MDCKII-MRP2-OATP1B1 cells. However, although expression and function of both OATP1B1 and ABCG2 was confirmed in the double transfected MDCKII cell line (Fig. 3A-B), we could not detect any transcellular transport of CB (Fig. 5A). These discrepancies can be explained by the conversion of CB in the cells (but not in IOVs) into a metabolite that is a higher affinity substrate of MRP2 than CB, but not recognized anymore by ABCG2. Mass spectrometry studies analyzing CB extruded from MDCKII-MRP2-OATP1B1 cells may clarify this issue. These results underline the relevance of cell-based assays, which are influenced by the intracellular metabolism of compounds that are also relevant in physiological drug transporter and drug-drug interactions.

Finally, since dual probes of OATP1B1 and ABCG2 suitable for transcellular transport measurements have not been identified, we also tested the transport of LDV, identified here as a substrate for ABCG2 (Fig. 2C). However, these experiments also failed to detect any vectorial transport in MDCKII-ABCG2-OATP1B1 cells (not shown). In addition, as LY has been described as a substrate of zebrafish drOatp1d1 (Faltermann et al., 2016), and our IOV experiments (Fig. 2D) showed high level of uptake of this compound by ABCG2, we tested LY transport in MDCKII-OATP1B1 cells. However, we found no detectable OATP1B1-mediated uptake of this compound (not shown), therefore LY was also excluded as a dual OATP1B1/ABCG2 probe. Although our efforts failed to set up an assay for vectorial transport of potential dual OATP1B1 and ABCG2 probes, LDV and CB can still be used to detect ABCG2 drug interactions in vesicular transport studies. As demonstrated in Fig. 6, uptake of these dyes in IOVs is inhibited in the presence of Ko143, a specific ABCG2 inhibitor (Fig. 6).

Although cell lines engineered to overexpress pairs of uptake and efflux transporter or even metabolic enzymes are an accepted model of *in vitro* drug interaction screens, to recapitulate *in vivo* conditions more complex models, e.g. human derived hepatocytes are needed. The dual OATP MRP2 substrates identified in our study are good candidates to monitor the function and drug interactions of these transporters in hepatocytes. Due to their low passive permeability, practically no uptake of pyranine, CB or SR101 is observed in mock transfected cells (Fig. 1B, and see also in Bakos et al., 2019; Patik et al., 2018), predicting low unspecific labeling in cellular assays/experiments. On the other hand, a plethora of transporters is present in hepatocytes, some of which may be involved in the uptake or efflux of these dyes. Based on our experiments, ABCG2 will not influence elimination of these dyes from the cells. In addition, based on our preliminary experiments performed with IOVs containing human ABCB1 (P-gp), no interaction with pyranine, CB or SR101 can be expected (not shown). However, it cannot be excluded that other ABC transporters, e.g. MRP3 (ABCC3), MRP4 (ABCC4), expressed in the sinusoidal membranes of hepatocytes, recognize these dyes and will limit their cellular accumulation. Similarly, the interaction of the fluorescent dyes with other solute carriers (SLCs) cannot be excluded. Future work will address the applicability of the fluorescence assays in more complex models. For example, toxicity of the test substrates may limit the applicability of these dyes in hepatocytes. However, when we investigated this issue in MDCKII cells we found no significant toxicity (Supplementary Fig. S2).

In conclusion we identify dual OATP1B1 MRP2 fluorescent probes, and also novel fluorescent substrates of ABCG2. To our best knowledge, pyranine, CB and SR101 are the first dual probes that can be applied for determining in a single, fluorescence-based assay the activity of OATP1B1 and MRP2 and for evaluating the DDI potential of drug candidates.

Authors' contribution

Virág Székely: performed the experiments, analyzed the data, helped in original draft preparation Izabel Patik: performed the

experiments, contributed to the design of the experiments, **Orsolya Ungvári**: performed the experiments, analyzed data **Ágnes Telbisz**: performed the experiments, helped in reviewing and editing the manuscript **Gergely Szakács**: helped in reviewing and editing the manuscript, **Éva Bakos**: Supervision, writing, original draft preparation **Csilla Özvegy-Laczka**: conceptualization, writing.

Declaration of Competing Interest

None.

Acknowledgements

This work has been supported by a research grant from the National Research, Development and Innovation Office [OTKA FK 128751]. Cs. Ö-L. is a recipient of the János Bolyai fellowship of the Hungarian Academy of Sciences.

Supplementary materials

Supplementary material associated with this article can be found, in the online version, at doi:10.1016/j.ejps.2020.105395.

References

Allen, J.D., van Loevezijn, A., Lakhai, J.M., van der Valk, M., van Tellingen, O., Reid, G., Schellens, J.H., Koomen, G.J., Schinkel, A.H., 2002. Potent and specific inhibition of the breast cancer resistance protein multidrug transporter in vitro and in mouse intestine by a novel analogue of fumitremorgin C. *Mol. Cancer Ther.* 1, 417–425.

Avnir, Y., Barenholz, Y., 2005. pH determination by pyranine: medium-related artifacts and their correction. *Anal. Biochem.* 347, 34–41.

Badee, J., Achour, B., Rostami-Hodjegan, A., Galetin, A., 2015. Meta-analysis of expression of hepatic organic anion-transporting polypeptide (OATP) transporters in cellular systems relative to human liver tissue. *Drug Metab. Disposition Biol. Fate Chem.* 43, 424–432.

Bakos, E., Evers, R., Sinko, E., Varadi, A., Borst, P., Sarkadi, B., 2000. Interactions of the human multidrug resistance proteins MRP1 and MRP2 with organic anions. *Mol. Pharmacol.* 57, 760–768.

Bakos, E., Nemet, O., Patik, I., Kucsma, N., Varady, G., Szakacs, G., Ozvegy-Laczka, C., 2019. A novel fluorescence-based functional assay for human OATP1A2 and OATP1C1 identifies interaction between third generation P-gp inhibitors and OATP1A2. *FEBS J.*

Barber, J.A., Stahl, S.H., Summers, C., Barrett, G., Park, B.K., Foster, J.R., Kenna, J.G., 2015. Quantification of drug-induced inhibition of canalicular Chylol-L-Lysyl-fluorescein excretion from hepatocytes by high content cell imaging. *Toxicol. Sci.* 148, 48–59.

Bednarczyk, D., 2010. Fluorescence-based assays for the assessment of drug interaction with the human transporters OATP1B1 and OATP1B3. *Anal. Biochem.* 405, 50–58.

Cantz, T., Nies, A.T., Brom, M., Hofmann, A.F., Keppler, D., 2000. MRP2, a human conjugate export pump, is present and transports fluo 3 into apical vacuoles of Hep G2 cells. *Am. J. Physiol. Gastrointest. Liver Physiol.* 278, G522–G531.

Clement, N.R., Gould, J.M., 1981. Pyranine (8-hydroxy-1,3,6-pyrenetrisulfonate) as a probe of internal aqueous hydrogen ion concentration in phospholipid vesicles. *Biochemistry* 20, 1534–1538.

Cui, Y., Konig, J., Keppler, D., 2001. Vectorial transport by double-transfected cells expressing the human uptake transporter SLC21A8 and the apical export pump ABCG2. *Mol. Pharmacol.* 60, 934–943.

Dawson, P.A., Lan, T., Rao, A., 2009. Bile acid transporters. *J. Lipid Res.* 50, 2340–2357.

de Waart, D.R., Hausler, S., Vlaming, M.L., Kunne, C., Hanggi, E., Gruss, H.J., Oude Elferink, R.P., Stieger, B., 2010. Hepatic transport mechanisms of chylol-L-lysyl-fluorescein. *J. Pharmacol. Exp. Ther.* 334, 78–86.

Deng, F., Sjostedt, N., Kidron, H., 2016. The effect of albumin on MRP2 and BCRP in the vesicular transport assay. *PLoS One* 11, e0163886.

Doyle, L.A., Yang, W., Abruzzo, L.V., Krogmann, T., Gao, Y., Rishi, A.K., Ross, D.D., 1998. A multidrug resistance transporter from human MCF-7 breast cancer cells. *PNAS* 95, 15665–15670.

Fahrmayr, C., Konig, J., Auge, D., Mieth, M., Fromm, M.F., 2012. Identification of drugs and drug metabolites as substrates of multidrug resistance protein 2 (MRP2) using triple-transfected MDCK-OATP1B1-UGT1A1-MRP2 cells. *Br. J. Pharmacol.* 165, 1836–1847.

Faltermann, S., Pretot, R., Pernthaler, J., Fent, K., 2016. Comparative effects of nodularin and microcystin-LR in zebrafish: 1. Uptake by organic anion transporting polypeptide Oatp1d1 (Slco1d1). *Aquat. Toxicol.* 171, 69–76.

Gan, B.S., Krump, E., Shrode, L.D., Grinstein, S., 1998. Loading pyranine via purinergic receptors or hypotonic stress for measurement of cytosolic pH by imaging. *Am. J. Physiol.* 275, C1158–C1166.

Giacomini, K.M., Balimane, P.V., Cho, S.K., Eadon, M., Edeki, T., Hillgren, K.M., Huang, S.M., Sugiyama, Y., Weitz, D., Wen, Y., Xia, C.Q., Yee, S.W., Zimdahl, H., Niemi, M.,

International Transporter, C., 2013. International transporter consortium commentary on clinically important transporter polymorphisms. *Clin. Pharmacol. Ther.* 94, 23–26.

Giacomini, K.M., Huang, S.M., 2013. Transporters in drug development and clinical pharmacology. *Clin. Pharmacol. Ther.* 94, 3–9.

Giacomini, K.M., Huang, S.M., Tweedie, D.J., Benet, L.Z., Brouwer, K.L., Chu, X., Dahlin, A., Evers, R., Fischer, V., Hillgren, K.M., Hoffmaster, K.A., Ishikawa, T., Keppler, D., Kim, R.B., Lee, C.A., Niemi, M., Polli, J.W., Sugiyama, Y., Swaan, P.W., Ware, J.A., Wright, S.H., Yee, S.W., Zamek-Gliszczynski, M.J., Zhang, L., 2010. Membrane transporters in drug development. *Nat. Rev. Drug Discov.* 9, 215–236.

Gui, C., Obaidat, A., Chaguturu, R., Hagenbuch, B., 2010. Development of a cell-based high-throughput assay to screen for inhibitors of organic anion transporting polypeptides 1B1 and 1B3. *Curr. Chem. Genomics* 4, 1–8.

Hagenbuch, B., Stieger, B., 2013. The SLCO (former SLC21) superfamily of transporters. *Mol. Aspects Med.* 34, 396–412.

Heredi-Szabo, K., Kis, E., Molnar, E., Gyorfi, A., Krajcsi, P., 2008. Characterization of 5(6)-carboxy-2',7'-dichlorofluorescein transport by MRP2 and utilization of this substrate as a fluorescent surrogate for LTC4. *J. Biomol. Screen* 13, 295–301.

Heyes, N., Kapoor, P., Kerr, I.D., 2018. Polymorphisms of the multidrug Pump ABCG2: a systematic review of their effect on protein expression, function, and drug pharmacokinetics. *Drug Metab. Disposition Biol. Fate Chem.* 46, 1886–1899.

Hirano, M., Maeda, K., Matsushima, S., Nozaki, Y., Kusuhara, H., Sugiyama, Y., 2005. Involvement of BCRP (ABCG2) in the biliary excretion of pitavastatin. *Mol. Pharmacol.* 68, 800–807.

Hirouchi, M., Kusuhara, H., Onuki, R., Ogilvie, B.W., Parkinson, A., Sugiyama, Y., 2009. Construction of triple-transfected cells [organic anion-transporting polypeptide (OATP) 1B1/multidrug resistance-associated protein (MRP) 2/MRP3 and OATP1B1/MRP2/MRP4] for analysis of the sinusoidal function of MRP3 and MRP4. *Drug Metab. Disposition Biol. Fate Chem.* 37, 2103–2111.

Hollo, Z., Homolya, L., Davis, C.W., Sarkadi, B., 1994. Calcein accumulation as a fluorometric functional assay of the multidrug transporter. *Biochim. Biophys. Acta* 1191, 384–388.

Hooijberg, J.H., Broxterman, H.J., Kool, M., Assaraf, Y.G., Peters, G.J., Noordhuis, P., Scheper, R.J., Borst, P., Pinedo, H.M., Jansen, G., 1999. Antifolate resistance mediated by the multidrug resistance proteins MRP1 and MRP2. *Cancer Res.* 59, 2532–2535.

Horsey, A.J., Cox, M.H., Sarwat, S., Kerr, I.D., 2016. The multidrug transporter ABCG2: still more questions than answers. *Biochem. Soc. Trans.* 44, 824–830.

Izumi, S., Nozaki, Y., Komori, T., Takenaka, O., Maeda, K., Kusuhara, H., Sugiyama, Y., 2016. Investigation of fluorescein derivatives as substrates of organic anion transporting polypeptide (OATP) 1B1 to develop sensitive fluorescence-based OATP1B1 inhibition assays. *Mol. Pharm.* 13, 438–448.

Jedlitschky, G., Hoffmann, U., Kroemer, H.K., 2006. Structure and function of the MRP2 (ABCC2) protein and its role in drug disposition. *Expert Opin. Drug Metab. Toxicol.* 2, 351–366.

Jetter, A., Kullak-Ublick, G.A., 2019. Drugs and hepatic transporters: a review. *Pharmacol. Res.* 104234.

Kimoto, E., Yoshida, K., Balogh, L.M., Bi, Y.A., Maeda, K., El-Kattan, A., Sugiyama, Y., Lai, Y., 2012. Characterization of organic anion transporting polypeptide (OATP) expression and its functional contribution to the uptake of substrates in human hepatocytes. *Mol. Pharm.* 9, 3535–3542.

Kitamura, S., Maeda, K., Wang, Y., Sugiyama, Y., 2008. Involvement of multiple transporters in the hepatobiliary transport of rosuvastatin. *Drug Metab. Disposition Biol. Fate Chem.* 36, 2014–2023.

Kock, K., Brouwer, K.L., 2012. A perspective on efflux transport proteins in the liver. *Clin. Pharmacol. Ther.* 92, 599–612.

Konig, J., Cui, Y., Nies, A.T., Keppler, D., 2000. A novel human organic anion transporting polypeptide localized to the basolateral hepatocyte membrane. *Am. J. Physiol. Gastrointest. Liver Physiol.* 278, G156–G164.

Konig, J., Nies, A.T., Cui, Y., Leier, I., Keppler, D., 1999. Conjugate export pumps of the multidrug resistance protein (MRP) family: localization, substrate specificity, and MRP2-mediated drug resistance. *Biochim. Biophys. Acta* 1461, 377–394.

Kovacsics, D., Patik, I., Ozvegy-Laczka, C., 2017. The role of organic anion transporting polypeptides in drug absorption, distribution, excretion and drug-drug interactions. *Expert Opin. Drug Metab. Toxicol.* 13, 409–424.

Kullak-Ublick, G.A., Ismail, M.G., Stieger, B., Landmann, L., Huber, R., Pizzagalli, F., Fattinger, K., Meier, P.J., Hagenbuch, B., 2001. Organic anion-transporting polypeptide B (OATP-B) and its functional comparison with three other OATPs of human liver. *Gastroenterology* 120, 525–533.

Lee, C.A., O'Connor, M.A., Ritchie, T.K., Galetin, A., Cook, J.A., Ragueneau-Majlessi, I., Ellens, H., Feng, B., Taub, M.E., Paine, M.F., Polli, J.W., Ware, J.A., Zamek-Gliszczynski, M.J., 2015. Breast cancer resistance protein (ABCG2) in clinical pharmacokinetics and drug interactions: practical recommendations for clinical victim and perpetrator drug-drug interaction study design. *Drug Metab. Disposition Biol. Fate Chem.* 43, 490–509.

Link, E., Parish, S., Armitage, J., Bowman, L., Heath, S., Matsuda, F., Gut, I., Lathrop, M., Collins, R., 2008. SLCO1B1 variants and statin-induced myopathy—a genome-wide study. *N. Engl. J. Med.* 359, 789–799.


Liu, L., Cui, Y., Chung, A.Y., Shitara, Y., Sugiyama, Y., Keppler, D., Pang, K.S., 2006. Vectorial transport of enalapril by Oatp1a1/Mrp2 and OATP1B1 and OATP1B3/MRP2 in rat and human livers. *J. Pharmacol. Exp. Ther.* 318, 395–402.

Liu, Y.H., Di, Y.M., Zhou, Z.W., Mo, S.L., Zhou, S.F., 2010. Multidrug resistance-associated proteins and implications in drug development. *Clin. Exp. Pharmacol. Physiol.* 37, 115–120.

Maliepaard, M., Scheffer, G.L., Faneyte, I.F., van Gastelen, M.A., Pijnburg, A.C., Schinkel, A.H., van De Vijver, M.J., Scheper, R.J., Schellens, J.H., 2001. Subcellular

- localization and distribution of the breast cancer resistance protein transporter in normal human tissues. *Cancer Res.* 61, 3458–3464.
- Mao, Q., Unadkat, J.D., 2015. Role of the breast cancer resistance protein (BCRP/ABCG2) in drug transport—an update. *AAPS J.* 17, 65–82.
- Mathew, G., Timm Jr., E.A., Sotomayor, P., Godoy, A., Montecinos, V.P., Smith, G.J., Huss, W.J., 2009. ABCG2-mediated DyeCycle Violet efflux defined side population in benign and malignant prostate. *Cell Cycle* 8, 1053–1061.
- Matsuo, H., Takada, T., Ichida, K., Nakamura, T., Nakayama, A., Ikebuchi, Y., Ito, K., Kusanagi, Y., Chiba, T., Tadokoro, S., Takada, Y., Oikawa, Y., Inoue, H., Suzuki, K., Okada, R., Nishiyama, J., Domoto, H., Watanabe, S., Fujita, M., Morimoto, Y., Naito, M., Nishio, K., Hishida, A., Wakai, K., Asai, Y., Niwa, K., Kamakura, K., Nonoyama, S., Sakurai, Y., Hosoya, T., Kanai, Y., Suzuki, H., Hamajima, N., Shinomiya, N., 2009. Common defects of ABCG2, a high-capacity urate exporter, cause gout: a function-based genetic analysis in a Japanese population. *Sci. Transl. Med.* 1, 5ra11.
- Matsushima, S., Maeda, K., Kondo, C., Hirano, M., Sasaki, M., Suzuki, H., Sugiyama, Y., 2005. Identification of the hepatic efflux transporters of organic anions using double-transfected Madin-Darby canine kidney II cells expressing human organic anion-transporting polypeptide 1B1 (OATP1B1)/multidrug resistance-associated protein 2, OATP1B1/multidrug resistance 1, and OATP1B1/breast cancer resistance protein. *J. Pharmacol. Exp. Ther.* 314, 1059–1067.
- Miller, D.S., Graeff, C., Droule, L., Fricker, S., Fricker, G., 2002. Xenobiotic efflux pumps in isolated fish brain capillaries. *Am. J. Physiol. Regul. Integr. Comp. Physiol.* 282, R191–R198.
- Miller, D.S., Nobmann, S.N., Gutmann, H., Toeroek, M., Drewe, J., Fricker, G., 2000. Xenobiotic transport across isolated brain microvessels studied by confocal microscopy. *Mol. Pharmacol.* 58, 1357–1367.
- Notenboom, S., Miller, D.S., Kuik, L.H., Smits, P., Russel, F.G., Masereeuw, R., 2005. Short-term exposure of renal proximal tubules to gentamicin increases long-term multidrug resistance protein 2 (Abcc2) transport function and reduces nephrotoxicant sensitivity. *J. Pharmacol. Exp. Ther.* 315, 912–920.
- Ozvegy, C., Varadi, A., Sarkadi, B., 2002. Characterization of drug transport, ATP hydrolysis, and nucleotide trapping by the human ABCG2 multidrug transporter. Modulation of substrate specificity by a point mutation. *J. Biol. Chem.* 277, 47980–47990.
- Patel, M., Taskar, K.S., Zamek-Gliszczynski, M.J., 2016. Importance of hepatic transporters in clinical disposition of drugs and their metabolites. *J. Clin. Pharmacol.* 56 (Suppl 7), S23–S39.
- Patik, I., Kovacsics, D., Nemet, O., Gera, M., Varady, G., Stieger, B., Hagenbuch, B., Szakacs, G., Ozvegy-Laczka, C., 2015. Functional expression of the 11 human Organic Anion Transporting Polypeptides in insect cells reveals that sodium fluorescein is a general OATP substrate. *Biochem. Pharmacol.* 98, 649–658.
- Patik, I., Szekely, V., Nemet, O., Szepesi, A., Kucsma, N., Varady, G., Szakacs, G., Bakos, E., Ozvegy-Laczka, C., 2018. Identification of novel cell-impermeant fluorescent substrates for testing the function and drug interaction of Organic Anion-Transporting Polypeptides, OATP1B1/1B3 and 2B1. *Sci. Rep.* 8, 2630.
- Prasad, B., Evers, R., Gupta, A., Hop, C.E., Salphati, L., Shukla, S., Ambudkar, S.V., Unadkat, J.D., 2014. Interindividual variability in hepatic organic anion-transporting polypeptides and P-glycoprotein (ABCB1) protein expression: quantification by liquid chromatography tandem mass spectroscopy and influence of genotype, age, and sex. *Drug Metab. Disposition Biol. Fate Chem.* 42, 78–88.
- Prevoo, B., Miller, D.S., van de Water, F.M., Wever, K.E., Russel, F.G., Flik, G., Masereeuw, R., 2011. Rapid, nongenomic stimulation of multidrug resistance protein 2 (Mrp2) activity by glucocorticoids in renal proximal tubule. *J. Pharmacol. Exp. Ther.* 338, 362–371.
- Roth, M., Obaidat, A., Hagenbuch, B., 2012. OATPs, OATs and OCTs: the organic anion and cation transporters of the SLC0 and SLC22A gene superfamilies. *Br. J. Pharmacol.* 165, 1260–1287.
- Saranko, H., Tordai, H., Telbisz, A., Ozvegy-Laczka, C., Erdos, G., Sarkadi, B., Hegedus, T., 2013. Effects of the gout-causing Q141K polymorphism and a CFTR DeltaF508 mimicking mutation on the processing and stability of the ABCG2 protein. *Biochem. Biophys. Res. Commun.* 437, 140–145.
- Sarkadi, B., Price, E.M., Boucher, R.C., Germann, U.A., Scarborough, G.A., 1992. Expression of the human multidrug resistance cDNA in insect cells generates a high activity drug-stimulated membrane ATPase. *J. Biol. Chem.* 267, 4854–4858.
- Shitara, Y., 2011. Clinical importance of OATP1B1 and OATP1B3 in drug-drug interactions. *Drug Metab. Pharmacokinet.* 26, 220–227.
- Shitara, Y., Itoh, T., Sato, H., Li, A.P., Sugiyama, Y., 2003. Inhibition of transporter-mediated hepatic uptake as a mechanism for drug-drug interaction between cerivastatin and cyclosporin A. *J. Pharmacol. Exp. Ther.* 304, 610–616.
- Siissalo, S., Hannukainen, J., Kolehmainen, J., Hirvonen, J., Kaukonen, A.M., 2009. A Caco-2 cell based screening method for compounds interacting with MRP2 efflux protein. *Eur. J. Pharm. Biopharm.* 71, 332–338.
- Sjostedt, N., van den Heuvel, J., Koenderink, J.B., Kidron, H., 2017. Transmembrane domain single-nucleotide polymorphisms impair expression and transport activity of ABC transporter ABCG2. *Pharm. Res.* 34, 1626–1636.
- Szakacs, G., Varadi, A., Ozvegy-Laczka, C., Sarkadi, B., 2008. The role of ABC transporters in drug absorption, distribution, metabolism, excretion and toxicity (ADME-Tox). *Drug Discov. Today* 13, 379–393.
- Telbisz, A., Muller, M., Ozvegy-Laczka, C., Homolya, L., Szente, L., Varadi, A., Sarkadi, B., 2007. Membrane cholesterol selectively modulates the activity of the human ABCG2 multidrug transporter. *Biochim. Biophys. Acta* 1768, 2698–2713.
- van de Steeg, E., Stranecky, V., Hartmannova, H., Noskova, L., Hrebicek, M., Wagenaar, E., van Esch, A., de Waart, D.R., Oude Elferink, R.P., Kenworthy, K.E., Sticova, E., al-Edreesi, M., Knisely, A.S., Kmoch, S., Jirsa, M., Schinkel, A.H., 2012. Complete OATP1B1 and OATP1B3 deficiency causes human Rotor syndrome by interrupting conjugated bilirubin reuptake into the liver. *J. Clin. Invest.* 122, 519–528.
- Woodward, O.M., Kottgen, A., Coresh, J., Boerwinkle, E., Guggino, W.B., Kottgen, M., 2009. Identification of a urate transporter, ABCG2, with a common functional polymorphism causing gout. *PNAS* 106, 10338–10342.
- Yamaguchi, H., Okada, M., Akitaya, S., Ohara, H., Mikkaichi, T., Ishikawa, H., Sato, M., Matsuura, M., Saga, T., Unno, M., Abe, T., Mano, N., Hishinuma, T., Goto, J., 2006. Transport of fluorescent chenodeoxycholic acid via the human organic anion transporters OATP1B1 and OATP1B3. *J. Lipid Res.* 47, 1196–1202.
- Zhou, S.F., Wang, L.L., Di, Y.M., Xue, C.C., Duan, W., Li, C.G., Li, Y., 2008. Substrates and inhibitors of human multidrug resistance associated proteins and the implications in drug development. *Curr. Med. Chem.* 15, 1981–2039.

A novel fluorescence-based functional assay for human OATP1A2 and OATP1C1 identifies interaction between third-generation P-gp inhibitors and OATP1A2

Éva Bakos¹, Orsolya Német¹, Izabel Patik¹, Nóra Kucsma¹, György Várady², Gergely Szakács^{1,3} and Csilla Özvegy-Laczka¹ 

¹ Membrane Protein Research Group, Institute of Enzymology, Research Centre for Natural Sciences, Hungarian Academy of Sciences, Budapest, Hungary

² Laboratory of Molecular Cell Biology, Institute of Enzymology, Research Centre for Natural Sciences, Hungarian Academy of Sciences, Budapest, Hungary

³ Institute of Cancer Research, Medical University Vienna, Wien, Austria

Keywords

central nervous system; drug interaction screen; fluorescent dye; OATP; P-gp inhibitor

Correspondence

C. Özvegy-Laczka, Membrane Protein Research Group, Institute of Enzymology, Research Centre for Natural Sciences, Hungarian Academy of Sciences, H-1117 Budapest, Magyar tudósok krt. 2., Hungary
 Tel: +3613826789
 E-mail: laczka.csilla@ttk.mta.hu

(Received 24 June 2019, revised 16 October 2019, accepted 22 November 2019)

doi:10.1111/febs.15156

Organic anion-transporting polypeptide 1A2 (OATP1A2), expressed in the human blood–brain barrier, promotes drug uptake from the blood and hence can be exploited for central nervous system-targeted drug delivery. The thyroid transporter OATP1C1, expressed in the choroid plexus and in astrocytes, is also a potential pharmacological target. Based on their established pharmacological relevance, screening the drug interaction profile of OATP1A2 and OATP1C1 is highly desirable. However, drug interaction screens require suitable model systems and functional assays. In the current study, uptake of a set of cell-impermeable fluorescent dyes was screened in HEK-293 and A431 cell lines overexpressing OATP1A2 and OATP1C1. Based on the uptake of fluorescent dye substrates, a functional assay was developed, which was used to characterize OATP inhibitors/substrates. We identify Live/Dead Green (LDG), Live-or-Dye 488, and sulforhodamines 101, G, and B as novel fluorescent substrates of OATP1A2 and OATP1C1. We show that LDG uptake is proportional to OATP1A2/1C1 expression, allowing the isolation of cells expressing high transporter levels. Additionally, dye uptake can be used to characterize the drug interaction pattern of OATP1A2 and OATP1C1. We demonstrate that third-generation P-glycoprotein inhibitors elacridar, tariquidar, and zosuquidar inhibit OATP1A2 function. Increased toxicity of elacridar in OATP1A2-expressing cells suggests that OATP1A2 may modulate the distribution of this compound. The fluorescence-based assays developed in the current study are a good alternative of radioligand-based tests and pave the way toward high-throughput screens for OATP1A2/1C1 drug interaction studies.

Introduction

Treatment of neurological diseases remains unsatisfactory, mostly due to the inadequate penetration of therapeutic agents through the blood–brain barrier

(BBB) [1,2]. Brain permeation of the majority of drugs is influenced by uptake and efflux transporters that are expressed in the membranes of endothelial

Abbreviations

ABC, ATP-binding cassette transporter; AF405, Alexa Fluor 405 dye; BBB, blood–brain barrier; BSP, bromosulphophthalein; CB, Cascade Blue hydrazide; CNS, central nervous system; CP, choroid plexus; CsA, cyclosporin A; DDI, drug–drug interaction; ES, estrone-3-sulfate; LDG, Live/Dead Green; LDV, Live/Dead Violet; LorD488, Live-or-Dye 488; OATP, organic anion-transporting polypeptide; P-gp, P-glycoprotein; SLC, solute carrier; ZV, Zombie Violet dye.

cells of the brain vasculature. An alternative route for drug delivery into the central nervous system (CNS) bypassing the BBB is through the choroid plexus (CP) [3,4]. However, similarly to the BBB, efflux and influx transporters of the CP also control the entry and exit of drugs, nutrients, and signaling molecules into the CNS. Members of the ATP-binding cassette family, including ATP-binding cassette transporter ABCB1 [P-glycoprotein (P-gp), multidrug resistance protein 1], ABCC1 (MRP1), and ABCG2, are the key sentinels of capillary endothelial cells of the BBB and CP epithelial cells [5]. Although various strategies have been developed to evade these transporters in order to increase drug permeation into the CNS, most of the trials failed due to toxic side effects or unpredictable pharmacokinetic consequences [1]. Recently, uptake transporters from the solute carrier (SLC) family have been targeted to promote drug delivery into the CNS. A prominent subgroup of the SLC transporter superfamily present in the BBB as well as the CP is organic anion-transporting polypeptides (OATPs). OATPs are membrane transporters that mediate the cellular entry of large amphipathic molecules in a sodium- and ATP-independent manner. In humans, 11 OATP encoding genes (termed SLCO) have been identified. The major physiological substrates of OATPs are steroid and thyroid hormones, prostaglandins, bile acids, and bilirubin [6]. However, several members of the OATP family, OATPs, 1A2, 1B1/1B3, and 2B1, are multispecific transporters that recognize a large variety of chemically diverse molecules, including not only endogenous substrates but also clinically applied drugs, for example, antivirals, chemotherapeutics, and statins [7,8]. These polyspecific OATPs therefore influence drug absorption, distribution, and toxicity, and have been in the focus of extensive research [9]. In particular, OATP1B1/1B3 has been intensively investigated, given their relevance in hepatic detoxification. The other two polyspecific OATPs, OATP1A2 and OATP2B1, are key determinants of drug absorption from the intestine and also control drug penetration through the BBB [10–12].

OATP1A2 is most abundantly expressed in the luminal side of endothelial cells of the BBB [13]. Additionally, OATP1A2 expression has been shown in neurons [14], in distal nephrons of the kidneys, in ciliary body epithelium [15], in syncytiotrophoblasts, and in cholangiocytes [6]. Although OATP1A2 has also been detected in the intestine, data concerning its relevance in intestinal drug uptake are controversial [10,16]. On the other hand, there is increasing evidence that OATP1A2 plays an important role in

drug penetration into the CNS by regulating drug entry into the BBB endothelial cells [11,17,18] and also in drug absorption/re-absorption in the bile duct and in the kidney [19]. Endogenous substrates of OATP1A2 include bile acids, bilirubin, steroid and thyroid hormones, prostaglandin E₂, and all-trans-retinol [7,19]. In addition, OATP1A2 mediates the cellular intake of numerous chemically unrelated compounds from antihistamines through statins to chemotherapeutic agents [8,12]. OATP1A2 may also be the site of drug–drug or food–drug interactions [11,12,17,19,20].

Compared to the multispecific OATPs, 1A2 and 2B1, OATP1C1 is one of the less characterized OATPs of the CNS. OATP1C1 is a thyroid hormone (T₄, T₄S, and rT₃) transporter, but it also recognizes estrone conjugates [21,22]. OATP1C1 is expressed in the CP [23], in astrocytes (mOatp1c1 [24]), in glial cells [25], and in Leydig cells of the testes [21], and low protein levels in the BBB have also been detected [23]. A recent study has shown that mutation of the SLCO1C1 gene is responsible for juvenile neurodegeneration characterized by hypothyroidism and neurodegeneration due to decreased neuronal T₄ uptake [26]. Therefore, the role of OATP1C1 in thyroid homeostasis of the brain can be far more important than previously thought. Despite its pharmacological relevance, little is known about the substrate recognition pattern or the structure–activity relationships behind the activity of OATP1C1.

The golden standard *in vitro* OATP drug interaction tests rely on radioactively labeled test substrates, for example, estrone-3-sulfate (ES) or estradiol 17 β -D-glucuronide. Recently, various fluorescent substrates have been identified as excellent alternatives of radiotracers in OATP drug interaction tests [27–30]. The general advantages of fluorescence-based assays include sensitivity, safety, and cost-effectiveness. In the case of OATP1B1, OATP1B3, and OATP2B1, several fluorescence-based drug screening assays have been developed. However, such assays for OATP1A2 or OATP1C1 have not yet been established.

In this study, we developed a fluorescence-based assay applicable for measuring the functionality and drug interactions of human OATP1A2 and OATP1C1. We identify a fluorescent viability dye [Live-or-Dye 488 (LorD488)] and sulforhodamines 101, R, and G, as excellent test substrates for OATP1A2 and OATP1C1 drug interaction tests. Using the novel assay, we detect for the first time inhibition of OATP1A2 activity by third-generation P-gp inhibitors elacridar, tariquidar, and zosuquidar.

Results

Increased uptake of fluorescent viability dyes and sulforhodamines in HEK-293 cells overexpressing human OATP1A2 or OATP1C1

Previously, we showed that fluorescent viability dyes such as Zombie Violet (ZV), Live/Dead Green (LDG), Live/Dead Violet (LDV), Cascade Blue hydrazide (CB), and Alexa Fluor 405 (AF405) are excellent substrates of hepatic OATPs [30]. Viability dyes cannot permeate healthy cells, unless the cells express OATP1B1, OATP1B3, or OATP2B1, which promote their cellular accumulation. The fluorescence of these dyes is largely independent of the pH, allowing the design of dedicated transport assays at acidic pH levels, which are often needed for maximum capacity OATP transport [31,32]. Our previous work has failed to identify a dye recognized by OATP1A2, and the interaction of OATP1C1 with viability dyes has never been investigated. Therefore, in the current study, we analyzed the uptake of further cell-impermeable dyes by OATP1A2 and OATP1C1. First, HEK-293 cells overexpressing OATP1A2 or OATP1C1 were generated (Fig. 1A). Using these cell lines, we analyzed the uptake of several viability dyes (LDG, LDV, and LorD488) by flow cytometry.

HEK-293-OATP1A2 and HEK-293-OATP1C1 cells showed LDG uptake, whereas mock-transfected controls remained negative (Fig. 1C). Since LDG is a dead cell marker, we added another viability dye ZV, which is not transported by either OATP1A2 or OATP1C1, to exclude dead cells. Figure 1D shows that a significant fraction of ZV-negative cells were in fact LDG-positive (lower right quadrant), suggesting that increased labeling by LDG is due to OATP1A2- or OATP1C1-mediated uptake, and not by cell death. To substantiate the role of OATP1A2 or OATP1C1 in LDG uptake, LDG-positive HEK-293-OATP1A2 or HEK-293-OATP1C1 cells were isolated by fluorescent cell sorting. Figure 1A,B shows that the sorting defined cells with very high levels of OATP1A2 or OATP1C1 expression. Importantly, high OATP1A2

and OATP1C1 levels were maintained for up to 10 passages (Fig. 1B).

After establishing HEK-293 cells with increased OATP1A2 or OATP1C1 expression, we analyzed the cellular accumulation of a set of viability dyes by these transporters. Figure 2A shows that in addition to LDG, LorD488 shows higher accumulation in OATP1A2- or OATP1C1-expressing cells, and LDV was transported by OATP1C1. In harmony with our previous findings, and in contrast to OATP2B1, AF405 and CB did not accumulate in HEK-293-OATP1A2 cells, but a weak uptake of ZV and LDV could be observed in cells with high OATP1A2 levels. We found that ZV, AF405, and CB are not substrates of OATP1C1.

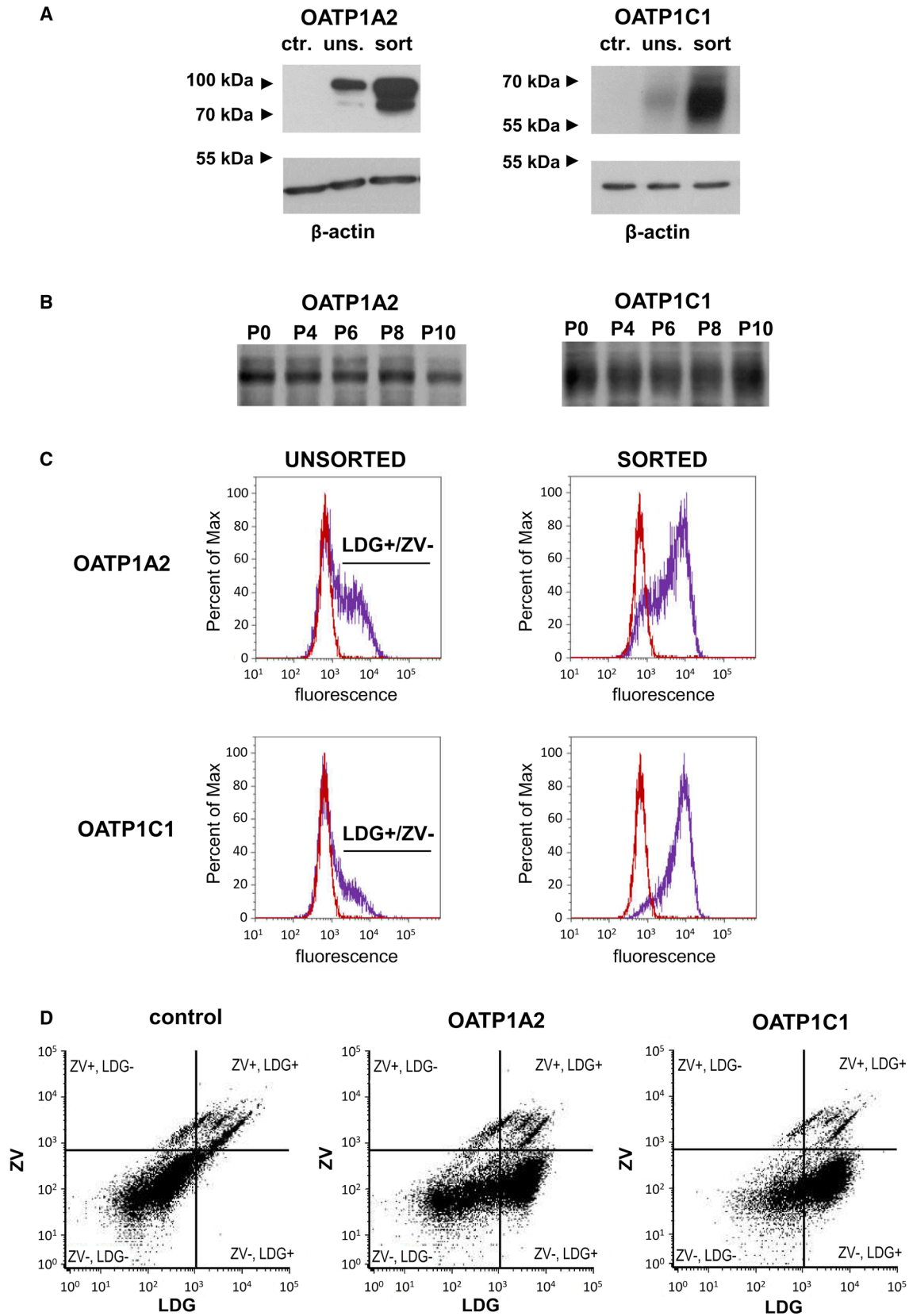
Since the major aim of this study was to establish a fluorescence-based assay for OATP1A2 and OATP1C1, we extended our investigation to sulforhodamines. We tested the uptake of SR101 and its structural analogs sulforhodamine B (SRB) and sulforhodamine G (SRG) by OATP1A2 and OATP1C1 in HEK-293 cells. Figure 2B demonstrates that OATP1C1 transports SR101 and that a moderate transport of SRB and SRG by OATP1C1 could also be detected. Interestingly, we found that SR101, SRB, and SRG are also substrates of OATP1A2, while OATP2B1-expressing cells did not accumulate the SRB and SRG dyes, and only a very weak SR101 transport could be observed (Fig. 2B).

Based on the above measurements, we conclude that LDG, LorD488, SR101, SRB, and SRG are novel substrates of OATP1A2 and OATP1C1, and LDV is transported by OATP1C1. Since neither the structure nor the concentration of LDG and LDV are available, we excluded these dyes from further investigations.

Typical transporter-mediated uptake of LorD488 and SR dyes in HEK-293-OATP1A2 and HEK-293-OATP1C1 cells

OATP-mediated transport is influenced by extracellular pH. Typically, acidic pH results in higher activity [31,32]. In order to find the optimal assay conditions

Fig. 1. Expression and LDG uptake in HEK-293 cells overexpressing human OATP1A2 and OATP1C1. (A, B) Western blot detection of human OATP1A2 or OATP1C1 expressed in HEK-293 cells. 20 μg of total cell lysates was analyzed by Western blot. Control (ctr.) represents mock-transfected HEK-293 cells, either before or after sorting. (B) OATP1A2 and OATP1C1 expression in sorted cells was followed up to 10 passages (P0–P10). Western blots (A and B) were repeated three times, and one representative image is shown from each experiment. (C, D) LDG uptake in HEK-293 cells. Uptake of 0.2 μL LDG in a final volume of 100 μL was measured at 37 $^{\circ}\text{C}$ in uptake buffer with pH 5.5 for 15 min. Intracellular fluorescence was measured by flow cytometry (Attune Acoustic Focusing Cytometer). Dead cells were identified based on ZV (0.1 $\mu\text{L}\cdot\text{mL}^{-1}$) staining. Experiments were repeated three times, and representative dot plots and histograms show the uptake of LDG into HEK-293 cells. Cells with the highest LDG fluorescence (LDG⁺/ZV⁻) were sorted, and after retrieval, they were again measured for LDG uptake (1C right panel). Mock-transfected controls are indicated by red histograms, and OATP1A2- or OATP1C1-expressing cells are labeled by purple histograms.



for the uptake of the newly identified fluorescent dye substrates of OATP1A2 and OATP1C1, we measured dye transport at several extracellular pH levels ranging from pH 5.5 to 8.4. Figure 2 shows that in the case of LorD488, transport activity by OATP1A2 and OATP1C1 was maximal at pH 5.5. Although the pH of the buffer had only a small influence on the uptake of the SR dyes, transport by OATP1A2 was highest at acidic pH, whereas OATP1C1 was most effective at neutral or basic pH levels (Fig. 2C,D). Therefore, further experiments were performed at pH 5.5 for LorD488, while pH 7.4 was used when the SR dyes were analyzed.

Next, we determined the time and concentration dependence of the uptake of LorD488 (at pH 5.5) and the SR dyes (at pH 7.4) by OATP1A2 and OATP1C1. Figures 3 and 4 demonstrate that a typical transporter-mediated uptake can be observed for all four dyes. Interestingly, we found that transport kinetics by the two transporters is similar (Table 1), with slowest

transport and lowest affinity for SRG, and the highest affinity for SR101.

SR dyes and LorD488 are applicable to test substrate/inhibitor interactions of OATP1A2 and OATP1C1

Fluorescent test substrates provide an alternative to radioactive assays for testing OATP drug interactions. In order to check whether the newly identified fluorescent dye substrates are applicable for such purposes, we tested the effect of known/potential interacting molecules on the uptake of these dyes in HEK-293-OATP1A2 and HEK-293-OATP1C1 cells. Figure 5A, B shows that most of the previously identified OATP1A2 substrates/inhibitors inhibit the uptake of the novel fluorescent substrates. Dye uptake in HEK-293-OATP1A2 and HEK-293-OATP1C1 cells can be inhibited by bromosulphophthalein (BSP), cyclosporin A (CsA), taurocholate (TC), ES, and benzbromarone

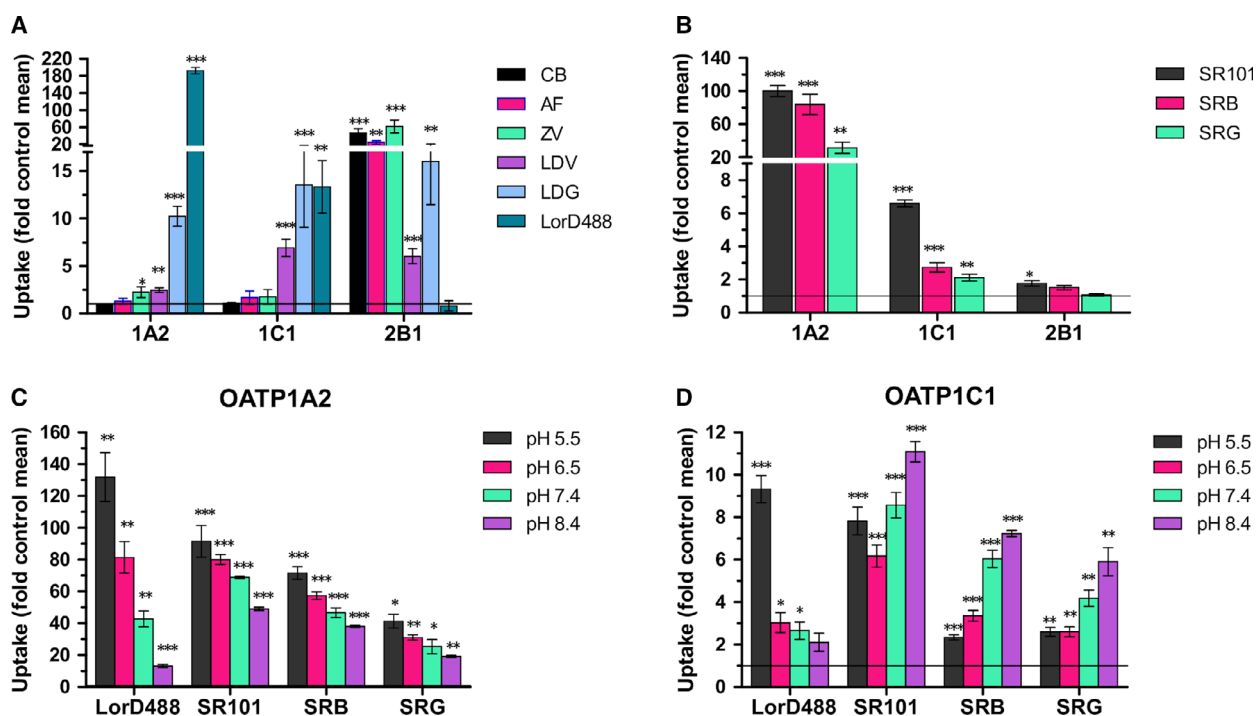


Fig. 2. Screening OATP-mediated transport of viability dyes (A) and sulforhodamines (B) by flow cytometry in HEK-293 cells. Cells were incubated with 0.2 μ L ZV or LDG, 0.5 μ M LorD488, 10 μ M CB, or AF405 (A) and 1 μ M SR101, 4 μ M SRB, or 4 μ M SRG (B) for 15 min at 37 $^{\circ}$ C in uptake buffer (pH 5.5) in final reaction volume of 100 μ L. Fluorescence was measured by flow cytometry. Uptake ratio was calculated by dividing fluorescence measured in OATP cells with mean fluorescence measured in mock-transfected cells. Average \pm SD values are shown, $n = 5$. (C, D) pH dependence of uptake of LorD488 and the SR dyes. HEK-293-OATP1A2 (C) and HEK-293-OATP1C1 (D) cells were incubated with 0.5 μ M LorD488, 1 μ M SR101, 4 μ M SRB, or 4 μ M SRG at 37 $^{\circ}$ C in uptake buffer with pH adjusted to 5.5, 6.5, 7.4, or 8.4. Incubation times applied were as follows: 1A2: LorD488 and SR101: 4 min; SRB and SRG: 15 min, and 1C1: LorD488 and SR101: 10 min; SRB and SRG: 15 min. Cellular fluorescence was determined by flow cytometry. Uptake ratios were calculated by dividing fluorescence measured in OATP cells with mean fluorescence measured in mock-transfected cells. Average \pm SD values are shown ($n = 3$). Statistical analysis was performed by Student's *t*-test (* $P < 0.05$, ** $P < 0.01$, *** $P < 0.001$).

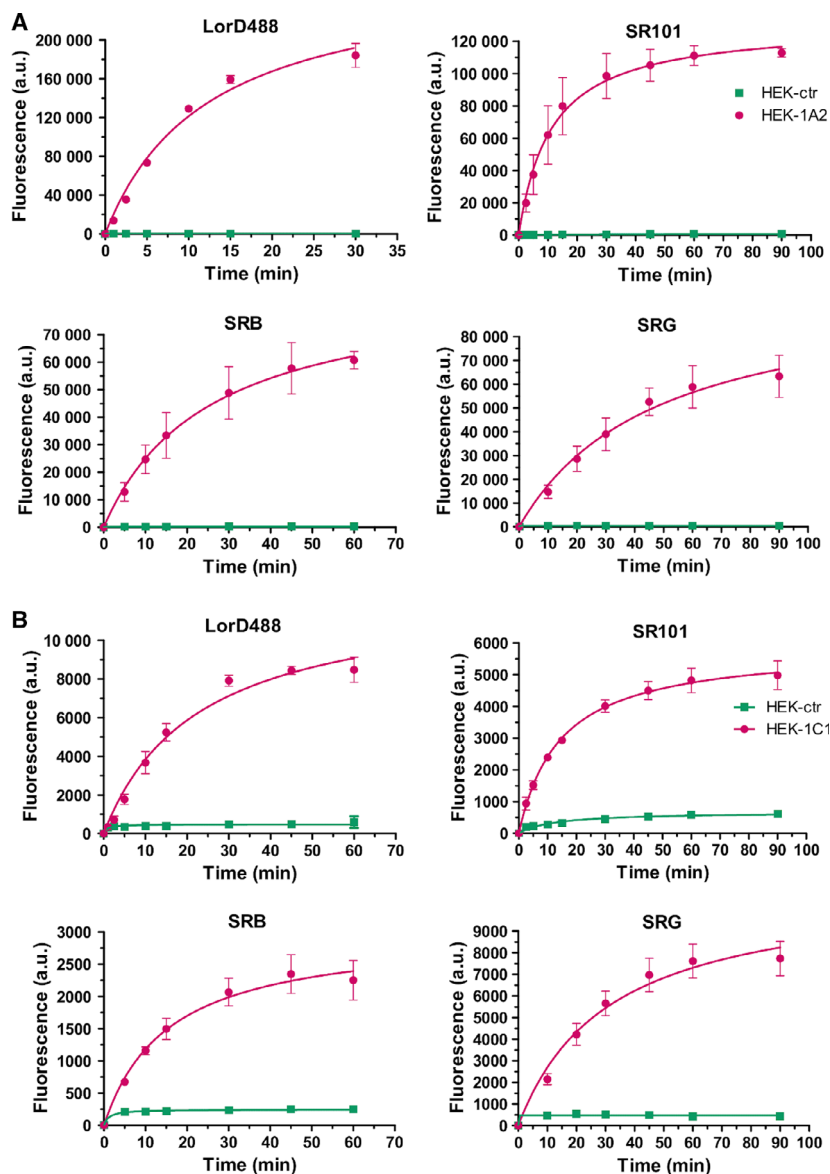


Fig. 3. Time dependence of LorD488 and SR dye uptake in HEK-293 cells overexpressing OATP1A2 or OATP1C1. HEK-293-OATP1A2 (A) and HEK-293-OATP1C1 (B) cells were incubated with 0.5 μM LorD488, 1 μM SR101, 4 μM SRB, or 4 μM SRG in buffer with pH 5.5 (LorD488) or pH 7.4 (SRs) for 30–60–90 min. Mock-transfected cells (HEK-ctr) were used as a control. Fluorescence was measured by flow cytometry. Each point represents the mean value \pm SD ($n = 3$).

[9,33–36]. Benzbromarone is a novel inhibitor of OATP1A2 and OATP1C1 function, and CsA is also a novel inhibitor of OATP1C1.

Drug–drug interaction (DDI) studies were repeated/extended using adherent A431 cells, which, due to their good adherence, are amenable for drug interaction tests in a multiwell plate-based setup [30,37]. A431 cells overexpressing OATP1A2 were generated, and the uptake of the novel fluorescent dye substrates was analyzed in detail using 96-well plates. In this semi high-throughput setup, we found similar kinetics of dye uptake as in HEK-293-OATP1A2 cells (Table 2 and Fig. 6). Moreover, the application of a fluorescent plate reader allowed the determination of transport capacity (V_{max} , see Table 2). Based on the V_{max}/K_m

values, SR101 has the highest OATP1A2-mediated uptake. Although we found high transport of LorD488, and its uptake was efficiently inhibited by known OATP inhibitors, this dye was omitted from further experiments, since its molecular structure is inaccessible.

In order to examine the suitability of the SR dyes as probes for OATP1A2 drug interaction tests, we determined the inhibitory potential of known inhibitors/substrates on SR dye uptake (Fig. 7A). The IC_{50} values obtained in the SR assay were similar to that found for well-established radioactive test compounds (Table 3) indicating that the SR dyes are good alternatives to radioligands.

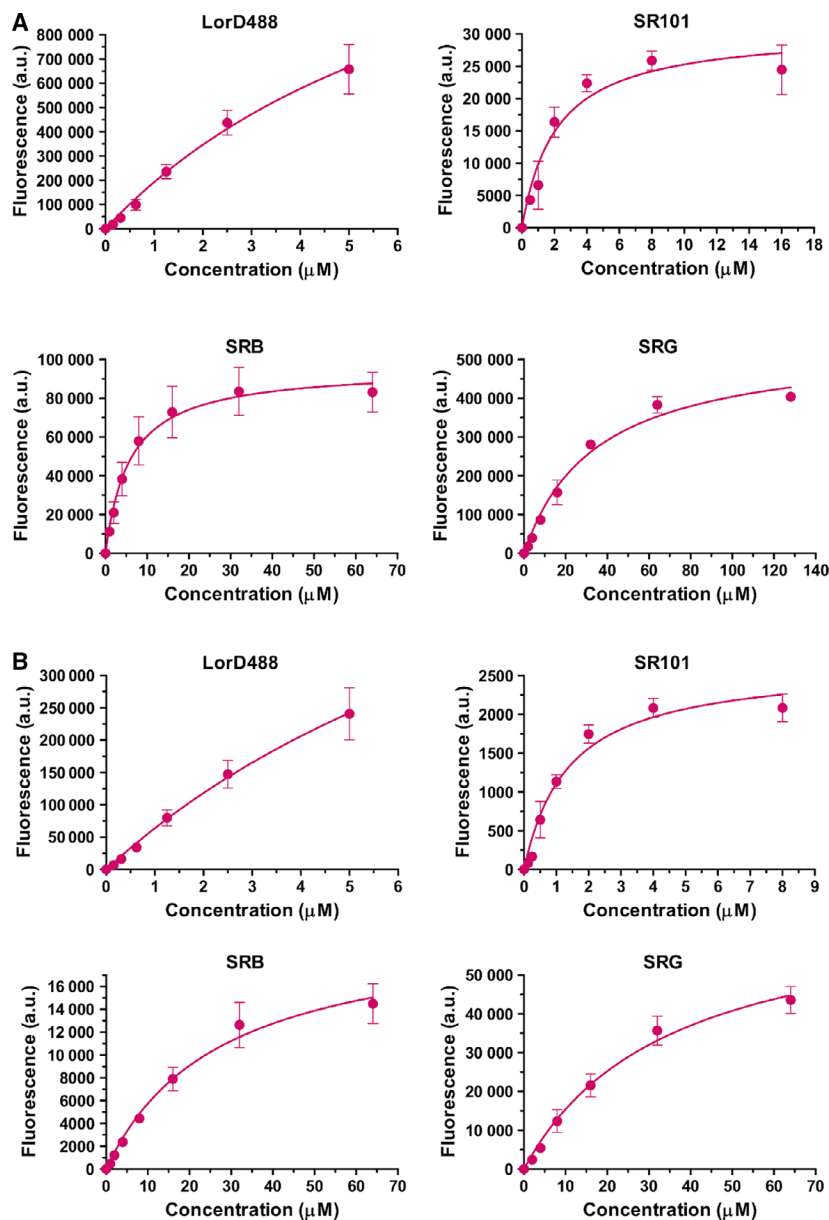


Fig. 4. Concentration dependence of LorD488 and SR dye uptake in HEK-293 cells overexpressing OATP1A2 or OATP1C1. HEK-293-OATP1A2 (A) and HEK-293-OATP1C1 (B) cells were incubated with increasing concentrations of the dyes at 37 °C in buffer with pH 5.5 (LorD488) or pH 7.4 (SRs) in the linear phase of uptake. Incubation times were applied as follows: 1A2: LorD488: 4 min; SR101: 2 min; SRB, SRG: 15 min, and 1C1: LorD488; SR101: 10 min; SRB, SRG: 15 min. Fluorescence was measured by flow cytometry. Transport data were obtained by subtracting the fluorescence in mock cells from that measured in OATP cells. Each point represents the mean value \pm SD ($n = 3$).

Although the expression levels of OATP1A2 and OATP1C1 cannot be compared, OATP1C1 showed a roughly 10-fold lower transport capacity of the fluorescent dyes than OATP1A2 (Fig. 2), and repeated sorting attempts failed to establish A431 cells with high enough expression levels, precluding 96-well plate-based transport measurements. Nevertheless, in order to test whether the SR dyes are also appropriate probes for testing substrate/inhibitor interactions with OATP1C1, we determined the inhibitory kinetics of BSP and ES, which were previously shown to interact with OATP1C1 in HEK-293-OATP1C1 cells (Fig. 7B). We found that the IC_{50} values obtained in the SR dye

assay were similar to those found using [^3H]E $_2$ 17 β G as a test substrate (Table 3).

Considering transport capacity and inhibitor sensitivity, SR101 is an ideal fluorescent substrate for OATP1A2 and OATP1C1 drug interaction tests. In order to test whether SR101 is also recognized by the other multispecific OATPs, 1B1/1B3 (transport by OATP2B1 was negligible, Fig. 2), we investigated SR101 transport in A431 cells overexpressing each of these transporters. Figure 8A shows that an increased uptake of SR101 by OATP1B1/1B3 can be observed as compared to mock-transfected cells or those overexpressing OATP2B1. Moreover, the uptake of SR101

Table 1. Kinetic parameters of OATP1A2- and OATP1C1-mediated LorD488 and SR dye uptake in HEK-293 cells. To determine the time dependence of dye uptake, the cells were incubated with 0.5 μM LorD488, 1 μM SR101, 4 μM SRB, or 4 μM SRG for 60 min in uptake buffer with pH 5.5 (LorD488) or pH 7.4 (SR dyes). The $t_{1/2}$ values were determined by nonlinear regression analysis (Fig. 3). The K_m values were calculated using data shown in Fig. 4.

	$t_{1/2}$ (min)		K_m (μM)	
	OATP1A2	OATP1C1	OATP1A2	OATP1C1
LorD488	12.42 \pm 2.62	24.88 \pm 7.32	8.04 \pm 2.02	11.64 \pm 2.51
SR101	11.06 \pm 0.97	14.51 \pm 0.58	2.14 \pm 0.67	1.39 \pm 0.35
SRB	25.70 \pm 2.25	19.38 \pm 3.90	5.83 \pm 0.68	27.41 \pm 4.51
SRG	37.87 \pm 12.27	33.99 \pm 11.17	34.62 \pm 6.74	34.95 \pm 6.13

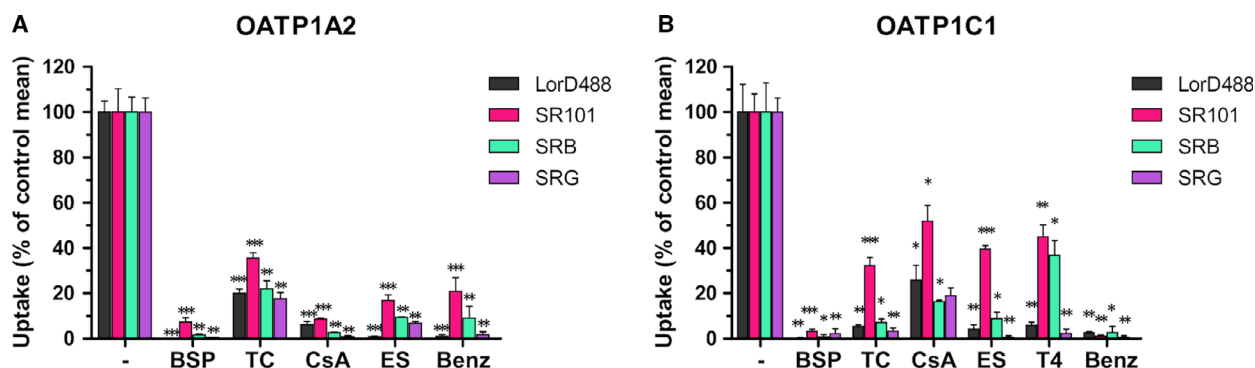


Fig. 5. Inhibition of LorD488 and SR dye uptake in HEK-293 cells overexpressing OATP1A2 (A) or OATP1C1 (B). Transport of 0.5 μM LorD488 (pH 5.5), 1 μM SR101, 2 μM SRB, and 4 μM SRG (pH 7.4) was measured for 10 min (LorD488, SR101) or 15 min (SRB, SRG) at 37 $^{\circ}\text{C}$ in the absence or presence of the investigated compounds. Fluorescence was measured by flow cytometry. Transport was determined by subtracting fluorescence in HEK-293-mock cells. Uptake rates were expressed as percent of the mean uptake measured in the absence of additional compounds. Effect of 100 μM BSP, 150 μM TC, 20 μM CsA, 100 μM ES, 10 μM thioresoxin (T4), and 40 μM benzbromarone (Benz) is shown. Data represent the mean values \pm SD ($n = 3$). Statistical analysis was performed by Student's t -test (* $P < 0.05$, ** $P < 0.01$, *** $P < 0.001$).

Table 2. Kinetic parameters of OATP1A2-mediated LorD488 and SR dye uptake in A431 cells. To determine $t_{1/2}$ values, A431-OATP1A2 cells were incubated with 0.5 μM LorD488, 1 μM SR101, 4 μM SRB, or 4 μM SRG for 60 min in uptake buffer with pH 5.5 (LorD488) or pH 7.4 (SRs). In order to determine K_m values, A431-OATP1A2 cells were incubated with increasing concentrations of dyes in buffer (pH 5.5, LorD488 or pH 7.4, SRs) at the following time: LorD488: 4 min; SR101: 5 min; SRB, SRG: 15 min. The transport values were fitted to the Michaelis–Menten equation, and kinetic parameters were determined using nonlinear regression analysis (Fig. 6). Data were calculated from at least three independent measurements.

	$t_{1/2}$ (min)	K_m (μM)	V_{max} (pmol \cdot min $^{-1}\cdot$ 10 $^{-6}$ cells)	V_{max}/K_m ($\mu\text{L}\cdot$ min $^{-1}\cdot$ 10 $^{-6}$ cells)
LorD488	10.25 \pm 2.15	12.04 \pm 3.52	4.69 \pm 1.06	0.39
SR101	8.70 \pm 1.00	1.87 \pm 0.24	5.94 \pm 0.25	3.18
SRB	21.58 \pm 4.36	4.99 \pm 0.50	3.13 \pm 0.06	0.63
SRG	29.91 \pm 6.98	15.02 \pm 4.91	2.19 \pm 0.25	0.15

by OATP1Bs can be inhibited by known inhibitors, CsA, BSP, and TC (Fig. 8B).

Third-generation P-gp inhibitors interact with OATP1A2

Elacridar (GF120918), tariquidar, and zosuquidar are third-generation P-gp inhibitors [38]. These inhibitors

were aimed to enhance brain distribution of P-gp and ABCG2 substrate drugs, for example, tyrosine kinase inhibitors. Since OATP1A2 and P-gp are both expressed in the BBB at high levels, we investigated whether OATP1A2 may interact with these inhibitors and therefore influence their distribution and availability. Using the SR101 assay, we analyzed the inhibitory potential of elacridar, tariquidar, and zosuquidar on

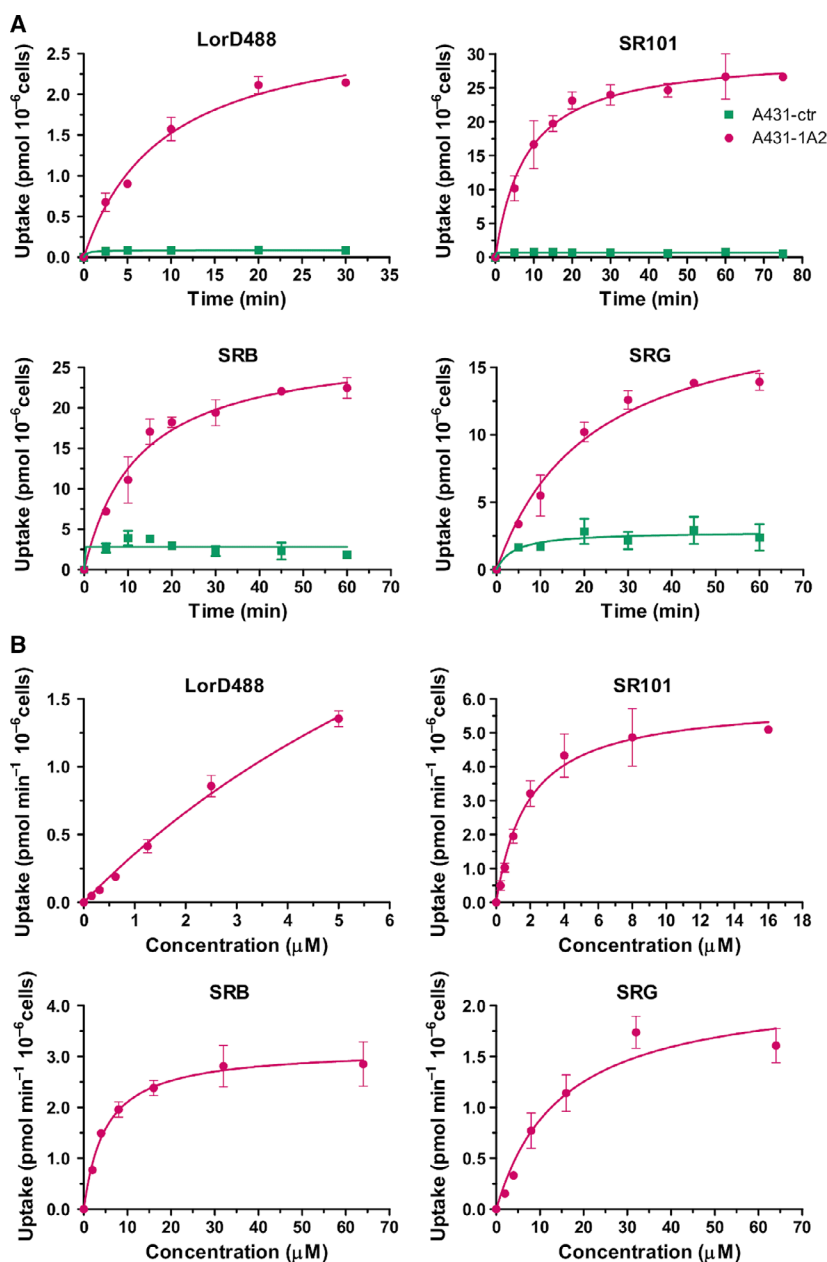


Fig. 6. Time and concentration dependence of LorD488 and SR dye uptake in A431 cells overexpressing OATP1A2. (A) A431-OATP1A2 or mock-transfected cells were incubated with 0.5 μM LorD488, 1 μM SR101, 4 μM SRB, or 4 μM SRG in buffer with pH 5.5 (LorD488) or pH 7.4 (SRs) for 30–60–75 min. (B) A431-OATP1A2 or mock-transfected cells were incubated with increasing concentrations of LorD488 (pH 5.5) or the SR dyes (pH 7.4) for the following time: LorD488: 4 min; SR101: 5 min; SRB, SRG: 15 min. Transport without the background signal (fluorescence in mock-transfected A431 cells) is shown. Fluorescence was measured in an EnSpire plate reader (Ex/Em: LorD488: 488/515 nm; SR101: 586/605 nm; SRB: 565/586 nm; SRG: 531/552 nm). Transport was calculated based on the fluorescence of known amounts of the dyes. Each point represents the mean value \pm SD ($n = 3$).

OATP1A2 function. Figure 9A shows that all three compounds are inhibitors of OATP1A2 function. Since both inhibitors and transported substrates can inhibit the uptake of the labeled test substrates, we investigated the toxicity of the P-gp inhibitors in A431-OATP1A2 cells. We hypothesized that transported substrates may be more toxic to A431-OATP1A2 cells as compared to the parental cell lines [37]. Figure 9B shows that indeed OATP1A2 expression sensitized the cells against elacridar. Compared to mock-transfected cells, a threefold sensitivity can be observed, which can be interpreted by increased uptake of elacridar by

OATP1A2. In the case of tariquidar and zosuquidar, no such effect was observed; therefore, these are most probably inhibitors and not substrates of OATP1A2.

Discussion

OATP1A2 is a multispecific uptake transporter that plays an important role in the distribution of CNS-targeted drugs, such as statins, (D-penicillamine 2,5) encephalin, deltorphin II, and K-strophanthosid [1,39,40]. Therefore, OATP1A2 may be exploited for increased uptake of CNS-targeted drugs, enabling the

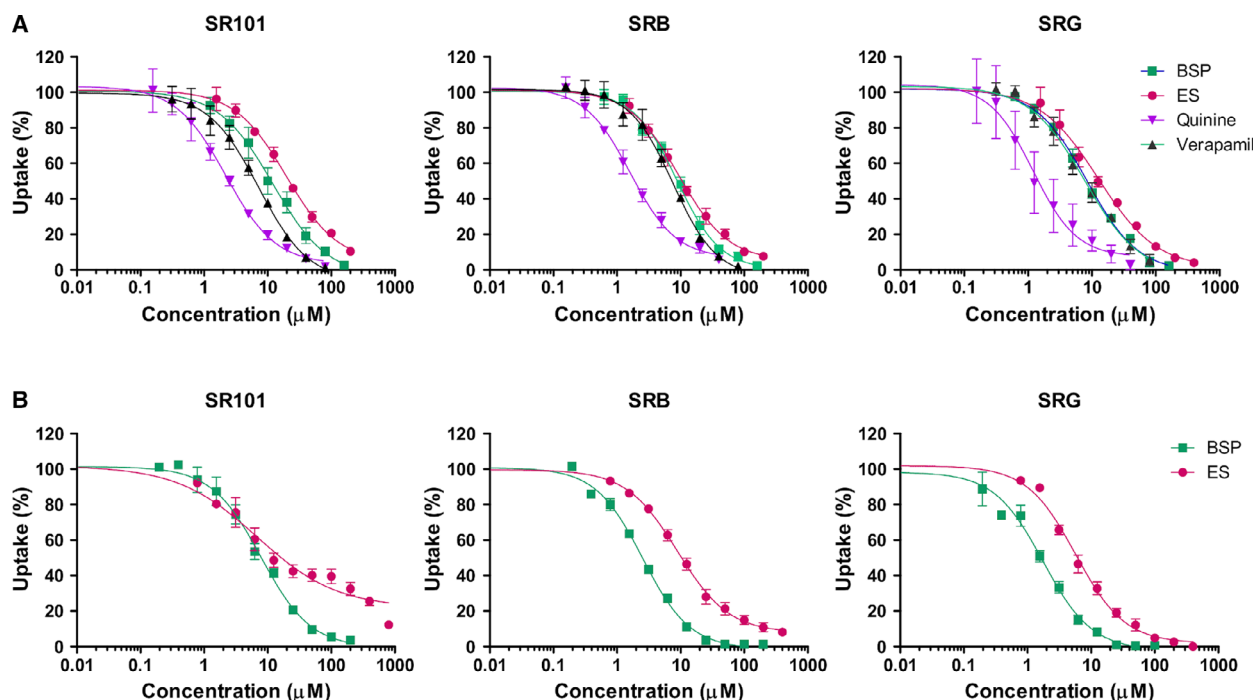


Fig. 7. Concentration-dependent inhibition of SR dye uptake in A431-OATP1A2 (A) or HEK-293-OATP1C1 (B) cells. Uptake of 1 μM SR101, 2 μM SRB, and 4 μM SRG was measured for 10 min (SR101) or 15 min (SRB, SRG) at 37 $^{\circ}\text{C}$ in the presence of increasing concentrations of BSP, ES, quinine, or verapamil. (A) Transport was determined in A431-OATP1A2 cells seeded in 96-well plates. Fluorescence was measured using an EnSpire fluorescent plate reader. (B) Uptake of SRs in HEK-OATP1C1 cells was measured by flow cytometry. Transport was determined by subtracting fluorescence in A431-mock (A) or HEK-293-mock (B) cells. Uptake rates were expressed as percent of the uptake measured in the absence of additional compounds. Data represent the mean values \pm SD ($n = 3$).

Table 3. Comparison of IC_{50} values obtained with the SR dye uptake assay with literature data. IC_{50} (μM) values were determined by nonlinear regression analysis using data shown in Fig. 7. Reported IC_{50} data were obtained in assays using [^3H]-ES, [^3H]-fexofenadine, or [^3H]-estradiol 17 β -D-glucuronide as probe substrates.

	SR101	SRB	SRG	Literature data
OATP1A2				
BSP	12.02 \pm 6.19	8.78 \pm 1.96	8.36 \pm 2.50	3.75 [46]
ES	19.70 \pm 5.92	9.39 \pm 1.73	12.53 \pm 2.73	16 ^a [60]
Quinine	2.18 \pm 0.17	1.62 \pm 0.24	1.20 \pm 0.60	0.7 [61]
Verapamil	7.18 \pm 0.56	7.58 \pm 0.29	7.70 \pm 0.09	2.6 [62]
OATP1C1				
BSP	7.86 \pm 0.87	2.53 \pm 0.27	1.75 \pm 0.56	4.18 ^b [36]
ES	6.57 \pm 2.47	8.93 \pm 1.84	5.74 \pm 1.58	6.63 ^b [36]

^a K_m value of direct transport experiments is shown, when transport inhibition data were not available; ^bIn the lack of inhibitory data for human OATP1C1 data measured for rat Oatp1c1 are shown.

successful treatment of various CNS diseases. On the other hand, since OATP1A2 also transports the neurosteroid DHEAS, modification of its function may influence DHEAS levels in the brain and hence influence neuron excitability [41]. Finally, CNS toxicity of drugs may also be related to OATP1A2-mediated transport, as documented in the case of several OATP1A2 substrates, including methotrexate,

levofloxacin, and microcystins [11]. Hence, OATP1A2-mediated DDIs should be considered upon the co-administration of OATP1A2 substrates [19]. In addition to OATP1A2, the less well-characterized thyroid transporter, OATP1C1, which is responsible for juvenile neurodegeneration [26], can also be a pharmacological target. However, in contrast to numerous studies dealing with the drug interaction pattern of OATP1A2

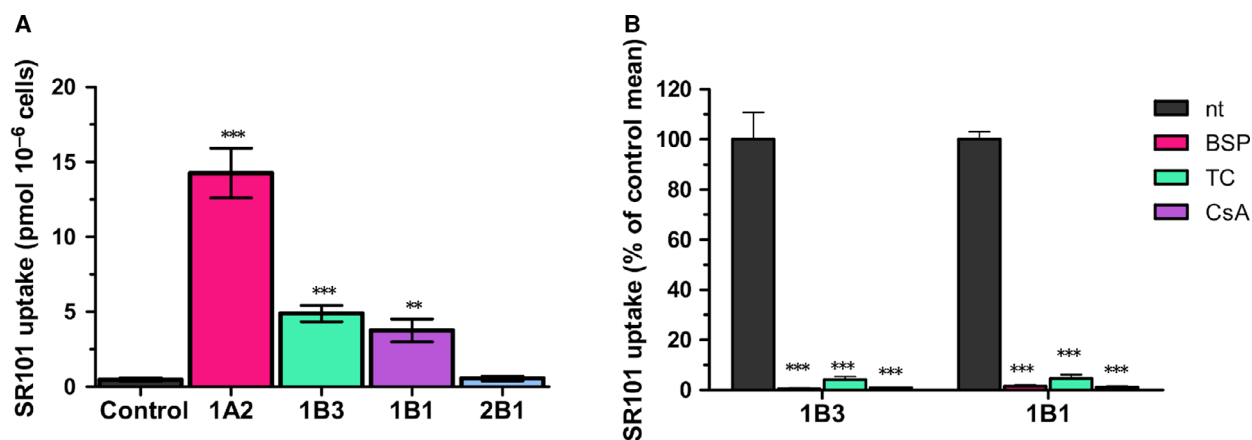


Fig. 8. SR101 uptake and inhibitor sensitivity of SR101 uptake in A431 cells overexpressing OATP1B1 or OATP1B3. (A) Uptake of 1 μ M SR101 (pH 7.4) was measured for 10 min at 37 °C on A431-OATP1A2, A431-OATP1B1, A431-OATP1B3, or A431-OATP2B1 cells seeded on 96-well plates. Fluorescence was measured in an EnSpire fluorescent plate reader. Transport was calculated based on a calibration curve. (B) Inhibition of SR101 uptake in A431-OATP1B1 or OATP1B3 cells. Transport of 1 μ M SR101 (pH 7.4) was measured for 10 min at 37 °C on A431 cells seeded on 96-well plates in the absence (nt) or presence of the investigated compounds. Fluorescence was measured in an EnSpire plate reader. Transport was determined by subtracting fluorescence in A431-mock cells. Uptake rates were expressed as percent of the mean uptake measured in the absence of inhibitors. Effects of 100 μ M BSP, 150 μ M TC, and 20 μ M CsA are shown. Data represent the mean values of three independent measurements \pm SD. Statistical analysis was performed by Student's *t*-test (** P < 0.01, *** P < 0.001).

(reviewed in Ref. [12]), the substrate specificity of OATP1C1 is not fully mapped.

Based on their established pharmacological relevance, screening the drug interaction profile of OATP1A2 and OATP1C1 is highly desirable. However, drug interaction screens require suitable model systems and functional assays. Application of fluorescent molecules as test substrates for drug transporters is a sensitive and cost-effective alternative of radiotracers [28]. Fluorescent assays are already available for the characterization of hepatic OATP1Bs [28–30]. In addition, we have recently identified Na-fluorescein as a general OATP substrate and fluorescein-methotrexate as an OATP1A2 substrate [35]. Unfortunately, due to its pH sensitivity and high passive uptake rate, fluorescein is not an ideal test substrate. Hence, in the current study we went on to screen further fluorescent dyes to develop sensitive assays for OATP1A2 and OATP1C1 drug interaction screens. We tested a panel of fluorescent viability dyes that can only accumulate in live cells as a result of transporter-mediated uptake. Interestingly, cells often do not tolerate forced expression of OATPs [42]. However, we have been able to circumvent this limitation by isolating the LDG⁺ fraction of HEK-293 cells overexpressing OATP1A2 or OATP1C1 (Fig. 1C,D). Establishment of HEK-293 cells with high levels of OATP1A2 or OATP1C1 expression allowed the systematic analysis of fluorescent dye uptake. In addition to cell-impermeable dyes,

we also investigated transport of SR dyes (Fig. 2). To our knowledge, SR transport by human OATPs has never been demonstrated. SR101 is a well-known astrocyte marker that has been previously suggested to be transported by rodent *Oatp1c1* [24,43], and SR101 transport by rodent *Oatp1a1*, *Oatp1a4*, and *Oatp2b1* has been recently demonstrated [44,45]. However, since both substrate/inhibitor recognition and expression patterns of rodent *Oatp1a*-s and human OATP1A2 show striking differences [15,46–48], rodent transporters do not necessarily model uptake mediated by human OATP1A2. For example, BSP, which inhibits most human OATPs (including OATP1A2, see Fig. 7), does not influence SR101 uptake by *Oatp1a4* [45].

We identified LorD488 and LDG as excellent substrates of OATP1A2 and OATP1C1, and also found that LDV is transported by OATP1C1 (Fig. 2A). Additionally, we unambiguously demonstrate that OATP1C1 is an SR101 transporter (Fig. 2B). SR101 is also a substrate of OATP1A2 and the hepatic transporters OATP1B1/1B3 (Figures 2B and 8). Although Tachikawa *et al.* previously found that *Oatp2b1* transports SR101 [44], in our hand SR101 transport by human OATP2B1 was negligible, again demonstrating that data obtained with rodent *Oatp*-s do not always correlate with human OATP data.

Interestingly, while SR101 is a widely applied astrocyte marker, its reliability largely depends on the cerebral region [24,49]. Although astrocytes do not

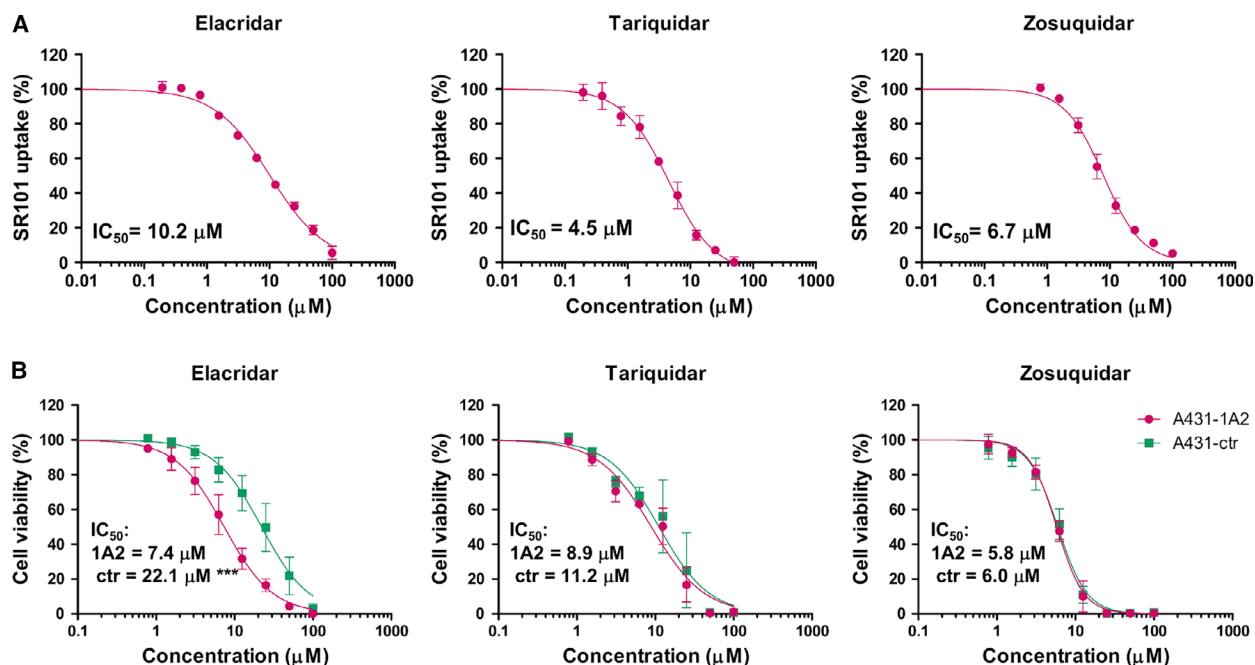


Fig. 9. Effect of third-generation P-gp inhibitors on OATP1A2-mediated transport and cell survival. (A) Inhibition of OATP1A2-mediated SR101 uptake by elacridar, tariquidar, or zosuquidar. Uptake of $1 \mu\text{M}$ SR101 was measured in A431-OATP1A2 cells seeded on 96-well plates for 10 min at 37°C in the presence of increasing concentrations of the P-gp inhibitors. Fluorescence was measured in an EnSpire plate reader. Transport was determined by subtracting fluorescence in A431-mock cells. Uptake rates were expressed as percent of the uptake measured in the absence of any inhibitor. (B) Cytotoxicity of elacridar, tariquidar, or zosuquidar in A431-OATP1A2 cells. A431-OATP1A2 cells and A431-mock cells were treated with increasing concentrations of the P-gp inhibitors followed by determination of cell viability by the SRB assay. IC_{50} values were determined by nonlinear regression analysis using data fitted on data points by the GRAPHPAD PRISM program. Data on the graphs show the average of at least three independent experiments \pm SD values. Statistical analysis was performed by Student's *t*-test (***) $P < 0.001$.

accumulate SR101 in *Oatp1c1* knock-out mice, residual staining of neurons can be observed that cannot be attributed to *Oatp1c1* function. Considering that OATP1A2 and *Oatp1a4* are expressed in neurons [14,50], we speculate that neuronal SR101 uptake may be mediated by *Oatp1a4*. Interestingly, hypoxia also induces neuronal SR101 staining, and opening of gap junction hemichannels was identified as a potential mechanism of increased dye uptake [51]. However, considering that hypoxia can also increase *Oatp1a4* expression [51], hypoxia-induced neuronal SR101 staining may also be attributed to *Oatp1a4* (or OATP1A2) function. Further studies using specific inhibitors or knock-out models will be necessary to clarify this issue. In addition, since rodent *Oatp1a4* is not an ortholog of human OATP1A2, experiments on human brain slices will be necessary to unambiguously demonstrate the involvement of OATP1A2 in neuronal SR101 uptake.

Selective substrates can be useful to distinguish the function of multispecific OATPs (OATP1A2, OATP1B1, OATP1B3, and OATP2B1) that have

largely overlapping substrate specificities, and also show an overlapping expression pattern (OATP1B3 and OATP2B1 are expressed in hepatocytes, while OATP1A2 and OATP2B1 are present in the BBB). Currently, the number of selective substrates is very limited [29,52]. Here, we show that SR101 can be used to measure OATP1A2 or OATP1B function without the influence of OATP2B1. Also, LorD488 or CB and AF405 can be used to distinguish between OATP2B1 and OATP1A2 function (Fig. 2).

Transport of the novel dye substrate LorD488 revealed a remarkable pH dependence by both OATP1A2 and OATP1C1 (Fig. 2C,D). Although the exact transport mechanism of OATPs is still not clarified, it has been demonstrated by numerous studies that an acidic extracellular milieu can trigger OATP-mediated transport [31,32]. However, previously Leuthold *et al.* found that uptake of T4 by OATP1C1 does not depend on extracellular pH due to the lack of a conserved His in the substrate binding site that is protonated at acidic pH [31]. In contrast to Leuthold *et al.*, we found that OATP1C1-mediated uptake of

LorD488 (Fig. 2D) is also triggered when an acidic extracellular pH milieu is created. Since the chemical structure of LorD488 is not known, the pH dependence of its transport may be due to an alteration in the charged state of the dye. Still, our results unambiguously show that OATP-mediated LorD488 uptake should be measured at acidic pH. On the other hand, we found that while OATP1A2 better transports the SR dyes at acidic pH, transport of the same dyes by OATP1C1 is slightly higher at neutral or basic pH (Fig. 2C,D). Since the pK value of the strongest base of the SR dyes is below 4, we do not expect a change in their charge in the applied pH range. Therefore, the difference in the pH sensitivity of SR transport may be attributed to other mechanisms, for example, the presence or the absence of the conserved His in the substrate binding site of OATP1A2 and OATP1C1, respectively.

Although HEK-293 cells are a generally accepted tool for the investigation of transporter activity, recently we have shown that A431 cells overexpressing hepatic OATPs, due to their better adherence, are more advantageous when a plate-based assay is needed [30]. Based on LDG uptake, we isolated A431 cells expressing high levels of OATP1A2, which allowed the design of a 96-well plate fluorescence assay measuring the uptake of the SR dyes (Table 2; Figs 6 and 7). By measuring the inhibitory effect of known OATP1A2 substrates/inhibitors in the SR assay, we found similar inhibitory constants as determined by radioactive test substrates (Table 3), indicating that our novel fluorescence-based assay is a sensitive alternative to ^3H -ES-based assays currently used to test drug interactions with OATP1A2. Considering the IC_{50} values determined in our current study (Table 3) and the physiological (*in vivo*) serum concentrations of these compounds, significant inhibition of OATP1A2 function can be expected following quinine treatment (plasma concentrations of quinine are 6–25 μM [53]). Based on our data, BSP may also interfere with OATP1A2 and OATP1C1 function *in vivo* (serum concentrations can reach 3 μM); however, BSP is no longer used in liver function tests for humans [54]. On the other hand, *in vivo* ES plasma concentrations are in the nanomolar range [55]; therefore, the *in vivo* relevance of OATP1A2 or OATP1C1 in ES transport may be less relevant. Similarly, the inhibitory effect of verapamil on OATP1A2 function may be negligible *in vivo*, since the maximal *in vivo* verapamil concentration is 0.21 μM [56] in contrast to the measured IC_{50} of 7.18 μM . Still, local concentrations may exceed serum levels; therefore, we cannot exclude the relevance of these interactions *in vivo*.

Elacridar, tariquidar, and zosuquidar were developed as third-generation P-gp inhibitors to overcome P-gp-mediated tumor multidrug resistance, and numerous *in vitro* and preclinical studies demonstrated their effectiveness [38]. However, clinical trials failed to meet these expectations. One of the reasons limiting the therapeutic benefit of P-gp modulation may be interaction with uptake transporters influencing their distribution. Second, unexpected toxicity was also observed upon the administration of third-generation P-gp inhibitors. Phase III clinical trial of tariquidar in non-small-cell lung cancer patients had to be stopped due to high toxicity [57]. Also, cerebellar toxicity was associated with oral administration of zosuquidar [58]. Our novel fluorescence-based assay identified elacridar as a putative OATP1A2 substrate, and potential transport by OATP1A2 was demonstrated in a cytotoxicity assay (Fig. 9). Therefore, OATP1A2 may be a good candidate influencing elacridar distribution. Though in view of the elacridar plasma concentrations measured in patients, the relevance of the OATP1A2 interaction may be limited. Also, the affinity of OATP1A2 toward elacridar, tariquidar, and zosuquidar (10.2, 4.5, and 6.7 μM , respectively) is far below to that observed for P-gp or ABCG2 (EC_{50} cca. 0.02 μM). Considering the range of maximum plasma concentrations of these inhibitors (1–2 μM) [38,59], only slight inhibition of OATP1A2 function can be expected. Further studies will be needed to clarify whether elacridar, tariquidar, and zosuquidar can alter the pharmacokinetics of OATP1A2 substrates. Still, local concentrations may be in the range inhibiting OATP1A2 function. Finally, based on the interaction of P-gp inhibitors with OATP1A2, other P-gp substrates, for example, chemotherapeutics, may also be identified as OATP1A2 inhibitors or substrates, and vice versa, the novel dye substrates may also be transported by P-gp or ABCG2. However, these would need further investigations. Nevertheless, we excluded that significant levels of P-gp or ABCG2 were present in the HEK-293 and A431 cell lines used in the current study (Fig. 10).

In conclusion, here we describe the development of fluorescence-based functional assays that, in combination with our high-expressing cell lines, provide a good alternative to radioligand-based tests in drug interaction screens for human OATP1A2 and OATP1C1. Since rodent *Oatp1a-s* are inappropriate models of human OATP1A2 in many regards, our assay may be used to detect novel drug interactions of OATP1A2, for example, demonstrated here for third-generation P-gp inhibitors. Our findings indicate that elacridar, tariquidar, and zosuquidar can participate in DDIs of

OATP1A2 and may also influence the transport of endogenous OATP1A2 substrates. Based on our findings, sulforhodamines are good candidate probes for *in vivo* imaging of OATP1A2/1C1 function.

Materials and methods

Materials

ZV was purchased from BioLegend® (San Diego, CA, USA). LIVE/DEAD® Fixable Cell Stain Dyes (Violet, Green), CB, and AF405 succinimidyl ester were bought from Thermo Fisher Scientific (Waltham, MA, USA); Live-or-Dye 488/515 was obtained from Biotium (Hayward, CA, USA); and sulforhodamine 101 (SR101), SRB, and SRG were obtained from Sigma-Aldrich (Budapest, Hungary). BSP, benzbromarone, TC, CsA, thyroxine (T4), and ES were purchased from Sigma-Aldrich. Restriction endonucleases were from New England Biolabs, Ltd. (Ipswich, MA, USA). All other materials, if not indicated otherwise, were purchased from Sigma-Aldrich.

Generation of plasmids

The cDNAs of human OATP1A2 (BC042452, HsCD00333163) and human OATP1C1 (BC022461, HsCD00332885) were amplified by HF PCR (Phusion® High-

Fidelity PCR Kit; NEB) from the pAcUW-21-L/OATP1A2 or OATP1C1 vectors [35] following the manufacturer's instructions and using the following primers: OATP1A2: forward 5' ATTAAGATCTGCGGCCGCGCCACCATG reverse 5' CATGTAAGTACTAGTTTACAATTTAGTTTTCAATTCATC; OATP1C1: forward 5' TAAAGGATCCGC CACCATGGACACTTC reverse 5' CATGTAAGTACTAGTCTAAAGTTGAGTTTCCTTGCC. After digestion with BglII and SpeI (OATP1A2) or BamHI and PstI (OATP1C1) enzymes, the PCR fragments were cloned to the corresponding sites of the pRRL-CMV-MCS-IRES-ΔCD4 vector [30]. The base order of the cDNAs in all constructs was verified by sequencing. Empty pRRLΔCD4 vector was used as a negative control.

Generation of cell lines

A431 cells expressing OATP1B1, OATP1B3, or OATP2B1 were generated as described elsewhere [30]. OATP1A2 and OATP1C1 overexpression in HEK-293 and A431 cells was achieved by recombinant lentiviruses. Retroviral transductions of A431 and HEK-293 cells were performed as described earlier [30]. All cell lines were cultured in Dulbecco's modified Eagle's medium supplemented with 10% fetal bovine serum, 2 mM L-glutamine, 100 units per mL penicillin, and 100 μg·mL⁻¹ streptomycin. No significant levels of endogenous P-gp or ABCG2 were found in the cell lines used in the experiments (Fig. 10).

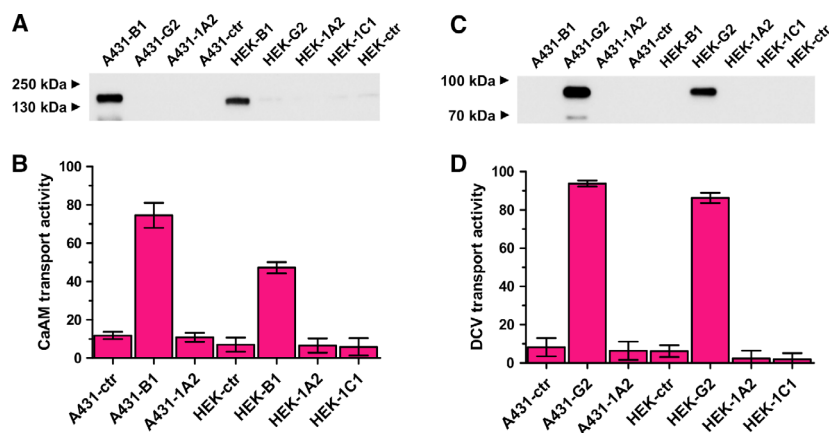


Fig. 10. Expression and function of ABCB1 (A, B) or ABCG2 (C, D) in A431 and HEK 293 cells. (A) Western blot image showing expression of ABCB1 in A431 and HEK 293 cells. 40 μg of whole-cell protein lysates was analyzed by Western blot using the MRK16 antibody. Ctr. stands for mock-transfected cells. Experiment was repeated three times. One representative image is shown. (B) Calcein-AM transport in A431 and HEK 293 cells. 3×10^5 cells were incubated with 0.25 μM calcein-AM (CaAM) for 10 min at 37 °C in transport buffer pH 7.4 in the presence or absence of 40 μM verapamil. The reaction was stopped by the addition of five volumes of ice-cold PBS. Fluorescence was detected in a flow cytometer. Transport activity was calculated as follows: (fluorescence with verapamil – fluorescence without verapamil)/fluorescence with verapamil × 100. Experiments were done in biological triplicates. Average ± SD values are shown. (C) Western blot image showing expression of ABCG2 in A431 and HEK 293 cells. 40 μg of whole-cell protein lysates was analyzed by western blot using the BXP-21 antibody. Ctr. stands for mock-transfected cells. A representative image from three independent Western blots is shown. (D) Dye cycle violet (DCV) transport in A431 or HEK 293 cells. Transport was performed as described for CaAM except that instead of CaAM, 1 μM DCV was applied and 1 μM Ko143 was used as an inhibitor. Transport activity was calculated as described above. Fluorescence was measured in a flow cytometer. Average ± SD values are shown.

Immunodetection of OATPs

Whole-cell lysates of HEK-293 and A431 cells (20 µg) were separated on 7.5% Laemmli SDS/PAGE gels and transferred onto PVDF membranes. Immunoblotting with appropriate antibodies was performed as described in Ref. [35]. The antibody raised against OATP1A2 (SAB2108577) was purchased from Sigma-Aldrich. The antibody recognizing OATP1C1 was a kind gift from Dr. Bruno Stieger [21] (Department of Clinical Pharmacology and Toxicology, University Hospital, 8091 Zurich, Switzerland). The secondary antibody was obtained from Jackson ImmunoResearch (Cambridgeshire, UK) (anti-rabbit peroxidase-conjugated donkey IgG, 20 000× diluted). Peroxidase-dependent luminescence on the blots was detected by the Luminol Enhancer Solution Kit by Thermo Scientific.

Determination of dye uptake by flow cytometry

Uptake of the fluorescent molecules in HEK-293 cells overexpressing OATPs was measured as described previously [30]. In brief, cells were trypsinized; 5×10^5 cells in suspension were pre-incubated in the presence or absence of inhibitors for 5 min at 37 °C. The reaction was started with the addition of the dyes. Transport experiments were carried out at 37 °C in the uptake buffer (125 mM NaCl, 4.8 mM KCl, 1.2 mM CaCl₂, 1.2 mM KH₂PO₄, 12 mM MgSO₄, 25 mM MES, and 5.6 mM glucose, with the pH adjusted to 8.5, 7.4, 6.5, or 5.5). The reaction was stopped by the addition of five volumes of ice-cold PBS, and the cells were kept on ice till the FACS analysis. Dead cells were excluded based on ZV labeling (0.1 µL·mL⁻¹). The cellular fluorescence of the cells was determined within an hour using an Attune Acoustic Focusing Cytometer (Applied Biosystems, Life Technologies, Carlsbad, CA, USA). The figures were generated using the FCS Express software.

Cell sorting

Function-based sorting was carried out based on the LDG uptake of HEK-293 and A431 cells expressing OATP1A2 or OATP1C1 as described previously [30]. Briefly, 2×10^6 cells were incubated with 0.8 µL LDG in 100 µL transport buffer pH 5.5 at 37 °C for 30 min. Cells with the highest fluorescence were collected using a BD FACSAria III Cell Sorter (BD Biosciences, San Jose, CA, USA).

Microplate-based uptake assay

The microplate-based assay was performed as described in Ref. [30]. 8×10^4 per well A431 cells overexpressing OATPs were seeded onto 96-well plates and cultured for 24 h at 37 °C. In the uptake experiments, cells were pre-incubated in uptake buffer in the presence or absence of

inhibitors for 5 min at 37 °C. The reaction was started with the addition of the SR dyes, and the plate was incubated at 37 °C for the indicated times. The reaction was stopped by the addition of excess ice-cold PBS, and the cells were washed with ice-cold PBS two more times. Finally, fluorescence of cells (in 200 µL PBS) was measured using an EnSpire fluorescent plate reader (PerkinElmer, Waltham, MA, USA) at the following wavelengths: LorD488: 488/515 nm; SR101: 586/605 nm; SRB: 565/586 nm; SRG: 531/552 nm. Additionally, in each experiment a calibration curve was generated by determining the fluorescence of increasing amounts of the given dye dissolved in 200 µL PBS. The amount of the dye in the cell samples was calculated based on the calibration curves (Figs 6 and 8A).

Cytotoxicity assay

Cells were seeded at a final cell density of 5000 cells per well in 96-well plates. Cells were incubated for 24 h at 37 °C and 5% CO₂ under humidified atmosphere prior to the addition of drugs. Elacridar, tariquidar, and zosuquidar were added in an 8-point dose-response format with two-fold dilution (the final volume was 100 µL, and DMSO did not exceed 1%). One hundred twenty hours after drug addition, cell number was measured using the SRB assay. Briefly, cells were fixed with 10% trichloroacetic acid and stained for 15 min with 0.4% (wt/vol) SRB dissolved in 1% acetic acid. The unbound dye was removed by repeated washing with 1% acetic acid. Finally, the protein-bound dye was dissolved in a solution containing 50 mM Tris pH 7.6, 150 mM NaCl, and 0.05 % Tween-20. Absorbance was measured at 570 nm using an EnSpire microplate reader.

Data and Statistical analysis

Results are presented as means ± SD from three or more independent experiments. Calculation of the kinetic parameters of dye uptake, half inhibitory concentrations (IC₅₀), and unpaired Student's *t*-test used for statistical analyses were performed using the GRAPHPAD PRISM software (GraphPad, La Jolla, CA, USA). **P* < 0.05, ***P* < 0.01, and ****P* < 0.001 were considered to be statistically significant.

Acknowledgements

We appreciate the financial support from the National Research Development and Innovation Office (OTKA, grant number FK 128751). CÖ-L is also grateful for the support by the János Bolyai Fellowship of the Hungarian Academy of Sciences.

Conflict of interest

The authors declare no conflict of interest.

Author contributions

Experiments were designed by ÉB, IP, CÖ-L, and GS. Plasmid constructs were generated by IP, ÉB, and ON. Transduction and sorting of the cells were performed by NK and GV. Transport experiments and cytotoxicity measurements were conducted by ÉB and ON. Data analysis was performed by ÉB, ON, GV, GS, and CÖ-L. The manuscript was written by ÉB, CÖ-L, and GS. All authors have read and approved the final draft of the manuscript.

References

- Abdullahi W, Davis TP & Ronaldson PT (2017) Functional expression of P-glycoprotein and organic anion transporting polypeptides at the blood-brain barrier: understanding transport mechanisms for improved CNS drug delivery? *AAPS J* **19**, 931–939.
- Pardridge WM (2017) Delivery of biologics across the blood-brain barrier with molecular Trojan horse technology. *BioDrugs* **31**, 503–519.
- Marques F, Sousa JC, Brito MA, Pahnke J, Santos C, Correia-Neves M & Palha JA (2017) The choroid plexus in health and in disease: dialogues into and out of the brain. *Neurobiol Dis* **107**, 32–40.
- Praetorius J & Damkier HH (2017) Transport across the choroid plexus epithelium. *Am J Physiol Cell Physiol* **312**, C673–C686.
- Girardin F (2006) Membrane transporter proteins: a challenge for CNS drug development. *Dialogues Clin Neurosci* **8**, 311–321.
- Hagenbuch B & Stieger B (2013) The SLCO (former SLC21) superfamily of transporters. *Mol Aspects Med* **34**, 396–412.
- Kovacsics D, Patik I & Ozvegy-Laczka C (2016) The role of organic anion transporting polypeptides in drug absorption, distribution, excretion and drug-drug interactions. *Expert Opin Drug Metab Toxicol* **13**, 409–424.
- Durmus S, van Hoppe S & Schinkel AH (2016) The impact of Organic Anion-Transporting Polypeptides (OATPs) on disposition and toxicity of antitumor drugs: insights from knockout and humanized mice. *Drug Resist Updat* **27**, 72–88.
- Giacomini KM, Huang SM, Tweedie DJ, Benet LZ, Brouwer KL, Chu X, Dahlin A, Evers R, Fischer V, Hillgren KM *et al.* (2010) Membrane transporters in drug development. *Nat Rev Drug Discov* **9**, 215–236.
- Shitara Y, Maeda K, Ikejiri K, Yoshida K, Horie T & Sugiyama Y (2013) Clinical significance of organic anion transporting polypeptides (OATPs) in drug disposition: their roles in hepatic clearance and intestinal absorption. *Biopharm Drug Dispos* **34**, 45–78.
- Urquhart BL & Kim RB (2009) Blood-brain barrier transporters and response to CNS-active drugs. *Eur J Clin Pharmacol* **65**, 1063–1070.
- Yu J, Zhou Z, Tay-Sontheimer J, Levy RH & Ragueneau-Majlessi I (2017) Intestinal drug interactions mediated by OATPs: a systematic review of preclinical and clinical findings. *J Pharm Sci* **106**, 2312–2325.
- Gao B, Hagenbuch B, Kullak-Ublick GA, Benke D, Aguzzi A & Meier PJ (2000) Organic anion-transporting polypeptides mediate transport of opioid peptides across blood-brain barrier. *J Pharmacol Exp Ther* **294**, 73–79.
- Gao B, Vavricka SR, Meier PJ & Stieger B (2015) Differential cellular expression of organic anion transporting peptides OATP1A2 and OATP2B1 in the human retina and brain: implications for carrier-mediated transport of neuropeptides and neurosteroids in the CNS. *Pflugers Arch* **467**, 1481–1493.
- Gao B, Huber RD, Wenzel A, Vavricka SR, Ismail MG, Reme C & Meier PJ (2005) Localization of organic anion transporting polypeptides in the rat and human ciliary body epithelium. *Exp Eye Res* **80**, 61–72.
- Drozdziak M, Groer C, Penski J, Lapczuk J, Ostrowski M, Lai Y, Prasad B, Unadkat JD, Siegmund W & Oswald S (2014) Protein abundance of clinically relevant multidrug transporters along the entire length of the human intestine. *Mol Pharm* **11**, 3547–3555.
- Ronaldson PT & Davis TP (2013) Targeted drug delivery to treat pain and cerebral hypoxia. *Pharm Rev* **65**, 291–314.
- Yang ZZ, Li L, Wang L, Xu MC, An S, Jiang C, Gu JK, Wang ZJ, Yu LS & Zeng S (2016) siRNA capsulated brain-targeted nanoparticles specifically knock down OATP2B1 in mice: a mechanism for acute morphine tolerance suppression. *Sci Rep* **6**, 33338.
- Zhou Y, Yuan J, Li Z, Wang Z, Cheng D, Du Y, Li W, Kan Q & Zhang W (2015) Genetic polymorphisms and function of the organic anion-transporting polypeptide 1A2 and its clinical relevance in drug disposition. *Pharmacology* **95**, 201–208.
- Bailey DG (2010) Fruit juice inhibition of uptake transport: a new type of food-drug interaction. *Br J Clin Pharm* **70**, 645–655.
- Pizzagalli F, Hagenbuch B, Stieger B, Klenk U, Folkers G & Meier PJ (2002) Identification of a novel human organic anion transporting polypeptide as a high affinity thyroxine transporter. *Mol Endocrinol* **16**, 2283–2296.
- van der Deure WM, Hansen PS, Peeters RP, Kyvik KO, Friesema EC, Hegedus L & Visser TJ (2008) Thyroid hormone transport and metabolism by organic anion transporter 1C1 and consequences of genetic variation. *Endocrinology* **149**, 5307–5314.
- Roberts LM, Woodford K, Zhou M, Black DS, Haggerty JE, Tate EH, Grindstaff KK, Mengesha W,

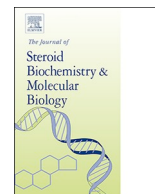
- Raman C & Zerangue N (2008) Expression of the thyroid hormone transporters monocarboxylate transporter-8 (SLC16A2) and organic ion transporter-14 (SLCO1C1) at the blood-brain barrier. *Endocrinology* **149**, 6251–61.
- 24 Schnell C, Shahmoradi A, Wichert SP, Mayerl S, Hagos Y, Heuer H, Rossner MJ & Hulsmann S (2015) The multispecific thyroid hormone transporter OATP1C1 mediates cell-specific sulforhodamine 101-labeling of hippocampal astrocytes. *Brain Struct Funct* **220**, 193–203.
- 25 Alkemade A, Friesema EC, Kalsbeek A, Swaab DF, Visser TJ & Fliers E (2011) Expression of thyroid hormone transporters in the human hypothalamus. *J Clin Endocrinol Metab* **96**, E967–E971.
- 26 Stromme P, Groeneweg S, Lima de Souza EC, Zevenbergen C, Torgersbraten A, Holmgren A, Gurcan E, Meima ME, Peeters RP, Visser WE *et al.* (2018) Mutated thyroid hormone transporter OATP1C1 associates with severe brain hypometabolism and juvenile neurodegeneration. *Thyroid* **28**, 1406–1415.
- 27 De Bruyn T, Fattah S, Stieger B, Augustijns P & Annaert P (2011) Sodium fluorescein is a probe substrate for hepatic drug transport mediated by OATP1B1 and OATP1B3. *J Pharm Sci* **100**, 5018–5030.
- 28 Gui C, Obaidat A, Chaguturu R & Hagenbuch B (2010) Development of a cell-based high-throughput assay to screen for inhibitors of organic anion transporting polypeptides 1B1 and 1B3. *Curr Chem Genomics* **4**, 1–8.
- 29 Izumi S, Nozaki Y, Komori T, Takenaka O, Maeda K, Kusuhara H & Sugiyama Y (2016) Investigation of fluorescein derivatives as substrates of organic anion transporting polypeptide (OATP) 1B1 to develop sensitive fluorescence-based OATP1B1 inhibition assays. *Mol Pharm* **13**, 438–448.
- 30 Patik I, Szekely V, Nemet O, Szepesi A, Kucsma N, Varady G, Szakacs G, Bakos E & Ozvegy-Laczka C (2018) Identification of novel cell-impermeant fluorescent substrates for testing the function and drug interaction of Organic Anion-Transporting Polypeptides, OATP1B1/1B3 and 2B1. *Sci Rep* **8**, 2630.
- 31 Leuthold S, Hagenbuch B, Mohebbi N, Wagner CA, Meier PJ & Stieger B (2009) Mechanisms of pH-gradient driven transport mediated by organic anion polypeptide transporters. *Am J Physiol Cell Physiol* **296**, C570–C582.
- 32 Marin JJ, Mangas D, Martinez-Diez MC, El-Mir MY, Briz O & Serrano MA (2003) Sensitivity of bile acid transport by organic anion-transporting polypeptides to intracellular pH. *Biochim Biophys Acta* **1611**, 249–257.
- 33 Roth M, Timmermann BN & Hagenbuch B (2011) Interactions of green tea catechins with organic anion-transporting polypeptides. *Drug Metab and Dispos* **39**, 920–926.
- 34 van Montfoort JE, Muller M, Groothuis GM, Meijer DK, Koepsell H & Meier PJ (2001) Comparison of "type I" and "type II" organic cation transport by organic cation transporters and organic anion-transporting polypeptides. *J Pharmacol Exp Ther* **298**, 110–115.
- 35 Patik I, Kovacsics D, Nemet O, Gera M, Várady G, Hagenbuch B, Stieger B, Szakács G & Özvegy-Laczka C (2015) Functional expression of the 11 human organic anion transporting polypeptides in insect cells reveals that sodium fluorescein is a general OATP substrate. *Biochem Pharmacol* **98**, 649–658.
- 36 Sugiyama D, Kusuhara H, Taniguchi H, Ishikawa S, Nozaki Y, Aburatani H & Sugiyama Y (2003) Functional characterization of rat brain-specific organic anion transporter (Oatp14) at the blood-brain barrier: high affinity transporter for thyroxine. *J Biol Chem* **278**, 43489–43495.
- 37 Windt T, Toth S, Patik I, Sessler J, Kucsma N, Szepesi A, Zdrzil B, Ozvegy-Laczka C & Szakacs G (2019) Identification of anticancer OATP2B1 substrates by an *in vitro* triple-fluorescence-based cytotoxicity screen. *Arch Toxicol* **93**, 953–964.
- 38 Dash RP, Jayachandra Babu R & Srinivas NR (2017) Therapeutic potential and utility of Elacridar with respect to P-glycoprotein inhibition: an insight from the published *in vitro*, preclinical and clinical studies. *Eur J Drug Metab Pharmacokinet* **42**, 915–933.
- 39 Furihata T & Anzai N (2017) Functional expression of organic ion transporters in astrocytes and their potential as a drug target in the treatment of central nervous system diseases. *Biol Pharm Bull* **40**, 1153–1160.
- 40 Froklage FE, Reijneveld JC & Heimans JJ (2011) Central neurotoxicity in cancer chemotherapy: pharmacogenetic insights. *Pharmacogenomics* **12**, 379–395.
- 41 Grube M, Hagen P & Jedlitschky G (2018) Neurosteroid transport in the brain: role of ABC and SLC transporters. *Front Pharmacol* **9**, 354.
- 42 Cesar-Razquin A, Snijder B, Frappier-Brinton T, Isserlin R, Gyimesi G, Bai X, Reithmeier RA, Hepworth D, Hediger MA, Edwards AM *et al.* (2015) A call for systematic research on solute carriers. *Cell* **162**, 478–487.
- 43 Hagos L & Hulsmann S (2016) Unspecific labelling of oligodendrocytes by sulforhodamine 101 depends on astrocytic uptake via the thyroid hormone transporter OATP1C1 (SLCO1C1). *Neurosci Lett* **631**, 13–18.
- 44 Tachikawa M, Sumiyoshiya Y, Saigusa D, Sasaki K, Watanabe M, Uchida Y & Terasaki T (2018) Liver Zonation index of drug transporter and metabolizing enzyme protein expressions in mouse liver acinus. *Drug Metab Dispos* **46**, 610–618.
- 45 Yaguchi Y, Tachikawa M, Zhang Z & Terasaki T (2019) Organic anion-transporting polypeptide 1a4

- (Oatp1a4/Slco1a4) at the blood-arachnoid barrier is the major pathway of sulforhodamine-101 clearance from cerebrospinal fluid of rats. *Mol Pharm* **16**, 2021–2027.
- 46 Lan T, Rao A, Haywood J, Davis CB, Han C, Garver E & Dawson PA (2009) Interaction of macrolide antibiotics with intestinally expressed human and rat organic anion-transporting polypeptides. *Drug Metab Dispos* **37**, 2375–2382.
- 47 Ose A, Kusuhara H, Endo C, Tohyama K, Miyajima M, Kitamura S & Sugiyama Y (2010) Functional characterization of mouse organic anion transporting peptide 1a4 in the uptake and efflux of drugs across the blood-brain barrier. *Drug Metab Dispos* **38**, 168–176.
- 48 Geyer J, Godoy JR & Petzinger E (2004) Identification of a sodium-dependent organic anion transporter from rat adrenal gland. *Biochem Biophys Res Commun* **316**, 300–306.
- 49 Hulsman S, Hagos L, Heuer H & Schnell C (2017) Limitations of sulforhodamine 101 for brain imaging. *Front Cell Neurosci* **11**, 44.
- 50 Ding J, Wang J, Xiang Z, Diao W, Su M, Shi W, Wan T & Han X (2017) The organic anion transporting polypeptide 1a5 is a pivotal transporter for the uptake of microcystin-LR by gonadotropin-releasing hormone neurons. *Aquatic Toxicol* **182**, 1–10.
- 51 Thompson RJ, Zhou N & MacVicar BA (2006) Ischemia opens neuronal gap junction hemichannels. *Science* **312**, 924–927.
- 52 Turkova A, Jain S & Zdrzil B (2018) Integrative data mining, scaffold analysis, and sequential binary classification models for exploring ligand profiles of hepatic organic anion transporting polypeptides. *J Chem Inf Model* **59**, 1811–1825.
- 53 Flieger J & Czajkowska-Zelazko A (2015) Aqueous two phase system based on ionic liquid for isolation of quinine from human plasma sample. *Food Chem* **166**, 150–157.
- 54 Flatland B, Leib MS, Warnick LD & Sponenberg DP (2000) Evaluation of the bromosulphophthalein 30-minute retention test for the diagnosis of hepatic disease in dogs. *J Vet Intern Med* **14**, 560–568.
- 55 Rizner TL, Thalhammer T & Ozvegy-Laczka C (2017) The importance of steroid uptake and intracrine action in endometrial and ovarian cancers. *Front Pharmacol* **8**, 346.
- 56 Frishman W, Kirsten E, Klein M, Pine M, Johnson SM, Hillis LD, Packer M & Kates R (1982) Clinical relevance of verapamil plasma levels in stable angina pectoris. *Am J Cardiol* **50**, 1180–1184.
- 57 Palmeira A, Sousa E, Vasconcelos MH & Pinto MM (2012) Three decades of P-gp inhibitors: skimming through several generations and scaffolds. *Curr Med Chem* **19**, 1946–2025.
- 58 Rubin EH, de Alwis DP, Pouliquen I, Green L, Marder P, Lin Y, Musanti R, Grospe SL, Smith SL, Toppmeyer DL *et al.* (2002) A phase I trial of a potent P-glycoprotein inhibitor, Zosuquidar. 3HCl trihydrochloride (LY335979), administered orally in combination with doxorubicin in patients with advanced malignancies. *Clin Cancer Res* **8**, 3710–3717.
- 59 Sandler A, Gordon M, De Alwis DP, Pouliquen I, Green L, Marder P, Chaudhary A, Fife K, Battiato L, Sweeney C *et al.* (2004) A Phase I trial of a potent P-glycoprotein inhibitor, zosuquidar trihydrochloride (LY335979), administered intravenously in combination with doxorubicin in patients with advanced malignancy. *Clin Cancer Res* **10**, 3265–3272.
- 60 Roth M, Obaidat A & Hagenbuch B (2012) OATPs, OATs and OCTs: the organic anion and cation transporters of the SLCO and SLC22A gene superfamilies. *Br J Pharmacol* **165**, 1260–1287.
- 61 Hubeny A, Keiser M, Oswald S, Jedlitschky G, Kroemer HK, Siegmund W & Grube M (2016) Expression of organic anion transporting polypeptide 1A2 in red blood cells and its potential impact on antimalarial therapy. *Drug Metab Dispos* **44**, 1562–1568.
- 62 Bailey DG, Dresser GK, Leake BF & Kim RB (2007) Naringin is a major and selective clinical inhibitor of organic anion-transporting polypeptide 1A2 (OATP1A2) in grapefruit juice. *Clin Pharmacol Ther* **81**, 495–502.



Contents lists available at ScienceDirect

Journal of Steroid Biochemistry and Molecular Biology

journal homepage: www.elsevier.com/locate/jsbmb

Structural dissection of 13-epiestrones based on the interaction with human Organic anion-transporting polypeptide, OATP2B1



Réka Laczkó-Rigó^a, Rebeka Jójárt^b, Erzsébet Mernyák^b, Éva Bakos^a, Alzbeta Tuerkova^c, Barbara Zdrzil^c, Csilla Özvegy-Laczka^{a,*}

^a Membrane Protein Research Group, Institute of Enzymology, RCNS, H-1117, Budapest, Magyar tudósok krt. 2, Hungary

^b Department of Organic Chemistry, University of Szeged, Dóm tér 8, H-6720, Szeged, Hungary

^c Department of Pharmaceutical Chemistry, Division of Drug Design and Medicinal Chemistry, University of Vienna, Althanstraße 14, A-1090, Vienna, Austria

ARTICLE INFO

Keywords:

Organic anion-transporting polypeptide
13-epiestrones
Inhibitor
SAR

ABSTRACT

Human OATP2B1 encoded by the *SLCO2B1* gene is a multispecific transporter mediating the cellular uptake of large, organic molecules, including hormones, prostaglandins and bile acids. OATP2B1 is ubiquitously expressed in the human body, with highest expression levels in pharmacologically relevant barriers, like enterocytes, hepatocytes and endothelial cells of the blood-brain-barrier. In addition to its endogenous substrates, OATP2B1 also recognizes clinically applied drugs, such as statins, antivirals, antihistamines and chemotherapeutic agents and influences their pharmacokinetics. On the other hand, OATP2B1 is also overexpressed in various tumors. Considering that elevated hormone uptake by OATP2B1 results in increased cell proliferation of hormone dependent tumors (e.g. breast or prostate), inhibition of OATP2B1 can be a good strategy to inhibit the growth of these tumors.

13-epiestrones represent a potential novel strategy in the treatment of hormone dependent cancers by the suppression of local estrogen production due to the inhibition of the key enzyme of estrone metabolism, 17 β -hydroxysteroid-dehydrogenase type 1 (HSD17 β 1). Recently, we have demonstrated that various phosphonated 13-epiestrones are dual inhibitors also suppressing OATP2B1 function. In order to gain better insights into the molecular determinants of OATP2B1 13-epiestrone interaction we investigated the effect of C-2 and C-4 halogen or phenylalkynyl modified epiestrones on OATP2B1 transport function. Potent inhibitors (with EC₅₀ values in the low micromolar range) as well as non-inhibitors of OATP2B1 function were identified. Based on the structure-activity relationship (SAR) of the various 13-epiestrone derivatives we could define structural elements important for OATP2B1 inhibition. Our results may help to understand the drug/inhibitor interaction profile of OATP2B1, and also may be a useful strategy to block steroid hormone entry into tumors.

1. Introduction

Organic anion-transporting polypeptides (OATPs) encoded by the *SLCO* (solute carrier for organic anions) genes are membrane proteins that mediate the cellular uptake of large (> 300 Da) organic molecules in a Na⁺- and ATP-independent manner [1]. 11 human OATPs are known, that are highly variable in their tissue distribution and substrate recognition. Some OATPs are ubiquitously expressed in the human body (OATP4A1, OATP3A1), while the expression of others is restricted to a given organ, like OATP1B1 and OATP1B3 expression which is restricted to hepatocytes [2,3]. Also, based on the substrate interaction

profile, multispecific OATPs (1A2, 1B1, 1B3, and 2B1) recognizing a plethora of organic compounds (including clinically applied drugs), and OATPs with a more limited substrate recognition (e.g., the thyroid transporter OATP1C1) can be distinguished. Although not all of the 11 OATPs are properly characterized with regard to their expression and function, steroids (e.g. bile acids, estrone-3-sulfate (E1S) and dehydroepiandrosterone sulfate (DHEAS)) can be considered as general OATP substrates [4]. Consequently, the OATPs 1A2, 1B1, 2B1 and 4A1 are supposed to be key participants in the cellular uptake of the steroid hormone conjugates E1S and DHEAS [3,5]. Besides their role in the maintenance of steroid hormone homeostasis, multispecific OATPs,

Abbreviations: OATP, Organic anion-transporting polypeptide; E1S, estrone-3-sulfate; HSD17 β 1, 17 β -hydroxysteroid-dehydrogenase type 1; SAR, structure activity relationship; STS, steroid sulfatase

* Corresponding author.

E-mail address: laczka.csilla@tk.mta.hu (C. Özvegy-Laczka).

<https://doi.org/10.1016/j.jsbmb.2020.105652>

Received 13 November 2019; Received in revised form 20 February 2020; Accepted 5 March 2020

Available online 06 March 2020

0960-0760/© 2020 The Authors. Published by Elsevier Ltd. This is an open access article under the CC BY-NC-ND license

(<http://creativecommons.org/licenses/by-nc-nd/4.0/>).

1A2, 1B1, 1B3 and 2B1 are important determinants of pharmacokinetics [6]. In addition, OATPs are often up-regulated in tumors [7–9]. Hence, they are promising targets for anti-tumor therapy.

OATP2B1 is a ubiquitously expressed transporter, with highest protein levels in pharmacologically relevant barrier tissues, like the intestine, liver and blood-brain barrier [1]. Besides, it is also expressed in the placenta, mammary gland and in skeletal muscle cells [1]. OATP2B1 is a multispecific transporter that recognizes molecules with largely variable size and structure. The most relevant endogenous substances transported by OATP2B1 are taurocholate, leukotriene C₄, E1S, DHEAS and prostaglandin E₂ [10]. OATP2B1 also promotes cellular uptake of clinically applied drugs, like statins, antibiotics, anti-hypertensives, anti-inflammatory drugs and chemotherapeutics [10]. Considering its tissue distribution and substrate recognition pattern, OATP2B1 may be a key player in intestinal drug absorption and also drug transport across the blood–brain barrier [11,12]. On the other hand, OATP2B1 overexpression has been detected in tumors of the colon, bone, breast, prostate and also in gliomas [13–15]. Considering its transport of anti-cancer agents, OATP2B1 is one of the main candidates of tumor-targeted drug delivery. On the other hand, it has been shown that increased steroid hormone (E1S, DHEAS) uptake by OATP2B1 promotes growth of steroid-dependent tumors. Matsumoto and colleagues demonstrated that overexpression of OATP2B1 results in increased survival of breast cancer cells *in vitro* [14]. Moreover, *in vivo* data revealed that DHEAS uptake by OATP2B1 has crucial role in prostate cancer progression [16]. Also, the SLCO2B1 rs12422149 GG (Arg312Gln) genotype resulting in increased OATP2B1 function correlates with shorter time to progression in prostate cancer patients who received androgen deprivation therapy [17,18]. Therefore, inhibition of OATP2B1 function presents a possible strategy to suppress steroid hormone uptake and hence the proliferation of hormone dependent cancers.

13-epiestrones are stereoisomers of natural estrone, lacking hormonal activity [19,20]. Previous work has demonstrated that certain 13-epiestrones are potent inhibitors of the 17 β -hydroxysteroid-dehydrogenase type 1 (HSD17 β 1) and steroid sulfatase (STS) enzymes crucial in estrone metabolism [21]. These enzymes are responsible for local estrogen formation and generation of the transcriptionally active estradiol therefore promoting proliferation of hormone dependent cancers [22,23]. Hence their inhibition e.g. by 13-epiestrones can be a potential anti-tumor strategy.

Recently we found that phosphonated 13-epiestrones inhibit the function of OATP2B1 [24]. In the current work, in order to get a better insight into the molecular determinants involved in this inhibition we analyzed the interaction between OATP2B1 and a large set of 13-epiestrones containing modifications on C-3 and C-2 or C-4. In addition, we systematically investigated the influence of certain substituents on inhibitory activity by correlation analysis.

2. Materials and methods

2.1. Materials

Materials if not stated otherwise were purchased for Sigma Aldrich (Budapest, Hungary). 13-epiestrones investigated in this study were synthesized as described elsewhere [21,25].

2.2. Generation and maintenance of the cell lines

A431 (human epidermoid carcinoma) cells overexpressing human OATP2B1 or mock transfected controls used in the current study were generated earlier as described in [26]. Briefly, OATP2B1 expressing cells were generated by transposase mediated genomic insertion of the OATP2B1 cDNA (BC041095.1, HsCD00378878). As a negative control mock transfected (pSB-CMV) cells were used. After 2 weeks of puromycin (1 μ g/ml) selection, cells were sorted based on Live/Dead Green

uptake. After recovery, cell were grown in DMEM (Gibco, Thermo Fischer Scientific (Waltham, MA, US)) without puromycin supplemented with 10 % fetal calf serum, 2 mM L-glutamine, 100 U/ml penicillin, and 100 μ g/ml streptomycin at 37 °C with 5% CO₂ and 95 % humidity.

2.3. Western blot detection of OATP2B1 expression

OATP2B1 expression was confirmed by Western blot as described earlier [26]. Briefly, whole cell lysates of A431 cells were separated on 7.5 % SDS-PAGE gels and transferred onto a PVDF membrane. OATP2B1 was detected by using an anti-OATP2B1 antibody (a courtesy of Dr. Bruno Stieger, Department of Clinical Pharmacology and Toxicology, University Hospital, 8091 Zurich, Switzerland) [27]. As a secondary antibody HRP-conjugated anti-rabbit antibody (Jackson ImmunoResearch, Suffolk, UK) was used in a dilution of 20,000 \times . An anti- β -actin antibody (A1978, Sigma) and HRP-conjugated anti-mouse antibody (Jackson ImmunoResearch, Suffolk, UK, 20,000 \times dilution) were used to detect β -actin. Luminescence was detected using the Luminer Enhancer Solution kit by Thermo Fisher Scientific (Waltham, MA, US).

2.4. Fluorescent dye uptake determined by flow cytometry

The transport function of OATP2B1 was determined by flow cytometry. A431 cells (mock and OATP2B1 overexpressing) were collected after 0.1 % trypsin treatment. The cells were washed in Uptake buffer (125 mM NaCl, 4.8 mM KCl, 1.2 mM CaCl₂, 1.2 mM KH₂PO₄, 12 mM MgSO₄, 25 mM MES, and 5.6 mM glucose, with the pH adjusted to 5.5 using 1 M HEPES and 1 N NaOH). After washing 5 \times 10⁵ cells were incubated for 15 min at 37 °C with Zombie Violet (BioLegend®, San Diego, CA, US) (0.4 μ l ZV/5 \times 10⁵ cell) in a final volume of 100 μ l. The reaction was stopped by the addition of 1 ml ice-cold PBS (phosphate buffered saline) and the cells were kept on ice until the flow cytometry analysis. The fluorescence of 10,000 living cells was determined using Attune NxT Flow Cytometer (Invitrogen, Carlsbad, CA). Dead cells were excluded by propidium iodide (1 μ g/ml) labeling.

2.5. 96 well plate-based transport assay

Effect of 13-epiestrones on OATP2B1 function was determined by measuring Zombie Violet (BioLegend®, San Diego, CA, US) fluorescent dye uptake on microplates [26]. Briefly, A431 cells were seeded on 96 well-plates (8 \times 10⁴ cells in 200 μ l final volume/well) and cultured for 16–24 h at 37 °C, 5% CO₂ prior to the transport measurements. Next day after repeated washing with 200 μ l PBS, cells were pre-incubated with 50 μ l Uptake buffer (125 mM NaCl, 4.8 mM KCl, 1.2 mM CaCl₂, 1.2 mM KH₂PO₄, 12 mM MgSO₄, 25 mM MES, and 5.6 mM glucose, with the pH adjusted to 5.5 using 1 M HEPES and 1 N NaOH) containing the appropriate concentrations of the 13-epiestrones (0–100 μ M) for 5 min at 37 °C. Reaction was started by the addition of 770 \times diluted Zombie Violet dye in 50 μ l/well Uptake buffer followed by a 30 min incubation at 37 °C. The reaction was stopped by the addition of 200 μ l ice-cold PBS. After repeated washing, 200 μ l ice-cold PBS was added to each well and fluorescence in the wells was determined in an Enspire fluorescent plate reader (Perkin Elmer, Waltham, MA) at Ex/Em: 405/423 nm. Experiments were repeated at least three times.

2.6. Measurement of ³H-E1S uptake

A431 control and A431-OATP2B1 cells (10⁶ cells/sample) were incubated in the absence or presence of 2-bromo-13-epiestrone (final concentration 50 μ M) for 5 min at 37 °C in uptake buffer pH 5.5. Transport reaction was started by the addition of ³H-E1S (250 mCi/ml, final concentration 9.65 nM (Perkin Elmer, Waltham, MA)). After incubation for further 10 min at 37 °C, the reaction was stopped by the addition of 1 ml ice-cold PBS and the cells were centrifuged at 300 g.

The cell pellet was collected in 100 μ l PBS and pipetted into 1 ml Opti-Fluor (Perkin Elmer, Waltham, MA). Radioactivity was measured in a Wallac Liquid Scintillator Counter. Experiments were repeated three times.

2.7. Data calculation

Transport data were obtained by subtracting the fluorescence in mock transfected cells from that measured in OATP2B1 cells. Kinetic parameters of dye uptake and half inhibitory concentrations (EC_{50}) obtained from at least three independent experiments were determined by Hill fit using the GraphPad prism software (GraphPad, La Jolla, CA, USA).

2.8. Structure-activity relationship (SAR) analysis

Compounds were drawn using the structure editor integrated into the ChemSpider chemical structure database webservice (freely available at <https://www.chemspider.com/About.aspx>). Daylight SMILES structural format was generated for every unique compound of the dataset. KNIME Analytics Platform (version 3.4) [28] was used to create an automated workflow for Structure-Activity Relationship (SAR) analysis of 13-epiestrones. First, Daylight SMILES format for input compounds was converted into the canonical form ('RDKit Canon SMILES' node). Murcko scaffolds were generated and the maximum common substructure (MCS) was derived from the retrieved Murcko scaffolds ('RDKit MCS' node). MCS was used as a structural query for substructure mining in order to perform R-group decomposition ('RDKit R Group Decomposition' node).

Physicochemical descriptors (RDKit) for the substituents (R groups) at position C-2 and C-4 were calculated. Descriptor values were normalized ('Normalizer' node using Z-score normalization). The Pearson correlation coefficient was calculated to identify positive or negative correlations between pEC_{50} values and respective physicochemical descriptors at a given R-group position ('Linear Correlation' node).

3. Results

3.1. Effect of C-2 or C-4 halogenated 13-epiestrones on the transport activity of OATP2B1

Recently, we have reported that various phosphonated 13-epiestrones are potent inhibitors of OATP2B1 function [24]. In order to gain better insights into the molecular determinants of this inhibition, we investigated the inhibitory effect of various 2- or 4-halogenated 3-hydroxy- (3-OH) or 3-methoxy (3-OMe) 13-epiestrones (Fig. 1).

Interaction was measured in A431 mock transfected (control) and OATP2B1 overexpressing cell lines using the Zombie Violet (ZV) assay. The A431 cell line overexpressing OATP2B1 was generated earlier [26]. Prior to the interaction tests OATP2B1 overexpression was confirmed by Western blot (Fig. 2A). ZV is one of the newly identified fluorescent dyes applicable for testing drug interactions and function of OATP2B1, and a good alternative to the generally used radioactive functional assays [26]. Fig. 2B shows that OATP2B1 overexpression results in increased uptake of the viability dye, ZV.

When testing the inhibitory effect of the epiestrone derivatives, ZV uptake was measured in A431-OATP2B1 (and control) cells seeded in 96-well plates in the presence of increasing amounts of the tested compounds. As shown in Fig. 3, the compounds showed various degrees of transport inhibition. The first striking difference could be observed between the C-3 OH and OMe compounds. 13-epiestrone (C-3 OH, termed as **compound 1**) had practically no effect on ZV transport (EC_{50} around 50 μ M), while its methylether counterpart (3-OMe derivative, **compound 2**) resulted in a quite effective inhibition (EC_{50} 2.98 μ M) (see Fig. 3 and Table 1).

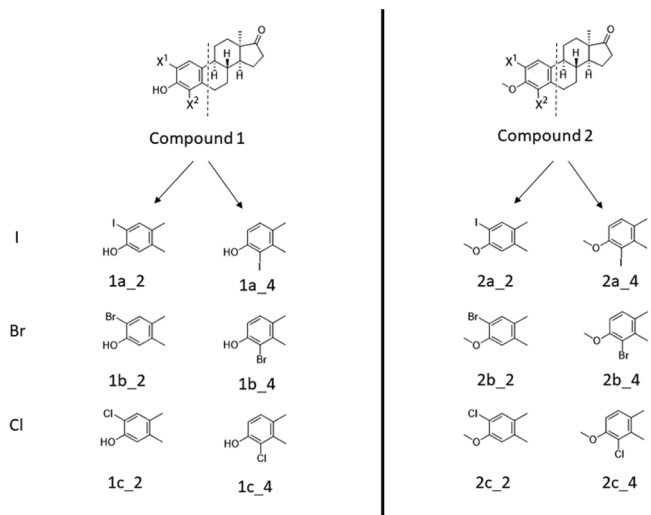


Fig. 1. Structure of the halogenated 13-epiestrones investigated in the current study. In the case of **compounds 1 and 2** $X^1 = H$ and $X^2 = H$.

Interestingly, introduction of a second modification, halogenation of either at C-2 or C-4 resulted in opposite changes in the inhibitory potential of 13-epiestrones. In the case of **compound 1**, halogenation at C-2 (compounds **1a_2**, **1b_2** and **1c_2**) resulted in a striking increase in inhibitory potential, with EC_{50} values between 0.5 and 2.1 μ M. However, the C-4 chlorinated derivative (compound **1c_4**) showed practically no effect on OATP2B1 transport function, while 4-iodo and 4-bromo 13-epiestrones (**1a_4** and **1b_4**) proved to be weak inhibitors. This reveals a strong dependence of the regioisomerism of the halogenated 3-OH compounds, the most potent inhibition detected with the 2-halogenated derivatives. In the case of 3-OMe derivatives, halogenation caused lower alteration in the inhibitory potential, although all of the compounds showed increased EC_{50} values compared to the initial compound. Iodinated derivatives (**2a_2** and **2a_4**) were more effective than the brominated or chlorinated compounds (**2b_2**, **2b_4** or **2c_2**, **2c_4**). Regioisomer specific inhibitory effect in the case of the 3-OMe variants could only be observed for the chlorinated compounds, with an approximately 5-fold increase in the EC_{50} of the C-4 vs. C-2 chlorinated epiestrones (**2c_2** and **2c_4**, Table 1).

3.2. Effect of C-2 or C-4 phenylalkynylated 13-epiestrones on the transport activity of OATP2B1

Next, we investigated the effect of the introduction of a phenylalkynyl group in position C-2 or C-4 on OATP2B1 function (Fig. 4).

In the case of 3-OH 13-epiestrones, introduction of a large ring resulted in various effects. In general, although some phenylalkynylated 13-epiestrones showed detectable interaction with OATP2B1, these compounds were less effective inhibitors than the C-2 halogenated epiestrones (see Table 2 and Fig. 5). The only exception is **1gS_4** containing a (4-methoxyphenyl)ethynyl substituent, that was almost as effective inhibitor as the C-2 halogenated 13-epiestrones. Interestingly, in the case of phenylalkynylated 3-OH 13-epiestrones no clear rule in preference in interaction with C-2 over C-4 modified compounds could be observed. Compounds **1eS_4** and **1gS_4** were more potent inhibitors than their C-2 counterparts (**1eS_2** and **1gS_2**). However, in the case of 13-epiestrones bearing fluorinated substituents (**1hS** and **1fS**), this tendency changed, C-2 compounds being slight inhibitors (EC_{50} around 10 μ M) compared to C-4 modified derivatives lacking any inhibitory potential (at least in the concentrations tested).

In the case of the 3-OMe compounds with a second, subst. phenylalkynyl modification, similarly to that observed for the halogenated

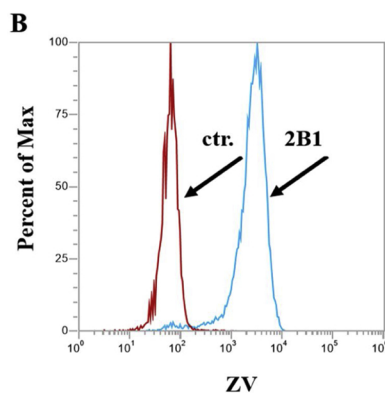
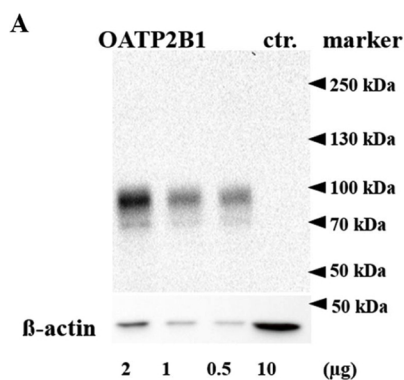


Fig. 2. A) Western blot detection of OATP2B1 expressed in A431 cells. OATP2B1 was detected by an anti-OATP2B1 antibody [27], and β -actin was used as a loading control. Control (ctr.) stands for mock transfected A431 cells. Multiple migratory bands may represent differentially glycosylated forms of OATP2B1. B) Zombie Violet uptake in A431-OATP2B1 and control cells. Histograms show the uptake of ZV (250x dilution) in the cells incubated with the fluorescent dye for 15 min at 37 °C in uptake buffer (pH 5.5). Living (propidium-iodide negative) cells are shown. Mock transfected cells are indicated with a red line and OATP2B1 transfected are with blue.

compounds, a decrease or even a complete loss of inhibition compared to the parental compound 3-OMe 13-epi estrone could be observed. The only exceptions were compounds **2gS_2** and **2gS_4** that proved to be effective inhibitors. A clear rule of regioselectivity could not be observed for the 3-OMe phenylalkynyl modified compounds.

3.3. Effect of 2-bromo 13-epi estrone on OATP2B1-mediated estrone-3-sulfate uptake

Inhibition of hormone uptake by OATP2B1 in tumor cells could be the major goal of the newly identified inhibitors. Therefore, in order to

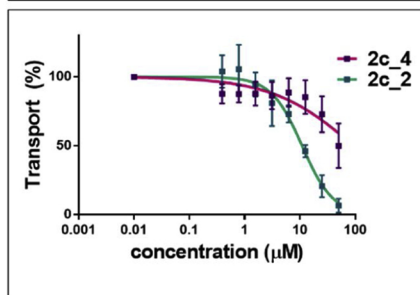
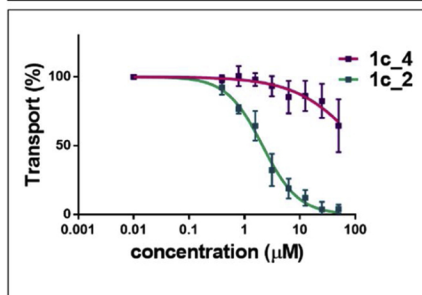
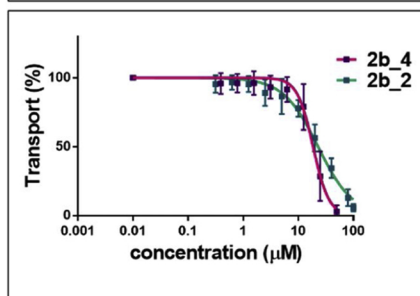
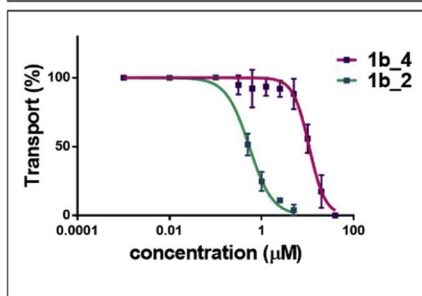
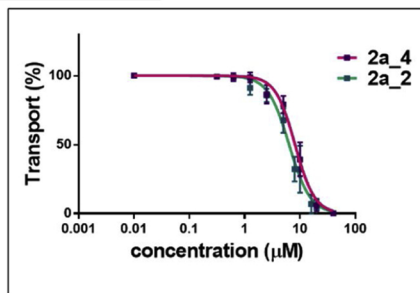
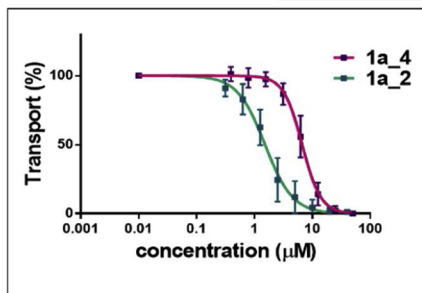
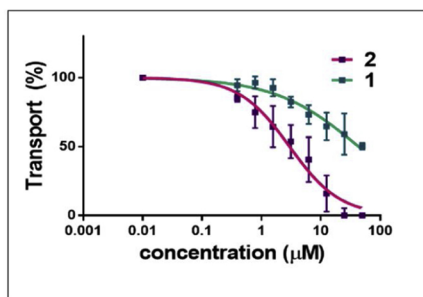


Fig. 3. Inhibition of dye uptake in A431-OATP2B1 cells by halogenated 13-epi estrones. A431-OATP2B1 cells and their mock transfected counterparts were incubated in the presence or absence of increasing amounts of the 13-epi estrones (1-100 μ M, as indicated on the x axis) with the Zombie Violet dye for 30 min at 37 °C. Fluorescence was measured in an Inspire plate reader. Fluorescence obtained in mock transfected A431 cells was subtracted from that measured in A431-OATP2B1 cells. Transport was calculated based on the fluorescence measured in the absence of 13-epi estrones (100 %). Data points show the average \pm SD values obtained in at least three independent biological replicates.

Table 1
Inhibition of OATP2B1 activity by C-2 or C-4 halogenated 13-epiestrones.

compound "name"	EC ₅₀ ± SD (μM)	compound "name"	EC ₅₀ ± SD (μM)	compound "name"	EC ₅₀ ± SD (μM)	compound "name"	EC ₅₀ ± SD (μM)
1	50			2	2.98 ± 0.05		
1a_2	1.52 ± 0.01	1a_4	6.63 ± 0.01	2a_2	6.34 ± 0.02	2a_4	8.14 ± 0.02
1b_2	0.54 ± 0.02	1b_4	10.8 ± 0.02	2b_2	22.88 ± 0.02	2b_4	18.6 ± 0.02
1c_2	2.11 ± 0.02	1c_4	> 50	2c_2	10.89 ± 0.03	2c_4	> 50

The inhibitory effect of 13-epiestrones was measured using *Zombie Violet* as a test substrate [26]. The kinetic parameters of inhibition shown on Fig. 3 were determined by the Graphpad Prism software.

determine whether the best performing newly identified inhibitor, 2-bromo-13-epiestrone (compound **1b_2**) can be applied to inhibit hormone uptake, we determined its effect on ³H-E1S uptake in A431 control and A431-OATP2B1 cells. Fig. 6 shows that compound **1b_2** can attenuate E1S uptake mediated by OATP2B1, therefore it is a good candidate to block hormone uptake in OATP2B1 expressing cells.

3.4. SAR analysis

Since the compounds under study do all possess a common core structure (scaffold) with largest variance in terms of different substituents in positions C-2 and C-4, it appears interesting to perform Structure-Activity Relationship (SAR) analysis for positions C-2 and C-4 separately. The rationale behind is that the increase or decrease of bioactivities within a congeneric SAR series of compounds can possibly be explained by the variations in physicochemical properties at a specific substitution site (R or X-group site). However, since the initial (parent) compounds 3-OH and 3-OMe are possessing very different inhibitory potential (EC₅₀ value of compound **1** (3-OH) is 50 μM while for compound **2** (3-OMe) is 2.98 μM), we have performed the SAR analysis for 3-OH and 3-OMe derivatives separately.

In the case of the 3-OH derivatives, the SAR analysis (Table 3) for substituents at position C-2 shows that the number of atoms and heavy atoms in the substituent is negatively correlated with activity (R = -0.89 and -0.84). Of equal effect is the number of aromatic carbocycles in that side chain: possessing no rings is more favorable (R = -0.90). Further, molar refractivity ('SMR') which reflects the charge distribution and hence corresponds to the polarizability of a given functional group is inversely correlated to bioactivity: less polarizable is more favourable (R = -0.88). Also Labute's Approximative Surface Area ('LabuteASA') (R = -0.82) [29] - a measure of the size of a molecules' surface area - as well as the partition coefficient ('SlogP') are negatively

correlated (R = -0.73) to activity, corresponding to a favorable lower size and lipophilicity of substituents at position C-2. Concrete values of Pearson correlation coefficients for given descriptors are listed in Table 3 (a heat map representation of correlation values is given in Supplementary Figure S1).

The only significant positive correlation at position C-2 was identified for the HallKier Alpha index ('HallKier α', R = 0.88), as introduced by Hall and Kier (equation nr. 58 in provided reference) [30]. HallKier α belongs to the class of topological descriptors which can quantify molecular shape similarity within a set of molecules. HallKier α relates to the size contribution of a query fragment to C(sp³)-hybridized atoms, which are taken as a reference (HallKier α for sp³ carbon equals to 0). HallKier α thus encodes the effect of both covalent radius and hybridization state of a given group of atoms. From Supplementary Table 1 it becomes clear that the halogenated derivatives are generally having positive HallKier α values and the phenylalkynyl compounds are showing negative values. Interestingly, in the case of 3-OMe derivatives none of the investigated physicochemical properties of the C-2 substituents showed a meaningful correlation with the bioactivity values of these compounds.

In contrast to substituents at position C-2, the SAR analysis for substituents at position C-4 did not allow to prioritize physicochemical features influencing the overall bioactivity on OATP2B1 (Table 3 and Supplementary Figure S1). In general, correlations of physicochemical features and bioactivity for substituents in position C-4 are comparable for both 3-OH and 3-OMe derivatives. Most strikingly, the number of heteroatoms of substituents at position C-4 is slightly negatively correlated with bioactivity for both 3-OH and 3-OMe derivatives (R = -0.47 and -0.45). Due to the chemical composition of our compounds, this effect points to an unfavorable effect of electronegative atoms at this position (Cl, I, Br, F) which is inverse to the trends observed for position C-2 (where halogens seem to be favorable).

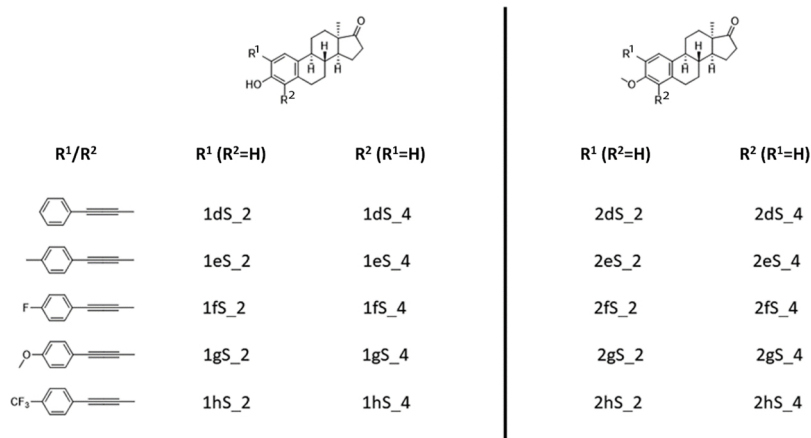


Fig. 4. Structure of the phenylalkynyl modified 13-epiestrones investigated in the current study.

Table 2
Inhibition of OATP2B1 activity by C-2 or C-4 phenylalkynylated 13-epiestrones.

compound "name"	EC ₅₀ ± SD (μM)	compound "name"	EC ₅₀ ± SD (μM)	compound "name"	EC ₅₀ ± SD (μM)	compound "name"	EC ₅₀ ± SD (μM)
1dS_2	15.53 ± 0.03	1dS_4	11.55 ± 0.02	2dS_2	> 50	2dS_4	12.83 ± 0.04
1eS_2	> 50	1eS_4	11.36 ± 0.02	2eS_2	20.77 ± 0.03	2eS_4	11.86 ± 0.02
1fS_2	12.95 ± 0.01	1fS_4	> 50	2fS_2	> 50	2fS_4	8.73 ± 0.02
1gS_2	11.08 ± 0.04	1gS_4	4.57 ± 0.01	2gS_2	3.79 ± 0.05	2gS_4	3.4 ± 0.02
1hS_2	9.27 ± 0.04	1hS_4	> 50	2hS_2	10.5 ± 0.03	2hS_4	46.09 ± 0.04

4. Discussion

Recognizing numerous clinically applied drugs and promoting their intestinal, hepatic and central nervous system (through the blood-brain-barrier) uptake, OATP2B1 is a key determinant of drug pharmacokinetics [31]. Hence understanding the mechanism of its substrate/inhibitor recognition can promote drug development and may also help in predicting/avoiding adverse effects caused by OATP2B1 mediated drug-drug interactions. In addition, OATP2B1 is a dedicated conjugated steroid hormone transporter. Its steroid hormone substrates are E1S, pregnenolone-sulfate and DHEAS [32,33]. OATP2B1 has been identified as a key uptake transporter of DHEAS and E1S in the placenta and mammary gland that are largely dependent on these hormone precursors [15,34]. In addition, OATP2B1 expressed in endothelial cells of the blood-brain barrier is considered as an important mediator of the uptake of the neuroactive steroids DHEAS and pregnenolone-sulfate into the brain [35]. On the other hand, increased steroid hormone uptake by OATP2B1 may also be favorable for tumor progression, as was demonstrated in breast and prostate cancer [36,37]. Therefore, inhibition of OATP2B1 function may be an alternative/successful strategy to inhibit the growth of various tumors.

During the last two decades, since OATP2B1 was cloned [27], numerous inhibitors of OATP2B1 have been described. Most of these are clinically applied drugs, like cyclosporin A, rifampicin and statins [38,39]. However these compounds are also inhibiting other drug transporters, like P-glycoprotein [40] and additional OATPs or even CYP enzymes [6,41], therefore they are lacking OATP2B1 specificity. In addition, various steroids, e.g. estrone or testosterone that are themselves not transported by OATP2B1 have been documented as OATP2B1 inhibitors [32]. However, besides again the lack of specificity, these steroids are not effective inhibitors, since only low levels of inhibition could be observed even at concentrations well above their physiological occurrence. Grube et al. documented only 20–30 % decrease in OATP2B1-mediated E1S uptake by the application of 10 or 100 μM testosterone or estrone, respectively [32].

13-epiestrones represent a new class of OATP2B1 inhibitors. They have no steroidogenic effect, hence their application may be void of side effects. In our preliminary work we found that phosphonated 13-epiestrones are potent inhibitors of OATP2B1 function, with EC₅₀ values in the micromolar range [24]. In order to map the molecular determinants of this inhibition, here we analyzed the inhibitory effect of a series of 3-hydroxy or 3-methylether 13-epiestrones containing a second, C-2 or C-4 halogen or phenylalkynyl modification. **Compound 1**, (3-OH 13-epiestrone) showed no interaction with OATP2B1 (EC₅₀ around 50 μM), but the 3-methoxy counterpart **compound 2** (3-OMe 13-epiestrone) performed a strong interaction (EC₅₀ 2.98 μM). Introduction of a second modification on C-2 or C-4 resulted in various effects. In the case of 3-OMe 13-epiestrones, the second modification issued in a decrease or loss of inhibitory activity with the exception of 2-iodo or 4-iodo (**2a_2** and **2a_4**), (4-fluorophenyl)ethynyl (**2fS_4**), (2-methoxyphenyl)ethynyl (**2gS_2**) and (4-methoxyphenyl)ethynyl

(**2gS_4**) derivatives having similar EC₅₀ values as the initial compound 3-OMe 13-epiestrone. In contrast, in the case of 13-epiestrone, the second modification had various effects depending on the site (C-2 or C-4) or nature (halogen or phenylalkynyl) of the substitution. In general, introduction of a phenylalkynyl substituent did not result in potent inhibitors. The only exception was the C-4 modified compound **1gS_4** having an EC₅₀ value well below 10 μM. However, the most striking change in the inhibitory effect was observed in the case of the 2-halogenated 13-epiestrones (**1a_2**, **1b_2** and **1c_2**). These compounds potently inhibited OATP2B1 function with EC₅₀ values between 0.5 and 2.1 μM. In addition, halogenated 13-epiestrones revealed a strong regioselectivity, 4-halogenated compounds showing no or very weak inhibition of OATP2B1 activity. This C-2 halogen preference has already been observed in the case of 2-iodo-estrone-3-sulfate [42]. Banerjee and colleagues have demonstrated that 2-[¹²⁵I]-estrone-3-sulfate is transported by OATP2B1 while transport in the case of its 4-iodo counterpart could not be observed.

SAR analysis by R-group decomposition was performed in order to elucidate molecular determinants potentially being responsible for bioactivity of 13-epiestrones. Different potency of respective compounds was correlated to the subtle changes in physico-chemical properties at a specific R or X -group position. It has to be emphasized that the observed trends are showing correlations of side chain features and bioactivity, but these correlations are not necessarily pointing to a causal relationship of activity and chemical descriptor value. In other words, some of the correlations we see might be artefacts caused by high intercorrelation of related features (e.g. molecular weight and lipophilicity are often intercorrelated). The presence of halogens in position C-2 was identified to drive the activity against OATP2B1. The importance of fluor and 4-fluorophenyl functional groups for OATP2B1 substrate activity was already demonstrated by the substructural fragment analysis performed by Shaikh et al. [43]. Our findings are suggesting the likelihood of halogen bond formation in OATP2B1-ligand binding complexes. As an outlook, we suggest to prove such a hypothesis by e.g. molecular docking combined with quantum mechanics techniques. SAR analysis of functional groups at position C-4 delivered negative correlation with the number of heteroatoms. These trends, however, appear to be less pronounced for position C-4 substituents and therefore it is required to repeat the analyses with a bigger data set showing a larger range of structural variations in this position for further investigations. SAR analysis revealed that 3-OH derivatives are showing more pronounced positive and negative correlation with different physicochemical properties at position C-2. In general, 3-OH derivatives are more sensitive to the substitutions at position C-2 when compared to 3-OMe derivatives.

In our previous study we investigated 3-hydroxy, 3-methylether and 3-benzylether (3-OBn) 13-epiestrones with a C-2 or C-4 diethyl phosphono or diphenylphosphine oxide substitution [24]. In that study, in accordance with our current findings, we found that the second (C-2 or C-4) modification results in dramatic increase in the inhibitory potential of 13-epiestrone (3-OH). Also in harmony with our current results,

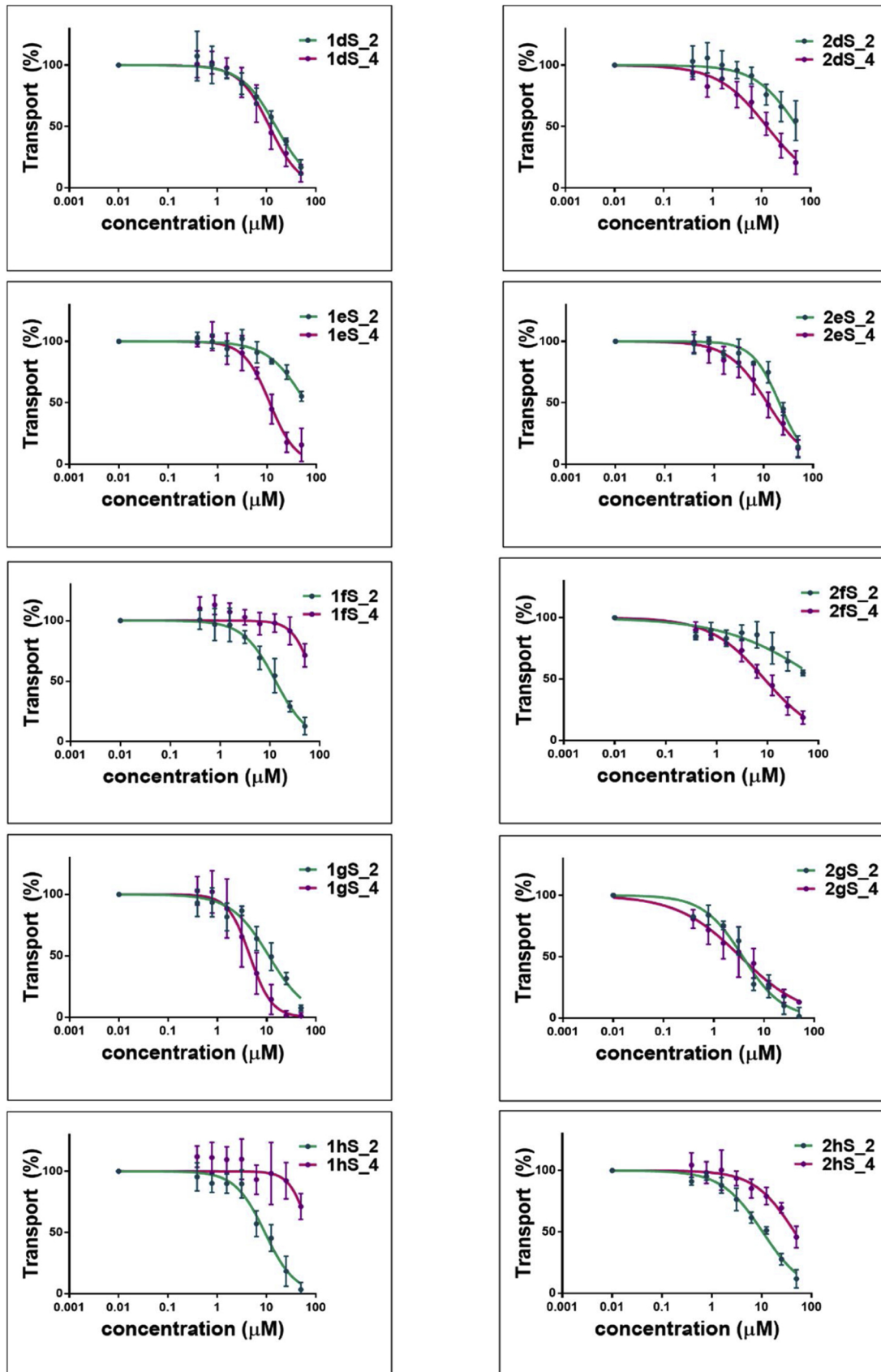


Fig. 5. Inhibition of dye uptake in A431-OATP2B1 cells by phenylalkynylated 13-epiandrosterones. Inhibition of Zombie Violet uptake in A431-OATP2B1 and mock transfected cells was measured as described at Fig. 3. Average \pm SD values obtained in at least three independent biological replicates are shown.

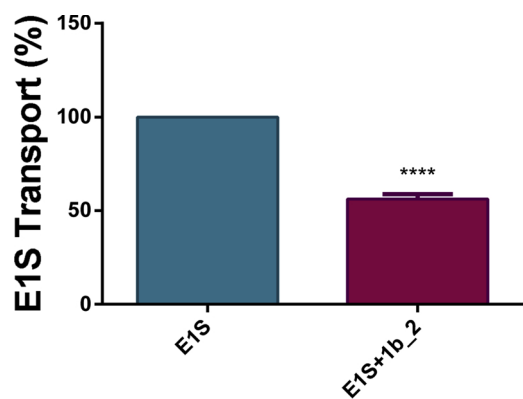


Fig. 6. Inhibition of ³H-E1S uptake in A431-OATP2B1 cells by 2-bromo-13-epiestrone (1b₂). A431-OATP2B1 cells and their mock transfected counterparts were incubated in the presence or absence of 50 μM 1b₂ with 9.65 nM ³H-E1S for 10 min at 37 °C. The radioactivity was measured by Wallac Liquid Scintillator Counter. Radioactivity obtained in mock transfected A431 cells was subtracted from that measured in A431-OATP2B1 cells. Transport was calculated based on the measured radioactivity of ³H-E1S in the absence of 2-bromo-13-epiestrone (100 %). Data points show the average +/- SD values obtained in three independent biological replicates. Significance was calculated with GraphPad Prism, using unpaired t-test, ****P < 0.0001.

Table 3

Pearson correlation coefficients for physico-chemical descriptors at position C-2 and C-4.

A) 3-OH derivatives		
Descriptor name	Pearson correlation coefficient	
	Position C-2	Position C-4
NumAtoms	-0.89	0.01
NumHeavyAtoms	-0.84	-0.13
NumHeteroAtoms	0.23	-0.47
NumAromaticCarbocycles	-0.90	-0.06
SMR	-0.88	0.08
LabuteASA	-0.82	-0.03
SlogP	-0.73	-0.26
HallKierAlpha	0.88	0.13

B) 3-Ome derivatives		
Descriptor name	Pearson correlation coefficient	
	Position C-2	Position C-4
NumAtoms	-0.05	0.31
NumHeavyAtoms	-0.06	0.20
NumHeteroAtoms	0.39	-0.45
NumAromaticCarbocycles	-0.21	0.30
SMR	-0.05	0.39
LabuteASA	-0.01	0.28
SlogP	-0.08	-0.04
HallKierAlpha	0.16	-0.23

the second modification could not further improve the potent inhibition by 3-Ome 13-epiestrone. However, in the case of phosphonated 13-epiestrones, the OATP2B1 inhibitory action did not substantially depend on the regioisomerism (C-2 vs. C-4).

HSD17β1 and STS are key enzymes in local estrogen production. Inhibition of their activity by specific or more desirably by dual inhibitors could be a good strategy to prevent tumor progression [44]. The most promising STS inhibitor STX-64, Irosustat performed well in phase I trial, however the phase II trial was not that satisfactory [44], suggesting the need for combined treatment with HSD17β1 inhibitors [45]. Moreover, it has been demonstrated that blocking the aromatase pathway resulted in the upregulation of the STS enzyme and OATPs [46]. Therefore, simultaneous blockage of the different estrogen metabolic pathways and the function of the steroid uptake transporter

Table 4

Comparison of the inhibitory effect of 13-epiestrones on OATP2B1, HSD17β1 and STS activity.

C-3	C-2	C-4	Inhibition of OATP2B1 (determined in the current study)	Inhibition of HSD17β1 (as described earlier in [21,25])	STS (as described earlier in [21])
OH	H	H	non	+	non
	halogen	H	+ / + +	+ +	non
	phenylalkynyl	H	non	+ +	+ / non
	H	halogen	+ / non	+	+ / non
Ome	H	phenylalkynyl	+ / non	non	non
	halogen	H	+	+	n.d.
	phenylalkynyl	H	+ / non	non	n.d.
	H	halogen	+ / non	+ +	n.d.
	H	phenylalkynyl	+ / non	non	n.d.

Columns labeled with C-2, C-3 or C-4 indicate modifications on the 2nd, 3rd or 4th carbon of 13-epiestrone. n.d.: no data available.

+ : EC50 below 10 μM.
+ + : EC50 below 1 μM.

OATPs could be the only successful strategy to inhibit hormone dependent cancers. Our experiments show that the newly identified best performing inhibitor, 2-bromo-13-epiestrone (compound 1b₂) can be used to inhibit OATP2B1-mediated E1S uptake (Fig. 6). Some of the inhibitors identified in our current study, including compound 1b₂, are also potent inhibitors of the HSD17β1 enzyme (see Table 4), therefore they can be good candidate dual inhibitors to be tested in hormone dependent cell lines.

Although OATP2B1 is not related evolutionally to the STS and HSD17β enzyme families, considering their overlapping inhibitor specificities, one may speculate that knowledge gathered from the inhibitor recognition profile of these enzymes can be used to design effective inhibitors of OATP2B1. This is especially important since a protein structure of OATPs is not yet available. Therefore, we have compared the inhibition data obtained in the current study for OATP2B1 with that previously measured for HSD17β1 and STS enzymes [21,25]. Table 4 shows, that inhibition of HSD17β1 reveals few similar features to that of the inhibition of OATP2B1.

Namey, HSD17β1 also has a C-2 preference and both 2-halogenated and phenylalkynyl conjugates potently inhibit HSD17β1 function. Also, similarly to OATP2B1, 3-Ome 13-epiestrones are less effective inhibitors of HSD17β1. However, C-4 halogenation of 3-Ome 13-epiestrones also results in effective inhibitors that is in contrast to that observed for OATP2B1. Unfortunately, data about the effect of the 13-epiestrones investigated in the current study on STS activity are incomplete. Nevertheless, although estrone-3-sulfate is a common substrate of OATP2B1 and STS, based on the interaction with halogenated 13-epiestrones, opposite inhibitor preference could be observed for OATP2B1 and STS. STS was only inhibited by some of the C-4 halogenated compounds that were not the most effective inhibitors of OATP2B1. We suggest that a larger data set of HSD17β1, STS, OATP and 13-epiestrone interactions should be generated in order to determine whether common trends in structural elements important for their inhibition can be observed. Also it would be interesting to investigate the inhibitory effect of 13-epiestrones on the function of other OATPs up-regulated in hormone dependent cancers, OATP1A2, OATP1B3, OATP3A1 and OATP4A1 [47]. On the other hand, hepatic OATPs, 1B1, 1B3 and 2B1 have overlapping substrate specificities, hence, although desirable, specific inhibitors amenable to distinguish between their function are scarce. The OATP2B1 inhibitor 13-epiestrones (1a₂, 1b₂ and 1c₂) identified in the current study can be good candidates to be tested for OATP1B interaction.

In summary, we identify potent inhibitors of OATP2B1. The EC₅₀ of the most potent inhibitor 2-bromo-13-epiestrone falls within the range

of previously documented OATP2B1 inhibitors (BSP 1.26 μM [26], antivirals: 0.5–1 μM , erlotinib: 0.03 μM [48] and EIS: 0.56 μM [26]. However, although potent inhibitors were identified, our assay cannot distinguish between an inhibition caused by transported substrates or non-competitive inhibitors. Further experiments, e.g. measurement of direct uptake of the best performing 13-epiestrones (showing the highest inhibition) are needed to clarify this issue. Still, one may speculate that if OATP2B1 can mediate the uptake of these HSD17 β 1 inhibitors, a more potent anti-tumor effect can be achieved in tumors expressing both HSD17 β 1 and OATP2B1. Since certain 2-halogenated-13-epiestrones, and the previously investigated phosphonated 13-epiestrones [24] are dual inhibitors of HSD17 β 1 and OATP2B1, their effect on the survival of hormone dependent cell lines with OATP2B1 overexpression, and/or HSD17 β 1 expression is reasonable to be investigated.

CRedit authorship contribution statement

Réka Laczkó-Rigó: Methodology, Visualization, Writing - original draft. **Rebeka Jójárt:** Resources. **Erzsébet Mernyák:** Resources, Writing - review & editing. **Éva Bakos:** Methodology, Supervision, Conceptualization. **Alzbeta Tuerkova:** Methodology, Formal analysis. **Barbara Zdrzil:** Methodology, Formal analysis, Writing - review & editing. **Csilla Özvegy-Laczka:** Conceptualization, Writing - review & editing.

Acknowledgements

This work has been supported by research grants from the National Research, Development and Innovation Office (OTKA FK 128751 and SNN 124329). E. M. and Cs. Ó-L. are recipients of the János Bolyai fellowship of the Hungarian Academy of Sciences. This work also received funding from the Austrian Science Fund (FWF) (Grant P 29712).

Appendix A. Supplementary data

Supplementary material related to this article can be found, in the online version, at doi:<https://doi.org/10.1016/j.jsbmb.2020.105652>.

References

- [1] B. Hagenbuch, B. Stieger, The SLCO (former SLC21) superfamily of transporters, *Mol. Aspects Med.* 34 (2013) 396–412.
- [2] J. König, Y. Cui, A.T. Nies, D. Keppler, A novel human organic anion transporting polypeptide localized to the basolateral hepatocyte membrane, *Am. J. Physiol. Gastrointest. Liver Physiol.* 278 (2000) G156–64.
- [3] M. Roth, A. Obaidat, B. Hagenbuch, OATPs, OATs and OCTs: the organic anion and cation transporters of the SLCO and SLC22A gene superfamilies, *Br. J. Pharmacol.* 165 (2012) 1260–1287.
- [4] A. Obaidat, M. Roth, B. Hagenbuch, The expression and function of organic anion transporting polypeptides in normal tissues and in cancer, *Annu. Rev. Pharmacol. Toxicol.* 52 (2012) 135–151.
- [5] A. Koenen, K. Kock, M. Keiser, W. Siegmund, H.K. Kroemer, M. Grube, Steroid hormones specifically modify the activity of organic anion transporting polypeptides, *Eur. J. Pharm. Sci.* 47 (2012) 774–780.
- [6] A. Kalliokoski, M. Niemi, Impact of OATP transporters on pharmacokinetics, *Br. J. Pharmacol.* 158 (2009) 693–705.
- [7] V. Buxhofer-Ausch, L. Secky, K. Wlcek, M. Svoboda, V. Kounnis, E. Briasoulis, A.G. Tzakos, W. Jaeger, T. Thalhammer, Tumor-specific expression of organic anion-transporting polypeptides: transporters as novel targets for cancer therapy, *J. Drug Deliv.* 2013 (2013) 863539.
- [8] R.R. Schulte, R.H. Ho, Organic anion transporting polypeptides: emerging roles in Cancer pharmacology, *Mol. Pharmacol.* 95 (2019) 490–506.
- [9] K. Wlcek, M. Svoboda, T. Thalhammer, F. Sellner, G. Krupitza, W. Jaeger, Altered expression of organic anion transporter polypeptide (OATP) genes in human breast carcinoma, *Cancer Biol. Ther.* 7 (2008) 1450–1455.
- [10] D. Kovacsics, I. Patik, C. Özvegy-Laczka, The role of organic anion transporting polypeptides in drug absorption, distribution, excretion and drug-drug interactions, *Expert Opin. Drug Metab. Toxicol.* 13 (2017) 409–424.
- [11] T. Nakanishi, I. Tamai, Genetic polymorphisms of OATP transporters and their impact on intestinal absorption and hepatic disposition of drugs, *Drug Metab. Pharmacokinet.* 27 (2012) 106–121.
- [12] B. Gao, S.R. Vavricka, P.J. Meier, B. Stieger, Differential cellular expression of

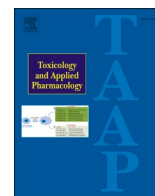
- organic anion transporting peptides OATP1A2 and OATP2B1 in the human retina and brain: implications for carrier-mediated transport of neuropeptides and neurosteroids in the CNS, *Pflugers Arch.* 467 (2015) 1481–1493.
- [13] J. Kindla, T.T. Rau, R. Jung, P.A. Fasching, R. Strick, R. Stoehr, A. Hartmann, M.F. Fromm, J. König, Expression and localization of the uptake transporters OATP2B1, OATP3A1 and OATP5A1 in non-malignant and malignant breast tissue, *Cancer Biol. Ther.* 11 (2011) 584–591.
- [14] J. Matsumoto, N. Ariyoshi, M. Sakakibara, T. Nakanishi, Y. Okubo, N. Shiina, K. Fujisaki, T. Nagashima, Y. Nakatani, I. Tamai, H. Yamada, H. Takeda, I. Ishii, Organic anion transporting polypeptide 2B1 expression correlates with uptake of estrone-3-sulfate and cell proliferation in estrogen receptor-positive breast cancer cells, *Drug Metab. Pharmacokinet.* 30 (2015) 133–141.
- [15] F. Pizzagalli, Z. Varga, R.D. Huber, G. Folkers, P.J. Meier, M.V. St-Pierre, Identification of steroid sulfate transport processes in the human mammary gland, *J. Clin. Endocrinol. Metab.* 88 (2003) 3902–3912.
- [16] S.M. Green, A. Kaipainen, K. Bullock, A. Zhang, J.M. Lucas, C. Matson, W.A. Banks, E.A. Mostaghel, Role of OATP transporters in steroid uptake by prostate cancer cells *in vivo*, *Prostate Cancer Prostatic Dis.* 20 (2017) 20–27.
- [17] N. Fujimoto, T. Kubo, H. Inatomi, H.T. Bui, M. Shiota, T. Sho, T. Matsumoto, Polymorphisms of the androgen transporting gene SLCO2B1 may influence the castration resistance of prostate cancer and the racial differences in response to androgen deprivation, *Prostate Cancer Prostatic Dis.* 16 (2013) 336–340.
- [18] M. Yang, W. Xie, E. Mostaghel, M. Nakabayashi, L. Werner, T. Sun, M. Pomerantz, M. Freedman, R. Ross, M. Regan, N. Sharifi, W.D. Figg, S. Balk, M. Brown, M.E. Taplin, W.K. Oh, G.S. Lee, P.W. Kantoff, SLCO2B1 and SLCO1B3 may determine time to progression for patients receiving androgen deprivation therapy for prostate cancer, *J. Clin. Oncol.* 29 (2011) 2565–2573.
- [19] D. Ayan, J. Roy, R. Maltais, D. Poirier, Impact of estradiol structural modifications (18-methyl and/or 17-hydroxy inversion of configuration) on the *in vitro* and *in vivo* estrogenic activity, *J. Steroid Biochem. Mol. Biol.* 127 (2011) 324–330.
- [20] B. Schonecker, C. Lange, M. Kotteritzsch, W. Gunther, J. Weston, E. Anders, H. Gørls, Conformational design for 13 α -steroids, *J. Org. Chem.* 65 (2000) 5487–5497.
- [21] I. Bacsa, B.E. Herman, R. Jójárt, K.S. Herman, J. Wolfling, G. Schneider, M. Varga, C. Tomboly, T.L. Rizner, M. Szecsi, E. Mernyák, Synthesis and structure-activity relationships of 2- and/or 4-halogenated 13 β - and 13 α -estrone derivatives as enzyme inhibitors of estrogen biosynthesis, *J. Enzyme Inhib. Med. Chem.* 33 (2018) 1271–1282.
- [22] J.M. Tian, B. Ran, C.L. Zhang, D.M. Yan, X.H. Li, Estrogen and progesterone promote breast cancer cell proliferation by inducing cyclin G1 expression, *Braz. J. Med. Biol. Res.* 51 (2018) 1–7.
- [23] M. Yang, J. Wang, L. Wang, C. Shen, B. Su, M. Qi, J. Hu, W. Gao, W. Tan, B. Han, Estrogen induces androgen-repressed SOX4 expression to promote progression of prostate cancer cells, *Prostate* 75 (2015) 1363–1375.
- [24] R. Jójárt, S. Pecszy, G. Keglevich, M. Szecsi, R. Rigo, C. Özvegy-Laczka, G. Kecskemeti, E. Mernyák, Pd-Catalyzed microwave-assisted synthesis of phosphonated 13 α -estrone derivatives as potential OATP2B1, 17 β -HSD1 and/or STS inhibitors, *Beilstein J. Org. Chem.* 14 (2018) 2838–2845.
- [25] I. Bacsa, R. Jójárt, J. Wolfling, G. Schneider, B.E. Herman, M. Szecsi, E. Mernyák, Synthesis of novel 13 α -estrone derivatives by Sonogashira coupling as potential 17 β -HSD1 inhibitors, *Beilstein J. Org. Chem.* 13 (2017) 1303–1309.
- [26] I. Patik, V. Szekely, O. Nemet, A. Szepesi, N. Kucsma, G. Varady, G. Szakacs, E. Bakos, C. Özvegy-Laczka, Identification of novel cell-impermeant fluorescent substrates for testing the function and drug interaction of Organic Anion-Transporting Polypeptides, OATP1B1/1B3 and 2B1, *Sci. Rep.* 8 (2018) 2630.
- [27] G.A. Kullak-Ublick, M.G. Ismail, B. Stieger, L. Landmann, R. Huber, F. Pizzagalli, K. Fattinger, P.J. Meier, B. Hagenbuch, Organic anion-transporting polypeptide B (OATP-B) and its functional comparison with three other OATPs of human liver, *Gastroenterology* 120 (2001) 525–533.
- [28] M.R.C. Berthold, N. Dill, F. Gabriel, T.R. Kotter, T.O. Meinel, P. Thiel, K. B. Wiswedel, KNIME - the konstanz information miner version 2.0 and beyond *AcM SIGKDD explorations Newsletter*, 11 (2009), pp. 26–31.
- [29] P. Labute, A widely applicable set of descriptors, *J. Mol. Graph. Model.* 18 (2000) 464–477.
- [30] L.H.K. Hall, L. B, The molecular connectivity chi indexes and kappa shape indexes in structure-property modeling, *Rev. Comput. Chem.* (1991) 367–422.
- [31] S.J. McFeely, L. Wu, T.K. Ritchie, J. Unadkat, Organic anion transporting polypeptide 2B1 - more than a glass-full of drug interactions, *Pharmacol. Ther.* 196 (2019) 204–215.
- [32] M. Grube, K. Kock, S. Karner, S. Reuther, C.A. Ritter, G. Jedlitschky, H.K. Kroemer, Modification of OATP2B1-mediated transport by steroid hormones, *Mol. Pharmacol.* 70 (2006) 1735–1741.
- [33] I. Tamai, T. Nozawa, M. Koshida, J. Nezu, Y. Sai, A. Tsuji, Functional characterization of human organic anion transporting polypeptide B (OATP-B) in comparison with liver-specific OATP-C, *Pharm. Res.* 18 (2001) 1262–1269.
- [34] M.V. St-Pierre, B. Hagenbuch, B. Ugele, P.J. Meier, T. Stallmach, Characterization of an organic anion-transporting polypeptide (OATP-B) in human placenta, *J. Clin. Endocrinol. Metab.* 87 (2002) 1856–1863.
- [35] M. Grube, P. Hagen, G. Jedlitschky, Neurosteroid transport in the brain: role of ABC and SLC transporters, *Front. Pharmacol.* 9 (2018) 354.
- [36] W. Al Sarakbi, R. Mokbel, M. Salhab, W.G. Jiang, M.J. Reed, K. Mokbel, The role of STS and OATP-B mRNA expression in predicting the clinical outcome in human breast cancer, *Anticancer Res.* 26 (2006) 4985–4990.
- [37] T. Nozawa, M. Suzuki, H. Yabuuchi, M. Irokawa, A. Tsuji, I. Tamai, Suppression of cell proliferation by inhibition of estrone-3-sulfate transporter in estrogen-dependent breast cancer cells, *Pharm. Res.* 22 (2005) 1634–1641.

- [38] J. König, H. Glaeser, M. Keiser, K. Mandery, U. Klotz, M.F. Fromm, Role of organic anion-transporting polypeptides for cellular mesalazine (5-aminosalicylic acid) uptake, *Drug Metab. Dispos.* 39 (2011) 1097–1102.
- [39] I.Y. Gong, R.B. Kim, Impact of genetic variation in OATP transporters to drug disposition and response, *Drug Metab. Pharmacokinet.* 28 (2013) 4–18.
- [40] R.B. Kim, Drugs as P-glycoprotein substrates, inhibitors, and inducers, *Drug Metab. Rev.* 34 (2002) 47–54.
- [41] A. Koenen, H.K. Kroemer, M. Grube, H.E. Meyer zu Schwabedissen, Current understanding of hepatic and intestinal OATP-mediated drug-drug interactions, *Expert Rev. Clin. Pharmacol.* 4 (2011) 729–742.
- [42] N. Banerjee, T.R. Wu, J. Chio, R. Kelly, K.A. Stephenson, J. Forbes, C. Allen, J.F. Valliant, R. Bendayan, (125)I-Labelled 2-Iodoestrone-3-sulfate: synthesis, characterization and OATP mediated transport studies in hormone dependent and independent breast cancer cells, *Nucl. Med. Biol.* 42 (2015) 274–282.
- [43] N. Shaikh, M. Sharma, P. Garg, Selective fusion of heterogeneous classifiers for predicting substrates of membrane transporters, *J. Chem. Inf. Model.* 57 (2017) 594–607.
- [44] X. Sang, H. Han, D. Poirier, S.X. Lin, Steroid sulfatase inhibition success and limitation in breast cancer clinical assays: an underlying mechanism, *J. Steroid Biochem. Mol. Biol.* 183 (2018) 80–93.
- [45] T.L. Rizner, T. Thalhammer, C. Ozvegy-Laczka, The importance of steroid uptake and intracrine action in endometrial and ovarian cancers, *Front. Pharmacol.* 8 (2017) 346.
- [46] T. Higuchi, M. Endo, T. Hanamura, T. Gohnno, T. Niwa, Y. Yamaguchi, J. Horiguchi, S. Hayashi, Contribution of estrone sulfate to cell proliferation in aromatase inhibitor (AI)-Resistant, hormone receptor-positive breast Cancer, *PLoS One* 11 (2016) e0155844.
- [47] N. Banerjee, N. Miller, C. Allen, R. Bendayan, Expression of membrane transporters and metabolic enzymes involved in estrone-3-sulphate disposition in human breast tumour tissues, *Breast Cancer Res. Treat.* 145 (2014) 647–661.
- [48] R.A. Johnston, T. Rawling, T. Chan, F. Zhou, M. Murray, Selective inhibition of human solute carrier transporters by multikinase inhibitors, *Drug Metab. Dispos.* 42 (2014) 1851–1857.



Contents lists available at ScienceDirect

Toxicology and Applied Pharmacology

journal homepage: www.elsevier.com/locate/taapSelective antiproliferative effect of C-2 halogenated 13 α -estrones on cells expressing Organic anion-transporting polypeptide 2B1 (OATP2B1)Réka Laczkó-Rigó^a, Éva Bakos^a, Rebeka Jójárt^b, Csaba Tömböly^c, Erzsébet Mernyák^b, Csilla Özvegy-Laczka^{a,*}^a Institute of Enzymology, Research Centre for Natural Sciences, Eötvös Loránd Research Center, Magyar tudósok körútja 2, H-1117 Budapest, Hungary^b Department of Organic Chemistry, University of Szeged, Dóm tér 8, H-6720 Szeged, Hungary^c Laboratory of Chemical Biology, Institute of Biochemistry, Biological Research Centre, Temesvári krt. 62, H-6726 Szeged, Hungary

ARTICLE INFO

Editor: Dr. Lawrence Lash

Keywords:

13 α -estrones
Selective antiproliferative effect
Steroid uptake
OATP

ABSTRACT

Organic anion-transporting polypeptide 2B1 (OATP2B1) is a multispecific transporter mediating the cellular uptake of steroids and numerous drugs. OATP2B1 is abundantly expressed in the intestine and is also present in various tumors. Increased steroid hormone uptake by OATP2B1 has been suggested to promote progression of hormone dependent tumors. 13 α -estrones are effective inhibitors of endogenous estrogen formation and are potential candidates to inhibit proliferation of hormone dependent cancers. Recently, we have identified a variety of 13 α / β -estrone-based inhibitors of OATP2B1. However, the nature of this interaction, whether these inhibitors are potential transported substrates of OATP2B1 and hence may be enriched in OATP2B1-overexpressing cells, has not yet been investigated. In the current study we explored the antiproliferative effect of the most effective OATP2B1 inhibitor 13 α / β -estrones in control and OATP2B1-overexpressing A431 carcinoma cells. We found an increased antiproliferative effect of 3-O-benzyl 13 α / β -estrones in both mock transfected and OATP2B1-overexpressing cells. However, C-2 halogenated 13 α -estrones had a selective OATP2B1-mediated cell growth inhibitory effect. In order to demonstrate that increased sensitization can be attributed to OATP2B1-mediated cellular uptake, tritium labeled 2-bromo-13 α -estrone was synthesized for direct transport measurements. These experiments revealed increased accumulation of [³H]2-bromo-13 α -estrone due to OATP2B1 function. Our results indicate that C-2 halogenated 13 α -estrones are good candidates in the design of anti-cancer drugs targeting OATP2B1.

1. Introduction

Organic anion-transporting polypeptides (OATPs) are membrane proteins mediating the cellular uptake of various endogenous and exogenous organic compounds in a Na⁺ and ATP independent manner (Hagenbuch and Stieger, 2013). The known 11 human OATPs vary in their tissue distribution and substrate specificity. Some members of the OATP family are expressed ubiquitously in the human body (Konig et al., 2000; Roth et al., 2012), while others possess a tissue specific expression, like OATPs, 1B1 and 1B3, expressed exclusively in hepatocytes (Konig et al., 2000). OATPs, 1A2, 1B1, 1B3 and 2B1 are multispecific transporters recognizing a plethora of organic compounds, while for e. g., OATP1C1, a thyroid transporter, has a more limited substrate recognition pattern (Kovacsics et al., 2017; Pizzagalli et al., 2002) at

least based on the available research data. Steroids, like bile acids and steroid hormones are common OATP substrates. OATPs, 1A2, 1B1, 2B1 and 4A1 are key participants in the cellular uptake of estrone-3-sulfate (E1S) and dehydroepiandrosterone-sulfate (DHEAS) and hence these OATPs are important in the maintenance of steroid hormone homeostasis (Rizner et al., 2017). On the other hand, altered expression of OATPs in tumors was documented by numerous studies (Buxhofer-Ausch et al., 2013; Thakkar et al., 2015). It has been proposed that elevated uptake of nutrients and hormones by OATPs provides a selective advantage of tumor cells over their healthy counterparts (Buxhofer-Ausch et al., 2013). For example, overexpression of OATPs, 1A2, 1B3 and 2B1 results in enhanced uptake of E1S and DHEAS and consequently issue in an increased survival of breast cancer cells in vitro (Arakawa et al., 2012; Matsumoto et al., 2015; Nozawa et al., 2004). Moreover, in

* Corresponding author.

E-mail addresses: rigo.reka@ttk.hu (R. Laczkó-Rigó), bakos.eva@ttk.hu (É. Bakos), tomboly.csaba@brc.hu (C. Tömböly), bobe@chem.u-szeged.hu (E. Mernyák), laczka.csilla@ttk.hu (C. Özvegy-Laczka).<https://doi.org/10.1016/j.taap.2021.115704>

Received 24 April 2021; Received in revised form 6 August 2021; Accepted 26 August 2021

Available online 30 August 2021

0041-008X/© 2021 The Authors.

Published by Elsevier Inc.

This is an open access article under the CC BY-NC-ND license

<http://creativecommons.org/licenses/by-nc-nd/4.0/>.

vivo data from prostate cancer patients also underline that OATP expression promotes tumor progression. Enhanced testosterone uptake by OATP1B3, or DHEAS by OATP2B1 stimulates prostate cancer progression (Hamada et al., 2008; Wright et al., 2011). Therefore, inhibition of the uptake of hormones or hormone precursors by OATPs may be a potential strategy in the treatment of hormone dependent cancers.

On the other hand, multispecific OATPs also recognize various medicines, encompassing chemotherapeutics. Hence, they can potentially be targeted to increase intratumor accumulation of chemotherapeutic agents. For instance, OATPs, 1B1 and 1B3 transport atrasentan, sorafenib-glucuronide, SN-38 (the active metabolite of irinotecan), docetaxel, methotrexate, paclitaxel, and doxorubicin (Durmus et al., 2016). Additionally, OATP2B1, overexpressed in several cancers, including tumors of the breast, colon, bone and gliomas (Kovacsics et al., 2017), promotes the intracellular accumulation of abiraterone (Mostaghel et al., 2017), erlotinib (Bauer et al., 2018), etoposide (Fahrmayr et al., 2012), teniposide (Schafer et al., 2018) and SN-38 (Fujita et al., 2016). OATP2B1 has been shown to sensitize tumor cells to various chemotherapeutics (e.g.: tamoxifen, cytarabine) (Windt et al., 2019).

Inhibition of local estradiol synthesis through the inhibition of the aromatase or steroid-sulfatase (STS) pathways (e.g. by Exemestane or Irosustat, respectively (Gupta et al., 2013; Sang et al., 2018)) is a medical strategy to treat hormone dependent breast cancer in postmenopausal women. Recently, various 13 α -estrone-derivatives have been developed that inhibit another key enzyme of local estradiol synthesis, 17 β -hydroxysteroid dehydrogenase 1 (HSD1) (Ayan et al., 2011; Bacsá et al., 2015). 13 α -estrone is the epimer of the natural 13 β -estrone that, due to a configurational change, cannot bind to the estrogen receptor and lacks hormonal activity (Ayan et al., 2011; Yaremenko and Khvat, 1994; Schonecker et al., 2000). Moreover, various 13 α -estrones have been shown to inhibit the steroid transporter OATP2B1 as well (Jojart et al., 2018; Jójárt et al., 2021). Therefore, these derivatives are a promising novel, dual-target tool for the treatment of hormone sensitive cancers. Furthermore, if 13 α -estrones were enriched in tumors by the function of OATP2B1 it could also potentially enhance their efficacy. Therefore, in the current study we investigated the antiproliferative effect of a set of previously identified 13 α -estrone derivative OATP2B1 inhibitors to identify potential OATP2B1-transported substrates.

2. Materials and methods

2.1. Materials

If not stated otherwise materials were purchased from Sigma Aldrich, Merck (St. Louis, MO, US). The investigated steroids were synthesized as described elsewhere (Bacsá et al., 2018; Jojart et al., 2018; Jójárt et al., 2021).

Tritium labeling was carried out in a self-designed vacuum manifold (Schafer et al., 2015), radioactivity was measured with a Packard Tri-Carb 2100 TR liquid scintillation analyzer using Hionic-Fluor scintillation cocktail of PerkinElmer. Radio-HPLC was performed on a Jasco HPLC system equipped with a Packard Radiomatic 505 TR Flow Scintillation Analyzer.

2.2. Synthesis of 2-bromo-13 α -estrone

2-Bromo- and 2,4-dibromo-13 α -estrone were synthesized as described elsewhere (Bacsá et al., 2018).

2.3. Preparation of [³H]2-bromo-13 α -estrone ([³H]2_2Br)

4.3 mg of 2,4-dibromo-13 α -estrone (10 μ mol) was dissolved in 0.6 mL of EtOAc in the presence of 5 mg of Pd/C (10% Pd) catalyst and 3 μ L of triethylamine (21 μ mol). The reaction mixture was degassed prior to tritium reduction by two freeze-thaw cycles, and then it was stirred under 0.18 bar of tritium gas for 2 h at rt. The excess tritium gas was then absorbed onto pyrophoric uranium and the catalyst was filtered off with a syringe filter.

The filtrate was evaporated in vacuo and the labile tritium was removed by repeated evaporations from EtOH solution. Finally, 10.6 GBq of [³H]13 α -estrone (2) was isolated as a white solid that was immediately used for the next step. 450 MBq of [³H]13 α -estrone (2) was dissolved in 200 μ L of dichloromethane and 28 μ L of 1,3-dibromo-5,5-dimethylhydantoin dissolved in dichloromethane (5 mg/mL, 0.45 μ mol) was added. The solution was stirred for 15 min then it was evaporated and the resulting solid was dissolved in tetrahydrofuran. HPLC purification resulted in 28 MBq of [³H] 2_2Br. The specific activity was determined by using an HPLC peak area calibration curve recorded with 2-bromo-13 α -estrone (2_2Br) and it was found to be 555 MBq/mmol. The tritium labeled [³H]2-bromo-13 α -estrone ([³H]2_2Br) was dissolved in EtOH (37 MBq/mL) and stored in liquid nitrogen.

2.4. Generation and maintenance of the cell lines

The A431 (human epidermoid carcinoma) cell line was purchased from ATCC. OATP2B1 and mock transfected A431 cell lines were generated as described previously (Patik et al., 2018). To generate cells with a fluorescent marker (green fluorescent protein, GFP or mCherry), A431 mock or A431-OATP2B1 cells were transduced with lentiviral supernatants produced with pRRL-EF1-mCherry or pRRL-EF1-eGFP expression plasmids (Windt et al., 2019). Cells were cultured in DMEM (Gibco, Thermo Fischer Scientific (Waltham, MA, US)) supplemented with 2 mM L-glutamine, 100 U/mL penicillin and 100 μ g/mL streptomycin and 10% fetal calf serum at 37 °C with 5% CO₂ and 95% humidity.

2.5. Detection of OATP2B1 expression by Western blot

OATP2B1 expression in the cell lines was confirmed by Western blot as previously described in (Patik et al., 2018). Shortly, whole cell lysate of the OATP2B1 and mock transfected cell lines were separated on 7.5% SDS-PAGE gels and proteins were transferred onto PVDF membranes. The presence of OATP2B1 was detected by an anti-OATP2B1 antibody (a kind gift of Dr. Bruno Stieger, Department of Clinical Pharmacology and Toxicology, University Hospital, 8091 Zurich, Switzerland (Kullak-Ublick et al., 2001) with an epitope of: LLVSGPGKKPEDSRV). As a secondary antibody 20,000 \times diluted HRP-conjugated anti-rabbit antibody (Jackson ImmunoResearch, Suffolk, UK) was used. Antibody raised against β -actin was applied as an internal control (anti- β -actin antibody (A1978, Sigma)) and in this case a HRP-conjugated anti-mouse secondary antibody was used (Jackson ImmunoResearch, Suffolk, UK) in 20,000 \times dilution. Luminescence was detected by Luminor Enhancer Solution kit by Thermo Fisher Scientific (Waltham, MA, US).

2.6. Functional measurements

OATP2B1 expression was regularly checked by Zombie Violet (ZV, BioLegend®, San Diego, CA, US) uptake by flow cytometry (Patik et al., 2018). A431-OATP2B1 and mock transfected cells were collected after 0.1% trypsin treatment. The cells were washed with 1 mL uptake buffer (125 mM NaCl, 4.8 mM KCl, 1.2 mM CaCl₂, 1.2 mM KH₂PO₄, 12 mM MgSO₄, 25 mM MES, and 5.6 mM glucose, with the pH adjusted to 5.5 using 1 N NaOH). 5 \times 10⁵ cells were incubated with ZV (0.4 μ L ZV/5 \times 10⁵ cells) for 15 min at 37 °C in a final volume of 100 μ L. The reaction was stopped by adding 500 μ L ice cold phosphate-buffered saline (PBS) and until the flow cytometry analysis the cells were kept on ice. The fluorescence of 10,000 living cells was determined by Attune NxT Flow Cytometer (Invitrogen, Carlsbad, CA).

2.7. Fluorescence-based measurement of cell proliferation

To measure the antiproliferative effect of the compounds, a fluorescence-based cell proliferation assay was performed as published in (Windt et al., 2019). The number of the fluorophore-labeled cells

(A431-mock-GFP and A431-OATP2B1-mCherry) is traceable over the incubation time, as the fluorescence is proportional with the number of the cells.

Cells were seeded in a density of 5×10^3 cells/well on 96-well plates in 100 μ L in DMEM supplemented with 2 mM L-glutamine, 100 U/mL penicillin and 100 μ g/mL streptomycin and 10% fetal calf serum. After 16–24 h the steroids diluted in 100 μ L DMEM (0–50 or 0–100 μ M final concentration) were added to the cells. As a control, 10 μ M PZ-08 (3-*N*-benzyltriaazolylmethyl-13 α -estrone) was applied, previously shown to inhibit growth of A431 cells by 100% (Szabo et al., 2016b). The cells were cultured for 120 h at 37 °C with 5% CO₂ after which cellular fluorescence was recorded by a Perkin Elmer Enspire microplate reader (GFP: ex/em 485/510 nm; mCherry: ex/em 585/610 nm) by scanning the plate at a resolution of five points per well. Cell number was calculated based on the fluorescence values measured in non-treated (100%) or PZ-08-treated (0%) wells. Experiments were repeated in at least 3 biological replicates with 3 parallels in each. Mean \pm SD values are shown.

2.8. Measurement of intracellular accumulation of 2,2Br

A431 mock control and A431-OATP2B1 cells (10^6 cells/sample) were incubated in the presence of 0.135 μ M [³H]2,2Br in a final concentration of 1 μ M (or higher, see below) in 100 μ L uptake buffer pH 5.5 for 10 min at 37 °C (or on ice, see Figure 8). The reaction was stopped by the addition of 1 mL ice-cold PBS and the cells were centrifuged at 300g. The cell pellet was collected in 100 μ L PBS and pipetted into 1 mL Opti-Fluor (Perkin Elmer, Waltham, MA, US). Radioactivity was measured in a Wallac Liquid Scintillation Counter. Experiments were repeated three times.

Concentration dependent uptake was determined as described above with the exception that increasing concentrations of [³H]2,2Br (1–100 μ M) were applied for 5 min. For specific inhibition of OATP2B1, the cells were preincubated for 5 min in the presence of 20 μ M bromo-sulphophthalein in uptake buffer pH 5.5. After 5 min 1 μ M [³H]2,2Br was added and the cells were further incubated for 10 min at 37 °C. Experiments were repeated in at least 3 biological replicates in which cells derived from different passages with 3 technical parallels.

2.9. Data analysis

All data are presented by calculating the mean \pm SD obtained from at least three independent measurements, with 3 technical replicates in each individual experiment. The IC₅₀ values were determined by sigmoidal curve fitting using the GraphPad Prism software (version 6 for Windows, GraphPad Software, San Diego, California, US). For statistical analyses unpaired Student's *t*-test was performed and the *p* value for statistical significance was set at **p* < 0.05, ***p* < 0.01 or ****p* < 0.001, *****p* < 0.0001.

3. Results

3.1. Enhanced antiproliferative effect of 2-halogenated 13 α -estrones on cells overexpressing OATP2B1

In our earlier studies we identified a series of 13 α - and 13 β -estrone derivatives that effectively inhibit the transport function of OATP2B1 (Jojart et al., 2018; Laczkó-Rigó et al., 2020; Jójárt et al., 2021). However, the nature of these interactions, whether these compounds are inhibitors or substrates of OATP2B1 was not investigated. Therefore, in the current study estrones with high affinity to OATP2B1 (IC₅₀ \leq 2 μ M, see Figs. 1 and 2, and Table 1) were further investigated in an in vitro cell proliferation assay. In addition, as controls, in the case of halogenated 13 α -estrones the less effective OATP2B1 inhibitor 4-C halogenated stereoisomers (2,4 series, see Table 1) were also tested.

We hypothesized that transported toxic or cytostatic substrates of

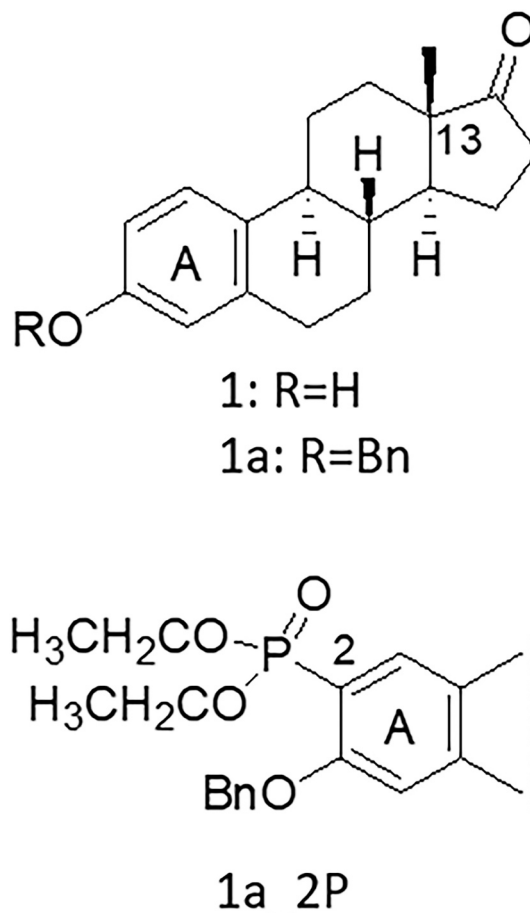


Fig. 1. Selected 13 β -estrone-based high affinity OATP2B1 inhibitor (1a_{2P}).

OATP2B1, due to their increased uptake by OATP2B1, will result in increased antiproliferative effect in cells expressing OATP2B1 (Windt et al., 2019). For this aim, we used the A431 cell line overexpressing OATP2B1, generated earlier in our laboratory. A431-OATP2B1 is an ideal tool for microplate based functional measurements (Patik et al., 2018) including that of measuring cytotoxicity (Windt et al., 2019). In addition, it has been shown earlier that A431 cells are sensitive to certain 13 α -estrone derivatives (Szabo et al., 2016b). In our study cell growth was followed by measuring the fluorescence of the protein used to tag the cells, GFP for mock transfected cells and mCherry for cells containing OATP2B1. We showed previously that fluorescence of GFP or mCherry is proportional to the cell number in the range of 5000–40,000 cells, and therefore this simple method can be used to monitor cell growth or death without the need of the addition of cell viability reagents (Windt et al., 2019). Expression and function of OATP2B1 was confirmed and regularly checked in the A431-OATP2B1-mCherry cell line (Fig. 3).

We found various degrees of cell proliferation inhibition of the OATP2B1 inhibitor 13 α - and 13 β -estrones. Estrone (1) had no significant antiproliferative effect on A431 cells, at least in the concentration range applied (Fig. 4). Similarly, 13 α -estrone (2) and 3-*O*-methyl-13 α -estrone (2b) had no effect on cell growth. However, 3-*O*-benzyl-13 α -estrone (2a) exerted a well-measurable antiproliferative effect with an IC₅₀ of 10.36 μ M (Fig. 4 and Table 1).

We have demonstrated earlier that modification of the 13 α - or 3 β -estrone on C-2 or C-4 with diethylphosphite enhances its OATP2B1 inhibitory action (Jojart et al., 2018; Jójárt et al., 2021). Here we found that C-2 or C-4 diethylphosphonate modification of 2a did not further increase cell growth inhibition as the IC₅₀ values of 2- and 4- diethylphosphonates (15.91 μ M and 10.52 μ M, respectively) were unaltered

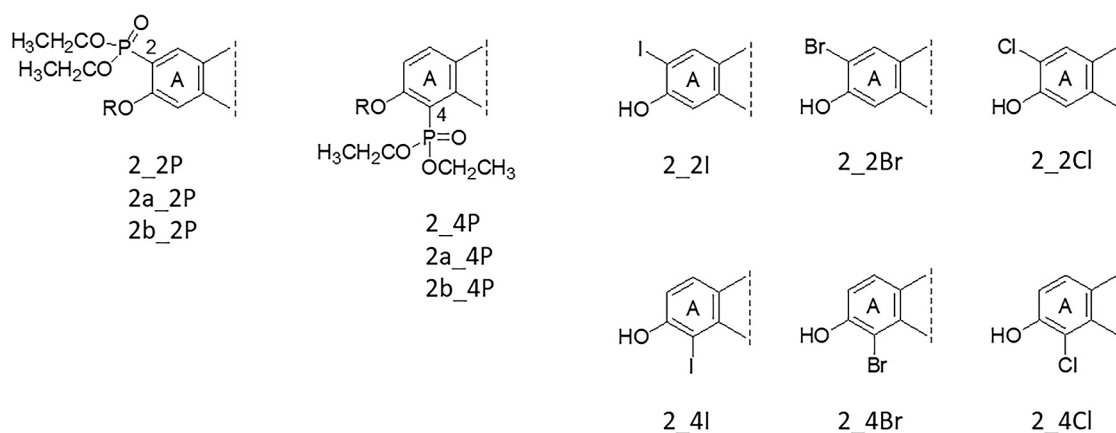
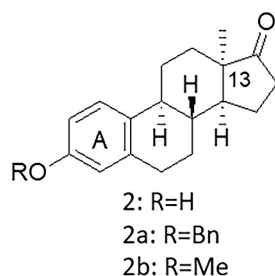


Fig. 2. Selected 13 α -estrone-based high affinity OATP2B1 inhibitors.

Table 1
Inhibitory effect of the investigated compounds.

Name	IC ₅₀ ± SD (μM)	Name	IC ₅₀ ± SD (μM)
1	2.06 ± 0.043	2^b	>50
1a_2P^a	0.041 ± 0.02	2_2P^b	2.8 ± 1.5
2b^b	3.4 ± 0.3	2_4P^b	1.4 ± 0.2
2b_2P^b	1.8 ± 0.3	2_2I^c	1.52 ± 0.01
2b_4P^b	2.8 ± 1.5	2_4I^c	6.63 ± 0.01
2a^b	1.7 ± 0.9	2_2Br^c	0.54 ± 0.02
2a_2P^b	0.2 ± 0.02	2_4Br^c	10.8 ± 0.02
2a_4P^b	0.3 ± 0.02	2_2Cl^c	2.11 ± 0.02
		2_4Cl^c	>50

Inhibitory effect of the compounds was described earlier, with the exception of compound **1**, a: (Jórárt et al., 2021), b: (Jórárt et al., 2018), c: (Laczkó-Rigó et al., 2020). Compounds were tested on A431-OATP2B1 cells in a transport assay using CascadeBlue hydrazide as test substrate. IC₅₀ values were determined by nonlinear regression analysis fitted to the data points by GraphPad Prism software. Bold indicates compound names, italics is for SD values.

compared to **2a** (Figs. 4 and 5 and Table 2). Similarly, 2- and 4-diethylphosphonate variants of **2** (**2_2P** and **2_4P**) and the 2-diethylphosphonated version of 3-O-methyl-13 α -estrone (**2b_2P**) were found to have no major effect on cell growth.

On the other hand, 3-O-benzyl-13 α - and 13 β -derivatives (**2a** series and **1a_2P**) resulted in significantly increased cell growth inhibition with IC₅₀ values of around 10 μM (Fig. 5 and Table 2). However, in spite of their high affinity inhibition of OATP2B1 function, none of these compounds showed increased cell growth inhibition in A431-OATP2B1

cells as compared to the mock-transfected controls.

Similarly to the diethylphosphonated derivatives, the halogen substituted derivatives of **2** (**2_2I**, **2_2Br**, **2_2Cl**, **2_4Br** or **2_4Cl**) had no or only marginal (**2_2I** or **2_4I**) effect on mock-transfected cells. However, the C-2 halogenated compounds showed increased cell growth inhibition (see Fig. 6 and Table 2) in cells overexpressing OATP2B1. The selective cell growth inhibition of C-2 halogenated 13 α -estrone in OATP2B1-overexpressing cells can be interpreted as the result of cellular enrichment of these compounds by OATP2B1. Indeed, we found that inhibiting OATP2B1 function with the OATP-specific inhibitor bromosulphophthalein (BSP) could partially block the effect of **2_2Br** in A431-OATP2B1 cells (Supplementary Fig. S2A).

3.2. Synthesis and tritium labeling of **2_2Br**

In order to investigate the possible OATP2B1-mediated transport of the most selective compound (with a 4-fold selectivity ratio, Table 2), radioactive labeling of 2-bromo-13 α -estrone (**2_2Br**) was performed. Tritium labeling was carried out by catalytic dehalogenation of the bis-brominated compound 2,4-dibromo-13 α -estrone in the presence of tritium gas followed by mono-bromination of [³H]**1** at the C-2 position. The regioselective bromination cannot be achieved under various conditions, and thus, a mixture of brominated compounds was obtained. Next, an HPLC method was developed for the separation of the compounds [³H]**2_2Br**, [³H]**2_4Br** and the bis-brominated **2_2/4Br**. The bromination of [³H]**1** was performed in the presence of DDH with an optimal yield of [³H]**2_2Br** that was isolated by HPLC separation (Supplementary Fig. S1).

3.3. OATP2B1-mediated accumulation of [³H]-2-bromo-13 α -estrone ([³H]**2_2Br**)

Cellular accumulation of [³H]**2_2Br** was measured in A431-OATP2B1 and mock control cells. We found that OATP2B1-overexpressing A431 cells accumulated twice more [³H]**2_2Br** than

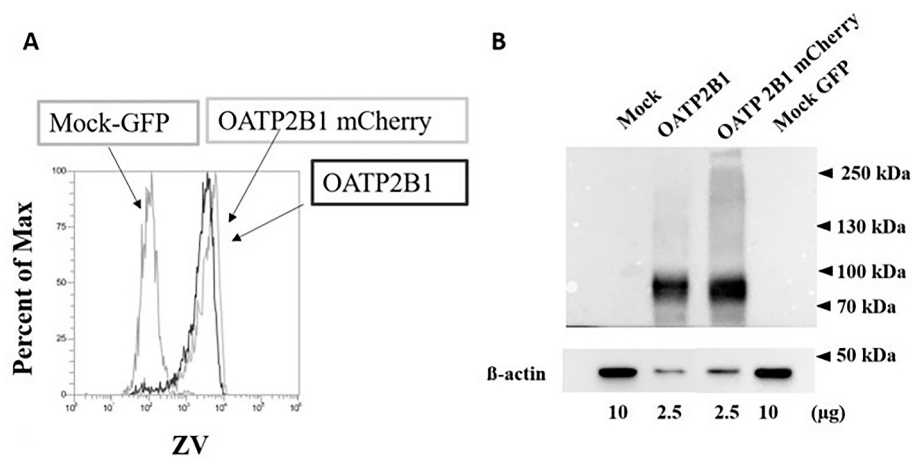


Fig. 3. A. Zombie Violet uptake in OATP2B1 and mock transfected cells. The histogram shows the uptake of the Zombie Violet (ZV, 250x diluted) fluorescent dye, a known substrate of OATP2B1 (Patik et al., 2018). A431 cells were incubated for 15 min at 37 °C in uptake buffer (pH 5.5). Fluorescence was monitored by flow cytometry. Experiments were repeated every week in order to control OATP2B1 expression. A representative histogram is shown. B. Expression of OATP2B1 in A431 cells confirmed by Western blot. OATP2B1 was detected by an anti-OATP2B1 antibody (Kullak-Ublick et al., 2001) and β -actin was used as loading control. Experiments were repeated at least three times. One representative blot is shown.

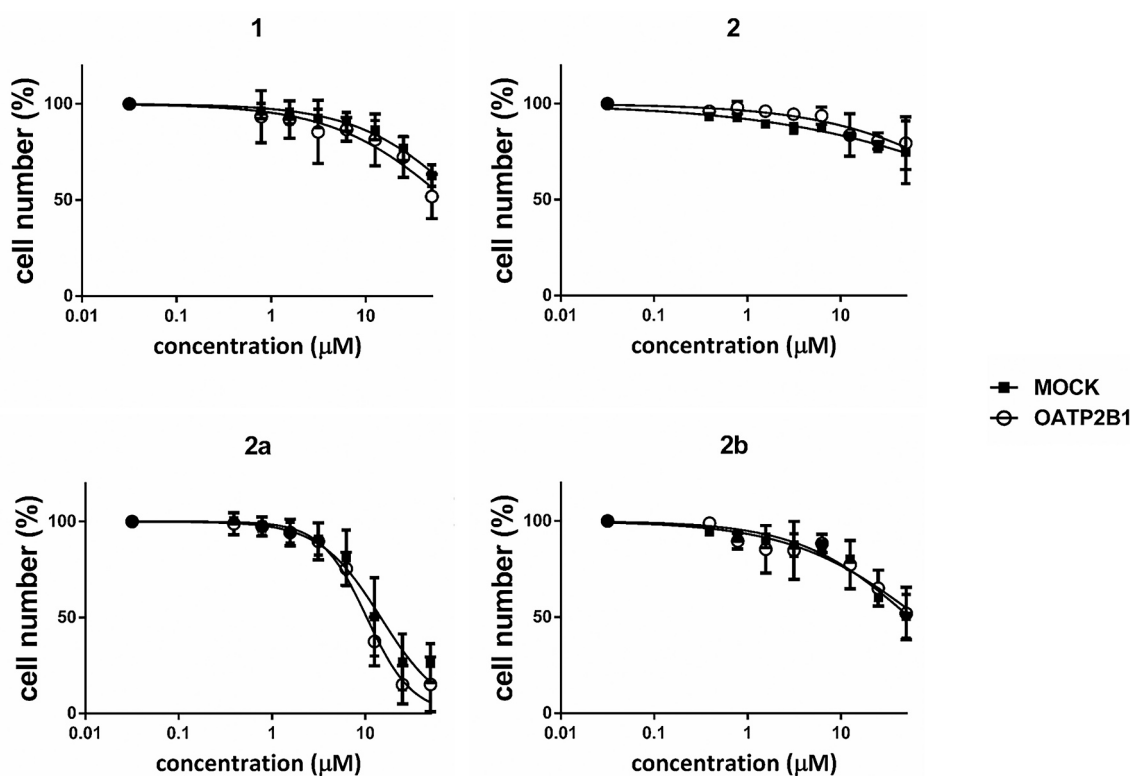


Fig. 4. Cell growth inhibition of compounds in A431 cells. A431 mock and A431-OATP2B1 cells were incubated with increasing steroid concentrations for 120 h on 96-well plates. Cell number was determined based on the fluorescence of mCherry or GFP measured in an Enspire fluorescence plate reader, 100%: in the absence of estrogens. Data show the mean \pm SD values obtained from at least three independent measurements.

the control A431 cells (Fig. 8A). The concentration dependence of the cellular uptake of [^3H] 2_2Br in the range of 1–100 μM (at both pH 5.5 (Fig. 8B) and pH 7.4 (Supplementary Fig. S3)) indicated a transporter mediated uptake mechanism that was further confirmed by the significantly decreased transport in the presence of the OATP-specific inhibitor bromosulphthalein, and by the lack of transport at 4 °C (Fig. 8C).

4. Discussion

OATP2B1 is a plasma membrane protein mediating intestinal and hepatic uptake of its substrates. On the other hand, OATP2B1 is also overexpressed in tumors of the colon, bone, breasts and gliomas (Kovacsics et al., 2017). Since OATP2B1 is a multispecific transporter recognizing a large set of chemically diverse compounds, including

various drugs, one anti-tumor strategy could be to exploit its activity to increase intra-tumor concentrations of its substrate chemotherapeutics. Indeed, we have recently shown that OATP2B1 can sensitize the cells toward chemotherapeutics (Windt et al., 2019).

Synthetic steroids, e.g. the estrogen receptor degrader Fulvestrant (Lee et al., 2017) and the aromatase inhibitor Exemestane (Van Asten et al., 2014) are frequently administered for hormone receptor positive breast cancers. However, steroid-based compounds face the challenge of lacking estrogenic activity. 13 α -estrone derivatives are good candidates for anticancer treatment, since they have no hormonal activity, but interfere with local estrogen synthesis by inhibiting the STS and/or HSD1 enzymes. Indeed, several 13 α -estrone derivatives were identified as antiproliferative agents against various cancer cell lines (Berenyi et al., 2013; Szabo et al., 2016a). However, for example, 3-benzyl ether

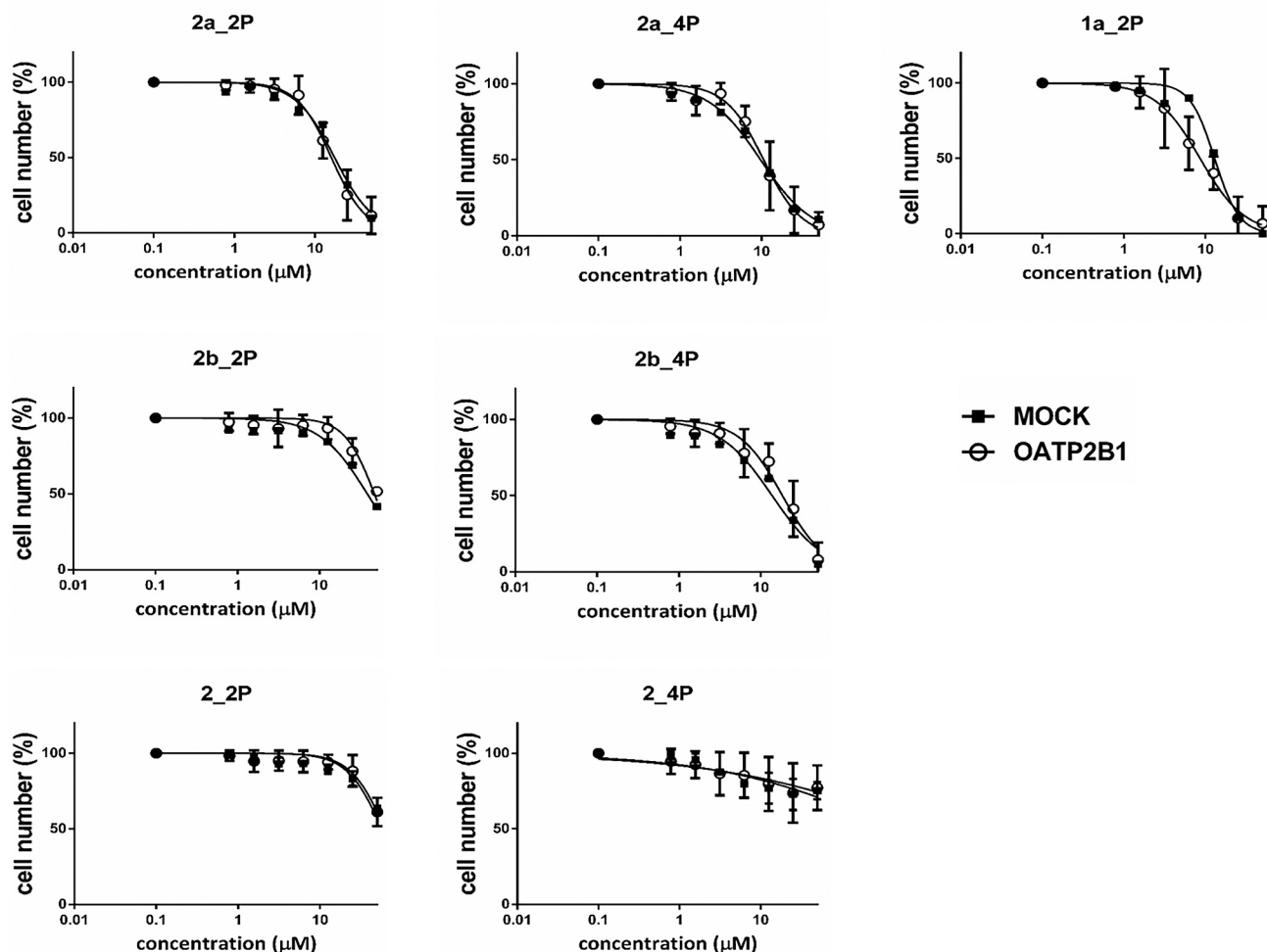


Fig. 5. Effect of C-2 or C-4 diethylphosphonated 13 α -estrone derivatives on the proliferation of A431 cells. A431 mock and A431-OATP2B1 cells were incubated with increasing steroid concentrations for 120 h. Cell number was determined based on mCherry or GFP fluorescence measured in an Enspire plate reader. Data show the mean values \pm SD calculated from at least three independent measurements.

Table 2

Antiproliferative effect of the compounds on OATP2B1 and mock transfected cells.

Name	IC ₅₀ \pm SD (μ M)		Name	IC ₅₀ \pm SD (μ M)		SR
	2B1	mock		2B1	mock	
1	42.01 ± 0.033	36.36 ± 0.029	2	>50	>50	
1a_2P	8.552 ± 0.05	12.89 ± 0.027	2_2P	>50	>50	
2b	>50	>50	2_4P	>50	>50	
2b_2P	46.42 ± 0.022	38.03 ± 0.028	2_2I	15.78 ± 0.051	36.57 ± 0.016	2.32****
2b_4P	18.32 ± 0.036	13.71 ± 0.036	2_4I	27.76 ± 0.022	28.48 ± 0.167	1.03
2a	10.36 ± 0.03	14.65 ± 0.042	2_2Br	32.4 ± 0.017	129.8^x ± 0.056	4.01****
2a_2P	15.91 ± 0.03	17.45 ± 0.039	2_4Br	77.52 ^x ± 0.051	95.83 ^x ± 0.084	1.24
2a_4P	10.52 ± 0.036	9.67 ± 0.038	2_2Cl	23.92 ± 0.014	51.21 ± 0.013	2.14*
			2_4Cl	67.01 ± 0.024	251.8 ^x ± 0.037	3.75

IC₅₀ values were determined by nonlinear regression analysis fitted to the data points by GraphPad Prism software. SR = selectivity ratio: IC₅₀ in mock/IC₅₀ in OATP2B1, ^x: data were predicted by GraphPad Prism software. Statistically significant difference between IC₅₀ values: *p < 0.05, ****p < 0.0001. Bold indicates compound names, italics is for SD values.

of the 16-oxime propionate in the 13 α -estrone series was shown to be toxic not only to HeLa and MCF-7 cells, but also to A431 cells lacking the STS and HSD1 enzymes (Szabo et al., 2016a). In addition, triazolyl-13 α -D-secoestrone derivatives exerted an excellent antiproliferative potential on human cervical (HeLa, C33), ovarian (A2780) and HR⁺ breast (MCF-7, T47D) cancer cell lines (Berenyi et al., 2013).

Previously, we have shown that 13 α - or 13 β -estrone derivatives, originally designed to inhibit the STS and HSD1 enzymes, are effective inhibitors of OATP2B1 function (Jóhart et al., 2018; Laczkó-Rigó et al., 2020; Jóhart et al., 2021). Hence, these estrones can be good candidate dual-targeted molecules simultaneously aiming a tumoric transporter as well as an enzyme. We hypothesized that if transported by OATP2B1 these compounds can be enriched in and be more toxic to the cells overexpressing the transporter. Hence, we further investigated a set of these OATP2B1 inhibitor 13 α -estrone (Fig. 2) and a recently identified OATP2B1 inhibitor with a nanomolar inhibitory constant, phosphonated 13 β -estrone (**1a_2P**, Fig. 1) (Jóhart et al., 2021), for their ability to inhibit the proliferation of OATP2B1-overexpressing cells. For this aim, the A431 cell line, a well-established model for the investigation of OATP function (Windt et al., 2019) was applied. Although the toxicity of 13 α -estrone in A431 cells has not yet been investigated in detail, various 13 α -estrone have been shown to be toxic in A431 cells (Szabo et al., 2016b).

From the set of the investigated compounds, we found that 3-O-benzyl derivatives (**2a**, **2a_2P**, **2a_4P**, **1a_2P** and **2a_4P**) had increased

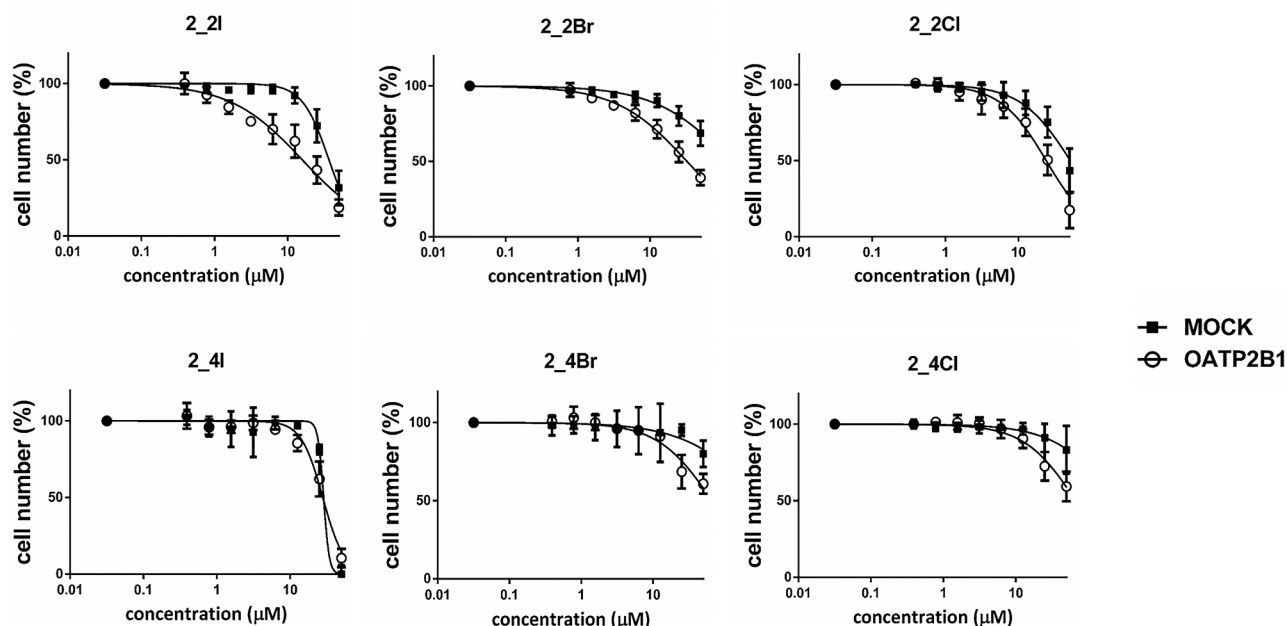


Fig. 6. Effect of C-2 or C-4 halogenated 13 α -estrone derivatives on growth of A431 cells. A431 mock and A431-OATP2B1 cells were incubated with increasing steroid concentrations for 120 h on 96-well plates. Cell number was determined based on the fluorescence of mCherry or GFP in an Enspire fluorescence plate reader. Data show the mean \pm SD values obtained from at least three independent measurements.

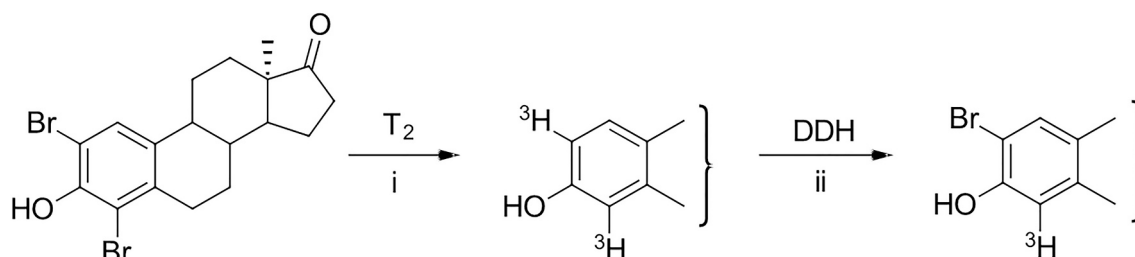


Fig. 7. Tritium labeling of **2_2Br**. (i) Pd/C (10% Pd), $^3\text{H}_2$, EtOAc, TEA; (ii) 1.2 equiv. DDH, CH_2Cl_2 , 15 min, rt.

antiproliferative effect on A431 cells (their IC_{50} values below 20 μM) irrespective of the presence of OATP2B1. This harmonizes with our previous findings, various 13 α -estrones with a C-3 *N*-benzyl-triazolylmethoxy moiety being toxic on A431 cells (Szabo et al., 2016b). In the current study C-2 or C-4 iodinated 13 α -estrones also resulted in a moderately increased antiproliferative effect (IC_{50} values around 30 μM) compared to the core 13 α -estrone. While here only a limited set of compounds was investigated, since our study focused on the highest affinity inhibitors of OATP2B1 function, we observed that the introduction of a large substituent on 3-hydroxy function of the initial compounds 13 α - or 13 β -estrone issued in enhanced cell growth inhibition effect.

The OATP2B1-selective antiproliferative effect was observed exclusively in the case of the 2-halogenated compounds. **2_2I**, **2_2Br** and **2_2Cl** resulted in a 2-, 4- and 2-fold decreased IC_{50} in A431-OATP2B1 cells, respectively (Fig. 6 and Table 1). The C-4 halogenated counterparts were less effective inhibitors of OATP2B1 function, accordingly, they did not result in an OATP2B1-selective anti-proliferative effect. Furthermore, the OATP2B1-selective antiproliferative effect of **2_2Br** could be inhibited by bromosulphophthalein (Supplementary Fig. S2A). In further experiments we demonstrated the OATP2B1-mediated uptake of the most selective compound **2_2Br** (Fig. 8) that may explain its enhanced antiproliferative effect in OATP2B1-overexpressing cells.

The 13 α -estrones investigated here have been designed to inhibit the HSD1 enzyme (Bacsá et al., 2015; Jojart et al., 2018), and hence

decrease the proliferation of hormone dependent tumors. A431 cells lack HSD1 and are hormone independent, however they are enriched in the 17 β -HSD type 2 (HSD2) enzyme (Blomquist et al., 1997). HSD2 has been shown to be inhibited by C18, C19 and C21 steroids (Blomquist et al., 1984), therefore, the investigated steroids may act through the inhibition of HSD2 in A431 cells. On the other hand, increased expression of estrogen-related receptor alpha ($\text{ERR}\alpha$) has been documented in A431 cells (Chen et al., 2018). $\text{ERR}\alpha$ is an orphan nuclear receptor, of which upregulation is involved in the development of estrogen-independent tumors (Chen et al., 2018). Accordingly, suppression of $\text{ERR}\alpha$ inhibited A431 cell proliferation (Chen et al., 2018). However, whether the antiproliferative effect of 13 α -estrones observed in our study can be related to the inhibition of the $\text{ERR}\alpha$ receptor needs further investigations. Interestingly, **2_2Br** had only a slightly increased antiproliferative effect in estrogen-dependent T47D breast cancer cells (also expressing the HSD1 enzyme, Supplementary Fig. S2B) indicating that the compound may exert its antiproliferative effect independent of the estrogen pathway. Recently, 13 α -estrones have been described as inhibitors of tubulin formation (Jojart et al., 2020), therefore this can be an alternative mechanism of cell growth inhibition in A431 cells.

Many illnesses including cancer treatment require the simultaneous action on multiple targets in order to avoid drug resistance mechanisms, to increase effectiveness and to prolong overall survival. This is often achieved by drug “cocktails”. However, by the application of “cocktail therapy” the incidence of drug-drug interactions and off-target effects

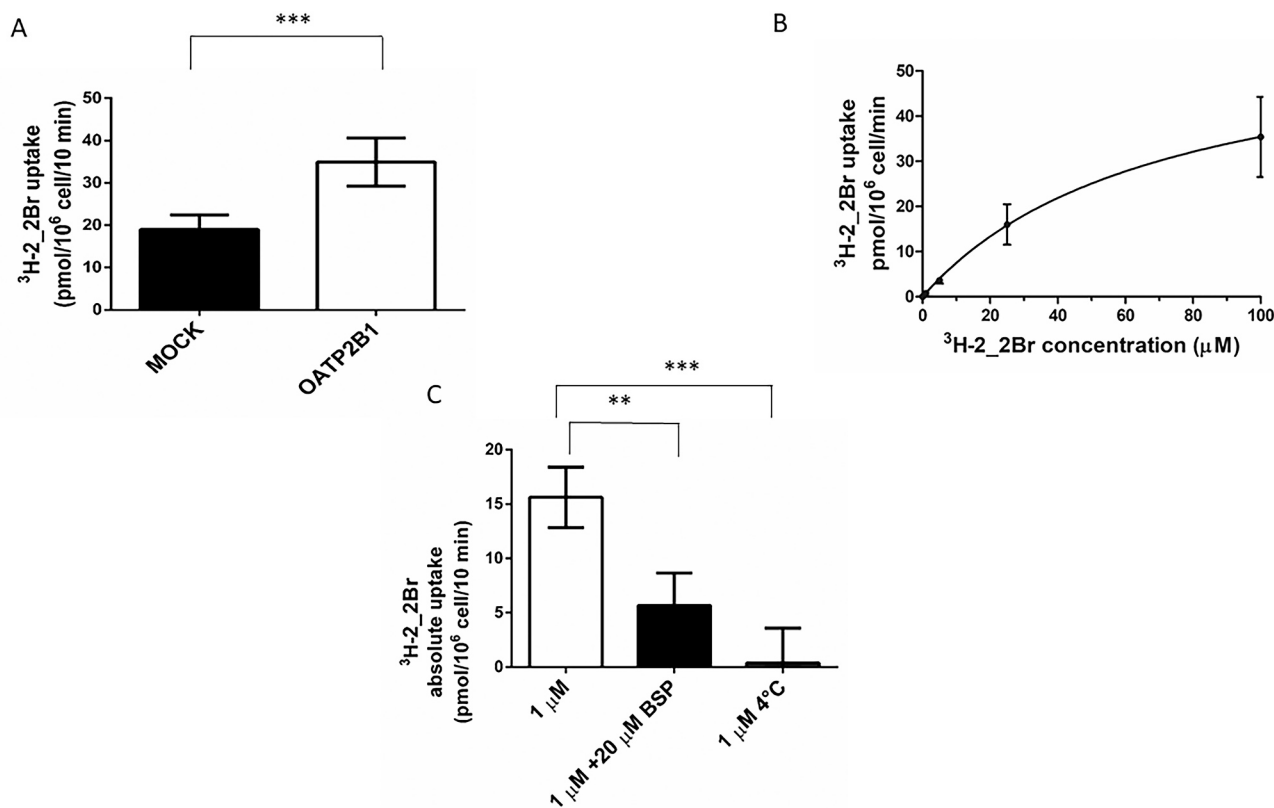


Fig. 8. A. Uptake of [³H] 2,2Br in A431 cells. A431-OATP2B1 cells and their mock transfected counterparts were incubated with 1 μM (A) or 1 μM–100 μM (B) [³H] 2,2Br for 10 (A) or 5 (B) min at 37 °C at pH 5.5. Radioactivity was measured by a Wallac Liquid Scintillator Counter. C. Uptake of [³H] 2,2Br was measured in the presence or absence of 20 μM BSP (bromosulfophthalein) for 10 min at 37 °C or 0 °C at pH 5.5. B) and C) signal measured in on mock cells were subtracted from that measured in A431-OATP2B1 cells. Data points show the average ± SD values obtained in three independent replicates. Statistical analysis was performed with unpaired t-test (***p* < 0.01 and ****p* < 0.001).

increases. Using a single chemical entity with multiple targets is a better strategy to avoid side effects (Meena et al., 2015). Multi-targeted drug design has not only been applied for anti-cancer treatment, but also for inflammatory conditions, Alzheimer’s disease and neurodegenerative disorders, as well (Geldenhuys and Van der Schyf, 2013).

Here we identified 2-halogenated-13α-estrones as (potential) OATP2B1 substrates. Since these compounds are also effective HSD1 inhibitors, their increased uptake mediated by OATP2B1 can potentially be exploited to achieve an enhanced anti-tumor effect in estrogen dependent tumors. Though further experiments on estrogen-dependent cell lines expressing the potential targets of 13α-estrones, the STS and/or HSD1 enzymes (e.g. T47D, MCF-7) with and without OATP2B1 overexpression would be needed to clarify this issue.

Author contribution statement

R. L.-R.: performed experiments, analyzed data, wrote manuscript draft, É. B.: performed experiments, analyzed data, wrote manuscript file, R. J.: synthesized purified and quality checked the steroids, Cs. T: synthesized tritiated steroids, wrote the manuscript, E. M.: designed and synthesized the steroids, wrote the manuscript, Cs. Ö-L.: conceptualized the work, analyzed data, wrote the manuscript.

Declaration of Competing Interest

The authors declare that they have no known competing financial interests or personal relationships that could have appeared to influence the work reported in this paper.

Acknowledgements

This work was supported by National Research, Development and Innovation Office-NKFIH through projects [OTKA SNN 124329 (E. M.) and OTKA FK 128751 (Cs. Ö-L.)]. The sponsors had no influence on the design of the experiments, on the interpretation of the data or on the publication.

Appendix A. Supplementary data

Supplementary data to this article can be found online at <https://doi.org/10.1016/j.taap.2021.115704>.

References

Arakawa, H., Nakanishi, T., Yanagihara, C., Nishimoto, T., Wakayama, T., Mizokami, A., Namiki, M., Kawai, K., Tamai, I., 2012. Enhanced expression of organic anion transporting polypeptides (OATPs) in androgen receptor-positive prostate cancer cells: possible role of OATP1A2 in adaptive cell growth under androgen-depleted conditions. *Biochem. Pharmacol.* 84, 1070–1077.

Ayan, D., Roy, J., Maltais, R., Poirier, D., 2011. Impact of estradiol structural modifications (18-methyl and/or 17-hydroxy inversion of configuration) on the in vitro and in vivo estrogenic activity. *J. Steroid Biochem. Mol. Biol.* 127, 324–330.

Bacsa, I., Jójart, R., Schneider, G., Wolfing, J., Maroti, P., Herman, B.E., Szecsi, M., Mernyak, E., 2015. Synthesis of A-ring halogenated 13alpha-estrone derivatives as potential 17beta-HSD1 inhibitors. *Steroids* 104, 230–236.

Bacsa, I., Herman, B.E., Jójart, R., Herman, K.S., Wolfing, J., Schneider, G., Varga, M., Tomboly, C., Rízner, T.L., Szecsi, M., Mernyak, E., 2018. Synthesis and structure-activity relationships of 2- and/or 4-halogenated 13beta- and 13alpha-estrone derivatives as enzyme inhibitors of estrogen biosynthesis. *J. Enzym. Inhib. Med. Chem.* 33, 1271–1282.

Bauer, M., Matsuda, A., Wulkersdorfer, B., Philippe, C., Traxl, A., Ozvegy-Laczka, C., Stanek, J., Nics, L., Klebermass, E.M., Poschner, S., Jager, W., Patik, I., Bakos, E., Szakacs, G., Wadsak, W., Hacker, M., Zeitlinger, M., Langer, O., 2018. Influence of

- OATPs on hepatic disposition of erlotinib measured with positron emission tomography. *Clin. Pharmacol. Ther.* 104, 139–147.
- Berenyi, A., Minorics, R., Ivanyi, Z., Ocsosvzki, I., Ducza, E., Thole, H., Messinger, J., Wolfing, J., Motyan, G., Mernyak, E., Frank, E., Schneider, G., Zupko, I., 2013. Synthesis and investigation of the anticancer effects of estrone-16-oxime ethers in vitro. *Steroids* 78, 69–78.
- Blomquist, C.H., Lindemann, N.J., Hakanson, E.Y., 1984. Inhibition of 17 beta-hydroxysteroid dehydrogenase (17 beta-HSD) activities of human placenta by steroids and non-steroidal hormone agonists and antagonists. *Steroids* 43, 571–586.
- Blomquist, C.H., Leung, B.S., Beaudoin, C., Poirier, D., Tremblay, Y., 1997. Intracellular regulation of 17 beta-hydroxysteroid dehydrogenase type 2 catalytic activity in A431 cells. *J. Endocrinol.* 153, 453–464.
- Buxhofer-Ausch, V., Secky, L., Wlcek, K., Svoboda, M., Kounnis, V., Briasoulis, E., Tzakos, A.G., Jaeger, W., Thalhammer, T., 2013. Tumor-specific expression of organic anion-transporting polypeptides: transporters as novel targets for cancer therapy. *J. Drug Deliv.* 2013, 863539.
- Chen, H., Pan, J., Zhang, L., Chen, L., Qi, H., Zhong, M., Shi, X., Du, J., Li, Q., 2018. Downregulation of estrogen-related receptor alpha inhibits human cutaneous squamous cell carcinoma cell proliferation and migration by regulating EMT via fibronectin and STAT3 signaling pathways. *Eur. J. Pharmacol.* 825, 133–142.
- Durmus, S., van Hoppe, S., Schinkel, A.H., 2016. The impact of Organic Anion-Transporting Polypeptides (OATPs) on disposition and toxicity of antitumor drugs: insights from knockout and humanized mice. *Drug Resist. Updat.* 27, 72–88.
- Fahrmayr, C., König, J., Auge, D., Mieth, M., Fromm, M.F., 2012. Identification of drugs and drug metabolites as substrates of multidrug resistance protein 2 (MRP2) using triple-transfected MDCK-OATP1B1-UGT1A1-MRP2 cells. *Br. J. Pharmacol.* 165, 1836–1847.
- Fujita, D., Saito, Y., Nakanishi, T., Tamai, I., 2016. Organic anion transporting polypeptide (OATP)2B1 contributes to gastrointestinal toxicity of anticancer drug SN-38, active metabolite of Irinotecan hydrochloride. *Drug Metab. Dispos.* 44, 1–7.
- Goldenhuy, W.J., Van der Schyf, C.J., 2013. Designing drugs with multi-target activity: the next step in the treatment of neurodegenerative disorders. *Expert Opin. Drug Discovery* 8, 115–129.
- Gupta, A., Kumar, B.S., Negi, A.S., 2013. Current status on development of steroids as anticancer agents. *J. Steroid Biochem. Mol. Biol.* 137, 242–270.
- Hagenbuch, B., Stieger, B., 2013. The SLCO (former SLC21) superfamily of transporters. *Mol. Asp. Med.* 34, 396–412.
- Hamada, A., Sissung, T., Price, D.K., Danesi, R., Chau, C.H., Sharifi, N., Venzon, D., Maeda, K., Nagao, K., Sparreboom, A., Mitsuya, H., Dahut, W.L., Figg, W.D., 2008. Effect of SLC01B3 haplotype on testosterone transport and clinical outcome in caucasian patients with androgen-independent prostatic cancer. *Clin. Cancer Res.* 14, 3312–3318.
- Jojart, R., Pecszy, S., Keglevich, G., Szecsi, M., Rigó, R., Ozvegy-Laczka, C., Kecskemeti, G., Mernyak, E., 2018. Pd-Catalyzed microwave-assisted synthesis of phosphonated 13alpha-estrones as potential OATP2B1, 17beta-HSD1 and/or STS inhibitors. *Beilstein J. Org. Chem.* 14, 2838–2845.
- Jojart, R., Ali, H., Horvath, G., Kele, Z., Zupko, I., Mernyak, E., 2020. Pd-catalyzed Suzuki-Miyaura couplings and evaluation of 13alpha-estrone derivatives as potential anticancer agents. *Steroids* 164, 108731.
- Jórárt, R., Laczkó-Rigó, R., Klement, M., Köhl, G., Kecskemeti, G., Özvegy-Laczka, C., Mernyak, E., 2021. Design, synthesis and biological evaluation of novel estrone phosphonates as high affinity organic anion-transporting polypeptide 2B1 (OATP2B1) inhibitors. *Bioorg. Chem.* 112, 104914.
- König, J., Cui, Y., Nies, A.T., Keppler, D., 2000. A novel human organic anion transporting polypeptide localized to the basolateral hepatocyte membrane. *Am. J. Physiol. Gastrointest. Liver Physiol.* 278, G156–G164.
- Kovacsics, D., Patik, I., Ozvegy-Laczka, C., 2017. The role of organic anion transporting polypeptides in drug absorption, distribution, excretion and drug-drug interactions. *Expert Opin. Drug Metab. Toxicol.* 13, 409–424.
- Kullak-Ublick, G.A., Ismail, M.G., Stieger, B., Landmann, L., Huber, R., Pizzagalli, F., Fattinger, K., Meier, P.J., Hagenbuch, B., 2001. Organic anion-transporting polypeptide B (OATP-B) and its functional comparison with three other OATPs of human liver. *Gastroenterology* 120, 525–533.
- Laczko-Rigo, R., Jojart, R., Mernyak, E., Bakos, E., Tuerkova, A., Zdrzil, B., Ozvegy-Laczka, C., 2020. Structural dissection of 13-epiestrones based on the interaction with human Organic anion-transporting polypeptide, OATP2B1. *J. Steroid Biochem. Mol. Biol.* 200, 105652.
- Lee, C.I., Goodwin, A., Wilcken, N., 2017. Fulvestrant for hormone-sensitive metastatic breast cancer. *Cochrane Database Syst. Rev.* 1, CD011093.
- Matsumoto, J., Ariyoshi, N., Sakakibara, M., Nakanishi, T., Okubo, Y., Shiina, N., Fujisaki, K., Nagashima, T., Nakatani, Y., Tamai, I., Yamada, H., Takeda, H., Ishii, I., 2015. Organic anion transporting polypeptide 2B1 expression correlates with uptake of estrone-3-sulfate and cell proliferation in estrogen receptor-positive breast cancer cells. *Drug Metab. Pharmacokinet* 30, 133–141.
- Meena, P., Nemaysh, V., Khatri, M., Manral, A., Luthra, P.M., Tiwari, M., 2015. Synthesis, biological evaluation and molecular docking study of novel piperidine and piperazine derivatives as multi-targeted agents to treat Alzheimer's disease. *Bioorg. Med. Chem.* 23, 1135–1148.
- Mostaghel, E.A., Cho, E., Zhang, A., Alyamani, M., Kaipainen, A., Green, S., Marck, B.T., Sharifi, N., Wright, J.L., Gulati, R., True, L.D., Loda, M., Matsumoto, A.M., Tamae, D., Penning, T.N., Balk, S.P., Kantoff, P.W., Nelson, P.S., Taplin, M.E., Montgomery, R.B., 2017. Association of tissue abiraterone levels and SLCO genotype with intraprostatic steroids and pathologic response in men with high-risk localized prostate cancer. *Clin. Cancer Res.* 23, 4592–4601.
- Nozawa, T., Suzuki, M., Takahashi, K., Yabuuchi, H., Maeda, T., Tsuji, A., Tamai, I., 2004. Involvement of estrone-3-sulfate transporters in proliferation of hormone-dependent breast cancer cells. *J. Pharmacol. Exp. Ther.* 311, 1032–1037.
- Patik, I., Szekely, V., Nemet, O., Szepesi, A., Kucsma, N., Varady, G., Szakacs, G., Bakos, E., Ozvegy-Laczka, C., 2018. Identification of novel cell-impermeant fluorescent substrates for testing the function and drug interaction of Organic Anion-Transporting Polypeptides, OATP1B1/1B3 and 2B1. *Sci. Rep.* 8, 2630.
- Pizzagalli, F., Hagenbuch, B., Stieger, B., Klenk, U., Folkers, G., Meier, P.J., 2002. Identification of a novel human organic anion transporting polypeptide as a high affinity thyroxine transporter. *Mol. Endocrinol.* 16, 2283–2296.
- Rizner, T.L., Thalhammer, T., Ozvegy-Laczka, C., 2017. The importance of steroid uptake and intracrine action in endometrial and ovarian cancers. *Front. Pharmacol.* 8, 346.
- Roth, M., Obaidat, A., Hagenbuch, B., 2012. OATPs, OATs and OCTs: the organic anion and cation transporters of the SLCO and SLC22A gene superfamilies. *Br. J. Pharmacol.* 165, 1260–1287.
- Sang, X., Han, H., Poirier, D., Lin, S.X., 2018. Steroid sulfate inhibition success and limitation in breast cancer clinical assays: an underlying mechanism. *J. Steroid Biochem. Mol. Biol.* 183, 80–93.
- Schafer, B., Orban, E., Kele, Z., Tomboly, C., 2015. Tritium labelling of a cholesterol amphiphile designed for cell membrane anchoring of proteins. *J. Label. Comp. Radiopharm.* 58, 7–13.
- Schafer, A.M., Bock, T., Meyer Zu Schwabedissen, H.E., 2018. Establishment and validation of competitive counterflow as a method to detect substrates of the organic anion transporting polypeptide 2B1. *Mol. Pharm.* 15, 5501–5513.
- Schonecker, B., Lange, C., Kotteritzsch, M., Gunther, W., Weston, J., Anders, E., Gørls, H., 2000. Conformational design for 13alpha-steroids. *J. Organomet. Chem.* 65, 5487–5497.
- Szabo, J., Jerkovics, N., Schneider, G., Wolfing, J., Bozsity, N., Minorics, R., Zupko, I., Mernyak, E., 2016a. Synthesis and in vitro antiproliferative evaluation of C-13 epimers of triazolyl-d-secoestrone alcohols: the first potent 13alpha-d-secoestrone derivative. *Molecules* 21.
- Szabo, J., Pataki, Z., Wolfing, J., Schneider, G., Bozsity, N., Minorics, R., Zupko, I., Mernyak, E., 2016b. Synthesis and biological evaluation of 13alpha-estrone derivatives as potential antiproliferative agents. *Steroids* 113, 14–21.
- Thakkar, N., Lockhart, A.C., Lee, W., 2015. Role of organic anion-transporting polypeptides (OATPs) in cancer therapy. *AAPS J.* 17, 535–545.
- Van Asten, K., Neven, P., Lintermans, A., Wildiers, H., Paridaens, R., 2014. Aromatase inhibitors in the breast cancer clinic: focus on exemestane. *Endocr. Relat. Cancer* 21, R31–R49.
- Windt, T., Toth, S., Patik, I., Sessler, J., Kucsma, N., Szepesi, A., Zdrzil, B., Ozvegy-Laczka, C., Szakacs, G., 2019. Identification of anticancer OATP2B1 substrates by an in vitro triple-fluorescence-based cytotoxicity screen. *Arch. Toxicol.* 93, 953–964.
- Wright, J.L., Kwon, E.M., Ostrander, E.A., Montgomery, R.B., Lin, D.W., Vessella, R., Stanford, J.L., Mostaghel, E.A., 2011. Expression of SLCO transport genes in castration-resistant prostate cancer and impact of genetic variation in SLC01B3 and SLC02B1 on prostate cancer outcomes. *Cancer Epidemiol. Biomark. Prev.* 20, 619–627.
- Yaremenko, Feodor G., Khvat, Alexandr V., 1994. A new One-pot synthesis of 17-oxo-13 α -steroids of the androstane series from their 13 β -analogues. *Mendelev Commun.* 4, 187–188.



Article

Interactions of Potential Anti-COVID-19 Compounds with Multispecific ABC and OATP Drug Transporters

Ágnes Telbisz^{1,†}, Csilla Ambrus^{2,3,†}, Orsolya Móznér^{1,3}, Edit Szabó¹, György Várady¹, Éva Bakos¹, Balázs Sarkadi^{1,4,*} and Csilla Özvegy-Laczka^{1,*}

¹ Institute of Enzymology, ELKH Research Centre for Natural Sciences, Magyar Tudósok krt. 2, 1117 Budapest, Hungary; telbisz.agnes@ttk.hu (Á.T.); moznér.orsolya@ttk.hu (O.M.); szabo.edit@ttk.hu (E.S.); varady.gyorgy@ttk.hu (G.V.); bakos.eva@ttk.hu (É.B.)

² SOLVO Biotechnology, Irinyi József Street 4-20, 1117 Budapest, Hungary; ambrus@solvo.com

³ Doctoral School of Molecular Medicine, Semmelweis University, Tűzoltó u. 37-47, 1094 Budapest, Hungary

⁴ Department of Biophysics and Radiation Biology, Semmelweis University, Tűzoltó u. 37-47, 1094 Budapest, Hungary

* Correspondence: sarkadi.balazs@ttk.hu (B.S.); laczka.csilla@ttk.hu (C.Ö.-L.)

† These authors contributed equally to this work.

Abstract: During the COVID-19 pandemic, several repurposed drugs have been proposed to alleviate the major health effects of the disease. These drugs are often applied with analgesics or non-steroid anti-inflammatory compounds, and co-morbid patients may also be treated with anticancer, cholesterol-lowering, or antidiabetic agents. Since drug ADME-tox properties may be significantly affected by multispecific transporters, in this study, we examined the interactions of the repurposed drugs with the key human multidrug transporters present in the major tissue barriers and strongly affecting the pharmacokinetics. Our in vitro studies, using a variety of model systems, explored the interactions of the antimalarial agents chloroquine and hydroxychloroquine; the antihelminthic ivermectin; and the proposed antiviral compounds ritonavir, lopinavir, favipiravir, and remdesivir with the ABCB1/Pgp, ABCG2/BCRP, and ABCC1/MRP1 exporters, as well as the organic anion-transporting polypeptide (OATP)2B1 and OATP1A2 uptake transporters. The results presented here show numerous pharmacologically relevant transporter interactions and may provide a warning on the potential toxicities of these repurposed drugs, especially in drug combinations at the clinic.

Keywords: anti-COVID-19 agents; repurposed drugs; APP-Binding Cassette (ABC) transporters; OATP transporters; in vitro functional studies



Citation: Telbisz, Á.; Ambrus, C.; Móznér, O.; Szabó, E.; Várady, G.; Bakos, É.; Sarkadi, B.; Özvegy-Laczka, C. Interactions of Potential Anti-COVID-19 Compounds with Multispecific ABC and OATP Drug Transporters. *Pharmaceutics* **2021**, *13*, 81. <https://doi.org/10.3390/pharmaceutics13010081>

Received: 21 November 2020

Accepted: 31 December 2020

Published: 9 January 2021

Publisher's Note: MDPI stays neutral with regard to jurisdictional claims in published maps and institutional affiliations.



Copyright: © 2021 by the authors. Licensee MDPI, Basel, Switzerland. This article is an open access article distributed under the terms and conditions of the Creative Commons Attribution (CC BY) license (<https://creativecommons.org/licenses/by/4.0/>).

1. Introduction

During the COVID-19 pandemic, based on in vitro experimental studies, a number of potential antiviral drugs have been proposed for the clinic. These potential treatments were rapidly brought to the attention of the medical community and the general public by the media, while in many cases, drug evaluation agencies could not properly investigate the pharmacokinetics, potential risks, and benefits. Despite this, clinicians and thousands or even millions of lay people started to compassionately use the advocated off-label compounds. The most notorious example is the wide range off-label use of the antimalarial agents **chloroquine** and **hydroxychloroquine**, in some cases together with zinc or the wide-spectrum antibacterial agent azithromycin. Chloroquine (CQ) and the less toxic analog hydroxychloroquine (HCQ) are efficient antimalarial drugs, increasing the endosomal pH in both the parasites and the host cells. HCQ is also clinically used in autoimmune diseases [1]. However, these compounds were previously found to have major toxicities, especially by prolonging the cardiac QT interval or causing hypoglycemia. CQ and HCQ were both reported to be moderate inhibitors of CYP2D6 and the ABCB1/Pgp transporter. Interestingly, azithromycin has a similar toxicity to CQ and HCQ to prolong the QT interval [2].

The potential use of CQ and HCQ in COVID-19 was initiated by *in vitro* studies, in which both compounds inhibited the fusion of SARS-CoV-2 with the cell membranes, and reduced ACE2 receptor glycosylation (the binding site of SARS-CoV-2) and the transfer of SARS-CoV-2 from early endosomes to lysosomes [3–5]. However, whilst CQ and HCQ—also in combinations with azithromycin—have been examined in several clinical trials, their use has not been approved by the EMA or FDA for the treatment of COVID-19. A recent statement of the NIH COVID-19 Treatment Guidelines Panel (NIH-CTGP) strongly advises against the use of CQ or HCQ because of inefficiency and the cardiac complications [6,7].

Another proposed anti-COVID-19 agent—**ivermectin**—is a broad-spectrum antiparasitic agent and widely used to treat neglected tropical diseases. The target of the antiparasitic action of ivermectin is a glutamate-gated chloride channel and a GABA receptor, specific for some invertebrates. However, in mammals, ivermectin may also inhibit GABAergic neurotransmission by promoting the release of GABA and acting as a GABA receptor agonist. This potentially neurotoxic drug is only absorbed in humans in a very small fraction, and this low-level ivermectin absorption is mainly caused by active extrusion in the intestine by the ABCB1/Pgp transporter. ABCB1, and probably other ABC transporters (especially ABCG2) in the blood–brain barrier (BBB), also have a significant role in protecting the mammalian central nervous system (CNS) against toxic ivermectin penetration. In mouse Pgp-knock-out models, in natural Pgp-knock-out Collie dogs, and also in some humans with low-level ABCB1/Pgp expression, ivermectin exerts major neurotoxicity [8,9]. In addition, both ABCB1 and several other multispecific transporters have been shown to be inhibited by micromolar concentrations of ivermectin [10–12], so ivermectin may influence the pharmacokinetics of several drugs or toxic compounds. Ivermectin was suggested to have anti-CoV-2 effects based on *in vitro* studies, indicating that this compound inhibits the importin alpha/beta-1 nuclear transporter, and thus in cell cultures, reduces the replication of various viruses [13–15], including SARS-CoV-2 [16,17]. However, the ivermectin plasma concentrations required to reach an *in vitro* antiviral efficacy (about 2–10 μ M) are highly toxic, and very high oral doses would be needed for antiviral use [18]. Therefore, in spite of some anecdotal clinical results, ivermectin has not been approved for the treatment of any viral diseases, including SARS-CoV-2 (see the NIH-CTGP). Moreover, in April, 2020, FDA issued a warning not to use ivermectin to treat COVID-19 in humans.

Several approved and clinically effective HIV protease inhibitors, including **ritonavir** and **lopinavir**, based on their potential for inhibiting other viral proteases, also entered clinical trials as anti-COVID-19 agents. SARS-CoV-2 virus replication requires the cleavage of viral polyproteins, and the proteases 3CLpro and PLpro are responsible for this cleavage. *In vitro*, lopinavir and ritonavir were found to inhibit 3CLpro, and thus reduce SARS-CoV-2 replication [19]. However, these drugs are poorly selective and high concentrations are required to achieve *in vivo* inhibition [20]. Therefore, the current NIH-CTGP recommends against the use of these compounds for COVID-19 treatment, except in a clinical trial. The NIH-CTGP also warns that the lopinavir/ritonavir combination is a strong inhibitor of cytochrome CYP3A, so co-treatment with numerous drugs metabolized by CYP3A may result in increased toxicities. Ritonavir induces CYP1A2 and inhibits CYP3A4 and CYP2D6. Therefore, it may cause serious drug–drug interactions. Ritonavir and lopinavir are inhibitors of ABC multidrug transporters [21,22], both *in vitro* and *in vivo* [23], and according to studies with labeled ritonavir and lopinavir, these agents are transported substrates of ABCB1/Pgp [24,25], but not of ABCG2/BCRP [26,27].

Recently developed antiviral agents, despite having been found to be minimally effective in earlier clinical studies and not approved for general use, have also been introduced in COVID-19 clinical trials. **Favipiravir** (Avigan) is a pyrazinecarboxamide derivative antiviral agent, administered as a prodrug in both oral and intravenous formulations. The active form is an inhibitor of the viral RNA-dependent RNA polymerase and thus reduces the viral load. Favipiravir was approved in Japan against special cases of influenza, although it was found to be ineffective in human airway cells [28]. Favipiravir degradation mostly occurs by aldehyde oxidase (AO) and xanthine oxidase. Since favipiravir was found

to inhibit CYP2C8, co-administration with CYP2C8 substrates may increase some drug effects. Since favipiravir is often used together with acetaminophen, it is important to note that favipiravir inhibits acetaminophen sulfate formation. In addition, favipiravir has been shown to have a teratogenic effect in animals [29]. Currently, the use of favipiravir in treating COVID-19, despite only having limited clinical data for its efficiency in this disease, has been approved in China, India, and for emergency use in Japan, while this agent remains unapproved in Europe and the USA.

Remdesivir (Veklury) is a broad-spectrum antiviral medication employed for intravenous injection provided in a sulfobutylether- β -cyclodextrin (SBECD) complex. Remdesivir (RDV) itself is a prodrug, and its active triphosphate metabolite is a ribonucleotide analogue inhibitor of viral RNA polymerase. Remdesivir was developed for the treatment of hepatitis C and Ebola virus diseases, while based on initial clinical trials, it has been authorized for emergency use in COVID-19 in numerous countries, especially for patients with severe symptoms. In October 2020, FDA authorized the clinical use of remdesivir against COVID-19, while the WHO still does not support its use in this disease. Preclinical studies indicated that remdesivir is not a substrate of CYP2C8, CYP2D6, or CYP3A4, and is not “significantly” transported by ABCB1/Pgp or the organic anion-transporting polypeptide (OATP)-type drug transporters [30], while detailed studies on remdesivir–drug interactions are not yet available. Remdesivir in *in vitro* studies was metabolized by CYP2C8, 2D6, and 3A4, while *in vivo* studies indicate its metabolism by hydrolases. Remdesivir at the clinic is applied in the form of a sulfobutyl ether beta-cyclodextrin (SBECD) complex, thus, in addition to remdesivir, we have also used this cyclodextrin complex in our *in vitro* studies.

In order to explore the multispecific drug transporter interactions of the above repurposed drugs (see Table 1), in this investigation, we performed a detailed *in vitro* study on their potential interaction with several key multidrug transporters. We focused on the potential role of the transporter–drug interactions in the important tissue barriers, especially the intestinal epithelium and the blood–brain barrier (BBB) endothelial cells (see <http://www.fda.gov/Drugs/DevelopmentApprovalProcess/DevelopmentResources/DrugInteractionsLabeling/ucm093664.htm#major> (2017)).

Table 1. Mechanism of action of the potential anti-COVID-19 drugs examined in this study.

Potential Anti-COVID-19 Compounds	Mechanism of Action
chloroquine	Antimalarial—endosomal pH increase
hydroxychloroquine	Antimalarial—endosomal pH increase
ivermectin	Antiparasitic—glutamate-gated chloride channel and a GABA receptor inhibitor
lopinavir	(HIV) protease inhibitor
ritonavir	(HIV) protease inhibitor
remdesivir	Viral RNA-polymerase inhibitor
favipiravir	Viral RNA-polymerase inhibitor

The ABCB1/Pgp and ABCG2/BCRP efflux transporters are key proteins for xenobiotic extrusion in the intestine and BBB, while they are also involved in toxin and drug metabolism in the liver and kidney [31–33]. In addition to several endogenous substrates, including conjugated metabolites, steroids, and uric acid, there is a wide range of environmental and food-related toxic molecules actively transported by these proteins. Therefore, they are major players in drug–drug interactions. While, in most model animals, Pgp is the major drug transporter in the BBB, in primates and humans, ABCG2 seems to be the key protective transporter in this tissue [34–36]. In addition, ABCC1 has a role in the blood–cerebrospinal barrier to avoid CNS toxicity [37].

Organic anion-transporting polypeptides (OATPs) belong to the Solute Carrier (SLC) family and some of them (e.g., OATP1A2, 1B1, 1B3, and 2B1) are well-documented multispecific plasma membrane xenobiotic and drug transporters involved in the cellular uptake

of various organic molecules (“uptake transporters”) [38]. OATP1B1 and OATP1B3 are important in liver drug metabolism, while OATP1A2 and OATP2B1 are expressed in a variety of human tissues [39]. These latter transporters are highly expressed in the intestine, while OATP1A2 is the key drug uptake transporter expressed in the BBB endothelial cells, promoting drug uptake from the blood plasma into the CNS [40–42]. Therefore, OATPs 1A2 and 2B1 are important players in the pharmacokinetics of numerous drugs, either being substrates or inhibitors of these transporters. Based on both in vitro and clinical data, OATP1A2 and OATP2B1 are key players in the intestinal uptake of a large variety of clinically important drugs, including statins, fexofenadine, sulfasalazine, steroids, and telmisartan, while they may be significantly inhibited by chemotherapeutics or antiviral compounds [42]. In addition, they contribute to the tissue penetration of numerous endogenous substrates, including steroid and thyroid hormones, prostaglandins, bile acids, and bilirubin [43]. Based on their important role in tissue barriers and drug pharmacokinetics, we studied the potential inhibition of the function of ABCB1, ABCG2, ABCC1, OATP2B1, and OATP1A2 by the clinically applied anti-COVID-19 agents. In these experiments, we used an array of in vitro functional transporter assays which, together, may provide important new information regarding the potential ADME-tox properties of these agents.

2. Materials and Methods

2.1. Materials

All basic laboratory reagents were obtained from Sigma Aldrich. The 5D3 antibody was a kind gift from B. Sorrentino, St. Jude Children Hospital, Memphis, USA, and remdesivir and remdesivir-SBECN were kind gifts from Lajos Szente, Cyclolab Ltd., Budapest, Hungary. Vesicular assay membranes and components were obtained from SOLVO Biotechnology, Budapest, Hungary (<https://www.solvobiotech.com/services/categories/>).

2.2. ABC Transporter Assays

For the ABC transporter assays, we used both cell-based and membrane-based functional assays. For assaying the function of the ABC transporters in cell-based assays, we applied stable cell lines expressing the transporters ABCG2 PLB-985, ABCB1 PLB-985, and ABCC1 HL-60, and their parental lines, which lack significant ABC transporter expression [44]. The respective transport activities were assayed by measuring the cellular fluorescence of the respective transported substrates PhenGreen (ABCG2) and Calcein (ABCB1 and ABCC1) [44]. For the ABCG2 transport assay, we also used HeLa cells stably expressing the wild-type or Q141K polymorphic variant of the ABCG2 protein (see below).

For studying ABCB1 and ABCC1 transport, 5×10^4 parental control or transporter-containing cells were incubated with 0.25 μM Calcein-AM (C3100MP ThermoFisher Scientific, Waltham, MA, USA) in phosphate buffered saline (PBS) containing 1 g/L D-glucose (DPBS) for 40 min at 37 °C. The test compounds were applied in 0.2–50 μM , and as specific transporter inhibitors, 0.25 μM tariquidar (TQ, which was a kind gift from Dr. S. Bates (NCI, NIH)) for ABCB1 and 10 μM indomethacin (IM, I0200000, Sigma-Aldrich-Merck, St. Louis, MO, USA) were used. The cells were kept on ice until the flow cytometry measurements. All experiments were performed in triplicate and in at least three biological parallels.

For examining the function of ABCG2, 5×10^4 parental control or ABCG2 transporter-expressing cells were incubated with 0.25 μM PhenGreen-SK diacetate (P14313, ThermoFisher Scientific, Waltham, MA, USA) in DPBS containing 1 μM EDTA, for 40 min at 37 °C. The test compounds were applied in 0.2–50 μM , and as a specific transporter inhibitor, 2.5 μM Ko143 (3241, Tocris Bioscience, Bristol, UK) was applied. The cells were kept on ice until the flow cytometry measurements. All experiments were performed in triplicate and in at least three biological parallels. Cellular fluorescence reflecting the transport activity was measured by an Attune Nxt cytometer (Thermo Fischer Scientific, Waltham, MA, USA) equipped with a blue (488 nm) laser. The PhenGreen (PG) or Calcein signal was detected in the BL1 channel (emission filter: 530/30 nm). Analysis of the data was carried out by the Attune Nxt Cytometer Software v3.1.2 (Thermo Fischer

Scientific, Waltham, MA, USA). The inhibition of transporter activity was calculated by comparing the fluorescence in the presence of the test compound to that in the presence of a specific inhibitor providing maximum inhibition. Higher concentrations of some of the investigated compounds also altered the fluorescence of Calcein in the parental cells in an ABC transporter-independent way (parental cells had no significant ABC transporter expression, as tested by specific inhibitors), and these data were used for correction of the data obtained in ABC transporter-expressing cells. Half-maximum inhibition (IC_{50}) values were calculated by using the Origin2019 software (9.6.5.169, OriginLab Corporation, Northampton, MA, USA). In addition to studies on the wild-type ABCG2 transporter, we also examined the effects of drugs on the function of a relatively frequent (present in up to 20–35% of the population) polymorphic variant—the Q141K-ABCG2 (SNP rs2231142) transporter. In these experiments, we measured Hoechst dye extrusion in HeLa cells stably expressing eGFP and the ABCG2 variants driven by the same promoter—the transgenic cells generated by the Sleeping Beauty transposon system. These cells were sorted based on similar levels of eGFP, and ABCG2 expression was examined by a monoclonal (5D3) antibody-based flow cytometry assay (Q141K-ABCG2 cell surface expression was approximately 80% of the wild-type ABCG2 expression. For details, see Zámbo et al. [45]). For the ABCG2 transporter inhibition assay, trypsinized HeLa cells expressing the ABCG2 wild-type (WT) or Q141K variant were incubated in a shaker for 20 min at 37 °C in HPMI buffer (20 mM HEPES, 132 mM NaCl, 3.5 mM KCl, 0.5 mM $MgCl_2$, 5 mM glucose, 1 mM $CaCl_2$ [pH 7.4]) with 0.2 μ M of Hoechst 33342 (H1399, Thermo Fisher Scientific, Waltham, MA, USA) dye, in the presence of the tested drugs or 1 μ M of the specific ABCG2 inhibitor Ko143 (3241, Tocris Bioscience, Bristol, UK). Following incubation, the cells were put on ice and Hoechst dye fluorescence was measured using the violet laser (405 nm) and VL1 detector on the Attune Nxt Cytometer. Cells showing similar eGFP fluorescence were gated in the case of the WT and Q141K variants. The maximum inhibition was defined for each variant as the fluorescence difference of the samples incubated with and without Ko143, respectively. All tested drugs (ivermectin, remdesivir, ritonavir, lopinavir, and Ko143) were dissolved in DMSO, and the same DMSO concentration (below 0.5%) was applied for all drug concentrations examined. Data analysis was performed using the Attune Nxt Cytometer Software v3.1.2. Two samples per condition and three biological replicates were examined in each experiment.

For studying the vesicular ATP-dependent transporter activity of the ABC transporters, we used ABCB1/Pgp or ABCG2/BCRP containing HEK-293 cell membrane vesicles, as well as ABCC1/MRP1 containing Sf9 membrane vesicles, prepared by Solvo Biotechnology. Membrane vesicles (12.5 μ g protein/sample) were incubated with transporter-specific substrates: For ABCG2, 5 μ M lucifer yellow (LY) as a fluorescent substrate and the radiolabeled substrate probes; for ABCB1, 1 μ M N-methyl quinidine (NMQ); and for ABCC1, 0.2 μ M estradiol-glucuronide (ETGB). These were employed at 37 °C for 10 min (ABCG2), 1 min (ABCB1), or 3 min (ABCC1), with or without 4 mM Mg-ATP, in a 50 μ L final volume. The known reference inhibitors of the transporters (1 μ M Ko143 for ABCG2, 1 μ M Valspodar for ABCB1, and 200 μ M Benzbromarone for ABCC1) served as controls. Each test compound was dissolved in DMSO and a 1 μ L volume was added to the samples. After incubation, the samples were filtered and washed, and the substrates in the vesicles were dissolved in 10% SDS and transferred onto another plate. After the addition of a stabilizer, the fluorescence was measured in plate readers (Victor X3 and Enspire Perkin-Elmer, Waltham, MA, USA), while the activity of the radiolabeled substrate was measured by liquid scintillation counting (Perkin Elmer MicroBeta2 liquid scintillation counter, Perkin Elmer, Waltham, MA, USA). ABC transporter-related vesicular transport was calculated by subtracting uptake measured in the presence of Mg-AMP from the values measured in the presence of Mg-ATP. No significant quenching by the test compounds was observed.

ABC transporter ATPase activity was measured in Sf9 membrane vesicles containing the respective human ABC transporters [46–50]. For ABCG2/BCRP, the cholesterol level in the vesicles was increased to the level of mammalian cell membranes for full activity [49].

For ABCB1/Pgp 20 µg/150 µL and for ABCG2/BCRP 10 µg/150 µL, vesicles were incubated with 3 mM Mg-ATP for 25 min at 37 °C. The test drugs were dissolved in DMSO and 1 µL was added to the samples. The ABC transporter-related ATPase activity was determined and reference activators (50 µM verapamil for ABCB1 and 5 µM quercetin for ABCG2) served as controls.

2.3. OATP Transporter Assays

For studying the function of the multispecific uptake transporters OATP1A2 and OATP2B1, we used A431 human tumor cells overexpressing these human proteins and mock transfected A431 cells as controls, generated as previously described [47,51]. The interaction between OATPs and the potential anti-COVID-19 agents was studied by employing fluorescent dye substrates: Pyranine for OATP2B1 and sulforhodamine 101 for OATP1A2 [51,52].

Briefly, A431 cells overexpressing OATP1A2 or OATP2B1 [47] were seeded on 96-well plates, washed three times with 200 µL phosphate buffered saline (PBS, pH 7.4), and pre-incubated with 50 µL uptake buffer (125 mM NaCl, 4.8 mM KCl, 1.2 mM CaCl₂, 1.2 mM KH₂PO₄, 12 mM MgSO₄, 25 mM MES (2-(N-morpholino) ethanesulfonic acid, and 5.6 mM glucose, pH 5.5 for OATP2B1 and pH 7.0 for OATP1A2) at 37 °C, with or without increasing concentrations of the tested compounds. The test compounds were dissolved in DMSO (maximum 0.5%), and the reaction was started by the addition of a final concentration of 20 µM pyranine (OATP2B1) or 0.5 µM sulforhodamine 101 (OATP1A2). After incubation at 37 °C for 15 min (OATP2B1) or 10 min (OATP1A2), the reactions were stopped and the cells were washed three times with ice-cold PBS. Fluorescence was measured in an Enspire plate reader (Perkin Elmer, Waltham, MA, USA) (ex/em: 403/5 and 517/5 nm (pyranine) or 586/5 and 605/5 nm (sulforhodamine 101)), and the OATP-dependent transport activity was determined by comparing the data to those obtained from mock transfected cells. In all experiments, three biological replicates were used and IC₅₀ values were calculated by using GraphPad prism software (version 5.01, GraphPad, La Jolla, CA, USA). Due to the high level of specific transporter expression, background transport was very low in these cells (see reference [47]).

3. Results

3.1. Interaction of Anti-COVID-19 Drug Candidates with ABCB1/MDR1/Pgp

In these experiments, we applied several independent in vitro methods to explore the drug interactions with this transporter. We measured ABCB1-related fluorescent substrate (Calcein-AM) transport inhibition in intact model cells, inhibition of the vesicular transport of an established ABCB1 substrate N-methyl quinidine (NMQ) in mammalian cell membrane vesicles, and drug-dependent ABCB1-ATPase activity in isolated insect (*Sf9*) cell membranes (see Figure 1). In all cases, previously well-characterized cells or membranes with highly expressed ABCB1 levels were applied, so the data can be compared to numerous similar studies in the relevant scientific literature.

3.1.1. Transport Assays in Intact Human PLB-985/ABCB1 Cells

ABCB1 is a high-affinity active efflux transporter of the viability dye Calcein-AM (CaAM). The cellular uptake of the non-fluorescent CaAM is strongly inhibited by the extrusion of this compound by the ABCB1 transporter, so the cellular fluorescence of the intracellularly formed free Calcein is strongly reduced in cells expressing ABCB1 [53]. Here, we applied this widely used cellular assay (see <https://www.solvobiotech.com/services/categories/dye-efflux-assays>) to characterize drug interactions of the applied compounds in intact PLB-985 cells, expressing high levels of the ABCB1 protein. Maximum inhibition of the transporter was achieved by 0.25 µM tariquidar (TQ), which is a third-generation specific inhibitor of ABCB1. ABCB1 inhibition by the test compounds was estimated by their relative (%) inhibition compared to full inhibition by TQ. As shown in Figure 1A,B, ivermectin caused a strong inhibition of the ABCB1-dependent CaAM

extrusion at low micromolar concentrations (estimated IC_{50} of 0.6 μM), while chloroquine and hydroxychloroquine had practically no effect on this ABCB1-dependent transport. Figure 1B documents the effects of lopinavir, ritonavir, favipiravir, and remdesivir on the CaAM extrusion by ABCB1. Favipiravir, remdesivir, and its cyclodextrin complex did not significantly inhibit the transport activity of ABCB1. In contrast, lopinavir and ritonavir caused a strong inhibition of the ABCB1-dependent CaAM extrusion at low micromolar concentrations (estimated IC_{50} values of 6.3 and 8.4 μM , respectively).

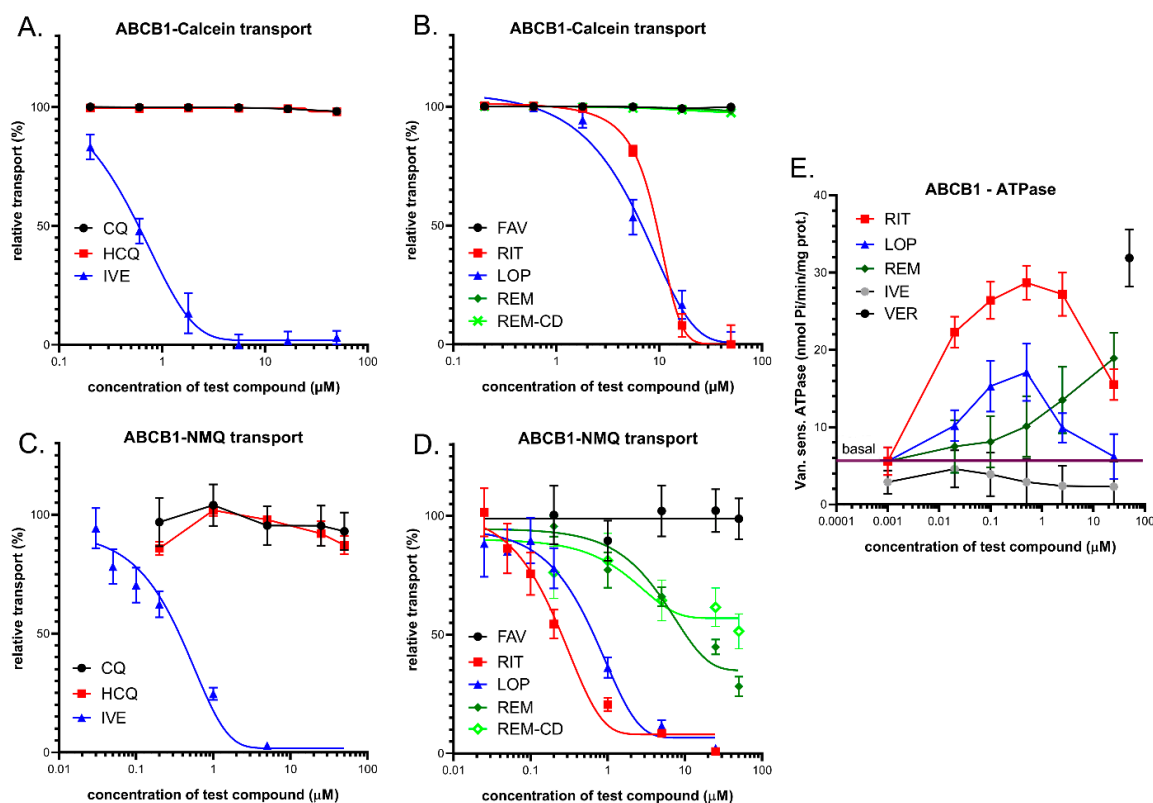


Figure 1. (A,B) Inhibition of ABCB1-mediated Calcein-AM (CaAM) extrusion in intact ABCB1 expressing PLB-985 cells. (A) Effects of ivermectin (IVE), chloroquine (CQ), and hydroxychloroquine (HCQ). (B) Effects of lopinavir (LOP), ritonavir (RIT), favipiravir (FAV), remdesivir (REM), and cyclodextrin formulated remdesivir (REM-CD). (C,D) Inhibition of ABCB1-mediated N-methyl quinidine (NMQ) transport in the vesicular transport assay. (E) ABCB1-ATPase activity in isolated Sf9 membrane vesicles. Effects of ivermectin, lopinavir, ritonavir, and remdesivir. As a reference substrate, verapamil (VER) was used. The basal line represents the ATPase activity level without the addition of any drug. Data on the graphs show the average of at least three independent experiments, +/- SD or SEM (E) values.

3.1.2. Vesicular Transport Studies in HEK/ABCB1 Membrane Vesicles

In these experiments, we studied the effects of the potential anti-COVID-19 compounds in a vesicular transport assay by using inverted membrane vesicles prepared from HEK-293 cells expressing high levels of the ABCB1 transporter. In the inverted membrane vesicle measurements, labeled substrates and the investigated compounds were both applied on the cytoplasmic side of the membrane, which excludes most of the complex intracellular drug interactions. The modulation of the ATP-dependent vesicular uptake of a specific ABCB1 probe substrate directly reveals drug interactions with the transporter. In the present work, we measured the uptake of 3H -N-methyl-quinidine (NMQ), which is a labeled low-permeability amphipathic substrate of the human ABCB1/MDR1/Pgp [54,55]. Transport inhibition (%) of this labeled substrate by the test compounds was calculated by setting probe substrate transport in the absence of test compounds as 100%. As shown in Figure 1C, in ABCB1 expressing membrane vesicles, ivermectin caused a strong inhibition of the ATP-dependent NMQ uptake at low micromolar concentrations (estimated IC_{50}

of 0.3 μM), while chloroquine and hydroxychloroquine had practically no effect on this transport activity. Figure 1D shows the effects of lopinavir, ritonavir, favipiravir, and remdesivir on the transport activity of ABCB1. As documented, lopinavir and ritonavir are strong inhibitors of this transport (estimated IC_{50} values are 0.6 and 0.3 μM , respectively), remdesivir and remdesivir-SBECED are weak inhibitors of ABCB1 (IC_{50} above 20 μM), and favipiravir had no inhibitory effect.

3.1.3. ABCB1-ATPase Activity Measurements in Sf9 Membranes

Drug-stimulated ATPase activity of the ABCB1 transporter is a well-documented functional assay employed to estimate the substrate or inhibitory features of various drugs. ATP-dependent substrate transport is reflected in the activation of this specific ATPase activity in most cases, and in many cases, drug-stimulated ABCB1-ATPase has been shown to correlate with the substrate affinity. In this assay, most transported substrates show a biphasic curve: Low concentrations stimulate, while higher concentrations inhibit, the ATPase activity [46]. In these experiments, we measured the vanadate-sensitive (ABC transporter-related) ABCB1-ATPase activity in membrane vesicles isolated from ABCB1 overexpressing Sf9 cells [46,49]. Sf9 cells exhibit low intrinsic membrane ATPase activity, so both the baseline and the drug-stimulated ATPase activity of the ABCB1 protein can be measured. High-level stimulation of this ATPase activity can be achieved by 50 μM of verapamil—a transported substrate of ABCB1—serving as a positive control in this assay. As shown in Figure 1E, several tested compounds significantly increased the ABCB1-ATPase activity in this assay. Low micromolar concentrations of ritonavir (EC_{50} less than 0.1 μM) stimulated the ATPase activity up to the level of verapamil activation, and both lopinavir (EC_{50} about 0.05 μM) and remdesivir (EC_{50} about 10 μM) showed significant ABCB1-ATPase stimulation. Ritonavir and lopinavir exhibited maximal stimulation at around 0.5 μM , whereas remdesivir only increased the ATPase activity at 10–50 μM . At higher concentrations, ritonavir and lopinavir displayed inhibitory effects. Ivermectin only showed ABCB1-ATPase inhibition.

3.2. Interaction of Anti-COVID-19 Drug Candidates with ABCC1/MRP1

3.2.1. Transport Assay in Intact Human Cells—HL60/ABCC1 Cells

ABCC1, similarly to ABCB1, is a high-affinity active efflux transporter for Calcein-AM and the cellular fluorescence of free Calcein is also reduced in cells expressing ABCC1 [56]. Therefore, we applied this assay to characterize the test drug interactions in intact HL60 cells expressing high levels of the ABCC1 protein. Maximum inhibition of the transporter was achieved by 10 μM of indomethacin (IM), which is a strong inhibitor of ABCC1. ABCC1 inhibition by the test compounds was estimated by their relative (%) inhibition compared to full inhibition by IM. As shown in Figure 2A, ivermectin caused a strong inhibition of the ABCC1-dependent CaAM extrusion at low micromolar concentrations (estimated IC_{50} of 3.3 μM), while chloroquine and hydroxychloroquine had practically no effect. As documented in Figure 2B, lopinavir and ritonavir had strong inhibitory effects, with estimated IC_{50} values of 10.7 and 7.7 μM , respectively. Favipiravir, remdesivir, and its cyclodextrin complex did not significantly inhibit the cellular transport activity of ABCC1 (a slight inhibition by higher concentrations of remdesivir was observed).

3.2.2. Vesicular Transport Studies in Sf9/ABCC1 Membrane Vesicles

In this study, we measured the effects of the test compounds in a vesicular transport assay by using inverted membrane vesicles prepared from Sf9 cells expressing high levels of the ABCC1 transporter. We measured the uptake of ^3H -estradiol-17 β -glucuronide (ETGB), which is a labeled substrate of the human ABCC1/MRP1 transporter [57]. Relative inhibition (%) was calculated by setting probe substrate transport in the absence of test compounds as 100%. As shown in Figure 2C, in ABCC1 expressing membrane vesicles, lopinavir caused an inhibition of the ATP-dependent ETGB uptake in a dose-dependent manner, with a maximum inhibition of 60% at the highest applied concentration. Ivermectin

inhibited the ABCC1-mediated ETGB accumulation, with a maximum inhibition of 80% at a 25 μM concentration. Ritonavir, favipiravir, chloroquine, and hydroxychloroquine had practically no effect on this transport activity (CQ and HCQ not shown), while, interestingly, remdesivir significantly stimulated the vesicular ETGB transport activity of ABCC1, although only at above 25 μM .

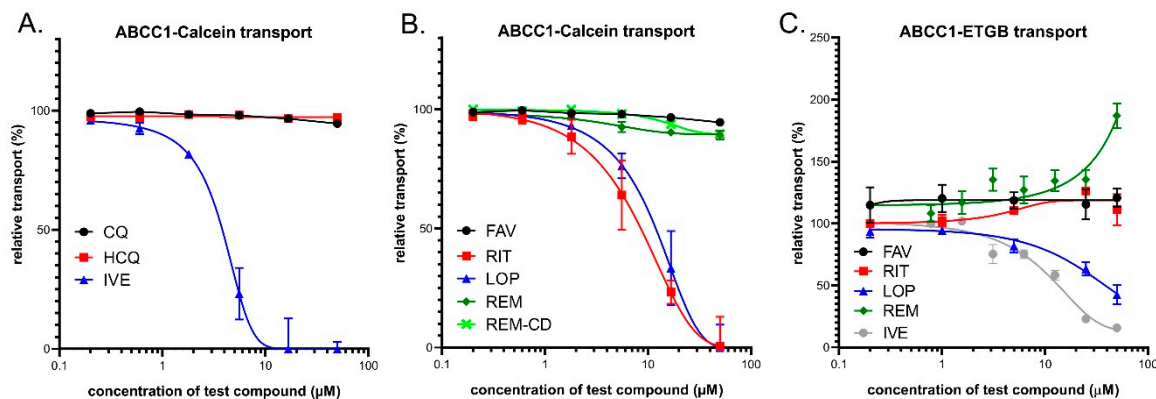


Figure 2. (A,B) Inhibition of ABCC1-mediated CaAM extrusion in intact HL60 cells. Panel C: Inhibition of ABCC1-mediated vesicular uptake of ^3H -estradiol-17 β -glucuronide (ETGB). Panel (A) Effects of ivermectin (IVE), chloroquine (CQ), and hydroxychloroquine (HCQ). (B) Effects of lopinavir (LOP), ritonavir (RIT), favipiravir (FAV), remdesivir (REM), and SEBCD-remdesivir (REM-CD). (C) Effects of ivermectin (IVE), lopinavir (LOP), ritonavir (RIT), favipiravir (FAV), and remdesivir (REM).

3.3. Interaction of Anti-COVID-19 Drug Candidates with ABCG2

3.3.1. Transport Measurements in Intact Human Cells—PLB/ABCG2 and HeLa/ABCG2

The ABCG2 protein does not transport Calcein AM, so this assay cannot be used for assaying ABCG2 activity in intact cells. In contrast, several fluorescent dyes, including Hoechst 33342 (Hst), DyeCycle violet (DCV), and PhenGreen-SK diacetate (PG-DA), are actively extruded by the ABCG2 transporter [44,58–63], providing an opportunity for fluorescence-based cellular assays. Here, we used both PhenGreen-SK diacetate and Hst dye for these measurements. The PhenGreen (PG) assay is a recently patented method applied for ensuring an efficient ABCG2 transport measurement, as the non-fluorescent PhenGreen diacetate (PG-DA) is actively extruded by ABCG2 and the cellular fluorescence is correlated with ABCG2 transport activity [44]. Therefore, we applied this assay to characterize the test drug interactions in intact PLB-985 cells expressing high levels of the ABCG2 protein. Maximum inhibition of the transporter was achieved by 2.5 μM of Ko143, which is a high-affinity specific inhibitor of ABCG2. ABCG2 inhibition by the test compounds was estimated by their relative (%) inhibition compared to full inhibition by Ko143. As shown in Figure 3A,B, ivermectin caused a strong inhibition of the ABCG2-dependent PG-DA extrusion at micromolar concentrations (estimated IC_{50} of 3.1 μM). Lopinavir and ritonavir also had strong inhibitory effects, with estimated IC_{50} values of 13.1 and 8.3 μM , respectively. Favipiravir, chloroquine, and hydroxychloroquine had practically no effect on this ABCG2-dependent transport. Remdesivir and its complex are relatively weak inhibitors of the ABCG2-dependent PG-DA extrusion at micromolar concentrations (estimated IC_{50} values are greater than 40–50 μM).

3.3.2. Vesicular Transport Studies in HEK/ABCG2 Membrane Vesicles

The effects of the test compounds on ABCG2 activity were also measured in a vesicular transport assay by using inverted membrane vesicles prepared from HEK-293 cells expressing high levels of the ABCG2 transporter. The ATP-dependent uptake of lucifer yellow (LY), which is a substrate of the human ABCG2/BCRP transporter [64], was measured, and inhibition of this fluorescent substrate uptake by the test compounds was compared to a full inhibition achieved by 1 μM of Ko143. As shown in Figure 3C,D, in ABCG2

containing HEK-293 cell membrane vesicles, ivermectin caused a strong inhibition of the ATP-dependent LY uptake at low micromolar concentrations (estimated IC_{50} of 1.1 μM), while chloroquine and hydroxychloroquine had practically no effect. Lopinavir, ritonavir, and remdesivir, as well as remdesivir-cyclodextrin, inhibited the transport activity of ABCG2, with estimated IC_{50} values of 4.2, 7.5, and more than 20 μM , respectively.

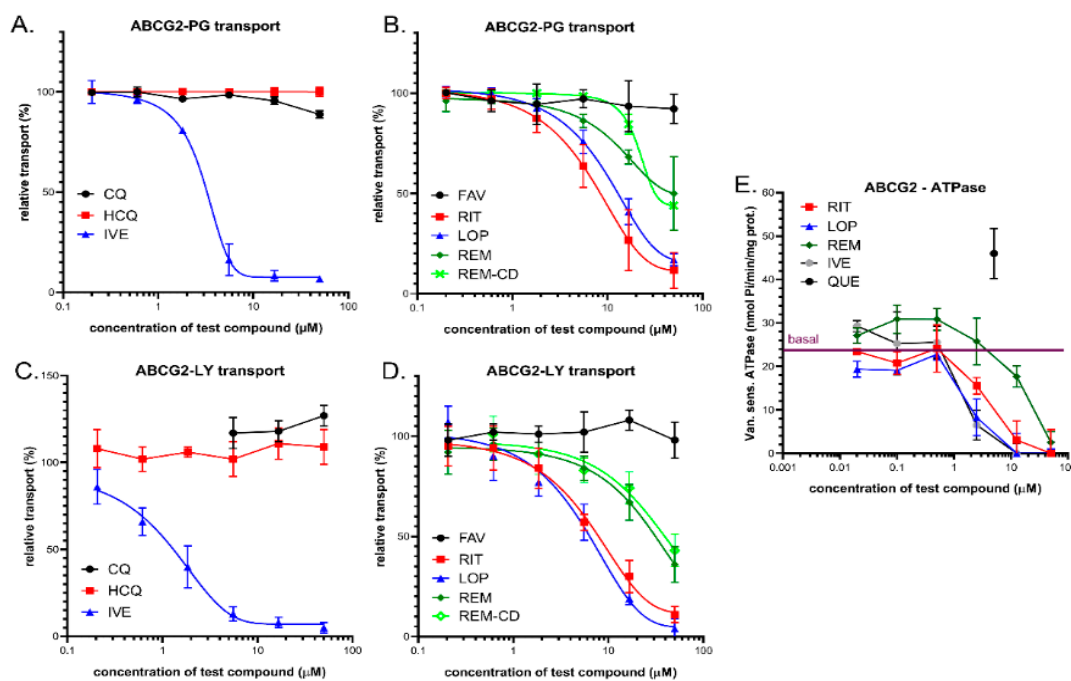


Figure 3. (A,B) Inhibition of ABCG2-mediated PhenGreen (PG)-AM extrusion in intact PLB-985 cells. Panel A: Effects of ivermectin (IVE), chloroquine (CQ), and hydroxychloroquine (HCQ). Panel B: Effects of lopinavir (LOP), ritonavir (RIT), favipiravir (FAV), remdesivir (REM), and SEBCD-remdesivir (REM-CD). (C,D) Inhibition of ABCG2-mediated lucifer yellow (LY) transport in the vesicular transport assay. (E) ABCG2-ATPase activity in isolated Sf9 membrane vesicles. Effects of ivermectin, lopinavir, ritonavir, and remdesivir. Maximum ATPase stimulation was obtained by 5 μM quercetin. Data on the graphs show the average of at least three independent experiments, \pm SD (A,B) or SEM (C–E) values.

3.3.3. ABCG2-ATPase Activity Measurements in Sf9 Membranes

Drug-stimulated ATPase activity of the ABCG2 transporter was also measured in the present study. This functional assay may be used to estimate the substrate/inhibitory features of various drugs (see 1.E, and [50]). Here, we measured the vanadate-sensitive ABCG2-ATPase activity in membrane vesicles isolated from ABCG2 overexpressing Sf9 cells [50], and the maximum stimulation of this ABCG2-ATPase activity was achieved by the transported substrate—5 μM quercetin—serving as a positive control in this assay. As shown in Figure 3E, ivermectin, ritonavir, and lopinavir at low micromolar concentrations, and remdesivir at higher concentrations (around 20–50 micromoles), significantly inhibited the baseline ABCG2-ATPase activity. None of the tested compounds displayed significant ABCG2-ATPase stimulation effects. Therefore, the assay was not informative regarding their potential transported substrate nature.

3.3.4. Effect of the Q141K-ABCG2 Polymorphism on the Inhibitory Potential of the Test Drugs

The very frequent (present in 12–35% in various populations) Q141K-ABCG2 polymorphic variant has been reported to have lower membrane expression levels and reduced transport activity in various assay systems [65]. Since ivermectin, lopinavir, ritonavir, and remdesivir resulted in well-measurable inhibition of the ABCG2-dependent PG dye extrusion activity (see above), we performed similar studies in HeLa cells stably expressing either the wild-type ABCG2 or the Q141K-ABCG2 variant [45]. In this case, we measured

the extrusion of the Hoechst 33342 dye, which is another transported substrate of ABCG2, and once again used the specific inhibitor Ko143 to achieve full inhibition of the transporter. As shown in Figure 4, ivermectin (A), ritonavir (B), and lopinavir (C) also inhibited Hst dye extrusion by ABCG2 in the HeLa cells, and remdesivir (D) had a slight effect at relatively high concentrations. An important finding was that Hst dye extrusion in HeLa cells expressing the Q141K-ABCG2 variant showed a higher sensitivity to all drug inhibition.

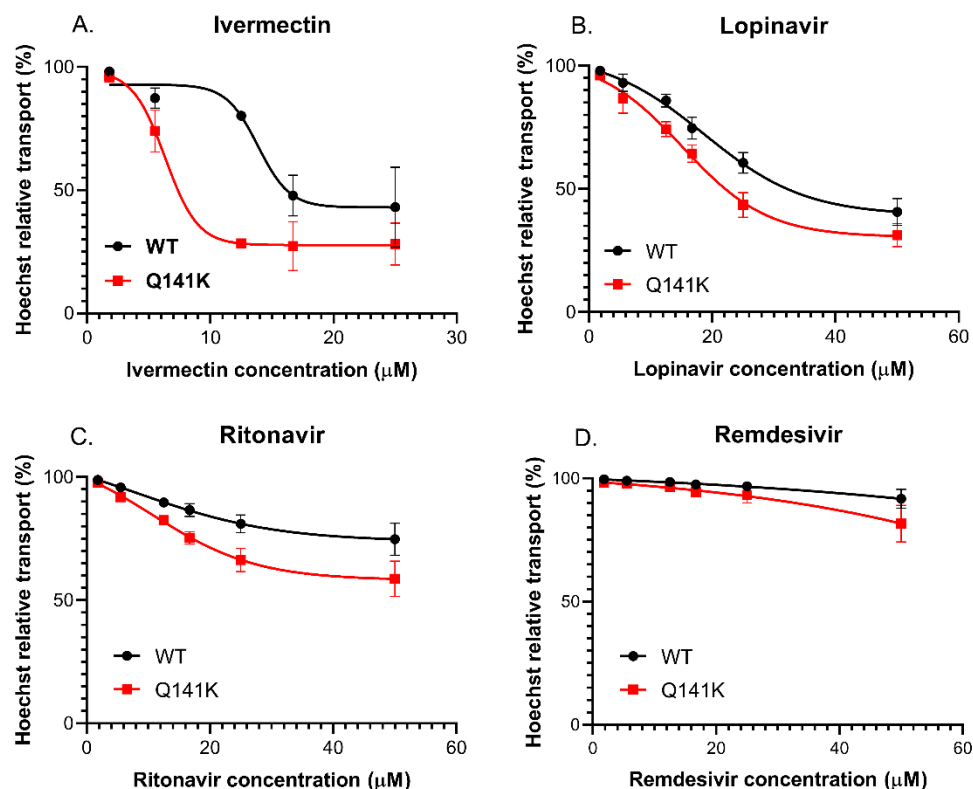


Figure 4. Hoechst 33342 dye extrusion in HeLa cells stably expressing the WT and Q141K variants of ABCG2. Different concentrations of ivermectin (A), lopinavir (B), ritonavir (C), and remdesivir (D) were used to determine their effect on ABCG2 function. Data on the graphs show the average of three independent experiments, \pm SD values.

3.4. Interaction of Anti-COVID-19 Candidates with OATP1A2 and OATP2B1 Transporters

In order to explore potential interactions between the potential anti-COVID-19 drugs and OATP1A2 or OATP2B1, the compounds were investigated in a fluorescence-based cellular transport assay recently developed by our laboratory [47,51]. The uptake of pyranine or sulforhodamine 101 as test substrates was measured in A431-OATP1A2 or A431-OATP2B1 cells, and mock transfected A431 were used as the negative control. As shown by Figure 5, with the exception of favipiravir, all of the compounds examined inhibited OATP1A2 function. Based on the IC_{50} values, the antivirals lopinavir, ritonavir, remdesivir, and the anti-parasitic ivermectin exhibited similar affinities towards OATP1A2. On the other hand, although still effective, chloroquine and hydroxychloroquine were 3–10-fold lower affinity inhibitors (see Table 2). Interestingly, cyclodextrin resulted in a slightly decreased inhibitory potential of remdesivir on OATP1A2 function (Figure 5, and Table 2). In the case of OATP2B1, a similar inhibitory potency was observed for the antiviral compounds, as in the case of OATP1A2. Lopinavir and ritonavir were the highest affinity inhibitors, with IC_{50} values of 1.0 and 1.4 μM , respectively, and remdesivir, the remdesivir-cyclodextrin complex, and ivermectin had lower inhibitory effects, with IC_{50} values of 3.8, 5.6, and 8.6 μM , respectively. Chloroquine and hydroxychloroquine exerted only modest inhibition of OATP2B1 activity, and favipiravir showed no interaction with this transporter.

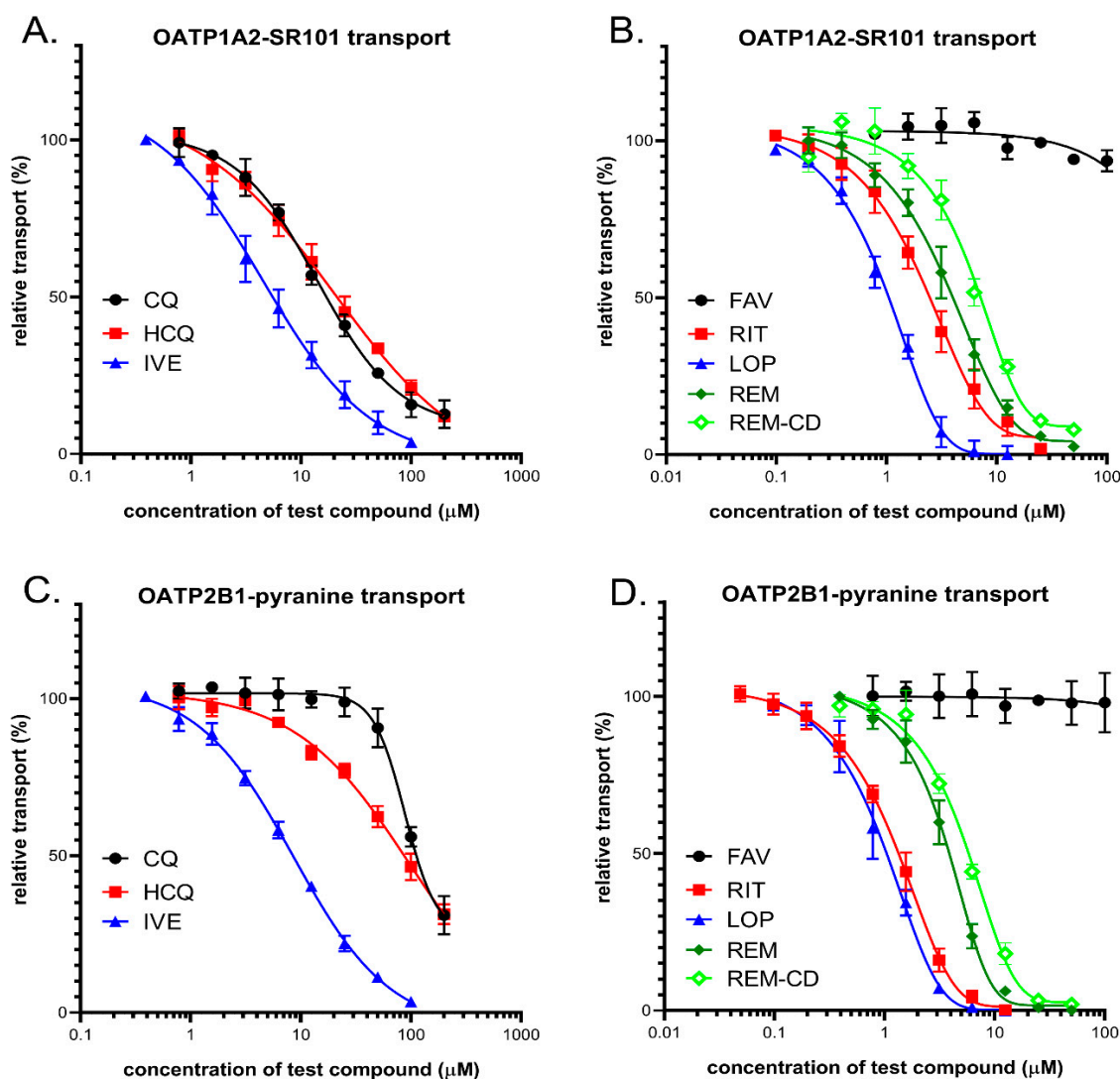


Figure 5. (A,B) Inhibition of OATP1A2-mediated sulforhodamine101 (SR101) uptake by potential antiviral compounds. Uptake of 0.5 μM SR101 was measured in A431-OATP1A2 cells seeded on 96-well plates for 10 min in the presence of increasing concentrations of ivermectin (IVE), chloroquine (CQ), hydroxychloroquine (HCQ), favipiravir (FAV), lopinavir (LOP), ritonavir (RIT), remdesivir (REM), and SEBCD-remdesivir. (C,D) Inhibition of OATP2B1-mediated pyranine uptake by different antiviral compounds. Uptake of 20 μM pyranine was measured in A431-OATP2B1 cells for 15 min in increasing concentrations of the tested compounds. In all cases, averages were obtained based on at least three biological replicates. \pm SD values are shown.

Table 2. Summary of the transporter inhibition properties of the drugs examined. Approximate IC_{50} (μM) values were determined by nonlinear regression analysis of the data shown in the results section, using GraphPad prism software (version 5.01, GraphPad, La Jolla, CA, USA).

Potential anti-COVID-19 compounds	Estimated Transporter Inhibition— IC_{50} (μM)						OATP Cellular Assays	
	ABCB1		ABCC1		ABCG2		OATP1A2	OATP2B1
	cellular assay	vesicular assay	cellular assay	vesicular assay	cellular assay	vesicular assay		
chloroquine	-	-	-	-	-	-	17.0	119
hydroxychloroquine	-	-	-	-	-	-	18.9	84
ivermectin	0.6	0.3	3.3	13.3	3.1	1.1	5.2	8.6
lopinavir	6.3	0.6	10.7	10	13.1	4.2	1.5	1.0

Table 2. Cont.

	Estimated Transporter Inhibition—IC ₅₀ (μM)						OATP Cellular Assays	
	ABCB1		ABCC1		ABCG2			
ritonavir	8.4	0.3	7.7	-	8.3	7.5	2.3	1.4
remdesivir	-	>20	-	*	>50	>50	3.8	3.8
remdesivir-SBECD	-	>20	-	NA	>50	>50	6.1	5.6
favipiravir	-	-	-	-	-	-	-	-

* Stimulation of substrate transport.

4. Discussion

Multispecific drug and xenobiotic transporters play a major role in the pharmacokinetics of numerous pharmacological agents, and any new drug candidates have to be tested for interactions with the key transporters in this regard [66,67]. However, several drugs rapidly repurposed in the past months for potential anti-COVID-19 activity may not have been analyzed in detail for these interactions. This lack of information is making their clinical use, especially in combination with other pharmacological agents, potentially dangerous for patients. Since SARS-CoV-2 virus infection causes severe clinical symptoms, especially in elderly patients and/or in those with existing co-morbidities, the ADME-Tox properties and the potentially harmful drug–drug interactions of the repurposed drugs may have major relevance in these cases. In addition, there are no current methods for correctly estimating the transporter–drug interactions by *in silico* approaches, and only detailed *in vitro* studies may answer these questions. Therefore, in the present study, we examined the interactions of the repurposed drug candidates with the key multispecific drug transporters, with the hope that our results help clinical applications in COVID-19 treatment. We have used a wide range of assay systems and transported substrates to provide comparative aspects for the transporter–drug interactions.

ABC transporters play a key role in the pharmacokinetics of numerous pharmacological agents, and they—especially ABCB1 and ABCG2—should be tested in early phases of drug development [66]. As shown in the results section and in the summary in Table 2, regarding the three ABC multispecific transporters examined, we found that chloroquine, hydroxychloroquine, and favipiravir displayed practically no potentially relevant interaction with any of these transporters. In contrast, ivermectin was found to exert a strong inhibitory effect in the case of the ABCB1, ABCC1, and ABCG2 transporter. Some of these interactions have already been explored; in particular, ivermectin inhibition of the human and animal Mdr1/Pgp/ABCB1 has been studied in detail [8,9,68]. As we show here, in all kinds of assays, a strong inhibition of both ABCC1 and ABCG2 transport activity was also observed by ivermectin, emphasizing the potentially dangerous effects of this compound at higher doses or with an impaired transporter function. The antiviral protease inhibitors lopinavir and ritonavir had a significant inhibitory effect on the three ABC transporters examined here, and a strong inhibition was observed for ABCB1/Pgp (Table 2). However, ABCC1 and ABCG2 were also inhibited by these compounds in potentially relevant concentrations. As suggested by the relevant FDA information (https://www.accessdata.fda.gov/drugsatfda_docs/label/2007/021226s018lbl.pdf, https://www.ema.europa.eu/en/documents/scientific-discussion/kalettra-epar-scientific-discussion_en.pdf), lopinavir in patients may reach plasma concentrations of about 13 μM, while ritonavir may peak at about 1 μM. Therefore, our *in vitro* data indicate that drug–drug interactions should be considered. Remdesivir was found to be a relatively weak inhibitor of all three ABC transporters, although the ABCB1/Pgp inhibition with an IC₅₀ of about 20 μM, which was observed in the vesicular transport assay, may be relevant under certain treatment conditions (reported peak plasma concentrations of remdesivir of about 5 μM). Interestingly, remdesivir significantly stimulated the vesicular transport of a test substrate ETGB by the ABCC1 transporter, so an allosteric effect of remdesivir on this transporter should be considered.

The experiments performed in intact cells expressing the polymorphic ABCG2 transporter variant Q141K, with impaired membrane localization and transport activity, suggest that, with lower transporter functions, some of the weak inhibitors may have a clinically important effect. In this case, both lopinavir and ritonavir exerted significantly stronger inhibition of this drug transporter variant. Considering that the allele encoding the ABCG2-Q141K variant (rs2231142) has an incidence of about 30% in the Asian population, this information is especially important for clinical interventions in these countries. In our studies, we also examined the membrane ATPase activity of the ABCB1 and ABCG2 transporters in isolated membranes. These assays may help to decipher the substrate vs. inhibitor nature of the test compounds. Although these results only provide a tentative answer in this regard, we found that the ABCB1-ATPase activity is significantly stimulated by low concentrations of lopinavir, ritonavir, and remdesivir, indicating that these drugs may be transported substrates. We observed no such stimulation in the case of the ABCG2 transporter in terms of these drugs. In addition to the ABC multidrug transporters, the role of drug-transporting OATPs in pharmacokinetics and drug–drug or food–drug interactions is increasingly being recognized [66]. While OATPs 1B1 and 1B3 are liver-specific proteins, OATP1A2 and OATP2B1 are highly expressed in the endothelial cells of the BBB. Therefore, these transporters are key modulators of the entry of their drug substrates into the central nervous system [41,69,70]. In addition, OATP2B1 also influences the absorption of its substrates from the intestine [40]. In the current study, we investigated the interactions between OATP1A2 and OATP2B1 and drugs repurposed to treat COVID-19 disease. We found high-affinity interactions between the antiviral protease inhibitors lopinavir and ritonavir with both OATP1A2 and OATP2B1. These interactions have already been documented [71–74]. Moreover, lopinavir and ritonavir are also inhibitors of OATP1B1 and OATP1B3, which are the key transporters in the liver [71]. The IC₅₀ values obtained in our study are in harmony with those observed by Tupova et al. [72] and Kis et al. [73]. Moreover, a previous study [74] showed that lopinavir is transported by OATP1A2, so OATP1A2 probably affects lopinavir absorption and blood to brain entry. Ivermectin, as reported previously [75], also inhibited OATP2B1, although in our experiments, with a higher affinity than that found by Karlgren et al. (20 μM, 39%—this may be explained by the different test substrates used). However, here, we document, for the first time, that ivermectin inhibits OATP1A2 function. Our experiments confirmed the relatively weak interactions between chloroquine and hydroxychloroquine with OATP1A2 and OATP2B1, and the observed IC₅₀ values are in harmony with those found by others [76,77]. We observed no interaction of favipiravir with the two OATPs examined here. There are no data available for the interaction of remdesivir—currently a major anti-COVID-19 drug candidate—with OATP1A2 and OATP2B1. Based on our data, showing a high-affinity interaction of remdesivir with both transporters, and the relatively high plasma concentrations of this drug (peak values in 3–5 μM [78,79]), remdesivir may significantly interfere with the pharmacokinetics of drug substrates of OATP1A2 and OATP2B1. Our current methods do not distinguish between transported and non-transported inhibitors, so further investigations are needed to decipher whether OATP1A2 and OATP2B1 can mediate the uptake of remdesivir. From the currently developed anti-COVID-19 drugs tested in our study, favipiravir is the most promising candidate for avoiding unexpected drug–drug interactions. Favipiravir, similar to what was found for the multispecific ABC transporters located in the tissue barriers (see above), did not inhibit the function of the investigated OATPs. Therefore, this compound is not expected to influence OATP-mediated drug pharmacokinetics. As a summary, our current data, summarized in Table 2, provide a detailed in vitro quantitative analysis on the interaction of the anti-COVID-19 agents with the key human multispecific drug transporters. These in vitro assays, which should be followed by careful clinical pharmacokinetic studies, may provide a strong warning against the compassionate use of some of these agents, especially when other relevant drugs are also applied to the patient, or in cases of endogenously impaired transporter activity.

Author Contributions: Á.T., C.Ö.-L., and B.S. wrote the draft, and C.A., O.M., E.S., É.B., Á.T., and G.V. performed the experiments and critically revised the manuscript. All authors have read and agreed to the published version of the manuscript.

Funding: This work has been supported by research grants from the National Research, Development and Innovation Office (OTKA, grant numbers FK 128751 (C.-Ö.L.), K-128011 (G.V.), KFI_16-1-2017-0232 (Á.T.), FIEK 16-1-2016-0005, and VEKOP-2.1.1-15-2016-00117 (B.S.)). O.M. was supported by the KDP doctoral scholarship from the Ministry for Innovation and Technology (National Research, Development and Innovation Fund).

Institutional Review Board Statement: Not applicable.

Informed Consent Statement: Not applicable.

Data Availability Statement: The data presented in this study are available on request from the corresponding author at the Researchgate website (https://www.researchgate.net/profile/Csilla_Ozvegy-Laczka, or https://www.researchgate.net/publication/347138768_Interactions_of_anti-COVID-19_drug_candidates_with_multispecific_ABC_and_OATP_drug_transporters). The data are not publicly available due to a company participation.

Acknowledgments: The 5D3 antibody was a kind gift from B. Sorrentino, St. Jude Children Hospital, Memphis, USA, and remdesivir and remdesivir-SBECED were kind gifts from Lajos Szente, Cyclolab Ltd., Budapest, Hungary.

Conflicts of Interest: The authors declare no conflict of interest. The funders had no role in the design of the study; in the collection, analyses, or interpretation of data; in the writing of the manuscript, or in the decision to publish the results.

References

1. Savarino, A.; Boelaert, J.R.; Cassone, A.; Majori, G.; Cauda, R. Effects of chloroquine on viral infections: An old drug against today's diseases? *Lancet Infect. Dis.* **2003**, *3*, 722–727. [[CrossRef](#)]
2. Singh, H.; Chauhan, P.; Kakkar, A.K. Hydroxychloroquine for the treatment and prophylaxis of COVID-19: The journey so far and the road ahead. *Eur. J. Pharmacol.* **2020**, 173717. [[CrossRef](#)] [[PubMed](#)]
3. Vincent, M.J.; Bergeron, E.; Benjannet, S.; Erickson, B.R.; Rollin, P.E.; Ksiazek, T.G.; Seidah, N.G.; Nichol, S.T. Chloroquine is a potent inhibitor of SARS coronavirus infection and spread. *Virology* **2005**, *2*, 69. [[CrossRef](#)] [[PubMed](#)]
4. Liu, J.; Cao, R.; Xu, M.; Wang, X.; Zhang, H.; Hu, H.; Li, Y.; Hu, Z.; Zhong, W.; Wang, M. Hydroxychloroquine, a less toxic derivative of chloroquine, is effective in inhibiting SARS-CoV-2 infection in vitro. *Cell Discov.* **2020**, *6*, 16. [[CrossRef](#)] [[PubMed](#)]
5. Wang, M.; Cao, R.; Zhang, L.; Yang, X.; Liu, J.; Xu, M.; Shi, Z.; Hu, Z.; Zhong, W.; Xiao, G. Remdesivir and chloroquine effectively inhibit the recently emerged novel coronavirus (2019-nCoV) in vitro. *Cell Res.* **2020**, *30*, 269–271. [[CrossRef](#)] [[PubMed](#)]
6. Simpson, T.F.; Kovacs, R.J.; Stecker, E.C. *Cardiology Magazine*. Available online: <https://www.acc.org/latest-in-cardiology/article/s/2020/03/27/14/00/ventricular-arrhythmia-risk-due-to-hydroxychloroquine-azithromycin-treatment-for-covid-19> (accessed on 20 November 2020).
7. Roden, D.M.; Harrington, R.A.; Poppas, A.; Russo, A.M. Considerations for Drug Interactions on QTc in Exploratory COVID-19 Treatment. *Circulation* **2020**, *141*, e906–e907. [[CrossRef](#)] [[PubMed](#)]
8. Schinkel, A.H.; Smit, J.J.; van Tellingen, O.; Beijnen, J.H.; Wagenaar, E.; van Deemter, L.; Mol, C.A.; van der Valk, M.A.; Robanus-Maandag, E.C.; te Riele, H.P. Disruption of the mouse *mdr1a* P-glycoprotein gene leads to a deficiency in the blood-brain barrier and to increased sensitivity to drugs. *Cell* **1994**, *77*, 491–502. [[CrossRef](#)]
9. Mealey, K.L.; Bentjen, S.A.; Gay, J.M.; Cantor, G.H. Ivermectin sensitivity in collies is associated with a deletion mutation of the *mdr1* gene. *Pharmacogenetics* **2001**, *11*, 727–733. [[CrossRef](#)]
10. Lespine, A.; Dupuy, J.; Orłowski, S.; Nagy, T.; Glavinas, H.; Krajcsi, P.; Alvinerie, M. Interaction of ivermectin with multidrug resistance proteins (MRP1, 2 and 3). *Chem. Biol. Interact.* **2006**, *159*, 169–179. [[CrossRef](#)]
11. Pouliot, J.F.; L'Heureux, F.; Liu, Z.; Prichard, R.K.; Georges, E. Reversal of P-glycoprotein-associated multidrug resistance by ivermectin. *Biochem. Pharmacol.* **1997**, *53*, 17–25. [[CrossRef](#)]
12. Didier, A.; Loor, F. The abamectin derivative ivermectin is a potent P-glycoprotein inhibitor. *Anticancer. Drugs* **1996**, *7*, 745–751. [[CrossRef](#)] [[PubMed](#)]
13. Wagstaff, K.; Sivakumaran, H.; Heaton, S.; Harrich, D.; Jans, D. Ivermectin is a specific inhibitor of importin α /beta-mediated nuclear import able to inhibit replication of HIV-1 and Dengue virus. *Biochem. J.* **2012**, *443*, 851–856. [[CrossRef](#)] [[PubMed](#)]
14. Lundberg, L.; Pinkham, C.; Baer, A.; Amaya, M.; Narayanan, A.; Wagstaff, K.M.; Jans, D.A.; Kehn-Hall, K. Nuclear import and export inhibitors alter capsid protein distribution in mammalian cells and reduce Venezuelan Equine Encephalitis Virus replication. *Antivir. Res.* **2013**, *100*, 662–672. [[CrossRef](#)] [[PubMed](#)]
15. Yang, S.N.Y.; Atkinson, S.C.; Wang, C.; Lee, A.; Bogoyevitch, M.A.; Borg, N.A.; Jans, D.A. The broad spectrum antiviral ivermectin targets the host nuclear transport importin α / β 1 heterodimer. *Antivir. Res.* **2020**, *177*, 104760. [[CrossRef](#)]

16. Bray, M.; Rayner, C.; Noël, F.; Jans, D.; Wagstaff, K. Ivermectin and COVID-19: A report in Antiviral Research, widespread interest, an FDA warning, two letters to the editor and the authors' responses. *Antivir. Res.* **2020**, *178*, 104805. [[CrossRef](#)]
17. Caly, L.; Druce, J.D.; Catton, M.G.; Jans, D.A.; Wagstaff, K.M. The FDA-approved drug ivermectin inhibits the replication of SARS-CoV-2 in vitro. *Antivir. Res.* **2020**, *178*, 104787. [[CrossRef](#)]
18. Chaccour, C.; Hammann, F.; Ramón-García, S.; Rabinovich, N.R. Ivermectin and COVID-19: Keeping Rigor in Times of Urgency. *Am. J. Trop. Med. Hyg.* **2020**, *102*, 1156–1157. [[CrossRef](#)]
19. Uzunova, K.; Filipova, E.; Pavlova, V.; Vekov, T. Insights into antiviral mechanisms of remdesivir, lopinavir/ritonavir and chloroquine/hydroxychloroquine affecting the new SARS-CoV-2. *Biomed. Pharmacother.* **2020**, *131*, 110668. [[CrossRef](#)]
20. Arshad, U.; Pertinez, H.; Box, H.; Tatham, L.; Rajoli, R.K.R.; Curley, P.; Neary, M.; Sharp, J.; Liptrott, N.J.; Valentijn, A.; et al. Prioritization of Anti-SARS-Cov-2 Drug Repurposing Opportunities Based on Plasma and Target Site Concentrations Derived from their Established Human Pharmacokinetics. *Clin. Pharmacol. Ther.* **2020**, *108*, 775–790. [[CrossRef](#)]
21. Weiss, J.; Rose, J.; Storch, C.H.; Ketabi-Kiyanvash, N.; Sauer, A.; Haefeli, W.E.; Efferth, T. Modulation of human BCRP (ABCG2) activity by anti-HIV drugs. *J. Antimicrob. Chemother.* **2007**, *59*, 238–245. [[CrossRef](#)]
22. Martinec, O.; Huliciak, M.; Staud, F.; Cecka, F.; Vokral, I.; Cervený, L. Anti-HIV and Anti-Hepatitis C Virus Drugs Inhibit P-Glycoprotein Efflux Activity in Caco-2 Cells and Precision-Cut Rat and Human Intestinal Slices. *Antimicrob. Agents Chemother.* **2019**, *63*. [[CrossRef](#)] [[PubMed](#)]
23. Corona, G.; Vaccher, E.; Sandron, S.; Sartor, I.; Tirelli, U.; Innocenti, F.; Toffoli, G. Lopinavir-ritonavir dramatically affects the pharmacokinetics of irinotecan in HIV patients with Kaposi's sarcoma. *Clin. Pharmacol. Ther.* **2008**, *83*, 601–606. [[CrossRef](#)] [[PubMed](#)]
24. Agarwal, S.; Pal, D.; Mitra, A.K. Both P-gp and MRP2 mediate transport of Lopinavir, a protease inhibitor. *Int. J. Pharm.* **2007**, *339*, 139–147. [[CrossRef](#)] [[PubMed](#)]
25. Janneh, O.; Jones, E.; Chandler, B.; Owen, A.; Khoo, S.H. Inhibition of P-glycoprotein and multidrug resistance-associated proteins modulates the intracellular concentration of lopinavir in cultured CD4 T cells and primary human lymphocytes. *J. Antimicrob. Chemother.* **2007**, *60*, 987–993. [[CrossRef](#)] [[PubMed](#)]
26. Gupta, A.; Zhang, Y.; Unadkat, J.D.; Mao, Q. HIV protease inhibitors are inhibitors but not substrates of the human breast cancer resistance protein (BCRP/ABCG2). *J. Pharmacol. Exp. Ther.* **2004**, *310*, 334–341. [[CrossRef](#)] [[PubMed](#)]
27. Bierman, W.F.W.; Scheffer, G.L.; Schoonderwoerd, A.; Jansen, G.; van Agtmael, M.A.; Danner, S.A.; Scheper, R.J. Protease inhibitors atazanavir, lopinavir and ritonavir are potent blockers, but poor substrates, of ABC transporters in a broad panel of ABC transporter-overexpressing cell lines. *J. Antimicrob. Chemother.* **2010**, *65*, 1672–1680. [[CrossRef](#)] [[PubMed](#)]
28. Yoon, J.-J.; Toots, M.; Lee, S.; Lee, M.-E.; Ludeke, B.; Luczo, J.M.; Ganti, K.; Cox, R.M.; Sticher, Z.M.; Edpuganti, V.; et al. Orally Efficacious Broad-Spectrum Ribonucleoside Analog Inhibitor of Influenza and Respiratory Syncytial Viruses. *Antimicrob. Agents Chemother.* **2018**, *62*. [[CrossRef](#)]
29. Furuta, Y.; Komeno, T.; Nakamura, T. Favipiravir (T-705), a broad spectrum inhibitor of viral RNA polymerase. *Proc. Jpn. Acad. Ser. B Phys. Biol. Sci.* **2017**, *93*, 449–463. [[CrossRef](#)]
30. Yang, K. What Do We Know About Remdesivir Drug Interactions? *Clin. Transl. Sci.* **2020**, *13*, 842–844. [[CrossRef](#)]
31. Szakács, G.; Váradi, A.; Ozvegy-Laczka, C.; Sarkadi, B. The role of ABC transporters in drug absorption, distribution, metabolism, excretion and toxicity (ADME-Tox). *Drug Discov. Today* **2008**, *13*, 379–393. [[CrossRef](#)]
32. Takada, T.; Ichida, K.; Matsuo, H.; Nakayama, A.; Murakami, K.; Yamanashi, Y.; Kasuga, H.; Shinomiya, N.; Suzuki, H. ABCG2 dysfunction increases serum uric acid by decreased intestinal urate excretion. *Nucleosides Nucleotides Nucleic Acids* **2014**, *33*, 275–281. [[CrossRef](#)] [[PubMed](#)]
33. Sarkadi, B.; Homolya, L.; Szakács, G.; Váradi, A. Human Multidrug Resistance ABCB and ABCG Transporters: Participation in a Chemoimmunity Defense System. *Physiol. Rev.* **2006**, *1179*–1236. [[CrossRef](#)] [[PubMed](#)]
34. Dauchy, S.; Dutheil, F.; Weaver, R.J.; Chassoux, F.; Daumas-Duport, C.; Couraud, P.-O.; Scherrmann, J.-M.; De Waziers, I.; Declèves, X. ABC transporters, cytochromes P450 and their main transcription factors: Expression at the human blood-brain barrier. *J. Neurochem.* **2008**, *107*, 1518–1528. [[CrossRef](#)] [[PubMed](#)]
35. Kamiie, J.; Ohtsuki, S.; Iwase, R.; Ohmine, K.; Katsukura, Y.; Yanai, K.; Sekine, Y.; Uchida, Y.; Ito, S.; Terasaki, T. Quantitative atlas of membrane transporter proteins: Development and application of a highly sensitive simultaneous LC/MS/MS method combined with novel in-silico peptide selection criteria. *Pharm. Res.* **2008**, *25*, 1469–1483. [[CrossRef](#)] [[PubMed](#)]
36. Uchida, Y.; Ohtsuki, S.; Katsukura, Y.; Ikeda, C.; Suzuki, T.; Kamiie, J.; Terasaki, T. Quantitative targeted absolute proteomics of human blood-brain barrier transporters and receptors. *J. Neurochem.* **2011**, *117*, 333–345. [[CrossRef](#)] [[PubMed](#)]
37. Daood, M.; Tsai, C.; Ahdab-Barmada, M.; Watchko, J.F. ABC transporter (P-gp/ABCB1, MRP1/ABCC1, BCRP/ABCG2) expression in the developing human CNS. *Neuropediatrics* **2008**, *39*, 211–218. [[CrossRef](#)]
38. Hagenbuch, B.; Gui, C. Xenobiotic transporters of the human organic anion transporting polypeptides (OATP) family. *Xenobiotica* **2008**, *38*, 778–801. [[CrossRef](#)]
39. Hagenbuch, B.; Stieger, B. The SLCO (former SLC21) superfamily of transporters. *Mol. Asp. Med.* **2013**, *34*, 396–412. [[CrossRef](#)]
40. Shitara, Y.; Maeda, K.; Ikejiri, K.; Yoshida, K.; Horie, T.; Sugiyama, Y. Clinical significance of organic anion transporting polypeptides (OATPs) in drug disposition: Their roles in hepatic clearance and intestinal absorption. *Biopharm. Drug Dispos.* **2013**, *34*, 45–78. [[CrossRef](#)]

41. Urquhart, B.L.; Kim, R.B. Blood-brain barrier transporters and response to CNS-active drugs. *Eur. J. Clin. Pharmacol.* **2009**, *65*, 1063–1070. [[CrossRef](#)]
42. Yu, J.; Zhou, Z.; Tay-Sontheimer, J.; Levy, R.H.; Ragueneau-Majlessi, I. Intestinal Drug Interactions Mediated by OATPs: A Systematic Review of Preclinical and Clinical Findings. *J. Pharm. Sci.* **2017**, *106*, 2312–2325. [[CrossRef](#)] [[PubMed](#)]
43. Kovacsics, D.; Patik, I.; Özvegy-Laczka, C. The role of organic anion transporting polypeptides in drug absorption, distribution, excretion and drug-drug interactions. *Expert Opin. Drug Metab. Toxicol.* **2017**, *13*, 409–424. [[CrossRef](#)] [[PubMed](#)]
44. Szabó, E.; Türk, D.; Telbisz, Á.; Kucsma, N.; Horváth, T.; Szakács, G.; Homolya, L.; Sarkadi, B.; Várady, G. A new fluorescent dye accumulation assay for parallel measurements of the ABCG2, ABCB1 and ABCC1 multidrug transporter functions. *PLoS ONE* **2018**, *13*, e0190629. [[CrossRef](#)] [[PubMed](#)]
45. Zámbo, B.; Móznér, O.; Bartos, Z.; Török, G.; Várady, G.; Telbisz, Á.; Homolya, L.; Orbán, T.I.; Sarkadi, B. Cellular expression and function of naturally occurring variants of the human ABCG2 multidrug transporter. *Cell. Mol. Life Sci.* **2020**, *77*, 365–378. [[CrossRef](#)] [[PubMed](#)]
46. Sarkadi, B.; Bauzon, D.; Huckle, W.R.; Earp, H.S.; Berry, A.; Suchindran, H.; Price, E.M.; Olson, J.C.; Boucher, R.C.; Scarborough, G.A. Biochemical characterization of the cystic fibrosis transmembrane conductance regulator in normal and cystic fibrosis epithelial cells. *J. Biol. Chem.* **1992**, *267*, 2087–2095. [[CrossRef](#)]
47. Patik, I.; Székely, V.; Német, O.; Szepesi, Á.; Kucsma, N.; Várady, G.; Szakács, G.; Bakos, É.; Özvegy-Laczka, C. Identification of novel cell-impermeant fluorescent substrates for testing the function and drug interaction of Organic Anion-Transporting Polypeptides, OATP1B1/1B3 and 2B1. *Sci. Rep.* **2018**, *8*, 2630. [[CrossRef](#)] [[PubMed](#)]
48. Ozvegy, C.; Litman, T.; Szakács, G.; Nagy, Z.; Bates, S.; Váradi, A.; Sarkadi, B. Functional characterization of the human multidrug transporter, ABCG2, expressed in insect cells. *Biochem. Biophys. Res. Commun.* **2001**, *285*, 111–117. [[CrossRef](#)]
49. Telbisz, A.; Müller, M.; Ozvegy-Laczka, C.; Homolya, L.; Szenté, L.; Váradi, A.; Sarkadi, B. Membrane cholesterol selectively modulates the activity of the human ABCG2 multidrug transporter. *Biochim. Biophys. Acta* **2007**, *1768*, 2698–2713. [[CrossRef](#)]
50. Ozvegy, C.; Váradi, A.; Sarkadi, B. Characterization of drug transport, ATP hydrolysis, and nucleotide trapping by the human ABCG2 multidrug transporter. Modulation of substrate specificity by a point mutation. *J. Biol. Chem.* **2002**, *277*, 47980–47990. [[CrossRef](#)]
51. Bakos, É.; Német, O.; Patik, I.; Kucsma, N.; Várady, G.; Szakács, G.; Özvegy-Laczka, C. A novel fluorescence-based functional assay for human OATP1A2 and OATP1C1 identifies interaction between third-generation P-gp inhibitors and OATP1A2. *FEBS J.* **2020**, *287*, 2468–2485. [[CrossRef](#)]
52. Székely, V.; Patik, I.; Ungvári, O.; Telbisz, Á.; Szakács, G.; Bakos, É.; Özvegy-Laczka, C. Fluorescent probes for the dual investigation of MRP2 and OATP1B1 function and drug interactions. *Eur. J. Pharm. Sci. Off. J. Eur. Fed. Pharm. Sci.* **2020**, *151*, 105395. [[CrossRef](#)] [[PubMed](#)]
53. Homolya, L.; Holló, Z.; Müller, M.; Mechetner, E.B.; Sarkadi, B. A new method for quantitative assessment of P-glycoprotein-related multidrug resistance in tumour cells. *Br. J. Cancer* **1996**, *73*, 849–855. [[CrossRef](#)] [[PubMed](#)]
54. Hooiveld, G.J.E.J.; Heegsma, J.; van Montfoort, J.E.; Jansen, P.L.M.; Meijer, D.K.F.; Müller, M. Stereoselective transport of hydrophilic quaternary drugs by human MDR1 and rat Mdr1b P-glycoproteins. *Br. J. Pharmacol.* **2002**, *135*, 1685–1694. [[CrossRef](#)] [[PubMed](#)]
55. Herédi-Szabó, K.; Palm, J.E.; Andersson, T.B.; Pál, Á.; Méhn, D.; Fekete, Z.; Beéry, E.; Jakab, K.T.; Jani, M.; Krajcsi, P. A P-gp vesicular transport inhibition assay—optimization and validation for drug-drug interaction testing. *Eur. J. Pharm. Sci. Off. J. Eur. Fed. Pharm. Sci.* **2013**, *49*, 773–781. [[CrossRef](#)] [[PubMed](#)]
56. Holló, Z.; Homolya, L.; Hegedűs, T.; Müller, M.; Szakács, G.; Jakab, K.; Antal, F.; Sarkadi, B. Parallel functional and immunological detection of human multidrug resistance proteins, P-glycoprotein and MRP1. *Anticancer Res.* **1998**, *18*, 2981–2987. [[PubMed](#)]
57. Slot, A.J.; Wise, D.D.; Deeley, R.G.; Monks, T.J.; Cole, S.P.C. Modulation of human multidrug resistance protein (MRP) 1 (ABCC1) and MRP2 (ABCC2) transport activities by endogenous and exogenous glutathione-conjugated catechol metabolites. *Drug Metab. Dispos.* **2008**, *36*, 552–560. [[CrossRef](#)] [[PubMed](#)]
58. Strouse, J.J.; Ivnitski-Steele, I.; Waller, A.; Young, S.M.; Perez, D.; Evangelisti, A.M.; Ursu, O.; Bologna, C.G.; Carter, M.B.; Salas, V.M.; et al. Fluorescent substrates for flow cytometric evaluation of efflux inhibition in ABCB1, ABCC1, and ABCG2 transporters. *Anal. Biochem.* **2013**, *437*, 77–87. [[CrossRef](#)]
59. Telford, W.G.; Bradford, J.; Godfrey, W.; Robey, R.W.; Bates, S.E. Side population analysis using a violet-excited cell-permeable DNA binding dye. *Stem Cells* **2007**, *25*, 1029–1036. [[CrossRef](#)]
60. Boesch, M.; Reimer, D.; Rumpold, H.; Zeimet, A.G.; Sopper, S.; Wolf, D. DyeCycle Violet used for side population detection is a substrate of P-glycoprotein. *Cytom. A* **2012**, *81*, 517–522. [[CrossRef](#)]
61. Nerada, Z.; Hegyi, Z.; Szepesi, Á.; Tóth, S.; Hegedűs, C.; Várady, G.; Matula, Z.; Homolya, L.; Sarkadi, B.; Telbisz, Á. Application of fluorescent dye substrates for functional characterization of ABC multidrug transporters at a single cell level. *Cytom. A* **2016**, *89*, 826–834. [[CrossRef](#)]
62. Zong, Y.; Zhou, S.; Fatima, S.; Sorrentino, B.P. Expression of mouse *Abcg2* mRNA during hematopoiesis is regulated by alternative use of multiple leader exons and promoters. *J. Biol. Chem.* **2006**, *281*, 29625–29632. [[CrossRef](#)] [[PubMed](#)]
63. Zhou, S.; Schuetz, J.D.; Bunting, K.D.; Colapietro, A.M.; Sampath, J.; Morris, J.J.; Lagutina, I.; Grosveld, G.C.; Osawa, M.; Nakauchi, H.; et al. The ABC transporter *Bcrp1/ABCG2* is expressed in a wide variety of stem cells and is a molecular determinant of the side-population phenotype. *Nat. Med.* **2001**, *7*, 1028–1034. [[CrossRef](#)] [[PubMed](#)]

64. Sjöstedt, N.; van den Heuvel, J.J.M.W.; Koenderink, J.B.; Kidron, H. Transmembrane Domain Single-Nucleotide Polymorphisms Impair Expression and Transport Activity of ABC Transporter ABCG2. *Pharm. Res.* **2017**, *34*, 1626–1636. [[CrossRef](#)] [[PubMed](#)]
65. Móznér, O.; Bartos, Z.; Zámbo, B.; Homolya, L.; Hegedűs, T.; Sarkadi, B. Cellular Processing of the ABCG2 Transporter-Potential Effects on Gout and Drug Metabolism. *Cells* **2019**, *8*, 1215. [[CrossRef](#)] [[PubMed](#)]
66. Giacomini, K.M.; Balimane, P.V.; Cho, S.K.; Eadon, M.; Edeki, T.; Hillgren, K.M.; Huang, S.-M.; Sugiyama, Y.; Weitz, D.; Wen, Y.; et al. International Transporter Consortium commentary on clinically important transporter polymorphisms. *Clin. Pharmacol. Ther.* **2013**, *94*, 23–26. [[CrossRef](#)]
67. Huang, S.-M.; Zhang, L.; Giacomini, K.M. The International Transporter Consortium: A collaborative group of scientists from academia, industry, and the FDA. *Clin. Pharmacol. Ther.* **2010**, *87*, 32–36. [[CrossRef](#)] [[PubMed](#)]
68. Geyer, J.; Gavrilova, O.; Petzinger, E. Brain penetration of ivermectin and selamectin in *mdr1a,b* P-glycoprotein- and *bcrp*-deficient knockout mice. *J. Vet. Pharmacol. Ther.* **2009**, *32*, 87–96. [[CrossRef](#)]
69. Gao, B.; Hagenbuch, B.; Kullak-Ublick, G.A.; Benke, D.; Aguzzi, A.; Meier, P.J. Organic anion-transporting polypeptides mediate transport of opioid peptides across blood-brain barrier. *J. Pharmacol. Exp. Ther.* **2000**, *294*, 73–79.
70. Billington, S.; Salphati, L.; Hop, C.E.C.A.; Chu, X.; Evers, R.; Burdette, D.; Rowbottom, C.; Lai, Y.; Xiao, G.; Humphreys, W.G.; et al. Interindividual and Regional Variability in Drug Transporter Abundance at the Human Blood-Brain Barrier Measured by Quantitative Targeted Proteomics. *Clin. Pharmacol. Ther.* **2019**, *106*, 228–237. [[CrossRef](#)]
71. Annaert, P.; Ye, Z.W.; Stieger, B.; Augustijns, P. Interaction of HIV protease inhibitors with OATP1B1, 1B3, and 2B1. *Xenobiotica* **2010**, *40*, 163–176. [[CrossRef](#)]
72. Tupova, L.; Hirschmugl, B.; Sucha, S.; Pilarova, V.; Székely, V.; Bakos, É.; Novakova, L.; Özvegy-Laczka, C.; Wadsack, C.; Ceckova, M. Interplay of drug transporters P-glycoprotein (MDR1), MRP1, OATP1A2 and OATP1B3 in passage of maraviroc across human placenta. *Biomed. Pharmacother.* **2020**, *129*, 110506. [[CrossRef](#)] [[PubMed](#)]
73. Kis, O.; Zastre, J.A.; Ramaswamy, M.; Bendayan, R. pH dependence of organic anion-transporting polypeptide 2B1 in Caco-2 cells: Potential role in antiretroviral drug oral bioavailability and drug-drug interactions. *J. Pharmacol. Exp. Ther.* **2010**, *334*, 1009–1022. [[CrossRef](#)] [[PubMed](#)]
74. Hartkoorn, R.C.; Kwan, W.S.; Shallcross, V.; Chaikan, A.; Liptrott, N.; Egan, D.; Sora, E.S.; James, C.E.; Gibbons, S.; Bray, P.G.; et al. HIV protease inhibitors are substrates for OATP1A2, OATP1B1 and OATP1B3 and lopinavir plasma concentrations are influenced by SLCO1B1 polymorphisms. *Pharmacogenet. Genom.* **2010**, *20*, 112–120. [[CrossRef](#)] [[PubMed](#)]
75. Karlgren, M.; Vildhede, A.; Norinder, U.; Wisniewski, J.R.; Kimoto, E.; Lai, Y.; Haglund, U.; Artursson, P. Classification of inhibitors of hepatic organic anion transporting polypeptides (OATPs): Influence of protein expression on drug-drug interactions. *J. Med. Chem.* **2012**, *55*, 4740–4763. [[CrossRef](#)] [[PubMed](#)]
76. Hubeny, A.; Keiser, M.; Oswald, S.; Jedlitschky, G.; Kroemer, H.K.; Siegmund, W.; Grube, M. Expression of Organic Anion Transporting Polypeptide 1A2 in Red Blood Cells and Its Potential Impact on Antimalarial Therapy. *Drug Metab. Dispos.* **2016**, *44*, 1562–1568. [[CrossRef](#)]
77. Xu, C.; Zhu, L.; Chan, T.; Lu, X.; Shen, W.; Madigan, M.C.; Gillies, M.C.; Zhou, F. Chloroquine and Hydroxychloroquine Are Novel Inhibitors of Human Organic Anion Transporting Polypeptide 1A2. *J. Pharm. Sci.* **2016**, *105*, 884–890. [[CrossRef](#)]
78. Cao, Y.-C.; Deng, Q.-X.; Dai, S.-X. Remdesivir for severe acute respiratory syndrome coronavirus 2 causing COVID-19: An evaluation of the evidence. *Travel Med. Infect. Dis.* **2020**, *35*, 101647. [[CrossRef](#)]
79. Jorgensen, S.C.J.; Kebriaei, R.; Dresser, L.D. Remdesivir: Review of Pharmacology, Pre-clinical Data, and Emerging Clinical Experience for COVID-19. *Pharmacotherapy* **2020**, *40*, 659–671. [[CrossRef](#)]



The role of organic anion transporting polypeptides in drug absorption, distribution, excretion and drug-drug interactions

Daniella Kovacsics, Izabel Patik & Csilla Özvegy-Laczka

To cite this article: Daniella Kovacsics, Izabel Patik & Csilla Özvegy-Laczka (2017) The role of organic anion transporting polypeptides in drug absorption, distribution, excretion and drug-drug interactions, Expert Opinion on Drug Metabolism & Toxicology, 13:4, 409-424, DOI: [10.1080/17425255.2017.1253679](https://doi.org/10.1080/17425255.2017.1253679)

To link to this article: <https://doi.org/10.1080/17425255.2017.1253679>



Accepted author version posted online: 26 Oct 2016.
Published online: 09 Nov 2016.



Submit your article to this journal [↗](#)



Article views: 461



View Crossmark data [↗](#)



Citing articles: 8 View citing articles [↗](#)



REVIEW

The role of organic anion transporting polypeptides in drug absorption, distribution, excretion and drug-drug interactions

Daniella Kovacsics, Izabel Patik and Csilla Özvegy-Laczka

Membrane protein research group, Institute of Enzymology, Research Centre for Natural Sciences, Hungarian Academy of Sciences, Budapest, Hungary

ABSTRACT

Introduction: The *in vivo* fate and effectiveness of a drug depends highly on its absorption, distribution, metabolism, excretion and toxicity (ADME-Tox). Organic anion transporting polypeptides (OATPs) are membrane proteins involved in the cellular uptake of various organic compounds, including clinically used drugs. Since OATPs are significant players in drug absorption and distribution, modulation of OATP function via pharmacotherapy with OATP substrates/inhibitors, or modulation of their expression, affects drug pharmacokinetics. Given their cancer-specific expression, OATPs may also be considered anticancer drug targets.

Areas covered: We describe the human OATP family, discussing clinically relevant consequences of altered OATP function. We offer a critical analysis of published data on the role of OATPs in ADME and in drug–drug interactions, especially focusing on OATP1A2, 1B1, 1B3 and 2B1.

Expert opinion: Four members of the OATP family, 1A2, 1B1, 1B3 and 2B1, have been characterized in detail. As biochemical and pharmacological knowledge on the other OATPs is lacking, it seems timely to direct research efforts towards developing the experimental framework needed to investigate the transport mechanism and substrate specificity of the poorly described OATPs. In addition, elucidating the role of OATPs in tumor development and therapy response are critical avenues for further research.

ARTICLE HISTORYReceived 23 May 2016
Accepted 24 October 2016**KEYWORDS**

Drug–drug interaction; hepatic clearance; intestinal absorption; organic anion transporting polypeptides; pharmacokinetics; pharmacogenetics; ADME; GWAS

1. Introduction

According to a 2012 survey, one in four Americans over the age of 40 is taking statins [1]. Prescribed to reduce the risk of heart disease, statins lower the serum levels of low-density lipoproteins by inhibiting the activity of HMG-CoA reductase, the rate-limiting enzyme of cholesterol synthesis [2]. As is the case with every drug, the efficacy of the treatment largely depends on the fate of the statins in the body. Studies on large patient populations have found significant interindividual differences in the pharmacokinetics (PK) of statins, and suggested the relevance of drug–drug interactions (DDI). Since many statins are substrates of uptake transporters of the organic anion-transporting polypeptide (OATP) family, it is not surprising that coadministration of cholesterol-lowering drugs with other OATP substrates has been associated with serious side effects, including potentially fatal rhabdomyolysis [3,4]. Expressed in barrier tissues and detoxifying organs, OATPs transport a wide variety of endogenous and exogenous compounds into the cell. OATPs are members of the solute carrier superfamily (SLC), a large group of transporters that facilitate the cellular mobility of various compounds. Similar to the efflux pumps of the ATP-binding cassette (ABC) family, uptake transporters of the SLC superfamily are now recognized as major determinants of the absorption, distribution, excretion, and toxicity (ADME-Tox) properties of clinically important drugs (Figure 1) [5].

Acknowledging the importance of transporters to the PK of drugs, the International Transporter Consortium (ITS), the US Food and Drug Administration (FDA) and the European Medicines Agency (EMA) have recommended investigating the interaction of new molecular entities with several ABC (ABCB1, ABCG2) and SLC transporters (OATP1B1, OATP1B3, OCT2, OAT1, OAT3) [6–8].

The dramatic rise in the number of reviews on the role of OATPs in drug absorption, distribution, and DDIs is reflective of the increasing recognition of these transporters as determinants of PK. Compared to these reviews, we give an additional overview of other members of the OATP family that are potentially involved in ADME and DDI. We also provide a critical overview of the *in vitro* and *in vivo* methods that are used to identify clinically relevant molecules as potential OATP substrates or inhibitors. We discuss disease association of OATPs and single-nucleotide polymorphisms (SNPs) that are relevant in PK. Finally, we review the *in vitro* and *in vivo* models that are currently available to interrogate OATP–drug interactions.

2. The human OATP family

2.1. OATP-mediated transport

The 11 human OATPs, encoded by the SLCO genes, are membrane proteins that mediate the sodium and ATP-independent

Article highlights

- OATPs 1A2, 1B1, 1B3 and 2B1 are multi-specific transporters involved in the absorption, distribution and elimination of widely used drugs
- The function of these OATPs can be altered by genetic variations and drug interactions that result in altered pharmacokinetics (PK) and toxicity
- Based on their expression in barrier tissues (blood-brain barrier, placenta) and in detoxifying organs, lesser known members of the OATP family may also influence PK
- Research efforts should be directed at the development of the experimental toolkit needed to elucidate the role of the less described OATPs in ADME
- Increased expression of selected OATPs in cancer may be exploited by novel anti-cancer therapy

This box summarizes key points contained in the article.

uptake of large (usually >300 Da) organic molecules. It is generally accepted that OATPs act as electroneutral exchangers, coupling substrate uptake to the efflux of a counter ion, such as glutathione, conjugated glutathione, bicarbonate, or glutamate [9,10]. Other lines of evidence suggest that OATP-mediated uptake may be driven by a proton gradient [11], although, the pH sensitivity of transport appears to be OATP and substrate dependent [12,13]. It is unclear whether OATPs are obligate uptake transporters or whether they have additional functions as efflux transporters [14].

2.2. Substrate recognition by OATPs

The substrates of these transporters are primarily organic anions, though OATPs are also capable of transporting uncharged (e.g. digoxin (4C1); ouabain (1B3)), zwitterionic (e.g. fexofenadine (1A2, 1B3, 2B1)), and positively charged molecules (e.g. doxorubicin (1A2/1B) and triptans (1A2)) [11,15–18]. Among the endogenous substrates of OATPs are bile acids, bilirubin, eicosanoids, prostaglandins, hormones, and their sulfated and glucuronated conjugates (summarized in Table 1). Hence, under physiological conditions, OATPs are important in

bile acid homeostasis (1A2, 1B, 1C1, 2B1, 4A1, 4C1), bilirubin elimination (1A2, 1B), inflammatory processes (4C1), and the regulation of hormonal levels (1A2, 1B, 1C1, 2A1, 2B1, 3A1, 4A1, 4C1) [11,15]. Many OATPs also recognize exogenous compounds such as statins, cardiac glycosides, antidiabetic agents, immune suppressants, antibiotics, antivirals (e.g. HIV protease inhibitors), and anticancer medications. The extensive body of literature on the OATP-mediated transport of chemotherapy drugs has been recently reviewed by Sprowl and Sparreboom [19].

Based on their substrate recognition pattern, OATPs can be divided into two groups. The first group includes OATP1A2, 1B1, 1B3, and 2B1, which have partially overlapping substrate specificities, similar to ABC efflux transporters (e.g. ABCB1, ABCG2, and ABCC2/3) [6]. The other members of the family (1C1, 2A1, 3A1, 4A1, 4C1, 5A1, and 6A1) recognize a much smaller set of compounds. This latter set of transporters has been less characterized; therefore, our current knowledge about their substrates may be incomplete. Nevertheless, the increasing number of genome-wide association studies (GWAS) and expanding repertoire of *in vitro* and *in vivo* assays are rapidly enhancing our knowledge on potential substrates. OATP substrates with the greatest clinical relevance are summarized in Tables 1 and 2. For a more exhaustive list of substrates, the reader is referred to excellent reviews in the literature [11,15]. Because most of the OATP-interacting compounds have been identified *in vitro*, often using concentrations that exceed those occurring *in vivo*, substrate recognition data should be carefully interpreted. Additionally, interacting compounds identified by indirect *in vitro* studies do not necessarily distinguish between a transported substrate and an inhibitor.

2.3. Tissue distribution and localization

OATPs are present in the cell membrane of epithelial and endothelial cells and display distinct expression patterns; some OATPs are broadly expressed while others are expressed in specific organs. The characterization of the tissue

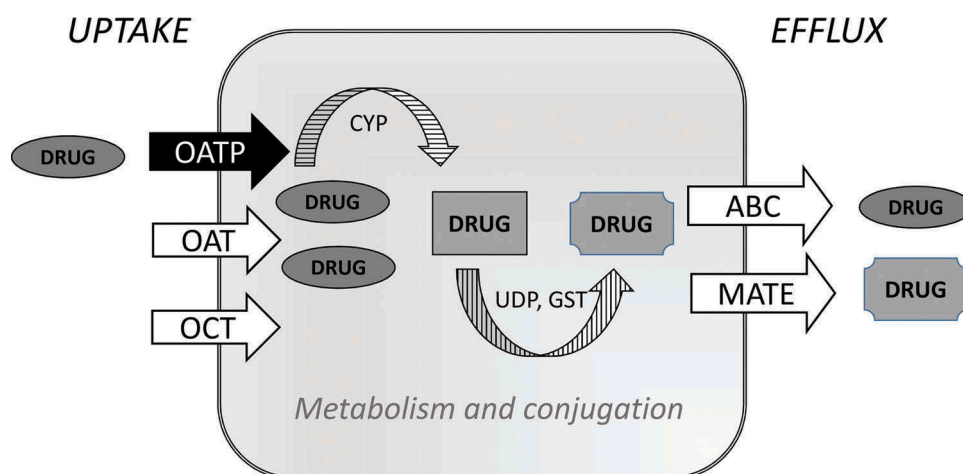


Figure 1. OATPs involved in drug uptake. Members of the OATP/SLCO (OATP1A2, 1B1, 1B3 and 2B1) and SLC22 (OCT2 and OAT1 and OAT3) transporter families are key determinants of drug uptake. Within the cell, drugs may undergo modifications by CYP (cytochrome P450), UDP (uridine diphospho-glucuronosyltransferase), GST (glutathione S-transferase) and SULT (sulphotransferase) enzymes. The most relevant transporters involved in the efflux of drugs and toxins are the ATP-binding cassette proteins (ABCB1, ABCG2, ABCC2 and 3) and member of the SLC47 family (MATE1 and MATE2-K).

Table 1. List of major endogenous and OATP test substrates.

OATP	Physiological substrates	Fluorescent or radioactive substrates
1A2	<ul style="list-style-type: none"> • atROL [20] • bile salts (taurocholate, cholate, ursodeoxycholic acid) [15,21] • bilirubin [15] • hormones (T4, DHEAS, ES) [15] • PGE₂ [15] • neuropeptides: SP, VIP [22] 	<ul style="list-style-type: none"> • [³H] atROL [20] • [³H] BSP [23] • [³⁵S] BSP [21] • [tyrosyl-3,5-³H] deltrophin II [24] • [³H] digoxin [25] • [³H] docetaxel [26] • [tyrosyl-2,6-³H(N)] DPDPE [24] • [³H] ES [25] • FI-MTX [13] • [³H] MTX [27] • [³H] nadolol [23] • Na-Fluo [13] • [³H] PGE² [25] • [³H] quercetin [28] • [³H] quinidine [29] • Rhodamine 123 [30] • [³H] N- methyl-quinine [25] • [¹⁴C] SQV [31] • [³H] TCL [32] • [³H] BSP [34] • [³H] BPS [35] • DCF and DBF [36] • [³H] docetaxel [37] • [³H] E17βG [38] • [³H] ES [34] • FI-MTX [39] • Fluo-3 [40] • Flutax-2 (oregon green 488-paclitaxel) [15] • Na-Fluo [41] • Oregon green [36]
1B1	<ul style="list-style-type: none"> • bile salts (taurocholate, tauroursodeoxycholate) [15] • bilirubin [15] • eicosanoids (LTC4, LTE4, PGE₂, thromboxane B2) [33] • hormones (ES, E17βG, T3, T4, DHEAS) [15] 	<ul style="list-style-type: none"> • [³H] TC [38] • [³H] BSP [44] • [³H] BPS [35] • [³H] CCK-8 [42] • DBF [36] • [³H] docetaxel [37] • [³H] E17βG [44] • [³H] ES [25] • FI-MTX [39] • Fluo-3 [36] • Na-Fluo [41] • Oregon green [36]
1B3	<ul style="list-style-type: none"> • bile salts (cholate, glycocholate, taurocholate, taurochenodeoxycholate, taurodeoxycholate, tauroursodeoxycholate) [15] • bilirubin [15] • CCK-8 [42] • hormones (T3, T4, ES, DHEAS, testosterone) [15] • LTC4 [15] • steroid conjugates [43] 	<ul style="list-style-type: none"> • [³H] TC [38] • [¹²⁵I]-T3 [25] • [¹²⁵I]-T4 [25] • [³H] BSP [45] • [³H] docetaxel [37] • [³H] E17βG [45] • [³H] ES [45] • Na-Fluo [13] • SR101 [46]
1C1	<ul style="list-style-type: none"> • hormones (ES, E17βG, thyroid hormones) [15,43] 	<ul style="list-style-type: none"> • Na-Fluo [13] • SR101 [46]
2A1	<ul style="list-style-type: none"> • PGs (PGE₁, PGE₂, PGD₂, PGF_{2α}) [47] 	<ul style="list-style-type: none"> • Na-Fluo [13] • [³H] PGE² [47] • [³H] PGE¹ [47] • [³H] quercetin [28]
2B1	<ul style="list-style-type: none"> • DHEAS [48] • ES [15] • LTC4 [48] • neuropeptides: SP, VIP [22] • PGE₂ [15] • taurocholate [48,49] • thromboxane B2 [47] 	<ul style="list-style-type: none"> • [³H] BSP [25] • DCF and DBF [36] • [³H]-ES [50] • FI-MTX [13] • Na-Fluo [13] • Oregon green [36] • [³H] quercetin [28] • [³H] PGE2 [50] • [³H]TC [49]
3A1	<ul style="list-style-type: none"> • ES [11] • PGE₁, PGE₂ [11] • T4 [48] • vasopressin [11] 	<ul style="list-style-type: none"> • [prolyl-3,4(N)-³H]-BQ-123 [51] • [³H]-ES [50] • Na-Fluo [13] • [³H] PGE² [51] • [³H] PGE¹ [51] • [tyrosyl-3,5(N)-³H]-vasopressin [51]

(Continued)

Table 1. (Continued).

OATP	Physiological substrates	Fluorescent or radioactive substrates
4A1	<ul style="list-style-type: none"> • E17βG [15] • ES [15] • PGE₂ [50] • thyroid hormones (T4, rT3(weak), T3, Taurocholate [52]) 	<ul style="list-style-type: none"> • [³H] ES [50] • [³H] PGE₂ [50] • Na-Fluo [13] • [³H] taurocholate [52] • [¹²⁵I] T4 [52]
4C1	<ul style="list-style-type: none"> • cAMP [53] • ES [54] • thyroid hormones [53] 	<ul style="list-style-type: none"> • [³H] digoxin [53] • [³H] ES [12,54] • Na-Fluo [13] • [¹⁴C] and [³H] sitagliptin [55]
5A1		<ul style="list-style-type: none"> • Na-Fluo [13]
6A1		<ul style="list-style-type: none"> • [³H] quercetin [28] • Na-Fluo [13]

atROL: all-trans-retinol; DHEAS-dehydroepiandrosterone sulfate; ES: estrone-3-sulphate; SP: substance P; VIP: vasoactive intestinal peptide; LTC4: leukotriene C4; PGE: prostaglandin E; BSP: bromsulphthalein/sulfobromophthalein; BPS: beraprost sodium; DPDPE: [D-penicillamine2,5]encephalin; MTX: methotrexate; SQV: saquinavir mesylate; TCL: trospium chloride; DBF: 4',5'-dibromofluorescein; DCF: 2',7'- dichlorofluorescein.

distribution of OATPs relies heavily on mRNA data. For example, mRNAs for OATP2A1, 3A1, and 4A1 have been detected in a broad number of tissues, while OATP1B1 and 1B3 are restricted to the liver and OATP6A1 is expressed in the testes [11]. A number of recent immunofluorescence analyses suggest unexpected localization patterns for some OATPs, such as the prostaglandin transporter OATP2A1, which was detected within the lysosomes of normal macrophages [87], and OATP2B1, 3A1 and the poorly characterized OATP5A1, which localized to the intracellular spaces within tumorous breast tissues [88]. As OATP expression has been thoroughly discussed in recent reviews [11,15], we discuss this information only in the context of ADME properties.

2.3.1. OATPs in hepatic clearance

OATP1A2 was the first human OATP isolated. Expressed in cholangiocytes, OATP1A2 is involved in bile acid, unconjugated bilirubin, and xenobiotic reabsorption [11]. The key role of OATP1B1 in hepatic drug uptake was recognized when it was realized that plasma statin levels increase in the presence of OATP1B1 inhibitors, such as cyclosporin A or gemfibrozil [3,73,89]. Several *in vitro* and *in vivo* experiments confirmed the relevance of OATP1B transporters in hepatic clearance [90,91]. OATP1B1 and 1B3 are almost exclusively expressed in the sinusoidal membranes of hepatocytes and are involved in the uptake of bilirubin, bile acids, and various drugs from the blood into hepatocytes. OATP2B1, which is ubiquitously expressed, may also be important in hepatic clearance [11]. It is difficult to estimate the relative contribution of OATP1B1, 1B3, and 2B1 to drug uptake *in vivo* due to their overlapping substrate/inhibitor specificity. However, based on mRNA and protein expression data, OATP1B1 is the most abundant and most relevant OATP in the liver [92].

2.3.2. OATPs in the kidney

In addition to the liver, the kidney is a relevant site of drug elimination. OATP4C1 is a kidney-specific transporter localized to the basolateral membranes of proximal tubules. OATP4C1 is involved in uremic toxin elimination [85,93] and mediates the uptake of certain heart medications (digoxin, ouabain), and anticancer drugs (methotrexate; MTX), from the blood [53,84]. Kidney-specific expression of the human OATP4C1 provided

protection against hypertension and inflammation in a rat renal failure model, demonstrating the role of OATP4C1 in renal toxin elimination [85,93]. In a recent study, bupropion (an antidepressant) decreased the area under the plasma concentration–time curve (AUC, a measure of drug exposure) of digoxin via the activation of OATP4C1-mediated renal clearance [84].

OATP1A2 is also expressed in the kidney, though it localizes to the distal tubules of the nephrons. OATP1A2 may play a role in the active tubular reabsorption of MTX and in MTX-induced toxicities [27]. Knauer et al. demonstrated that mRNA expression levels of OATP2B1 in the kidney were comparable to expression levels in the small intestine [94]. However, OATP2B1 protein expression in the kidney has not yet been confirmed.

2.3.3. OATPs in the intestine

Several ubiquitously expressed OATPs (1A2, 2B1, 3A1, and 4A1) have been detected in the intestine. Based on quantitative mRNA data, OATP2B1 is the most abundantly expressed OATP in the intestine [95] and the expression of this transporter on the apical side of enterocytes has also been confirmed by immunofluorescent labeling [96]. Based on these data, OATP2B1 is the dominant OATP involved in first-line drug absorption and a significant determinant of the oral availability of drugs.

2.3.4. Other blood–tissue barriers

The blood–brain barrier (BBB) provides a tight control of the cerebral entry of molecules. Due to many medications aimed at targeting the brain, the BBB is the most extensively investigated blood–tissue barrier. OATP1A2 and 2B1 are expressed on the apical surface of brain capillary endothelial cells [22] with similar mRNA expression levels. A recent study demonstrated that both 1A2 and 2B1 are present in the retina, mediating neurotransmitter and neurosteroid uptake in this tissue [22]. OATP1A2 is also expressed in neurons and may influence neuronal statin and MTX levels [97]. In the choroid plexus, OATP1C1 and OATP3A1 protein expression has been detected [45,51].

OATPs may also be involved in drug transport across the blood–testes (1A2, 1C1, 3A1, 6A1) [11,15,98], blood–ocular (1A2, 1C1, 2B1, 1A2, 3A1, 4A1) [20,99], and maternal–fetal barriers (1A2, 1B1, 1B3, 2B1, 2A1, 4A1) [15,100]. OATPs that

Table 2. OATP–drug interactions.

OATP (human)	Substrates and inhibitors <i>in vitro</i>	Drug interactions <i>in vivo</i> ^a
1A2	Antibiotics • direct TBPM-PI (β -lactam antibiotic) uptake [56] Anesthetics and analgesics • direct dextropropriphol II and DPDPE transport [24] • direct rocuronium transport inhibited by APM, taurocholate, K-strophanthoside, QD, and NMQD [29] Anticancer drugs • ES uptake inhibited by MTX [27] • imatinib transport inhibited by naringin [57] Antihypertensive drugs • direct nadolol uptake inhibited by green tea, naringin, verapamil [23] • direct talinolol uptake [58] Antihistaminic drugs • direct fexofenadine uptake [59] • direct fexofenadine uptake inhibited by naringin and hesperidin [60] Antiretroviral drugs • direct SQV uptake [31] Statins • direct pravastatin uptake [61] Toxins • direct microcystin transport [62] Others • direct ES uptake inhibited by atROL, direct atROL transport [20] • direct TCL uptake [32] • direct uptake measurements with triptans [17] For further list of interacting molecules see [5,15,63]	<ul style="list-style-type: none"> • reduced fexofenadine AUC by citrus juices [59,64] • imatinib pharmacokinetics affected by SLCO1A2 SNPs in CML patients [57] • green tea ingestion decreases plasma concentrations of nadolol in humans, presumably in part by inhibition of OATP1A2-mediated intestinal absorption of nadolol [23] • docetaxel transport in humanized mice [26]
1B1	Antibiotics • ES uptake inhibited by several anti-TB drugs [65] • E17 β G uptake inhibited by novobiocin [66] Anticancer • direct docetaxel uptake [37] • direct flavopiridol uptake and increased toxicity [67] • involved in toxicity and disposition of platinum anticancer drugs [68] • TKIs as 1B substrates (e.g. direct sorafenib transport) [69] Antihypertensive drugs • direct bosentan uptake inhibited by CsA and rifampicin [70] • direct valsartan uptake [71] Anti-inflammatory drugs • direct mesalazine transport inhibited by budesonide, cyclosporine A, rifampin [72] Statins • transport inhibitors: lovastatin acid, pravastatin acid, and simvastatin acid [66] • direct cerivastatin uptake inhibited by CsA [3] • cerivastatin-mediated toxicity caused by 1B1 inhibition with gemfibrozil [73] Toxins • direct microcystin transport and cytotoxicity [62,74] For further interacting molecules, see: [5,15,48,63,66,75]	<ul style="list-style-type: none"> • rifampicin as an inhibitor of OATP1B1 and OATP1B3 • Oral or intravenous dose of rifampicin increases exposure of rosuvastatin and pitavastatin [76] • docetaxel transport (humanized mice) [26] • role for OATP1Bs in the elimination of sorafenib (humanized mice) [69]
1B3	Antibiotics • ES uptake inhibited by several anti-TB drugs [65] • direct E17 β G uptake inhibited by novobiocin [66] Anticancer drugs • direct paclitaxel transport [77] • transport inhibitors: mitoxantrone and vincristine 27 [66] • direct docetaxel transport [37] • direct flavopiridol uptake and increased toxicity [67] • 1B3-linked toxicity and disposition of cisplatin, carboplatin, and oxaliplatin [68] • TKIs as 1B substrates (e.g. direct sorafenib transport) [69] Anti-inflammatory drugs • direct mesalazine transport inhibited by budesonide, cyclosporine, rifampin [72] Antihypertensive drugs • direct bosentan uptake inhibited by CsA and rifampicin [70] • direct valsartan uptake [71] Toxins • direct microcystin transport and cytotoxicity [62,74] For an exhaustive list of interacting molecules see: [5,15,48,63,66]	<ul style="list-style-type: none"> • imatinib pharmacokinetics affected by SNPs in CML patients [78] • paclitaxel pharmacokinetics affected by SNPs [77] • docetaxel transport (humanized mice) [26] • role for OATP1Bs in the elimination of sorafenib (humanized mice) [69] • rifampicin as an inhibitor of OATP1B1 and OATP1B3 [76] • rifampicin as an inhibitor of OATP1B1 and OATP1B3 • Oral or intravenous dose of rifampicin increases exposure of rosuvastatin and pitavastatin [76]
1C1 2A1	Anti-inflammatory drugs • direct PGE ₂ uptake inhibited by diclofenac and lumiracoxib [79] • direct PGE ₂ uptake induced by indomethacin, ketoprofen, and naproxen [79] Flavonoids • direct quercetin transport [28] Prostaglandin analogs • direct latanoprost acid uptake [80]	

(Continued)

Table 2. (Continued).

OATP (human)	Substrates and inhibitors <i>in vitro</i>	Drug interactions <i>in vivo</i> ^a
2B1	Antibiotics <ul style="list-style-type: none"> • direct ES uptake inhibited by several anti-TB drugs [65] • direct TBPM-PI (β-lactam antibiotic) uptake [56] • direct ES uptake inhibited by novobiocin [66] Anticancer drugs <ul style="list-style-type: none"> • transport inhibitor: erlotinib [66] • direct flavopiridol uptake and increased toxicity [67] Anti-inflammatory drugs <ul style="list-style-type: none"> • direct mesalazine transport inhibited by budesonide, cyclosporine, rifampin [72] • direct DCF-AG transport and toxicity [81] Antihypertensive drugs <ul style="list-style-type: none"> • direct talinolol uptake [58] Prostaglandin analogs <ul style="list-style-type: none"> • direct latanoprost acid uptake [80] Statins <ul style="list-style-type: none"> • transported by 2B1 [5] • involved in increased cytotoxicity of statins [82] For further interacting molecules see: [5,15,48,63,66]	
3A1	Antibiotics <ul style="list-style-type: none"> • direct benzylpenicillin transport [50] Antihypertensive drugs <ul style="list-style-type: none"> • direct BQ-123 transport [51] 	<ul style="list-style-type: none"> • 3A1 as a novel CD-associated gene, results higher incidence of bowel perforation in CD patients [83]
4A1	Antibiotics <ul style="list-style-type: none"> • direct benzylpenicillin transport [50] 	
4C1	Antidiabetics <ul style="list-style-type: none"> • direct sitagliptin transport [55] Cardiac glycosides <ul style="list-style-type: none"> • direct digoxin transport [53,55] • direct digoxin transport increased by bupropion [84] Statins <ul style="list-style-type: none"> • statins increase the expression and function of OATP4C1 [85] 	<ul style="list-style-type: none"> • OATP4C1 overexpression reduced hypertension, cardiomegaly, and inflammation in a rat renal failure model [85]
5A1	Anticancer drugs <ul style="list-style-type: none"> • 5A1 expressing cells showed higher resistance to satraplatin [86] Flavonoids <ul style="list-style-type: none"> • direct quercetin uptake [28] 	
6A1		

^aHuman OATP transporter activity and OATP-related disposition of drugs measured *in vivo* (human clinical or rodent data).

TBPM-PI: tebipenem pivoxil; DPDPE: [D-penicillamine_{2,5}]encephalin; ES: estrone-3-sulphate; E17βG: estradiol-17-β-glucuronide; atROL: all-trans-retinol; TCL: trospium chloride; TKI: tyrosine kinase inhibitors; PGE: prostaglandin E; CsA: cyclosporin A; DCF-AG: diclofenac acyl glucuronide; SQV: saquinavir mesylate; CD: Crohn's disease; CML: chronic myeloid leukemia; MTX: methotrexate.

are present in the placenta are important for steroid sulfate (2B1) [101] and thyroid hormone (4A1) [102] transport but the role of placental OATPs in fetal exposure to drugs is poorly understood. OATP expression may be significantly altered in tumor tissues compared to healthy cells (see chapter 2.4.); however, the functional consequences of this phenomenon are not yet well understood.

2.4. The role of OATPs in disease

To date, few diseases have been associated with mutations in OATP genes. Rotor syndrome (RS) is a rare, benign disorder marked by elevated levels of bilirubin in the blood and coproporphyrin in the urine [103]. The role of OATP1B1/1B3 in bilirubin transport has been indicated in a number of GWAS, including families with RS whose GWAS results revealed simultaneous mutations in OATP1B1 and 1B3 that rendered both transporters non-functional [103,104]. These data were further confirmed in mice harboring mutations in genes for the 1A/1B family of OATPs, which resulted in hyperbilirubinemia [105].

Mesomelia-synostoses syndrome (MSS) is a rare, autosomal-dominant disease characterized by limb shortening and various congenital malformations. A study of five patients in four families identified an interstitial deletion in chromosome 8q13

spanning two genes: SULF1 (heparan sulfate 6-O-sulfatase 1) and SLCO5A1 (OATP5A1) [106]. OATP5A1 is expressed in the adult heart and in fetal brain but its function is currently unknown. The contribution of OATP5A1 to MSS requires further investigation, as a partial deletion of SLCO5A1 was reported in a healthy individual.

Primary hypertrophic osteoarthropathy (PHO) is a rare genetic disease affecting skin and bone formation. A study of three individuals with PHO indicated that inactivating mutations in SLCO2A1 cause PHO by impairing prostaglandin E₂ (PGE₂) transport [107]. Loss of SLCO2A1 function has also been implicated in a form of hereditary enteropathy that is characterized by chronic ulcers in the small intestine [108]. Furthermore, a study using a mouse model of pulmonary fibrosis suggested that SLCO2A1 may also be critical to lung tissue restoration [109]. Given the multiple roles of PGE₂ in the body, prostaglandin transport-inactivating SLCO2A1 mutations will likely remain intensely investigated.

A GWA study of over 1100 patients with progressive supranuclear palsy (PSP), a rare neurodegenerative movement disorder similar to Parkinson's disease, revealed a putative association with SLCO1A2 [110]. OATP1A2 is located in the brain, eyes, kidney, liver, and intestine. Bile acids, bilirubin, and dehydroepiandrosterone sulfate (DHEAS), a precursor of

steroid hormones, are among the physiological substrates of OATP1A2 [111]. The possible role of this OATP in PSP has not been investigated. Another GWA study of Crohn's disease within an Ashkenazi Jewish population found a variant of SLCO6A1 [111].

OATPs have become the focus of considerable attention because of the altered expression of these transporters in various types of cancer (Table 3). The liver-specific transporters 1B1 and 1B3 were found to be downregulated in liver cancers and significantly upregulated in tumors of the ovaries (1B1, 1B3), colon (1B1, 1B3), breast (1B3), prostate (1B3), and lung (1B3) [43]. Similarly, OATP6A1 expression, normally limited to the testes, was detected in tumors of the brain, bladder, and lung [43]. Many of the widely distributed OATPs have also been reported to be upregulated in certain malignant cells.

Because OATPs are able to transport a wide variety of substrates, including hormones, one would hypothesize that an upregulated or atypical OATP expression could lead to the proliferation of estrogen- and androgen-dependent tumors.

Indeed, OATP expression levels correlate with tumor growth. Estrone-3-sulfate uptake by OATPs 1A2 [117], 1B3 [133], 3A1, and 4A1 has been implicated in the survival of hormone-dependent breast cancer cells [126]. These data suggest that targeting these transporters in the treatment of hormone-responsive breast cancer may have beneficial effects and improved survival [117,126].

OATPs also influence disease progression in androgen-dependent prostate cancers (PC). OATP1B3 transports testosterone and the 334T allelic variant of 1B3, which efficiently transports testosterone, is associated with decreased patient survival [134]. In another study of PC patients, presence of a testosterone transport-deficient variant of OATP1B3 (haplotype 334GG/699AA) was associated with better survival over 10 years [135]. Similarly, an OATP2B1 variant, with increased DHEAS transport, was correlated with increased patient mortality [134].

In summary, changes in OATP expression have been demonstrated in numerous cancers. However, conflicting

Table 3. OATP expression in normal and cancerous tissues.

OATP	Normal expression		Cancer	
		Localization	Downregulated	Upregulated
1A2	Ubiquitous: BBB [112,113] eye (retina) [20,22] intestine [95] kidney (distal tubule) [112] liver (cholangiocytes) [112] neurons [22] Liver (hepatocytes) [50]	Apical	Breast* [114] colon [115] gliomas [113]	Bone [116] breast*[43,117] prostate [118]
1B1	Liver (hepatocytes) [50]	Basolateral (sinusoidal)	Liver cancer [43]	Colon [43,119] ovaries [119]
1B3	Liver (hepatocytes) [44] pancreas (Langerhans islets) [120]	Basolateral (sinusoidal)	Liver cancer [43]	Breast [119] colon [43,119] lung [43,119] pancreas [43,119] prostate [43,119] ovaries [119,121] Malignant bone cysts [116]
1C1	Brain (choroid plexus) testis (Leydig cells) [11,45]	Basolateral		
2A1	Ubiquitous: eye (retina, ciliary epithelium) [80] endometrium [122] neurons [123]			Bile duct [124] bone [116] breast [114] liver [124]
2B1	Ubiquitous: BBB [113] intestine [96] liver (hepatocytes) [25] skeletal muscle [82]	Apical (enterocytes) basolateral (hepatocytes)	Breast* [114]	Colon [50] bone [116] breast* [125] gliomas [113]
3A1	Brain (choroid plexus, neurons) [51] testis [51]	Apical (3A1_v2) basolateral (3A1_v1)		Colon [125] bone [116] breast (altered localization) [88,126–128] liver [124] lung [125] pancreas [125] Lung [130] liver [124] colon [50] pancreas [50] breast [126,127] bone [116] Breast (altered localization) [88,114] lung [130] Breast (altered localization) [88] liver [124] lung [130]
4A1	Ubiquitous: eye (ciliary body) [99] kidney [52] pancreas [52] placenta [129]	Apical		pancreas [50] breast [126,127] bone [116] Breast (altered localization) [88,114] lung [130] Breast (altered localization) [88] liver [124] lung [130]
4C1	Kidney (human OATP4C1 expressed in rats localizes to proximal tubule cells) [85]	Basolateral		Bladder, brain, and esophagus [132] lung [43,130]
5A1	Heart [131] fetal brain [131] breast [88]			
6A1	Testis (Sertoli cells) [132]			

Most data are based on mRNA expression. Protein data are indicated by bold letters.

*: Controversial reports.

reports on the tumor-specific expression of OATP1A2 and 2B1 suggest that the therapeutic or prognostic value of expression changes should be cautiously interpreted. Nevertheless, mounting evidence supports the hypothesis that OATPs are upregulated in tumors, potentially to meet the increased nutritional demand of cancer cells.

2.5. Methods and models to investigate OATP–drug interactions

2.5.1. Test substrates of OATPs

OATP function is commonly investigated in whole-cell-based systems by measuring the uptake of radioactively labeled substrates. Estrone-3-sulfate, bromosulfophthalein, and estradiol 17 β -D-glucuronide are among the most extensively used tritiated substrates and have been used to investigate the function of multiple OATPs [15]. However, due to the cost and limited availability of radiolabeled substrates, their utility in large-scale substrate-screening experiments is impeded and recent efforts have focused on fluorescent substrates as safe, simple, and cost-effective alternatives. A multitude of fluorescent probes (Na-fluorescein, fluorescein-methotrexate, fluorescein-cAMP, various fluorescent bile acids [39,41,136,137]) have been used to uncover interacting compounds of OATP1B transporters; however, until recently, no fluorescent assay has been available for other OATPs. Recently, expression of the 11 human OATPs in insect cells revealed that, under acidic conditions, Na-fluorescein is a general OATP substrate, suitable for the characterization of the entire human OATP family [13]. A pan-OATP substrate is of particular importance for the characterization of the poorly characterized members of the OATP family, 5A1, and 6A1. The advantage of fluorescein derivatives in developing substrate inhibition assays for OATP1B and 2B1 transporters was also demonstrated in mammalian cells [36]. Typical and newly developed test substrates of OATPs are listed in Table 1.

Because indirect transport assays cannot reveal the nature of the interaction between molecule and OATP, the transport of candidate substrates should be confirmed by direct transport measurements, such as mass spectrometry or direct labeling.

2.5.2. *In vitro* models

2.5.2.1. Engineered cell lines. The preferred model systems for the investigation of OATPs are mammalian cell lines with exogenous OATP expression, although transiently transfected *Xenopus* oocytes and insect cells have also been used [6,13]. While many stable OATP-expressing cell lines have been generated to date, evidence suggests that the overexpression of certain OATPs in standard mammalian laboratory cell lines is not straightforward (our own unpublished results). This may be due to metabolic perturbation of the cells, although the exact mechanism behind this phenomenon is still unclear.

2.5.2.2. Pharmacological models. The individual role of a transporter in the transmembrane movement of drugs is most easily assessed in cell lines engineered to express a single OATP. Additionally, cotransfected cell lines with simultaneous OATP and ABC expression have also been established [138]. However, because the transport of drugs occurs in an

elaborate network of uptake and efflux transporters as well as drug metabolizing enzymes, a closer approximation of the *in vivo* environment requires more complex *in vitro* model systems. Caco-2 cells, which form monolayers resembling the intestinal epithelium, are currently considered the ‘gold standard’ in studying intestinal absorption. Nonetheless, Caco-2 cells do not fully reflect the transporter profile of the natural intestinal environment and are unable to recapitulate *in vivo* organization at a tissue level [139]. These limitations led to the proposal of stem cell-derived organoids [140] and precision cut intestinal slices [141] as ADME models; however, the application of these methods to the investigation of drug transport is limited [141]. Polarized cells (e.g. MDCKII or LLCPK) have been successfully used to model renal processes. However, establishing *in vitro* models that recapitulate the complexity of the liver has proved challenging. Several hepatic models exist, ranging from immortalized cell lines (HepG2, HepaRG), liver slices, and stem cell-derived hepatocytes to 3D cell cultures and bioreactors [142,143]. These models vary in maintenance costs, accessibility, and transporter expression pattern [144]; therefore, the appropriate models should be selected based on these considerations and the pharmacological goal.

2.5.3. OATP-mediated ADME *in vivo*

To predict DDI during the preclinical phase is of major importance; however, the extrapolation of *in vitro* data to more relevant *in vivo* processes is a difficult task [91]. Therefore, *in vivo* data gained from pharmacogenetic/pharmacogenomic studies, clinical trials involving volunteers, and animal models are crucial in modeling the *in vivo* fate of a drug.

2.5.3.1. Animal studies. Recognizing the importance of liver-specific transporters in drug disposition, *Oatp1a/1b* knockout (KO) mice have been widely used to study the PK of clinically applied drugs [145] as well as natural OATP substrates [145,146]. For example, *Oatp1b2* (a homolog of OATP1B1/1B3) single KO mice have been used to study the liver and plasma distribution of toxins (phalloidin, microcystin-LR), cholesterol-lowering drugs (cerivastatin, lovastatin acid, pravastatin, and simvastatin acid), and antibiotics (rifampicin and rifamycin SV) [145,147,148]. Mice with a deletion of the 1a/1b locus (missing all established mouse 1a/1b transporters) were used to elucidate the hepatic clearance of bilirubin, bile acids, and drugs from the blood [105]. In addition, 1a/1b KO mice have been used to establish coproporphyrin (CP) I and III as endogenous biomarkers for the assessment of transporter activity during early drug development [146]. The applicability of CPs as endogenous probes for liver transport was also confirmed in cynomolgous monkeys by administering *oatp1a/1b* inhibitors [146].

There are significant species differences that hinder the interpretation of data from mouse models. OATP1Bs and 1A2 have no rodent orthologs and the homology between OATP2B1 and its mouse ortholog is only 77% [33]. As exemplified by the rat *Oatp4c1*, which localizes to the apical, instead of the basolateral, membrane of the proximal tubules of the kidney, the localization of some rodent OATP orthologs may also differ [149]. To address these issues, van de Steeg et al. generated humanized mice with liver-specific expression

of human OATP1B1, 1B3, and 1A2 in a mouse *oatp1a/1b* KO background [150,151]. OATP1A2-humanized mice do not mimic normal conditions in the liver as OATP1A2 is expressed in hepatocytes [151], not cholangiocytes. Further limiting the *in vivo* assessment of hepatic clearance, a KO mouse model for OATP2B1 has not been established.

Nevertheless, humanized mice are an invaluable tool for studying the *in vivo* disposition of drugs and have been used to study the PK of anticancer medications (e.g. methotrexate, paclitaxel, and docetaxel [26,151]) and to detect DDIs (e.g. between methotrexate and the antibiotic rifampicin, or the antihypertensive drug, telmisartan [152]).

2.5.3.2. Human studies. The majority of *in vivo* data on the role of OATPs in drug PK arose from unexpected toxicity due to either coadministration of OATP substrates/inhibitors or altered OATP function/expression caused by SNPs.

2.5.3.2.1. Drug interaction studies. A striking example of OATP-mediated DDIs is the potentially lethal interaction between cerivastatin and gemfibrozil (used to treat hypercholesterolemia and hypertriglyceridemia, respectively), which led to the withdrawal of cerivastatin from the market [90]. Retrospective *in vitro* analyses revealed that the major mechanism of cerivastatin-mediated toxicity was the inhibition of both OATP1B1 and the metabolizing enzyme CYP2C8 by gemfibrozil glucuronide [73]. Many additional clinical data indicated statin-mediated toxicity upon the simultaneous administration of OATP substrates/inhibitors (cyclosporin A, rifampicin, lopinavir) and statins [3,90,91]. The role of OATP2B1 in muscular toxicity of statins was proposed due to its expression in skeletal muscle [82]. In addition to statins, the AUC of bosentan, an endothelin receptor antagonist, is influenced by the OATP1B inhibitors rifampicin, cyclosporin A, and sildenafil [70].

Considering the physiological role of OATPs, drugs inhibiting the transport of endogenous substrates may disrupt bile acid or hormone homeostasis. Indeed, it has been documented that the administration of tyrosine kinase inhibitors or high doses of cyclosporine A result in hyperbilirubinemia, probably due to the inhibition of bilirubin uptake by OATP1B1/3 [153,154].

2.5.3.2.2. GWA and genotype panel studies. Pharmacogenetic studies have made an enormous contribution to our understanding of the role of OATPs in PK and revealed various SNPs in OATP genes (SLCO) that cause interindividual differences in drug efficacy and safety. While GWAS and genotype panels highlighted the importance of certain SLCO polymorphisms, detailed functional analyses required *in vitro* follow-up studies.

The most clinically relevant SLCO SNPs are summarized in Table 4.

SLCO1B1: Given its recognized role in hepatic transport, the pharmacological consequences of SLCO1B1 SNPs have been extensively investigated. The two most common polymorphisms of SLCO1B1 are c.521T > C (p.174V > A, rs4149056), and c.388A>G (p.130N > D, rs2306283), though more than 14 SNPs in SLCO1B1 have been analyzed.

The c.521T > C variant (allele *5) results in decreased OATP1B1 activity [159], leading to increased plasma levels of various OATP1B1 substrates including drugs used in the

treatment of high cholesterol (statins), high blood pressure (olmesartan), diabetes (atrasentan), heart disease (torsemide), HIV (lopinavir), cancer (SN-38), allergy (fexofenadine), and immune diseases (tacrolimus) [5,160,161]. Accordingly, elevated plasma levels of these medications may increase the risk of toxicity. Indeed, a GWA study of 85 patients with myopathy and 90 matched controls indicated that an SLCO variant in near-complete linkage disequilibrium with the *SLCO1B1**5 allele is the most important predictor of myopathy in patients taking high doses of simvastatin [161]. The association between the *SLCO1B1**5 allele and adverse drug reactions upon statin treatment (simvastatin, pravastatin, lovastatin) was confirmed in multiple GWA studies [171,172] and genotype panels revealed that the *SLCO1B1**5 allele may markedly affect the PK of various statins (simvastatin, atorvastatin, rosuvastatin, pravastatin) [89,172,173]. However, the c.521 T > C variant did not influence *in vivo* fluvastatin clearance, indicating a substrate-specific transport alteration by this variant [172]. Alternatively, minor effects of the c.521 T > C variant on fluvastatin clearance were not detected due to study power limitations.

While *in vitro* and *in vivo* data on the c.388A>G polymorphism are controversial (haplotype *b), this SNP was associated with decreased AUC of several drugs including the non-statin cholesterol-lowering medication ezetimibe, the antidiabetic repaglinide [156,157] and lovastatin acid (the active metabolite of lovastatin) [5,162,174]. Contrastingly, the c.388A>G polymorphism did not alter response to statin therapy in a study of 386 adults of Greek origin [158]. The c.388A>G polymorphism is often linked to c.521 T > C, resulting in the *15 haplotype (the most frequent of the 18 documented haplotypes). Similarly to the effect of haplotype *5, *15 is associated with increased plasma levels of pravastatin and lovastatin [5,6,162,163]. In addition, lower methotrexate clearance has been associated with variations in noncoding regions of SLCO1B1.

In summary, based on the extensive clinical data available for SLCO1B1, haplotype information can be a good predictive marker in personalized medication.

SLCO1B3: The two most common mutations of SLCO1B3 are c.334T > G (p.112S>A, rs4149117) and c.699G>A (p.233M > I, rs7311358). Allele frequency data indicate that 334G and 699A are the most frequent variants in the Caucasian and Asian populations. Because the 334G and 699A polymorphisms are in near-complete linkage disequilibrium, with an allele frequency above 70% (Table 4), the haplotype encoding 112A and 233I should be regarded as dominant in these populations [165]. *In vitro* studies show that the single variants have no effect on transporter function, while the 112A/233I variant has reduced activity compared to the reference sequence [135,165]. Likely due to the compensatory effect of other OATPs, clinical data about the effect of SLCO1B3 SNPs are scarce and controversial (summarized in [91]). While the c.699G>A variant was associated with decreased docetaxel clearance in Chinese nasopharyngeal cancer patients [167], the c.334T > G polymorphism increased the clearance of imatinib in chronic myeloid leukemia patients in a Japanese population [166]. As described in the disease section, PC patients harboring the 334GG/

Table 4. List of the most relevant SLCO SNPs altering *in vivo* PK.

Gene	dbSNP ID	Allele	Mutant allele frequency (%)			Nucleotide change	AA change	Functional consequences		
			Caucasian	Afro-American	Asian			<i>In vitro</i>	<i>In vivo</i>	
SLCO1A2	rs10841795	*2	13–16	2–4	<1	113 T	c.38 T > C	Increased ³ H-MTX and ³ H-EIS uptake [27] unaltered ³ H-EIS transport [112]	Increased AUC of methotrexate [97]	
SLCO1B1	rs3764043		2	9	17		c.361G>A	promoter region	Increased imatinib clearance [57]	
	rs2306283	*1b	30–45	72–83	59–86		c.388A>G	N130D	Unaltered transport function [155]	Decreased AUC of repaglinide, ezetimibe, and simvastatin acid [156, 157] No alteration in statin response [158]
	rs4149056	*5	8–20	1–8	8–16		c.521 T > C	V174A	Decreased function [159]	Increased AUC of statins, sartans, torsemide, lopinavir, fexofenadine, and tacrolimus [5, 160, 161]
SLCO1B3		*15	16–25	2–16	12		c.388A>G, c.521 T > C	N130D + V174A	Decreased function [155]	Increased plasma levels of pravastatin and simvastatin [162, 163] and increased risk of rifampin-induced liver injury [164]
	rs4149117		65–80	<50%	75–86		c.334 T > G	S112A	Unaltered transport function [135, 165]	Increased the clearance of imatinib [166]
	rs7311358		81–84	<50%	64–81		c.699G>A	M233I	Unaltered transport function [135, 165]	Decreased docetaxel clearance [167]
SLCO2B1		*1	>70%	>70%	>70%		c.334G, c.699A	S112A + M233I	Decreased function [135, 165]	Better survival in prostate cancer [135]
	rs11045585		14	22	18		IVS12-5676A>G	Intronic		Increased AUC of docetaxel and telmisartan [167]
	rs12422149		8–14	13	37		c.935G>A	R312Q		Increased survival in prostate cancer [168] decreased AUC of montelukast [169]
	rs2306168	*3	3	19	31		c.1457C>T	S486 F	Decreased transport of ³ H-ES [170]	Increased AUC of a beta blocker celiprolol [5]

699AA haplotype showed longer median survival than patients carrying the TT/AA and TG/GA haplotypes [135]. Interestingly, an intronic variant, harboring an extra intron, was found to be associated with increased AUC of telmisartan and docetaxel [167].

SLCO2B1: The expression pattern and pH sensitivity of OATP2B1 suggest that it contributes to intestinal drug absorption although, current data are insufficient to firmly support this hypothesis. The c.1457C>T variant (p.S486F), which has a 31% frequency in the Japanese population, decreases *in vitro* transport activity [170] and results in a decreased AUC of the beta-blocker celiprolol [5,175]. These data indicate that OATP2B1 contributes to intestinal absorption, rather than hepatic uptake. OATP2B1 variants also influence the progression of androgen-dependent PC as a function of DHEAS transport activity [134,168]. Accordingly, time to progression was increased in patients with the androgen transport-deficient variant c.935G>A (rs12422149) [168].

SLCO1A2: Although several SLCO1A2 SNPs have been characterized *in vitro*, allele frequency data suggest that the clinical significance of these polymorphisms may be limited. The only allele with potential *in vivo* significance is c.38T > C (p.131>T). Based on *in vitro* analyses, the c.38T > C variant exhibits normal transporter function [27,112]. However, a twofold increase in methotrexate uptake was documented *in vivo*, supporting increased transport by this variant [97]. Additionally, a mutation in the promoter region of SLCO1A2 (c.361G>A) resulted in increased imatinib clearance in chronic myeloid leukemia patients [57].

3. Conclusions

The role of OATPs in PK is increasingly recognized. OATPs transport large, primarily anionic, compounds into cells and are known to influence the absorption and elimination of common medications, such as statins, antivirals, antidiabetic, and anticancer molecules. The four OATPs that are proven to have a major impact on the *in vivo* fate of drugs are 1A2, 1B1, 1B3, and 2B1. Hepatic OATPs 1B3 and, the more abundant, 1B1 have a key role in the hepatic clearance of drugs, bile acids, and bilirubin. OATP2B1 is also expressed in the liver. However, the exact contribution of this transporter to hepatic clearance is not yet elucidated. Increasing evidence suggests that OATP2B1 is involved in the intestinal absorption of orally administered drugs. In addition, cerebral and muscular drug levels may be determined by OATP1A2 and OATP2B1, respectively. Recently, the digoxin transporter, OATP4C1, has emerged as a determinant of the renal elimination of drugs, although the substrate recognition pattern of this transporter is not fully mapped.

Until now, OATP research has focused on OATP1A2, 1B1, 1B3, and 2B1 because of the profound pharmacological significance of these transporters. The rest of the OATP family, however, received less attention, despite emerging evidence that OATPs in the blood–testes (1A2, 1C1, 3A1, 6A1 [11,15,98] and maternal–fetal barrier (2A1, 4A1) are also involved in hormone transport and drug absorption [15,100–102]. The hiatus in our knowledge about the other members of the OATP family arises from the following: (1) the lack of established expression systems and suitable functional assays and,

(2) the scarcity of *in vivo* data. Therefore, to uncover the substrate recognition pattern of the poorly investigated OATPs, research efforts should focus on developing novel *in vitro* methods that allow for high-throughput substrate screening and the further collection of *in vivo* data.

Finally, as many OATPs show *de novo* expression in tumors, they may be important in influencing local, intra-tumor concentrations of therapeutic compounds. Thus, the mapping of drug–OATP interactions would be critical to tumor-specific drug delivery.

4. Expert opinion

OATPs 1A2, 1B1, 1B3, and 2B1 participate in the absorption and distribution of various medications and are sites of DDI leading to altered drug efficacy or unexpected toxicity. Altered transporter function, as a result of interindividual variations in OATP-encoding genes (i.e. polymorphisms), may lead to altered drug exposure over time. Food components and solubilizing agents, such as polysorbate 80 [19], may also affect transporter function. Finally, drugs may alter the OATP-mediated transport of endogenous compounds (bilirubin, bile salts, or hormones). Therefore, the International Transporter Consortium (ITS) recognizes OATP1A2, 1B1, 1B3, and 2B1 as major determinants of drug PK and recommends the investigation of these transporters during drug development.

To investigate OATP–drug interactions, various *in vitro* methods have been established. OATP function is commonly investigated using radioactively labeled test substrates, although the use of fluorescently labeled compounds would be simpler, safer, and more cost-effective. Indeed, several fluorescence-based OATP1B assays have been established. For OATP1A2 and 2B1, however, fluorescent assays have been described only recently, and there are no established assays for the large-scale measurement of drug interactions with the other members of the OATP family. A potential solution would be to screen the available library of fluorescent molecules for OATP substrates with low passive cell permeability. Alternatively, known OATP substrates could be conjugated to fluorescent molecules. Appropriate and well-characterized *in vitro* assays would aid the characterization of the entire OATP family by allowing for the reproducible comparison of OATP variants and the further mapping of OATP-mediated DDIs.

When designing *in vitro* assays to determine OATP-mediated DDIs, the following should be considered: (1) because of the complexity of the substrate binding site of the transporter, the function of each OATP should be tested using multiple substrates, (2) due to the promiscuous nature of OATPs, it is almost impossible to measure all potential OATP-mediated DDIs, (3) substrates/inhibitors should be used at physiologically relevant concentrations.

In the body, OATPs are part of a complex system of influx and efflux transporters as well as metabolizing enzymes; therefore, the effect of these transporters on PK should be interpreted in the context of the entire organism. Attempts at mimicking the *in vivo* environment varied from the development of pharmacological models to the use of humanized mice. While these models have been profoundly useful in studying the function of OATPs, they still

suffer from major limitations. Pharmacological models, however complex, cannot fully recapitulate the *in vivo* environment and data acquired from Oatp KO mice are limited by species differences. One solution to these problems would be to rely on pharmacogenetic/pharmacogenomic data to evaluate the relevance of OATPs, however, with the exception of OATP1B1, these studies are scarce. In addition, although results obtained from pharmacogenetic studies do faithfully represent the *in vivo* environment, these data should be interpreted by considering interindividual genetic differences and the potential compensatory effect of other transporters.

Because OATPs also influence local drug concentrations, the differential expression of OATPs may be exploited in several ways. Liver-specific OATPs may be exploited in hepatic drug targeting or in noninvasive diagnostic techniques (e.g. positron emission tomography) [176]. In addition, OATPs that show cancer-specific expression could be used for tumor-selective drug delivery. However, tumor-selective drug delivery would require the use of selective substrates to minimize systemic toxicity. In addition, tumors could also be targeted using a different approach: as the physiological function of OATPs is hormone and nutrient transport, cancer cells could be deprived of these factors using OATP-specific inhibitors.

OATPs 1A2, 1B1, 1B3, and 2B1 are relatively well characterized; however, less is known about the other members of the OATP family including a liver-specific OATP2B1 variant [94], and a cancer-specific 1B3 isoform [121]. An increasing number of GWAS is likely to elucidate which members of the OATP family are most critical to ADME. However, discovering OATP-specific substrates for targeted drug delivery requires the establishment of *in vitro* assays suitable for large-scale substrate screening experiments.

Funding

This research has been supported by research grants from the Hungarian Scientific Research Fund (OTKA, K 109423) and MedInProt. C Özvegy-Laczka is a recipient of the János Bolyai Scholarship of the Hungarian Academy of Sciences.

Declaration of interest

The authors have no other relevant affiliations or financial involvement with any organization or entity with a financial interest in or financial conflict with the subject matter or materials discussed in the manuscript apart from those disclosed.

References

Papers of special note have been highlighted as either of interest (*) or of considerable interest (***) to readers.

- Gu Q, Paulose-Ram R, Burt VL, et al. Prescription cholesterol-lowering medication use in adults aged 40 and over: United States, 2003-2012. NCHS Data Brief. 2014;177:1-8.
- Wenner Moyer M. The search beyond statins. Nat Med. 2010;16:150-153.
- Shitara Y, Itoh T, Sato H, et al. Inhibition of transporter-mediated hepatic uptake as a mechanism for drug-drug interaction between cerivastatin and cyclosporin A. J Pharmacol Exp Ther. 2003;304:610-616.
- First study demonstrating DDI between cyclosporin A and cerivastatin due to the inhibition of OATP1B1.**
- Elsby R, Hilgendorf C, Fenner K. Understanding the critical disposition pathways of statins to assess drug-drug interaction risk during drug development: it's not just about OATP1B1. Clin Pharmacol Ther. 2012;92:584-598.
- Gong IY, Kim RB. Impact of genetic variation in OATP transporters to drug disposition and response. Drug Metab Pharmacokinet. 2013;28:4-18.
- A comprehensive review on OATP SNPs.**
- Giacomini KM, Huang S, Tweedie DJ, et al. Membrane transporters in drug development. Nature. 2012;9:215-236.
- The white paper on the role of OATPs (and other transporters) in pharmacokinetics.**
- Huang S-M, Zhang L, Giacomini KM. The international transporter consortium: a collaborative group of scientists from academia, industry, and the FDA. Clin Pharmacol Ther. 2010;87:32-36.
- Major guidelines to study the interaction of transporters with new molecular entities.**
- Yu J, Ritchie TK, Mulgaonkar A, et al. Drug disposition and drug-drug interaction data in 2013 FDA new drug applications: a systematic review. Drug Metab Dispos. 2014;42:1991-2001.
- Li L, Meier PJ, Ballatori N. Oatp2 mediates bidirectional organic solute transport: a role for intracellular glutathione. Mol Pharmacol. 2000;58:335-340.
- The first study demonstrating a novel mechanism for OATP transport.**
- Satlin LM, Amin V, Wolkoff AW, et al. Organic anion transporting polypeptide mediates organic anion /HCO₃⁻ exchange *. J Biol Chem. 1997;272:26340-26345.
- The first study demonstrating a novel mechanism for OATP transport.**
- Hagenbuch B, Stieger B. The SLCO (former SLC21) superfamily of transporters. Mol Aspects Med. 2013;34:396-412.
- A comprehensive review about OATP expression, function, and physiological relevance.**
- Leuthold S, Hagenbuch B, Mohebbi N, et al. Mechanisms of pH-gradient driven transport mediated by organic anion polypeptide transporters. Am J Physiol Cell Physiol. 2009;296:C570-82.
- A comprehensive study about the pH dependence of various human and rodent OATPs.**
- Patik I, Kovacsics D, Németh O, et al. Functional expression of the 11 human organic anion transporting polypeptides in insect cells reveals that sodium fluorescein is a general OATP substrate. Biochem Pharmacol. 2015;98:649-658.
- The first study demonstrating transport of a fluorescent substrate for all human OATPs.**
- Masuda S, Ibaramoto K, Takeuchi A, et al. Cloning and functional characterization of a new multispecific organic anion transporter, OAT-K2, in rat kidney. Mol Pharmacol. 1999;55:743-752.
- Roth M, Obaidat A, Hagenbuch B. OATPs, OATs and OCTs: the organic anion and cation transporters of the SLCO and SLC22A gene superfamilies. Br J Pharmacol. 2012;165:1260-1287.
- A review with an excellent overview of OATP substrates.**
- Durmus S, Naik J, Buil L, et al. In vivo disposition of doxorubicin is affected by mouse OATP1a/1b and human OATP1A/1B transporters. Int J Cancer. 2014;135:1700-1710.
- Cheng Z, Liu H, Yu N, et al. Hydrophilic anti-migraine triptans are substrates for OATP1A2, a transporter expressed at human blood-brain barrier. Xenobiotica. 2012;42:880-890.
- Gozalpour E, Greupink R, Wortelboer HM, et al. Interaction of digitalis-like compounds with liver uptake transporters NTCP, OATP1B1, and OATP1B3. Mol Pharm. 2014;11:1844-1855.
- Sprowl JA, Sparreboom A. Uptake carriers and oncology drug safety. Drug Metab Dispos. 2014;42:611-622.
- A review giving a good overview of chemotherapeutics transported by OATPs.**
- Chan T, Zhu L, Madigan MC, et al. Human organic anion transporting polypeptide 1A2 (OATP1A2) mediates cellular uptake of all-trans-retinol in human retinal pigmented epithelial cells. Br J Pharmacol. 2015;172:2343-2353.

21. Kullak-Ublick GA, Hagenbuch B, Stieger B, et al. Molecular and functional characterization of an organic anion transporting polypeptide cloned from human liver. *Gastroenterology*. 1995;109:1274–1282.
22. Gao B, Vavricka SR, Meier PJ, et al. Differential cellular expression of organic anion transporting peptides OATP1A2 and OATP2B1 in the human retina and brain: implications for carrier-mediated transport of neuropeptides and neurosteroids in the CNS. *Pflügers Arch Eur J Physiol*. 2014;467:1481–1493.
23. Misaka S, Yatabe J, Müller F, et al. Green tea ingestion greatly reduces plasma concentrations of nadolol in healthy subjects. *Clin Pharmacol Ther*. 2014;95:432–438.
24. Gao B, Hagenbuch B, Kullak-Ublick GA, et al. Organic anion-transporting polypeptides mediate transport of opioid peptides across blood-brain barrier. *J Pharmacol Exp Ther*. 2000;294:73–79.
25. Kullak-Ublick GA, Ismail MG, Stieger B, et al. Organic anion-transporting polypeptide B (OATP-B) and its functional comparison with three other OATPs of human liver. *Gastroenterology*. 2001;120:525–533.
26. Iusuf D, Hendrikx JJMA, van Esch A, et al. Human OATP1B1, OATP1B3 and OATP1A2 can mediate the in vivo uptake and clearance of docetaxel. *Int J Cancer*. 2015;136:225–233.
27. Badagnani I, Castro RA, Taylor TR, et al. Interaction of methotrexate with organic-anion transporting polypeptide 1A2 and its genetic variants. *J Pharmacol Exp Ther*. 2006;318:521–529.
- **First study characterizing new OATP1A2 SNPs.**
28. Glaeser H, Bujok K, Schmidt I, et al. Organic anion transporting polypeptides and organic cation transporter 1 contribute to the cellular uptake of the flavonoid quercetin. *Naunyn Schmiedebergs Arch Pharmacol*. 2014;387:883–891.
29. Van Montfoort JE1, Müller M, Groothuis GM, et al. Comparison of 'Type I' and 'Type II' organic cation transport by organic cation transporters and organic anion-transporting polypeptides. *J Pharmacol Exp Ther*. 2001;298:110–115.
30. Forster S, Thumser AE, Hood SR, et al. Characterization of rhodamine-123 as a tracer dye for use in in vitro drug transport assays. *PLoS One*. 2012; 7: e33253.
31. Su Y, Zhang X, Sinko PJ. Human organic anion-transporting polypeptide OATP-A (SLC21A3) acts in concert with P-glycoprotein and multidrug resistance protein 2 in the vectorial transport of Saquinavir in Hep G2 cells. *Mol Pharm*. 2004;1:49–56.
32. Bexten M, Oswald S, Grube M, et al. Expression of drug transporters and drug metabolizing enzymes in the bladder urothelium in man and affinity of the bladder spasmolytic trospium chloride to transporters likely involved in its pharmacokinetics. *Mol Pharm*. 2015;12:171–178.
33. Hagenbuch B, Meier PJ. The superfamily of organic anion transporting polypeptides. *Biochim Biophys Acta*. 2003;1609:1–18.
34. Izumi S, Nozaki Y, Komori T, et al. Substrate-dependent inhibition of organic anion transporting polypeptide 1B1: comparative analysis with prototypical probe substrates estradiol-17 β -glucuronide, estrone-3-sulfate, and sulfobromophthalein. *Drug Metab Dispos*. 2013;41:1859–1866.
35. Oshida K, Shimamura M, Seya K, et al. Identification of transporters involved in beraprost sodium transport in vitro. *Eur J Drug Metab Pharmacokinet*. 2016. DOI:10.1007/s13318-016-0327-4
36. Izumi S, Nozaki Y, Komori T, et al. Investigation of fluorescein derivatives as substrates of Organic Anion Transporting Polypeptide (OATP) 1B1 to develop sensitive fluorescence-based OATP1B1 inhibition assays. *Mol Pharm*. 2016;13:438–448.
37. Lee HH, Leake BF, Teft W, et al. Contribution of hepatic organic anion-transporting polypeptides to docetaxel uptake and clearance. *Mol Cancer Ther*. 2015;14:994–1003.
38. Abe T, Kakyō M, Tokui T, et al. Identification of a novel gene family encoding human liver-specific organic anion transporter LST-1. *J Biol Chem*. 1999;274:17159–17163.
39. Gui C, Obaidat A, Chaguturu R, et al. Development of a cell-based high-throughput assay to screen for inhibitors of organic anion transporting polypeptides 1B1 and 1B3. *Curr Chem Genomics*. 2010;4:1–8.
- **The first study to establish a high-throughput functional assay for OATPs.**
40. Gui C, Miao Y, Thompson L, et al. Effect of pregnane X receptor ligands on transport mediated by human OATP1B1 and OATP1B3. *Eur J Pharmacol*. 2008;584:57–65.
41. De Bruyn T, Fattah S, Stieger B, et al. Sodium fluorescein is a probe substrate for hepatic drug transport mediated by OATP1B1 and OATP1B3. *J Pharm Sci*. 2011;100:5018–5030.
42. Ismail MG, Stieger B, Cattori V, et al. Hepatic uptake of cholecystokinin octapeptide by organic anion-transporting polypeptides OATP4 and OATP8 of rat and human liver. *Gastroenterology*. 2001;121:1185–1190.
43. Obaidat A, Roth M, Hagenbuch B. The expression and function of organic anion transporting polypeptides in normal tissues and in cancer. *Annu Rev Pharmacol Toxicol*. 2012;52:135–151.
- **A review summarizing OATP expression in normal and malignant tissues.**
44. König J, Cui Y, Nies AT, et al. Localization and genomic organization of a new hepatocellular organic anion transporting polypeptide. *J Biol Chem*. 2000;275:23161–23168.
45. Pizzagalli F, Hagenbuch B, Stieger B, et al. Identification of a novel human organic anion transporting polypeptide as a high affinity thyroxine transporter. *Mol Endocrinol*. 2002;16:2283–2296.
46. Schnell C, Shahmoradi A, Wichert SP, et al. The multispecific thyroid hormone transporter OATP1C1 mediates cell-specific sulforhodamine 101-labeling of hippocampal astrocytes. *Brain Struct Funct*. 2013;220:193–203.
47. Lu R, Kanai N, Bao Y, et al. Cloning, in vitro expression, and tissue distribution of a human prostaglandin transporter cDNA(hPGT). *J Clin Invest*. 1996;98:1142–1149.
48. Hagenbuch B, Gui C. Xenobiotic transporters of the human organic anion transporting polypeptides (OATP) family. *Xenobiotica*. 2008;38:778–801.
49. Nozawa T, Imai K, Nezu J-I, et al. Functional characterization of pH-sensitive organic anion transporting polypeptide OATP-B in human. *J Pharmacol Exp Ther*. 2004;308:438–445.
50. Tamai I, Nezu J, Uchino H, et al. Molecular identification and characterization of novel members of the human organic anion transporter (OATP) family. *Biochem Biophys Res Commun*. 2000;273:251–260.
51. Huber RD, Gao B, Sidler Pfändler M-A, et al. Characterization of two splice variants of human organic anion transporting polypeptide 3A1 isolated from human brain. *Am J Physiol Cell Physiol*. 2007;292: C795–C806.
52. Fujiwara K, Adachi H, Nishio T, et al. Identification of thyroid hormone transporters in humans: different molecules are involved in a tissue-specific manner. *Endocrinology*. 2001;142:2005–2012.
53. Mikkaichi T, Suzuki T, Onogawa T, et al. Isolation and characterization of a digoxin transporter and its rat homologue expressed in the kidney. *Proc Natl Acad Sci U S A*. 2004;101:3569–3574.
54. Yamaguchi H, Sugie M, Okada M, et al. Transport of estrone 3-sulfate mediated by organic anion transporter OATP4C1: estrone 3-sulfate binds to the different recognition site for digoxin in OATP4C1. *Drug Metab Pharmacokinet*. 2010;25:314–317.
55. Chu XY, Bleasby K, Yabut J, et al. Transport of the dipeptidyl peptidase-4 inhibitor sitagliptin by human organic anion transporter 3, organic anion transporting polypeptide 4C1, and multidrug resistance P-glycoprotein. *J Pharmacol Exp Ther*. 2007;321:673–683.
56. Kato K, Shirasaka Y, Kuraoka E, et al. Intestinal absorption mechanism of tebipenem pivoxil, a novel oral carbapenem: involvement of human OATP family in apical membrane transport. *Mol Pharm*. 2010;7:1747–1756.
57. Yamakawa Y, Hamada A, Shuto T, et al. Pharmacokinetic impact of SLC01A2 polymorphisms on imatinib disposition in patients with chronic myeloid leukemia. *Clin Pharmacol Ther*. 2011;90:157–163.
58. Shirasaka Y, Kuraoka E, Spahn-Langguth H, et al. Species difference in the effect of grapefruit juice on intestinal absorption of talinolol between human and Rat. *J Pharmacol Exp Ther*. 2010;332:181–189.

59. Glaeser H, Bailey DG, Dresser GK, et al. Intestinal drug transporter expression and the impact of grapefruit juice in humans. *Clin Pharmacol Ther.* 2007;81:362–370.
60. Bailey DG, Dresser GK, Leake BF, et al. Naringin is a major and selective clinical inhibitor of organic anion-transporting polypeptide 1A2 (OATP1A2) in grapefruit juice. *Clin Pharmacol Ther.* 2007;81:495–502.
61. Shirasaka Y, Suzuki K, Nakanishi T, et al. Intestinal absorption of HMG-CoA reductase inhibitor pravastatin mediated by organic anion transporting polypeptide. *Pharm Res.* 2010;27:2141–2149.
62. Fischer WJ, Altheimer S, Cattori V, et al. Organic anion transporting polypeptides expressed in liver and brain mediate uptake of microcystin. *Toxicol Appl Pharmacol.* 2005;203:257–263.
63. König J, Seithel A, Gradhand U, et al. Pharmacogenomics of human OATP transporters. *Naunyn Schmiedebergs Arch Pharmacol.* 2006;372:432–443.
64. Dresser GK, Bailey DG, Leake BF, et al. Fruit juices inhibit organic anion transporting polypeptide-mediated drug uptake to decrease the oral availability of fexofenadine. *Clin Pharmacol Ther.* 2002;71:11–20.
65. Parvez MM, Jung J-A, Shin H-J, et al. Characterization of 22 anti-tuberculosis drugs for the inhibitory interaction potential on organic anionic transporter polypeptides (OATPs) mediated uptake. *Antimicrob Agents Chemother.* 2016;60:3096–3105.
66. Karlgren M, Vildhede A, Norinder U, et al. Classification of inhibitors of hepatic Organic Anion Transporting Polypeptides (OATPs): influence of protein expression on drug – drug interactions. *J Med Chem.* 2012;55:4740–4763.
67. Brenner S, Riha J, Giessrigl B, et al. The effect of organic anion-transporting polypeptides 1B1, 1B3 and 2B1 on the antitumor activity of flavopiridol in breast cancer cells. *Int J Oncol.* 2015;46:324–332.
68. Lancaster CS, Sprowl JA, Walker AL, et al., Sparreboom and AS. Modulation of OATP1B-type transporter function alters cellular uptake and disposition of platinum chemotherapeutics. *Mol Cancer Ther.* 2013;12:1537–1544.
69. Zimmerman EI, Hu S, Roberts JL, et al. Contribution of OATP1B1 and OATP1B3 to the disposition of sorafenib and sorafenib-glucuronide. *Clin Cancer Res.* 2013;19:1458–1466.
70. Treiber A, Schneider R, Häusler S, et al. Bosentan is a substrate of human OATP1B1 and OATP1B3: inhibition of hepatic uptake as the common mechanism of its interactions with cyclosporin A, rifampicin, and sildenafil. *Drug Metab Dispos.* 2007;35:1400–1407.
71. Yamashiro W, Maeda K, Hirouchi M, et al. Involvement of transporters in the hepatic uptake and biliary excretion of valsartan, a selective antagonist of the angiotensin II AT1-receptor, in humans. *Drug Metab Dispos.* 2006;34:1247–1254.
72. König J, Glaeser H, Keiser M, et al. Role of organic anion-transporting polypeptides for cellular mesalazine (5-aminosalicylic acid) uptake. *Drug Metab Dispos.* 2011;39:1097–1102.
73. Shitara Y, Hirano M, Sato H, et al. Gemfibrozil and Its glucuronide inhibit the organic anion transporting polypeptide 2 (OATP2/OATP1B1: SLC21A6)-mediated hepatic uptake and cyp2c8-mediated metabolism of cerivastatin: analysis of the mechanism of the clinically relevant drug-drug interaction. *J Pharmacol Exp Ther.* 2004;311:228–236.
74. Monks NR, Liu S, Xu Y, et al. Potent cytotoxicity of the phosphatase inhibitor microcystin LR and microcystin analogues in OATP1B1- and OATP1B3-expressing HeLa cells. *Mol Cancer Ther.* 2007;6:587–598.
75. Karlgren M, Ahlin G, Bergström CAS, et al. In vitro and in silico strategies to identify OATP1B1 inhibitors and predict clinical drug-drug interactions. *Pharm Res.* 2012;29:411–426.
76. Prueksaritanont T, Chu X, Evers R, et al. Pitavastatin is a more sensitive and selective organic anion-transporting polypeptide 1B clinical probe than rosuvastatin. *Br J Clin Pharmacol.* 2014;78:587–598.
77. Smith NF, Marsh S, Scott-Horton TJ, et al. Variants in the SLCO1B3 gene: interethnic distribution and association with paclitaxel pharmacokinetics. *Clin Pharmacol Ther.* 2007;81:76–82.
78. Nambu T, Hamada A, Nakashima R, et al. Association of SLCO1B3 polymorphism with intracellular accumulation of imatinib in leukocytes in patients with chronic myeloid leukemia. *Biol Pharm Bull.* 2011;34:114–119.
79. Mandery K, Bujok K, Schmidt I, et al. Influence of cyclooxygenase inhibitors on the function of the prostaglandin transporter organic anion-transporting polypeptide 2A1 expressed in human gastroduodenal mucosa. *J Pharmacol Exp Ther.* 2010;332:345–351.
80. Kraft ME, Glaeser H, Mandery K, et al. The prostaglandin transporter OATP2A1 is expressed in human ocular tissues and transports the antiglaucoma prostanoid latanoprost. *Invest Ophthalmol Vis Sci.* 2010;51:2504–2511.
81. Scialis RJ, Manautou JE. Elucidation of the mechanisms through which the reactive metabolite diclofenac acyl glucuronide can mediate toxicity. *J Pharmacol Exp Ther.* 2016;357:167–176.
82. Knauer MJ, Urquhart BL, Meyer Zu Schwabedissen HE, et al. Human skeletal muscle drug transporters determine local exposure and toxicity of statins. *Circ Res.* 2010;106:297–306.
83. Wei SC, Tan YY, Weng MT, et al. SLCO3A1, a novel Crohn's disease-associated gene, regulates NF- κ B activity and associates with intestinal perforation. *PLoS One.* 2014;9:e100515.
84. He J, Yu Y, Prasad B, et al. Mechanism of an unusual, but clinically significant, digoxin-bupropion drug interaction. *Biopharm Drug Dispos.* 2014;35:253–263.
85. Toyohara T, Suzuki T, Morimoto R, et al. SLCO4C1 transporter eliminates uremic toxins and attenuates hypertension and renal inflammation. *Ther Res.* 2010;31:1221–1223.
- **First study about the potential role of OATP4C1 in the kidney.**
86. Hamilton U, Olszewski M, Svoboda M, et al. Organic anion transporting polypeptide 5A1 (OATP5A1) in Small Cell Lung Cancer (SCLC) cells: possible involvement in chemoresistance to satraplatin. *Biomark Cancer.* 2011;3:31–40.
87. Shimada H, Nakamura Y, Nakanishi T, et al. OATP2A1/SLCO2A1-mediated prostaglandin E2 loading into intracellular acidic compartments of macrophages contributes to exocytotic secretion. *Biochem Pharmacol.* 2015;98:629–638.
- **The first study demonstrating the intracellular expression of an OATP.**
88. Kindla J, Rau TT, Jung R, et al. Expression and localization of the uptake transporters OATP2B1, OATP3A1 and OATP5A1 in non-malignant and malignant breast tissue. *Cancer Biol Ther.* 2011;11:584–591.
89. Mäki P, Neuvonen M, Neuvonen P. SLCO1B1 polymorphism markedly affects the pharmacokinetics of simvastatin acid. *Pharmacogenet Genomics.* 2006;16:873–879.
90. Maeda K. Organic anion transporting polypeptide (OATP)1B1 and OATP1B3 as important regulators of the pharmacokinetics of substrate drugs. *Biol Pharm Bull.* 2015;38:155–168.
91. Shitara Y, Maeda K, Ikejiri K, et al. Clinical significance of organic anion transporting polypeptides (OATPs) in drug disposition: their roles in hepatic clearance and intestinal absorption. *Biopharm Drug Dispos.* 2013;34:45–78.
- **Review summarizing data about the role of OATPs in the intestine.**
92. Kunze A, Huwyler J, Camenisch G, et al. Prediction of organic anion-transporting polypeptide 1B1- and 1B3- mediated hepatic uptake of statins based on transporter protein expression and activity data. *Drug Metab Dispos.* 2014;42:1514–1521.
93. Masereeuw R, Mutsaers HAM, Toyohara T, et al. The kidney and uremic toxin removal: glomerulus or tubule? *semin. Nephrol.* 2014;34:191–208.
94. Knauer MJ, Girdwood AJ, Kim RB, et al. Transport function and transcriptional regulation of a liver-enriched human organic anion transporting polypeptide 2B1 transcriptional start site variant. *Mol Pharmacol.* 2013;83:1218–1228.
- **The first study about the functional characterization of an OATP2B1 transcript variant.**
95. Meier Y, Eloranta J, Darimont J. Regional distribution of solute carrier mRNA expression along the human intestinal tract. *Drug Metab.* 2007;35:590–594.
96. Kobayashi D, Nozawa T, Imai K, et al. Involvement of human organic anion transporting polypeptide OATP-B (SLC21A9) in pH-dependent transport across intestinal apical membrane. *J Pharmacol Exp Ther.* 2003;306:703–708.

97. Urquhart BL, Kim RB. Blood-brain barrier transporters and response to CNS-active drugs. *Eur J Clin Pharmacol.* **2009**;65:1063–1070.
98. Su L, Mruk DD, Lee WM, et al. Drug transporters and blood–testis barrier function. *J Endocrinol.* **2015**;2:337–351.
99. Gao B, Huber RD, Wenzel A, et al. Localization of organic anion transporting polypeptides in the rat and human ciliary body epithelium. *Exp Eye Res.* **2005**;80:61–72.
100. Wang H, Yan Z, Dong M, et al. Alteration in placental expression of bile acids transporters OATP1A2, OATP1B1, OATP1B3 in intrahepatic cholestasis of pregnancy. *Arch Gynecol Obstet.* **2012**;285:1535–1540.
101. Grube M, Reuther S, Meyer Zu Schwabedissen H, et al. Organic anion transporting polypeptide 2B1 and breast cancer resistance protein interact in the transepithelial transport of steroid sulfates in human placenta. *Drug Metab Dispos.* **2007**;35:30–35.
102. Hagenbuch B. Cellular entry of thyroid hormones by organic anion transporting polypeptides. *Best Pract Res Clin Endocrinol Metab.* **2007**;21:209–221.
103. Memon N, Weinberger BI, Hegyi T, et al. Inherited disorders of bilirubin clearance. *Pediatr Res.* **2016**;79:378–386.
104. Van De Steeg E, Stránecký V, Hartmannová H, et al. Complete OATP1B1 and OATP1B3 deficiency causes human Rotor syndrome by interrupting conjugated bilirubin reuptake into the liver. *J Clin Invest.* **2012**;122:519–528.
105. Van De Steeg E, Wagenaar E, van der Kruijssen CMM, et al. Organic anion transporting polypeptide 1a/1b-knockout mice provide insights into hepatic handling of bilirubin, bile acids, and drugs. *J Clin Invest.* **2010**;120:2942–2952.
106. Isidor B, Pichon O, Redon R, et al. Mesomelia-synostoses syndrome results from deletion of *slc1* and *slco5a1* genes at 8q13. *Am J Hum Genet.* **2010**;87:95–100.
107. Zhang Z, Xia W, He J, et al. Exome sequencing identifies *SLCO2A1* mutations as a cause of primary hypertrophic osteoarthropathy. *Am J Hum Genet.* **2012**;90:125–132.
108. Umeno J, Hisamatsu T, Esaki M, et al. A hereditary enteropathy caused by mutations in the *SLCO2A1* gene, encoding a prostaglandin transporter. *PLoS Genet.* **2015**;11:1–15.
109. Nakanishi T, Hasegawa Y, Mimura R, et al. Prostaglandin transporter (PGT/*SLCO2A1*) protects the lung from bleomycin-induced fibrosis. *PLoS One.* **2015**;10:1–19.
110. Höglinger GU, Melhem NM, Dickson DW, et al. Identification of common variants influencing risk of the tauopathy progressive supranuclear palsy. *Nat Genet.* **2011**;43:699–705.
111. Kenny EE, Pe'er I, Karban A, et al. A genome-wide scan of Ashkenazi Jewish Crohn's disease suggests novel susceptibility loci. *PLoS Genet.* **2012**;8:e1002559.
112. Lee W, Glaeser H, Smith LH, et al. Polymorphisms in human organic anion-transporting polypeptide 1A2 (OATP1A2): implications for altered drug disposition and central nervous system drug entry. *J Biol Chem.* **2005**;280:9610–9617.
113. Bronger H, König J, Kopplow K, et al. ABC drug efflux pumps and organic anion uptake transporters in human gliomas and the blood-tumor barrier. *Cancer Res.* **2005**;65:11419–11428.
114. Wlcek K, Svoboda M, Thalhammer T, et al. Altered expression of organic anion transporter polypeptide (OATP) genes in human breast carcinoma. *Cancer Biol Ther.* **2008**;7:1450–1455.
115. Ballester MR, Monte MJ, Briz O, et al. Expression of transporters potentially involved in the targeting of cytostatic bile acid derivatives to colon cancer and polyps. *Biochem Pharmacol.* **2006**;72:729–738.
116. Liedauer R, Svoboda M, Wlcek K, et al. Different expression patterns of organic anion transporting polypeptides in osteosarcomas, bone metastases and aneurysmal bone cysts. *Oncol Rep.* **2009**;22:1485–1492.
117. Meyer Zu Schwabedissen HE, Tirona RG, Yip CS, et al. Interplay between the nuclear receptor pregnane X receptor and the uptake transporter organic anion transporter polypeptide 1A2 selectively enhances estrogen effects in breast cancer. *Cancer Res.* **2008**;68:9338–9347.
118. Arakawa H, Nakanishi T, Yanagihara C, et al. Enhanced expression of organic anion transporting polypeptides (OATPs) in androgen receptor-positive prostate cancer cells: possible role of OATP1A2 in adaptive cell growth under androgen-depleted conditions. *Biochem Pharmacol.* **2012**;84:1070–1077.
119. Thakkar N, Lockhart AC, Lee W. Role of organic anion-transporting polypeptides (OATPs) in cancer therapy. *AAPS J.* **2015**;17:535–545.
120. Zu Schwabedissen HEM, Boettcher K, Steiner T, et al. OATP1B3 is expressed in pancreatic b-islet cells and enhances the insulinotropic effect of the sulfonylurea derivative glibenclamide. *Diabetes.* **2014**;63:775–784.
121. Furihata T, Sun YCK. Cancer-type organic anion transporting polypeptide 1B3: current knowledge of the gene structure, expression profile, functional implications and future perspectives. *Curr Drug Metab.* **2015**;16:474–485.
- **A recent review demonstrating that a cancer-type OATP1B3 variant is present in most tumor tissues and cell lines.**
122. Kang J, Chapdelaine P, Parent J, et al. Expression of human prostaglandin transporter in the human endometrium across the menstrual cycle. *J Clin Endocrinol Metab.* **2005**;90:2308–2313.
123. Choi K, Zhuang H, Crain BDS. Expression and localization of prostaglandin transporter in Alzheimer disease brains and age-matched controls. *J Neuroimmunol.* **2008**;195:81–87.
124. Wlcek K, Svoboda M, Riha J, et al. The analysis of organic anion transporting polypeptide (OATP) mRNA and protein patterns in primary and metastatic liver cancer. *Cancer Biol Ther.* **2011**;11:801–811.
125. Al Sarakbi W, Mokbel R, Salhab M, et al. The role of STS and OATP-B mRNA expression in predicting the clinical outcome in human breast cancer. *Anticancer Res.* **2006**;26:4985–4990.
126. Nozawa T, Suzuki M, Takahashi K, et al. Involvement of estrone-3-sulfate transporters in proliferation of hormone-dependent breast cancer cells. *J Pharmacol Exp Ther.* **2004**;311:1032–1037.
127. Pizzagalli F, Varga Z, Huber RD, et al. Identification of steroid sulfate transport processes in the human mammary gland. *J Clin Endocrinol Metab.* **2003**;88:3902–3912.
128. Nozawa T, Suzuki M, Yabuuchi H, et al. Suppression of cell proliferation by inhibition of estrone-3-sulfate transporter in estrogen-dependent breast cancer cells. *Pharm Res.* **2005**;22:1634–1641.
129. Sato K, Sugawara J, Sato T, et al. Expression of organic anion transporting polypeptide E (OATP-E) in human placenta. *Placenta.* **2003**;24:144–148.
130. Brenner S, Klameth L, Riha J, et al. Specific expression of OATPs in primary small cell lung cancer (SCLC) cells as novel biomarkers for diagnosis and therapy. *Cancer Lett.* **2015**;356:517–524.
131. Okabe M, Szakács G, Reimers MA, et al. Profiling *SLCO* and *SLC22* genes in the NCI-60 cancer cell lines to identify drug uptake transporters. *Mol Cancer Ther.* **2008**;7:3081–3091.
132. Lee S-Y, Williamson B, Caballero OL, et al. Identification of the gonad-specific anion transporter *SLCO6A1* as a cancer/testis (CT) antigen expressed in human lung cancer. *Cancer Immunol.* **2004**;4:13.
133. Muto M, Onogawa T, Suzuki T, et al. Human liver-specific organic anion transporter-2 is a potent prognostic factor for human breast carcinoma. *Cancer Sci.* **2007**;98:1570–1576.
134. Wright JL, Kwon EM, Ostrander EA, et al. Expression of *SLCO* transport genes in castration-resistant prostate cancer and impact of genetic variation in *SLCO1B3* and *SLCO2B1* on prostate cancer outcomes. *Cancer Epidemiol Biomarkers Prev.* **2011**;20:619–627.
135. Hamada A, Sissung T, Price DK, et al. Effect of *SLCO1B3* haplotype on testosterone transport and clinical outcome in caucasian patients with androgen-independent prostatic cancer. *Clin Cancer Res.* **2008**;14:3312–3318.
136. Yamaguchi H, Okada M, Akitaya S, et al. Transport of fluorescent chenodeoxycholic acid via the human organic anion transporters OATP1B1 and OATP1B3. *J Lipid Res.* **2006**;47:1196–1202.
137. de Waart DR, Häusler S, Vlaming MLH, et al. Hepatic transport mechanisms of cholestyramine-L-lysyl-fluorescein. *J Pharmacol Exp Ther.* **2010**;334:78–86.
138. Kopplow K, Letschert K, König J, et al. Human hepatobiliary transport of organic anions analyzed by quadruple-transfected cells. *Mol Pharmacol.* **2005**;68:1031–1038.
139. Sun D, Lennernas H, Welage LS, et al. Comparison of human duodenum and Caco-2 gene expression profiles for 12,000 gene

- sequences tags and correlation with permeability of 26 drugs. *Pharm Res.* 2002;19:1400–1416.
140. Sato T, Vries RG, Snippet HJ, et al. Single Lgr5 stem cells build crypt-villus structures in vitro without a mesenchymal niche. *Nature.* 2009;459:262–265.
141. Li M, de Graaf IAM, Groothuis GMM. Precision-cut intestinal slices: alternative model for drug transport, metabolism, and toxicology research. *Expert Opin Drug Metab Toxicol.* 2016;5255:1–16.
142. Soldatow VVY, Lecluyse EEL, Griffith LLG, et al. In vitro models for liver toxicity testing. *Toxicol Res (Camb).* 2013;2:23–39.
143. Herzog N, Hansen M, Miethbauer S, et al. Primary-like human hepatocytes genetically engineered to obtain proliferation competence display hepatic differentiation characteristics in monolayer and organotypical spheroid cultures. *Cell Biol Int.* 2016;40:341–353.
144. Godoy P, Hewitt NJ, Albrecht U, et al. Recent advances in 2D and 3D in vitro systems using primary hepatocytes, alternative hepatocyte sources and non-parenchymal liver cells and their use in investigating mechanisms of hepatotoxicity, cell signaling and ADME. *Arch Toxicol.* 2013;87:1315–1530.
- **An excellent overview of the limitations of the current hepatic models and possible novel strategies to model hepatic transport processes.**
145. Evers R, Chu XY. Role of the murine organic anion-transporting polypeptide 1b2 (OATP1b2) in drug disposition and hepatotoxicity. *Mol Pharmacol.* 2008;74:309–311.
146. Shen H, Dai J, Liu T, et al. Coproporphyrins I and III as functional markers of OATP1B activity: in vitro and in vivo evaluation in preclinical species. *J Pharmacol Exp Ther.* 2016;357:382–393.
147. Lu H, Choudhuri S, Ogura K, et al. Characterization of organic anion transporting polypeptide 1b2-null mice: essential role in hepatic uptake/toxicity of phalloidin and microcystin-LR. *Toxicol Sci.* 2008;103:35–45.
148. Zaher H, Meyer Zu Schwabedissen HE, Tirona RG, et al. Targeted disruption of murine organic anion-transporting polypeptide 1b2 (OATP1b2/SLCO1b2) significantly alters disposition of prototypical drug substrates pravastatin and rifampin. *Mol Pharmacol.* 2008;74:320–329.
149. Kuo K-L, Zhu H, McNamara PJ, et al. Localization and functional characterization of the Rat OATP4c1 Transporter in an in vitro cell system and rat tissues. *PLoS One.* 2012;7:e39641.
150. van de Steeg E, van der Kruijssen CM, Wagenaar E, et al. Methotrexate pharmacokinetics in transgenic mice with liver-specific expression of human organic anion-transporting polypeptide 1B1 (SLCO1B1). *Drug Metab Dispos.* 2009;37:277–281.
151. van de Steeg E, van Esch A, Wagenaar E, et al. Influence of human OATP1B1, OATP1B3, and OATP1A2 on the pharmacokinetics of methotrexate and paclitaxel in humanized transgenic mice. *Clin Cancer Res.* 2013;19:821–832.
152. Durmus S, Lozano-Mena G, van Esch A, et al. Preclinical mouse models to study human OATP1B1- and OATP1B3-mediated drug-drug interactions in vivo. *Mol Pharm.* 2015;12:4259–4269.
153. List AF, Spier C, Greer J, et al. Phase I/II trial of cyclosporine as a chemotherapy-resistance modifier in acute leukemia. *J Clin Oncol.* 1993;11:1652–1660.
154. Khurana V, Minocha M, Pal D, et al. Role of OATP-1B1 and/or OATP-1B3 in hepatic disposition of tyrosine kinase inhibitors. *Drug Metabol Drug Interact.* 2014;29:179–190.
155. Nozawa T, Minami H, Sugiura S, et al. Role of organic anion transporter OATP1B1 (OATP-C) in hepatic uptake of irinotecan and its active metabolite, 7-ethyl-10-hydroxycamptothecin: in vitro evidence and effect of single nucleotide polymorphisms. *Drug Metab Dispos.* 2005;33:434–439.
156. Oswald S, König J, Lütjohann D, et al. Disposition of ezetimibe is influenced by polymorphisms of the hepatic uptake carrier OATP1B1. *Pharmacogenet Genomics.* 2008;18:559–568.
157. Kalliokoski A, Neuvonen M, Neuvonen PJ, et al. Different effects of SLCO1B1 polymorphism on the pharmacokinetics and pharmacodynamics of repaglinide and nateglinide. *J Clin Pharmacol.* 2008;48:311–321.
158. Giannakopoulou E, Ragia G, Kolovou V, et al. No impact of SLCO1B1 521T>C, 388A>G and 411G>A polymorphisms on response to statin therapy in the Greek population. *Mol Biol Rep.* 2014;41:4631–4638.
159. Tirona RG, Leake BF, Merino G, et al. Polymorphisms in OATP-C: identification of multiple allelic variants associated with altered transport activity among European- and African-Americans. *J Biol Chem.* 2001;276:35669–35675.
160. Niemi M, Pasanen MK, Neuvonen PJ. Organic anion transporting polypeptide 1B1: a genetically polymorphic transporter of major importance for hepatic drug uptake. *Pharmacol Rev.* 2011;63:157–181.
161. Link E, Parish S, Armitage J, et al.; SEARCH Collaborative Group. SLCO1B1 variants and statin-induced myopathy — A genomewide study. *N Engl J Med.* 2008;359:789–799.
162. Tornio A, Vakkilainen J, Neuvonen M, et al. SLCO1B1 polymorphism markedly affects the pharmacokinetics of lovastatin acid. *Pharmacogenet Genomics.* 2015;25:382–387.
163. Gerloff T, Schaefer M, Mwinyi J, et al. Influence of the SLCO1B1*1b and *5 haplotypes on pravastatin's cholesterol lowering capabilities and basal sterol serum levels. *Naunyn Schmiedebergs Arch Pharmacol.* 2006;373:45–50.
164. Li LM, Chen L, Deng GH, et al. SLCO1B1*15 haplotype is associated with rifampin-induced liver injury. *Mol Med Rep.* 2012;6:75–82.
165. Letschert K, Keppler D, König J. Mutations in the SLCO1B3 gene affecting the substrate specificity of the hepatocellular uptake transporter OATP1B3 (OATP8). *Pharmacogenetics.* 2004;14:441–452.
166. Yamakawa Y, Hamada A, Nakashima R, et al. Association of genetic polymorphisms in the influx transporter SLCO1B3 and the efflux transporter ABCB1 with imatinib pharmacokinetics in patients with chronic myeloid leukemia. *Ther Drug Monit.* 2011;33:244–250.
167. Chew SC, Sandanaraj E, Singh O, et al. Influence of SLCO1B3 haplotype-tag SNPs on docetaxel disposition in Chinese nasopharyngeal cancer patients. *Br J Clin Pharmacol.* 2012;73:606–618.
168. Fujimoto N, Kubo T, Inatomi H, et al. Polymorphisms of the androgen transporting gene SLCO2B1 may influence the castration resistance of prostate cancer and the racial differences in response to androgen deprivation. *Prostate Cancer Prostatic Dis.* 2013;16:336–340.
169. Mougey EB, Feng H, Castro M, et al. Absorption of montelukast is transporter mediated: a common variant of OATP2B1 is associated with reduced plasma concentrations and poor response. *Pharmacogenet Genomics.* 2009;19:129–138.
170. Nozawa T, Nakajima M, Tamai I, et al. Genetic polymorphisms of human organic anion transporters OATP-C (SLC21A6) and OATP-B (SLC21A9): allele frequencies in the Japanese population and functional analysis. *J Pharmacol Exp Ther.* 2002;302:804–813.
171. Deepak V, Svati HS, Spasojevic I, et al. The SLCO1B1* 5 genetic variant is associated with statin-induced side effects. *J Am Coll Cardiol.* 2009;54:1609–1616.
172. Donnelly LA, Doney a SF, Tavendale R, et al. Common nonsynonymous substitutions in SLCO1B1 predispose to statin intolerance in routinely treated individuals with type 2 diabetes: a go-DARTS study. *Clin Pharmacol Ther.* 2011;89:210–216.
173. Pasanen MK, Fredrikson H, Neuvonen PJ, et al. Different effects of SLCO1B1 polymorphism on the pharmacokinetics of atorvastatin and rosuvastatin. *Clin Pharmacol Ther.* 2007;82:726–733.
174. Generaux GT, Bonomo FM, Johnson M, et al. Impact of SLCO1B1 (OATP1B1) and ABCG2 (BCRP) genetic polymorphisms and inhibition on LDL-C lowering and myopathy of statins. *Xenobiotica.* 2011;41:639–651.
175. Tamai I. Oral drug delivery utilizing intestinal OATP transporters. *Adv Drug Deliv Rev.* 2012;64:508–514.
176. Solon EG. Use of radioactive compounds and autoradiography to determine drug tissue distribution. *Chem Res Toxicol.* 2012;25:543–555.